

**1.3.3 Research Projects and Internships****P.G. Department of Commerce and Management**

<b>S.No</b>	<b>Course Name</b>	<b>Course Code</b>	<b>Roll No.</b>	<b>Student Name</b>	<b>Project Title</b>
1	B.Com (Hon) (Sem-III)	BCH	232701	Nazia	Tally ERP 9
2	B.Com (Hon) (Sem-III)	BCH	232702	Amanpreet Kaur	Tally ERP 9
3	B.Com (Hon) (Sem-III)	BCH	232703	Anjali Devi	Income Tax
4	B.Com (Hon) (Sem-III)	BCH	232704	Ramneet Kaur	Tally ERP 9
5	B.Com (Hon) (Sem-III)	BCH	232705	Hardeep Kaur	Income Tax
6	B.Com (Hon) (Sem-III)	BCH	232707	Manjot Kaur	Tally ERP 9
7	B.Com (Hon) (Sem-III)	BCH	232708	Dilpreet Kaur	Income Tax Returns
8	B.Com (Hon) (Sem-III)	BCH	232709	Tejveer Singh	Income Tax
9	B.Com (Hon) (Sem-III)	BCH	232710	Deepanshi	GST, Tally ERP 9 and Income Tax
10	B.Com (Hon) (Sem-III)	BCH	232711	Ritika	Material Manangement in NFL
11	B.Com (Hon) (Sem-III)	BCH	232712	Malkeet	Tally ERP 9
12	B.Com (Hon) (Sem-III)	BCH	232713	Kalpana	Purchase Management
13	B.Com (Hon) (Sem-III)	BCH	232714	Harsh	Income Tax
14	B.Com (Hon) (Sem-III)	BCH	232715	Mansimar Kaur	Internship
15	B.Com (Hon) (Sem-III)	BCH	232716	Mehakpreet Kaur	Tally ERP 9
16	B.Com (Hon) (Sem-III)	BCH	232717	Palak	Office Routine work in BBMB
17	B.Com (Hon) (Sem-III)	BCH	232718	Bhoomika	Income Tax and Tally Erp 9
18	B.Com (Hon) (Sem-III)	BCH	232719	Naspreet Kaur	Tally ERP 9
19	B.Com (Hon) (Sem-III)	BCH	232720	Jaswinder Kaur	Tally ERP 9
20	B.Com (Hon) (Sem-III)	BCH	232721	Mandeep Kaur	Tally ERP 9
21	B.Com (Hon) (Sem-III)	BCH	232722	Neelam Rani	Office Routine work in BBMB
22	B.Com (Hon) (Sem-III)	BCH	232723	Jasmeen Kaur	Tally ERP 9
23	B.Com (Hon) (Sem-III)	BCH	232724	Malika Sharma	Tally ERP 9
24	B.Com (Hon) (Sem-III)	BCH	232725	Amandeep Kaur	Tally ERP 9
25	B.Com (Hon) (Sem-III)	BCH	232726	Rani Devi	Tally ERP 9
26	B.Com (Hon) (Sem-III)	BCH	232727	Baljeet Kaur	Material Manangement
27	B.Com (Hon) (Sem-III)	BCH	232728	Sukhwinder Kaur	Tally ERP 9
28	B.Com (Hon) (Sem-III)	BCH	232729	Jasleen Kaur	Tally ERP 9
29	B.Com (Hon) (Sem-III)	BCH	232730	Parveen Kaur	Income Tax
30	B.Com (Hon) (Sem-III)	BCH	232732	Damanpreet Kaur	Income Tax and Tally Erp 9
31	B.Com (Hon) (Sem-III)	BCH	232733	Suman	Tally ERP 9
32	B.Com (Hon) (Sem-III)	BCH	232734	Aditi	Office Routine work in BBMB
33	B.Com (Hon) (Sem-III)	BCH	232735	Simarjot Kaur	Tally ERP 9
34	B.Com (Hon) (Sem-III)	BCH	232736	Aashima	Tally ERP 9
35	B.Com (Hon) (Sem-III)	BCH	232737	Ishika	Tally ERP 9
36	B.Com (Hon) (Sem-III)	BCH	232739	Gurnaman Singh	Income Tax
37	B.Com (Hon) (Sem-III)	BCH	232740	Kinderpreet Kaur	Store Management in NFL
38	B.Com (Hon) (Sem-III)	BCH	232742	Shivali	Tally ERP 9
39	B.Com (Hon) (Sem-III)	BCH	232743	Palak	Tally ERP 9

40	B.Com (Hon) (Sem-III)	BCH	232744	Taranpreet Kaur	Internship
41	B.Com (Hon) (Sem-III)	BCH	232745	Harsimran Kaur	Internship
42	B.Com (Hon) (Sem-III)	BCH	232746	Harsh Kumar	Income Tax
43	B.Com (Hon) (Sem-III)	BCH	232747	Supriya	Accounts and Finance Department at NFL
44	B.Com (Hon) (Sem-III)	BCH	232749	Tamnna Sharma	Income Tax
45	B.Com (Hon) (Sem-III)	BCH	232750	Vanshita	Internship
46	B.Com (Hon) (Sem-III)	BCH	232751	Ishan Chaudhary	Tally ERP 9
47	B.Com (Hon) (Sem-III)	BCH	232752	Harshit Mahajan	Income Tax
48	B.Com (Hon) (Sem-III)	BCH	232753	Pragati	Tally ERP 9
49	B.Com (Hon) (Sem-III)	BCH	232754	Anjali Rana	Accounts and Finance Department at NFL
50	B.Com (Hon) (Sem-III)	BCH	232755	Gurwinder Kaur	Tally ERP 9
51	B.Com (Hon) (Sem-III)	BCH	232756	Charandeep Singh	Tally ERP 9
52	B.Com (Hon) (Sem-III)	BCH	232757	Sethi	Income Tax
53	B.Com (Hon) (Sem-III)	BCH	232758	Gurdeep Singh	Income Tax
54	B.Com (Hon) (Sem-III)	BCH	232760	Komalpreet	Tally ERP 9
55	B.Com (Hon) (Sem-III)	BCH	232762	Sahilpreet Singh	Tally ERP 9
56	B.Com (Hon) (Sem-III)	BCH	232764	Manjot Kaur	Tally ERP 9
57	B.Com (Hon) (Sem-III)	BCH	232766	Mahir Sharma	Tally ERP 9
58	B.Com (Hon) (Sem-III)	BCH	232767	Mandeep Kaur	Tally ERP 9
59	B.Com (Accounting & Finance) (Sem-III)	BCAF	231201	Anchal Saini	GST
60	B.Com (Accounting & Finance) (Sem-III)	BCAF	231202	Manish Kumar	Income Tax
61	B.Com (Accounting & Finance) (Sem-III)	BCAF	231203	Shubam	Gem Portal and MS Word
62	B.Com (Accounting & Finance) (Sem-III)	BCAF	231205	Gurbachan Singh	Tally ERP 9
63	B.Com (Accounting & Finance) (Sem-III)	BCAF	231206	Tanisha	Material Handling
64	B.Com (Accounting & Finance) (Sem-III)	BCAF	231207	Nitin	Income Tax
65	B.Com (Accounting & Finance) (Sem-III)	BCAF	231209	Raman	Tally ERP 9
66	B.Com (Accounting & Finance) (Sem-III)	BCAF	231210	Barinder Singh	BBMB
67	B.Com (Accounting & Finance) (Sem-III)	BCAF	231212	Shweta	Inventory Management
68	B.Com (Accounting & Finance) (Sem-III)	BCAF	231214	Abha	Working Capital Management
69	B.Com (Accounting & Finance) (Sem-III)	BCAF	231217	Janvi	Income Tax Returns
70	B.Com (Accounting & Finance) (Sem-III)	BCAF	231218	Sadhna	Stock Control
71	BBA (Sem-VI)	BBA	211401	Simranpreet Kaur	National Fertilizers Limited, Nangal
72	BBA (Sem-VI)	BBA	211402	Anshita	National Fertilizers Limited, Nangal
73	BBA (Sem-VI)	BBA	211404	Soni Kumari	Jupiter multi fruit processor,Tahliwal
74	BBA (Sem-VI)	BBA	211405	Tanu	National Fertilizer Limited, Nangal
75	BBA (Sem-VI)	BBA	211406	Jasmeet Kaur	Jupiter multi fruit processor,Tahliwal
76	BBA (Sem-VI)	BBA	211407	Navneet Kaur	SML Isuzu ltd , Rupnagar
77	BBA (Sem-VI)	BBA	211408	Chhavi Vashisht	Jupiter multi fruit processor, Tahliwal
78	BBA (Sem-VI)	BBA	211409	Nancy Rana	Royal Enfield Aaray motors Amritsar
79	BBA (Sem-VI)	BBA	211410	Ashima	CA Gurjinder singh firm , Anandpur Sahib
80	BBA (Sem-VI)	BBA	211411	Pardeep Kaur	Ropar Central Co-oparative Bank,Nangal
81	BBA (Sem-VI)	BBA	211412	Yash	Nestle India Limited, Tahliwal

82	BBA (Sem-VI)	BBA	211416	Jashanpreet Kaur	Ropar Central Co-operative Bank, Nangal
83	BBA (Sem-VI)	BBA	211417	Riya	CA Gurjinder Singh firm, Anandpur Sahib
84	BBA (Sem-VI)	BBA	211421	Gurnoor Singh	Wipro enterprises pvt. Ltd. Baddi
85	BBA (Sem-VI)	BBA	211422	Harpreet Kaur	Wisdom Infosoft, Mohali
86	BBA (Sem-VI)	BBA	211424	Varun	Ambuja Cements Limited, Rupnagar
87	BBA (Sem-VI)	BBA	211425	Neha	Ambuja Cements Limited, Rupnagar
88	BBA (Sem-VI)	BBA	211426	Jyoti	Ambuja Cements Limited, Rupnagar
89	BBA (Sem-VI)	BBA	211427	Navjot	<b>Wipro enterprises pvt.ltd.Baddi</b>
90	BBA (Sem-VI)	BBA	211431	Rana Veer Pratap	Wipro enterprises pvt.ltd. Baddi
91	BBA (Sem-VI)	BBA	211434	Komal	Jupiter multi fruit processor, Tahliwal
92	BBA (Sem-VI)	BBA	211435	Simranjeet Singh	CA Gurjinder Singh firm, Anandpur Sahib
93	BBA (Sem-VI)	BBA	211439	Anurag	Jupiter multi fruit processor, Tahliwal
94	BBA (Sem-VI)	BBA	211430	Kamalpreet	Jupiter multi fruit processor, Tahliwal
95	BBA (Sem-VI)	BBA	211440	Bikram Singh	Wisdom Infosoft, Mohali
96	M.Com (Sem-IV)	MCOM	222204	Hardeep Kaur	Study of How Service and Product Quality Effects on Customer satisfaction in Café 21
97	M.Com (Sem-IV)	MCOM	222205	Sabita Sharma	Study of Effectiveness of Digital Marketing Strategies for Clothing Products by Customers (A Case study in Kiratpur Sahib)
98	M.Com (Sem-IV)	MCOM	222206	Simran Singh	to Study customer satisfaction towards E-banking services ( A Case study of Una)
99	M.Com (Sem-IV)	MCOM	222207	Manpreet Kaur	Customer Satisfaction Towards Banking Services of co-operative Bank in Rural Areas
100	M.Com (Sem-IV)	MCOM	222208	Maninder Kaur	Patients satisfaction towards Government Hospital in Bharatgarh
101	M.Com (Sem-IV)	MCOM	222209	Sukhwinder Kaur	General Attitude of Students Towards online learning
102	M.Com (Sem-IV)	MCOM	222210	Ritika	To study the impact of packaging on consumers buying Behaviour
103	M.Com (Sem-IV)	MCOM	222211	Nitika Dutta	A Study On Work Life And Job Performance Of Employees
104	M.Com (Sem-IV)	MCOM	222212	Riya	Brand Preference of Mobile Phones Among Students
105	M.Com (Sem-IV)	MCOM	222213	Priyanka Rani	Factors Behind The Plastic Money (A Case Study Of Sgth Khalsa College Sri Anandpur Sahib)
106	M.Com (Sem-IV)	MCOM	222214	Gagandeep Kaur	Factor Affecting Consumer Preferences Towards The Organic Food Purchase ( A Case Study Of Sgth Khalsa College Sri Anandpur Sahib)
107	M.Com (Sem-IV)	MCOM	222216	Simran Kaur	Causes Of Stress Among, Youth And Its Management ( A Case Study Of Sgth Khalsa College Sri Anandpur Sahib)
108	M.Com (Sem-IV)	MCOM	222217	Shivani Sharma	Awareness Of Stock Market In Rural Areas"
109	M.Com (Sem-IV)	MCOM	222218	Monika	Investment Pattern Of Salaried Employees ( A Case Study Of Nurpur Bedi)
110	M.Com (Sem-IV)	MCOM	222219	Arshdeep Kaur	Customer Satisfaction Towards Flipkart (A Case Study Of Sgth Khalsa College Sri Anandpur Sahib)

111	M.Com (Sem-IV)	MCOM	222220	Ramanjeet Kaur	Consumer Satisfactions Behaviour Verka Milk & Milk Products( A Case Study O F Sri Anandpur Sahib)
112	M.Com (Sem-IV)	MCOM	222221	Bhawna	Customer's Satisfaction In Airtel
113	M.Com (Sem-IV)	MCOM	222222	Meenakshi	Customer Satisfaction Regarding Banking Services Of Punjab National Bank Shri Anandpur Sahib
114	M.Com (Sem-IV)	MCOM	222225	Komalpreet Kaur	Impact Of Social Media On Youngsters (Punjabi University, Patiala)
115	M.Com (Sem-IV)	MCOM	222226	Megha Sharma	Effect Of Fast Food On Human Health
116	M.Com (Sem-IV)	MCOM	222227	Pargat Singh	Customer Satisfaction on Mobile Service Provider Networks
117	B.Voc Retail Management (Sem-VI)	BVRM	214101	Razat Singh Rayat	Color Bucket Store
118	B.Voc Retail Management (Sem-VI)	BVRM	214102	Anchal	Hamir Real Estate Private Ltd at Fun Plaza Multiplex Mall
119	B.Voc Retail Management (Sem-VI)	BVRM	214103	Sourav Sharma	Soni Auto Delaers LLP (Suzuki)
120	B.Voc Retail Management (Sem-VI)	BVRM	214104	Tania	Happy Shopping Complex Dher
121	B.Voc Retail Management (Sem-VI)	BVRM	214107	Ashma Devi	Reliance Centro
122	B.Voc Retail Management (Sem-VI)	BVRM	214110	Diksha Devi	Aditya Birla Fashion And Retail (Pantaloon)
123	B.Voc Retail Management (Sem-VI)	BVRM	214111	Neha	Aditya Birla Fashion And Retail (Pantaloon)
124	B.Voc Retail Management (Sem-VI)	BVRM	214115	Kiranjot Kaur	Hotel Mirage Mohali
125	B.Voc Retail Management (Sem-VI)	BVRM	214116	Seema Mehta	Action Clothing Co. Ltd.
126	B.Voc Retail Management (Sem-VI)	BVRM	214118	Manpreet	Aditya Birla Fashion And Retail (Pantaloon)
127	B.Voc Retail Management (Sem-VI)	BVRM	214121	Hardeep Kaur	Mohit Motors Dher
128	B.Voc Retail Management (Sem-VI)	BVRM	214122	Gursimrat	Click World Mohali
129	B.Voc Retail Management (Sem-VI)	BVRM	214123	Kunal Rana	Rehal Garments(Octave Metal)
130	B.Voc Retail Management (Sem-VI)	BVRM	214125	Mehak Pama	Happy Shopping Complex Dher
131	B.Voc Retail Management (Sem-VI)	BVRM	214126	Mohit Nadda	Boany Technology Pvt Ltd
132	B.Voc Retail Management (Sem-VI)	BVRM	214129	Jashanpreet	Training
133	B.Voc Retail Management (Sem-VI)	BVRM	214133	Harahpreet Singh	Training
134	B.Voc Retail Management (Sem-VI)	BVRM	214137	Paramvir Singh	Maruti Suzuki
135	B.Voc Retail Management (Sem-VI)	BVRM	214140	Abhishek Gulati	TVS Motors
136	B.Voc Retail Management (Sem-VI)	BVRM	214141	Harmanjot Singh	Aditya Birla Fashion And Retail (Pantaloon)
137	B.Voc Retail Management (Sem-VI)	BVRM	214143	Onkar Singh	Goldi Boot House, Nangal
138	B.Voc Retail Management (Sem-VI)	BVRM	214147	Lovepreet	Mohit Motors Dher
139	B.Voc Retail Management (Sem-VI)	BVRM	214150	Taranpreet singh	Mohit Motors Dher
140	B.Voc Retail Management (Sem-VI)	BVRM	214154	Simranpreet Kaur	Color Bucket Store
141	B.Voc Hospitality and Tourism Management (Sem-VI)	BVHT	214001	Jatin Kumar	Hotel Operations of Hotel SEA, Patiala
142	B.Voc Hospitality and Tourism Management (Sem-VI)	BVHT	214008	Sharuti	Hotel Operation of Hotel Miraj, SAS Nager Mohali
143	B.Voc Hospitality and Tourism Management (Sem-VI)	BVHT	214014	Gurwinder Singh	New Taj Hotel & Restaurant, Sri Anandpur Sahib
144	B.Voc Hospitality and Tourism Management (Sem-VI)	BVHT	214024	Kuljinder Kaur	Hotel Operation of Surya Classic Hotel & Restaurant, Mohali.
145	B.Voc Hospitality and Tourism Management (Sem-VI)	BVHT	214031	Jaspreet singh	Hotel Operation of Hotel Miraj,Sec-70 SAS Nager Mohali
146	B.Voc Hospitality and Tourism Management (Sem-VI)	BVHT	214040	Nitish	Hotel Operation of Hotel S. Rattan, Sri Anandpur Sahib.
147	B.Voc Hospitality and Tourism Management (Sem-VI)	BVHT	214044	Gurkarandeep Singh	Hotel Operation of Hotel S. Rattan, Sri Anandpur Sahib.





**A PROJECT REPORT ON  
SUMMER INTERNSHIP TRAINING  
BATCH 2023-24**

**SUBMITTED BY:**

**NAME- NAZIA** *Nazia*

**CLASS-BCOM(HONS)3sem**

**ROLL NO-232701**

**SUBMITTED TO:**

**DR. NAVJEET KAUR** *Navjeet*

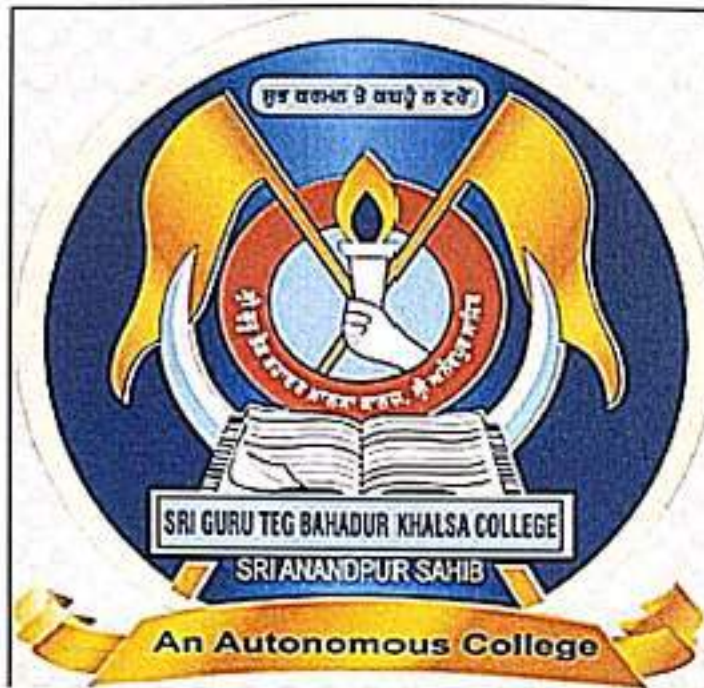
**(PG DEPARTMENT**

**OF COMMERCE AND**

**MANAGEMENT )**

**SRI GURU TEG BAHADUR  
KHALSA COLLEGE ANANDPUR SAHIB**

# SRI GURU TEGH BAHADUR KHALSA COLLEGE, SRI ANANDPUR SAHIB



## A PROJECT REPORT ON SUMMER TRAINING

**BATCH 2023-2024**

**SUBMITTED BY :-**

**NAME :- AMANPREET KAUR**

**CLASS :- BCOM.HONOURS 1<sup>st</sup> YEAR**

**ROLL NO. :- 232702**

**SUBMITTED TO :-**

**DR. NAVJEET KAUR**

**(PG DEPARTMENT**

**OF COMMERCE**

**& MANAGEMENT)**

*Amanpreet Kaur*



**A PROJECT ON SUMMER INTERNSHIP TRAINING BATCH**

**Submitted By:-** *Anjali Devi*

**Name:** Anjali Devi

**Roll.No:** 232703

**Class:** B.com (Honours) 2<sup>nd</sup> Year

**Submitted To:-**

Dr. Navjeet Kaur

(P.G. Department of

Commerce and

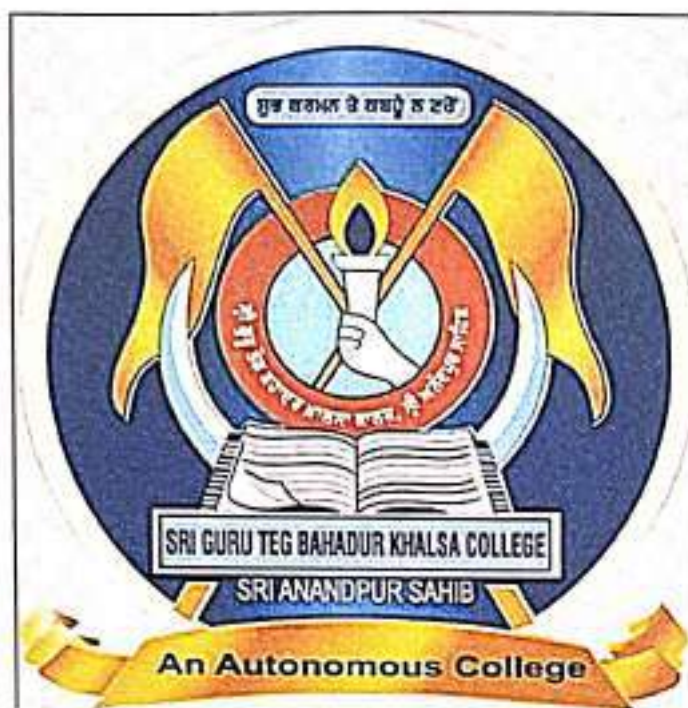
Management)

**Sri Guru Tegh Bahadur Khalsa  
College**

**Sri Anandpur Sahib**



# SRI GURU TEGH BAHADUR KHALSA COLLEGE, SRI ANANDPUR SAHIB



## A PROJECT REPORT ON SUMMER TRAINING

**BATCH 2023-2024**

**SUBMITTED BY :-**

**NAME :- RAMNEET KAUR**

**CLASS :- BCOM.HONOURS 1<sup>st</sup> YEAR**

**ROLL NO. :- 232704**

**SUBMITTED TO :-**

**DR. NAVJEET KAUR**

**(PG DEPARTMENT**

**OF COMMERCE**

**& MANAGEMENT)**

*Ramneet Kaur*



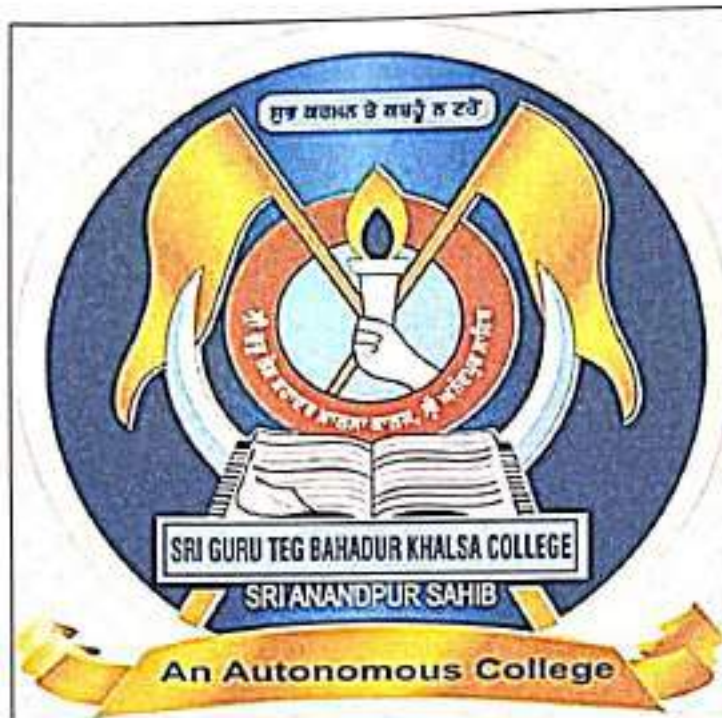
## A PROJECT ON SUMMER INTERNSHIP TRAINING BATCH

Submitted By:- *Hardeep Kaur*  
Name: Hardeep Kaur  
Roll.No:232705  
Class: B.com (Honours) 2<sup>nd</sup> Year

Submitted To:- *NKaur*  
Dr. Navjeet Kaur  
(P.G. Department of  
Commerce and  
Management)

**Sri Guru Tegh Bahadur Khalsa  
College Anandpur Sahib**

# SRI GURU TEGH BAHADUR KHALSA COLLEGE, SRI ANANDPUR SAHIB



## A PROJECT REPORT ON SUMMER TRAINING

**BATCH 2023-2024**

**SUBMITTED BY :-**

**NAME :- MANJOT KAUR**

*Manjot Kaur*

**CLASS :- BCOM.HONOURS 1<sup>st</sup> YEAR**

**ROLL NO. :- 232707**

**SUBMITTED TO :-**

**DR. NAVJEET KAUR**

**(PG DEPARTMENT**

**OF COMMERCE**

**& MANAGEMENT)**





**A PROJECT ON SUMMER INTERNSHIP TRAINING BATCH**

**Submitted By:-** *Dilpreet Kaur.*  
**Name:** Dilpreet Kaur  
**Roll.No:** 232708  
**Class:** B.com (Honours) 2<sup>nd</sup> Year

**Submitted To:-**  
Dr. Navjeet Kaur *NKaur*  
(P.G. Department of  
Commerce and  
Management)

**Sri Guru Tegh Bahadur Khalsa  
College  
Sri Anandpur Sahib**

# SHRI GURU TEG BAHADUR KHALSA COLLEGE ANANDPUR SAHIB



## A PROJECT REPORT ON SUMMER INTERNSHIP TRAINING BATCH 2023-24

**SUBMITTED BY:-**

**NAME: TEJVEER SINGH** Tejveer Singh

**ROLL NO:232709**

**CLASS:B.COM(HONS)2<sup>ND</sup> YEAR**

**SUBMITTED TO:-**

**DR. NAVJEET KAUR** *NKaur*

**(P.G. DEPARTMENT OF  
COMMERCE )**

**[SGTB KHALSA COLLEGE,  
ANANDPUR SAHIB]**



# PROJECT REPORT ON SUMMER TRAINING

Submitted To:

Dr. Navjeet kaur *Nav*

[P.G. Department of commerce  
and Management.]

Submitted By:

Deepanshi *Deepanshi*

B.com (Honours) 2<sup>nd</sup> year

Class Roll no: 232710

University Roll no: 2409

## SHRI GURU TEG BAHADUR KHALSA COLLEGE



# PROJECT REPORT ON SUMMER TRAINING

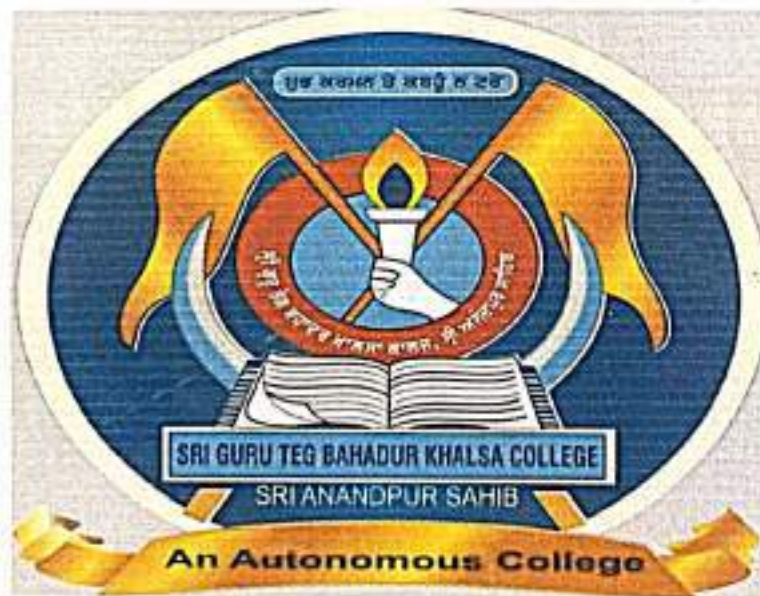
Submitted To:

Dr Navjeet Kaur *Navjeet*  
[P.G. Department of Commerce and  
Management]

Submitted By:

Ritika *Ritika*  
B.Com [Honours]  
Class Roll No. 232711  
University Roll No. 2410

## SRI GURU TEG BAHADUR KHALSA COLLEGE SRI ANANDPUR SAHIB



# Project Report On Summer Training



Submitted by:

Malkeet : Malkeet

Bcom (Honours) 3rd se.

Class Roll no. 232712.

University Roll no

2411

Submitted To:

Dr. Navjeet kaur *NKaur*

[Asst. Professor ]

PG Department of  
Commerce and  
Management

## SRI GURU TEG BAHADUR KHALSA COLLEGE





# PROJECT REPORT ON SUMMER TRAINING



2024-2025

**SRI GURU TEG BAHADUR KHALSA COLLEGE**  
**SRI ANANDPUR SAHIB**

**An Autonomous College**  
**Affiliated to Punjabi University, Patiala**

Submitted to  
Dr. NAVJEET KAUR  
P.G Department of  
Commerce and mgt

Submitted by-  
NAME:- KALPANA  
B.COM(H)2<sup>nd</sup> Year  
Uni. Roll No- 2412  
Class Roll No- 232713

Kalpana

# SHRI GURU TEG BAHADUR KHALSA COLLEGE ANANDPUR SAHIB



## A PROJECT REPORT ON SUMMER INTERNSHIP TRAINING BATCH 2023-24

**SUBMITTED BY:-**

**NAME: HARSH** *Harsh*

**ROLL NO: 232714**

**CLASS: B.COM (HONS) 2<sup>ND</sup> YEAR**

**SUBMITTED TO:-**

**DR. NAVJEET KAUR** *Navjeet*

**(P.G. DEPARTMENT OF  
COMMERCE)**

**[SGTB KHALSA COLLEGE,  
ANANDPUR SAHIB]**

# SHRI GURU TEG BAHADUR KHALSA COLLEGE

SHRI ANANDPUR SAHIB

(AN AUTONOMOUS COLLEGE)

Affiliated To Punjabi University Patiala



## PROJECT REPORT ON SUMMER TRAINING

SUBMITTED TO :-

ASST.PROFESSOR

NAVJEET KAUR

*Navjeet*

(PG DEPARTMENT OF

COMMERCE AND

MANAGEMENT)

SUBMITTED BY:-

MEHAKPREET KAUR

*Mehakpreet Kaur*

ROLL NO.232716

UNI.ROLL NO. 2414



**A PROJECT REPORT ON  
SUMMER INTERSHIP TRAINING BATCH 2024-25**



**SRI GURU TEG BAHADUR KHALSA COLLEGE  
SRI ANANDPUR SAHIB**

**Submitted To:-** *Navjeet Kaur*

**Prof. NAVJEET KAUR**

**(PG Dept. of**

**Commerce and management)**

**Submitted By:-** *Palak*

**Name : PALAK**

**Class : BCH SEM 3**

**Roll No. : 232717**

# Project Report on summer Training



Summer Training

Batch 2023-2024

Submitted by:

Bhoomika *Bhoomika*

B.com(honours) 2nd year

Class Roll no :232718

University roll no: 2416

Submitted to:

Dr. Navjeet Kaur *NKaur*

[Assistant professor]

[P.G Department of commerce

And Management]

Sri Guru Teg Bahadur Khalsa College

Sri Anandpur sahib





**SHRI GURU TEG BAHADUR KHALSA COLLEGE**  
**SRI ANANDPUR SAHIB**  
**AN AUTONOMOUS COLLEGE**  
**ASSIGNMENT ON TALLY ERP9**



**A PROJECT REPORT ON SUMMER TRAINING**



**SUBMITTED TO:**  
Asst. Prof. Dr. Navjeet kaur *NKaur*  
P.G. Department of Commerce  
And Management

**SUBMITTED BY:** *Naspreet Kaur*  
**NASPREET KAUR**  
**B.COM (honours)**  
**UNI .ROLL NO.2417**  
**CLASS ROLL NO. 232719**

## REPORT ON SUMMER TRAINING (2024-2025)

### Tally.ERP 9-with GST

Submitted to:

Dr.NAVJEET KAUR

*NKaur*

(Pg department of

commerce and management )

Submitted by:

JASWINDER KAUR

*Jaswinder kaur*

B.com(H)-3rd sem

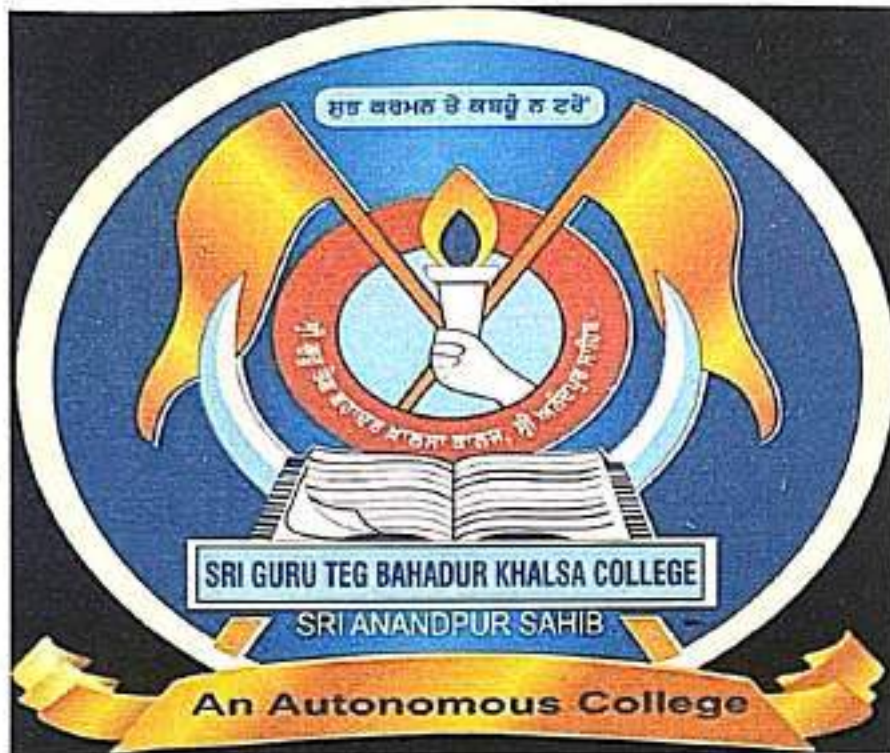
Roll no.232720



**SRI GURU TEG BAHADUR KHALSA COLLEGE**  
**SRI ANANDPUR SAHIB**  
**An Autonomous College**



# SRI GURU TEGH BAHADUR KHALSA COLLEGE , SRI ANANDPUR SAHIB



## A PROJECT REPORT ON SUMMER TRAINING

BATCH 2023-24

SUBMITTED BY :-

NAME :- MANDEEP KAUR *Mandeep Kaur*

CLASS:- B.COM HONOURS

ROLL NO:- 232721

SUBMITTED TO :-

DR. NAVJEET KAUR *NKaur*

P.G DEPARTMENT

OF COMMERCE

& MANAGEMENT

**A PROJECT REPORT ON**  
**SUMMER INTERNSHIP TRAINING BATCH 2024-25**



**SRI GURU TEG BAHADUR KHALSA COLLEGE**  
**SRI ANANDPUR SAHIB**

**SUBMITTED TO**

**Prof. NAVJEET KAUR** *Nkam*  
**(PG department of**  
**Commerce and management)**

**SUBMITTED BY**

*Neelam Rani*

**NEELAM RANI**

**Class-BCH SEMESTER 3**

**Roll no.232722**

# PROJECT REPORT ON SUMMER TRAINING

Submitted To:

Dr. Navjeet Kaur *NKaur*

[P.G Department of

Commerece and Management]

Submitted By:

Jasmeen kaur

B.com(Honours)2nd year

Class Roll no: 232723

University Roll no: 2421

## SHRI GURU TEG BAHADUR KHALSA COLLEGE

*Jasmeen Kaur*





## PROJECT REPORT ON SUMMER TRAINING

Submitted To:

Dr.Navjeet Kaur

[P.G Department of

Commerece and Management]

Submitted By: *Malika Sharma*

Malika Sharma

B.com(Honours)2nd year

Class Roll no: 232724

University Roll no: 2422

## SHRI GURU TEG BAHADUR KHALSA COLLEGE



# SHRI GURU TEG BAHADUR KHALSA COLLEGE

SHRI ANANDPUR SAHIB

(AN AUTONOMOUS COLLEGE)

Affiliated To Punjabi University Patiala



## PROJECT REPORT ON SUMMER TRAINING

SUBMITTED TO :-

ASST.PROFESSOR

NAVJEET KAUR

(PG DEPARTMENT OF

COMMERCE AND

MANAGEMENT)

SUBMITTED BY:-

AMANDEEP KAUR

ROLL NO.232725

UNI.ROLL NO. 2423

# PROJECT REPORT ON SUMMER TRAINING



2024-2025

Submitted To: *NKaur*  
Dr. Navjeet kaur  
[P.G. Department of commerce  
and Management.]

Submitted By:  
Rani Devi  
B.com(Honours)2<sup>nd</sup> year  
Class Roll no:232726  
University Roll no:2424

**SHRI GURU TEG BAHADUR KHALSA COLLEGE**  
**SRI ANADPUR SAHIB**

*Rani Devi*



# PROJECT REPORT ON SUMMER TRAINING



2024-2025

Submitted To:

Asst. Professor

Dr. Navjeet Kaur

*Navjeet Kaur*

[ P. G. Department of

Commerce and Management.]

Submitted By:

Baljeet Kaur

B. Com(Honours) 2<sup>nd</sup> year

Class Roll No.: 232727

University Roll No : 2425

**SHRI GURU TEG BAHADUR KHALSA COLLEGE**  
**SRI ANANDPUR SAHIB**

*Baljeet Kaur*



**PROJECT REPORT ON SUMMER TRAINING**  
**Batch (2024-2025)**

***Submitted BY :-***

Name : Sukhwinder Kaur  
Roll no. 232728 *Sukhwinder Kaur*  
Class : Bcom (Honours).  
3<sup>rd</sup> sem.

***Submitted To:-***

Dr. Navjeet kaur *NKaur*  
{ PG DEPARTMENT OF  
COMMERCE AND  
MANAGEMENT }

**SRI GURU TEG BAHADUR KHALSA**  
**COLLEGE SRI ANANDPUR SAHIB**

**SRI GURU TEG BAHADUR KHALSA COLLEGE**

**SRI ANANDPUR SAHIB.**



**ASSIGNMENT ON  
INCOME TAX AND TALLY ERP 9.**



**SUBMITTED TO: -**

Dr. Prof. Navjeet Kaur

P.G. Department of Commerce  
and Management.

*Navjeet Kaur*

**SUBMITTED BY: -**

Name:- Parveen Kaur

Class:- B.Com (Hons) 3<sup>rd</sup> Sem

Roll No:- 232730 or 2428

*Parveen Kaur*



# PROJECT REPORT ON SUMMER TRAINING



Summer Training  
Batch 2023-24

**Tally**  
POWER OF SIMPLICITY

**Submitted To :**

Dr. Navjeet kaur

[ Assistant professor ]

[ P.G department of Commerce  
And Management ]

**Submitted By :**

Suman Suman

Bcom [honours] 2<sup>nd</sup> year

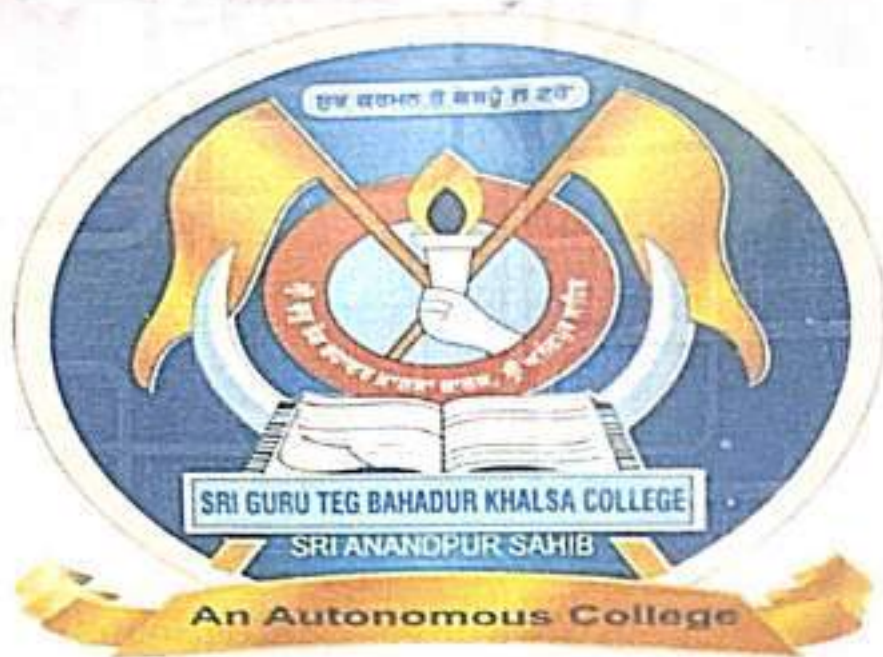
Class Roll no : 232733

University Roll no : 2430

**Sri Guru Teg Bahadur khalsa College**

**Sri Anandpur Sahib**





**A PROJECT REPORT ON**  
**SUMMER INTERNSHIP TRAINING BATCH 2023-24**

**SUBMITTED BY:-**

**NAME:-** ISHIKA *Ishika*

**CLASS:-** B.COM(HONS) 2<sup>nd</sup> YEAR

**ROLL NO:-** 232737

**SUBMITTED TO:** *NKaur*

**DR. NAVJEET KAUR**

**{ PG DEPARTMENT**

**OF COMMERCE**

**AND**

**MANAGEMENT}**

**SRI GURU TEG BAHADUR KHALSA COLLEGE**  
**SRI ANANDPUR SAHIB**



**SHRI GURU TEG BAHADUR  
KHALSA COLLEGE  
ANANDPUR SAHIB**



**PROJECT REPORT ON**

**SUMMER INTERNSHIP TRAINING BATCH 2023-24**

**SUBMITTED BY:-**

**NAME: GURNAMAN SINGH**

**ROLL NO.: 232739**

**CLASS: B.COM(H)2<sup>nd</sup>)YEAR**

**SUBMITTED TO:-**

**DR.NAVJEET KAUR**

**(P.G DEPARTMENT**

**OF COMMERCE)**

**(SGTB KHALSA  
COLLEGE),SHRI  
ANANDPUR SAHIB**

# PROJECT REPORT ON

## SUMMER TRAINING

SUBMITTED TO - *NKaur*  
Dr. NAVJEET KAUR  
[P.G.DEPARTMENT OF COMMERCE  
AND MANAGEMENT]

SUBMITTED BY-  
KINDERPREET KAUR *Kinderpreet Kaur*  
B.COM [HONOURS] 3<sup>rd</sup> SEM  
CLASS ROLLNO.232740  
UNIVERSITY ROLL NO.2435

**SRI GURU TEG BAHADUR KHALSA COLLEGE**

**SHRI ANANDPUR SAHIB**





# SRI GURU TEGH BAHADUR KHALSA COLLEGE, SRI ANANDPUR SAHIB



## A PROJECT REPORT ON SUMMER TRAINING BATCH 2023-2024

SUBMITTED BY :- *Jasleen Kaur*  
NAME :- JASLEEN KAUR  
CLASS :- BCOM.HONOURS 1<sup>st</sup> YEAR  
ROLL NO. :- 232729

SUBMITTED TO :- *Navjeet Kaur*  
DR. NAVJEET KAUR  
(PG DEPARTMENT  
OF COMMERCE  
& MANAGEMENT)



# SRI GURU TEG BAHADUR KHALSA COLLEGE

SRI ANANDPUR SAHIB  
(AN AUTONOMOUS COLLEGE)  
Affiliated to Punjabi University Patiala



(2024-25)

## ASSIGNMENT ON INCOME TAX AND TALLY ERP 9.



**Submitted To:-**

**Dr.Prof. Navjeet Kaur**

**P.G. Department Of commerce**

**And Management**

**Submitted By:-**

*Damanpreet Kaur*  
**Damanpreet Kaur**

**B.com (Hons) Sem 3<sup>rd</sup>**

**Roll No. 232732**

**Uni.Roll No. 2429**

**A PROJECT REPORT ON**  
**SUMMER INTERNSHIP TRAINING BATCH 2024-25**



**SRI GURU TEG BAHADUR KHALSA COLLEGE**  
**SRI ANANDPUR SAHIB**

**SUBMITTED TO**

**Prof. NAVJEET KAUR** *Navjeet*  
(PG department of  
Commerce and management)

**SUBMITTED BY**

**ADITI** *Aditi*  
Class-BCH SEMESTER 3  
Roll no.232734



# PROJECT SUMMER TRAINING REPORT

Page | 1



## Submitted To:

Dr. Navjeet Kaur *NKaur*

(Assistant Professor)

(P.G. Department of Commerce and Management)

## Submitted By:

Simarjot Kaur *Simarjot Kaur*

B.com Honours (1<sup>st</sup> year)

Class Roll No. 232735

University Roll no. 2432

**SRI GURU TEG BAHADUR KHALSA COLLEGE**  
**SHRI ANANDPUR SAHIB**

**A PROJECT REPORT ON**  
**SUMMER INTERNSHIP TRAINING**  
**BATCH (2023-2024)**



**SUBMITTED BY:**

NAME: AASHIMA. *Aashima.*

ROLL NO: 232736

Class: B.com (HONOURS)

**SUBMITTED TO:**

DR. NAVJEET KAUR. *Navjeet*

(Assistant professor)

(P.G. Department of commerce)

**SHRI GURU TEG BAHADUR KHALSA COLLEGE**  
**(SHRI ANANDPUR SAHIB)**



# PROJECT REPORT ON SUMMER TRAINING



Shri Guru Teg Bahadur khalsa College

Sri Anandpur Sahib

Submitted by : Shivali  
B.com(Honours)2<sup>nd</sup> year  
Class Roll no:232742  
University Roll no:2436

*Shivali*

Submitted To:Dr.Navjeet kaur

*Navjeet*

[P.G. Department of commerce  
and management]

# REPORT ON SUMMER TRAINING

Tally.ERP 9



(2024-20225)

**Submitted to:**

Dr. Navjeet kaur *NKaur*

**Submitted by:**

Palak *Palak*

B.com(H)-3rd sem

Roll no.232743

University Roll no :2437

**SRI GURU TEG BAHADUR KHALSA COLLEGE**  
**SRI ANANDPUR SAHIB**  
**An Autonomous College**

# SHRI GURU TEG BAHADUR KHALSA COLLEGE ANANDPUR SAHIB



## A PROJECT REPORT ON SUMMER INTERNSHIP TRAINING BATCH 2024-25 TOPIC:-INCOME TAX

**SUBMITTED BY:-**

**NAME: Harsh Kumar** *Harsh Kumar*

**ROLL NO: 232746**

**CLASS: B.COM(HONS) 2<sup>ND</sup> YEAR**

**SUBMITTED TO:-**

**DR. NAVJEET KAUR** *N. Kaur*

**(P.G. DEPARTMENT OF  
COMMERCE)**

**[SGTB KHALSA COLLEGE,  
ANANDPUR SAHIB]**



# SHRI GURU TEG BHADUR KHALSA COLLEGE SHRI ANANDPUR SAHIB



## A PROJECT REPORT ON SUMMER INTERNSHIP TRAINING BATCH 2024 – 2025

SUBMITTED BY:

Name: Tamnna Sharma

Roll NO. :232749

Class: B.COM(hons)2<sup>nd</sup> YEAR

SUBMITTED TO

ASSI PROF.:- NAVJEET KAUR

[PG Department OF COMMERCE]

[STGB KHALSA COLLEGE

ANANDPUR SAHIB]

**SHRI GURU TEG BAHADUR KHALSA**  
**COLLEGE ANANDPUR SAHIB**



---

**A PROJECT REPORT ON SUMMER INTERNSHIP TRAINING BATCH  
2023-2024.**

*Ishan Chaudhary*  
**SUBMITTED BY:-Ishan Chaudhary**  
**ROLL NO:- 232751**  
**CLASS:-B.com(Honours)**

*Navjeet Kaur*  
**SUBMITTED TO:-DR.Navjeet Kaur**  
**(P.G. Department of commerce)**  
**(SGTB Khalsa College)**



**SHRI GURU TEG BAHADUR KHALSA**  
**COLLEGE ANANDPUR SAHIB**



---

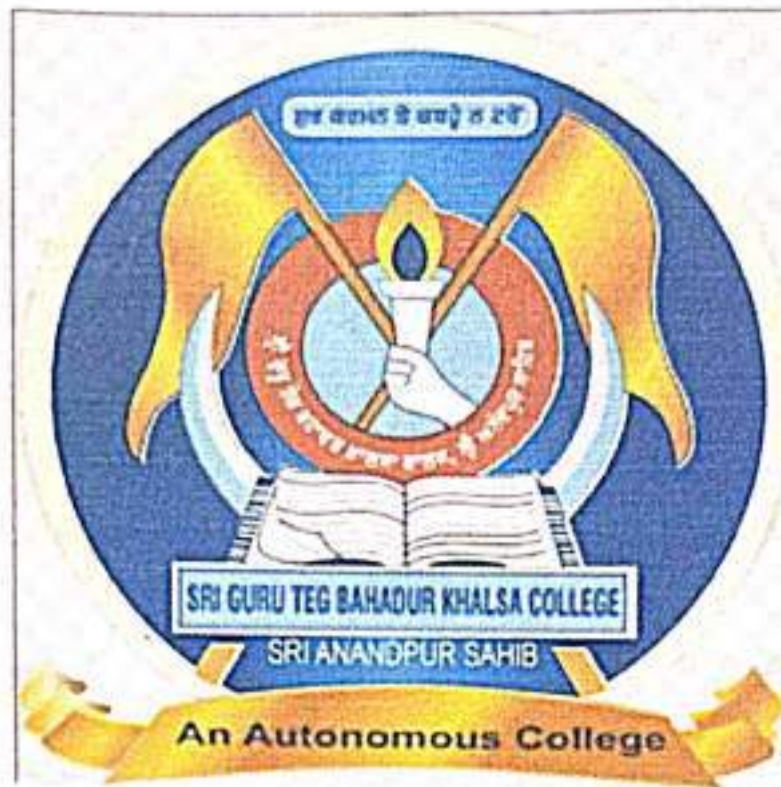
**A PROJECT REPORT ON SUMMER INTERNSHIP TRAINING BATCH**

**2023-2024.**

<b>SUBMITTED BY:-Harshit Mahajan</b>	<b>SUBMITTED TO:-DR.Navjeet Kaur</b>
<b>ROLL NO:- 232752</b>	<b>(P.G. Department of commerce)</b>
<b>CLASS:-B.com(Honours)</b>	<b>( SGTB Khalsa College)</b>



# SRI GURU TEGH BAHADUR KHALSA COLLEGE, SRI ANANDPUR SAHIB



## A PROJECT REPORT ON SUMMER TRAINING

**BATCH 2023-2024**

**SUBMITTED BY :-**

**NAME :-PRAGATI** *Pragati*

**CLASS :- BCOM.HONOURS 1<sup>st</sup> YEAR**

**ROLL NO. :- 232753**

**SUBMITTED TO :-**

*Navjeet*  
**DR. NAVJEET KAUR**

**(PG DEPARTMENT**

**OF COMMERCE**

**& MANAGEMENT)**

**SRI GURU TEG BAHADUR KHALSA**  
**COLLEGE, SRI ANANDPUR SAHIB**



**A PROJECT REPORT ON**  
**SUMMER INTERNSHIP TRAINING**  
**BATCH 2023-2024**

**SUBMITETED BY:-**

**NAME: ANJALI RANA** *Anjali Rana*

**ROLL NO: 232754**

**CLASS: B.COM. (HONS.)**

**SUBMITTED TO:-**

**DR. NAVJEET KAUR** *NKaur*

**{P.G. DEP. OF COMMERCE  
AND MANAGEMENT}**

**[SGTB KHALSA COLLEGE  
ANANDPUR SAHIB]**



**SUMMER TRAINING REPORT  
ON  
WORKING CAPITAL MANAGEMENT  
(NFL)**




**SRI GURU TEG BAHADUR KHALSA COLLEGE,  
SHRI ANANDPUR SAHIB**

**BATCH : 2023-2024**

**SUBMITTED TO:**

  
**DR. NAVJEET KAUR**

**SUBMITTED BY :**

  
**SUPRIYA SAINI**  
**B. COMM (HONS) SEM-III**  
**UNIVERSITY ROLL NO.-2440**





**A PROJECT REPORT ON  
SUMMER INTERNSHIP TRAINING BATCH 2023-24**

**SUBMITTED BY :-**

**NAME: GURWINDER KAUR**  
*Gurwinder Kaur*

**CLASS : BCOM(HON)2<sup>ND</sup> YEAR**

**ROLL NO: 232755**

**SUBMITTED TO :-**

**DR. NAVJEET KAUR** *N. Kaur*

**{P.G.DEPARTMENT**

**OF COMMERCE**

**AND**

**MANAGEMENT}**

**SRI GURU TEG BAHADUR KHALSA  
COLLAGE SRI ANANDPUR SAHIB**

# SHRI GURU TEG BAHADUR KHALSA COLLEGE ANANDPUR SAHIB



## A PROJECT REPORT ON SUMMER INTERNSHIP TRAINING BATCH 2023-24

**SUBMITTED BY:-**

**NAME: CHARANDEEP SINGH** *Charandeep Singh*

**ROLL NO: 232756**

**CLASS: B.COM (HONS) 2<sup>ND</sup> YEAR**

**SUBMITTED TO:-**

**DR. NAVJEET KAUR** *Navjeet*

**(P.G. DEPARTMENT OF  
COMMERCE)**

**[SGTB KHALSA COLLEGE,  
ANANDPUR SAHIB]**

**SHRI GURU TEG BAHADUR KHALSA  
COLLEGE ANANDPUR SAHIB**



**A PROJECT REPORT ON  
SUMMER INTERNSHIP TRAINING BATCH 2023-24**

**SUBMITTED BY:-**

**NAME: SE THI** Sethi

**ROLL NO:232757**

**CLASS:B.COM(HONS)2<sup>ND</sup> YEAR**

**SUBMITTED TO:-**

Navjeet Kaur  
**DR. NAVJEET KAUR**

**(P.G. DEPARTMENT OF  
COMMERCE )**

**[SGTB KHALSA COLLEGE,  
ANANDPUR SAHIB]**

Sethi



SHRI GURU TEG BAHADUR KHALSA  
COLLEGE ANANDPUR SAHIB



A PROJECT REPORT ON  
SUMMER INTERNSHIP TRAINING BATCH 2023-24

SUBMITTED BY:-

NAME: GURDEEP SINGH Gurdeep Singh

ROLL NO: 232758

CLASS: B.COM(HONS) 2<sup>ND</sup> YEAR

SUBMITTED TO:-

DR. NAVJEET KAUR

(P.G. DEPARTMENT OF  
COMMERCE)

[SGTB KHALSA COLLEGE,  
ANANDPUR SAHIB]

# PROJECT REPORT ON SUMMER TRAINING



SUBMITTED TO:

Dr. NAVJEET KAUR

[P.G. Department of commerce

And management ]

SUBMITTED BY:

KOMALPREET *Komalpreet*

Bcom(hons.) 2<sup>nd</sup> year

(2024-25)

class roll no.:232760

University roll no: 2446

**SRI GURU TEG BAHADUR KHALSA COLLEGE**

**SRI ANANDPUR SAHIB**

# PROJECT REPORT ON SUMMER TRAINING



Shri Guru Teg Bahadur khalsa College

Sri Anandpur Sahib

Submitted by : Sahilpreet singh

Submitted To: Dr. Navjeet kaur

B.com(Honours) 2<sup>nd</sup> year  
Class Roll no: 232762

[P.G. Department of commerce  
and management]

University Roll no: 2458

*Sahilpreet Singh*



# PROJECT REPORT ON SUMMER TRAINING

## SRI GURU TEG BAHADUR KHALSA COLLEGE SRI ANANDPUR SAHIB



Submitted To:-  
Navjeet Kaur *NKaur*  
(PG Deptt. of Commerce & Management)

Submitted by:-  
Manjot Kaur *Manjot Kaur*  
B.Com Honours (IInd Year)  
Class Roll No. 232764  
Uni. Roll No. 2447

**SHRI GURU TEG BAHADUR KHALSA**  
**COLLEGE ANANDPUR SAHIB**



---

**A PROJECT REPORT ON SUMMER INTERNSHIP TRAINING BATCH  
2023-2024.**

*Mahir*  
**SUBMITTED BY:-Mahir Sharma**  
**ROLL NO:- 232766**  
**CLASS:-B.com(Honours)**

*Navjeet*  
**SUBMITTED TO:-DR.Navjeet Kaur**  
**(P.G. Department of commerce)**  
**( SGTB Khalsa College)**

*Arjun*

# REPORT ON SUMMER TRAINING

TALLY.ERP 9



(2024-2025)

**Submitted to**  
Dr. Navjeet kaur  
PG Department of  
Commerce and Management

**Submitted by-**  
Mandeep kaur *Mandeep kaur*  
B.COM (H)- 3<sup>rd</sup> SEM  
Uni. Roll No- 2448  
Class roll no - 232767

**SRI GURU TEG BAHADUR KHALSA COLLEGE**  
**SRI ANANDPUR SAHIB**  
**An Autonomous College**  
**Affiliated to Punjabi University, Patiala**




# SUMMER TRAINING REPORT

ON

G.S.T.

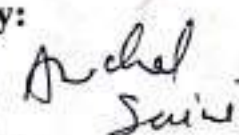


  
Submitted to:

**Dr. Manpreet Kaur**  
(Assistant professor)

P.G. department of commerce  
and management

Submitted by:

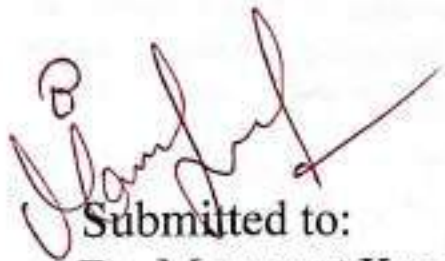
Anchal Saini   
Roll No. 231201

B.A.F. 1<sup>st</sup> year

**SHRI GURU TEG BHADUR KHALSA COLLEGE**  
**SHRI ANANDPUR SAHIB**

# SUMMER TRAINING REPORT ON INCOME TAX





Submitted to:  
Dr. Manpreet Kaur  
(P.G. Dept. of Com. )

Submitted By:  
Manish Kumar *Manish Kumar*  
Class: B.Com(A&F)  
Roll no.231202

Shri Guru Teg Bahadur Khalsa College  
Anandpur Shaib

**Summer Training Report**  
**ON**  
**Gem Portal And MS WORD**



*A*  
*Manpreet Kaur*  
Submitted to:

**Dr. Manpreet Kaur**

**(P.G. Department of Commerce )**

Submitted By:

*Shubham Anand*  
**Shubham Anand**

**Class;B.com A&F**

**Roll no. 231203**

**SHRI GURU TEG BAHADUR KHALSA COLLEGE**  
**ANANDPUR SHAIB**



# SHRI GURU TEG BAHADUR KHALSA COLLEGE ANANDPUR SAHIB



## Summer Training Report On Tally .ERP 9

**SUBMITTED BY:-**

*Gurbachan Singh*  
**NAME: GURBACHAN SINGH**

**ROLL NO: 231205**

**CLASS: B.COM(A&F) 2<sup>ND</sup> YEAR**

**SUBMITTED TO:-**

**PROF. MANPREET KAUR**

**{P.G. DEPARTMENT OF  
COMMERCE}**

**SGTB KHALSA COLLEGE**

# SUMMER TRAINING REPORT ON MATERIAL HANDLING



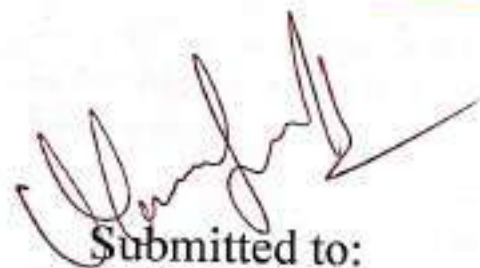
*(Signature)*  
Submitted to:  
Dr. Manpreet Kaur  
(P.G.Dept.of Commerce. )

Submitted By:  
Tanisha Arora *Tanisha Arora*  
Class: B.Com(A&F)  
Roll no.231206

Shri Guru Teg Bahadur Khalsa College  
Anandpur Shaib

# SUMMER TRAINING REPORT ON INCOME TAX





Submitted to:  
Dr. Manpreet Kaur  
(P.G. Dept. of Com.)

Submitted By:

Nitin Kumar *Nitin Kumar*  
Class: B.Com(A&F)  
Roll no.231207

Shri Guru Teg Bahadur Khalsa College  
Anandpur Shaib



# SUMMER TRAINING REPORT ON TALLY ERP- 9



B  
Submitted to:  
Dr. Manpreet Kaur  
(P.G.Dept.of Commerce. )

Submitted By:  
Raman Saini *Raman Saini*  
Class: B.Com(A&F)  
Roll no.231209

Shri Guru Teg Bahadur Khalsa College  
Anandpur Shaib

## Summer Training project on BBMB



*Dr. Manpreet Kaur*  
Submitted to:

Dr. Manpreet Kaur

(P.G. Department of Commerce)

Submitted By:

Barinder Singh *Barinder Singh*

Class: B.Com(A&F)

Roll no.231210

Shri Guru Teg Bahadur Khalsa College Anandpur Shaib

# SUMMER TRAINING REPORT ON INVENTORY MANAGEMENT



*AX* Submitted To:

Dr. Manpreet Kaur

[Assistant Professor]

[P. G. Department Of Commerce  
And Management]

Submitted By:

Shweta *Shweta*

Class: B.com[A&F] [Sem-3]

Class Roll No.: 231212

University Roll No.: 2353

**SRI GURU TEGH BAHADUR KHALSA COLLEGE,  
SRI ANANDPUR SAHIB**



**SUMMER TRAINING REPORT  
ON  
WORKING CAPITAL MANAGEMENT  
(NFL)**



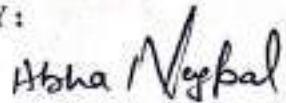
**SRI GURU TEG BAHADUR KHALSA COLLEGE,  
SHRI ANANDPUR SAHIB**

**BATCH : 2023-2024**

  
**SUBMITTED TO:**

Dr. Manpreet Kaur.  
(Assistant professor)  
PG Department of Commerce and management.

**SUBMITTED BY :**

Abha Nagpal   
BCOM. (SEM :3)  
(Accounting and finance)  
University Roll No: 2354  
Class Roll No: 231214

SUMMER TRAINING REPORT ON ITR(INCOME TAX RETURN)



A  
SUBMITTED TO :  
21/11/2024

Dr. MANPREET KAUR

(ASSISTANT PROFESSOR)

(P.G. DEPARTMENT OF COMMERCE AND MANAGEMENT)

SUBMITTED BY :

JANVI MANKOTIA

Janvi Mankotia  
B.COM (A&F)(3<sup>rd</sup> SEM.)

C. ROLL NO. - 2312 17

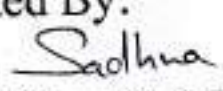
**SHRI GURU TEG BAHADUR KHALSA COLLEGE**

**SHRI ANANDPUR SAHIB**

# SUMMER TRAINING REPORT ON STOCK CONTROL



A/   
Submitted to:  
Dr. Manpreet Kaur  
(P.G.Dept.of Commerce. )

Submitted By:  
Sadhna   
Class: B.Com(A&F)  
Roll no.231218

Shri Guru Teg Bahadur Khalsa College  
Anandpur Shaib



**PROJECT REPORT**

**A STUDY ON OPTIMIZING LEAVE ATTENDANCE MANAGEMENT IN NESTLE INDIA  
LIMITED, TAHLIWAL**

**SUBMITTED TO:**

**PUNJABI UNIVERSITY PATIALA**

**IN THE PARTIAL FULLFILMENT OF THE REQUIREMENT FOR THE DEGREE OF  
BACHELOR OF BUSINESS ADMINISTRATION**

**(2021-2024)**



**SUBMITTED TO :**

**ASSISTANT PROF. AMANPREET KAUR**

**(P.G. DEPARTMENT OF COMMERCE**

**& MANAGEMENT)**

**SUBMITTED BY** *Simran Preet Kaur*

**SIMRANPREET KAUR**

**B.B.A(SEM - 6<sup>th</sup>)**

**UNI. ROLL NO.15651**

**CLASS ROLL NO.211401**

**SRI GURU TEG BAHADUR KHALSA COLLEGE**

**SRI ANANDPUR SAHIB**

**(AN AUTONOMOUS COLLEGE) .**

**PROJECT REPORT**  
**A STUDY ON VARIOUS SERVICES PERFORMED BY A CA FIRM**  
**IN PARTIAL FULFILLMENT OF THE REQUIREMENTS FOR THE**  
**DEGREE OF BACHELOR OF BUSINESS ADMINISTRATION**  
**(2023-2024)**



SUBMITTED TO:  
ASSISTANT PROF. AMANPREET KAUR  
(P. G. DEPARTMENT OF COMMERCE  
AND MANGEMENT)

SUBMITTED BY: Anshita  
ANSHITA SAINI Saini  
B.B.A (SEM 6<sup>TH</sup>)  
UNI. ROLL NO.15652  
CLASS ROLL NO.211402

**SRI GURU TEGH BAHADHUR KHAKSA COLLEGE**  
**SRI ANANDPUR SAHIB**  
**(AN AUTONOMUS COLLEGE)**

# PROJECT REPORT

## A STUDY ON EMPLOYEE HEALTH, SAFETY, AND WELFARE MEASURES AT AMBUJA CEMENTS LIMITED, RUPNAGAR

In partial fulfillment of the requirements for the degree of  
Bachelor of Business Administration  
(Session 2023- 2024)



### SUBMITTED TO:

Assistant Prof. Amanpreet Kaur  
(P.G Department of Commerce &  
Management)

### SUBMITTED BY:

Soni Kumari  
B.B.A (Sem- VI)  
Roll No. 211404  
Univ. Roll No. 15654

SRI GURU TEG BAHADUR KHALSA COLLEGE  
SRI ANANDPUR SAHIB  
(AN AUTONOMOUS COLLEGE)

27/5/24

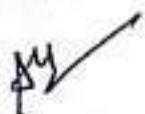


**PROJECT REPORT**  
**ON**  
**A STUDY ON EMPLOYEE ENGAGEMENT AT AMBUJA CEMENTS**  
**LIMITED, RUPNAGAR**

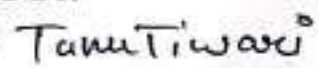
In partial fulfillment of the requirements for the degree of  
Bachelor of Business Administration  
(Session 2023- 2024)



**SUBMITTED TO:**

Assistant Prof. Amanpreet Kaur   
(P.G Department of Commerce & Management)

**SUBMITTED BY:**


Tanu Tiwari   
B.B.A (Sem- VI)  
Roll No. 211405  
Univ. Roll No. 15655

  
27/5/24

**SRI GURU TEG BAHADUR KHALSA COLLEGE**  
**SRI ANANDPUR SAHIB**  
**(AN AUTONOMOUS COLLEGE)**

**PROJECT REPORT**  
**A STUDY ON WORK PERFORMED IN A CA FIRM**  
**SUBMITTED TO:**  
**PUNJABI UNIVERSITY PATIALA**  
**IN PARTIAL FULFILLMENT OF THE REQUIREMENTS FOR THE**  
**DEGREE OF BACHELOR OF BUSINESS ADMINISTRATION**  
**(2021-2024)**



**SUBMITTED TO:**  
**PROF. AMANPREET KAUR**   
**(PG DEPARTMENT OF COMMERCE**  
**&MANAGEMENT)**

**SUBMITTED BY:** *Jasmeet Kaur*  
**JASMEET KAUR**  
**B.B.A (SEM 6<sup>TH</sup>)**  
**UNI.ROLL.NO-15656**  
**CLASS ROLLNO-211406**

**SRI GURU TEG BAHADHUR KHALSA COLLEGE**  
**SRI ANANDPUR SAHIB**  
**(AN AUTONOMOUS COLLEGE)**

**PROJECT REPORT**  
**A STUDY ON CREDIT RISK MANAGEMENT IN ROPAR CENTRAL**  
**CO-OPERATIVE BANK LTD, NANGAL**  
**IN PARTIAL FULFILMENT OF THE REQUIREMENTS FOR THE DEGREE OF**  
**BACHELOR OF BUSINESS ADMINISTRATION**  
**(2023-2024)**



SUBMITTED TO:

ASSISTANT PROF. AMANPREET KAUR

(P.G. DEPARTMENT OF COMMERCE

& MANAGEMENT)

SUBMITTED BY:

NAVNEET KAUR Navneetkaur

BBA (SEM-6<sup>TH</sup>)

UNI.ROLL NO. 15657

CLASS ROLL NO.211407

**SRI GURU TEG BAHADUR KHALSA COLLEGE**

**SRI ANANDPUR SAHIB**

**(AN AUTONOMOUS COLLEGE)**




**PROJECT REPORT**

**A STUDY ON MARKETING STRATEGIES AT ROYAL ENFIELD IN AARAY  
MOTORS PVT LTD, AMRITSAR**

**SUBMITTED TO:  
PUNJABI UNIVERSITY PATIALA  
IN THE PARTIAL FULLFILMENT OF THE REQUIREMENT FOR THE DEGREE OF  
BACHELOR OF BUSINESS ADMINISTRATION**

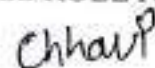
**(2021-2024)**




**SUBMITTED TO:**   
**ASSISTANT PROF. AMANPREET KAUR**  
**(P.G. DEPARTMENT OF COMMERCE  
& MANAGEMENT)**

**SUBMITTED BY**  
**CHHAVI VASHISHT**  
**B.B.A(SEM - 6<sup>th</sup>)**  
**UNI. ROLL NO.15658**

**CLASS ROLL NO.211408**



  
27/5/24

**SRI GURU TEG BAHADUR KHALSA COLLEGE**  
**SRI ANANDPUR SAHIB**  
**(AN AUTONOMOUS COLLEGE)**

**PROJECT REPORT**  
**A STUDY ON CUSTOMER RELATIONSHIP MANAGEMENT IN ROPAR CENTRAL**  
**CO-OPERATIVE BANK LTD, NANGAL**  
**IN PARTIAL FULFILMENT OF THE REQUIREMENTS FOR THE DEGREE OF**  
**BACHELOR OF BUSINESS ADMINISTRATION**

(2023-2024)



SUBMITTED TO:

ASSISTANT PROF. AMANPREET KAUR

(P.G. DEPARTMENT OF COMMERCE

& MANAGEMENT)

SUBMITTED BY:

NANCY RANA

BBA (SEM-6<sup>TH</sup>)

UNI.ROLL NO. 15659

CLASS ROLL NO. 211409

**SRI GURU TEG BAHADUR KHALSA COLLEGE**

**SRI ANANDPUR SAHIB**

**(AN AUTONOMOUS COLLEGE)**


**PROJECT REPORT  
ON**

**A STUDY ON TRAINING AND DEVELOPMENT IN  
NATIONAL FERTILIZER LIMITED**

**IN PARTIAL FULFILLMENT OF THE REQUIREMENTS FOR THE  
DEGREE OF BACHELOR OF BUSINESS ADMINISTRATION  
(2021-2024)**



SUBMITTED TO:

PROF.: AMANPREET KAUR   
(P.G. DEPARTMENT OF COMMERCE.  
& MANAGEMENT)

SUBMITTED BY: Ashima

ASHIMA

B.B.B (SEM.6<sup>th</sup>)

UNI.R.No.-15660

CLASS R.NO.-211410

**SRI GURU TEG BAHADUR KHALSA COLLEGE  
SRI ANANDPUR SAHIB  
(AN AUTONOMOUS COLLEGE)**



# **Research Project Report On Performance Appraisal**

**SUBMITTED TO:**

**Sri Guru Teg Bahadur Khalsa College  
Sri Anandpur Sahib  
Punjabi University, Patiala**

**In the partial fulfillment of the requirements for full time training in  
Bachelors of Business Administration  
(Session 2023-2024)**



Under the Guidance of:  
Prof. Amanpreet Kaur  
(PG Dept. of Commerce and Management)

Submitted By:  
Pardeep Kaur  
B.B.A. (6th SEM.)  
Roll no. 211411  
University roll no. 15661

**PROJECT REPORT**  
**ON**  
**A STUDY ON MARKETING STRATEGIES AND BRAND**  
**LOYALTY OF HIMPA IN INDIA**

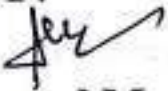
**In partial fulfilment of the requirements for the degree Bachelor**  
**of Business Administration**

**(Session 2021-2024)**

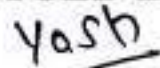
**PUNJABI UNIVERSITY, PATIALA**



**UNDER GUIDANCE OF:**

**Prof. Amanpreet Kaur**   
**(PG Dept. of Commerce and Management)**

**SUBMITTED BY**

**Yash**   
**BBA (6<sup>th</sup> Sem)**

**Roll no. 21412**

**Uni Roll no.**

**(15670)**



**SRI GURU TEG BAHADUR KHALSA COLLEGE**


**SRI ANANDPUR SAHIB**

**(AN AUTONOMOUS COLLEGE)**


**PROJECT REPORT**  
**A STUDY ON STRESS MANAGEMENT**  
**AT**  
**NATIONAL FERTILIZER LIMITED**  
**IN THE PARTIAL FULFILLMENT OF THE REQUIREMENTS FOR**  
**THREE MONTHS FULL TIME TRAINING IN**  
**BACHELOR OF BUSINESS ADMINISTRATION**




SUMMITTED TO:

PROF. AMANPREET KAUR   
(PG DEPT. OF COMMERCE & MANAGEMENT)

SUBMITTED BY:

JASHANPREET KAUR   
BBA 6<sup>TH</sup> SEM  
UNI. R.NO.- 15662  
CLASS R.NO.-211416

**SRI GURU TEG BAHADUR KHALSA COLLEGE**  
**SRI ANANDPUR SAHIB**  
**(AN AUTONOMOUS COLLEGE)**

  
27/5/24




**PROJECT REPORT  
ON  
EMPLOYEE WELFARE  
AT  
NATIONAL FERTILIZERS LIMITED**

**IN THE PARTIAL FULFILLMENT OF THE REQUIREMENTS FOR  
THE DEGREE OF BACHELOR OF BUSINESS ADMINISTRATION  
(2021-2024)**



**SUMMITTED TO:**

**PROF. AMANPREET KAUR**   
(PG DEPT. OF COMMERCE & MANAGEMENT)

**SUBMITTED BY:**

**RIYA SHARMA** *Riya Sharma*  
BBA 5<sup>TH</sup> SEM

UNI. R.NO.- 15663

CLASS R.NO. – 211417

**SRI GURU TEG BAHADUR KHALSA COLLEGE  
SRI ANANDPUR SAHIB  
(AN AUTONOMOUS COLLEGE)**

**PROJECT REPORT**  
**A STUDY ON MARKETING STRATEGIES AND BRAND LOYALTY OF**  
**HIMPA IN INDIA**

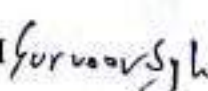
**SUBMITTED TO:**  
**PUNJABI UNIVERSITY, PATIALA**

**IN PARTIAL FULFILLMENT OF THE REQUIREMENTS FOR THE DEGREE OF**  
**BACHELOR OF BUSINESS ADMINISTRATION**

**(Session 2021-2024)**



**SUBMITTED TO:**  
**ASSISTANT PROF.**  
**AMANPREET KAUR**   
**(P.G. Department of Commerce and**  
**Management)**

**SUBMITTED BY:**  
**GURNOOR SINGH**   
**B.B.A(6th SEM)**  
**UNI. Roll No. 15672**  
**CLASS Roll No. 211421**

**SRI GURU TEG BAHADUR KHALSA**  
**SRI ANANDPUR SAHIB**  
**(AN AUTONOMOUS COLLEGE)**

**PROJECT REPORT**  
**ON**  
**A STUDY ON WORKMEN ABSENTEEISM OF WIPRO**  
**ENTERPRISES PRIVATE LIMITED BADDI UNIT**  
**In partial fulfilment of the requirements for the degree**  
**Bachelor of Business Administration**  
**(Session 2021-2024)**  
**PUNJABI UNIVERSITY, PATIALA**



**UNDER GUIDANCE OF:**

**Prof. Amanpreet Kaur**

**(PG Dept. of Commerce and Management)**

**SUBMITTED BY**

**Harpreet Kaur**

**B.B.A(6<sup>th</sup> SEM)**

**Roll No.211422**

**Univ. Roll No.**

**(15664)**

**SRI GURU TEG BAHADUR KHALSA COLLEGE**  
**SRI ANANDPUR SAHIB**  
**(AN AUTONOMOUS COLLEGE)**



# PROJECT REPORT

## CUSTOMER SATISFACTION REGARDING DIFFERENT PRODUCTS BY HIMPA

IN PARTIAL FULFILMENT OF THE REQUIREMENT FOR THE  
DEGREE OF BACHELOR OF BUSINESS ADMINISTRATION

(2021-2024)



SUBMITTED TO  
ASSISTANT PROF  
AMANPREET KAUR *[Signature]*  
(PG DEPARTMENT OF COMMERCE  
& MANAGEMENT)

SUBMITTED BY  
VARUN SHARMA *[Signature]*  
B.B.A (SEM-6)  
UNI. ROLL NO. 15673  
CLASS RPLL NO. 211424

*Pam 1*  
*27/5/24*

**SRI GURU TEG BAHADUR KHALSA COLLEGE**  
**SRI ANANDPUR SAHIB**  
**(AN AUTONOMOUS COLLEGE)**

**PROJECT REPORT**  
**A STUDY ON STRESS MANAGEMENT**  
**MEASURES AT WISDOM INFOSOFT, MOHALI**  
In partial fulfillment of the requirement for the degree of  
**Bachelor Of Business Administration**  
(Session 2023-2024)



**SUBMITTED TO:**

Assistant Prof. Amanpreet Kaur  
(P. G Department Of Commerce & Management)

Univ. Roll no. - 15665

**SUBMITTED BY:**

Neha

B.B.A(Sem-4th)

Roll no. - 211425

Neha

Pass  
27/5/24

**SRI GURU TEG BAHADUR KHALSA COLLEGE**  
**SRI ANANDPUR SAHIB**  
(AN AUTONOMOUSE COLLEGE)

# PROJECT REPORT

## A STUDY ON EMPLOYEE MOTIVATION AND ITS TECHNIQUES

IN PARTIAL FULFILMENT OF THE REQUIREMENT FOR THE  
DEGREE OF BACHELOR OF BUSINESS ADMINISTRATION

(2023-2024)



**SUBMITTED TO:**

ASSISTANT PROF: AMANPREET KAUR

(PG DEPARTMENT OF COMMERCE

& MANAGEMENT)

**SUBMITTED BY:**

JYOTI KUMARI *Jyoti Kumari*

BBA (SEM-6<sup>TH</sup>)

UNLROLL NO 15666

CLASS ROLL NO. 211426

**SHRI GURU TEG BAHADUR KHALSA COLLEGE**

**SHRI ANANDPUR SAHIB**

**(AN AUTONOMOUS COLLEGE)**

*Pam*  
27/5/24



**RESEARCH PROJECT REPORT  
ON**

**TRAINING AND DEVELOPMENT**

**SUBMITTED TO:-**

**Sri Guru Teg Bahadur Khalsa College**

**Sri Anandpur Sahib**

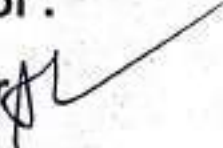
**Punjabi University, Patiala**

**In partial fulfilment of the requirements for the Degree of  
Bachelor of Business Administration (BBA)**

**(Session 2023-2024)**




**Under the Guidance of :**

**Prof. Amanpreet Kaur**   
**(PG Dept.of Comm. and Mgt )**

  
27/5/24

**Submitted By:**

  
**Kamalpreet Kaur**

**B.B.A.(6thSEM.)**

**Roll no. 211430**

**Univ roll no.15668**

**PROJECT REPORT**  
**ON**  
**A STUDY ON MARKETING STRATEGIES AND BRAND**  
**LOYALTY OF HIMPA IN INDIA**

**In partial fulfilment of the requirements for the degree Bachelor**  
**of Business Administration**

**(Session 2021-2024) PUNJABI**  
**UNIVERSITY, PATIALA**



**SUBMITTED TO:**  
**Prof. Amanpreet Kaur** *AK*  
**(PG Dept. of Commerce and Management)**

**SUBMITTED BY:** *Veer Partap Singh*  
**Rana veer partap singh**  
**BBA (6<sup>th</sup> Sem)**

**Roll no. 211431**

**Uni Roll no. (15674)**

**SRI GURU TEG BAHADUR KHALSA COLLEGE**  
**SRI ANANDPUR SAHIB**  
**(AN AUTONOMOUS COLLEGE)**

## **PROJECT REPORT**

**A STUDY ON TRAINING AND DEVELOPMENT IN WIPRO**

**ENTERPRISES PVT LTD, BADDI**

**IN PARTIAL FULFILMENT OF THE REQUIREMENTS FOR DEGREE OF BACHELOR  
OF BUSINESS ADMINISTRATION**

**(2021-2024)**



**SUBMITTED TO:**

**ASSISTANT PROF: Ms. AMANPREET KAUR**

**(P.G.DEPARTMENT OF COMMERCE**

**& MANAGEMENT)**

**SUBMITTED BY:**

**KOMAL KUMARI** *Komal Kumari*

**B.B.A(SEM-6)**

**UNL.ROLLNO.15669**

**CLASS ROLL.211434**

**SRI GURU TEG BAHADUR KHALSA COLLEGE**

**SRI ANANDPUR SAHIB**

**(AN AUTONOMOUS COLLEGE)**



**PROJECT REPORT**  
**ON**  
**A STUDY ON MARKETING STRATEGIES AND BRAND**  
**LOYALTY OF HIMPA IN INDIA**

**In partial fulfilment of the requirements for the degree Bachelor  
of Business Administration**

**(Session 2021-2024) PUNJABI**  
**UNIVERSITY, PATIALA**

23-24



**SUBMITTED TO:**  
**Prof. Amanpreet Kaur**  
**(PG Dept. of Commerce and Management)**

**SUBMITTED BY:**  
**Simarjeet singh**  
**BBA (6<sup>th</sup> Sem)**

Simarjeet  
Singh

**Roll no. 211435**

**Uni Roll no. (15676)**

Pam  
27/5/24

**SRI GURU TEG BAHADUR KHALSA COLLEGE**  
**SRI ANANDPUR SAHIB**  
**(AN AUTONOMOUS COLLEGE)**

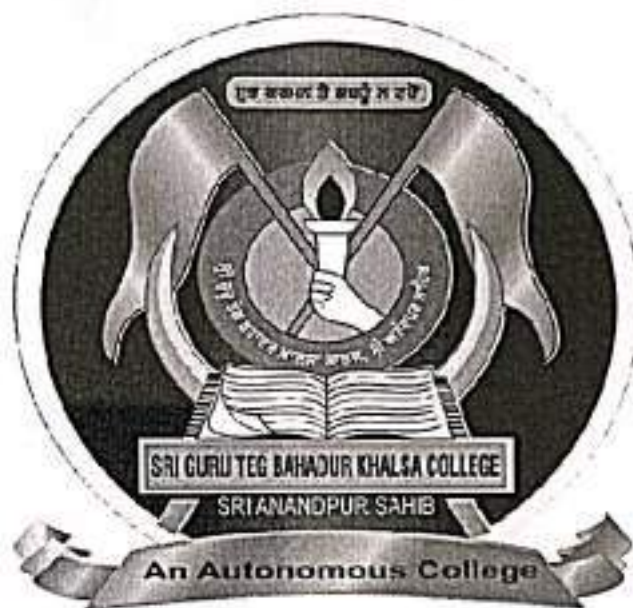
# **PROJECT REPORT**

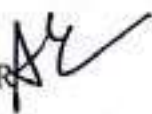
## **CUSTOMER SATISFACTION REGARDING DIFFERENT PRODUCTS BY HIMPA**


IN PARTIAL FULFILMENT OF THE REQUIREMENT FOR THE  
DEGREE OF BACHELOR OF BUSINES ADMINISTRATION

PUNJABI UNIVERSITY, PUNJABI

(2021-2024)



SUBMITTED TO  
ASSISTANT PROF  
AMANPREET KAUR   
(PG DEPARTMENT OF COMMERCE  
& MANAGEMENT)

SUBMITTED BY  
ANURAG GILL   
B.B.A (SEM-6)  
UNI. ROLL NO. 15680  
CLASS ROLL NO. 211439

**SRI GURU TEG BAHADUR KHALSA COLLEGE**  
**SRI ANANDPUR SAHIB**  
**(AN AUTONOMOUS COLLEGE)**

**RESEARCH PROJECT**  
**ON**  
**STUDY OF HOW SERVICE AND PRODUCT QUALITY**  
**EFFECTS ON CUSTOMER SATISFACTION IN CAFE21**  
**(IN ANANDPUR SAHIB)**



**SRI GURU TEG BAHADUR KHALSA COLLEGE**  
**ANANDPUR SAHIB**  
**(2022-24)**

**SUBMITTED TO:**  
**DR.MANJEET SINGH**  
**(HEAD OF PG DEPT.OF**  
**COMMERCE AND MANAGEMENT)**

**SUBMITTED BY:**  
  
**HARDEEP KAUR**  
**M.COM 4<sup>TH</sup> SEM**  
**ROLL NO:222204**  
**UNI ROLL NO:4701**



**RESEARCH PROJECT  
ON  
STUDY OF EFFECTIVENESS OF DIGITAL MARKETING  
STRATEGIES FOR CLOTHING PRODUCTS BY  
CUSTOMERS  
( A CASE STUDY IN SRI KIRATPUR SAHIB)**



**MASTERS OF COMMERCE  
(2022-2024)**

**SUBMITTED TO:-  
DR. MANJEET SINGH  
(HEAD OF PG DEPARTMENT OF  
COMMERCE AND MANAGEMENT )**

**SUBMITTED BY:**  
*Sabita*  
**SABITA SHARMA  
M.COM ( SEM -4<sup>TH</sup> )  
ROLL NO 222205  
UNI. ( ROLL NO) 4702**

**SRI GURU TEG BAHADUR KHALSA COLLEGE  
SRI ANANDPUR SAHIB**

**RESEARCH PROJECT REPORT**  
**ON**  
**TO STUDY CUSTOMER SATISFACTION**  
**TOWARDS E-BANKING SERVICES**  
**(A CASE STUDY OF UNA)**  
**TO**  
**PG Department of Commerce & Management**  
**(In partial fulfilment of the requirement for the degree)**  
**OF MASTERS OF COMMERCE**



**(SESSION 2022-2024)**

**SUBMITTED TO.**

**DR. MANJEET SINGH**

**(HEAD OF PG DEPARTMENT OF  
COMMERCE & MANGEMENT)**

**SUBMITTED BY**

**SIMRAN SINGH**

**M.COM (SEM-4<sup>TH</sup>)**

**ROLL NO. 222206**

**UNI. ROLL NO. 4703**

*Simran Singh.*

**SRI GURU TEG BAHADUR KHALSA COLLEGE**

**SRI ANANDPURSAHIB**

**RESEARCH PROJECT REPORT  
ON  
CUSTOMER SATISFACTION TOWARDS BANKING  
SERVICES OF CO-OPERATIVE BANK IN RURAL  
AREAS  
TO**

**PG Department of Commerce & Management  
(In partial fulfilment of the requirement for the degree)  
OF MASTERS OF COMMERCE**



**MASTER OF COMMERCE  
(SESSION 2022-2024)**

**SUBMITTED TO.** *Navjeet Kaur*  
**DR. NAVJEET KAUR**  
**(PG DEPARTMENT OF  
COMMERCE & MANGEMENT)**

*Manpreet Kaur*  
**SUBMITTED BY**  
**MANPREET KAUR**  
**M.COM (SEM-4<sup>TH</sup>)**  
**ROLL NO. 222207**  
**UNI. ROLL NO. 4704**

**SRI GURU TEG BAHADUR KHALSA COLLEGE  
SRI ANANDPURSAHIB**



**RESEARCH PROJECT  
ON  
PATIENTS SATISFACTION TOWARDS GOVERNMENT  
HOSPITAL IN BHARATGARH  
TO  
PG DEPARTMENT OF COMMERCE & MANAGEMENT  
(IN PARTIAL FULFILLMENT OF THE REQUIREMENT FOR  
THE DEGREE)**



**MASTERS OF COMMERCE  
(2022-2024)**

**SUBMITTED TO:-  
DR. NAVJEET KAUR**  
(PG DEPARTMENT OF COMMERCE  
AND MANAGEMENT )

**SUBMITTED BY:** *Maninder Kaur*  
**MANINDER KAUR**  
**M.COM ( SEM -4<sup>TH</sup> )**  
**ROLL NO 222208**  
**UNI. ( ROLL NO) 4705**

**SRI GURU TEG BAHADUR KHALSA COLLEGE  
SRI ANANDPUR SAHIB**

**RESEARCH PROJECT REPORT**  
**ON**  
**GENERAL ATTITUDES OF STUDENTS TOWARDS**  
**ONLINE LEARNING**  
**PG DEPARTMENT OF COMMERCE & MANAGEMENT**  
**(IN PARTIAL FULFILMENT OF THE REQUIREMENT FOR THE DEGREE)**



**MASTERS OF COMMERCE**

**(SESSION 2022-2024)**

**SUBMITTED TO**

**DR. NAVJEET KAUR**

**(PG DEPARTMENT OF COMMERCE**

**AND MANAGEMENT)**

**SUBMITTED BY:**

**SUKHWINDER KAUR**

**M.COM(4<sup>TH</sup> SEM)**

**ROLL NO 222209**

**UNL.( ROLL NO) 4706**

**RESEARCH PROJECT  
REPORT ON  
TO STUDY THE IMPACT OF  
PACKAGING ON CONSUMERS  
BUYING BEHAVIOR  
SUBMITTED TO**



**SRI GURU TEG BAHADUR KHALSA  
COLLEGE SRI ANANDPUR SAHIB  
MASTER OF COMMERCE**

**SESSION: 2022-2024**

**SUPERVISOR**

**Dr.MANPREET KAUR**

**(PG DEPARTMENT OF COMMERCE & MANAGEMENT)**

**SUBMITTED BY**

**RITIKA** *Ritika*

**M.COM 4<sup>TH</sup> semester**



**RESEARCH PROJECT REPORT  
ON  
A STUDY ON WORK LIFE AND  
JOB PERFORMANCE OF EMPLOYEES  
SUBMITTED TO**



**SRI GURU TEG BAHADUR KHALSA COLLEGE  
SRI ANANDPUR SAHIB**

**MASTER OF COMMERCE  
SESSION: 2022-2024**

**SUPERVISOR  
Dr. MANPREET KAUR  
(PG DEPARTMENT OF COMMERCIAL & MANAGEMENT)**


**SUBMITTED BY:**  
*Nitika Dutta*  
**NITIKA DUTTA  
UNIVERSITY ROLL NO. 4708  
CLASS ROLL NO. 222211  
M.COM 4<sup>th</sup> semester**

**RESEARCH PROJECT REPORT**  
**ON**  
**BRAND PREFERENCE OF**  
**MOBILE PHONES AMONG STUDENTS**  
**SUBMITTED TO**



**SRI GURU TEG BAHADUR KHALSA COLLEGE**  
**SRI ANANDPUR SAHIB**  
**MASTER OF COMMERCE**  
**SESSION: 2022-2024**

**SUPERVISOR**  
**Prof. MANPREET KAUR**  
**(PG DEPARTMENT OF COMMEREC & MANAGEMENT)**

**SUBMITTED BY:**  
**RIYA**   
**UNIVERSITY ROLNO.-4709**  
**CLASS ROLL NO.222212**  
**M.COM 4<sup>th</sup> semester**

**RESEARCH PROJECT REPORT  
ON  
FACTORS BEHIND THE PLASTIC MONEY  
(A CASE STUDY OF SGTB KHALSA COLLEGE  
SRI ANANDPUR SAHIB)**

**TO  
PG Department of Commerce & Management  
(In partial fulfilment of the requirement for the degree)  
OF MASTERS OF COMMERCE**



**(SESSION 2022-2024)**

**SUBMITTED TO.  
PROF. POONAM *Pm*  
(PG DEPARTMENT OF  
COMMERCE & MANGEMENT)**

**SUBMITTED BY  
PRIYANKA RANI *Priyanka Rani*  
M.COM (SEM-4<sup>TH</sup>)  
ROLL NO. 222213  
UNI. ROLL NO. 4710**

**SRI GURU TEG BAHADUR KHALSA COLLEGE  
SRI ANANDPURSAHIB**



**RESEARCH PROJECT  
ON  
FACTOR AFFECTING CONSUMER PREFERENCES  
TOWARDS THE ORGANIC FOOD PURCHASE  
( A CASE STUDY OF SGTB KHALSA COLLEGE  
SRI ANANDPUR SAHIB)**



**MASTERS OF COMMERCE  
(2022-2024)**

**SUBMITTED TO:-  
PROF. POONAM *Poonam*  
(PG DEPARTMENT OF COMMERCE  
AND MANAGEMENT )**

**SUBMITTED BY: *Gagandeep*  
GAGANDEEP KAUR  
M.COM ( SEM -4<sup>TH</sup> )  
ROLL NO 222214  
UNI. ( ROLL NO) 4711**

**SRI GURU TEG BAHADUR KHALSA COLLEGE  
SRI ANANDPUR SAHIB**

**RESEARCH PROJECT  
ON  
CAUSES OF STRESS AMONG, YOUTH AND ITS  
MANAGEMENT  
( A CASE STUDY OF SGTB KHALSA COLLEGE  
SRI ANANDPUR SAHIB)**



**MASTERS OF COMMERCE  
(2022-2024)**

**SUBMITTED TO:-  
PROF. POONAM** *Poonam*  
**(PG DEPARTMENT OF COMMERCE  
AND MANAGEMENT )**

**SUBMITTED BY:  
SIMRAN KAUR** *Simran*  
**M.COM ( SEM -4<sup>TH</sup> )  
ROLL NO 222216  
UNI. ( ROLL NO) 4712**

**SRI GURU TEG BAHADUR KHALSA COLLEGE  
SRI ANANDPUR SAHIB**

**PROJECT REPORT  
ON  
“AWARENESS OF STOCK  
MARKET IN RURAL AREAS”**



**SUBMITTED TO:**

**DR. PARAMPREET SINGH  
(PG DEPARTMENT OF  
COMMERCE & MANAGEMENT**

**SUBMITTED BY:**

**SHIVANI SHARMA**  
**M.COM-4<sup>RD</sup> SEM.**  
**ROLL NO. 222217**  
**UNI.ROLL NO. 4713**

*Shivani  
Sharma*

**SRI GURU TEG BAHADUR KHALSA COLLEGE,  
SRI ANANDPUR SAHIB**



**RESEARCH PROJECT  
ON  
INVESTMENT PATTERN OF SALARIED EMPLOYEES  
( A CASE STUDY OF NURPUR BEDI )**



**MASTERS OF COMMERCE  
(2022-2024)**

**SUBMITTED TO:-  
DR. PARAMPREET SINGH  
(PG DEPARTMENT OF COMMERCE  
AND MANAGEMENT)**

**SUBMITTED BY:**  
*Monika*  
**MONIKA  
M.COM ( SEM -4<sup>TH</sup> )  
ROLL NO 222218  
UNI. ( ROLL NO) 4714**

**SRI GURU TEG BAHADUR KHALSA COLLEGE  
SRI ANANDPUR SAHIB**

**RESEARCH PROJECT  
ON  
CUSTOMER SATISFACTION TOWARDS FLIPKART  
( A CASE STUDY OF SGTB KHALSA COLLEGE  
SRI ANANDPUR SAHIB)**



**MASTERS OF COMMERCE  
(2022-2024)**

**SUBMITTED TO:-  
DR. PARAMPREET SINGH  
(PG DEPARTMENT OF COMMERCE  
AND MANAGEMENT)**

**SUBMITTED BY:  
ARSHDEEP KAUR  
M.COM ( SEM -4<sup>TH</sup> )  
ROLL NO 222219  
UNI. ( ROLL NO) 4715**

**SRI GURU TEG BAHADUR KHALSA COLLEGE  
SRI ANANDPUR SAHIB**

**RESEARCH PROJECT  
ON  
CONSUMER SATISFACTIONS BEHAVIOUR VERKA MILK  
& MILK PRODUCTS  
( A CASE STUDY OF SRI ANANDPUR SAHIB)**



**MASTERS OF COMMERCE  
(2022-2024)**

**SUBMITTED TO:-**  
**DR. HARDEEP KAUR**  
**(PG DEPARTMENT OF COMMERCE  
AND MANAGEMENT)**

**SUBMITTED BY:**  
**RAMANJEET KAUR**  
**M.COM ( SEM -4<sup>TH</sup> )**  
**ROLL NO 222220**  
**UNI. ( ROLL NO) 4716**

**SRI GURU TEG BAHADUR KHALSA COLLEGE  
SRI ANANDPUR SAHIB**



**A PROJECT REPORT  
ON  
CUSTOMER'S SATISFACTION IN AIRTEL**



**MASTER OF COMMERCE  
(2022-2024)**

**SUBMITTED TO:**

*Hardeep*  
**Dr. Hardeep Kaur**

**Assistant professor**

**PG Department of commerce  
& Management**

**SUBMITTED BY:**

*Bhawna*  
**BHAWNA KAUMARI**

**University Roll no. 4717**

**M.com 4<sup>th</sup> semester**

**A PROJECT REPORT  
ON  
CUSTOMER SATISFACTION REGARDING BANKING SERVICES OF  
PUNJAB NATIONAL BANK SHRI ANANDPUR SAHIB**



**MASTER OF COMMERCE  
(2022-2024)**

**SUBMITTED TO:**

*Hardeep*  
**Dr. Hardeep Kaur**

**Assistant professor**

**PG Department of commerce**

**& Management**

**SUBMITTED BY:**

*Meenakshi*  
**Meenakshi Rani**

**University Roll no. 4718**

**M.com 4<sup>th</sup> semester**

**RESEARCH PROJECT REPORT**  
**ON**  
**IMPACT OF SOCIAL MEDIA ON YOUNGSTERS**  
**(PUNJABI UNIVERSITY, PATIALA)**



**SUBMITTED TO:**

**DR. TEJINDER KAUR**

(Assistant Professor )

(Post Graduation of commerce

And management)

**SUBMITTED BY:**

**KAMALPREET KAUR**

University roll no.4719

*Kamalpreet Kaur*

**SRI GURU TEG BAHADUR KHALSA COLLEGE**  
**SRI ANANDPUR SAHIB**  
**(An Autonomous College)**



# EFFECT OF FAST FOOD ON HUMAN HEALTH

RESEARCH PROJECT REPORT  
SUBMITTED TO  
PUNJABI UNIVERSITY, PATIALA



SUBMITTED TO

DR. TEJINDER KAUR *Tejinder Kaur*  
(Assistant Professor)  
PG DEPARTMENT OF COMMERCE  
AND MANAGEMENT

SUBMITTED BY

MEGHA SHARMA  
Roll No. 222226  
University Roll no. 4720

*Megha Sharma*

SRI GURU TEG BAHADUR KHALSA COLLEGE

SRI ANANDPUR SAHIB

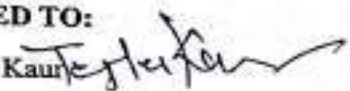
(AN AUTONOMOUS COLLEGE)

2024

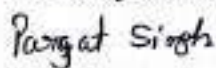
**RESEARCH PROJECT REPORT**  
**ON**  
**Customer Satisfaction on Mobile Service Provider Networks**  
**SUBMITTED TO:**  
**Punjabi University, Patiala**



**SUBMITTED TO:**

Dr. Tejinder Kaur   
(Assistant Professor)  
Post Graduation of commerce & management

**SUBMITTED BY:**

Pargat Singh  
University Rollno:4723  


**SRI GURU TEG BAHADUR KHALSA COLLEGE**  
**SRI ANANDPUR SAHIB**  
**(An Autonomous College)**

AN  
INDUSTRIAL TRAINING REPORT  
AT  
**(MOHIT MOTORS)**

In the partial fulfillment of the requirement of the  
Degree of B.Voc Retail Management  
(2021-2024)



Submitted to:  
PROF SHUBNEET KAUR

*Shubneet*

Submitted by: TARANPREET SINGH  
B.VOC RETAIL MANAGEMENT  
UNIVERSITY ROLL NO:- 14448

*Taranpreet Singh*

**SRI GURU TEG BAHADUR KHALSA COLLEGE**  
**SRI ANANDPUR SAHIB**



AN  
INDUSTRIAL TRAINING REPORT  
AT

**"TVS Motors"**

In the partial fulfillment of the requirement of the  
Degree of B.Voc Retail Management  
(2021-2024)



Submitted to:

Prof. Shubhneet Kaur

*Shubhneet*

Submitted by

Abhishek Gulati

B.Voc (Retail Management) sem 6<sup>th</sup>

Uni. Roll No. 14438

*Abhishek Gulati*

**SRI GURU TEG BAHADUR KHALSA COLLEGE**  
**SRI ANANDPUR SAHIB**

AN  
INDUSTRIAL TRAINING REPORT  
AT

Boang Technology Pvt. Ltd.

In the partial fulfillment of the requirement of the  
“BACHELOR OF VOCATION IN RETAIL MANAGEMENT”

(2021-2024)



**SRI GURU TEG BAHADUR KHALSA COLLEGE**  
**SRI ANANDPUR SAHIB**  
**AN AUTONOMOUS COLLEGE**

**SUPERVISED BY:-**

**Prof. Shubneet Kaur**

*Shubneet*

**SUBMITTED BY:-**

**Mohit Nadda**

**B.Voc (Retail Management)**

**Uni. Roll No. 14424**

*Mohit Nadda*

AN  
INDUSTRIAL TRAINING REPORT  
AT  
"MARUTI SUZUKI"

In the partial fulfillment of the requirement of the  
Degree of B.Voc Retail Management  
(2021-2024)



Submitted to:

Prof. Shubhneet Kaur

*Shubhneet Kaur*

Submitted by

Paramvir Singh

B.Voc (Retail Management) sem 6<sup>th</sup>

Uni. Roll No. 14435

*Paramvir Singh*

**SRI GURU TEG BAHADUR KHALSA COLLEGE**  
**SRI ANANDPUR SAHIB**



AN  
INDUSTRIAL TRAINING REPORT  
AT  
**VR PUNJAB MALL MOHALI**

In the partial fulfillment of the requirement of the  
**“BACHELOR OF VOCATION IN RETAIL MANAGEMENT”**  
(2021-2024)



**SRI GURU TEG BAHADUR KHALSA COLLEGE**  
**SRI ANANDPUR SAHIB**  
**AN AUTONOMOUS COLLEGE**

**SUPERVISED BY:-**

**Prof. Jatinder Singh**

**SUBMITTED BY:-**

**Ashma Devi**

**B.Voc (Retail Management)**

**Uni. Roll No. 14403**

AN  
INDUSTRIAL TRAINING REPORT  
AT  
**MOHIT MOTORS DHER**

In the partial fulfillment of the requirement of the  
“BACHELOR OF VOCATION IN RETAIL MANAGEMENT”

(2021-2024)



**SRI GURU TEG BAHADUR KHALSA COLLEGE**  
**SRI ANANDPUR SAHIB**  
**AN AUTONOMOUS COLLEGE**

**SUPERVISED BY:-**

**Prof. Jatinder Singh**

**SUBMITTED BY:-**

**Hardeep kaur** Hardeep Kaur

**B.Voc (Retail Management)**

**Uni. Roll No. 14410**

AN  
INDUSTRIAL TRAINING REPORT  
AT  
**COLOUR BUCKET STORE**

In the partial fulfillment of the requirement of the  
Degree of B.Voc Retail Management  
(2021-2024)



Submitted to:

Prof. Jatinder Singh

Submitted by:

Razat Singh Rayat

Uni. Roll. No.: 14415

**SRI GURU TEG BAHADUR KHALSA COLLEGE**  
**SRI ANANDPUR SAHIB**



AN

**INDUSTRIAL TRAINING REPORT AT  
REHAL GARMENTS (OCTAVE METTLE)**

In the partial fulfillment of the requirement of the

**"BACHELOR OF VOCATION IN RETAIL MANAGEMENT"**

**(2021-2024)**



**SRI GURU TEG BAHADUR KHALSA COLLEGE  
ANANDPUR SAHIB  
AN AUTONOMOUS COLLEGE**

**SUPERVISED BY:-**

**Prof. Jatinder Singh**

**SUBMITTED BY:-**

**Kunal Rana**

**B.Voc (Retail Management)**

**Uni. Roll No. 14423**

AN  
INDUSTRIAL TRAINING REPORT  
AT  
**SONI AUTO DEALERS LLP (SUZUKI)**

In the partial fulfillment of the requirement of the  
**“BACHELOR OF VOCATION IN RETAIL MANAGEMENT”**  
(2021-2024)



**SRI GURU TEG BAHADUR KHALSA COLLEGE**  
**SRI ANANDPUR SAHIB**  
**AN AUTONOMOUS COLLEGE**

**SUPERVISED BY:-**

**Prof. Jatinder Singh**

**SUBMITTED BY:-**

**Sourav Sharma**

**B.Voc (Retail Management)**

**Uni. Roll No. 14416**

AN

**INDUSTRIAL TRAINING REPORT AT**  
**FUN PLAZA MULTIPLEX MALL KKP**  
**(HAMIR REAL ESTATE PRIVATE LIMITED)**

In the partial fulfillment of the requirement of the  
**“BACHELOR OF VOCATION IN RETAIL MANAGEMENT”**

(2021-2024)



**SRI GURU TEG BAHADUR KHALSA COLLEGE**  
**SRI ANANDPUR SAHIB**  
**AN AUTONOMOUS COLLEGE**

**SUPERVISED BY: -**

Prof. Jatinder Singh  


**SUBMITTED BY:-**

Anchal   
**B.Voc (Retail Management)**  
**Uni. Roll no. 14401**



AN  
INDUSTRIAL TRAINING REPORT  
AT  
**ADITYA BIRLA FASHION AND RETAIL (PANTALOONS)**

In the partial fulfillment of the requirement of the  
**"BACHELOR OF VOCATION IN RETAIL MANAGEMENT"**

(2021-2024)



**SRI GURU TEG BAHADUR KHALSA COLLEGE**  
**SRI ANANDPUR SAHIB**  
**AN AUTONOMOUS COLLEGE**

**SUPERVISED BY:-**

Prof. Jatinder Singh

**SUBMITTED BY:-**

Harmanjot Singh

**B.Voc (Retail Management)**

**Uni. Roll No. 14439**

*Harmanjot*

AN  
INDUSTRIAL TRAINING REPORT  
AT  
**GOLDI BOOT HOUSE, NANGAL**

In the partial fulfillment of the requirement of the  
**“BACHELOR OF VOCATION IN RETAIL MANAGEMENT”**

(2021-2024)



**SRI GURU TEG BAHADUR KHALSA COLLEGE**  
**SRI ANANDPUR SAHIB**  
**AN AUTONOMOUS COLLEGE**

**SUPERVISED BY:-**

**Prof. Jatinder Singh**

**SUBMITTED BY:-**

**Onkar Singh**

**B.Voc (Retail Management)**

**Uni. Roll No. 14441**

AN  
INDUSTRIAL TRAINING REPORT  
AT  
**ADITYA BIRLA FASHION AND RETAIL**  
**(PANTALOONS)**

In the partial fulfillment of the requirement of the  
Degree of B.Voc Retail Management

(2021-2024)



Manpreet Kaur  
27/05/24

**SUPERVISED BY:-**

Prof. Jatinder Singh

**SUBMITTED BY:-**

Manpreet Kaur Manpreet Kaur

B.Voc (Retail Management)

Uni. Roll No. 14409

**SRI GURU TEG BAHADUR KHALSA COLLEGE**  
**SRI ANANDPUR SAHIB**



**AN  
INDUSTRIAL TRAINING REPORT  
AT  
HAPPY SHOPPING COMPLEX DHER**

**In the partial fulfillment of the requirement of the  
“BACHELOR OF VOCATION IN RETAIL MANAGEMENT”**

**(2021-2024)**



**SRI GURU TEG BAHADUR KHALSA COLLEGE  
SRI ANANDPUR SAHIB  
AN AUTONOMOUS COLLEGE**

**SUPERVISED BY:-**

**Prof. Jatinder Singh**

**SUBMITTED BY:-**

**Tania Tania**

**B.Voc (Retail Management)**

**Uni. Roll No. 14402**

AN  
INDUSTRIAL TRAINING REPORT  
AT  
**ADITYA BIRLA FASHION AND RETAIL  
(PANTALOONS)**

In the partial fulfillment of the requirement of the  
**“BACHELOR OF VOCATION IN RETAIL MANAGEMENT”**  
(2021-2024)



**SRI GURU TEG BAHADUR KHALSA COLLEGE  
SRI ANANDPUR SAHIB  
AN AUTONOMOUS COLLEGE**

**SUPERVISED BY:-**

**Prof. Jatinder Singh**

**SUBMITTED BY:-**

**Neha**

**B.Voc (Retail Management)**

**Uni. Roll No. 14406**

AN  
INDUSTRIAL TRAINING REPORT  
ON  
**ACTION CLOTHING CO. LIMITED**  
**(KHARAR)**

In partial fulfillment of the requirement of full-time training in  
**“BACHELOR OF VOCATION IN RETAIL MANAGEMENT”**



**SRI GURU TEG BAHADUR KHALSA COLLEGE**  
**SRI ANANDPUR SAHIB**  
**AN AUTONOMOUS COLLEGE**

**SUPERVISED BY:-**  
Asst. Prof. Jatinder Singh

**SUBMITTED BY:-**  
Seema Mehta *Seema Mehta*  
**B.Voc (Retail Management)**  
**Uni. Roll No. 14408**



AN  
INDUSTRIAL TRAINING REPORT  
AT  
**COLOUR BUCKET STORE**

In the partial fulfillment of the requirement of the  
Degree of B.Voc Retail Management  
(2021-2024)



Submitted to:

Prof. Jatinder Singh

Submitted by:

Simranpreet Kaur

Uni. Roll. No.: 14414

**SRI GURU TEG BAHADUR KHALSA COLLEGE**  
**SRI ANANDPUR SAHIB**

AN  
INDUSTRIAL TRAINING REPORT  
AT  
**ADITYA BIRLA FASHION AND RETAIL  
(PANTALOONS)**

In the partial fulfillment of the requirement of the  
“**BACHELOR OF VOCATION IN RETAIL  
MANAGEMENT**”

(2021-2024)



**SRI GURU TEG BAHADUR KHALSA COLLEGE  
SRI ANANDPUR SAHIB  
AN AUTONOMOUS COLLEGE**

**SUPERVISED BY:-**

**Prof. Jatinder Singh**

**SUBMITTED BY:-**

**Diksha Devi**

**B.Voc (Retail Management)**

**Uni. Roll No. 14405**



AN  
INDUSTRIAL TRAINING REPORT  
AT  
**HAPPY SHOPPING COMPLEX DHER**  
In the partial fulfillment of the requirement of the  
“BACHELOR OF VOCATION IN RETAIL  
MANAGEMENT”

(2021-2024)



**SRI GURU TEG BAHADUR KHALSA COLLEGE**  
**SRI ANANDPUR SAHIB**  
**AN AUTONOMOUS COLLEGE**

**SUPERVISED BY:-**

**Prof. Jafinder Singh**

**SUBMITTED BY:-**

**Mehak Pama**

**B.Voc (Retail Management)**

**Uni. Roll No. 14412**



AN  
INDUSTRIAL TRAINING REPORT  
AT  
"HOTEL MIRAGE MOHALI"

In partial fulfillment of the requirement of the degree of  
"BACHELOR OF VOCATION IN RETAIL MANAGEMENT"



**SUPERVISED BY:-**  
Prof. Jatinder Singh

**SUBMITTED BY:-**  
Kiranjot Kaur  
B.Voc (Retail Management)  
Uni. Roll No. 14407

**SRI GURU TEG BAHADUR KHALSA COLLEGE**  
**SRI ANANDPUR SAHIB**  
**AN AUTONOMOUS COLLEGE**

**AN  
INDUSTRIAL TRAINING REPORT  
AT  
MOHIT MOTORS**

**In the partial fulfillment of the requirement of the  
Degree of B.Voc Retail Management  
(2021-2024)**



**Submitted to:**

Ms. Subhneet Kaur

**Submitted by:**

Lovepreet

B.Voc (Retail Management)

Uni. Roll No. 14445

*Submitt*

**SRI GURU TEG BAHADUR KHALSA COLLEGE  
SRI ANANDPUR SAHIB**

AN  
INDUSTRIAL TRAINING REPORT  
AT

CLICK WORLD ONLINE

In the partial fulfillment of the requirement of the  
“BACHELOR OF VOCATION IN RETAIL  
MANAGEMENT”

(2021-2024)



**SRI GURU TEG BAHADUR KHALSA COLLEGE**  
**SRI ANANDPUR SAHIB**  
**AN AUTONOMOUS COLLEGE**

**SUPERVISED BY:-**  
**Prof. Jatinder Singh**

**SUBMITTED BY:-**

Jashanpreet Singh *Jashanpreet Singh*

**B.Voc (Retail Management)**  
Roll No. 214129



AN  
INDUSTRIAL TRAINING REPORT  
AT

CLICK WORLD ONLINE

In the partial fulfillment of the requirement of the  
“BACHELOR OF VOCATION IN RETAIL  
MANAGEMENT”

(2021-2024)



**SRI GURU TEG BAHADUR KHALSA COLLEGE**  
**SRI ANANDPUR SAHIB**  
**AN AUTONOMOUS COLLEGE**

**SUPERVISED BY:-**

**Prof. Jatinder Singh**

**SUBMITTED BY:-**

**Harshpreet Singh**

*Harshpreet*

**B.Voc (Retail Management)**

Roll No. 214133

AN  
INDUSTRIAL TRAINING REPORT  
AT  
CLICK WORLD ONLINE

In the partial fulfillment of the requirement of the  
"BACHELOR OF VOCATION IN RETAIL  
MANAGEMENT"

(2021-2024)



**SRI GURU TEG BAHADUR KHALSA COLLEGE**  
**SRI ANANDPUR SAHIB**  
**AN AUTONOMOUS COLLEGE**

**SUPERVISED BY:-**

**Prof. Jatinder Singh**

**SUBMITTED BY:-**

Gursimrat Singh *Gursimrat Singh*


**B.Voc (Retail Management)**

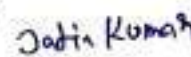
Roll No. 214122

**A**  
**Industrial Training Report**  
**On**  
**Hotel Operations of Hotel Sea, Patiala**

Submitted in partial fulfillment of the requirement for the  
degree

Of  
**BACHELOR OF VOCATION**  
**In**  
**Hospitality and Tourism**  
**(2021-2024)**

  
**Submitted to:**  
**Dr. Kamaljeet Singh**  
**Assistant Professor**  
**Tourism**  
**Hospitality and Tourism**  
**14304**

**Submitted By:**   
**Jatin Kumar**  
**B.Voc. Hospitality and**  
**Semester VI, Uni. Roll No. 14304**



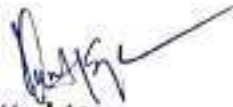
**PG Department of Commerce and Management**  
**Sri Guru Teg Bahadur Khalsa College, Sri Anandpur Sahib**  
**Rupnagar, Punjab**  
**May, 2024**

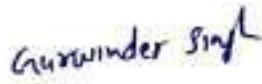


A  
**Industrial Training Report**  
**On**  
**New Taj Hotel, Sri Anandpur Sahib**

Submitted in partial fulfillment of the requirement for the  
degree

Of  
**BACHELOR OF VOCATION**  
**In**  
**Hospitality and Tourism**  
**(2021-2024)**

  
**Submitted to:**  
**Dr. Kamaljeet Singh**  
**Assistant Professor**  
**Hospitality and Tourism**

  
**Submitted By:**  
**Gurwinder Singh**  
**B.Voc. Hospitality and Tourism**  
**Semester VI, Uni. Roll No. 14314**




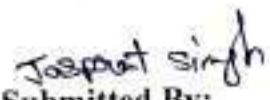
**PG Department of Commerce and Management**  
**SriGuruTegBahadurKhalsaCollege, SriAnandpurSahibRupnagar,**  
**Punjab**

**A**  
**Industrial Training Report**  
**On**  
**Hotel Operations of Hotel Mirage Sector 70 SAS**

Submitted in partial fulfillment of the requirement for the  
degree

**Of**  
**BACHELOR OF VOCATION**  
**In**  
**Hospitality and Tourism**  
**(2021-2024)**

  
Submitted to:  
**Dr. Kamaljeet Singh**  
Assistant Professor  
Hospitality and Tourism

  
Submitted By:  
**Jaspreet Singh**  
B.Voc.Hospitality and Tourism  
Semester VI, Uni. Roll No. 14327



**PG Department of Commerce and Management**  
**Sri GuruTeg Bahadur Khalsa College, Sri Anandpur Sahib**  
**Rupnagar, Punjab**

**A**  
**Industrial Training Report**

**On**

**Hotel Operations of Hotel S. Rattan, Sri Anandpur Sahib**

Submitted in partial fulfillment of the requirement for the degree

of

**BACHELOR OF VOCATION**

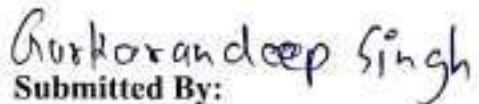
**In**

**Hospitality and Tourism**

**(2021-2024)**

  
Submitted to:

**Dr. Kamaljeet Singh**  
**Assistant Professor**  
**Hospitality and Tourism**

  
Submitted By:

**Gurkaran Singh**  
**B.Voc. Hospitality and Tourism**  
**Semester VI, Uni. Roll No.**



**PG Department of Commerce and Management**  
**Sri Guru Teg Bahadur Khalsa College, Sri Anandpur Sahib**  
**Rupnagar, Punjab**  
**May, 2024**



**A**  
**Industrial Training Report**

**On**

**Hotel Operations of Hotel S. Rattan, Sri Anandpur Sahib**

Submitted in partial fulfillment of the requirement for the degree

of

**BACHELOR OF VOCATION**

**In**

**Hospitality and Tourism**

**(2021-2024)**

  
Submitted to:

**Dr. Kamaljeet Singh**  
**Assistant Professor**  
**Hospitality and Tourism**

  
Submitted By:

**Nitish**  
**B.Voc. Hospitality and Tourism**  
**Semester VI, Uni. Roll No.14336**

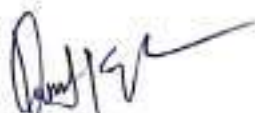


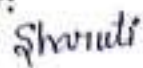
**PG Department of Commerce and Management**  
**Sri Guru Teg Bahadur Khalsa College, Sri Anandpur Sahib**  
**Rupnagar, Punjab**  
**May, 2024**

**A**  
**Industrial Training Report**  
**On**  
**Hotel Operations of Hotel Mirage, SAS Nager, mohali 70 (sector)**

Submitted in partial fulfillment of the requirement for the  
degree

Of  
**BACHELOR OF VOCATION**  
**In**  
**Hospitality and Tourism**  
**(2021-2024)**

  
**Submitted to:**  
**Dr. Kamaljeet Singh**  
**Assistant Professor**  
**Hospitality and Tourism**

**Submitted By:**  
**Sharuti**   
**B.Voc. Hospitality and Tourism**  
**Semester VI, Uni. Roll No. 14302**



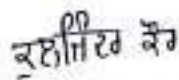
**PG Department of Commerce and Management**  
**Sri Guru Teg Bahadur Khalsa College, Sri Anandpur Sahib**  
**Rupnagar, Punjab**

**A**  
**Industrial Training Report**  
**On**  
**Hotel Operations of Surya Classic Hotel & Restaurant, Mohali**

Submitted in partial fulfillment of the requirement for the  
degree

Of  
**BACHELOR OF VOCATION**  
**In**  
**Hospitality and Tourism**  
**(2021-2024)**

  
**Submitted to:**  
**Dr. Kamaljeet Singh**  
**Assistant Professor**  
**Hospitality and Tourism**

**Submitted By:**  
**Kuljinder Kaur**   
**B.Voc.Hospitality and Tourism**  
**Semester VI, Uni. Roll No.14303**



**PG Department of Commerce and Management**  
**Sri GuruTeg Bahadur Khalsa College, Sri Anandpur Sahib**  
**Rupnagar, Punjab**  
**May, 2024**



**Sri Guru Teg Bahadur khalsa college**

(An Autonomous College)

**PlayTube**

A Project

Submitted in partial fulfillment for the award of the degree

of

**BACHELOR OF VOCATION**

**IN**

**SOFTWARE DEVELOPMENT**



Submitted To: *[Signature]*  
Prof. GaganDeep Singh

Submitted By : *Karandeep Singh*  
Karandeep Singh (14226)  
Karanveer (14228) *Karanveer*  
B.Voc (S.D.) Sem-6<sup>th</sup>

**P.G DEPT. OF COMPUTER SCIENCE**

**SRI GURU TEGH BAHADUR KHALSA COLLEGE**

**SRI ANANDPUR SAHIB (RUPNAGAR), PUNJAB (INDIA) - 140118**

**(AFFILIATED TO PUNJABI UNIVERSITY PATIALA, PUNJAB (INDIA))**

**May, 2024**

Research Report

On

Asp.Net Core through Ecommerce Application

In the Fulfilment for the Requirement of the Degree of (B.Voc) Bachelor of Vocation in  
Software Development



Submitted To :  
Prof. Gagan Deep Singh

Submitted By :  
Ritik Sharda & Ayush Bhardwaj

B.Voc(S.D.)Sem-6<sup>th</sup>

Roll No.-14234, 14224

Ayush Bhardwaj  
Ritik Sharda

RESEARCH REPORT  
ON  
MERN STACK (WEB DEVELOPMENT AND WEB  
DEPLOYMENT)  
AT



ThinkNEXT Technologies Pvt. Ltd.

In The Fulfillment for the Requirement of the Degree of B.voc  
(Bachelor of Vocational Education) in Software Development



Submitted to  
Prof. Gagandeep Singh.

Submitted by-

B.voc(S.D) Sem-6<sup>th</sup>

Roll No-14202 Tanujcet Kaur  
14204 Manpreet Kaur  
14206 Rangna Devi



**Sri Guru TegBahadurKhalsa College**  
(An Autonomous College)

**Graphics designing**

A Project Report

Submitted in partial fulfillment for the award of the degree  
of

**BACHELOR OF VOCATION**

**IN**

**SOFTWARE DEVELOPMENT**



Under the Guidance Of :-  
Prof Gagandeep Singh

Submitted By:-

Keshav(14236) &

Baljeet kumar(14222)

Keshav  
Baljeet Kumar

**P.G DEPT. OF COMPUTER SCIENCE**

**SRI GURU TEGH BAHADUR KHALSA COLLEGE**

**SRI ANANDPUR SAHIB (RUPNAGAR) PUNJAB (INDIA) – 140118,**

**AFFILIATED TO PUNJABI UNIVERSITY PATIALA, PUNJAB (INDIA))**

**May, 2024**

**Sri Guru TegBahadurKhalsa College**  
(An Autonomous College)  
**SEARCH ENGINE OPTIMIZATION(SEO)**

A Project Report  
Submitted in partial fulfillment for the award of the degree  
of  
**BACHELOR OF VOCATION**  
IN  
**SOFTWARE DEVELOPMENT**



Under the Guidance Of:  
Prof Gagandeep Singh

Submitted By:

Harshit(14227) & Harshit  
Tajinder Singh(14221)

P.G DEPT. OF COMPUTER SCIENCE

**SRI GURU TEGH BAHADUR KHALSA COLLEGE**  
SRI ANANDPUR SAHIB (RUPNAGAR), PUNJAB (INDIA) – 140118  
(AFFILIATED TO PUNJABI UNIVERSITY PATIALA, PUNJAB (INDIA))

**SRI GURU TEG BAHADUR KHALSA COLLEGE SRIANANDPUR SAHIB  
(AN AUTONOMOUS COLLEGE)**



**A REPORT OF SEMESTER TRAINING**

at

**THINKNEXT TECHNOLOGIES., MOHALI**

SUBMITTED IN PARTIAL FULFILLMENT OF THE REQUIREMENT FOR THE AWARD OF THE  
DEGREE OF

**BACHELOR OF VOCATIONAL IN SOFTWARE DEVELOPMENT**

FEB-JUNE, 2024

**UNDER THE GUIDANCE OF:-**  
MR. AHSAAN (PROJECT MANAGER)  
THINKNEXT TECHNOLOGIES

**SUBMITTED BY:** *Navneet Kaur*  
NAME: NAVNEET KAUR (14243)

&  
ANJIT (14207) *Anju*

P.G. DEPT. OF COMPUTER SCIENCE  
SRI GURU TEG BAHADUR KHALSA COLLEGE  
SRIANANDPUR SAHIB (RUPNAGAR), PUNJAB (INDIA) – 140118  
(AFFILIATED TO PUNJAB )



# RESEARCH REPORT

ON

Digital marketing

AT



ThinkNEXT Technologies Pvt. Ltd.

In The Fulfillment for the Requirement of the Degree of B.voc  
(Bachelor of Vocational Education) in Software Development



Submitted to-  
*Gagandeep Singh*  
Prof. Gagandeep Singh.

Submitted by-  
B.voc(S.D) Sem-6<sup>th</sup>

Roll No-14232 *Anil Singh*  
14212 *Simran*  
14211 *Simran*

**SRI GURU TEG BAHADUR KHALSA COLLEGE**

**SRI ANANDPUR SAHIB**

**(AN AUTONOMOUS COLLEGE)**



**PROJECT REPORT**

**SUBMITTED TO:**

**PROF. RAMANDEEP KAUR**

**(PG DEPT. OF COMPUTER SCIENCE)**

**SUBMITTED BY:**

**POOJA (14052)**

**SHRUTI (14057)**

**CLASS: B.SC(H)AI&DS**

**(SEM. VI)**

# Sri Guru Teg Bahadur Khalsa College

Sri Anandpur Sahib

( An Autonomous college )



**Project Report**

**On**

**Bus Booking Tour & Travels Website**

**(Batch: 2021-24)**

**Submitted To:**

*Rxaur*  
**Asst. Prof. Ramandeep Kaur Mam**  
(PG Department of Com. Sci.)

**Submitted By:**

*Taranpreet Singh*  
**Name: Taranpreet Singh**

**Class: BSc Hons A.I & D.S**

**Sem - 6 (Final-Year)**

**Roll no – 14064**



**SRI GURU TEG BAHADUR KHALSA COLLEGE**  
**SRI ANANDPUR SAHIB**  
**An Autonomous College**  
**Affiliated to Punjabi University, Patiala**



**2023-2024**

**Project File**  
**Of**  
**Food Ordering**

**Submitted to**  
Prof. Ramandeep Kaur  
*RKaur*

**Submitted by-**  
Palvi Sharma-14063 *Palvi Sharma*  
Gagandeep Kaur-14055 *Gagandeep Kaur*  
Harinder Kaur-14053 *Harinder Kaur*  
Ekta-14062 *Ekta*  
Riya-14059 *Riya Thakur*  
Bsc[H]AI&DS[Sem-6<sup>th</sup>]

## Project File Of Joining Gym

Рхан

Rahul- 14065 Rahul  
 Vinod Kumar- 14083 Vinod Kumar  
 Neha-14051 Neha  
 Dilpreet singh- 14084 Dilpreet Singh  
 Gurkaran Singh-14068 Gurkaran Singh  
 BSc(H)AI&DS(Sem-6<sup>th</sup>)

**SRI GURU TEG BAHADUR KHALSA COLLEGE**  
**SRI ANANDPUR SAHIB**

*An Autonomous College*

*Affiliated to Punjabi University Patiala*



**Project FILE**

**OF**

**PHP**

**Art Gallery Management System**

*Session - May 2024*

**SUBMITTED TO:**

**Prof. Ramandeep Kaur**

**P.G. Dept. of Computer Science**

**SUBMITTED BY:**

**Harsimran Kaur (14056)**

**Harpreet Kaur (14060)**

**Gagandeep (14061)**

**BSc (Hon's) AI&DS-III**



**SRI GURU TEG BAHADUR KHALSA  
COLLEGE**

**SRI ANANDPUR SAHIB**

**An Autonomous College**



**Affiliated To Punjabi University, Patiala**

**Web Development Using PHP**

**SESSION 2023-24**

Submitted To : Ramandeep Kaur *Ramandeep Kaur*

Submitted By: Siya Sharma (14058) *Siya Sharma*

Manan Mohindroo (14088) *Manan Mohindroo*

Durgeshwar Rana (14082) *Durgeshwar Rana*

Nikhil Agyal (14078) *Nikhil Agyal*

Class B.Sc (Hons) AI & DS Sem 6<sup>th</sup>

**SRI GURU TEG BAHADUR KHALSA COLLEGE**  
**SRI ANANDPUR SAHIB**

*An Autonomous College*

*Affiliated to Punjabi University Patiala*



(2023-2024)

**PROJECT FILE**  
**OF**  
**EMPLOYEE DATABASE AND PAYROLL MANAGAMENT SYSTEM**

**SUBMITTED TO:**

Prof. Ramandeep Kaur *RKaur*  
P.G. Dept. of Computer Science

**SUBMITTED BY:**

Manish(14092) *Manish*  
Narinder Singh(14087) *Narinder Singh*  
Rahul(14071) *Rahul*  
B.Sc (Hon's) AI&DS Sem:6<sup>th</sup>

**SRI GURU TEG BAHADUR KHALSA COLLEGE**

**SRI ANANDPUR SAHIB**

*An Autonomous College*

*Affiliated to Punjabi University Patiala*



**PROJECT FILE**

**OF PHP**

**LIBRARY MANAGEMENT SYSTEM**

*Session - May 2024*

**SUBMITTED TO:**

*Prof. Ramandeep Kaur*

*P.G. Dept. of Computer Science*

**SUBMITTED BY:**

*Dilpreet Kaur*

*BSc (Hon's) AI&DS, Sem:6th*

*University Roll No.- 14089*



**SRI GURU TEG BAHADUR KHALSA COLLEGE**

**SRI ANANDPUR SAHIB**

*An Autonomous College*

*Affiliated to Punjabi University Patiala*



**PROJECT FILE  
OF PHP**

**LIBRARY MANAGEMENT SYSTEM**

*Session - May 2024*

**SUBMITTED TO:**

**Prof. Ramandeep Kaur** *Ramandeep Kaur*

**P.G. Dept. of Computer Science**

**SUBMITTED BY:**

**Aarti Devi** *Aarti Devi*

**BSc (Hon's) AI&DS, Sem:6th**

**University Roll No. - 14090**

# SRI GURU TEG BAHADUR KHALSA COLLEGE

SRI ANANDPUR SAHIB

**An Autonomous College**



**Affiliated to Punjabi University, Patiala**

**Web Development Using PHP**

**SESSION 2023-24**

Submitted To: Ramandeep Kaur *Ramandeep Kaur*

Submitted By: Nitin Sharma (14079) *Nitin Sharma*

Ramandeep Singh (14081) *Ramandeep Singh*

Prince (14091) *Prince*

Devinder Thakur (14076) *Devinder Thakur*

Dilpreet Singh (14085) *Dilpreet Singh*

Class: B.Sc (Hons) AI & DS Sem 6<sup>TH</sup>

**SRI GURU TEG BAHADUR KHALSA  
COLLEGE**

**SRI ANANDPUR SAHIB**

**An Autonomous College**



**Affiliated To Punjabi University, Patiala**

**Web Development Using PHP**

**SESSION 2023-24**

Submitted To : Ramandeep Kaur *RKaur*

Submitted By: Muskan Sabharwal (14054) *Muskan Sabharwal*

Ansh Sharma (14086) *Ansh Sharma*

Jasveer Singh (14075) *Jasveer Singh*

Puneet Dhiman (14074) *Puneet Dhiman*

Class: B.Sc (Hons) AI & DS Sem 6<sup>th</sup>



**SRI GURU TEG BAHADUR KHALSA COLLEGE**

**SRI ANANDPUR SAHIB**

**AN AUTONOMOUS COLLEGE**



**PROJECT REPORT**

**SUBMITTED TO:**

PROF. RAMANDEEP KAUR *RKaur*  
(PG DEPT. COMPUTER SCIENCE)

**SUBMITTED BY:**

AVNISH RAI (14067) *Avnish Rai*  
VIKAS DOGRA (14073) *Vikas Dogra*  
**CLASS:** B.SC.(H) AI& DS  
**SEM-6TH**

**SRI GURU TEG BAHADUR KHALSA COLLEGE**  
**SRI ANANDPUR SAHIB**  
*An Autonomous College*  
Affiliated to Punjabi University Patiala



**PROJECT FILE**

**OF**  
**PHP on AJ Fit**

**SUBMITTED TO:**

**Prof. Ramandeep Kaur**

*RKaur*

**P.G. Dept. of Computer Science**

**SUBMITTED BY:**

*Armanpreet Singh Jaspreet*  
**Armanpreet Singh, Jaspreet,**

**Jagwinder Singh** *Jagwinder Singh*

**Uni. Roll no. 14069,14093,14072**

**BSc. (Hons) AI & DS (Sem-6th)**

**SRI GURU TEG BAHADUR KHALSA COLLEGE**  
**SRI ANANDPUR SAHIB**  
*An Autonomous College*  
Affiliated to Punjabi University Patiala



**PROJECT FILE**

**OF**

*PHP on website for coffee*

**SUBMITTED TO:**

**Prof. Ramandeep Kaur** *PKaur*  
**P.G. Dept. of Computer Science**

**SUBMITTED BY:**

*Davinder Singh Dilpreet Singh*  
**Davinder Singh, Dilpreet Singh**  
**Uni. Roll no. 14077,14066**  
**BSc. (Hons) AI & DS (Sem-6)**



**SRI GURU TEG BAHADUR KHALSA COLLEGE,  
SRIANANDPUR SAHIB,**

**(AN AUTONOMOUS COLLEGE)  
Affiliated to Punjabi University Patiala**



**2023-24**

**Project of PHP  
Trending Fashion**

**Submitted To :**

**Prof. Ramandep kaur**

*Rkaur*

**Submitted By:**

**Harsimran Kaur (4357)** *Harsimran Kaur*

**Gurpreet Kaur (4367)** *Gurpreet Kaur*

**Mandeep Kaur (4361)** *Mandeep Kaur*

**Dilkar Singh (4382)** *Dilkar Singh*

**Amritdeep Singh (4375)** *Amritdeep Singh*

**Class B.voc (SD)sem 4th**

A  
MINOR PROJECT REPORT BASED ON PHP  
Car Rental System

SUBMITTED TO:

(PUNJABI UNIVERSITY, PATIALA)



SUBMITTED TO:

Prof. RAMANDEEP KAUR

(Assistant Professor)

(PG Department of

Computer Science)

SUBMITTED BY:

JASKARAN SINGH B.Voc SD IV (4383)

ANSHDEEP B.Voc SD IV (4392)

SANEHPREET SINGH B.Voc SD IV (4387)

KARTIK B.Voc SD IV (4388)

SRI GURU TEG BAHADUR KHALSA COLLEGE

SRI ANANDPUR SAHIB

(An Autonomous College)

# SRI GURU TEG BAHADUR KHALSA COLLEGE

SRI ANANDPUR SAHIB  
(AN AUTONOMOUS COLLEGE)  
Affiliated to Punjabi University Patiala



(2023-24)

## PROJECT FILE OF SCOPIE'S CAFFE

Submitted To:-  
Prof. Ramandeep Kaur

*R Kaur*

Submitted By:-

Jasmeen Kaur (4360)

Rajdeep Kaur (4359)

Simranjeet Kaur (4351)

B.Voc (SD) Sem IV



# SRI GURU TEG BAHADUR KHALSA COLLEGE

SHRI ANADPUR SAHIB

(AN AUTONOMOUS COLLEGE)

Affiliated to Punjabi University Patiala



## PROJECT FILE

OF

"Travel Freeks" a travel company

Session- May, 2024

### SUBMITTED TO:-

Prof. Ramandeep kaur *Ramandeep*  
Department of computer science

### SUBMITTED BY:-

Ruhani (4353) *Ruhani*  
Prianshu Sharma *Prianshu Sharma*  
(4390)  
B.voc (SD) sem-IV

# SRI GURU TEG BAHADUR KHALSA COLLEGE

SRI ANANDPUR SAHIB  
(AN AUTONOMOUS COLLEGE)  
Affiliated to Punjabi University Patiala



(2023-24)

## PROJECT FILE OF RESTAURANT

Submitted To:-

Prof. Ramandeep Kaur *R. Kaur*  
PG Dept. Of Computer Sci.

Submitted By:-

Dilpreet Kaur (4356) *Dilpreet Kaur*  
Jashanpreet Kaur (4373) *Jashanpreet Kaur*  
Sukhchitinder Kaur (4368) *Sukhchitinder Kaur*  
B.voc (SD) Sem IV

# SRI GURU TEG BAHADUR KHALSA COLLEGE

SRI ANANDPUR SAHIB  
(AN AUTONOMOUS COLLEGE)  
Affiliated to Punjabi University Patiala



(2023-24)

## PROJECT FILE OF FAMOUS TOUR PLACES IN INDIA

Submitted To:-  
Prof. Ramandeep Kaur  
PG Dept. Of Computer Sci.

*RKaur*

Submitted By:-  
Priya (4352) - *Priya*  
Navneet Kaur (4354) *Navneet Kaur*  
B.voc (SD) Sem IV



**SRI GURU TEG BAHADUR KHALSA COLLEGE**  
**SRI ANANDPUR SAHIB**  
**AN AUTONOMOUS COLLEGE**



**Project File of**  
**Clothing Store**

Submitted To:

Prof. Ramandeep Kaur

*Rxaur*

Submitted By:

Jaswinder Singh (4384) *Jaswinder Singh*

Manpreet Singh (4380) *Manpreet Singh*

Jaspreet Singh (4376) *Jaspreet Singh*

Gagandeep Singh (4386) *Gagandeep Singh*

B.Voc(SD) Sem-4th

**SRI GURU TEG BAHADUR KHALSA COLLEGE**

**SRI ANANDPUR SAHIB**

**(AN AUTONOMOUS COLLEGE)**



**2023-24**

**PROJECT FILE OF PHP**

**SUBMITTED TO:**

**PROF. Ramandeep Kaur**

*RKaur*

**SUBMITTED BY:**

**NAME: Harkirtan Singh (4375)** *Harkirtan Singh*

**Jaspreet Kaur (4364)** *Jaspreet Kaur*

**CLASS: B.voc (Sd) 2<sup>nd</sup> Sem-4<sup>th</sup>**



# SRI GURU TEG BAHADUR KHALSA COLLEGE

SRI ANANDPUR SAHIB  
(AN AUTONOMOUS COLLEGE)  
Affiliated to Punjabi University Patiala



(2023-24)

## PROJECT FILE OF GROCERY MANAGEMENT SYSTEM

Submitted To:-  
Prof. Ramandeep Kaur

Submitted By:-

Hardeep Kaur *Hardeep Kaur*

B.Voc (SD) Sem- IV

Uni. Roll No-4370



Sri Guru Teg Bahadur Khalsa College  
Sri Anandpur Sahib  
( An Autonomous college)



PROJECT FILE USING PHP AND MYSQL  
(Based on Online Grocery Store)

Submitted To:  
Prof. Rajwinder Kaur  
(PG Department of Com. Sci.)

Submitted by:  
Amandeep Kaur(13935)  
Harpreet Kaur (13936)  
Harpreet Kaur (13938)  
Mandeep Kaur(13939)  
Amanjot Kaur(13964)  
Simranpreet Kaur(14025)  
Class: BCA 6<sup>th</sup> Sem

# SGTB KHALSA COLLEGE SRI ANANDPUR SAHIB



## Project Report

On

## PHP & MySQL

(COMPANY- Vanced solutions pvt. Ltd.)

Submitted as a part of course curricula for


**Prof. Rajwinder Kaur**

in

Bachelor of Computer Science

Under the guidance of

Submitted to:

  
Asst. Prof. Rajwinder Kaur  
( PG department of computer science)

Submitted by:

Rajwinder kaur(13924)  
Naveen(13979)  
Sanjana(13915)  
Arshdeep(13975)  
Inderjeet(13954)

**SRI GURU TEG BAHADUR KHALSA COLLEGE  
SRI ANANDPUR SAHIB  
AN AUTONOMOUS COLLEGE**



**A PRACTICAL FILE IN THE PARTIAL FULFILMENT OF THE  
REQUIREMENTS FOR THE AWARD OF DEGREE OF  
BACHELOR'S OF COMPUTER APPLICATIONS**

**BCA - 316 : MAJOR PROJECT - Registration Form**

**SUBMITTED TO**

Prof. Rajwinder Kaur

P. G. department of Computer science

**SUBMITTED BY**

Bharti(13919)

Harpreet(14010)

Nrinder(13995)



**SRI GURU TEG BAHADUR KHALSA COLLEGE  
SRI ANANDPUR SAHIB  
AN AUTONOMOUS COLLEGE**



A PRACTICAL FILE IN THE PARTIAL FULFILMENT OF THE  
REQUIREMENTS FOR THE AWARD OF DEGREE OF  
BACHELOR'S OF COMPUTER APPLICATIONS

**BCA - 316 : MAJOR PROJECT - Registration Form**

**SUBMITTED TO**

*R. Kaur*  
Prof. Rajwinder Kaur

P. G. department of Computer science

**SUBMITTED BY**

Neha(13956)

Natasha(13948)

Reetika(13957)

Babeeta(14037)

Baljeet(13958)

Jaspreet Kaur(13970)

# SRI GURU TEG BAHADUR KHALSA COLLEGE

SRI ANANDPUR SAHIB  
(AN AUTONOMOUS COLLEGE)  
Affiliated to Punjabi University Patiala



(2023-24)

## MAJOR PROJECT ON COFFEE

Submitted To: *Rajwinder Kaur*  
Prof. Rajwinder Kaur  
PG Dept. Of Computer Sci.

Submitted By:-  
Varinder Singh (13980)  
Aarti (13951)  
Diksha (13960)  
Simranjeet Kaur(13959)  
HarsimranKaur(14038)  
B.C.A – III (Sem- VI)

**Sri Guru Teg Bahadur Khalsa College**  
**Sri Anandpur Sahib**  
**(An Autonomous college)**



SESSION: 2023-24

**BCA-316: MAJOR PROJECT-**  
**CREATE PROJECT ON**  
**RESTAURANT WEBSITE**

Submitted To:

Asst. Prof. *Rajwinder Kaur*  
(PG department of computer science)

Submitted By:

Rajni (13963)  
Harmandeep Kaur (13955)  
Kamaljeet Kaur (13952)  
Anjali Sharma (13953)



**SRI GURU TEG BAHADUR KHALSA COLLEGE**

**SRI ANANDPUR SAHIB**



**PROJECT FILE**

**HOTEL MANAGEMENT**

**SESSION: MAY 2024**

**SUBMITTED TO:**

**PROF. RAJWINDER KAUR**

**SUBMITTED BY:**

**ISHA SAINI(13909)**

**ANKITA SHARMA(13942)**

**SIMRAN RANA(13968)**

**HARSIMRAN KAUR(13965)**

**RAM KAUR(13961)**

**BCA SEM-6<sup>TH</sup>**

**Sri Guru Teg Bahadur Khalsa College**  
**Sri Anandpur Sahib**  
**(An Autonomous college)**



SESSION: 2023-24

**BCA-316: MAJOR PROJECT-**  
**CREATE PROJECT ON**  
**FASHION WEBSITE**

Submitted To:

Asst. Prof. *Rajwinder Kaur*

(PG department of computer science)

Submitted By:

Randeep Kaur (13904)

Pardeep Kaur (13907)

Tanvi Saini (13902)

Indu Saini (13925)



# **SGTB Khalsa College Sri Anandpur Sahib**

## **Project Report**

### **COLLEGE WEBSITE**

Submitted as a part of course curricula for

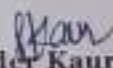
**Prof. Rajwinder Kaur**

in

Bachelor of Computer Science

Under the guidance of

**Submitted To :**

Prof.   
Rajwinder Kaur  
(Department of Computer Science)

**Submitted By :**

Vanshika(13947)  
Simran Rani (13949)  
Tamana Sharma(13946)  
Manvir Kaur (13934)  
Deepali (13940)  
Gurleen (13941)



# SRI GURU TEG BAHADUR KHALSA COLLEGE

SRI ANANDPUR SAHIB  
(AN AUTONOMOUS COLLEGE)  
Affiliated to Punjabi University Patiala



(2023-24)

## MAJOR PROJECT ON RESTURTANT

Submitted To:-  
Prof. Rajwinder Kaur  
PG Dept. Of Computer Sci.

Submitted By:-  
Anshul Sharma(14002)  
Dheeraj Bharwdwaj (14003)  
Himanshu Sanan(14000)  
B.C.A – III (Sem- VI)

**Sri Guru Teg Bahadur Khalsa College**  
**Sri Anandpur Sahib**  
**(An Autonomous college)**



SESSION: 2023-24

**BCA-316: MAJOR PROJECT-**  
**CREATE PROJECT ON**  
**FOOD ORDERING WEBSITE**

Submitted To:

Asst. Prof. Rajwinder Kaur  
(PG department of computer science)

Submitted By:

Jaswinder singh (13974)  
Harjeet Singh (13976)  
Sahil Kumar (13981)  
Paryag duvedi (13987)  
Harpal Singh (13991)

**SRI GURU TEG BAHADUR KHALSA COLLEGE  
SRI ANANDPUR SAHIB  
AN AUTONOMOUS COLLEGE**



**PRACTICAL file  
OF  
Art Gallery Management System  
Project in PHP**

**SUBMITTED TO**

Prof. Rajwinder Kaur

P. G. department of Computer science

**SUBMITTED BY**

Harmanpreet Singh, Arshnoor Singh, Abhinav





# **SGTB Khalsa College Sri Anandpur Sahib**

## **Project Report**

On

### **Burger King WEBSITE**

Submitted as a part of course curricular for

**Prof. Rajwinder Kaur**

in

Bachelor of Computer Science

Under the guidance of

**Submitted to:**

Asst.Prof. <sup>RKaur</sup>Rajwinder Kaur

(PG Department of Computer Science)

**Submitted by:**

Shivangi, Diksha, Arti

# **SRI GURU TEG BAHADUR KHALSA COLLEGE**

**SRI ANANDPUR SAHIB**  
**(AN AUTONOMOUS COLLEGE)**  
Affiliated to Punjabi University Patiala



**(2023-24)**

## **MAJOR PROJECT OF JUJUTSU KAISEN PRODUCTS**

**Submitted To:-**  
Prof. Rajwinder Kaur  
PG Dept. Of Computer Sci.

**Submitted By:-**  
Tanveer Singh (14028)  
Harmanpreet Singh(14009)  
Fateh Singh (14019)  
Devansh Chandel (14015)  
Deepak Rana (14013)  
B.C.A – III (Sem- VI)

**SRI GURU TEG BAHADUR KHALSA COLLEGE SRI ANANDPUR**  
**SAHIB AN AUTONOMOUS COLLEGE**



**PROJECT REPORT**

**ON**

**Bank Locker Management System**

Submitted as a part of course curricula for

Prof. Rajwinder Kaur

In

Bachelor of computer Science

Under the guidance of

Submitted to:

Asst.Prof. *Rajwinder Kaur*

Submitted by:

*Anushka, Komal,  
Amanjot, Lalita, Harpreet*

Roll No. *3901, 908, 910,  
926, 931*



**SRI GURU TEG BAHADUR KHALSA COLLEGE SRI ANANDPUR**  
**SAHIB AN AUTONOMOUS COLLEGE**



**PROJECT REPORT**

**ON**

**Bank Locker Management System**

Submitted as a part of course curricula for

Prof. Rajwinder Kaur

**In**

**Bachelor of computer Science**

**Under the guidance of**

Submitted to:

Asst.Prof.Rajwinder Kaur

Submitted by:

Harjinder ,Swapana

Raman,Manisha,Siya

Roll No<sup>13921</sup>...,13927, 13906  
13989, 13917

# SRI GURU TEG BAHADUR KHALSA COLLEGE

SRI ANANDPUR SAHIB  
(AN AUTONOMOUS COLLEGE)  
Affiliated to Punjabi University Patiala



(2023-24)

## MAJOR PROJECT OF DEMON SLAYER PROJECT

Submitted To:-  
Prof. Rajwinder Kaur  
PG Dept. Of Computer Sci.

Submitted By:-  
Amritpal Singh (14018)  
Amandeep (14017)  
Parchant Bhatia (14005)  
Navjot Singh (14021)  
B.C.A – III (Sem- VI)



# **SGTB Khalsa College Sri Anandpur Sahib**

## **Project Report**

On

### **Data of college students**

Submitted as a part of course curricular for

**Prof. Rajwinder Kaur**

in

Bachelor of Computer applications

Under the guidance of

Submitted to:

Asst.Prof. Rajwinder Kaur

Submitted by:

Dishant kumar (13985)

Hitesh kumar (14026)

Abhishek sharma (13984)

Aman deep soni (13986)

Nikhil (13992)

(PG Department of Computer Science )



**Sri Guru Teg Bahadur Khalsa College**  
**Sri Anandpur Sahib**  
**(An Autonomous college)**



2023-24

BCA -316

Major project on KFC

Submitted To:

Asst. Prof. *Rajwinder Kaur*

(PG Department of Com. Sci.)

Submitted By:

Aniket (13972)

Manpreet kaur (13911)

Sneha (13918)

Abhishek (13982)

Shivam (14029)

**Sri Guru Teg Bahadur Khalsa College**  
**Sri Anandpur Sahib**  
**(An Autonomous college)**



SESSION: 2023-24

**Project Report**

On

**Library Management System**

Submitted as a part of course curricula for

**Prof. Rajwinder Kaur**

In

Bachelor of computer Science

Under the guidance of

**Submitted To:**

**Asst. Prof. Rajwinder Kaur**

(PG department of computer science)

**Submitted By:**

**Satwinder kaur (13905)**

**Harwinder Kaur (13914)**

# SGTB KHALSA COLLEGE SRI ANANDPUR SAHIB



## Project Report

On

## PHP & MySQL

(Library Management System)

Submitted as a part of course curricula for

*Ran*  
**Prof. Rajwinder Kaur**

in

Bachelor of Computer Science

Under the guidance of

Submitted to:

Asst.Prof. Rajwinder Kaur  
( PG department of computer science)

Submitted by:

Amandeep Kaur(13928)  
Soma Devi (13930)  
Manpreet Kaur(13903)  
Simardeep Singh(13978)  
Jashandeep Singh(13973)



**Sri Guru Teg Bahadur Khalsa College**  
**Sri Anandpur Sahib**  
**(An Autonomous college)**



2023-24

**PROJECT FILE**

**ON**

**ART GALLERY MANAGEMENT SYSTEMN USING PHP AND  
MYSQL**

Submitted To:

Asst. Prof. Rajvinder Kaur

(PG Department of Com. Sci.)

Submitted By:

Sukhjeet Singh(14031)

Harpavneet Singh (14036)

Mohit Saini( 14022)

Hardeep Singh (13999)

Dharampreet Singh(14027)

**SRI GURU TEG BAHADUR KHALSA COLLEGE**  
**SRI ANANDPUR SAHIB**  
**(AN AUTONOMOUS COLLEGE)**



**PROJECT FILE ON WEB DEVELOPMENT USING**  
**PHP AND MYSQL**  
**SESSION 2021-22**

**SUBMITTED TO:-**

*R. Kaur*  
**Prof. Rajwinder Kaur**  
**Department of Computer Science**

**SUBMITTED BY :-**

**Name -Bharti Rani**  
**Himani Sharma**  
**Class: B.C.A 6<sup>TH</sup> Sem**  
**Roll No - 13923, 13916**

**SRI GURU TEG BAHADUR KHALSA COLLEGE**  
**SRI ANANDPUR SAHIB**  
**An Autonomous College**



**Affiliated to Punjabi University, Patiala**  
**NLP Project FILE**  
**ON**  
**TEXT SUMMARIZATION**  
**UNDERDATA ANALYSIS USING PYTHON**  
**SESSION 2023-24**

**\*SUBMITTED TO:**

**PROF.GAGANDEEP SINGH**

**PG. DEPT. OF COMPUTER SCIENCE**

**SUBMITTED BY:**

**SUKHBINDER KAUR,**

**AARTI**  
**RAJVEER SINGH**  
**MSC AI & DS SEM 4<sup>TH</sup>**  
**Roll no: 5751, 5755, 5760**



**SRI GURU TEG BAHADUR KHALSA COLLEGE**  
**SRI ANANDPUR SAHIB**  
**An Autonomous College**



**Affiliated to Punjabi University, Patiala**  
**Project on Sentiment Analysis**  
**Of Indian Elections**  
**SESSION 2023-24**

SUBMITTED TO:  
*Gagan*  
PROF. GAGANDEEP SINGH  
PG DEPT. OF COMPUTER  
SCIENCE

SUBMITTED BY:  
VANDANA KUMARI,5754  
SIMRANJEET KAUR,5752  
NATASHA SEHGAL,5758  
MSC AI & DS SEM 4<sup>th</sup>

**SRI GURU TEG BAHADUR KHALSA COLLEGE**  
**SRI ANANDPUR SAHIB**  
**An Autonomous College**



**Affiliated to Punjabi University, Patiala**  
**NLP Project FILE**  
**ON**  
**TEXT CLASSIFICATION**  
**UNDER DATA ANALYSIS USING PYTHON**  
**SESSION 2023-24**

SUBMITTED TO:  
PROF. GAGANDEEP SINGH  
PG.DEPT. OF COMPUTER  
SCIENCE

SUBMITTED BY:  
MAMTA DEVI  
ROLL NO. 5756  
PARMINDER KAUR  
ROLL NO. 5753

# **DERIVATIVE AND APPLICATION OF DERIVATIVES**

Project report submitted to  
**Sri Guru Teg Bahadur Khalsa college**  
For the award of the degree  
of  
**Bachelors of science**  
by

**Simaran, Harsimran, Shruti**

Under the guidance of  
**Dr. Mandeep Kaur**



**Department of Mathematics**  
**Sri Guru Teg Bahadur Khalsa College**  
**Sri Anandpur Sahib**



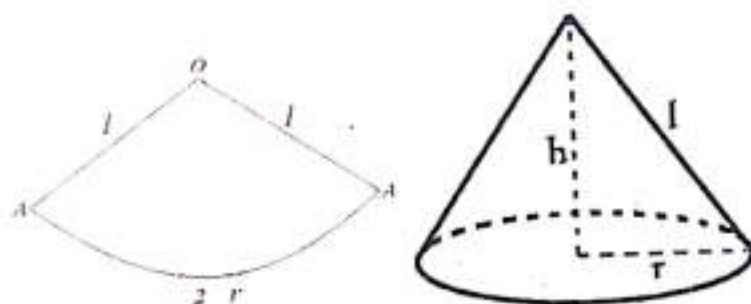
# CONTENTS

Sr no.	Title
1.	Introduction
2.	Preliminary
3.	Chapter 1- Derivatives
4.	Chapter 2- Application of derivatives
5.	Conclusion
6.	Bibliography

Sri Guru Teg Bahadur Khalsa College,

Sri Anandpur Sahib

Topic: Curves and Surfaces



$$\text{Slant height } l = \sqrt{r^2 + h^2}$$

$$\text{Volume } V = \frac{1}{3} \pi r^2 h$$

$$\text{Curved surface area CSA} = \pi r l$$

Submitted To -Prof. Jaspreet Kaur

Submitted by -Jatinder Singh & Dhruv Sharma

Class : Bsc. Non Med , BSc Honors Mathematics sem 3

Roll number: 210607,213535

Session 2023-2024

## Projects for Mathematics Students

### Curves and surfaces

#### Prerequisites:

Programming skills in C, ability to use a standard function library, and mathematics skills to understand simple functions and their graphs

#### Graphics to be learned from these projects:

Defining an image using viewing projections and an eye point; use of graphics primitives and transformations for modeling; rendering features of a graphics API such as lighting and transparency; various callbacks and interactions that control changes in both modeling and rendering; the use of capabilities such as clipping and alpha blending in rendering images.

The projects we have developed for mathematics students in the first computer graphics course focus around curves and surfaces based on various formulas. These give students a chance to become more familiar with some standard kinds of shapes and to build their intuition about how functions work.

One of the interesting opportunities for mathematical explorations is to consider surfaces that have singularities or discontinuities in the domain being examined. The display of these functions will not itself have any of these, but it should be possible to find places where they would occur.

Surfaces may be graphs of a real-valued function of two variables, or they may arise from other processes that work on a two-dimensional domain. Real functions of two variables are common in multivariate calculus and in actual applications; you will find examples in the set of physics projects, for example. Parametric surfaces are created by functions from real two-space into real three-space. They can define surfaces with more complex behaviors, such as multiple sheets, as shown in Figure 3, as well as surfaces such as the torus. This is the source of another kind of graphics project in which the student is asked to display a surface defined by parametric functions of two variables: one for each of the three coordinates in the 3-space that will contain the surface. It may even be possible for some classes to examine higher-dimensional surfaces through functions from a two-dimensional domain into higher-dimensional space, with the displayed surface being projected down into three-space for viewing.

Surfaces are plotted as illustrated in Figure 1 by creating a grid on a rectangular domain in two-space and applying a function or functions to the points in the grid to determine points in three-space. This figure illustrates the fundamental principal for surfaces that are given by a function of two variables; it shows a coarse grid on the domain (a 6x6 grid instead of 125x125) for the actual surface in Figure 2 so you may see the underlying grid and the relationship of the function's value to the surface more clearly. Those points are used to determine rectangles in three-space that can be displayed with standard OpenGL functions. The gridded surfaces we create in this way are only approximations of the real surfaces, of course, and it will be instructive to the students to consider what happens when they try to work with functions whose surfaces includes discontinuities of various kinds.

Parametric surfaces are plotted in much this same way, but they are slightly more difficult for the student to grasp because they do not have the close relationship between the domain grid and the surface components shown in the figure. Some motivating examples may help students understand how the function surface process extends to parametric surfaces.



# **GRAPH COLORING**

**Project report  
(Under DBT)**

**Submitted by**

**Kriti Devi (213524)**

**Rinkal Bala(213526)**

**Submitted to**

**Prof. Pallvi**

**Department of Mathematics**

**Sri Guru Teg Bahadur Khalsa College**

**Sri Anandpur Sahib**

## CONTENTS

Sl no.	Title	Page No.
01	Introduction	1
02	Basic Concepts	2
03	Chapter 1-Coloring	3 – 6
04	Chapter 2-Chromatic Number	7 – 16
05	Chapter 3-Applications Of Graph Colouring	17 – 19
06	Conclusion	20
07	Bibliography	21

# **PLANARITY IN GRAPH THEORY**

**Project report  
(Under DBT)**

**Submitted by**

**Khushi (213527)**

**Gauri (213525)**

**Submitted to**

**Prof. Kamaljeet Kaur**

**Department of Mathematics**

**Sri Guru Teg Bahadur Khalsa College**

**Sri Anandpur Sahib**



## CONTENTS

Sl No	Title	Page No
1	Introduction	1
2	Chapter 1 - Basic Concepts	2 - 9
3	Chapter 2 – Planar Graph	10 - 17
4	Chapter 3 – Euler's Formula	18 – 19
5	Chapter 4 – Dual of a Plane Graph	20
6	Conclusion	21
7	Bibliography	22

# **EFFECT OF AN AQUEOUS EXTRACT FROM *MURRAYA KOENIGII* AGAINST THE WHEAT STORAGE PEST, *TRIBOLIUM CASTANEUM***

A Dissertation submitted to  
Sri Guru Teg Bahadar Khalsa College, Sri Anandpur Sahib, Punjab  
In Partial fulfillment of the requirement  
For the award of the Degree of

**MASTER OF SCIENCE  
IN  
ZOOLOGY**

Submitted By  
**LATASHA**  
ROLL NO. 4972



**SRI GURU TEG BAHADAR KHALSA COLLEGE, SRI ANANDPUR SAHIB, PUNJAB, INDIA**  
(AN AUTONOMOUS COLLEGE)  
(Affiliated to [Punjabi University, Patiala, Punjab](#))  
[Session: 2023-2024](#)

### **CERTIFICATE-I**

This is to be certified that this dissertation entitled “**Effect of an aqueous extract from *Murraya koenigii* against the wheat storage pest, *Tribolium castaneum***” submitted by Latash in partial fulfilment of the requirement for the award of degree of **Master of Science in Zoology**, is a bonafide research work carried by her under my supervision during fourth semester of **Academic Year 2023-24**. No part of this work has been published / carried for any other degree or diploma.

**Dr. Amandeep Kaur**  
Supervisor  
Assistant Professor & Head  
PG Department of Zoology  
Sri Guru Teg Bahadar Khalsa College  
Sri Anandpur Sahib



## **CERTIFICATE-2**

This is to be certified that the dissertation entitled “**Effect of an aqueous extract from *Murraya koenigii* against the wheat storage pest, *Tribolium castaneum***” Submitted to Sri Guru Teg Bahadar Khalsa College, Sri Anandpur Sahib, Affiliated to Punjabi University, Patiala in the partial fulfillment of the degree of **Master of Science in Zoology** has been jointly evaluated by us.

**External Examiner**

**Head of the Department**

PG Department of Zoology

Sri Guru Teg Bahadar Khalsa College, Sri Anandpur Sahib

## **ACKNOWLEDGEMENT**

*First of all, I offer my humble thanks with folded hands and bowed head to the “**Almighty**” Lord for his grace, kindness and blessings due to which I have been able to accomplish this important task of my life.*

*I feel proud being a student of SGTB Khalsa College, Sri Anandpur Sahib and at the same time, I acknowledge the help provided by the PG Department of Zoology.*

*Though the debt of learning cannot be repaid, it is my sovereign privilege to express my gratitude and moral obligation to my esteemed Major Advisor, **Dr. Amandeep Kaur**, Assistant Professor and HOD, Department of Zoology for her enlightened, invaluable and inspiring guidance. I shall remain ever indebted for her care and affection during the course of research as well as in the preparation of this manuscript. Her multifaceted personality and commitment to work motivated and encouraged me to work, even harder and hence developed right attitude not only for my research work but also as a managed human being.*

*In my opinion, God would not be everywhere, therefore, he made loving parents. A formal acknowledgement of my emotions is inadequate to convey the depth of my feelings of gratitude to my loving parents. I am forever indebted to my parents for their understanding, endless patience and encouragement when it was most required and for providing me the means to learn and understand.*

*I have been fortunate to come across my good friends without whom life would be bleak. I am happy to acknowledge the shadow support and moral upliftment showered upon me by my friends.*

*Last but not the least, I duly acknowledge my sincere thanks to all those who love and care for me. Every name may not be mentioned but none is forgotten.*

**Date:**

**Place: Anandpur Sahib**

**(LATASHA)**

**Title of the Dissertation** : Effect of an aqueous extract from *Murraya koenigii* against the wheat storage pest, *Tribolium castaneum*

**Name of the Student and Roll No.** : Latasha (4972)

**Major Subject** : Zoology

**Name and Designation of Major Advisor** : Dr. Amandeep Kaur  
Assistant Professor and HOD

**Degree to be Awarded** : M.Sc.

**Year of award of Degree** : 2024

**Total Pages in Dissertation** : 45

**Name of College** : Sri Guru Teg Bahadur Khalsa College, Sri Anandpur Sahib-140118  
Punjab, India

### ABSTRACT

Pest attack is the major cause that leads to the reduced productivity of field crops and stored grains. Insecticides and pesticides are applied to crops and stored grains in an effort to decrease the economic losses. In addition to control an insect or pest, these chemicals also possess some negative impacts on humans. In view of these considerations the assaying for toxicity of aqueous extract of *Murraya koenigii* was initiated. Data obtained for adulticidal, larvicidal, residual efficacy and repellency effect of aqueous extracts against *T. castaneum* was observed as with concentrations 2ppm>1.75ppm>1.50ppm>1.25ppm> 1ppm. The aqueous extract was found to be significantly effective in terms of all four parameters. The reason for the same could be the presence of phenolic compounds such as; Rutin, Quercetin-3-glycoside, Myrecetin, and Quercetin & some volatile compounds such as;  $\beta$ -Caryophyllene,  $\alpha$ -cedrene,  $\alpha$ -copaene,  $\beta$ -cubebene, and germacrene D which may exhibit insecticidal properties against the *T. castaneum*. These observations could be the first step towards exploring possibilities of usefulness of chosen plant on commercial basis, as a source of organic insecticides against *T. castaneum*.

**Key words:** Extract, Economic loss, Insecticides, Pest, Plant

---

Signature of Major Advisor

---

Signature of the Student



## CONTENTS

CHAPTER	TITLE	PAGE NO.
I	INTRODUCTION	8-11
II	REVIEW OF LITERATURE	12-22
III	MATERIALS AND METHODS	23-28
IV	RESULTS AND DISCUSSION	29-37
V	SUMMARY	38-39
VI	REFERENCES	40-45

## LIST OF TABLES

TABLE NO.	TITLE	PAGE
1	Toxicity of aqueous extract against Adults of <i>Tribolium castaneum</i>	29
2	Toxicity of aqueous extract against Larvae of <i>T. castaneum</i>	30
3	Repellency Data of Aqueous extract against adults of <i>T. castaneum</i>	31
4	Repellency percentage of aqueous extract against adults of <i>T. castaneum</i>	31
5	Residual toxicity: Mean Mortality of <i>T.castaneum</i> by aqueous extract at various Hrs AT	32

## LIST OF FIGURES

FIGURE NO.	TITLE	PAGE
1	Toxicity of aqueous extract against Adults of <i>Tribolium castaneum</i>	29
2	Toxicity of aqueous extract against Larvae of <i>T. castaneum</i>	30
3	Repellency percentage of aqueous extract against adults of <i>T. castaneum</i>	32
4	Residual toxicity: Mean Mortality of <i>T.castaneum</i> by aqueous extract at various Hrs AT	33

## CHAPTER-I

### INTRODUCTION

Food security means to have a dependable and constant access for all people to an adequate supply of healthy food that satisfies their nutritional needs and preferences in order to lead active and healthy lives <sup>1</sup>. A prosperous nation requires a reliable access to food on daily basis. Food security is composed of three essential elements: food availability, food access, and food utilization. Hazards such as; Climate change, Increased population, and Pest attacks may affect the food availability and access.

Pest attack is the major cause that leads to the reduced productivity of field crops and stored grains. The word ‘Pest’ is derived from a Latin word ‘Pestis’ which means Plague. ‘Pest’ is defined as an insect or any other organism that causes damage to crops, stored products and animals. An insect reaches the status of a pest when its population increases to an extent that it causes a significant loss of economy. Pests cause major damage to stored seeds, pulses and cereal grains etc. Some pests attack and damage the cultivating crops while some feed upon the stored grains and contaminate them.

Storage insect pests are of two types; Primary storage pests (internal & external feeders) and Secondary storage pests (damage already damaged or broken grains). Some major primary storage pests are; Rice weevil (*Sitophilus oryzae*), lesser grain borer (*Rhyzopertha dominica*), Angoumois grain moth (*Sitotroga cerealella*), Pulse beetle (*Callosobruchus chinensis*), Tamarind beetle (*Pachymeres gonagra*), Sweet potato beetle (*Cylas formicarius*), Potato tuber moth (*Phthorimaea operculella*), Red flour beetle (*Tribolium castaneum*), Khapra beetle (*Trogoderma granarium*) etc. Major secondary storage pests are; Saw toothed grain beetle (*Oryzaephilus surinamensis*), Long headed flour beetle (*Latheticus oryzae*), Flat grain beetle (*Cryptolestus minutus*), Grain mite (*Acarus siro*), Rice moth (*Corcyra cephalonica*) etc.

Among all, *T. castaneum* causes the most damage to Cereal items such as; grain, flour, porridge oats, and rice bran etc. It is a cosmopolitan pest which is found worldwide. Temperature of 35°C and 60–80% relative humidity is considered ideal for the development of each stage of its life cycle. Life cycle of red flour beetle comprises of four major stages; Egg, Larva, Pupa, Adult. The females of *T. castaneum* produce about 300-400 eggs in 4-5 months of their life span. After about 3 days of egg laying, eggs hatch into larvae and feed upon flour during different instars.



After a number of molts, an inactive stage occurs which is known as Pupa. It does not show feeding and moving activity during this stage. Sometimes, the pupa forms a cocoon like structure around its body. The developing organism inside the cocoon undergoes certain changes in morphology. After a few molts, a completely viable and actively feeding adult emerges out. It is reported that approximately 5–15% of the total weight of all grains, oilseeds, and pulses is damaged by adult *T. castaneum*.<sup>2</sup> These can cause economic loss and may also lead to food scarcity. Pest status of *T. castaneum* as a stored grain and milled product of wheat has been well established. Information's regarding developmental stages and life history helps in manoeuvring infestation led by *T. castaneum* (Herbst). The adult insect is of tapering form, tiny, flat, reddish brown beetle with antennae ending in abrupt clubs. Adults and grub are active whole year and these stages cause damage. From eggs to adult stage is completed in 50 days. An adult female lays about 300 eggs in pits, cracks and crevices in the soil or in cavity in the grain. When eggs are freshly laid, they are very small and white in colour, but they become bright red before hatching. Hatching takes 3 to 8 days, more eggs hatch in low humidity than higher. The grub covered with fine hairs is yellowish white and it has six legs. The young caterpillar makes, it way into the grain through some crack or hole in it. Larval instars are six in number and larval period lasts for 21 -28 days. When it is fully developed, it starts pupating, at the expiry of 3 to 10 days, adult comes up. Adults are 3.5mm long and 1.2mm in width. A generation of this insect takes 80 to 125 days to cover life span subjected to the effect of climate. 4 to 7 generations of them may evolve in a year. These beetles have chewing mouth parts but do not bite or sting. It spends whole life outside the grain kernels. It has high reproductive potential and breed through the year in warm area. *T. castaneum* pest status is considered as secondary, requiring prior infestation by an internal feeder. Adults and larvae cause serious damage to stored grains. The larvae feeds upon endosperm of seed, leaving only the seed coat. The seed thus completely loses its viability as well as its nutritive value. So the grain is rendered unfit for human consumption. Larvae also produce a large quantity of whitish powdery excreta, which makes the grain more dusty and imparts an unpleasant smell. The use of insecticides is first line of defence in controlling the insect pests. Although, Insecticides and pesticides are applied to crops and stored grains in an effort to decrease the economic losses. A pesticide is defined as any substance or a mixture of a number of substances, expected to prevent, repel, destroy or mitigate a pest. Before 1947, few synthetic insecticides used in crop protection were stomach poisons based on

heavy metals such as lead and arsenic, which killed only if eaten, were known as first – generation insecticides. Some botanical extracts, such as rotenone and pyrethrum, both of which quickly degrade in the environment, were also used. After Second World War varieties of artificially synthesised compounds were recognised. These, were effective in killing insects by mere physical contact known as second- generation insecticides, beginning with DDT in 1947 and these often killed natural enemies more efficiently than they killed targeted pest, are known as wide spectrum insecticides. Generally chemical insecticides like malathion, fenitrothion, permethrin, deltamethrin, cypermethrin have been used as grain protectant for stored grain. These are hazardous, being toxic to the flora and fauna of the ecosystem and also leading to abiotic and biotic environmental pollution. Insecticide was entering in the food chains and bio-magnification took place at different trophic levels. They indirectly increased the cost of application, pest resurgence and ability to develop resistance to insecticides. In addition to control an insect or pest, these chemicals also possess some negative impacts on humans. These impacts include; skin irritability, irritation in eyes, painful breathing, and prolonged contact of pesticides may lead to death of human beings. Pesticides in water supplies also have negative impacts on ecosystem. According to good agricultural practices (GAP), a legally authorized maximum concentration of pesticide residue after its use is known as Maximum Residual Limit (MRL). It aims to observe and prevent any unacceptable harm to human health. This concentration is expressed in milligrams per kilograms (mg/kg). If a residual level crosses standards of MRL, the pesticide/insecticide is no more permitted to be sold, imported or exported. Hence, an alternative and healthy approach is required to prevent the postharvest losses and health hazards. Plant extracts are considered suitable for this purpose. A variety of plant-based extracts are utilized to combat insects that affect the stored grains, due to their insecticidal and fragrant repellent qualities. Plant extracts such as oil, methanol, ethanol & hexane extracts are used to control pest attacks in households. There is a wide variety of plants that possess repellent and insecticidal properties against the insect pests of stored grains. Plants include; *Azadirachta indica* (Neem), *Tamarindus indicus* (Tamarind), *Cucumis sativus* (cucumber), *Psidium guajava* (guava), *Artemisia vulgaris* (common mugwort), *Murraya koenigii* (curry leaves), *Prosopis juliflora* (kikar), *Matricaria chamomilla* (chamomile), *Solanum sisymbriifolium* (red buffalo- bur) etc. One of the plants that is significant both commercially and physiologically is *M. koenigii*. This plant belongs to Rutaceae family and it is indigenous to Sri Lanka, India, and other south

Asian countries. It is an edible, therapeutic and a good source of vitamins A, B, C, and vitamin E<sup>3-7</sup>. It is also known as "curry-leaf" tree worldwide and "Mitha Neem" in northern states of India. *M. koenigii* is an unarmed, semi-deciduous, aromatic shrub. It has glabrous, imparipinnate, highly scented leaves, a thin but robust wooden stem, and dark grey colored bark on branches. Leaflets are gland-dotted, alternating, short-stemmed, and highly aromatic, with nine to twenty-five or more. When leaves mature, they contain 63.2% moisture, 1.5% total nitrogen, 6.5% fat, 18.92% total sugars, 14.6% starch, 6.8% crude fiber, ash (13.16%), 1.35 % acid-insoluble ash, 1.82% alcohol-soluble extractive, 27.33% extractive at cold water (20°C), and a maximum of 33.45% extractive at hot water <sup>8</sup>. In former studies, insecticidal activities of plant extract of *M. koenigii* against *Bemisia tabaci*, *C. chinensis* is reported. The main objective of this research is to investigate the effect of an aq. extract of *M. koenigii* against the storage pest of wheat i.e., *T. castaneum*. This study may report about the significant repellent and insecticidal activities of this plant extract against red flour beetles and was conducted during 2024 with following objectives:

- (i) To study the toxicity of aqueous extract against Adults of *T. castaneum*
- (ii) To study the toxicity of aqueous extract against Larvae of *T. castaneum*
- (iii) To repellency percentage of aqueous extract against adults of *T. castaneum*
- (iv) To study the Residual toxicity of aqueous extract



*Review*

# **THE JOURNEY OF BIOACTIVE GLASS FROM ORDINARY GLASS: CURRENT STATUS AND FUTURE CHALLENGES**

**PROJECT REPORT**

*Submitted in partial fulfillment of the  
requirements for the award of the degree of*

**MASTER OF SCIENCE**

**in**

**PHYSICS**

*By*

**Navneet Kaur**  
**(Regn. No. 8114-2022-1791)**



**DEPARTMENT OF PHYSICS**  
**SRI GURU TEG BAHADUR KHALSA COLLEGE, SRI ANANDPUR**  
**SAHIB**  
(An Autonomous College)  
**ANANDPUR SAHIB– 140118, PUNJAB (INDIA)**



SRI GURU TEG BAHADUR KHALSA COLLEGE, SRI ANANDPUR SAHIB  
(An Autonomous College)  
ANANDPUR SAHIB-140118, PUNJAB (INDIA)

## CERTIFICATE

It is certified that the work contained in the project report entitled "JOURNEY OF BIOACTIVE GLASS FROM ORDINARY GLASS, CURRENT STATUS AND FUTURE CHALLENGES" is an original contribution by me and has not been submitted in part or full for any other degree at this or other University/ Institute.

The assistance and help received during the course of the thesis work have been acknowledged.

Navneet Kaur

Regn. No. 8114-2022-1791.

I, the undersigned, Supervisor of **Navneet Kaur**, Regn. No. 8114-2022-1791, a candidate for the degree of **Master of Science**, agree that the project report entitled, "The JOURNEY OF BIOACTIVE GLASS FROM ORDINARY GLASS, CURRENT STATUS AND FUTURE CHALLENGES", may be submitted in partial fulfillment of the requirements for the award of degree.

This is to certify that the above statement made by the candidate is correct to the best of my knowledge.

**Dr. Randev Singh**  
Head of Department  
Department of Physics  
S.G.T.B. Khalsa College  
Sri Anandpur Sahib

**Dr. Devinder Singh**  
Assistant Professor  
Department of Physics  
S.G.T.B. Khalsa College  
Sri Anandpur Sahib

**Prof. Prabhjot Kaur**  
Assistant Professor  
Department of Physics  
S.G.T.B. Khalsa College  
Sri Anandpur Sahib

## ACKNOWLEDGEMENT

Firstly, I would like to thank almighty for giving me opportunity and guidance to achieve my goals then I would like to express my gratitude to my supportive Dr. Randev Singh Sandhu and Dr. Devinder Singh professor at department of physics Sri Guru Teg Bahadur Khalsa College Sri Anandpur Sahib. Who has resourcefully guided me throughout this research project. I'm extremely grateful for his motivating discussions while enable me to accomplish this task successfully. Without his active guidance, support and encouragement I would not have made headway in this project.

I also thankful to Dr. Randev Singh Sandhu HOD and assistant professor at Sri Guru Teg Bahadur Khalsa College Sri Anandpur Sahib for his moral support and suggestions to improve the dissertation work. I'm also thankful to other faculty members in the department for their encouragement and fruitful academic discussions. A special thanks to Proff. Prabhjot Kaur assistant professor at Sri Guru Teg Bahadur Khalsa College Sri Anandpur Sahib for the help and their valuable suggestions whenever I needed out of their busy schedule. I'm also thankful to my classmates and my friends who was directly or indirectly help me to complete this project report.

Anandpur Sahib,

  
Navneet Kaur



## **ABSTRACT**

The journey of ordinary glass to bioactive glass change the direction of modern biomedical studies. The first 45S5 active glass invented by Larry Hench around 50 years ago which was bio compatible and bioactive and able to make bonds to bones by the formation of hydroxyapatite layer.

Over the years many other bioactive glasses were composed for purpose of innovation biomedical application such as tissue repair, drug delivery, dental filling and cancer treatment. Many of today researches were unthinkable when the first bioactive glass were introduced to the world. That is the reason researchers are still trying to achieve the full potential of bioactive glass by facing future challenges such as fast degradability, mechanical strength, Reliable coating and Multiple properties performance.

This papers represent the whole journey of bioactive glass from ordinary glass, current status and future challenges.

## CONTENTS

<b>1. INTRODUCTION</b>	<b>1</b>
<b>2. GLASS</b>	<b>2</b>
2.1 DEFINITION OF GLASS	2
2.1.1 HISTORY OF GLASS	3
2.1.2 CHEMICAL COMPOSITION OF THE OLDEST GLASS	4
2.2 PRINCIPLE AND MANUFACTURING OF GLASS	6
2.2.1 MANUFACTURING OF GLASS	7
2.3 DIFFERENT TECHNIQUES OF FORMATION OF GLASS	9
<b>3. BIOACTIVE GLASS</b>	<b>11</b>
3.1 BIOMATERIALS	11
3.2 GLASS AS BIOMATERIAL	14
3.3 DEFINITION OF BIOACTIVE GLASS	14
3.4 HISTORY OF BIOACTIVE GLASS	15
3.5 METHODES OF SYNTHESIS OF BIOACTIVE GLASS	20
3.5.1 MELTING AND QUENCHING METHOD	20
3.5.2 SOL-GEL METHOD	23
3.6 BONE COMPOSITION	25
3.7 TYPES OF BIO ACTIVE GLASS	28
3.7.1 SILICATE-BASED BIOACTIVE GLASS	29
3.7.2 PHOSPHATE-BASED BIOACTIVE GLASS	30
3.7.3 BORATE-BASED BIOACTIVE GLASS	32
3.7.4 TITANIUM DIOXIDE CONTANING BIOACTIVE GLASS	33
3.7.5 ZINC DIOXIDE CONTAINING BIOACTIVE GLASS	34
3.7.6 SILVER DOPED BIOACTIVE GLASS	35
3.7.7 COPPER DOPPED BIOACTIVE GLASS	36
3.7.8 STRONTIUM DOPPED BIOACTIVE GLASS	37

3.8	CURRENT STATUS OF BIOACTIVE GLASS	38
3.9	FUTURE CHALLENGES OF BIOACTIVE GLASS	42
4.	CONCLUSION	52
5.	REFERENCES	53



# INTRODUCTION

## 1. Introduction

The journey of glass to bioactive glass is a great revolution in the field of glass and biomaterials. Centuries have spent in scientific discoveries and technology advancements. It begins with the ancient art of glass making, back then the glass were used only for particular purposes such as decoration, jewellery making, arrow head, containers and knives.

As the time progressed, lots of researches have done. Industrial revolution played a crucial role in advancement of glass and production techniques. Advancement like mass manufacturing and creation of glass on the large scale in possible easy way by different techniques and refinement of glasses.

In mid 20th century the field of bio material was exploring materials capability with the human body. In 1960 a young scientist named Larry hench successfully combined both the fields and introduced a special type of glass which was biomaterial biocompatible and bioactive. The name of the glass is "BIOACTIVE GLASS" changed the entire journey of a bio materials. The composition of bioactive glass resembled with the composition of human bones which makes it more compatible for human body, bioactive glass encourage the formation of hydroxyapatite layer, So it is use as implant device on the place of damage bones.

The earliest application of bioactive glass is in the field of dentistry. Today we are using bio active glasses as dental filling, implants.

Over subsequent decades bioactive class application found beyond dentistry such as ability to support cell growth, tissue regeneration and replacement of Cancerous tissues (commonly bones), bioactive glass in drug delivery system and spinal cord repair.

The future challenges is of bioactive glass could enhance its Mechanical properties, Reliable bioactive coating, Refined manufacturing, Fast degradability and multiple properties performance while maintaining bio compatibility and bioactivity.

# CHAPTER – 1

## GLASS

### 2. DEFINITION OF GLASS

"Glass is an organic product of fusion which has been cooled to a rigid condition without crystallization"

Glass is amorphous, hard, brittle, translucent or transparent, super cooled liquid of infinite viscosity having no definite melting point and obtained by fusing a mixture of silicates or borates with sodium, potassium, calcium and lead.

- ❖ Super cooled liquid.
- ❖ Hard rigid, transparent or Translucent, brittle.
- ❖ Non crystalline substance with no definite melting point
- ❖ It has very high viscosity which prevents Crystallization.
- ❖ Chemically it is a fused mixture of silicate of alkali and alkaline earth compounds and other Constituents like CaO, MgO, SnO, PbO, etc.

**Ordinary glass composition :**  $\text{Na}_2\text{O}$ .  $\text{CaO}$ .  $6\text{SiO}_2$

**Properties of glass :**

1. Amorphous solid.
2. No definite melting point.
3. Brittle in nature.
4. Soften on heating.
5. Bad conductor of heat and electricity.
6. Can absorb, reflect and transmit light.
7. Not affected by chemicals.

**Elements used in manufacturing of glasses :**

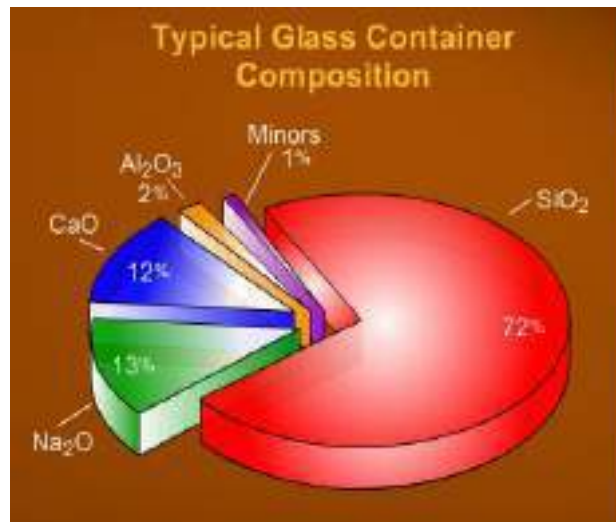
72%  $\text{SiO}_2$

13%  $\text{Na}_2\text{O}$

2%  $\text{Al}_2\text{O}_3$

12%  $\text{CaO}$

1% minors



Composition of glass

## 2.1 HISTORY OF GLASS

Obsidian, a natural volcanic glass, served as primitive tools and adornments for stone age people. Although Pliny credited Phoenician merchants in Syria with creating the first glass around 5000BC, archaeological evidence points to Eastern Mesopotamia and Egypt [1] as the origins of man-made glass around 3500BC. The initial glass vessels emerged circa 1500BC. Over the next 300 years, the glass industry experienced rapid growth, followed by a decline. It revived in Mesopotamia around 700BC and in Egypt during the 500s BC. For the next 500 years, Egypt, Syria, and surrounding regions were glass manufacturing hubs.

Initially, glass production was slow and challenging due to small furnaces with insufficient heat. In the 1st century BC, Syrian craftsmen introduced the blow pipe, revolutionizing glassmaking by making it easier, faster, and more cost-effective. While stone age people used obsidian, black volcanic glass, for tools and ornaments, Venice became a prominent glassmaking center during the Crusades. The first U.S. glass factory emerged in Jamestown, Virginia, in 1608.

The late 19th century marked a surge in glass development, driven by machinery advancements. In 1959, Sir Alastair Pilkington introduced the revolutionary float glass production, still constituting 90% of flat glass manufacturing today.

### ***2.1.1 Chemical composition of oldest glass***

The most familiar and historical oldest type of manufactured glass are “**silicate glass**” Based on the chemical compound silica (Silicon dioxide or quartz). The primary constitution was sand, sodium carbonate (Soda), limestone (Chalk) Over centuries, Various civilization refined glass recipe introducing additives like potash or lead oxide for introducing different properties.

In 17<sup>th</sup> century, George Ravenscroft Added led to create lead glass which enhanced the clarity of the glass [2].

Today innovations Continue with smart glass Incorporating technology for dynamic transparency. The advanced manufacturing technique, recycling efforts and a focus on sustainability Shape the modern glass industry from smartphone of architectural marvels glass remains an integral part of our lives.

### ***2.1.2 Evolution in the types of glass***

The evolution of glass types spans thousands of years, showcasing human ingenuity and technological advancements. The journey begins with the oldest known glass, dating back to around 3500 BCE in Mesopotamia.

#### **Ancient Glass:**

Ancient civilizations like the Mesopotamians and Egyptians discovered the art of making glass by heating a mixture of silica, soda ash, and lime. This resulted in basic glass objects, primarily beads and small vessels. The technique spread across cultures, with the Romans advancing glassmaking, introducing blown glass around the 1st century BCE.

#### **Medieval Stained Glass:**

During the medieval period, stained glass gained prominence. Artisans created intricate windows for cathedrals, using colored glass pieces assembled into stunning designs. This process involved hand-blown glass, giving each piece a unique character.

#### **Renaissance and Venetian Glass:**



The Renaissance brought a renewed focus on craftsmanship, and Venice became a hub for glass innovation in the 13th century. Murano glassmakers refined techniques, such as crystalline glass and millefiori (a thousand flowers) patterns. The Venetians also mastered the art of clear glass mirrors.

#### Industrial Revolution and Crown Glass:

The 18th century marked the Industrial Revolution, impacting glass production. Crown glass, made by blowing a large bubble and spinning it into a flat disc, became popular for window panes. This method persisted until the 19th century.

#### Early Modern Advancements (1600 CE - 1800 CE):

The 17th and 18th centuries marked a period of increased glass production. Improved kilns and the use of lead oxide contributed to the creation of lead glass, renowned for its brilliance and optical properties. Glassmaking centers, such as Murano in Venice, became hubs of innovation and craftsmanship.

#### Industrial Revolution Impact (1800 CE - 1900 CE):

The Industrial Revolution brought about a revolution in glass production. The invention of the glass bottle machine in 1903 marked a significant milestone, streamlining the manufacturing process and enabling mass production of glass containers. This period saw glass becoming an integral part of daily life.

#### Mid-20th Century Modernism (1900 CE - 1950 CE):

The mid-20th century witnessed the influence of modernist design on glassware. Artists and designers embraced minimalist forms, exploring new shapes and functions. The development of studio glass art in the mid-20th century allowed individual artists to express their creativity in unique and innovative ways.

#### Contemporary Glass (1950 CE - Present):

In the latter half of the 20th century and into the 21st century, glass has evolved with cutting-edge technologies. Tempered and laminated glass have become standard in architecture and automotive applications, providing safety and durability. Artists

continue to push the boundaries of fused glass techniques, creating stunning works of art with intricate patterns and textures.

Smart glass : The smart glass was a great revolution in the history of glass it has adjustable transparency energy efficient and modern aesthetic but the cost of manufacturing is really high [3].

Fiber glass : Fiber glass is lightweight strong corrosion Resistance the strength of fiber glass is really good the fiberglass were more expensive than traditional glass [4].

Colored glass : It is aesthetic, solar heat reduction it alters natural light and has limited transparency.

In conclusion, the evolution of glass types is a rich tapestry of human innovation, artistic expression, and technological progress. From the ancient origins of basic glassmaking to the contemporary fusion of art and science, glass continues to captivate and inspire across cultures and centuries.

## **2.2 Principle of Glass formation**

The principle of glass formation involves the rapid cooling of molten material to prevents its molecule from arranging into a crystalline structure resulting in an amorphous, glassy state [5]. This prevents the atoms from settling into a regular pattern and characteristic of crystalline solid, The principle of glass formation is rooted in the kinetic and thermodynamic aspect of material behaves during cooling. When a substance transition from a liquid to a solid state it typically forms a crystalline structure where atom or molecule arrange in a repeating pattern glass however defies this conventional solid state order.

The key lies in the rapid cooling bend a molten material is cooled quickly, its constituents particles lack sufficient time to arrange into order structure of a crystal. Instead, particles become “Frozen” in a disordered random arrangement.

This rapid cooling prevents The system from reaching its equilibrium state, Where particle would have arranged themselves into a crystalline structure imparts unique property to glass such as transparency and the absence of the distinct melting point is

also grants glass its amorphous nature making it more flexible and less brittle compared to crystalline solid.

In summary, The principle of glass formation involves manipulating the cooling process to hinder the formation of crystalline structure resulting in an amorphous solid with distinctive properties that find application in various industries from window to optical fiber.

### ***2.2.1 Manufacturing of glass***

Glass manufacturing involves melting raw materials like silica, soda ash, and limestone at high temperatures. The molten glass is then shaped through processes like blowing, pressing, or drawing before undergoing annealing to relieve stress. Further treatments like coating or cutting may follow.

#### **1. Raw Material Selection:**

The main raw materials include silica (sand), soda ash, and limestone. Other additives may be used depending on the desired properties of the glass.

#### **2. Batching:**

Precise proportions of raw materials are mixed together. This mixture is known as the batch.

#### **3. Melting:**

The batch is then fed into a furnace and heated to extremely high temperatures (around 1700°C). This heat causes the raw materials to melt and form molten glass.

#### **4. Clarification:**

Any impurities or bubbles present in the molten glass are removed or reduced through processes like settling or the addition of refining agents.

#### 5. Forming:

The molten glass is shaped into the desired form. This can be done through various techniques such as blowing, pressing, rolling, or drawing.

#### 6. Annealing:

The formed glass is slowly cooled in a controlled environment to relieve internal stresses. This process ensures uniform thickness and strength.

#### 7. Cutting and Finishing:

After annealing, the glass may undergo cutting, polishing, or other finishing processes to achieve the final product specifications.

#### 8. Inspection:

The finished glass is inspected for defects or imperfections. Quality control measures are taken to ensure the glass meets specific standards.





Steps of formation of glass

### Why annealing is important?

Annealing is the process of cooling down the molten slowly and gradually. It is important when we discuss the manufacturing the glass because if we cool down the molten instantly than the outer layer of the glass will be cool down but the inner layer will remain hot and this temperature difference creates internal strain in the glasses. This internal strain can result into sudden breaking of glass and also decrease the durability [6].

## 2.3 Different techniques of formation of glass

There are various techniques and method use in formation of glass

Some of the most used methods are:

- 1) **FLOT GLASS METHOD:** In the process the molten glass is powdered onto a pool of molten tin, forming a continuous ribbon that is gradually cooled and solidified resulting in a flat and uniform glass sheet.
- 2) **SOL- GEL METHOD:** This involves the chemical synthesis of glass from a solution that undergoes a gelation process to form a three dimensional network which is then heated to produce solid glass [7].
- 3) **VAPOUR DEPOSITION METHOD:** Thin layer of glass can be deposit onto a substrate using technique like chemical vapour deposition (CVD) or physical vapour deposition (PDV). This method allows the precise control over thickness and properties.
- 4) **MELT-QUENCHING METHOD:** The melt-quenching method involves heating a material to its molten state and then rapidly cooling it to create an amorphous or glassy structure instead of a crystalline one. This process is commonly used in glass formation for various materials like metals, polymers, and oxides. It allows the material to bypass the regular crystallization process, resulting in unique properties such as transparency and increased hardness.

## **CHAPTER – 2**

### **BIOACTIVE GLASS**

#### **3.1 BIOMATERIALS**

“The natural or man-made materials which are used to replace the function of living tissues known as bio materials” [8].

Biomaterials are substances engineered to interact with biological systems, serving a crucial role in various medical and healthcare applications. These materials play a pivotal role in the development of devices, implants, and drug delivery systems. The design of biomaterials involves careful consideration of their compatibility with living tissues, promoting desired biological responses while minimizing adverse reactions.

One primary category of biomaterials includes polymers, either natural or synthetic. Natural polymers, such as collagen and hyaluronic acid, exhibit biocompatibility but may lack mechanical strength. In contrast, synthetic polymers like polyethylene and polyurethane offer tunable properties but may trigger immune responses. The balance between these factors is crucial for successful biomaterial development.

Metals, another class of biomaterials, find application in orthopedic implants due to their mechanical strength. Titanium and stainless steel, for instance, are commonly used in joint replacements. However, concerns about corrosion and potential toxicity necessitate careful selection and surface modification to enhance biocompatibility.

Ceramics, including hydroxyapatite and alumina, are employed in bone grafts and dental implants. Their bioinert nature can be advantageous, but efforts to enhance their bonding with surrounding tissues continue. Composites, combining different materials, aim to leverage the strengths of each component while minimizing weaknesses. For instance, combining polymers with ceramics can produce materials with improved mechanical properties and biocompatibility.

Biomaterials are extensively used in the field of tissue engineering, where the goal is to create functional biological substitutes. Scaffolds made from biomaterials provide a framework for cells to grow and organize into tissues. Biodegradable polymers, like polylactic acid, are often used to construct such scaffolds, gradually breaking down as new tissue forms.

In drug delivery, biomaterials enable controlled release of therapeutic agents. Nanoparticles, micelles, and hydrogels made from various biomaterials can encapsulate drugs, protecting them from degradation and ensuring targeted delivery to specific tissues. This enhances treatment efficacy while minimizing side effects.

Biomaterials also play a crucial role in regenerative medicine, aiming to restore damaged tissues and organs. Stem cells combined with biomaterial scaffolds offer a promising avenue for tissue regeneration. The biomaterial provides physical support, while the cells contribute to the formation of new tissue.

Despite the advancements, challenges persist in the field of biomaterials. Immunogenic responses, degradation issues, and the need for long-term stability pose ongoing research challenges. Innovations in surface modifications, nano-structuring, and bioactive coatings are continuously explored to address these issues and improve the performance of biomaterials in clinical settings.

In conclusion, biomaterials represent a diverse and evolving field with applications ranging from medical implants to drug delivery and tissue engineering. As technology advances, the development of biomaterials continues to be driven by the pursuit of materials that seamlessly integrate with the complexities of the human body, facilitating better therapeutic outcomes and improving the quality of healthcare.

Biomaterials can be classified into several types based on their origin, composition, and use. Common types include:



#### Natural Biomaterials:

Derived from living organisms.

Examples: Collagen, chitosan, silk, and hyaluronic acid.

#### Synthetic Biomaterials:

Man-made materials designed for specific biomedical applications.

Examples: Polyethylene glycol (PEG), polylactic acid (PLA), and polyethylene terephthalate (PET).

#### Hybrid Biomaterials:

Combine natural and synthetic components to leverage the advantages of both.

Example: Hydrogels incorporating both natural and synthetic polymers.

#### Ceramic Biomaterials:

Inorganic materials often used for hard tissue replacements.

Examples: Hydroxyapatite, alumina, and zirconia.

#### Metallic Biomaterials:

Metals and alloys used in orthopedic implants and other medical devices.

Examples: Titanium, stainless steel, and cobalt-chromium alloys.

Polymeric Biomaterials:

Organic polymers with diverse applications in drug delivery, tissue engineering, and more.

Examples: Polyethylene, polyvinyl alcohol (PVA), and polycaprolactone (PCL).

Composite Biomaterials:

Combine two or more types of materials to achieve specific properties.

Example: Fiber-reinforced composites for enhanced strength and flexibility.

These classifications help researchers and engineers choose the most suitable biomaterial for a particular medical application.

### **3.2 Glass as Biomaterial**

Glass has limited use as traditional bio material due to its rigidity and lack of biocompatibility.

However researchers has explored BIOACTIVE Glass that can bound with biological tissues promotes healing. These glass may find an application in bone regeneration and wound healing. The field of bio glass development is evolving with ongoing efforts to enhance compatibility with living tissues.

### **3.3 DEFINITION OF BIOACTIVE GLASS**

Bio active glass is a unique man made material which has various abilities of bio materials such as bond making with living tissues, biocompatibility, bioactivity which makes it useful for bone and tissue repair [9].

When the bio glass comes into contact with the body it forms a strong chemical bond with bones which encourages the growth of new bone tissue. This property makes it valuable in application such as dental implants [10], bone grafts and other orthopaedic

and medical procedures. Bioactive glass can also release certain ions that have therapeutic effect such as promoting bone regeneration.

The property of formation of a hydroxyapatite layer on glass surface makes it bioactive. This offers excellent biocompatibility, bioactivity, less hardness and density[22].

Since cancer is uncontrolled growth of abnormal cells in the body. The goal of treatment is to kill as many as Cancerous cells while reducing the damage to normal cell nearby. Now a days the incorporation of radio nuclides such as 90 yttrium in bioactive glass could generate a revolution era for cancer therapy [11].

Before discovery of bioactive glasses be used autogenous bone graft in the procedure of surgery [12] for many years because of optimal osteoconductive and osteogenic properties.

However the autogenous bone graft has still many disadvantages such as the source of autogenous graft is very limited. It adds the overall surgical procedure and cause secondary trauma and pain in addition autograft brings some complications like blood loss nerve injury, hernia formation, infection, cosmic defect etc.

So researchers have been exploring variety of synthetic biomaterials which can be grafted in body to replace autogenous bone grafting.

### **3.4 HISTORY OF BIOACTIVE GLASS**

Medical science has made huge strides in aiding and repairing the human body and tried to reverse the irreversible restore that been permanently lost because of damage and decay. Before 1960 fixing broken bones and flash was problematic and very challenging. The immune system of bodies reacted to the artificial materials available before the discovery of bioactive glass. These artificial materials were producing scarring and artificial parts were often rejected by the body this was challenge for the scientists could they produce the materials that the body would naturally except. The credit for the discovery of bioactive glasses (BGs) goes to Larry Hench, a distinguished Research Professor in the Department of Materials Science and Engineering at the University of Florida. Later, he became the Director of the Bioglass Research Centre at

the same institution. Often, the genesis of scientific discoveries appears to be serendipitous, and the uncovering of BGs is no exception.

The foundational moment occurred during a friendly conversation between Larry Hench and a U.S. Army colonel who had recently returned from the Vietnam War in 1967. The focal point of their discussion was the challenges associated with the rejection of polymeric and metal implants, prevalent at the time for replacing living tissues due to their chemical inertness. These materials, once introduced into the physiological environment, were surrounded by a fibrous capsule of scar tissue, compromising their integration with the host tissue.

The catalyst for Hench's exploration into bioactive glasses came from studies on gamma rays applied to vanadia-phosphate semiconductors, conducted by him and his coworkers. The colonel posed a simple yet profound question: "If you can make a material that will survive exposure to high energy radiation, can you make a material that will survive exposure to the human body?" This inquiry set Hench on a path of scientific inquiry with significant implications for the post-war era, where the need for materials capable of replacing amputated limbs and compromised tissues without rejection became a critical concern for the social reintegration of survivors.

Hench developed the "hypothesis of bioactive glass" based on two fundamental pillars. Firstly, metals and synthetic polymers triggered a "foreign body reaction" due to their components being radically different from those constituting living tissues. Secondly, he postulated that a material capable of forming a bone-like hydroxyapatite layer on its surface would not be rejected by the body, considering hydroxyapatite as the primary mineral phase of natural bone tissue.

From 1969 to 1971, Hench and his team embarked on designing and studying various glass formulations based on the  $\text{SiO}_2\text{-Na}_2\text{O-CaO-P}_2\text{O}_5$  oxide system. After meticulous exploration, they settled on the composition  $45\text{SiO}_2\text{-}24.5\text{Na}_2\text{O-}24.5\text{CaO-}6\text{P}_2\text{O}_5$  (wt %). This composition, known as 4555, featured high levels of  $\text{Na}_2\text{O}$  and  $\text{CaO}$ , along with a



relatively high CaO/P<sub>2</sub>O<sub>5</sub> ratio, rendering the material highly reactive in physiological environments. Notably, the 4555 composition possessed the added advantage of being exceptionally easy to melt, thanks to its proximity to the ternary eutectic.

To distinguish this groundbreaking composition, the name Bioglass® was officially trademarked by the University of Florida. It's crucial to note that the term Bioglass® specifically refers to the original 4555 composition, and it shouldn't be used generically to indicate bioactive glasses as a whole.

The extensive studies conducted by Hench on the 4555 Bioglass have been thoroughly reviewed by Montazerian and Zanotto in a recent publication, providing a comprehensive understanding of the advancements and implications of this innovative material in the realm of biomaterials and tissue engineering. In essence, the journey from a casual conversation to the development of bioactive glasses has not only marked a scientific milestone but also contributed significantly to addressing real-world challenges in healthcare and rehabilitation.

In 1969, the pioneering discovery of the first melt-derived bioactive glass, known as Bio-Glass 45S5, marked a significant advancement in medical materials. This breakthrough was followed by the introduction of active gel-derived glasses proposed by Hench in 1991. When bioactive glass is strategically placed near a damaged bone within the body, it initiates a gradual and controlled reaction. This reaction results in the formation of a remarkably strong bond with the surrounding bones. Moreover, the bioactive glass releases ions that serve as stimulants for cells, promoting the regeneration of bone tissue.

Over time, this remarkable material undergoes a controlled degradation process, gradually disappearing as new bone growth takes place. The intricate interplay between the bioactive glass and the body's natural processes highlights its biocompatible nature. By fostering bone regeneration and integration, bioactive glass has become a crucial component in the realm of orthopedic and reconstructive medicine. Its ability to stimulate cellular activity and seamlessly integrate with the body's biology underscores its role as a dynamic and innovative solution for enhancing bone healing and tissue regeneration.

The first melt-driven bioactive glass was bio glass 45S5 discovered in 1969 followed by active gel derived glasses also proposed by Hench in 1991.

When we put bioactive glass inside the body near the damaged bone, it starts slightly react and form a really tight bond to bones and release ions that stimulate the cell to regrow more bones. This material degrades overtime and disappear as a new bone grows.

Bioactive glasses are bio compatible, biodegradable and multifunctional material which has been shown to promote osteogenic, angiogenic and antibacterial activities and also it induce various tissue regenerative process [13].

Bioactive glass shows both osteoconduction and osteoinduction properties and can be used in variety of applications such as bone grafting, scaffolding, drug delivery coating and in soft tissue engineering. However despite of excellent properties there are some disadvantages of bioactive glass such as low mechanical strength and low fracture toughness.

To overcome these disadvantages the various type of glasses that undergo the precipitation of different crystalline phase under heat treatment known as bioactive glass has been developed.

The first bioactive glass BG 45S5 with composition

$45\text{SiO}_2$ ,  $24.5\text{Na}_2\text{O}$ ,  $24.5\text{CaO}$  and  $6\text{P}_2\text{O}_5$  (wt%) was introduced in Florida [14].

First bioactive glass was silica based glass. The glass transition temperature for 45S5 bioactive glass is typically  $550^\circ\text{C}$ .

### ***Three generations of bioactive glass***

1. First Generation: The original bioactive glass, developed by Larry Hench in the 1969s, was composed mainly of  $\text{SiO}_2$ ,  $\text{Na}_2\text{O}$ ,  $\text{CaO}$ , and  $\text{P}_2\text{O}_5$ . It exhibited bioactivity by forming a hydroxyapatite layer on its surface when in contact with biological fluids.

2. Second Generation: Improvements were made in terms of composition to enhance the bioactivity and mechanical properties. Strontium and fluoride were sometimes added to influence bone formation and reduce degradation, respectively.

3. Third Generation: Continued refinement led to the development of bioactive glasses with more tailored compositions.

Researchers focused on optimizing the release of specific ions to stimulate bone regeneration and modulate the biological response.

1. 1969: Dr. Larry Hench and his team developed the first bioactive glass 4885 Bioglass.
2. 1970-1980s: Continued research led to the development of various composition of bioactive glass with improved properties.
3. 1992-2000s: Bioactive Glass started finding application in medical devices such as bone grafts dental filling [15] and coating for metallic implants [16].
4. Recent Years: Ongoing research is focused on enhancing the performance of bioactive glass, exploring new compositions, and expanding its applications in tissue engineering, drug delivery, and regenerative medicine and for small bone defect repair [17]. Revolution in the field of bioactive glass [18] is given below:

Year (First Experimental Use)	Achievement/Application
1969	Invention of the 45S5 glass composition (45S5 Bioglass®)
1977	Treatment of ear diseases by using Ceravital® glass-ceramics (replacement of middle ear small bones)
1978	Ocular implant (biocompatibility with corneal tissue)
1985	Approval by Food and Drug Administration (FDA) of the first 45S5 Bioglass® implant (MEP® implant for middle ear ossicular repair)
1987	Treatment of liver cancer (radioactive glasses)
1988	Clinical use of the 45S5 Bioglass®-based Endosseous Ridge Maintenance Implant (ERMI) in human patients
1993	FDA approval of PerioGlas (45S5 Bioglass® particulate used for bone and dental repair)
1998	Peripheral nerve repair
1999	FDA approval of radioactive glasses (TheraSphere®) for cancer treatment
2000	Wound healing
2002	FDA approval of Medpor®-Plus™ (polyethylene/45S5 Bioglass® composite porous orbital implants)
2003	Antibacterial (Zn-containing) bone/dental cements
2004	Lung tissue engineering
2004	Use of mesoporous bioactive glass (MBG) as a drug delivery system
2005	Skeletal muscle and ligament repair
2005	Treatment of gastrointestinal ulcers
2010	Cardiac tissue engineering
2011	Commercialization of a cotton-candy borate bioactive glass for wound healing in veterinarian medicine. FDA approval is pending.
2012	Embolization of uterine fibroids
2012	Spinal cord repair
2015	Use of radioactive glasses (TheraSphere®) in patients with metastatic colorectal carcinoma of the liver

## 3.5 METHODS OF SYNTHESIS OF BIOACTIVE GLASS

### 3.5.1 MELTING AND QUENCHING METHOD:

The synthesis of bioactive glass through melting and quenching is a sophisticated process that involves several steps, each step is crucial to achieving the desired properties of biomedical applications.

This method is widely employed due to its ability to produce a material with enhanced bioactivity, makes it suitable for use in bone grafts, dental implants and in other medical devices.



## **Procedure**

### **1. Raw Material Selection:**

The synthesis begins with the careful selection of raw materials, typically including silica ( $\text{SiO}_2$ ), calcium oxide ( $\text{CaO}$ ), phosphorous pentoxide ( $\text{P}_2\text{O}_5$ ), and sometimes additional trace elements. The choice of these components is pivotal in achieving a glass composition that closely mimics the mineral composition of natural bone, promoting better integration with biological tissues.

### **2. Weighing and Mixing:**

Accurate weighing and precise mixing of the raw materials are crucial to achieving the desired glass composition. The proportions are carefully controlled to ensure the optimal balance of structural integrity, bioactivity, and other essential properties. Silica provides the glass with structural stability, calcium enhances bone regeneration, and phosphorous contributes to bioactivity.[22]

### **3. Melting Process:**

The mixed raw materials are then subjected to a high-temperature melting process, typically carried out in a specialized furnace. The temperature is precisely controlled to allow for the complete homogenization of the components. During this melting phase, the solid raw materials transform into a molten glass, a crucial step in the synthesis.

#### 4. Quenching:

Following the melting process, the molten glass undergoes rapid quenching. Quenching is the sudden cooling of the material, and it can be achieved through various methods, such as air quenching or water quenching. This rapid cooling is a critical step that imparts unique characteristics to the bioactive glass.

#### 5. Amorphous Structure Formation:

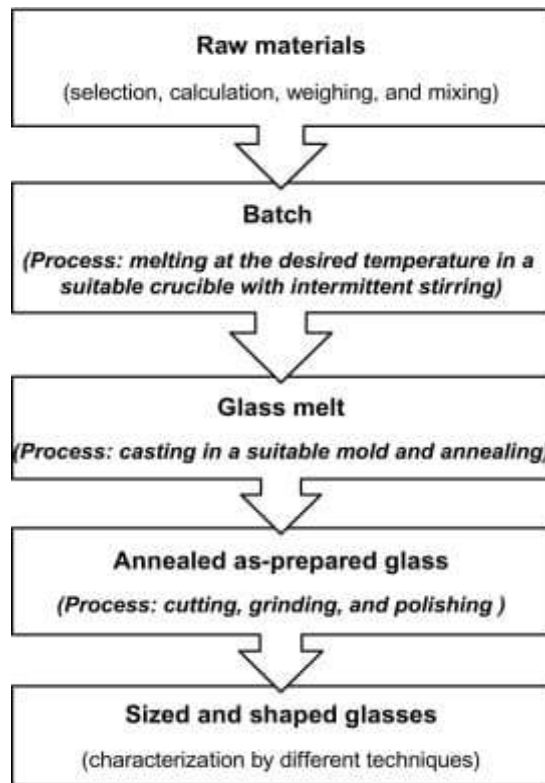
Quenching prevents the formation of large crystalline structures in the glass, resulting in an amorphous structure.

#### 6. Annealing :

Glass annealing is a heat treatment process where the glass is slowly cooled to relieve internal stresses and increase its strength and durability. This is typically done in a controlled environment called an annealing oven. The slow cooling process allows the glass to reach a state of equilibrium, minimizing internal tensions. Annealed glass is less prone to breaking and shattering compared to untreated glass.

#### 7. Shaping:

Shaping and sizing glass typically involve processes like cutting, grinding, and polishing. Glass can be cut using tools like glass cutters or diamond saws, and then shaped through grinding or other techniques. Sizing involves ensuring the glass fits specific dimensions, often achieved through precision cutting or shaping. The methods vary based on the type of glass and desired outcome.



Steps of synthesis of bioactive glass by melting and quenching techniques.

### 3.5.2 SOL-GEL METHOD :

The sol-gel method [19] is versatile and widely used technique in material science, particularly in the synthesis of bioactive glasses.

bioactive glasses have gained significant attention due to their unique property including ability to form a strong bond with tissues. This property is attributed to the formation of a hydroxyapatite layer [20] on the glass surface, this process is known as bioactivity.

The sol-gel method provides a flexible and controllable route for synthesizing bioactive glass allowing precise manipulation of composition and structure.

The sol-gel process involves the transformation of a colloidal suspension (sol) into a gel, ultimately leading to the formation of glassy materials. The fundamental steps include

## **Procedure**

### **1. Selection of Precursors**

The choice of precursor compounds significantly influences the properties of the resulting bioactive glass. Commonly used precursors include silicon alkoxides (e.g., tetraethyl orthosilicate, TEOS), calcium alkoxides, and phosphorus-containing compounds.

### **2. Sol Preparation**

The selected precursors are dissolved in a solvent, often ethanol or water, to form the sol. Careful control of precursor concentrations and solvent conditions is crucial for achieving the desired properties in the final glass.

### **3. Gelation**

The sol undergoes gelation through hydrolysis and condensation reactions. This process is influenced by factors such as pH, temperature, and the presence of catalysts. Gelation results in the formation of a three-dimensional network structure.

### **4. Aging**

The gel is allowed to age, promoting further polymerization and strengthening of the network. Aging conditions play a vital role in controlling the final structure and properties of the bioactive glass.

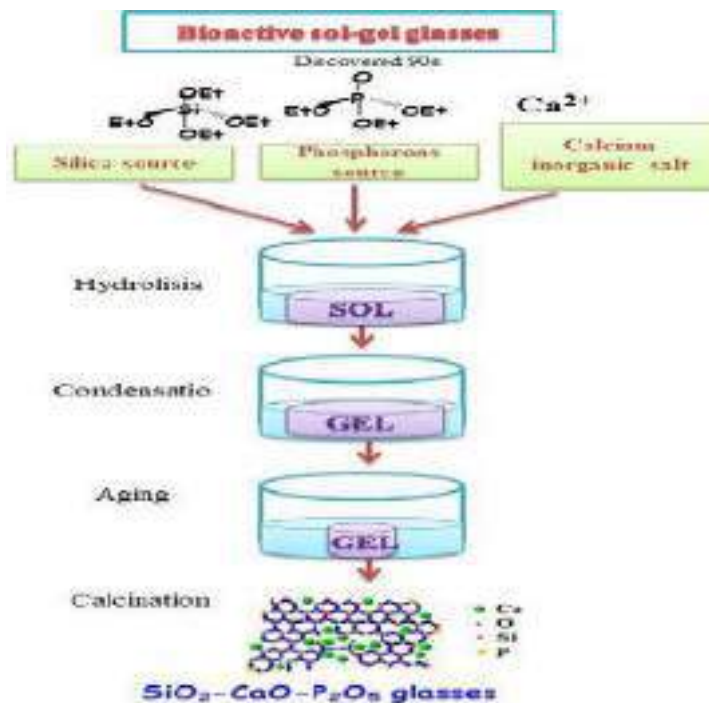
### **5. Drying**

Excess solvent is removed through drying, leaving a porous structure. The drying conditions impact the porosity and morphology of the resulting material.



## 6. Sintering

The dried gel is subjected to high temperatures in a process called sintering. This step eliminates remaining organic components, densifies the material, and induces crystallization, leading to the formation of bioactive glass.



Steps of synthesis of bioactive glass by sol-gel technique

This method allows precise control over composition and structure.

Characterization of bioactive glass prepared by sol-gel method can be done by XRD, EDX and SEM [21].

## 3.6 BONE COMPOSITION:

Bone, a dynamic and vital tissue in the human body, is a complex composition of various elements that contribute to its structure, strength, and functionality. Understanding the intricate makeup of bone involves exploring its mineral and organic components, along with the crucial role of bone marrow.

### Mineral Components:

1. Hydroxyapatite: The predominant mineral in bone, hydroxyapatite, forms a crystalline structure composed of calcium and phosphate. This compound provides rigidity and strength to bone tissue, contributing to its hardness. Hydroxyapatite crystals align along collagen fibers, creating a sturdy matrix that resists compression forces. This mineralization process is essential for the skeletal system's ability to support the body and withstand mechanical stress.

2. Calcium: Beyond hydroxyapatite, calcium is a fundamental element in bone composition. Approximately 99% of the body's calcium resides in bones and teeth, playing a pivotal role in bone density and strength. Calcium ions participate in signaling processes that regulate bone remodeling, influencing the balance between bone formation and resorption.

3. Phosphorus: Alongside calcium, phosphorus forms the phosphate component of hydroxyapatite. Phosphorus is integral to the mineralization process, enhancing bone density and hardness. It plays a vital role in maintaining the structural integrity of bone, ensuring its resistance to fractures and deformities.

4. Magnesium: Although present in smaller amounts than calcium and phosphorus, magnesium is essential for bone health. It influences the activity of bone-forming cells (osteoblasts) and bone-resorbing cells (osteoclasts), contributing to the dynamic process of bone remodeling. Magnesium deficiency can impact bone mineral density, highlighting its significance in maintaining skeletal integrity.

Other elements such as potassium(0.2%), sodium(0.8%), carbonate(9.8%) also present in chemical composition of bone.

### Organic Components:

1. Collagen: The organic component of bone is primarily composed of collagen, a fibrous protein that provides flexibility and tensile strength. Collagen fibers are interwoven within the mineralized matrix, creating a framework that enhances the bone's resilience to bending and stretching forces. This intricate network of collagen also contributes to the bone's ability to absorb energy, preventing fractures.
2. Proteoglycans: Alongside collagen, proteoglycans are essential organic molecules present in bone. These large molecules consist of a protein core with attached carbohydrates. Proteoglycans contribute to the compressive strength of bone by attracting water molecules, maintaining hydration within the bone matrix. This hydration aspect is crucial for resisting compression forces and ensuring the overall structural integrity of the bone.
3. Glycoproteins: Various glycoproteins, including osteocalcin and osteonectin, play roles in regulating bone mineralization and remodeling. Osteocalcin, for example, facilitates the binding of calcium and phosphate ions during the mineralization process. These glycoproteins contribute to the coordination of cellular activities involved in bone formation and maintenance.

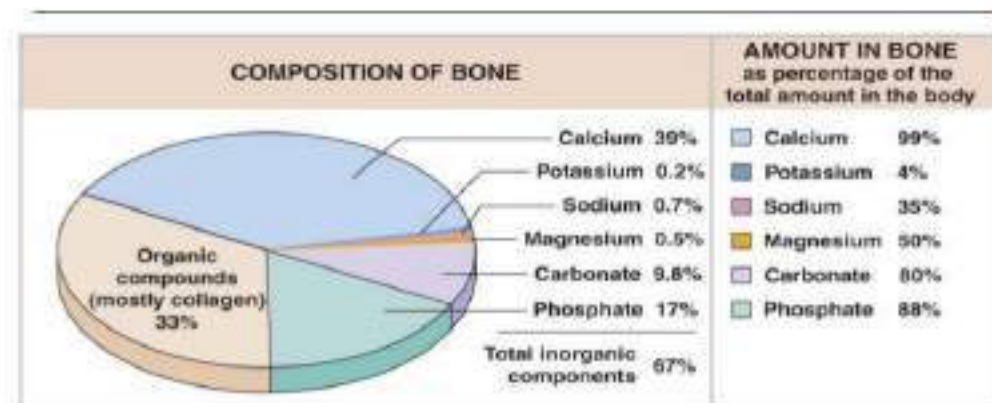
### Cellular Components:

1. Osteoblasts: These specialized cells are responsible for synthesizing and depositing new bone matrix during the process of bone formation (ossification). Osteoblasts play a crucial role in mineralizing the organic matrix with hydroxyapatite, contributing to bone density and strength.
2. Osteoclasts: In contrast to osteoblasts, osteoclasts are involved in bone resorption. These large, multinucleated cells break down bone tissue, releasing minerals into the bloodstream. This process is vital for calcium homeostasis and the removal of old or damaged bone during the constant remodeling that bones undergo.

3. Osteocytes: Osteocytes are mature bone cells embedded within the mineralized matrix. Connected by cellular extensions in tiny channels called canaliculi, osteocytes form a communication network within the bone. They sense mechanical forces and regulate bone remodeling by signaling to osteoblasts and osteoclasts.



## Chemical Composition of Bone



Chemical Composition of Bone.

Few types of Bioactive glasses is determined by the selection of doping and most of the selection of doping depends upon the composition of bones.

### 3.7 TYPES OF BIOACTIVE GLASS

There are several types of bioactive glass, each with unique compositions tailored for specific biomedical applications. Common types include:



### **3.7.1 SILICATE-BASED BIOACTIVE GLASS**

Silica-based bioactive glass is a distinctive biomaterial that has garnered significant attention in the medical field due to its unique properties and applications. The term "silica-based" refers to the predominant presence of silica ( $\text{SiO}_2$ ) in the glass composition, which plays a pivotal role in imparting bioactivity and biocompatibility to the material [24].

At the forefront of silica-based bioactive glass is the well-known 45S5 Bioglass, developed by Dr. Larry Hench in the 1960s. Comprising 45%  $\text{SiO}_2$ , 24.5%  $\text{Na}_2\text{O}$ , 24.5%  $\text{CaO}$ , and 6%  $\text{P}_2\text{O}_5$ , this composition was a groundbreaking innovation. Silica, as the primary component, serves as a key player in the glass's bioactive behavior, facilitating interactions with living tissues.

The bioactivity of silica-based bioactive glass is rooted in its ability to form a hydroxyapatite layer on its surface when exposed to bodily fluids. This process, known as bioactive bonding, involves the exchange of ions between the glass and the surrounding biological environment. Silica's contribution to this ion-exchange mechanism is crucial, as it initiates the formation of hydroxyapatite—a mineral closely resembling the natural structure of bone.

Silica, in its amorphous form within the glass structure, creates a highly reactive surface. When implanted in the body, the glass undergoes dissolution, releasing bioactive ions such as silicon (Si), calcium (Ca), and sodium (Na). These ions create a microenvironment that promotes the nucleation and growth of hydroxyapatite crystals. The resultant hydroxyapatite layer acts as a scaffold for bone cells, encouraging bone regeneration and integration with the surrounding tissues.

Silica-based bioactive glass finds widespread use in orthopedic and dental applications. In orthopedics, the material is employed in bone grafts and repair procedures to address skeletal defects resulting from trauma, diseases, or

surgeries. The bioactivity of the glass accelerates the natural healing processes, enhancing bone formation and integration at the implantation site. The compatibility of silica-based bioactive glass with the physiological environment minimizes the risk of adverse reactions, making it a preferred choice for orthopedic interventions.

Dentistry benefits significantly from silica- based bioactive glass, particularly in the realm of dental implants. The material's ability to bond with both hard and soft tissues is advantageous for implant stability and long-term success. As dental implants aim to replicate the natural structure of teeth, the bioactive glass facilitates osseointegration, ensuring a robust connection between the implant and the jawbone.

The glass can serve as a carrier for drugs or growth factors, enabling controlled release at the implantation site. This targeted drug delivery enhances tissue regeneration while minimizing systemic side effects.

Research endeavors continue to refine and expand the applications of silica-based bioactive glass. Modifications in composition and structure are explored to tailor the material for specific clinical needs. For instance, variations like 58S Bioactive Glass with increased silica content have been developed, offering improved mechanical properties and bioactivity compared to earlier compositions.

### ***3.7.2 PHOSPHATE-BASED BIOACTIVE GLASS***

Phosphate-based bioactive glass is a specialized category of biomaterials with a distinct composition that includes a significant proportion of phosphorous oxide ( $P_2O_5$ ). This composition imparts unique properties to the glass, making

it particularly suitable for various biomedical applications, especially in the field of bone regeneration.

The inclusion of phosphorous in the glass composition enhances its bioactivity, as phosphorous is a vital element in the formation of hydroxyapatite-the main mineral component of natural bone. The ability to form hydroxyapatite on the glass surface is a key characteristic that facilitates the integration of phosphate-based bioactive glass with living tissues.

One notable phosphate-based bioactive glass is known as PG (Phosphosilicate Glass). PG glass typically contains silica ( $\text{SiO}_2$ ), sodium oxide ( $\text{Na}_2\text{O}$ ), calcium oxide ( $\text{CaO}$ ), and phosphorous oxide ( $\text{P}_2\text{O}_5$ ). This combination is carefully balanced to optimize the bioactive properties of the glass. The presence of phosphorous not only contributes to the formation of hydroxyapatite but also enhances the overall bioactivity of the material.

When phosphate-based bioactive glass is implanted in the body, it undergoes dissolution in the physiological environment. This dissolution process releases ions, including phosphorous ions, into the surrounding tissues. These released ions create a favorable environment for the deposition of hydroxyapatite, mimicking the natural mineralization process of bone. The resulting hydroxyapatite layer acts as a scaffold for cell attachment and bone regeneration.

The bioactive bonding capability of phosphate-based bioactive glass is particularly advantageous in orthopedic applications. It is commonly used in bone grafting procedures where the goal is to stimulate bone formation and repair bone defects. The material provides structural support while promoting the regeneration of bone tissue, aiding in the healing process.

Phosphate glass exhibiting less pronounced bioactivity but High solubility once comes in the contact of body fluids and it dissolves harmlessly in the body [25].

### **3.7.3 BORATE-BASED BIOACTIVE GLASS**

Contains boron oxide ( $B_2O_3$ ) in addition to silica and other oxides. Used for wound healing and tissue engineering applications.

While there isn't a widely recognized category of "Borate-based" bioactive glass, it's possible that you meant "Borate-based" bioactive glass. Borate-based bioactive glass is indeed an area of research and development within the broader field of biomaterials. Borate glasses typically contain boron oxide ( $B_2O_3$ ) as a significant component, and they have shown promise in various biomedical applications.

Borate-based bioactive glasses offer certain advantages due to the unique properties of boron. Boron is known to stimulate bone formation and is involved in various physiological processes. Here are some key points about borate-based bioactive glass. Boron oxide along with other components such as silica ( $SiO_2$ ), sodium oxide ( $Na_2O$ ), calcium oxide ( $CaO$ ), and phosphorous oxide ( $P_2O_5$ ).

The specific composition can vary based on the desired properties for a particular application.

In summary, borate-based bioactive glasses show promise in various biomedical applications, particularly in bone regeneration and wound healing. Their unique properties make them valuable candidates for further exploration in the development of advanced biomaterials.

Borate-based bioactive glass has found diverse applications in the field of biomaterials due to its unique properties. This glass composition, typically containing boron, silica, and other elements, exhibits excellent biocompatibility



and bioactivity. When implanted in the body, it forms a hydroxyapatite layer on its surface, promoting bone integration.

In orthopedics, borate-based bioactive glass is utilized for bone regeneration and repair. Its ability to stimulate osteogenesis and support the growth of new bone makes it valuable in treating fractures or bone defects. Moreover, its controlled release of therapeutic ions, like boron, provides antimicrobial properties, reducing the risk of infections.

The glass also finds application in dentistry, where it can be used in dental fillings or implants. Its bioactive nature encourages the formation of a strong bond with surrounding tissues, enhancing the longevity of dental restorations. Additionally, borate-based bioactive glass has potential applications in drug delivery systems, leveraging its ability to release therapeutic agents in a controlled manner.

Overall, the versatile properties of borate-based bioactive glass make it a promising material in the development of advanced biomaterials for orthopedic and dental applications, contributing to the field of regenerative medicine

### ***3.7.4 TITANIUM DIOXIDE CONTAINING BIOACTIVE GLASS***

Titanium-containing bioactive glass is a specialized type of biomaterial that combines the properties of bioactive glass with the benefits of titanium. This hybrid material is designed to leverage the positive characteristics of both components, offering advantages in terms of mechanical strength [26], biocompatibility, and osteoconductivity.

Here are key points about titanium- containing bioactive glass:

1. **Composition:** The composition typically includes silica ( $\text{SiO}_2$ ), sodium oxide ( $\text{Na}_2\text{O}$ ), calcium oxide ( $\text{CaO}$ ), phosphorous oxide ( $\text{P}_2\text{O}_5$ ), and the incorporation of titanium dioxide ( $\text{TiO}_2$ ). The addition of titanium dioxide enhances the mechanical properties of the bioactive Mass, making it suitable for load-bearing applications.
2. **Mechanical Strength:** Titanium is renowned for its exceptional mechanical strength and biocompatibility. When integrated into bioactive glass, it contributes to the overall durability and stability of the material. This makes titanium-containing bioactive glass suitable for applications in orthopedics, where load-bearing capabilities are essential.
3. **Bioactivity:** Similar to other bioactive glasses, titanium-containing bioactive glass exhibits bioactivity by forming a hydroxyapatite layer on its surface when exposed to bodily fluids. The bioactivity promotes the integration of the glass with surrounding tissues, facilitating bone bonding and regeneration.

### ***3.7.5 ZINC DIOXIDE CONTAINING BIOACTIVE GLASS***

Incorporates zinc oxide for antimicrobial properties.

Addresses concerns related to bacterial infections in implantation sites. Zinc oxide-containing bioactive glass is a specialized type of biomaterial that incorporates zinc oxide ( $\text{ZnO}$ ) into its composition. This addition of zinc oxide brings unique properties to the bioactive glass, making it suitable for specific biomedical applications. Here are some key aspects of zinc oxide-containing bioactive glass:

#### **1. Composition:**

The glass composition includes silica ( $\text{SiO}_2$ ), sodium oxide ( $\text{Na}_2\text{O}$ ), calcium oxide ( $\text{CaO}$ ), phosphorous oxide ( $\text{P}_2\text{O}_5$ ), and the distinctive addition of zinc oxide ( $\text{ZnO}$ ). The specific ratios can vary based on the desired properties and intended applications.

## 2. Antimicrobial Properties:

Zinc oxide is known for its antimicrobial properties [27]. Its inclusion in bioactive glass imparts the ability to inhibit the growth of bacteria and other microorganisms. This antimicrobial effect is particularly beneficial in applications where preventing infections at the implantation site is crucial.

## 3. Bioactivity:

Similar to other bioactive glasses, zinc oxide-containing bioactive glass exhibits bioactivity by forming a hydroxyapatite layer on its surface when exposed to bodily fluids, which helps in bone regeneration and promotes tissue bonding

### ***3.7.6 SILVER DOPED BIOACTIVE GLASS***

Silver-doped bioactive glass is a amazing material that has gained significant attention in the field of biomaterials and medical applications. This unique composite material merges the advantageous properties of bioactive glass and the antimicrobial effects of silver, creating a versatile substance with a wide range of potential uses [28].

Bioactive glass, in its conventional form, has been extensively studied for its ability to bond with biological tissues. When in contact with bodily fluids, bioactive glass can form a hydroxyapatite layer on its surface, facilitating the integration of the material with surrounding tissues. This bioactivity is especially beneficial for applications in boke regeneration and repair

The incorporation of silver into bioactive glass introduces an additional layer of functionality. Silver is well-known for its antimicrobial properties, which have been utilized for centuries. In the context of biomaterials, the release of silver ions from the glass can effectively inhibit the growth of bacteria and other microorganisms. This antimicrobial action is particularly crucial in medical devices and implants, where preventing infections is of utmost importance.

One of the primary advantages of silver- doped bioactive glass is its versatility in different medical applications. For instance, in orthopedics, it can be employed in bone grafts and implants to promote bone regeneration while simultaneously preventing bacterial colonization. The antimicrobial effects become particularly significant in reducing the risk of postoperative infections, a common concern in orthopedic surgeries.

In dentistry, silver-doped bioactive glass has shown promise in applications such as dental implants and restorative materials. The material's ability to encourage the formation of hydroxyapatite enhances its integration with natural tooth structures, while the silver component helps combat oral bacteria, minimizing the risk of infections and improving overall oral health.

In conclusion, silver-doped bioactive glass stands at the intersection of material science, medicine, and biotechnology. Its dual functionality, combining the bioactivity of glass with the antimicrobial prowess of silver, opens up new possibilities for innovative medical solutions. As research progresses, this material holds the potential to revolutionize various fields, from orthopedics to dentistry and wound care, contributing to improved patient outcomes and advancing the frontier of biomaterials.

### ***3.7.7 COPPER DOPED BIOACTIVE GLASS***

Copper-doped bioactive glass is a compelling material that merges the benefits of bioactive glass with the unique properties of copper. This composite material has garnered attention in the realm of biomaterials and medical applications due to its potential for promoting tissue regeneration and exhibiting antimicrobial properties.

Bioactive glass, known for its ability to form a hydroxyapatite layer when in contact with bodily fluids, is widely used in various medical applications, particularly in bone



regeneration and repair. The incorporation of copper into bioactive glass introduces an additional layer of functionality, expanding its capabilities and potential applications.

Copper has been recognized for its

antimicrobial properties throughout history. In the context of biomaterials, the release of copper ions from the glass can effectively inhibit the growth of bacteria and other microorganisms. This antimicrobial action is crucial in medical applications where preventing infections is paramount

copper-doped bioactive glass represents a promising intersection of material science and medicine. Its dual functionality, combining the bioactivity of glass with the antimicrobial properties of copper, opens up new avenues for medical applications. As research advances, this material holds the potential to revolutionize orthopedics, dentistry, and wound care, offering innovative solutions for improved patient outcomes and pushing the boundaries of biomaterials.

### ***3.7.8 STRONTIUM DOPED BIOACTIVE GLASS***

Introduces strontium doped bioactive glass

Shows potential in promoting bone formation and reducing bone resorption [29].

Strontium (Sr) based bioactive glass is a material used in biomedical applications, known for its ability to promote bone regeneration. It contains strontium ions, which have been shown to enhance osteogenesis and inhibit bone resorption. This makes it valuable for bone tissue engineering and implants, contributing to improved bone healing and integration.

The effect of Sr-doped BG has also been examined for the treatment of osteoporotic bone in order to deliver a steady supply of  $\text{Sr}^{2+}$  ions to the bone defect site. In fact the studies have shown an inhibition in osteoclastic activity as the strontium content increases [30].

### 3.8 CURRENT STATUS

The journey of glass to bioactive glass is a great evolution that spans centuries, marked by scientific discovery and technological advancements. It begins with the ancient art of glassmaking, where artisans crafted glass objects for various purposes. Initially, glass was primarily used for decorative and functional items, such as containers and jewelry.

As time progressed, the industrial revolution played a pivotal role in advancing glass production techniques. Mass manufacturing allowed for the creation of glass on a larger scale, transforming it into a ubiquitous material in daily life. Innovations like the glassblowing technique further expanded the possibilities of glass applications.

In the mid-20th century, the field of biomaterials emerged, exploring materials compatible with the human body. Scientists recognized the potential of glass due to its inert nature and started investigating ways to enhance its biological interactions. This led to the development of bioactive glass, a revolutionary material with the ability to bond with living tissues.

The key breakthrough came in the 1960s when Dr. Larry Hench, an American scientist, pioneered the concept of bioactive glass. His research aimed to find materials that could integrate with the human body and stimulate bone regeneration. Bioactive glass, unlike traditional glass, is designed to elicit a biological response when in contact with bodily fluids. Its composition typically includes elements like silicon, calcium, and phosphorus, resembling the mineral composition of bone.

One of the earliest applications of bioactive

glass was in the field of dentistry. Researchers found that bioactive glass could encourage the formation of hydroxyapatite, a mineral essential for bone formation. This property made it an ideal material for dental fillings and implants, as it could promote the regeneration of natural tooth structure.

Over subsequent decades, bioactive glass found applications beyond dentistry. Orthopedic implants, such as bone screws and plates, began incorporating bioactive glass to enhance the integration with surrounding bone tissue. The material's versatility

allowed for modifications in composition to suit different medical needs, opening doors to diverse applications in regenerative medicine.

As research continued, scientists explored the potential of bioactive glass in drug delivery systems. The porous nature of the material proved advantageous for controlled release of therapeutic agents. This innovation expanded the utility of bioactive glass to include not only structural applications but also pharmaceutical advancements.

In recent years, bioactive glass has gained prominence in tissue engineering. Its ability to support cell growth and tissue regeneration has led to the development of bioactive glass scaffolds. These scaffolds serve as frameworks for the growth of new tissues, making them valuable in repairing and replacing damaged organs or bones.

The ongoing exploration of bioactive glass continues to unveil new possibilities in medicine and beyond, promising a future where the boundaries between inert materials and living tissues blur for the betterment of human health.

The first bio glass implant was performed in USA, aimed to replace a bone of middle in the ear in order to treat hearing loss [31] the sample was created by melting and quenching technique. This implant was non-porous truncated cone of fixed size which allow sound conduction from both its ends this was successful implantation.

45S5 bioglass was also used to anchor cochlear implants to temporal bone of the patient this implantation was also successful. In 1988 the bioactive glass has been used in dentistry as fillers.

In the late 1980s, a breakthrough in bioactive glass was achieved with the implantation of S53P4 plates ( $53\text{SiO}_2\text{-}20\text{CaO-}23\text{Na}_2\text{O-}4\text{P}_2\text{O}_5$  wt%) for fracture repair, stimulating new orbital bone growth. Subsequently, this bioactive glass gained widespread acceptance, reaching over 35 countries.

Enhancing its properties involved incorporating modifiers and doping in specific proportions. For instance, SrO was added to reduce bone resorption ( $44.5\text{SiO}_2\text{-}4\text{Na}_2\text{O-}4\text{K}_2\text{O-}7.5\text{MgO-}17.8\text{CaO-}4.5\text{P}_2\text{O}_5\text{-}17.8\text{SrO}$  mol%), while MgO contributed to fast bone regeneration ( $53\text{SiO}_2\text{-}6\text{Na}_2\text{O-}12\text{K}_2\text{O-}5\text{MgO-}20\text{CaO-}4\text{P}_2\text{O}_5$  wt%), particularly for repairing large bone defects. To further refine the properties, researchers shifted to the

sol-gel process for powdered bioactive glass synthesis, which exhibited faster bone healing than metal-derived counterparts. Notably, 45S5 powder is now utilized in toothpaste for treating sensitivity.

Zinc-containing bioactive glass demonstrated enhanced mechanical properties, bone bonding, and antibacterial effects, promoting regrowth and regeneration. Silver-containing bioactive glass showcased antimicrobial properties, reducing infection risks.

Bioactive hydrogels have recently emerged as a groundbreaking solution for repairing spinal cord injuries. These hydrogels create a supportive environment for cell growth, release healing substances, facilitate beneficial cell transplantation, and promote tissue regeneration and functional recovery.

Traditionally, bioactive glass, derived through a melting and quenching process, faced challenges with inflammation during bonding to living bones. The introduction of the sol-gel synthesis method addressed this issue, giving rise to a new generation of bioactive glasses with enhanced properties.

The sol-gel method has further paved the way for the development of nano-system-based bioactive glasses, utilizing nanoparticles and nanofibers. A notable advancement includes mesoporous bioactive glass, exhibiting outstanding texture and properties with quicker responses compared to previous iterations.

Nanoparticle bioactive glass represents a significant stride in medical and materials science. Its small size enhances bioactivity and integration with biological tissues, proving highly effective in applications such as bone regeneration and drug delivery. The increased surface area of nanoparticles fosters better tissue bonding and healing, unlocking new possibilities in biomedicine and biomaterials.

In the realm of cancer treatment, bioactive glasses are now employed for both tumor restriction and bone reconstruction. These glasses serve as drug carriers and implants.



with the drug combined with bioactive glass and implanted at the site after removing cancerous tissues and damaged bone. Initially used solely as an implant, the evolution of drug delivery technologies has led to bioactive glass being utilized as a carrier for

Like SrO has been used to reduce bone resorption [32]

(44.5SiO<sub>2</sub>- 4Na<sub>2</sub>O-4K<sub>2</sub>O-7.5MgO-17.8CaO-4.5P<sub>2</sub>O<sub>5</sub>-17.8SrO) mol%

And MgO has been used for fast bone regeneration (53SiO<sub>2</sub>-6Na<sub>2</sub>O-12K<sub>2</sub>O-5MgO-20CaO-4P<sub>2</sub>O<sub>5</sub>)wt% This was reported to repair the large bond defects.

Later on to enhance properties the synthesis methods has been changed. In order to create powdered bioactive glass researcher use sol-gel process. The Powdered bioactive glass was able to perform fast bone healing as compared to metal-driven bioactive glass. The powered 45S5 is currently used in toothpaste in order to treat the sensitivity [33].

Zinc containing bioactive glass were proved as properties enhancer in certain ways. Zinc containing exhibit mechanical properties, bone bonding ability and antibacterial effect. Zinc also present in bone which promotes regrowth and regeneration [34] [35].

The silver containing bioactive glass are known for its antimicrobial property which decrease the chances of infection.

The recent advancement is "bioactive hydrogel" which helps repair spinal cord injury by providing a supportive environment for cell growth releasing healing substances, facilitating the transplantation of beneficial cell and promotes tissue regeneration and function recovery [37].

The bioactive glass drive from melting and quenching process was causing the problem of inflammation while bonding to living bones. Thus new method of synthesis named sol-gel was introduced to the world. The sol-gel gave rise to new generation of bioactive glasses. This method developed a great potential to enhance the property of bioactivity glass.

Moreover this advancement allowed to obtain Nano system based bioactive glasses by using nanoparticle and Nano fibres.

Recently a mesoporous bioactive glass has developed which has outstanding texture, properties and this bioactive glass responses quicker than previous mentioned bioactive glasses [38].

Nanoparticle bioactive glass has been a significant advancement in medical and materials science. Its small size allows for enhanced bioactivity and improved integration with biological tissues, making it highly effective in applications like bone regeneration and drug delivery. The increased surface area of nanoparticles enhances reactivity, fostering better tissue bonding and healing. This innovation has opened new possibilities in biomedicine and biomaterials.

Nowadays the bioactive glasses are used in the treatment of cancer. The treatment of cancer involves tumor restriction and bone reconstruction. The bone-cancer treatment based on bioactive glass helps as drug carrier and implant. In this process the drug is combined with bioactive glass and implant on the site after removing Cancerous tissues and damaged bone.

Initially the bioactive glass was only used as implant after removing Cancerous tissues and affected bone however with the advancement of drug delivery technologies, they start using bioactive as carrier of bone-cancer drugs as well [36].

### **3.9 FUTURE CHALLENGES**

Bioactive glass a material with unique properties that promotes biological interactions faces several challenges and opportunities as it evolves in medical field. The future challenges of bioactive glass may include optimizing it's Mechanical properties, reliable coating, fast and simple way of fabrication, fast biodegradability, multiple properties performance while maintaining it's bio activity.

#### ***RELIABLE BIOACTIVE COATING:***

Developing a reliable bioactive coating has been a longstanding challenge in dentistry, especially with the prevalent use of metallic implants. Metal implants are susceptible

to encapsulation within fibrous tissue in the body, posing a threat to their stability. In addressing this issue, bioactive coatings play a crucial role by enhancing the implant's stability through bonding it to the host bone.

One key function of bioactive coatings is to act as a protective barrier for the metal implant, preventing corrosion. Corrosion, in this context, is a significant concern as it can release toxic ions from the metal surface, potentially causing adverse effects within the body. The bioactive coating acts as a shield, mitigating the risk of corrosion and subsequent release of harmful ions [39].

However, it's important to acknowledge a limitation associated with bioactive coatings, namely their biodegradability. Different coatings exhibit varying dissolution rates, leading to a potential challenge. The term "bioactive coating" suggests a coating that is biologically active, but this activity may come at the cost of rapid degradation over time. The issue arises when the coating degrades too quickly, exposing the underlying metal implant.

This biodegradability concern highlights the delicate balance that must be struck in designing bioactive coatings. Ideally, the coating should be stable enough to provide long-term protection against corrosion, yet it should not degrade so rapidly that it compromises the integrity of the implant. Striking this balance is crucial for ensuring the efficacy and safety of bioactive coatings in the realm of dental implants.

In summary, the quest for a reliable bioactive coating in dentistry revolves around achieving a delicate equilibrium between enhancing implant stability, protecting against corrosion, and addressing the challenge of biodegradability to ensure long-term success in dental implantology. Therefore this is the great challenge for the next few years and the aim is to slow down the dissolution rate of bioactive coating and optimized to improve the coating performance [40].

In dentistry, a significant challenge with bioactive coatings is ensuring long-term stability and durability, especially in the harsh oral environment. Factors like saliva,

acidic conditions, and mechanical stresses can impact the effectiveness of the coating over time. Researchers are actively working on improving the resilience of bioactive coatings to enhance their performance in dental applications.

#### *MECHANICAL PROPERTIES:*

The mechanical properties of bioactive glass are crucial in determining its suitability for various biomedical applications. Bioactive glass, composed of silica-based materials, exhibits unique characteristics that make it attractive for use in medical devices, tissue engineering, and bone regeneration. However, several challenges exist in optimizing its mechanical properties to meet the diverse demands of these applications.

One primary challenge is achieving a balance between strength and bioactivity. Bioactive glass is renowned for its ability to bond with living tissues through the formation of a hydroxyapatite layer, promoting integration with the surrounding biological environment. However, enhancing bioactivity often involves trade-offs with mechanical strength. The challenge lies in developing formulations that maintain sufficient strength while still allowing for effective bioactivity.

Another challenge is addressing brittleness, a common limitation in traditional bioactive glass compositions. The brittleness of bioactive glass can hinder its performance in load-bearing applications, such as orthopedic implants. Researchers are exploring various strategies, including compositional modifications and processing techniques, to mitigate brittleness and improve the fracture toughness of bioactive glass.

Furthermore, the mechanical properties of bioactive glass must be tailored to specific applications within dentistry and orthopedics. Dental applications, for instance, require materials with suitable hardness and wear resistance to withstand the dynamic and abrasive nature of the oral environment. Orthopedic implants, on the other hand, demand materials with adequate strength and fatigue resistance to endure the mechanical stresses associated with bodily movement.

Controlling the degradation rate poses another challenge in optimizing the mechanical properties of bioactive glass. While a controlled degradation rate is desirable for gradual integration with surrounding tissues, it is crucial to prevent premature failure. Achieving a delicate balance in degradation kinetics requires a surrounding tissues, it



is crucial to prevent premature failure. Achieving a delicate balance in degradation kinetics requires a thorough understanding of the interplay between composition, processing conditions, and the surrounding biological environment.

The influence of processing techniques on the mechanical properties of bioactive glass adds another layer of complexity[41]. Factors such as sintering temperature, cooling rate, and particle size distribution can significantly impact the final mechanical characteristics of the material. Optimizing these parameters is essential to ensure uniformity and reproducibility in the mechanical performance of bioactive glass across different batches.

Moreover, the challenge of achieving sufficient mechanical interlocking with host tissues must be addressed. While the bioactivity of the glass facilitates bonding with bone, optimizing the mechanical interlocking at the implant-tissue interface is crucial for long-term stability and functionality. Surface modifications and the incorporation of bioactive particles are being explored to enhance the mechanical interlocking capability of bioactive glass implants.

An additional challenge lies in adapting the mechanical properties of bioactive glass to match the natural properties of bone. Bone is a complex tissue with a hierarchical structure, and replicating its mechanical behavior is essential for the long-term success of bioactive glass implants.

Achieving biomimicry in mechanical properties involves a deep understanding of the structure-function relationship in bone and translating these principles into the design of bioactive glass materials.

Furthermore, the challenge of ensuring compatibility with existing medical imaging techniques is vital [42]. The mechanical properties of bioactive glass should not compromise the accuracy of diagnostic imaging modalities such as X-rays or magnetic resonance imaging (MRI). Developing bioactive glass formulations that are both mechanically robust and compatible with common imaging techniques is an ongoing challenge in the field.

Optimizing the mechanical properties of bioactive glass presents a multifaceted challenge in the realm of biomaterials. Balancing bioactivity with mechanical strength, addressing brittleness, tailoring properties for specific applications, controlling degradation rates, optimizing processing techniques, enhancing interlocking with host tissues, achieving biomimicry, and ensuring compatibility with medical imaging are all critical aspects that researchers are actively addressing.

Overcoming these challenges will pave the way for the widespread use of bioactive glass in various biomedical applications, contributing to advancements in regenerative medicine, orthopedics, and dentistry. The fabrication of 45S5 scaffolds was pioneering however these macro porous scaffolds produced by sponge replication per brittle (compressive strength 0.3-0.4Mpa) were not suitable for implantation.

This is the limitation of 45S5 i.e it's poor sinterability. The mechanical properties of porous like bioactive scaffolds can improve by applying a polymer coating on the surface and the polymer acts as glue that holds by active particle together. The presence of hydroxyapatite coating allows the compressive strength of 45S5 tripling the untreated scaffolds' strength.<sup>(41)</sup> Recent strides in additive manufacturing techniques (AMTs) offer promise, producing porous bioactive glasses (BGs) akin to cancellous bone at a reasonable cost. AMTs excel in crafting hierarchical scaffolds from mesoporous BGs (MBGs), featuring a nano-porous texture (2-50 nm). Initial attempts relied on foaming or dipping a template into sol, yielding brittle structures (<1 MPa compressive strength). Substantial improvement is achievable.

Bioactive glasses shine in bone and tissue repair, bonding to both hard and soft tissues, promoting regeneration. Despite mechanical limitations—brittleness, low bending strength, and fracture toughness—bioactive glasses find application as coatings on metallic implants. This fusion capitalizes on metallic implants. This fusion capitalizes on the mechanical robustness of metal alloys and the bioactivity and biocompatibility of bioactive glasses.

Overcoming these challenges is crucial for the widespread use of bioactive glass in regenerative medicine, orthopedics, and dentistry. The pioneering 45S5 scaffolds, despite their initial promise, faced limitations due to poor sinterability, resulting in brittle structures unsuitable for implantation. Addressing this, a polymer coating acts as

a structural adhesive, elevating compressive strength to 1.5 MPa through hydroxyapatite coating.

Recent advancements in additive manufacturing techniques show promise in creating porous bioactive glasses comparable to cancellous bone. However, initial attempts resulted in brittle structures with insufficient compressive strength. Ongoing improvements aim to overcome these limitations and enhance the mechanical properties of bioactive glass scaffolds.

Bioactive glasses stand out for their ability to bond with both hard and soft tissues, stimulating regeneration. Despite mechanical drawbacks, they find application as coatings on metallic implants, leveraging the strength of metal alloys alongside the bioactivity of glass. The ongoing efforts to refine fabrication techniques and enhance mechanical properties underscore the potential of bioactive glass in revolutionizing biomedical applications.

#### *DISCOVERING FAST AND SIMPLE WAYS OF FABRICATION:*

The fast fabrication of bioactive glass presents a formidable challenge, primarily driven by the intricate balance required between speed, precision, and maintaining the desired bioactive properties. Bioactive glass, known for its ability to bond with living tissues, finds applications in various medical and dental fields, necessitating a swift and reliable production process. Several factors contribute to the complexity of this challenge, ranging from the intricacies of the synthesis methods to the need for consistent quality in the final product.

One prevalent method for bioactive glass fabrication is the sol-gel process, which involves the conversion of precursor solutions into a gel followed by high- temperature treatment. However, the challenge lies in achieving rapid gelation without compromising the compositional control essential for the desired bioactivity. Accelerating gelation often results in non- uniform structures or incomplete incorporation of bioactive ions, impacting the glass's overall performance. Researchers

grapple with optimizing reaction kinetics and precursor concentrations to strike a balance between speed and precision.

Moreover, the challenge extends to the subsequent heat treatment phase, where controlled crystallization is crucial. Hastening this step without sacrificing the quality of the crystalline structure poses significant hurdle. The balance between speed and crystal growth control is intricate, as rapid processing may lead to undesired phase transformations or uneven crystalline distribution, jeopardizing the glass's bioactivity and mechanical properties.

In the pursuit of rapid fabrication, researchers explore alternative techniques such as microwave-assisted synthesis. Microwave irradiation offers the advantage of accelerated heating, potentially reducing processing times. However, adapting conventional sol-gel chemistry to microwave conditions requires meticulous adjustments to avoid overheating and ensure homogenous bioactive ion distribution.

Achieving reproducibility and scalability in this context remains a persistent challenge.

Continuous flow processing emerges as another avenue to expedite bioactive glass fabrication. Unlike batch processes, continuous flow setups allow for real-time control of reaction conditions, potentially enhancing production speed. Nonetheless, establishing optimal parameters for continuous flow synthesis demands careful consideration of residence times, flow rates, and mixing efficiency to ensure consistent product quality. Overcoming challenges related to scalability and equipment compatibility further complicates the integration of continuous flow techniques into large-scale production settings.

Ultimately, the challenge of fast fabrication of bioactive glass underscores the intricate interplay between speed, precision, and product quality. Continuous advancements in synthesis techniques, coupled with a deep understanding of the underlying chemistry and physics, are imperative to overcome these challenges. As research in this field progresses, the development of streamlined and efficient fabrication methods for



bioactive glass holds the promise of revolutionizing medical and dental applications, providing faster access to advanced biomaterials with enhanced bioactivity.

#### *MULTIPLE PROPERTIES PERFORMANCE:*

Bioactive glass, a versatile material with applications in biomedical engineering, faces the intricate challenge of optimizing multiple properties to meet the diverse requirements of various medical applications. The concurrent pursuit of biocompatibility, mechanical strength, degradation rate, and bioactivity poses a complex dilemma for researchers and engineers.

One of the primary challenges is achieving a delicate equilibrium between biocompatibility and mechanical strength. Bioactive glass is intended for use within the human body, demanding a material that seamlessly integrates with biological tissues. However, this biocompatibility cannot come at the expense of mechanical integrity. Balancing the fine line between these properties requires meticulous material design, exploring compositional variations, and employing advanced manufacturing techniques.

The second challenge revolves around the degradation rate of bioactive glass. A material's ability to degrade over time is crucial for applications like bone regeneration, where gradual dissolution facilitates ion release, promoting osteogenesis. However, excessive degradation may compromise structural integrity, undermining the mechanical strength of the material. Striking the optimal degradation rate requires a deep understanding of the interplay between material composition, structure, and the surrounding biological environment.

Furthermore, the challenge extends to achieving a high level of bioactivity. Bioactive glass is celebrated for its ability to form a hydroxyapatite layer on its surface, promoting osseointegration. However, enhancing this bioactivity without compromising other

essential properties poses a significant hurdle. Researchers must explore novel formulations, surface modifications, and processing techniques to boost bioactivity while maintaining overall material performance.

The multifaceted challenge also involves considering external factors, such as sterilization methods and long-term stability. Bioactive glass intended for implantation must withstand sterilization processes without compromising its properties. Moreover, ensuring the long-term stability of the material within the body is critical, demanding comprehensive studies on degradation mechanisms and their implications over extended periods.

In overcoming these challenges, collaborative efforts among researchers, material scientists, and biomedical engineers are crucial. Advanced characterization techniques, computational modeling, and innovative synthesis methods play pivotal roles in unraveling the complexities associated with optimizing multiple performance properties. The iterative process of design, experimentation, and analysis becomes paramount in refining bioactive glass for diverse applications.

#### *FAST DEGRADABILITY:*

The fast biodegradability of bioactive glass poses a challenge due to its inherent stability. Bioactive glass, often composed of silica, calcium, and phosphorus, is designed for biomedical applications such as bone regeneration. While its bioactivity accelerates tissue integration, its slow degradation hinders optimal resorption and replacement by natural bone over time. The challenge lies in balancing the material's therapeutic benefits with the need for timely degradation. Researchers are exploring strategies to enhance the biodegradability of bioactive glass, such as modifying its composition or structure. Tailoring these aspects can influence dissolution rates enabling a more controlled and accelerated breakdown. Achieving fast biodegradability is crucial to ensure that the material supports tissue healing without lingering in the body for extended periods. This pursuit involves a delicate trade-off, demanding a nuanced understanding of material science and biological interactions to overcome the challenge and advance the effectiveness of bioactive glass in medical applications.

Bioactive glass for drug delivery poses a formidable challenge due to its inherent degradable nature within a biological environment. The intricacies of its biodegradation are intricately tied to both its composition and the pH of the surrounding environment. These factors wield significant influence over the amount of drug released during the biodegradation process. The delicate balance between maintaining structural integrity and achieving controlled drug release hinges on meticulous composition adjustments[43].

$0.45\text{P}_2\text{O}_5 - \text{XCaO} - (0.55 - \text{X}) \text{Na}_2\text{O}$ ;  $\text{X}=0.2, 0.3, 0.4 \text{ mol\%}$

Their result shows the drug released from the composite was strongly determined by the dissolution rate of glass.

In some cases we require less disintegration. One of the case is bioactivity coating where the disintegration rate of coating must be really slow or almost removed.

So that teeth coating cannot come off and it reduces the chance of corrosion to metal [44].

## **CHAPTER - 3**

### **4. CONCLUSION**

The revolution from conventional glass to bioactive glass represents a groundbreaking paradigm shift in materials engineering. Bioactive glass, designed to interact with biological systems, has transformed the landscape of medical applications. Its unique ability to form a bond with living tissues has propelled innovations in fields like orthopedics and dentistry. Unlike traditional glass, bioactive glass actively participates in biological processes, promoting tissue regeneration and integration. This transition has ushered in a new era of biomaterials, where the boundaries between inert materials and living organisms blur. The profound impact of bioactive glass is evident in its use for bone grafts, dental implants, and wound healing. Its biocompatibility and therapeutic potential have opened avenues for advanced medical interventions, contributing to enhanced patient outcomes. As we witness this revolution, the convergence of materials science and biomedicine paves the way for further discoveries, shaping a future where bioactive materials play a pivotal role in improving human health and well-being.

In summary we forecast a bright future for the use of Bioactive glasses in medica which will expand the glass age.



## 5. REFERENCES

1. C.R Kurkjain, W.R. Prindle (1998) Perspective on the history of glass composition. *Journal of American ceramic society* 81(4), 795-813.
2. Z. Li, P. Lu, G. Wang, J. Li, Z. Yan, Y. Ma, H. Wang (2023) Analysis of the composition of Ancient glass and its identification based on the Daen-LR, ARIMA-LSTM and MLR combined Process. *Journal of applied Science* 13(11) 6639.
3. N. Zuidhof, S. B. Alloch, O. Peters, P. P. Verbeek (2021) Defining Smart glasses: A Rapid Review of state-of-the-art perspectives and future challenges from a social science perspective. *Augmented Human Research* 6(1).
4. G. Jain, T. Sonkar, N. Kamar, N. Kumar (2019) A Study of Fiber glass Material with different compositions. *SSRN Electronic journal*.
5. B. Hlaváček, J. Šesták, L. Koudelka (1986) Some Thermodynamic aspects of the glassy state. *Thermodynamic Acta*, 95, 459-471.
6. Q. Wang, H. Chen, Y. Wang, J. Sun (2013) Thermal Shock effect on the glass thermal Stress response and crack propagation. *Procedia Engineering* 62, 717-724.
7. S. P. Mukherjee (1980) Sol-gel process in glass science and technology. *Journal of Non- Crystalline solids*, vol 42, 477-488.
8. E. Marin, F. Boschetto, G. Pezzotti (2020) Biomaterials and Biocompatibility: An historical overview. *Journal of biomedical material Research* 108(8), 1617-1633.
9. M.N. Rahaman, D. E. Day, B. S. Bal, Q. Fu, S. B. Jung, L. F. Bonewald, A. P. Tomsia (2011) Bioactive glass in Tissues Engineering. *Acta Biomaterials* 7(6) 2355-2373.

10. A. Polini, H. Bai, A. P. Tomsia (2013) Dental Application of nanostructured Bioactive glass and it's composites. *Wiley interdisciplinary reviews nanomedicine and nano-biotechnology* 5(4), 399-410.
11. Y. Lin, J. C. Mauro, G. Kaur (2019) Bioactive glasses for Cancer therapy. *Woodhead Publishing Series in Biomaterial*, 273-312.
12. O. S. Janjua, S. M. Qureshi, M. S. Shaikh, A. Alnazzauri, F. J. Rodriguez-Lozano, M. P. Pecci-Llorel, M. S. Zafar (2020) Autogenous tooth bone grafts for Repair and Regeneration of Maxillofacial Defects: A narrative review. *International Journal of Environmental Research and Public Health* 19(6): 3690.
13. K. Zheng, W. Niu, B. Lei, A.R. Boccaccini (2021) Immunomodulatory bioactive glasses for tissue regeneration. *Acto Biomaterial*, vol 133. 168-186.
14. L. Hench, J. R. Jones (2015) Bioactive glasses: Frontier and challenges. *Frontiers in Bioengineering and Biotechnology section biomaterial*, Vol 13.
15. H. E. Skallefold, D. Rokaya, Z. Khurshid, M. S. Zafur (2019) Bioactive glass Application in dentistry. *International journal of molecular sciences* 20(23): 5960.
16. J. N. Oliver, Y. Su, X. Lu, P. Kuo, J. Du, D. Zhuc (2019) Bioactive glass coatings on Metallic implants for Biomedical applications. *Bioactive Material*, Vol 14, 261-270.
17. M. Sohrabi, B. E. Yekta, H. R. Rezaie, M. R. Naimi-Jamal (2020) Enhancing mechanical properties and biological performance of injectable bioactive glass by gelatin and chitosan for bone small defect repair. *Biomedicines* 8(13): 616.

18. F. Baino, S. Hamzehloce, S. Kargozar (2018) Bioactive glasses: Where Are we and where are we going? *Journal of Functional Biomaterial* 9(1): 25.
19. L. P. Singh, S. K. Bhattacharya, R. Kumar, G. Mishra, U. Sharma, G. Singh, S. Ahalawat (2014) Sol-gel processing of silica nanoparticles and their application. *Advances in colloid and interface Science*, Vol 214, 17-34.
20. S. Mistry, D. Kundu, S. Datta, D. Basu (2012) Effect of Bioactive glass, hydroxyapatite and Bioactive glass hydroxyapatite composite graft particles in the treatment of infrabony defects. *Journal of Indian Society of Periodontology* 16(2), 241-246.
21. A. Balamarugan, G. Sockalingum, J. Michel, J. Fauri, V. Banchet, L. Wortham, S. Bouthors, D. Laurent-Maquin, G. Balossier (2006) Synthesis and Characterization of sol-gel derived Bioactive glass for Biomedical application. *Materials letter* 60, 3752-3757.
22. M. Tavonit, M. Dapporto, A. Tampieri, S. Sprio (2021) Bioactive Calcium Phosphate-Based Composites for Bone Regeneration. *Biomaterial Research*, article no. 4.
23. D. G. Filip, V. Surdu, A. V. Paduraru, E. Andronescu (2022) Current development in Biomaterial Hydroxyapatite and Bioglass for applications in biomedical field: A review. *Journal of Functional Biomaterial* 13(4): 248.
24. N. Al-Harbi, H. Mohammed, Y. Al-Hadeethi, A.S. bakery, A. Umar, M. A. Hussein, M. A. Abbassy, K. G. Vaidya, G. A. Berakdar, E. M. Mkawi, M. Nune (2021) silica-based Bioactive glasses and their Applications in hard tissues Regeneration: A review *pharmaceuticals (Basel)* 14(2): 75.
25. J. K. Christie, R. I. Ainsworth, S. E. Ruiz-Hernandez, N.H. De Leeuw (2005) Structure and properties of phosphate based bioactive glasses from computer simulation: A review. *Journal of material chemistry B*.

26. J. Lian, X. Lu, X. Zheng, Y. R. Li, X. Y. Geng, K. Sun, H. Cai, Q. Jai, H. B. Jiang, K. Lier (2023) Modification of titanium orthopaedic implants with Bioactive glass: A Systematic Review of in vivo and vitro studies. *Frontiers in Bioengineering and Biotechnology, sec. Biomaterial*, vol 17.
  
27. R. Nagasaki, K. Nagano, T. M. Lijima (2023) Synthesis and Characterization of Bioactive glass and zinc oxide nanoparticles with enamel remineralization and antimicrobial capabilities. *Materials (Basel)* 16(21): 6878.
  
28. S. Akhtach, Z. Tabia, M. Bricha, K. El Mubrouk (2021) Structural characterization in vitro bioactivity and antibacterial evaluation of low silver-Doped bioactive glasses. *Ceramics international*, vol 47, 29036-29046.
  
29. L. L. Dai, F. Nudelma, C. H. Chu, E. M. Lo, M. L. Mei (2021) The effect of strontium-Doped Bioactive glass and Fluoride on hydroxyapatite crystallization. *Journal of Dentistry*, vol 105, 103581.
  
30. Y. Li, X. Shui, L. Zhang, J. Hu (2015) Cancellous Bone healing around strontium doped hydroxyapatite in Osteoclastic rats previously treated with zoledronic acid. *Journal of biomedical material Research part B, applied biomaterials*.
  
31. J. R. Jones, D. S. Braver, L. Hupa, D. C. Greenspan (2016) Bioglass and Bioactive glass and their impact on healthcare. *International journal of applied glass Science*, vol 7, 423-434.
  
32. S. Kargozar, M. Montazerian, E. Fiume, F. Baino (2019) Multiple and promising application of strontium- containing bioactive glass in Bone tissue engineering. *Frontiers in bioengineering, biotechnology, sec- biomaterial*, Vol 7.



33. D. G. Gilliam, J. Y Tang, N. J. Mordan, H. N. Newman (2022) The effect of a novel Bioglass dentifrice on dentine sensitivity: a scanning electron microscopic investigation. *Journal of oral Rehabilitation*, Vol 29, 305-313.
34. M. Molenda, J. Kolmas (2023) The role of zinc in bone Tissue health and regeneration: A review *Biological Trace Element Research* 201(12): 5640-5651.
35. J. P. O'Connor, D. M. Teitelbau, S. S. Lin, J. A. Cottrell (2020) Zinc as a Therapeutic Agent in bone regeneration. *Material (Basel)* 13(10): 2211.
36. R. Borges, A. M. Pelosine, A. S. Souza, J. M. Junior, G. Z. Justo, L. F. Gamarra, J. Marchi (2022) Cancer-Targeted drugs challenges and opportunities in bone cancer treatment. *Journal of material* 15(24) 9082.
37. Z. Sun, D. Zhu, H. Zhao, J. Liu, P. He, X. Luan, H. Hu, X. Znang, G. Wei, Y. Xi (2023) Recent advance bioactive hydrogel for repairing spinal cord injury material design biofunctional regulation and application. *Journal of nano-biotechnology* 21, article no. 238.
38. I. Izquierdo- Barba, A. Salinas, M. Vallet-Regi (2013) Bioactive glasses: From Macro to Nano. *International journal of applied glass Science* 4(2).
39. B. J. Mcentire, B. S. Bal, M. N. Rahaman, J. Chevalier, G. Pezzotti (2015) Ceramics and ceramic coating in orthopaedic. *Journal of the European ceramic society*, vol. 35, 4327-4369.
40. F. Baino, E. Verñe (2017) Glass-based Coatings on biomedical implants: A state-of-the-art review. *Biomedical glasses* (3), 1-17.

41. L. Řehořek, Z. Chlup, D. Meng, D. M. Yunous, A. R. Boccaccini, I. Dlouhy (2013) Response of 45S5 Bioglass foam to tensile loading. *Ceramics international*, vol. 39, 8015-8020.
42. G. Kaur, V. Kumar, F. Baino, J. C. Mauro, G. Pickrell, I. Evans, O. Bretcanu (2019) Mechanical properties of Bioactive glasses, ceramic, glass-ceramics and composites: State off-the-art review and future Challenges. *Material Science and engineering C*, Vol. 104, 109895.
43. H. Kim, E. Lee, I. Jun, H. Kim, J. C. Knowles (2005) Degradation and drug release of phosphate glass/polycaprolactone biological composites for hard tissue regeneration. *Journal biomedical material Research part B applied biomaterials*.
44. R. Sergi, D. Bellucci, V. Cannillo (2020) A Comprehensive review of Bioactive glass coating: State of the art, Challenges and future perspective. *Journal of Coating* 10(8), 757.

# **Synthesis and characterization of lead Sulphide PbS thin Film**

## **PROJECT REPORT**

*Submitted in partial fulfillment of the  
requirements for the award of the degree of*

**MASTER OF SCIENCE**

**in**

**PHYSICS**

**By**

**Shivani**

(Regn. No. 8114-19-776)



**DEPARTMENT OF PHYSICS**

**SRI GURU TEG BAHADUR KHALSA COLLEGE, SRI ANANDPUR SAHIB**

(An Autonomous College)

**ANANDPUR SAHIB– 140118, PUNJAB (INDIA)**



SRI GURU TEG BAHADUR KHALSA COLLEGE, SRI ANANDPUR SAHIB  
(An Autonomous College)  
ANANDPUR SAHIB-140118, PUNJAB (INDIA)

### CERTIFICATE

It is certified that the work contained in the project report entitled "Synthesis and characterization of lead Sulphide (PbS) thin Film" is an original contribution by me and has not been submitted in part or full for any other degree at this or other University/ Institute.

The assistance and help received during the course of the thesis work have been acknowledged.

*Shivani*  
Shivani

Regn. No. 8114-19-776

I, the undersigned, Supervisor of Shivani, Regn. No.8114-19-776, a candidate for the degree of Master of Science, agree that the project report entitled, "Synthesis and characterization of lead Sulphide (PbS) thin Film", may be submitted in partial fulfillment of the requirements for the award of degree.

This is to certify that the above statement made by the candidate is correct to the best of my knowledge.

*Randeve Singh*  
**Dr. Randeve Singh**  
Head of Department  
Department of Physics  
S.G.T.B. Khalsa College  
Sri Anandpur Sahib

*DeepShikha*  
**Dr. DeepShikha**  
Assistant Professor  
Department of Physics  
S.G.T.B. Khalsa College  
Sri Anandpur Sahib  
Supervisor

*Kajal*  
**Prof. Kajal**  
Assistant Professor  
Department of Physics  
S.G.T.B. Khalsa College  
Sri Anandpur Sahib



## ACKNOWLEDGEMENT

I wish to thank the Principal **Dr. Jasvir Singh** of my college for permitting me to use all the facilities available in the institution for my project work. I would also thank to Head of the Physics Department **Dr. Randev Singh.**, the teacher faculty for their support in completing the work successfully.

I am grateful to my Guide **Dr. DeepShikha** for her encouragement, guidance and supervision of my project work during the semester. I'm extremely grateful for his motivating discussions while enable me to accomplish this task successfully. Without his active guidance, support and encouragement I would not have made headway in this project.

A special thanks to Prof. Kajal assistant professor at Sri Guru Teg Bahadur Khalsa College Sri Anandpur Sahib for the help and their valuable suggestions whenever I needed out of their busy schedule. I'm also thankful to my classmates and my friends who was directly or indirectly help me to complete this project report.

Anandpur Sahib

Shivani

## CONTENTS

Title	page no.
Abstract	5
Chapter-1 Introduction	6- 7
Chapter-2 Thin film deposition	8-21
2.1 Thin film	8
2.2 Growth of film and nucleation	9-10
2.3 Deposition techniques	11-16
2.4 why chemical bath deposition used?	17-18
Chapter -3 Characterization techniques	19-27
3.1 X-Ray diffraction	19-20
3.2 UV-Vis spectrometer	21-23
3.3 SEM	23-25
3.4 TEM	26-27
Chapter -4 Synthesis and characterization of lead Sulphide PbS thin Film	28-34
4.1 Introduction	28
4.2 Experiment	28-29
4.3 Result and discussion	30-34
4.4 Conclusion	34
References	35-36

### **Abstract:**

Thin films are everywhere in modern world with many of technologies depend upon daily life. The films are considered as backbone for advanced application in various field such as telecommunication devices, energy storage device, optical devices and so on. Thin films are deposited by physical deposition and chemical deposition. The thin film of lead Sulphide PbS was prepared by chemical bath deposition. Chemical bath deposition includes principle of chemical vapour depositions. The structural properties of thin films were studied by X-Ray diffraction (XRD) technique. The crystal size and strain values are calculating from data of X-Ray Diffraction.

- The peaks from XRD pattern of Pbs indicate its cubic structure.
- Crystallite size of PbS thin film and powder form was measured and found to be ~62.5nm and ~90.9nm respectively.
- From W-H plot we calculate the crystallite size and strain value.

## Chapter-1

### Introduction

Nowadays, most of technologies are used for minimizing the material into nano size as well as nano thickness. Research on nanocrystalline materials is due to their distinctive properties and future applications in semiconductor devices. They are used for study of semiconductor communication, integrated circuit, photoconductors, light emitting diode etc. Lead Sulphide (PbS) belongs to group IV-VI compound semiconductor. Due to their properties, research groups have shown great interest in study and development of material by various deposition techniques such as electrodeposition, spray pyrolysis, atomic layer deposition, spin coating method, sputtering, chemical bath deposition, SILAR method etc. Chemical bath deposition is presently attracting considerable attention, as it does not require advanced instrumentation.

Lead Sulphide is an inorganic compound with formula PbS. PbS also known as galena, it is most important ore and most important compound of lead. Galena is one of the most abundant widely distributed Sulphide.

Molecular formula: PbS

Molecular mass: 239.30g/mol

Melting point: 1118 °C

Boiling point: 1281 °C

Crystal structure: cubic





Crystal structure of PbS

### **Application of lead Sulphide: -**

Lead Sulphide is semiconductor material. It is oldest and common detection element material in various infrared detectors. It has been extensively used in optoelectronic devices working in infrared region. Lead Sulphide find application in following:

- Infrared detectors
- Photo optic applications
- Tunable near infrared detectors
- Solid state laser
- Biological sensing



## **Chapter-2**

### **Thin film deposition**

#### **2.1 Thin film:**

Thin film deposition is a process of depositing thin film coating on glass substrate. Whenever growth of material is only in two dimensions that third dimension is negligible to other dimensions, is called thin films. Thin film is a layer of material ranging from nanometer to several micrometers in thickness. Thin film deposition is an important manufacturing step in production of solid state and optoelectronic device. Thin films have directly or indirectly advanced in area of search in solid state physics which based on phenomena of thickness, geometry and structure of thin film. Thin films are used because their properties are different than bulk material. There are different properties of thin film such as optical, magnetic, electrical, thermal, chemical, mechanical properties. The properties of thin films are more affected by surface to volume ratio.

There are several methods used for deposition of thin film. Thin film deposition is mainly classified by physical and chemical methods. lead Sulphide thin film is prepared by both physical and chemical deposition. In physical deposition process electromechanical and thermodynamic methods are used to produce thin film. Physical deposition system requires low-pressure vapor environment to function properly. In chemical deposition technique, a fluid precursor undergoes chemical change at solid surface and leaving solid layer. Among all these chemical bath deposition methods was chosen for preparation of thin film because physical methods are costly and required advanced instrumentation.

Any thin film deposition method process involves three main steps:

1. Production of appropriate atomic, molecular species.
2. Transport of these species to substrate.
3. Condensation on substrate

## **2.2 GROWTH OF THIN FILM AND NUCLEATION**

The phenomenon of formation of a stable nucleus is called Nucleation. The initial process that occurs in the formation of a crystal from a solution, a liquid, or a vapor, in which a small number of ions, atoms, or molecules becomes arranged in a pattern characteristic of a crystalline solid, forming a site upon which additional particles are deposited as the crystal grows. There are two stages in the crystallization process: nucleation and growth.

In the first nucleation stage, a small nucleus containing the newly forming crystal is created. Nucleation occurs relatively slowly as the initial crystal components must impinge on each other in correct orientation and placement for them to adhere and form the crystal. After successful formation of a stable nucleus, a growth stage ensues in which free particles (atoms or molecules) adsorb onto the nucleus and propagate its crystalline structure outwards from the nucleating site. This process is significantly faster than nucleation. The reason behind such rapid growth is that crystals contain dissociations and other defects, which act as a catalyst for the addition of particles to the existing crystalline structure. By contrast, perfect crystals (lacking defects) would grow exceedingly slowly. Most often, the properties of the film are affected by the underlying properties of the substrate and can vary drastically depending on the thickness of the film and the deposition technique employed for deposition.

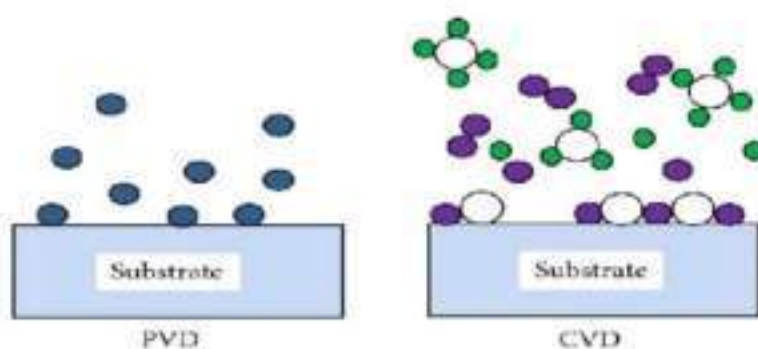
There are three major steps required in thin film growth and nucleation. The first step involves the creation of deposition species, i.e., the substrates and the target material, followed by the transportation from the target to the substrate using any deposition technique and the final stage involves the growth of the target on the substrate to form the thin film. A nucleus can grow in the two modes named parallel and perpendicular depending on the configuration of the substrates and target, and the two scenarios can be experienced in a single deposition. Parallel growth occurs on the substrate by surface diffusion of the absorbed atoms while perpendicular growth is because of direct impingement of the incident species. However, the rate of parallel growth is sometimes called lateral growth, at this stage is much higher than perpendicular growth and the grown nuclei are called islands.

## 2.3 Deposition techniques

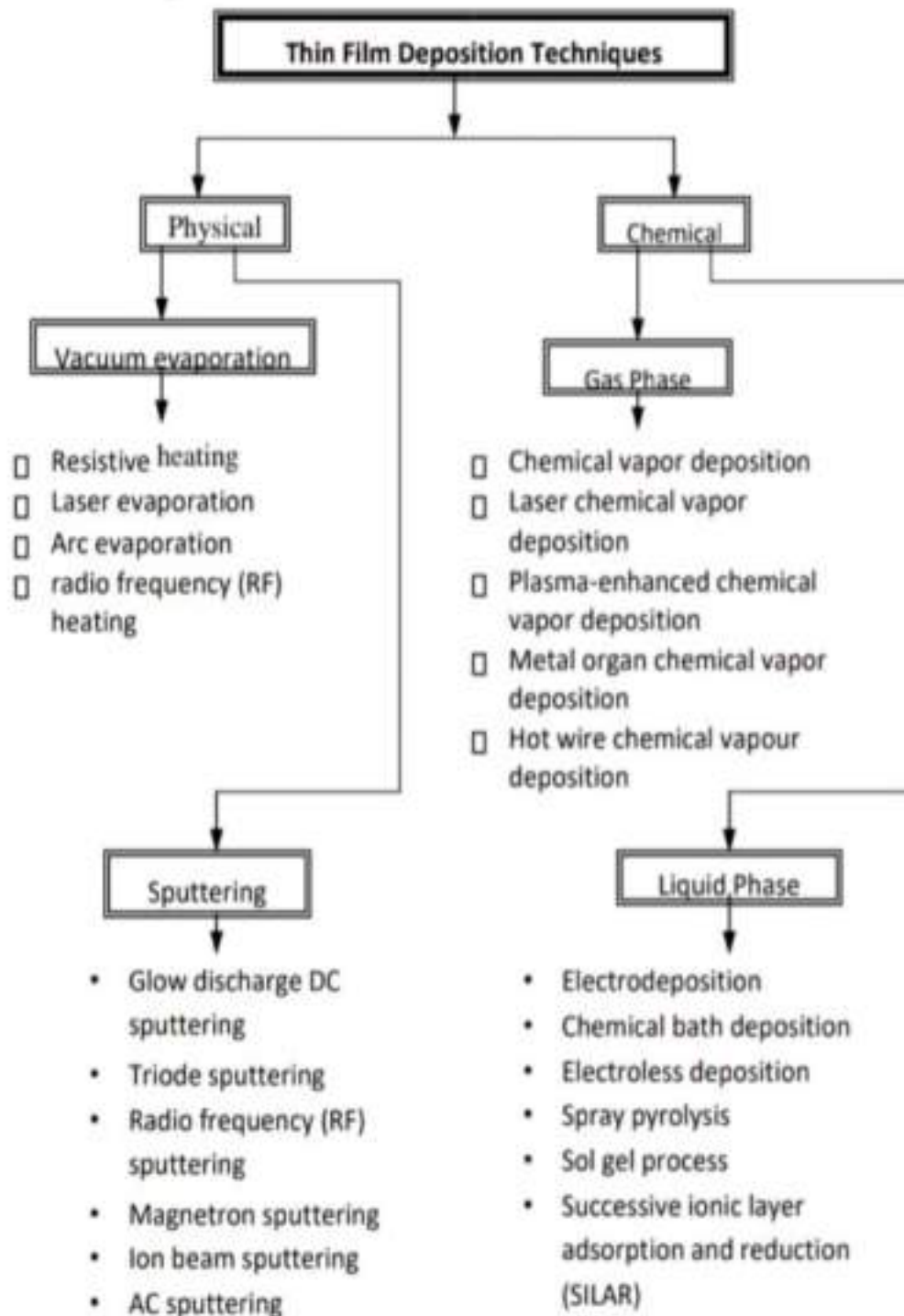
Thin films have distinct advantages over bulk material. Most of deposition techniques are used for formation of thin films. A deposition technique is considered as integral key for creation of thin film new materials due to increasing demand from industries for versatile and multi-dynamics materials. The deposition techniques all properties of thin film and can also be modify the existing properties. Combination of different techniques can also be used to form a hybrid deposition with each contributing to outcome of thin film. In the present time thin films can be fabricated in various method.

There are several types of thin film deposition techniques. The subset of deposition techniques are physical vapour deposition (PVD) and chemical vapour deposition (CVD). The distinguishing between PVD and CVD is in vapour. In PVD, the vapour is made up of atom and molecule simply in condense on substrate, and for CVD the vapour undergoes chemical reaction on substrate which resulted into thin film. Physical deposition system requires low-pressure vapor environment to function properly. In chemical deposition technique, a fluid precursor undergoes chemical change at solid surface and leaving solid layer.

In PVD uses physical processes and use pure source material while in CVD uses chemical process and mixed source material.







### **2.3.1 ELECTRODEPOSITION:**

Electrodeposition is widely utilized in making metallic coating. This technique is very old process which involve coating a thin layer of metal on top of different metal.it can be understood as extraordinary electrolysis resulting in deposition of solid material on electrode. This process involves

- Saturated solution of charged development species through arrangement when external electric field is applied.
- reduction of charge development species at growth and deposition surface which also such as electrode.

This process is also known as electroplating.

### **2.3.2 ELECTROLESS DEPOSITION**

In electroless deposition film of metal may deposit directly without any electrode potential being involved by suitable compound in solution. This is also called chemical reduction plating. In electroless deposition film can be grown on glass substrate by dipping them in appropriate solution of metal salt and reducing agent without any electric field. Deposition may occur by homogenous chemical reaction; reduction of metal ion in solution by reducing of metal ion in solution by reducing agent. There are three types of reaction take place:

- Noncatalytic reaction where types of substrates used.
- Catalytic reactions were used where film formation takes place on metallic substrates.
- Catalytic reaction using activator where deposition takes place with help of activate non catalytic surface.

### **2.3.3 CHEMICAL BATH DEPOSITION**

It is also called solution growth technique. CBD is method of deposition of thin film and nanoparticles is based on formation of solid phase from liquid solution. This

technique is easy. In CBD two steps are involved in formation of phase from precursors solution as formation of nucleation particle growth. The necessary step for precipitation is the formation of nucleation. The concept nucleation in solution is that molecules cluster form undergoes rapid decomposition and particles combine to form film on substrate. Formation of film also depends on deposition condition such as bath temp, stirring rate, ph. concentration of solution. Growth may occur through ion concentration of material. This technique is mostly used to prepare Chalcogenide (Sulphur, selenium etc.) film as well as metal oxide film

#### **2.3.4 SOL GEL METHOD:**

This technique is broadly used for synthesis of oxide material. Sol gel processing is high purity and uniform nanostructure achievable at low temperature. In this method molecule precursors are dissolved in water or alcohol and converted to gel by heating and stirring by hydrolysis. The gel we obtained from hydrolysis process is wet, it should be dried. After drying we get powdered and calcinated. The Sol gel method can be used in the process of making ceramics as molding material and used as intermediate by thin film of metal oxides in various application. A sol gel process involves formation of sol in liquid and then connecting sol particles to form porous network by drying liquid possible to obtained powder thin films.

#### **2.3.5 SPRAY PYROLYSIS METHOD:**

Spray coating technique may be one of the most useful coverings surfaces. In this method thin film is deposited by spraying solution on heated surfaces where constituent react to form chemical compound. Spray pyrolysis equipment consist of atomizer, precursor sol. Substrate heater and temperature controller. This technique involves spraying a metal salt solution onto a heated surface. Spray pyrolysis is a process in which nanostructure is obtained when a solution contained a precursor is spray using nano porous nebulizer on hot substrate in furnace. It is an aerosol process that atomizes a solution and heats the droplet to produce solid

particles. Pyrolysis means decomposition of chemical compound under action of heat at higher temperature

- Transform liquid precursor or sol precursor into ionized droplets.
- Making solvent to evaporate
- Allowing solute to condense
- Making solute decompose and react
- Sintering the solid particles

### **2.3.6 SILAR METHOD:**

SILAR is successive ionic layer absorption and reaction.

This is one of the most suitable for preparing semiconductor material. In Silar method thin films are obtained by immersing substrate into separately placed cationic and anionic precursor and rinsing between every immersion with ion exchanged bath. Rinsing time in ion exchange bath is critical for ionic layers formation.

- Immersion of substrate in cationic
- Immersion of substrate in distilled water
- Immersion of substrate in anionic
- Immersion of substrate in distilled water

### **2.3.7 SPIN COATING TECHNIQUE:**

This method has ability to quickly and easily produce very uniform films

- Deposition
- Spin up
- Spin off
- Evaporation

Initially solution is cast on to substrate using pipette, whether substrate is already spinning after deposition, the centrifugal motion will spread the solution across substrate. Most of the solutions are expelled from substrate. The fluid now begins to



thin film will change color due to interference effect, when color stops changing, this will indicate that film is mostly dry, fluid out of flow stops and thinning is dominated by evaporation of solvent.

### **2.3.8 ELECTRO BEAM EVAPORATION:**

In electron beam evaporation where intensive beam of electrons is generated from filament and steered through both electric and magnetic fields to hit target and vaporize it under vacuum environment. Thin film prepared by electron beam evaporation is good quality and purity. Large categories of materials can be prepared by electron beam evaporation technique. The electron system only heats the target source material, not the entire container resulting in lower degree of contamination from the container by concentrating energy on target rather than entire vacuum chamber, it helps reduce the possibility of heat damage substrate E-beam evaporation used in variety of application ranging from high performance aerospace and automobiles industries.

### **2.3.9 SPUTTERING:**

Sputtering is usually understood as sputter deposition. It is a physical vapors deposition process. It is the process of directing high energy ions to target in vacuum and remove target atoms. The deposition of these emitted atoms on surface is called sputter deposition. The requirement for sputtering deposition is ion beam and potential low pressure (less than 5m torr), good vacuum. Sputtering is a process in which particles are ejected from solid target materials due to bombarding of target by energetic particles. The kinetic energy of incident particles should be greater than thermal energy.

### **2.3.10 PULSED LASER DEPOSITION:**

It is a powerful method to grow thin films and multilayers complex material. It is technique where high power laser beam focused inside vacuum chamber to strike target of desired composition material is then vaporized from target as deposited

as thin film on substrate such as silicon wafer facing target. The process can occur in ultra-high vacuum or in presence of background gas such as oxygen which is commonly used when depositing oxide to fully oxygenated deposited films. The process of Pulse laser deposition can schematically be divided into four stages:

- Laser analysis of target material and creation of plasma.
- Dynamics of plasma under vacuum.
- Deposition of material on substrate.
- Nucleation and growth of film on substrate surface.

### **2.3.11 CATHODIC ARC DEPOSITION (ARC-PVD):**

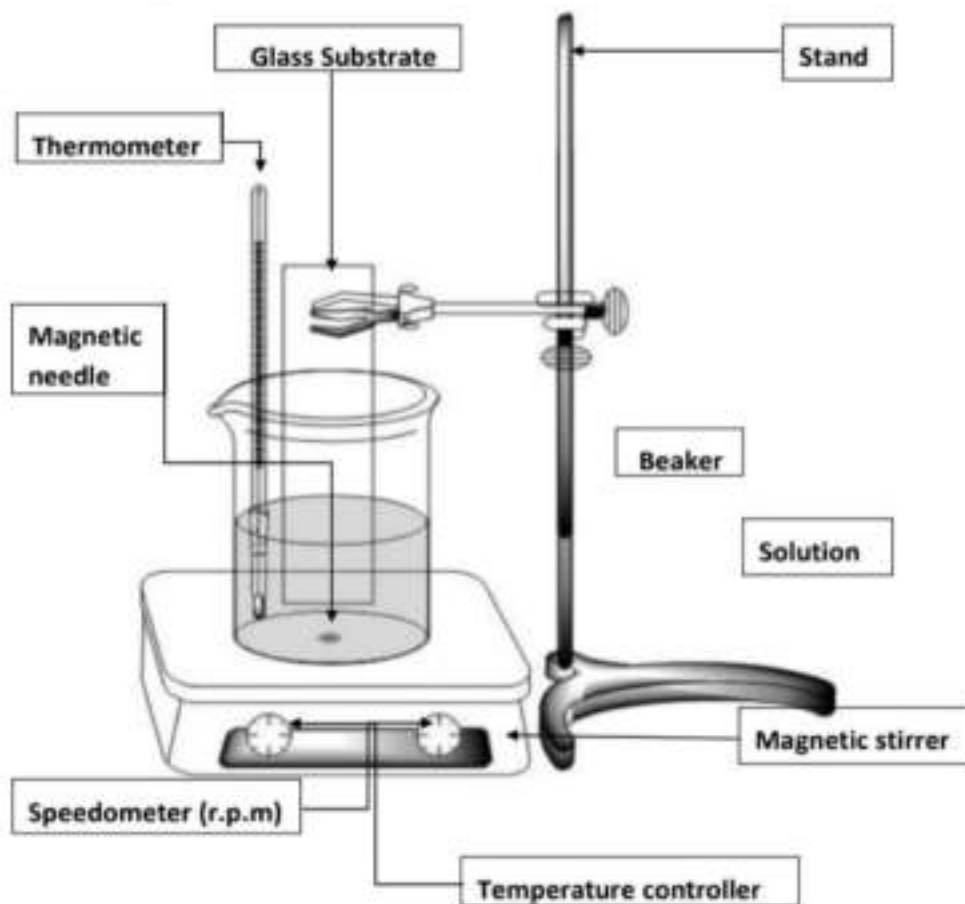
This is a physical vapor deposition technique in which an electric arc is used to vaporize material from a cathode target. The vaporized materials are then condensed on a substrate and form a thin film. This technique is being done to deposit metallic, ceramics, and composite films.

### **2.3.12 ELECTRO HYDRODYNAMICS DEPOSITION (ELECTRO SPRAY DEPOSITION):**

This is a relatively new process of film deposition. The liquid can be deposited either in the form of nanoparticles solution or simply a solution and it is fed to small capillary nozzle (usually metallic) which is connected to high power sources. The substrate on which the film will be deposited is connected to the ground terminal of the power source. Through the influence of electric field, the liquid comes out of the nozzles and takes a conical shape (Taylor cone) and at the apex of the cone a thin jet emanates which disintegrates into very fine and small positively charged droplets. The droplets keep getting smaller and smaller and finally get deposited on the substrate as a uniform thin layer.

## 2.4 Why chemical bath deposition?

This is chemical liquid phase method. Chemical bath deposition is one of the most suitable methods to get uniform, good reproducibility thin film. It is one of the cheapest methods to deposit thin film. As it does not depend upon expensive equipment and scalable technique that can be employed for large area batch processing or continuous deposition.



The major advantage of chemical bath deposition is that requires only solution container and substrate mounting device. The substrate is stirred with help of

magnetic stirrer. Water or paraffin bath with constant stirring are used to heat the chemical bath to desired temperature. In some case stirring is continuous from room temperature the beaker containing precursor. Solution and deionized water are alternately placed. Films produced by chemical bath deposition are used in semiconductor, photovoltaic cells and supercapacitor and there is increasing interest in using chemical bath deposition to create nanoparticles thin films.

### **Advantages of chemical bath deposition method**

- This method is presently attracting considered attention as it does not require an instrumentation like vacuum system other expensive equipment simple equipment like water bath with temperature indicator, magnetic stirrer, solution breaks used in this method. The starting chemical are commonly available and cheap with this method, large number of depositions of thin film can done with number of cycles. It is low cost-efficient methods and easy to scale up industrial purpose. They have advantages:
- low cost
- simplicity
- Uniformity
- controlled growth

### **USES:**

- I. Chemical bath deposition is used to deposit buffer layer in photovoltaic cells because chemical bath deposition does not damage substrate.
- II. Chemical bath deposition has possible application in antireflection, optical fiber, total reflector, LED, solar cells etc.
- III. Use in field of nanomaterials because properties of nanostructure of chemical bath deposition films can be precisely controlled because of uniform thickness, composition.



## **Chapter -3**

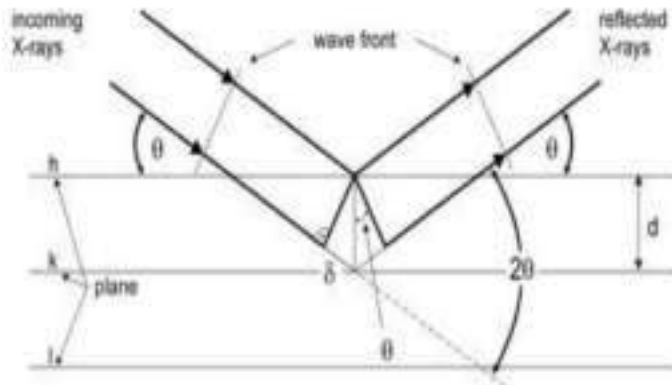
### **Characterization techniques**

Thin films are widely used in the electronic, optical and magnetic devices. In order to study different properties of these semiconducting materials in form of thin films. Various characterization techniques are used. These techniques include thickness measured structural morphology by X-Ray diffraction, surface morphology by scanning electron microscopy, optical absorption and transmission by UV visible spectrophotometer, electrical resistivity measurement etc.

#### **3.1 X-RAY DIFFRACTION (XRD)**

XRD is well known technique to obtain the information of composition, phase and crystalline orientation of material. It gives information about crystal structure, chemical composition and physical properties of material and thin film. This technique based on observing the scattering intensity of an X-Ray beam hitting a sample as a function of incident and scattered angle and, wavelength of energy. Interaction of incident ray with sample produce constructive when condition satisfy Bragg's law

$$n\lambda = 2d \sin \theta$$



$n$  = integer

$d$  = interplanar spacing

$\lambda$  = wavelength

$\theta$  = diffraction angle

It measures average spacing between layer of atoms, find structure of unknown materials. The different phase can be analyzed by X Ray analysis. It determines the orientation of single crystal or grain. X ray is generated in a cathode ray tube by heating filament to produce electron accelerating electron toward target by applying voltage and bombarding target material with electron have sufficient energy to dislodge inner shell electron of target material. Characteristics of X- Ray spectra are produced. As sample and detector are rotated intensity of reflected X-Ray is recorded when geometry of incident X -Ray satisfies. Bragg equation, constructive interface occurs and peak in intensity occur.

Application of X-Ray diffraction:

- Analysis of phase change under other special conditions such as temperature, humidity.
- Analysis of physical properties such crystallite size, orientations.
- Determination of unit cell dimension.
- Measurement of sample purity.

### 3.2 UV-Vis Spectroscopy

It involves the spectroscopy of photons and spectrophotometer. It uses the light in visible and adjacent near ultraviolet and near infrared ranges. It refers absorption spectroscopy and reflectance spectroscopy in ultraviolet region. UV-Vis spectroscopy is an analytical method which used to measure sample quantity depending on the amount of light received by analyte. UV-Vis measurement span wavelength from 200 nm -800 nm. This technique is suitable for a large spectrum of organic compounds and some inorganic species. UV-Vis spectroscopy is used in qualitative determination of solution in transmission metal ions and highly conjugated organic compounds.

- 1) Solution of transmission metal ion can be colored with electrons within the metal atoms can be excited from one electronic state to another.
- 2) Organic compounds also absorb light in UV or visible region of electromagnetic spectrum solvents.
- 3) While charge transfer complexes also give rise to color are often too intense to be used for qualitative measurement.

The instrument used in UV-spectroscopy is called UV-Vis spectrophotometer. It measures the intensity of light passing through the sample ( $I$ ), and compare it to intensity of light before it passes through the sample ( $I_0$ ). The ratio of  $I/I_0$  is called *Transmittance* and it is expressed as percentage. The absorbance  $A$  is expressed as Beer's law:

$$A = \log(I/I_0)$$

The optical bandgap of material is a very important parameter to determine the applications of thin films. It is evaluated using formula:

$$\alpha = [A/h\nu](h\nu - E_g)^n$$

where  $\alpha$  is absorption coefficient,  $A$  is parameter depends on transition probability,  $\nu$  is frequency of incident beam,  $h$  is planks constant,  $h\nu$  is photon energy. The plot of  $\alpha^2$  versus  $h\nu$  with extrapolation gives the straight-line portion of to zero absorption coefficient gives the band gap energy.

The spectrophotometer consists of light source (deuterium arc lamp in UV), a sample holder, diffraction grating and detector. These detectors are typically photodiode or CCD (silicon based multichannel array detector of UV, visible

And near infrared light). Photodiode are used with monochromatic which filter the light so that only light of single wavelength reaches the sample difference grating are used with CCD's which collect light of different wavelength on different pixels.

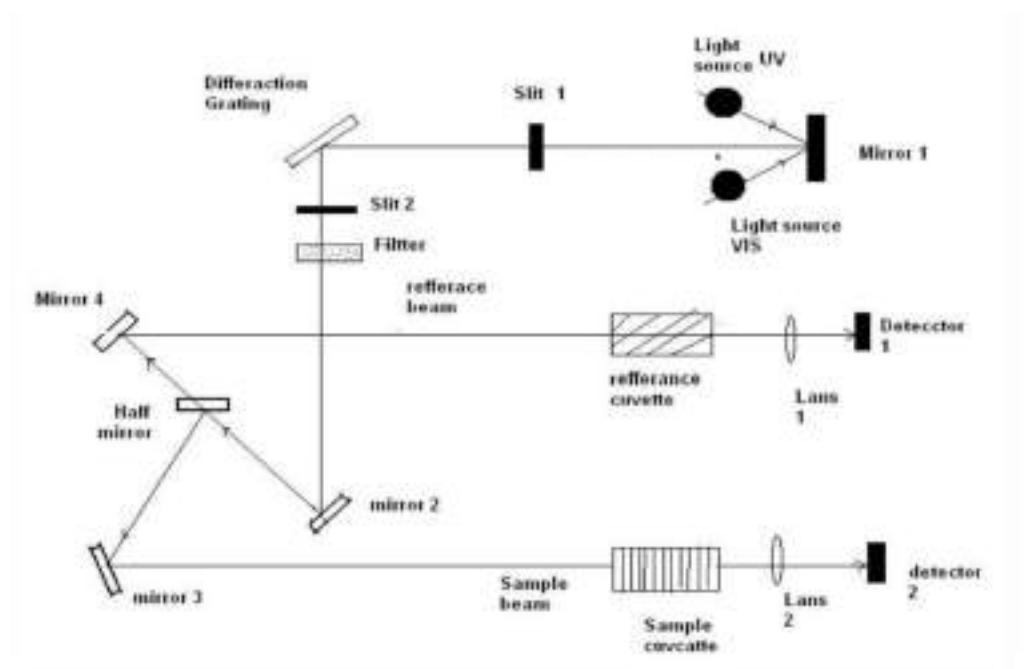


Fig: Block diagram of UV-Vis spectrophotometer

Applications of UV-Vis spectroscopy:

1) Detection of impurity

- It is best method for determination of impurities in organic molecules.
- Additional peaks can be observed due to impurities and it can be compared with that of standard raw material.



- 2) It is useful in structural explanation of organic molecules, such as in detecting presence and absence of unsaturation and presence of hetero atoms.
- 3) It can be used for qualitative determination of compound that absorb the UV radiation.
- 4) This technique is used to detect the presence of functional group in compound.
- 5) Kinetic of reaction can be studied using UV spectroscopy.
- 6) Molecular weight of compounds can be measured spectrophotometrically by preparing suitable derivative of these compound.
- 7) UV spectrophotometer may be used as detector for HPLCs

### **3.3 SEM (SCANNING ELECTRON MICROSCOPY)**

A scanning electron microscope is type of electron microscope that produces image of sample by scanning it with focused beam electrons. The electron interacts with atoms in sample, producing various signals that can be detected and contain information about the samples surface topography and composition. The electron beam is generally scanned in roaster scan pattern, and the beams position is combined with detected signal to produce image.

- SEM can achieve resolution better than 1 nanometer. It provides precise control over the degree of magnification because it uses electromagnets rather than lenses.
- The SEM allowed researchers to study a much variety of specimens.
- Scanning electron microscopes have development new areas of study in the medical and physical science communities.
- Specimen can observe in high vacuum, in low vacuum, in wet condition and at a wide range of elevated temperature.

When beam of electrons strikes the surface and specimen and interact with the atoms of sample signals in the form of secondary electrons, back scattered electron and characteristics X-rays are generated that contain information about the sample's surface topography, composition, etc. The SEM can produce a high-

resolution images of sample surface, revealing detail about 1-5 nm in its primary detection mode i.e. secondary electron imaging.

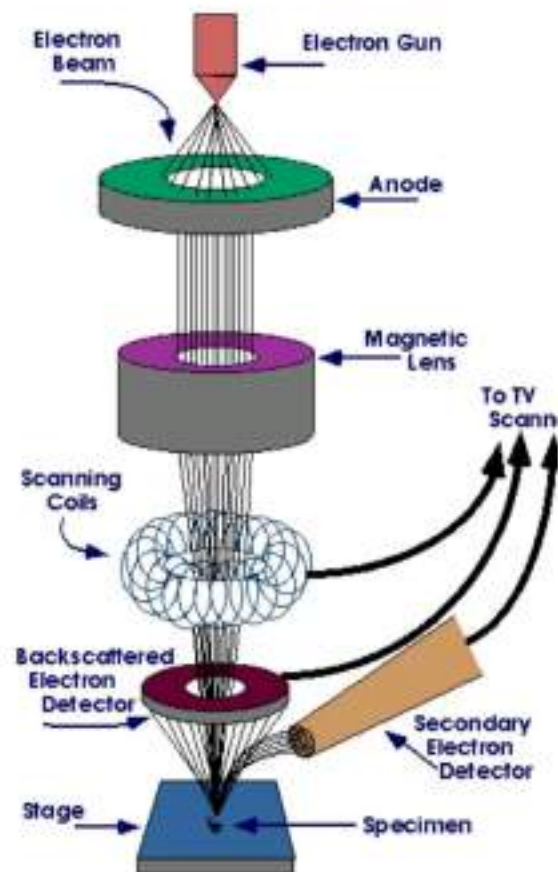


Fig: schematic diagram of scanning electron microscope

When electron beam hits the surface of sample, it penetrates the sample to depth of few microns depending on the accelerating voltage and the density of the sample. The three types of signals produced by SEM include secondary electrons, backscattered electrons and characteristic X-rays. Secondary electrons are electrons that interact with the top surface of the sample. Backscattered electrons are generated from elastic and inelastic collisions.

between electron and the atoms within the sample. The energy of the characteristics X-ray can be captured by Electron-dispersive X-rays spectrometer to qualitatively analyze the chemical character of the sample.

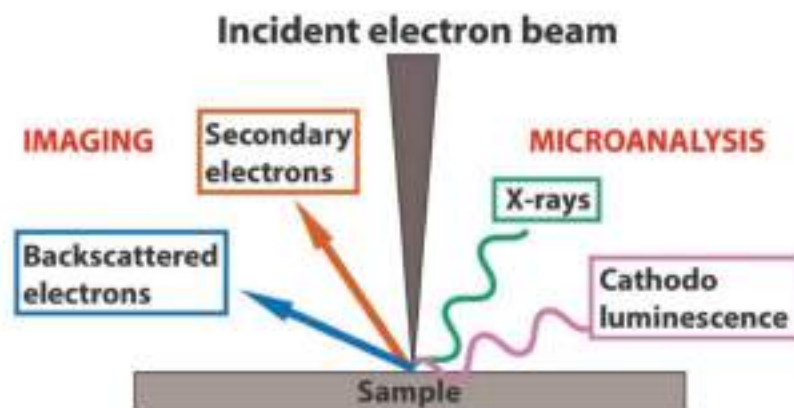


Fig: types of interaction of incident beam in SEM

The spatial resolution of SEM depends on size of electron spot, which in turn depends on both the wavelength of electrons and electron-optical system that produce the scanning beam. The resolution is also limited by size of interaction volume, volume of specimen material that interacts with electron beam.

### Application of SEM:

- Image morphology of sample
- Image compositional and some bonding difference
- Generate X-ray from sample for micro analysis
- Scanning electron microscopes are essential in quality control process.
- It is used to analyze filament bulb at traffic accident side.
- They are supporting development of nanowires by improving fabrication method.
- SEMs have practical, industrial and technological applications such as semiconductor inspection and assembly of microchips in computers.

### 3.2.4 Transmission electron microscopy (TEM)

Transmission electron microscopy is good complementary technique to XRD for evaluating the crystallography of materials using high electron beam ( $>200\text{keV}$ ). A high energy beam of electron is shone through a very thin sample, and interaction between electron and the atoms can be used to observe feature such as crystal structure. TEM can be used to study the growth of layer, their composition and defect. It is one of the most powerful microscopes with respect to its magnification and resolution, it is applied in wide range of applications can be utilized in variety of different scientific, educational and industrial fields.

The TEM operates on the same basic principle as light microscope but uses electrons instead of light. Because wavelength of electron is much smaller than that of light. TEM can reveal finest details of internal structure.

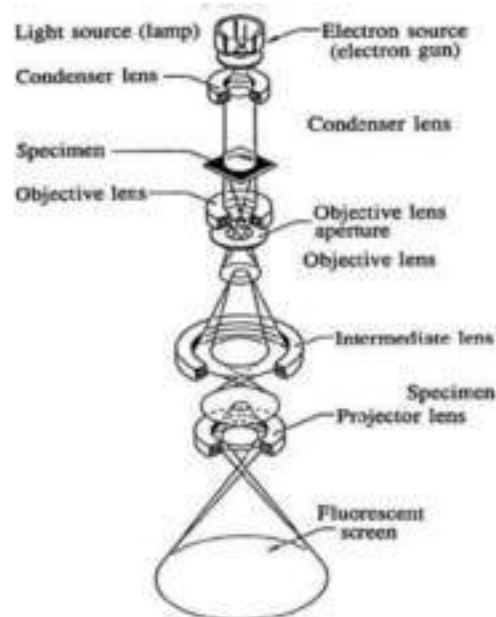


Fig: schematic diagram of transmission electron microscopy

In transmission electron microscope the electron gun, fires a beam of electrons. The gun accelerates the electrons to extremely high-speed using electromagnetic



coils and high voltage. The electron beam is focused into a thin, small beam by condenser lens has a high aperture that eliminates high angle electrons. The beam then strikes the specimen and part are transmitted depending upon thickness and electron transparency of specimen. The objective lens focuses the portion of the beam that is emitted from sample into an image. Another component of TEM is vacuum system. The transmitted portion is focused by objective lens into an image on phosphorous screen or charged coupled device (CCD) camera. The darker area of image represents those area of sample that fewer electrons are transmitted through while the lighter area of image represent those areas of sample that more electrons were transmitted through. The image produced by TEM, called micrograph.

### **Applications of TEM:**

It can be used for study of:

- Cancer research
- Semiconductor research
- Electronic structure
- Crystal orientation
- Chemical identity

## **Chapter-4**

### **Synthesis and characterization of lead Sulphide PbS thin Film**

#### **Introduction**

Research on nanocrystalline materials is due to their distinctive properties and future applications in semiconductor devices. They are used for study of semiconductor communication, integrated circuit, photoconductors, light emitting diode etc. lead Sulphide (PbS) belongs to group IV-VI compound semiconductor with its smaller band gap. PbS also low -toxicity and cost-effective materials. These properties indicate uses of PbS in solar cells, IR detector material ,photothermal conversion of solar energy, For these reasons many search groups have shown great interest in study and development of material by various deposition techniques such as electrodeposition, spray pyrolysis atomic layer deposition ,spin coating method ,sputtering, chemical bath deposition ,SILAR method etc. Chemical bath deposition is presently attracting considerable attention, as it does not require advanced instrumentation. It is relatively inexpensive, easy to handle, large area deposition, capable of good quality thin film. The characteristics of chemical bath deposited PbS thin film depend upon growth conditions.

#### **Experiment:**

With help of chemical bath deposition (CBD) method thin film of polycrystalline lead Sulphide deposited on the glass slab. The glass substrate degreased in hydrochloric acid solution (200ml deionized water and 100ml HCl) for 24 hours and then cleaned in chromic acid solution. Finally rinsed in deionized water and dry in air. Cleaning of glass slab due to remove hydrocarbons and other particle from glass slab. The bath was prepared by sequential addition of 5ml of 0.5M lead acetate anhydrate, 5ml of 2M sodium hydroxide, 6ml of 1M thiourea and 2ml of 1M triethanolamine. Deionized water was used to make up solution of 100ml in beaker. The solution was stirred before substrate was clamped vertically into bath. The

solution was transferred to 25ml glass beaker. Pre cleaned glass substrate were inserted and inclined at  $90^\circ$  with wall of beaker. The temperature of solution growth was  $30^\circ - 37^\circ$  celcius. The pH of mixture was nearly 11. The whole setup was allowed to stand for 5-6 hours. Thereafter substrate coated PbS was removed and dried in air and then dried in oven.



*Fig4.1: Experimental arrangement for deposition of PbS thin film by chemical bath deposition*

## Result and Discussion



Fig4.2.1: lead Sulphide (PbS) thin film by chemical bath deposition



Fig4.2.2: lead Sulphide (PbS) powder



## X-Ray Diffraction

X-Ray diffraction is the powerful and non-destructive technique for characterizing crystal material. Structural characterization was carried out with the help of XRD. XRD pattern of PbS thin film deposited by chemical bath deposition. The XRD pattern were collected with XPERT-PRO diffraction pattern. The intensity of diffracted x-rays measured as function of diffraction angle. The intensities of the spots provide information about the atomic basis. The sharpness and shape of spots are related to the perfection of crystal. The structure of material can be obtained from plot between intensity vs diffraction angle. The diffraction peaks provide the information about lattice plane and crystal structure. In fig (4.3.1) and (4.3.2) shows XRD spectra of lead Sulphide thin film and powder form respectively. All the diffraction peaks (111), (200), (220), (311), (222) are matched to standard data. So, it is confirmed that formation of PbS takes place cubic structure.

The Full Width Half Maximum (FWHM) ( $\beta$ ) can be related to strain ( $\epsilon$ ) and crystallite size (D) as:

$$\beta(\cos\theta)/\lambda = 1/D + \epsilon(\sin\theta)/\lambda$$

The plot of  $\beta(\cos\theta)/\lambda$  vs  $\sin\theta/\lambda$  are shown in Fig. 4.4.1 and 4.4.2. The reciprocal of the intercept on y axis in these graphs provides particle size, and the slope of graph will give strain value. The plot of  $\beta(\cos\theta)/\lambda$  vs  $\sin\theta/\lambda$  known as W-H plot. Williamson and Hall proposed this method for obtaining size and grain. The size and strain graph of lead Sulphide thin film and powder form are shown in fig (4.4.1) and (4.4.2) respectively. From these graphs we find the particle size and strain value.

Dislocation density denotes the number of dislocation line per unit volume of crystal, which is size of crystal defects possessed by a crystal. In other words, the dislocation value will illustrate the degree of crystallinity of nanoparticles.

$$\delta = 1/D^2$$

small dislocation density had high degree of crystallite.

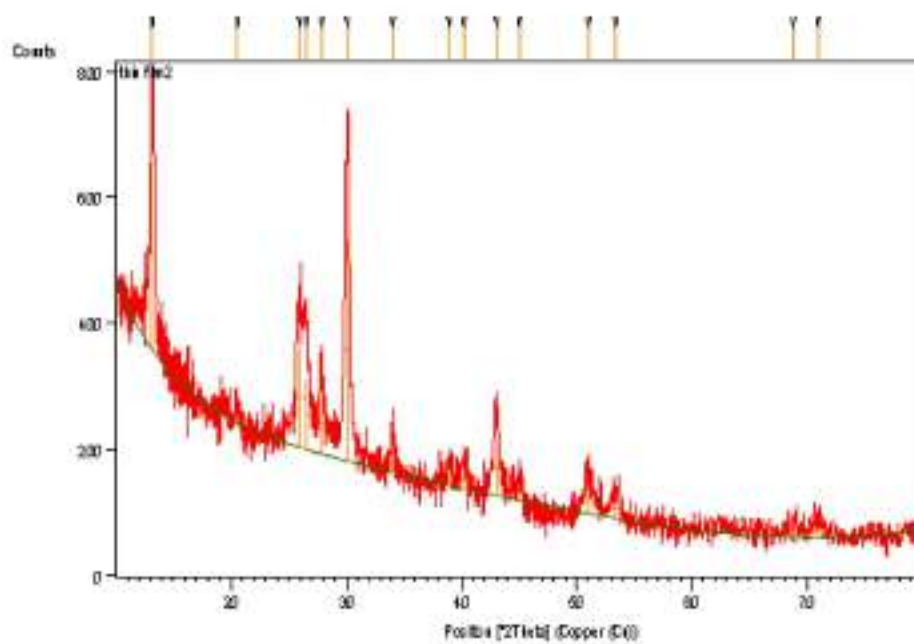


Fig4.3.1: XRD spectra of lead Sulphide thin film

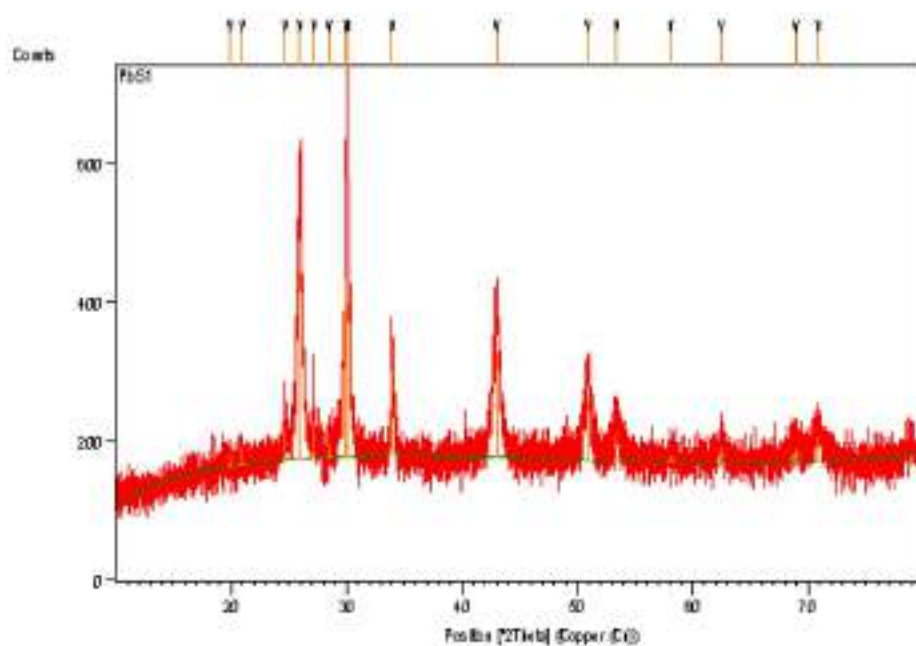


Fig4.3.2: XRD spectra of lead Sulphide powder

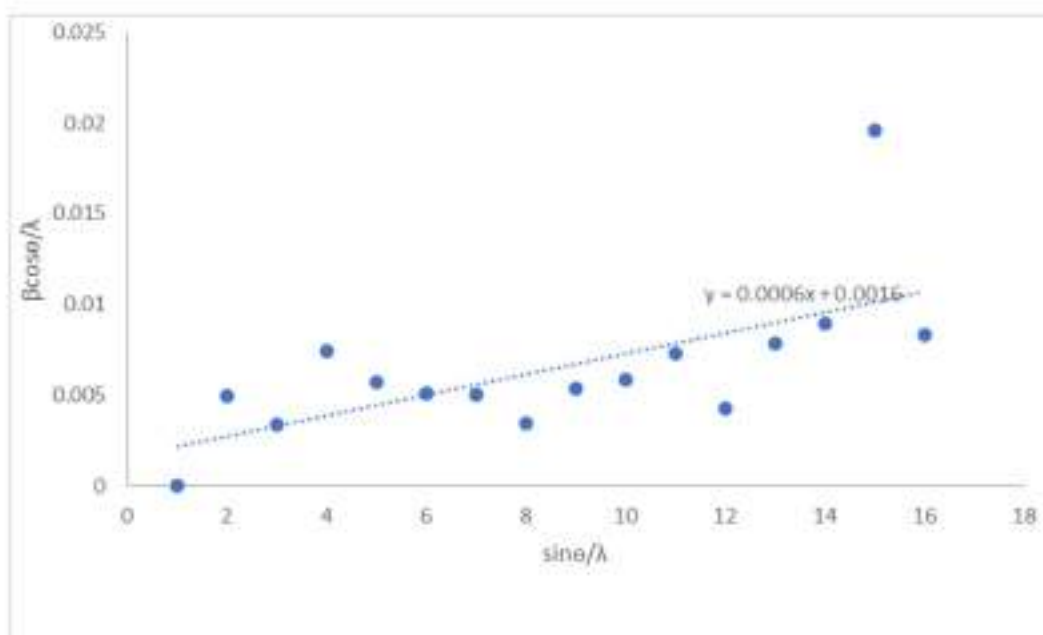


Fig4.4.1: size and strain graph of PbS thin film

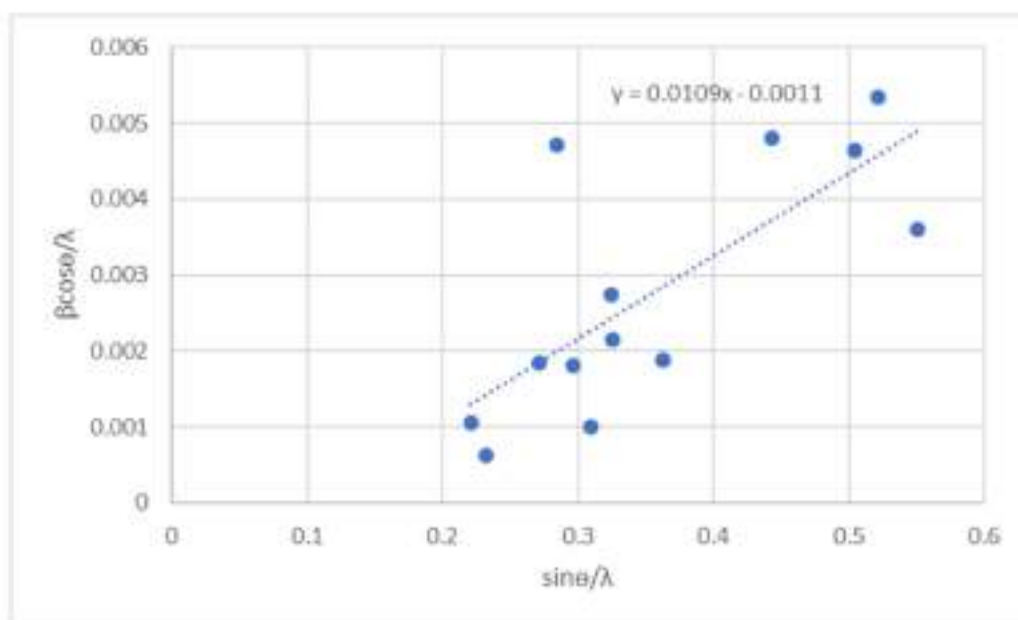


Fig4.4.2: size and strain graph of PbS powder

Type of material	Particle size(nm)	Strain ( $\epsilon$ )	Dislocation density( $m^{-2}$ )
PbS thin film	62.5	$6 \times 10^{-4}$	$2.56 \times 10^{14}$
PbS powder	90.9	$1 \times 10^{-2}$	$1.21 \times 10^{14}$

## Conclusion

In this, PbS Thin films can be successfully deposited by chemical bath deposition method. Structural characterization was carried out with the help of XRD. The XRD pattern were collected with XPERT-PRO diffraction pattern.

- XRD confirms the cubic structure of lead Sulphide.
- The particle size of PbS thin film  $\sim 62.5$  nm and particle size of PbS powder is  $\sim 90.0$  nm.
- The strain value for PbS thin film and powder forms are found to be  $6 \times 10^{-4}$  and  $1 \times 10^{-2}$  respectively.
- The Dislocation density of PbS thin film and powder form are found to be  $2.56 \times 10^{14} m^{-2}$  and  $1.21 \times 10^{14} m^{-2}$  respectively.
- Size of particle of thin film and powder are different due to surface area to volume ration increase. The confinement effect resulting from decrease in crystal size in grown nanocrystalline sample is responsible for blue shift.
- Lead Sulphide thin film have many applications in solar cell and photovoltaic cells.



## References

1. K. P. Bhandari, P. J. Roland, H. Mahabaduge, N. O. Haugen, C. R. Grice, S. Jeong, T. Dykstra, J. Gao, R. J. Ellingson, *Sol. Energy Mater. Sol. Cells* 117 (2013) 476.
2. M. S. Ghamsari, M. K. Araghi, S. J. Farahani, *Mater. Sci. Eng., B* 133 (2006) 113.
3. A. M. Malyarevich, M. S. Gaponenko, V. G. Savitski, K. V. Yumashev, G. E. Rachkovskaya, G. B. Zakharevich, *J. Non-Cryst. Solids* 353 (2007) 1195.
4. S. Seghaier, N. Kamoun, et al. *Mater. Chem. Phys.* 97 (2006) 71.
5. Y. Gülen, M. Alanyalıoğlu, K. Ejderha, Ç. Nuhoğlu, A. Turut, *J. Alloys Compd.* 509(6)(2011) 3155.
6. B. Thangaraju, P. Kaliannan, *Semicond. Sci. Technol.* 15 (2000) 849–853.
7. K.C. Preetha, T.L. Remadevi, *Mater. Sci. Semicond. Process.* 24 (2014) 179.
8. Y. Dong, J. Wen, F. Pang, Z. Chen, J. Wang, Y. Luo, G. Peng, T. Wang, *Appl. Surf. Sci.* 320 (2014) 372.
9. N.R. Mathews, C. Á. Chávez, M.A. Cortés-Jácome, J.A. Toledo Antonio, *Electrochim. Acta* 99 (2013) 76.
10. T. Tohidi, K. J. Ghaleh, A. Namdar, R. A. Ghaleh, *Mater. Sci. Semicond. Process.* 25(2014) 197.
11. B. Altıokka, M. C. Baykul, M. R. Altıokka, *J. Cryst. Growth* 384 (2013) 50.
12. Livage J, Ganguli D. Sol-gel electrochromic coatings and devices: A review. *Sol. Ener. Mater. Sol. Cells.* 2001;68: 365-381.
13. Mane RS, Lokhande CD. Chemical bath deposition method for metal chalcogenide thin films. *Mater. Chem. Phys.* 2011;11(2): 117-161
14. Hammad AH, Elmandouh ZS, Elmellegi HA. Structure and some physical properties and chemical properties of film In : Processing of 4<sup>th</sup> international Congress APMAS 2014; 901-903
15. Mahan JE (2000) physical vapour deposition of thin films ,Wiley –VCH
16. Wasa K, Hayakawa S(1992) Handbook of sputter deposition technology ,Noyes publication
17. Wasa K Kitabatake M, Adachi H (2004) Thin film processes , Norwich,Ny: Willian Andrew Publishing 17-69

18. T.Yamamoto H. Igarashi,K. Okazaki,J Am.Ceram. soc.,66(1983) 363-365
19. Seghair , S; kamoun N.;Brini , R.; Amara A.B. Structural and optical properties by chemical bath deposition .Mater. Chem .Phys.2006,97,71-80
- 20.Obaid, A.S; Mahdi,M.A.; Zainuraih,H. Mater.Res.2013,620,1-6
- 21.Mohammad G.Faraj and HaloD.Omer properties of thin fil (2014)2-3

**INVESTIGATIONS OF SHIELDING PROPERTIES OF  
LEAD-ZIRCONATE-TITANATE BASED GLASS**

**PROJECT REPORT**

*Submitted in partial fulfillment of the  
requirements for the award of the degree of*

**MASTER OF SCIENCE**

**in**

**PHYSICS**

*By*

**Ritika**

**Regn. No. 8114-19-1029**



**DEPARTMENT OF PHYSICS  
SRI GURU TEG BAHADUR KHALSA COLLEGE, SRI  
ANANDPUR SAHIB  
(An Autonomous College)  
ANANDPUR SAHIB– 140118, PUNJAB (INDIA)**



**SRI GURU TEG BAHADUR KHALSA COLLEGE, SRI ANANDPUR SAHIB**  
(An Autonomous College)  
**ANANDPUR SAHIB-140118. PUNJAB (INDIA)**

---

## **CERTIFICATE**

It is certified that the work contained in the project report entitled **“INVESTIGATIONS OF SHIELDING PROPERTIES OF LEAD-ZIRCONATE-TITANATE BASED GLASS”** is an original contribution by me and has not been submitted in part or full for any other degree at this or other University/ Institute.

The assistance and help received during the course of the thesis work have been acknowledged.

**Ritika**

Regn. No. **8114-19-1029**

I, the undersigned, Supervisor of **Ritika, Regn. No. 8114-19-1029**, a candidate for the degree of **Master of Science**, agree that the project report entitled, **“INVESTIGATIONS OF SHIELDING PROPERTIES OF LEAD-ZIRCONATE-TITANATE BASED GLASS”**, may be submitted in partial fulfillment of the requirements for the award of degree.

This is to certify that the above statement made by the candidate is correct to the best of my knowledge.

**Supervisor**

**Dr. Amrit Singh**

Assistant Professor

Department of Physics

Sri Guru Teg Bahadur Khalsa College

Sri Anandpur Sahib



## ACKNOWLEDGEMENT

Firstly, I had like to express my gratitude to my Supervisor, Dr. Amrit Singh Assistant Professor at Department of physics Sri Guru Teg Bahadur Khalsa College Sri Anandpur Sahib, who has resourcefully guided me throughout this research project. I'm extremely grateful for his motivating discussions while enable me to accomplish this task successfully. Without his active guidance, support and encouragement I would not have made headway in this project.

I also thankful to my Parents for their moral support and suggestions to improve the dissertation work. I'm also thankful to other faculty members in the department for their encouragement and fruitful academic discussions.

A special thanks to Ms. Monika Sharma Assistant Professor at Department of Physics for the help and their valuable suggestions whenever I needed out of their busy schedule. I'm also thankful to my classmates and my friends who was directly or indirectly help me to complete this project report.

Ritika

## ABSTRACT

The Gamma ray shielding parameters using WinXcom computer software have been investigated with change in lead doping in the glass structure. Accordingly, the influence of lead on the Gamma ray shielding properties of lead Zirconium titanite glasses  $xPbO:14TiO_2:16ZrO_2:(40 - 0.5x)B_2O_3:(40 - 0.5x)SiO_2$ , ( $x = 0, 10, 20, 30, 40$ ) was examined using WinXcom computer software. Several significant radiation shielding parameters were evaluated. The ceramic density was increased from 5.5102 to 7.6003 g/cm<sup>3</sup> with increasing lead content.

At each energy within the spectrum of interest in this research MAC generally trends in the order that (S1) MAC<(S2) MAC<(S3) MAC<(S4) MAC<(S5) MAC. The maximum and minimum values of LAC were obtained at 15KeV and 8MeV respectively with values of 30.93 and 0.074 cm<sup>-1</sup>; 111.54 and 0.108 cm<sup>-1</sup>; 175.19 and 0.133 cm<sup>-1</sup>; 249.21 and 0.167 cm<sup>-1</sup>; 322.08 and 0.201 cm<sup>-1</sup> for S1 to S5 respectively. The minimum and maximum values of HVL were obtained at 15KeV and 8MeV respectively with values of 0.022 and 8.55 cm; 0.066 and 6.52cm :0.004 and 5.60 cm :0.003 and 4.58 cm :0.002 and 3.89 cm for S1 to S5 respectively. The maximum and minimum values of Z effective were obtained at 15 KeV and 8 MeV respectively with values of 20.64 and 10.81; 47.46 and 15.40; 58.75 and 20.06; 64.98 and 24.82; 68.93 and 29.67 for S1 to S5 respectively. The trend of variation of electron density N effective as a function of photon energy for BZT ceramic is S1>S2>S3>S4>S5 for all photon energy range 0.015 MeV to 15 MeV.

# CONTENTS

CHAPTER	Page No.
<b>1. Introduction.</b>	<b>1-15</b>
1.1 Introduction.	
1.1.1 Photoelectric effect.	
1.1.2 Compton scattering.	
1.1.3 Pair production.	
1.1.4 Rayleigh scattering.	
1.1.5 Thomson scattering by nucleus.	
1.1.6 Delbruck scattering.	
1.1.7 Nuclear resonance scattering	
1.1.8 Photo disintegration of the nuclei	
1.2 Fundamental parameters related to Attenuation of Gamma rays	
1.2.1 Linear Attenuation coefficient of the material.	
1.2.2 Mass Attenuation coefficient.	
1.2.3 Mean free path	
1.2.4 Half value layer.	
1.2.5 Tenth value layer.	
1.2.6 Effective atomic number.	
1.2.7 Electron density.	
1.2.8 Energy build-up factors (EBF and EABF	
1.2.9 Computation of G-P fitting parameters.	
1.2.10 Computations of Buildup Factors	
<b>2. Literature survey.</b>	<b>16-22</b>
<b>3. Results and discussions.</b>	<b>23-36</b>
3.1 Introduction.	
3.2 Shielding properties.	
<b>4. Conclusions.</b>	<b>37-38</b>
<b>5. References</b>	<b>39-45</b>

# LIST OF FIGURES

**S. No.      Name of the Figure**

---

<b>Fig.1.1</b>	Schematic representation of photoelectric absorption
<b>Fig.1.2</b>	Schematic representation of pair production.
<b>Fig.3.1</b>	Variation of mass Attenuation coefficient values as a function of photon energy for given glasses
<b>Fig.3.2</b>	Variation of linear Attenuation coefficient values as a function of photon energy for given glasses
<b>Fig.3.3</b>	Variation of effective atomic number as a function of photon energy for given glasses samples
<b>Fig.3.4</b>	Half value layer against photon energy for investigated Glass samples
<b>Fig.3.5</b>	Tenth value layer against photon energy for given glasses samples
<b>Fig.3.6</b>	Mean free path against photon energy for given glasses samples
<b>Fig.3.7</b>	Variation of electron density number values as a function of photon energy for given glasses samples
<b>Fig.3.8</b>	Variation of atomic cross section values as a function of photon energy for given glasses samples
<b>Fig.3.9</b>	Variation of electron cross section values as a function of photon energy for given glasses samples
<b>Fig 3.10:</b>	Variations of the exposure buildup factors (EBF) with photon energy for S1 glass sample as a function of mean free path.
<b>Fig. 3.11:</b>	Variations of the exposure buildup factors (EBF) with photon energy for S2 glass sample as a function of mean free path
<b>Fig. 3.12:</b>	Variations of the exposure buildup factors (EBF) with photon energy for S3 glass sample as a function of mean free path
<b>Fig. 3.13:</b>	Variations of the exposure buildup factors (EBF) with photon energy for S4 glass sample as a function of mean free path
<b>Fig. 3.14:</b>	Variations of the exposure buildup factors (EBF) with photon energy for S5 glass sample as a function of mean free path



## LIST OF TABLES

S. No.	Name of the Table
<b>Table 3.1</b>	Sample codes , densities and chemical composition of glass samples

# CHAPTER-1

## INTRODUCTION

### 1.1 Introduction

The study of interaction of gamma-rays with matter is of great importance in the field of science and technology due to its vast applications in the fields of medicine, engineering, bio-technology, electric power generation plants and in non-destructive spectroscopic analysis, etc.

Around 1920s, de-Broglie developed the theory of matter-wave duality which introduced the concept of photon. Radiation emission, in the form of photon is the release of discrete amount of energy by a system as it moves from one state to other. Energy of the photon is the function of its frequency  $\nu$  (or wavelength  $\lambda$ ) and can be expressed as  $E = h\nu$ , where  $h$  is Plank's constant. Nature of radiation mainly depends upon its origin. When nucleus makes transition from high energy state to low energy state gamma-rays are emitted. Characteristic X-rays have atomic origins which are emitted when an electron makes transition from high energy state to low energy state. Continuous X-rays or Bremsstrahlung radiations are emitted due to the accelerated motion of the charged particles. The manner of interaction of X-rays and gamma-rays with matter is entirely different from the interaction of energetic charged particles because X-rays and gamma-rays are uncharged and massless (rest mass=0). During the interaction of the gamma-ray photon with matter, it either disappears entirely or is scattered through a significant angle. But the charged particles slow down gradually because of continuous interaction with many absorber atoms. As a result, range and specific energy loss concepts can't be applied in the same way on X-rays and gamma-rays as can be done on charged particles.

Incident gamma ray photons may interact with atomic electrons, with nucleons, with electric field surrounding the nuclei or with meson field surrounding the nucleons. These interactions may lead to complete or partial absorption of the incident photons and there is possibility of the scattering also. The most prominent incident energy range of photons is 0.01 to 5 MeV in which mainly photoelectric absorption, Compton scattering and pair production takes place. Brief introduction to various possible interactions is given below (Evans, 1955);

### **1.1.1 Photoelectric effect**

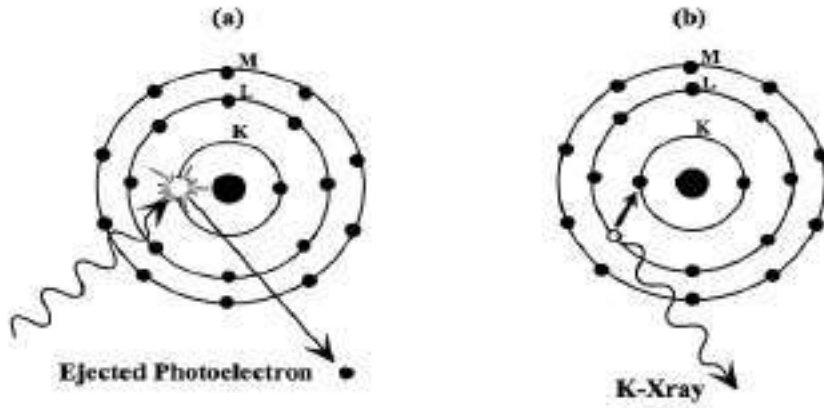
The photoelectric effect is the most important interaction in the 1-100 keV energy range of incident gamma ray. In this process, energy of the incident gamma ray photon gets completely transferred to the bounded electron of the atom. The necessary condition for the photoelectric emission is that the energy of the incident photon should be greater than the binding energy of the electron under consideration. If the incident energy is comparable with the binding energy of the electron photoelectric effect takes place more readily.

If  $E_\gamma$  is the energy of the incident gamma ray photon and  $E_b$  is the binding energy of the electron then kinetic energy of the ejected electron  $E_k$  is given as

$$E_k = E_\gamma - E_b \quad (1.01)$$

After the photoelectric emission of electron from the inner shell, the residual atom is in the ionized state with a vacancy in the inner shell. This vacancy gets filled by transition of the next higher shell electron with a lower binding energy as shown in Figure 1.1. This results in the shifting of the vacancy to the next higher shell, which in turn gets filled by electron from an even lower binding energy shell. So, we can say photoelectric effect triggers an electron cascade from outer to inner shell of the atom. These transitions of electrons from lower binding energy shells to high binding energy

shells appear as characteristic X-rays or Auger electrons. However, the probability of the characteristic X-ray emission is more for high atomic number (Z) targets.



**Figure 1.1: Schematic representation of photoelectric absorption**

K-shell has greatest contribution to the photoelectric effect while L, M and N shells have decreasing order of the importance. If the energy of the incident gamma ray photon is less than the binding energy of K shell electron then there will be interaction of the L, M or N shell electrons with gamma rays. So, there will be sharp decrease in the photoelectric cross-sections ( $\tau_{PE}$ ) with the decrease in the incident photon energy. The photoelectric cross-sections ( $\tau_{PE}$ ) or the photoelectric coefficient is defined as the probability of this interaction to take place.  $\tau_{PE}$  is a function of energy of the incident gamma rays ( $E_\gamma$ ), atomic number (Z) and atomic mass number (A) is given in equation 1.02,

$$\tau_{PE} \propto (N_t) \frac{Z^n}{E_\gamma^m} \quad (1.02)$$

The values of  $m$  and  $n$  lies from 3 to 5, which is a function of  $E_\gamma$ . The number of atoms/m<sup>3</sup> ( $N_t$ ) in the material through which the photon transverses and can be calculated mathematically as

$$N_t = \rho \frac{N_A}{A} \quad (1.03)$$

Such as,  $\rho$  is the bulk density,  $N_A$  is the Avogadro's number and  $A$  is atomic weight of the target (Tsoulfanidis, 1995).

### 1.1.2 Compton scattering

Compton scattering is the process in which the incident gamma ray photon interacts directly with the outermost shell electron of the target material. In Compton scattering incident gamma ray photon losses, a fraction of its energy contrary to photoelectric effect in which complete absorption of the photon takes place. Assuming the electron at rest before the collision, kinetic energy ( $K_e$ ) acquired by recoiled electron after the collision can be represented as (Dyson (2005))

$$K_e = E_{\gamma_i} - E_{\gamma_f} \quad (1.04)$$

Here  $E_{\gamma_i}$  and  $E_{\gamma_f}$  is the energy of the gamma photon before and after the interaction with the electron. To obtain expression for  $E_{\gamma_f}$ , laws of conservation of momentum can be applied and it is found that  $E_{\gamma_f}$  is the function of the scattering angle  $\theta$  as

$$E_{\gamma_f} = \frac{E_{\gamma_i}}{1 + (1 - \cos\theta) \frac{E_{\gamma_i}}{m_0 c^2}} \quad (1.05)$$

Equation 1.04 & 1.05 are used to obtain the kinetic energy  $K_e$  of the electron as

$$K_e = \frac{(1 - \cos\theta) \frac{E_{\gamma_i}}{m_0 c^2}}{1 + (1 - \cos\theta) \frac{E_{\gamma_i}}{m_0 c^2}} E_{\gamma_i} \quad (1.06)$$

Here  $m_0 c^2$  is the rest mass energy of the electron (0.511MeV). For  $\theta = \pi$  minimum energy is carried by the scattered photon, i.e.



$$E_{\gamma_f}^{min} = \frac{E_{\gamma_i}}{1 + 2 \frac{E_{\gamma_i}}{m_0 c^2}} \quad (1.07)$$

If  $\theta = 0^\circ$  there will be maximum energy taken by the scattered photon, i.e.,

$$E_{\gamma_f}^{max} = E_{\gamma_i} \quad (1.08)$$

From equation (1.07), it can be concluded that minimum energy of the scattered photon is greater than zero. So, in Compton scattering it is not possible that whole of the incident energy is carried by the ejected electron. From equation (1.08), we can say that there will be no interaction between the incident photon and the outer electron, as energy of the scattered photon remains unaffected.

Compton cross-section  $\sigma_C$  or Compton coefficient is defined as the probability of Compton interaction to take place per unit distance.  $\sigma_C$  is a complicated function of  $E_{\gamma_i}$ . Such that,

$$\sigma_C = NZ.f(E_{\gamma_i}) \quad (1.09)$$

Here  $f(E_{\gamma_i})$  is a function of  $E_{\gamma_i}$  and  $N$  is the atom density, which can be obtained using equation (1.03).

$$\sigma_C = \rho \frac{N_A}{A} Z.f(E_{\gamma_i}) \quad (1.10)$$

In most of the materials except Hydrogen, value of  $A \approx 2Z$  to  $2.6Z$ , so equation (1.10) can be modified as (Tsoufanidis, 1995)

$$\sigma_C \sim \rho \left( \frac{N_A}{2} \right).f(E_{\gamma_i}) \quad (1.11)$$

### 1.1.3 Pair production

Pair production is the third type of the interaction of highly energetic gamma ray with matter which becomes energetically possible if the incident gamma energy is more than twice of rest mass energy of the electron (1.02 MeV). In this type of interaction electron-positron pair appears on the cost of gamma ray photon. The

presence of the nucleus is must in this type of interaction; however it does not involve any change.

Kinetic energies  $K_e^-$  and  $K_e^+$  of electron and positron respectively can be obtained from the following equation using the law of conservation of mass and energy as (Tsoulfanidis (1995))

$$K_e^- + K_e^+ = E_\gamma - (mc^2)_{e^-} - (mc^2)_{e^+} = E_\gamma - 1.022\text{MeV} \quad (1.12)$$

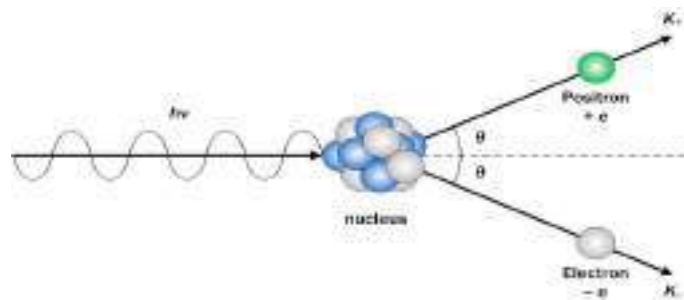
This energy is shared by electron and positron equally, so

$$K_e^- = K_e^+ = \frac{1}{2}(E_\gamma - 1.022\text{MeV}) \quad (1.13)$$

Pair production cross section ' $\kappa_{PP}$ ' or pair-production coefficient is the probability for pair production to occur which a complicated function is of  $E_\gamma$  and  $Z$  and can be written as

$$\kappa_{PP} = NZ^2 f(E_\gamma, Z) \quad (1.14)$$

It is important to note that  $\kappa_{PP}$  has threshold at 1.022 MeV and increases with  $E_\gamma$  and  $Z$ .



**Figure 1.2 Schematic representation of Pair-production**

#### 1.1.4 Rayleigh scattering

Rayleigh scattering is also known as coherent scattering in which the incident gamma ray photon interacts coherently with the all electrons of the absorber atom. In this scattering event, the energy is retained by the gamma ray photon after the interaction as a result target atom neither excites nor ionizes. Rayleigh scattering is

mainly due to the electric polarizability of the interacting atoms as a result this start oscillating with the same frequency of the incident radiation. The atoms behave like small radiating dipoles. Rayleigh scattering is most predominant at low incident photon energy, small scattering angles and high Z absorbers. So, in contrast to Compton scattering, Rayleigh scattering is negligible.

### **1.1.5 Thomson scattering by the nucleus**

Thomson scattering of the incident gamma ray is explained on the basis of classical electromagnetism in which nucleus is considered as a point charge. This involves scattering of the gamma rays by free electrons and nucleus as a whole (nuclear Thomson scattering). In this scattering process, there will be no change in the particle kinetic energy and the photon frequency before and after the scattering. However, this remains valid till the photon energy remains very- very small in contrast to the rest mass energy of the particle., i.e.,  $\nu \ll \frac{mc^2}{h}$ .

### **1.1.6 Delbruck scattering**

Delbruck scattering is also known as the elastic nuclear potential scattering in which there is coherent elastic scattering of photons in the Coulomb field of high Z nuclei. It is the deflection of highly energetic photons because of virtual electron pair formation in the coulomb field of nucleus. It is one of the two nonlinear effects of quantum electrodynamics (QED) in the Coulomb field investigated experimentally, which involves the splitting of single photon into two photons. However, this effect is quite small and cannot be detected in experiments done to measure it effectively. But these interactions are of good importance as it explain the inconsistencies between experimental and theoretical values of Compton scattering experiments on high Z elements.

### **1.1.7 Nuclear resonance scattering**

Nuclear resonance scattering depends upon the properties of the nuclear excited states. When there is resonance between the incident gamma ray photons and absorbing nuclei, then it gets excited to the higher energy levels. So, there will be absorption and re-emission of the photon by the nuclear energy levels of the resonant atom. This type of scattering occurs at energies near a resonance level, where the incident particle can easily form a compound nucleus and a similar particle may be emitted before any other competing emission or radiative process takes place in the compound nucleus.

### **1.1.8 Photo-disintegration of the nuclei**

Photo-disintegration or photo-transmutation is a process in which high energy gamma ray (nearly 8 MeV) is absorbed by an atomic nucleus. As a result, it gets excited and further decays immediately by emitting a subatomic particle like proton, neutron or alpha particle. This process is possible when the incident gamma ray photon has energy more than that of the separation energy of neutron or proton.

## **1.2 Fundamental parameters related to attenuation of gamma rays**

Attenuation is the removal of the incident photons from the collimated beam of monoenergetic photons during their passage through given target material. Linear attenuation coefficient, mass attenuation coefficient, effective atomic number and intensity ratios are the important fundamental parameters which describe the attenuation of the gamma rays through materials.

### **1.2.1 Linear attenuation coefficient of the materials**

Linear attenuation coefficient ( $\mu$ ) of a material is defined as a measure of the probability of interaction of the photons per unit linear path length in the absorber that leads to their elimination from the incident photon beam. Typically, it has the units of  $cm^{-1}$ . The number of removed photons  $n$  from the beam after traversing thickness  $x$  can be given as,

$$n = \mu N_o x \quad (1.15)$$

Here,  $N_o$  is the total number of incident photons.

Depending upon the energy of photon and atomic number of the target, incident photon interacts in different ways with matter. There are mainly three interaction mechanisms, i.e., photoelectric effect, Compton scattering and pair production with which a photon interacts with matter (explained in section 1.1).

The probability of a photon traversing a given amount of absorber without any kind of interaction is just the product of the probabilities of survival for each interaction. The probability of traversing a thickness  $x$  of absorber without a Compton collision is  $e^{-\sigma_C x}$  where  $\sigma_C$  is linear attenuation coefficient for the Compton process. Similarly, the probability of no photoelectric interaction is  $e^{-\tau_{PE} x}$ , where  $\tau_{PE}$  is the linear attenuation coefficient for the Photoelectric process and for probability of no pair-production collision is  $e^{-\kappa_{PP} x}$ , where  $\kappa_{PP}$  is the linear attenuation coefficient for the pair-production process. A collimated gamma-ray beam of initial intensity  $I_o$  after traversing a thickness  $x$  of absorber will have a residual or transmitted intensity  $I$  which is a function of incident gamma-ray energy, absorber composition and absorber thickness. Such that,

$$I = I_o(e^{-\sigma_C x} + e^{-\tau_{PE} x} + e^{-\kappa_{PP} x}) \quad (1.16)$$

$$= I_o e^{-(\sigma_C + \tau_{PE} + \kappa_{PP})x} \quad (1.17)$$

$$= I_o e^{-\mu x} \quad (1.18)$$



Where the quantity

$$\mu = \sigma_C + \tau_{PE} + \kappa_{PP} \quad (1.19)$$

is the total linear attenuation coefficient. The reciprocal of the attenuation coefficient has the units of length and is often known as mean free path, i.e., average distance a gamma ray travels in the absorber before interacting. Equation (1.19) establishes a linear relationship between the absorbance, density of an absorbing species and path length of the target and it is known as Beer-Lambert's law.

For the application of the Beer-Lambert law the target material must have uniform thickness and density. The linear relationship between absorption coefficient and thickness  $x$  of the material does not holds well, in case photons reaching the detector have unequal chances of absorption in the target material. This may happen due to the difference in the density or thickness of the target under study. Another reason behind it is the presence of impurity atoms in the target or some chemical change taking place in it, which causes non-uniformity in the density of the target.

Later, Silva et al. (2000) modified the general Beer-Lambert's law theoretically and proposed new method, i.e., Two Media Method for the measurement of the linear attenuation coefficient for materials having non-uniform thickness.

### **1.2.2 Mass attenuation coefficient**

When a collimated and monoenergetic beam of photons interact with the given thickness of the target material, the probability of interaction depends on the number of atoms per unit volume. This dependence can be normalised by defining linear attenuation coefficient per unit density of the target material, which is known as mass attenuation coefficient ( $\mu_m$ ) of the target. It can be calculated by dividing the linear

attenuation coefficient of the material under study by the density of the same material as;

$$\mu_m = \mu/\rho \quad (1.20)$$

Here  $\rho$  is the density of the target material in  $g/cm^3$ . So, the expression of Beer-Lambert's law becomes

$$I = I_0 e^{-\mu_m \rho x} \quad (1.21)$$

Here  $\rho x$  is the mass thickness of the material which is measured as mass per unit area.

In case of the compounds or homogenous mixtures, mass attenuation coefficient can be calculated by finding the weighted sum of the coefficients for the elements using simple rule as

$$\mu_m = \sum_i w_i \left( \frac{\mu}{\rho} \right)_i \quad (1.22)$$

In the above equation  $\left( \frac{\mu}{\rho} \right)_i$  is the mass attenuation coefficient for the  $i^{th}$  element and  $w_i$  is its weight fraction. For a chemical compound with formula  $(A_{x1}B_{x2}C_{x3} \dots \dots D_{xn})$  the weight fraction for the  $i^{th}$  element is given by

$$w_i = \frac{x_i A_i}{\sum_{i=1}^n x_i A_i} \quad (1.23)$$

Here,  $A_i$  is the atomic weight of the  $i^{th}$  element.

### 1.2.3 Mean Free Path

The mfp is defined as the average distance a gamma ray photon travels in the target absorbing material before any interaction with it. The  $\mu$  has the units  $cm^{-1}$ . Its reciprocal, possessing the units of length, represents the mfp. The mfp may also be defined as the thickness of the interacting substance which produces a gamma ray transmission as:

$$\frac{I}{I_0} = \frac{1}{e} = 0.37$$

In shielding process, considering samples of same thickness and targeted by the same gamma ray photon energy, the samples with lower mfp values are better gamma ray

shielders than high mfp value samples. Generally GP fitting parameters are utilized to calculate the gamma ray energy absorption buildup factor at various mean free path penetration depths for different incident photon energies.

#### 1.2.4 Half Value Layer

HVL or half value distance of an interacting target material is the width of material required at which the intensity of incident radiation narrow beam entering the target material is reduced to half of its original value. The HVL is given as:

$$HVL = \frac{\ln 2}{\mu} = \frac{0.693}{\mu} \quad (1.24)$$

The units of HVL are reciprocal of units of  $\mu$ . Normally, HVL is expressed in cm as the  $\mu$  is given in  $cm^{-1}$ . The lower value of HVL either indicates low photon energy or a better shielding material in terms of required thickness.

#### 1.2.5 Tenth Value Layer

The tenth value layer (TVL) of shielding is defined as a thickness of absorbing material that will reduce incident gamma radiation beam to tenth value of its initial intensity. Like HVL, the TVL thickness is also measured in units of distance i.e. mm or cm. The tenth value layer is given as:

$$TVL = \frac{\ln 10}{\mu} = \frac{2.303}{\mu} \quad (1.25)$$

#### 1.2.6 Effective atomic number

As attenuation of gamma photons is a function of the energy of incident photon, density and atomic number of the target element, so it is not possible to assign a single atomic number to a compound material for innumerable incident energies (Hine, 1952). However, for particular energy interaction of radiation with compound material is identical to the interaction of radiation with a single element whose atomic number is equivalent to the effective atomic number ( $Z_{eff}$ ) of the material.  $Z_{eff}$  can be obtained from atomic numbers of constituent elements, weighted according to the different partial photon interaction processes. Mathematically,  $Z_{eff}$  can be calculated from the following relation

$$Z_{eff} = \frac{\sigma_{t,a}}{\sigma_{t,el}} \quad (1.26)$$

Here  $\sigma_{t,a}$  is total atomic cross-section and  $\sigma_{t,el}$  is effective electronic cross-section. Total molecular cross-section can be obtained from mass attenuation coefficient according to following relation.

$$(\sigma_{t,m}) = \mu_m \left( \frac{M}{N_A} \right)$$

Where  $M = \sum_i n_i A_i$  is molecular weight of compound,  $n_i$  is total number of atoms in the molecule and  $A_i$  is the atomic weight of the  $i^{th}$  element.

Further, total atomic cross section can be calculated as

$$(\sigma_{t,a}) = \frac{1}{N_A} \sum_i f_i A_i (\mu_m)_i \quad (1.27)$$

Effective electronic cross-section is calculated by using the relation (Singh et al. (2002))

$$(\sigma_{t,el}) = \frac{1}{N} \sum_i \frac{f_i A_i}{Z_i} (\mu_m)_i \quad (1.28)$$

Here  $f_i = n_i / \sum_j n_j$  is fractional abundance and  $Z_i$  is atomic number of  $i^{th}$  constituent element,  $\sum_j n_j$  is the total number of atoms present in the molecular formula and  $N_A$  is Avogadro's number.

#### 1.2.4 Electron Density

The  $N_e$  is also a significant parameter for understanding and visualizing the incident radiation photon interactions probability with a particular absorbing substance. It is the more trustworthy parameter in comparison to the effective atomic number as it is directly associated with number of charged particles present in a unit mass of the material however its large values make the analysis process somewhat cumbersome. Higher is the value of  $N_e$  more is the probability of photon interaction and better is the sensing and shielding material.  $Z_{eff}$  offers similar information regarding mixed compositions as does the simple atomic number for single elements

$N_e$ , expressed as number of electrons in unit mass of the target interacting material. It exhibits the probability of incident photon interaction with target atom electrons. The higher  $N_e$  values mean that there are more chances of incident photon interaction with target shielding sample electrons. Thus  $Z_{eff}$  and  $N_e$  are the parameters which indicate the energy radiation incident photon interaction probabilities with various shielding materials. The  $N_e$  is closely related to the  $Z_{eff}$  and is given as:

$$N_e = \frac{\left(\frac{\mu}{\rho}\right)_{comp} Z_{eff}}{\sigma_a} \quad (1.29)$$

### 1.2.5 Energy build-up factors (EBF and EABF)

By placing a thick shield of material around any gamma source, all radiation is completely absorbed. However, Lambert-Beer's law was not obeyed because, as shielding material thickness increased, there was a greater chance of beam divergence. the buildup factor (B), often known as the corrective factor. Concerning the buildup factor, the following relation provides Lambert-Beer's law:

$$I = B I_0 e^{-\mu x} \quad (1.30)$$

The buildup factor "B" must be more than or equal to one (1), that is,  $B \geq 1$ . The equivalent atomic number ( $Z_{eq}$ ) of the ceramic samples has been derived using the interpolation approach as the initial step in evaluating the buildup factor for the synthesized glass samples[49]:

$$Z_{eq} = \frac{Z_1 (\log R_2 - \log R) + Z_2 (\log R - \log R_1)}{(\log R_2 - \log R_1)} \quad (1.31)$$

where,

$$R = \mu_c \mu_T \quad (1.32)$$

Here,  $\mu_c$  and  $\mu_T$  correspond to the Compton attenuation coefficient as well as the total mass attenuation coefficient. Ratio 'R' for the ceramic sample should be lies among  $R_1$  and  $R_2$  for consecutive elements related to  $Z_1$  and  $Z_2$  atomic numbers respectively.



### 2.2.3 Computation of G-P fitting parameters

In the photon energy range of 0.015 to 15.0 MeV and up to a penetration depth of 40 mfp, American National Standards [46] provided the energy absorption G.P. fitting parameters of 23 pure elements (Be, O, Na, S, Ar, Ca, Fe, Cu, Mo, Sn, La, Gd, W, Pb, and U), one compound (water), and two mixtures (air and concrete). Using the following logarithmic interpolation formula, the computed values of  $Z_{\text{eff}}$  for the chosen ceramic samples were used to interpolate G.P. fitting parameters ( $b$ ,  $c$ ,  $a$ ,  $X_k$ , and  $d$ ) for the energy absorption accumulation factor:

$$P = \frac{P_1(\log Z_2 - \log Z_{\text{eff}}) + P_2(\log Z_{\text{eff}} - \log Z_1)}{\log Z_2 - \log Z_1} \quad (1.33)$$

where  $Z_1$  and  $Z_2$  are the elemental atomic numbers between which the  $Z_{\text{eff}}$  of the chosen ceramic sample lies.  $P_1$  and  $P_2$  are the values of G.P. fitting parameters corresponding to the atomic numbers  $Z_1$  and  $Z_2$ , respectively, at a given energy. Using the above-given interpolation formula, G.P. fitting parameters for energy absorption buildup factors were computed at the selected incident photon energies for given ceramic samples.

### 2.2.4 Computations of Buildup Factors

The energy absorption building factors for the chosen ceramic samples in the incident photon energy range of 0.015 to 15.0 MeV and up to the penetration depth of 40 mfp were calculated using the computed G.P. fitting parameters ( $b$ ,  $c$ ,  $a$ ,  $X_k$ , and  $d$ ) using the following equations:

$$B(E, X) = 1 + \frac{b-1}{K-1}(K^X - 1) \quad K \neq 1 \quad (1.34)$$

$$B(E, X) = 1 + (b-1)X \quad K = 1 \quad (1.35)$$

$$\text{Where, } K(E, x) = cX^a + d \frac{\tanh\left(\frac{X}{X_k} - 2\right) - \tanh(-2)}{1 - \tanh(-2)} \quad \text{for } X \leq 40 \text{ mfp} \quad (1.36)$$

## CHAPTER – 2

### LITERATURE SURVEY

Lead titanate ( $\text{PbTiO}_3$ ) is a perovskite type ferroelectric material with high Curie temperature of  $490^\circ\text{C}$  which make them attractive for high-temperature and high-frequency piezoelectric applications [1–2]. Above  $T_c$ , the material has a simple cubic structure with lead atoms at the corners of the cubic unit cell, the titanium is at the body center position and oxygens are at the face-centered positions. Below  $T_c$ , the structure is tetragonal with the atoms distorted from the cubic arrangement by small relative displacements along the (polar) tetragonal  $c$  axis exhibiting a large tetragonality ( $c/a = 1.064$ ). It is reported in the literature that large ionic displacements in PT lead to a large spontaneous polarization of the order of  $453 \text{ mC/cm}^2$  at room temperature [3]. However, it is difficult to sinter pure lead titanate ceramics because of its large lattice anisotropy of  $c/a = 1.063$ .  $\text{PbTiO}_3$  ceramics prepared by conventional route usually have microcracks and fracture on cooling below crystallization temperature ( $T_c$ ) as a result of the large spontaneous strain generated due to phase transition from cubic to tetragonal. This has constrained the applications of undoped lead titanate ceramics. The glass–ceramic route therefore offers the possibility of fabricating lead titanate without cracking. The other advantages of this method, such as no ageing or depoling problems and good stability at high temperature, high-pressure and in harsh environments can be achieved [4]. In this method, a glass medium consisting of glass network formers and ferroelectric constituents is prepared by conventional melt-quenching technique. Ferroelectric phase is then precipitated within the glass matrix during subsequent heat treatment [5–6]. The advantages of glass–ceramic processing over traditional ceramic route include

ease of forming complicated shapes free from porosity, voids and microcracks [7]. The amount of ferroelectric phase and its microstructure can be controlled by choosing a suitable initial glass composition and a heat treatment schedule [8]. Ferroelectric glass-ceramics with uniform fine-grained structure have attracted much attention and, in many applications, like transducers [9–24]. Composition of the glass, proper proportion of glass forming oxides like  $B_2O_3$  and  $SiO_2$  and glass preparation methods plays very important role to develop ferroelectric phases in the glass-ceramics [25]. The phase diagram of  $PbO-TiO_2-B_2O_3$  shows that the glass compositions  $PbO-B_2O_3$  and  $2PbO-B_2O_3$  is suitable for crystallization of  $PbTiO_3$  and the glass system,  $5PbO-B_2O_3-SiO_2$  for the crystallization of PZT [26].

Gamma radiations are used in a number of applications which include apparatus sterilization in medical field [27-28] protecting the food articles by irradiation [29-30] in diagnosing and treatment of cancer and some other medical conditions [31-32] element analysis [33-34] checking any flaws in welded materials [35-36] and in agriculture and engineering fields. At the same time these high energy and most penetrating radiation exposure for longer time period on any living being may also cause radiation sickness, mutation and cancer. Thus, for the effective use of gamma radiation in scientific, engineering, medical and agricultural applications, there is an urgent requirement to develop materials that can act as good radiation shield to avoid the unnecessary harmful effect on human body and environment. These shielding materials are may also be useful to protect reactor vessel from overheating due to continuous gamma ray absorption.

The study of absorption of gamma radiations in any material is valuable in formulating accurate semi-empirical formulations [37]. Understanding  $\mu_m$  has great significance as gamma ray absorption is dependent upon  $Z_{eff}$  and density of the

absorbing/shielding material. Using  $\mu_m$  various parameters like the mass energy-absorption coefficient, the total interaction cross-section, the  $Z_{eff}$ , and the  $N_e$  can be derived. Mass attenuation coefficients of many elements and compounds are available in tabulated form published by Hubbell [38] for photon energy range 1 keV-20 MeV. However, these tables consisted of only 40 elements and 45 compounds only. A new tabulation by Hubbel and Seltzer [39], consisted all elements from atomic number 1-92 and 48 additional compounds and substances. Berger and Hubbel [40] have further updated these values. Chantler [41] has recently provided wide ranging tabulated values of mass attenuation coefficients.

$Z_{eff}$  of any amalgamated and complex absorbing material is a very handy parameter in various technological and engineering applications. This parameter has a physical meaning and allows many characteristics of absorbing material to be envisaged by using it just as a number. However, the value of  $Z_{eff}$  during its measurement changes with different measurement techniques. After many efforts to formulate rules for finding  $Z_{eff}$  of any composite material, the available formulas have limited validity subject to the experimental conditions used in the particular work. As the technology advances there is a need to develop shielding materials that can work even in unforgiving gamma radiation exposure situations [42]. In the process many glass systems have been developed for nuclear engineering applications [43]. Glasses have been developed which accomplish the double task. Glasses are not only transparent to visible light but also protect us by absorbing high energy gamma radiations [44]. Cadmium and boron containing glasses are used to absorb slow neutrons [45]. In general, any absorbing glass material should be chemically, mechanically and optically inert to irradiation effects having radiation absorption cross section to be extra ordinary.

For using glasses as shielding materials, their effective atomic numbers and gamma attenuation coefficients study possess considerable importance. A. Khanna et al. [46] has done previous measurements in some heavy metal oxide borate glasses. This study is performed on lead alumino borophosphate glasses.

There is also a constant need to develop better and better absorbing materials which can act as a good radiation shield in extreme unfriendly environment [47]. In this regard, glasses are promising materials because of their homogeneity and range of composition. Typical applications of radiation shielding glasses are in hospital X-ray rooms, radiation therapy rooms, airport security X-ray screens, for materials testing, nuclear facilities, dental clinics, laboratories, X-ray and radiation protection spectacles. Glasses are also used in space technology for protecting human beings and equipment from harmful radiation such as gamma and cosmic rays. Glass has also been suggested for the containment of radioactive waste products [48]. In general, the Heavy Metal Oxide glasses based on for example PbO or  $Bi_2O_3$  [49-53], have potential applications in radiation shielding, since they have large absorption cross section for radiation and at the same time small irradiation effects on their mechanical and optical properties. HMO glasses are better shields and may be used as transparent radiation shielding materials [54].

The transmitted intensity of a gamma ray beam through a medium follows Lambert's Beer law ( $I = I_0 e^{-\mu t}$ ) where  $I$ ,  $I_0$  are transmitted and incident intensities of photons for thickness  $t$  of the medium having linear attenuation coefficient,  $\mu$  under three conditions: (i) monochromatic ray (ii) thin absorbing material, and (iii) narrow collimated beam. The law becomes invalid in case all these three conditions are not exactly fulfilled. The law can be made valid by using a correction factor, called as "buildup factor". The buildup factor is defined as the ratio of total value of specified



radiation quantity at any point to the contribution to that value from radiation reaching to the point without having undergone a collision. To evaluate the shielding and exposure of gamma radiations a comprehensive and reliable buildup factor data is very useful for analysis and control [55]. Buildup factors are shielding material and geometry dependent parameters which are applied to correct the attenuation calculations by including the contribution to the radiation field produced by the collided part of the incident beam. Many researchers have studied gamma ray buildup factors for concretes/flyash concretes [56], soil and ceramic [57,58], human tissues [59], gaseous mixture [60], building materials [61] and found that G-P fitting method is quite useful in valuation of energy absorption and exposure buildup factors. Geometrical-Progression (GP) fitting formula has been developed by Harima et al [62]. This formula can reproduce data over full range of distance, energy and atomic number. Harima et al [63] have demonstrated the applicability of G-P method to generate buildup factor data for a wide range of energy and distance.

The shielding properties of the glasses can be modified by change in the chemical compositions. Gamma ray shielding properties of the glasses have been carried out for phosphate glass [64], lead silicate [65] and lead borate and silicate glass [66-69]. In nuclear reactors and other facilities where neutron radiations also exist alongside gamma radiations, neutron absorbing glasses must also possess elements such as Li, H, C, B etc. In the nuclear reactors the energy of neutron ranges up to 8 MeV [70] and gamma ray in range of 0.10–10 MeV. Therefore, boron containing glass shielding materials are found to be a promising and potential shielding candidate. The gamma ray attenuation coefficient of borate glasses has been investigated for photon energy 1173 and 1332 keV [71]. There is no such study for gamma ray and neutron shielding

by the borophosphate glasses in the literature. This encouraged us to investigate the shielding efficiencies of gamma ray and neutron.

Lead zirconate titanate glasses with composition  $xPbO:14TiO_2:16ZrO_2:(40 - 0.5x)B_2O_3:(40 - 0.5x)SiO_2$ , ( $x = 0, 10, 20, 30, 40$ ) have been investigated for their shielding properties in the present work. It has been determined through theoretical calculations if they can serve as gamma ray shielding. The WinXcom programme was used to theoretically estimate the mass attenuation coefficient ( $\mu_m$ ) for this goal. The ratio of the entire value of the prescribed radiation quantity at any location reaching the point without any collision is known as the buildup. The buildup factor has been classified as;

(i) EBF: Exposure Buildup Factor: It is referred to as the photon accumulation factor, with exposure as the quantity of interest and air absorption as the detector response function.

(ii) EABF, or energy absorption buildup factor: The quantity of interest is the absorbed or deposited energy in the interacting material, and the detector response function is that of absorption in the interacting material. It is the photon buildup factor.

There are few reports in the literature on the analysis of the EBF for glass using the G-P fitting approach. Therefore, it has become vital to understand the polymer's gamma-ray interaction properties when developing materials for radiation shielding applications. The present work focuses on examining the EBF of various types of glasses in light of the necessary knowledge of the radiation interaction of gamma-ray with the matter in various fields. Using the G-P approach, the obtained EBF and EABF data were assessed for incident photon energies ranging from 0.15 to 15 MeV up to a penetration depth of 40 mfp. The prepared glass samples are also subject to structural determinations. The findings of this study will offer details about the suitability of glasses as radiation shields and suggestions for developing new shielding materials. Further, the interaction of radiation with the atoms of the shielding material is described by the shielding characteristic known as the mean free path (MFP). The material that exhibits a low MFP is better at shielding. The MFP for

the chosen glass samples was calculated from the simulated linear attenuation coefficient values.

## CHAPTER-3

### RESULTS AND DISCUSSION

#### 3.1 Introduction

Present work is focused on theoretically exploring radiation shielding properties of lead zirconium titanate glasses viz.  $xPbO:14TiO_2:16ZrO_2:(40 - 0.5x)B_2O_3:(40 - 0.5x)SiO_2$ , ( $x = 0, 10, 20, 30, 40$ ). The radiation shielding parameters such as mass attenuation coefficient, linear attenuation coefficient, effective atomic number, electron density, half value layer and exposure buildup factor were obtained theoretically as preliminary data for preparing sample of required thickness.

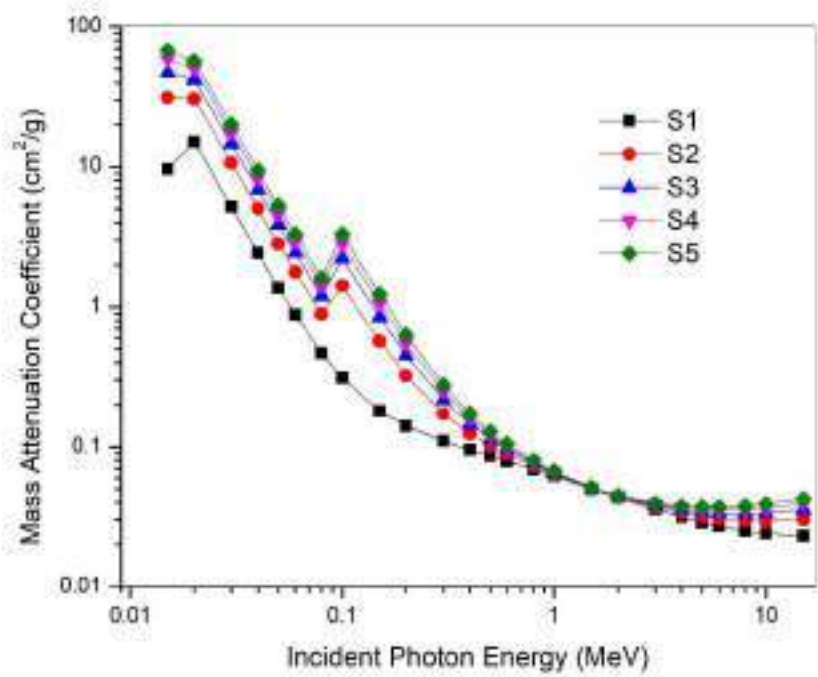
#### 3.2 Shielding Properties

In this study, the gamma-ray attenuation properties of lead zirconate titanate samples were investigated. The molar and elemental mass percentages and densities of the samples analyzed are listed in Table 1. According to Table 1, the density of the glasses increased from 5.5102 g/cm<sup>3</sup> to 7.6003 g/cm<sup>3</sup>. The sample with the highest structural lead oxide content, had the highest density.

**Table 3.1:** Sample codes, densities and chemical compositions of glasses

Sample Code	PbO	TiO <sub>2</sub>	ZrO <sub>2</sub>	B <sub>2</sub> O <sub>3</sub>	SiO <sub>2</sub>	Density (g/cm <sup>3</sup> )
S1	0	14	16	40	40	5.5102
S2	10	14	16	35	35	5.9216
S3	20	14	16	30	30	6.3217
S4	30	14	16	25	25	6.7105
S5	40	14	16	20	20	7.6003

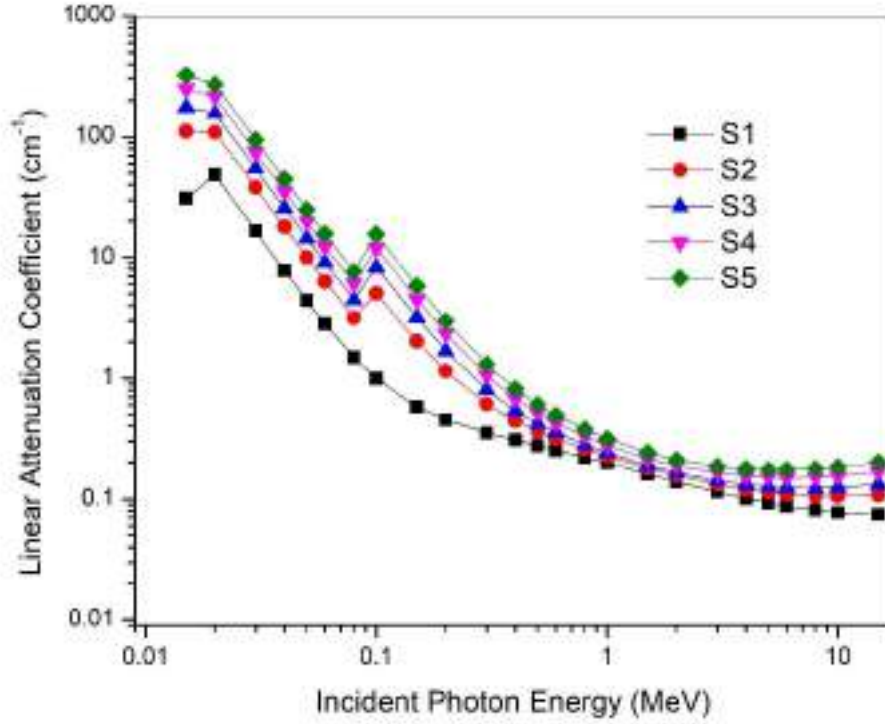
The WinXcom program's theoretical results were first used to obtain the  $\mu_m$  values in order to explore the gamma-ray attenuation properties of the selected glasses. Gamma energy was increased up to 15 MeV, and this caused a sharp fall in the  $\mu_m$  values (Fig. 3.1). Photoelectric absorption (PEA) was the reason for this decrease. The main influence on absorption in this sector regime came from the PEA. The  $\mu_m$  values changed more slowly after 1 MeV. This was caused by the strength of the linear Z-dependent Compton scattering (CS), which was present at this range of energy. Pair production (PP), which was the main mechanism above 5 MeV, caused the influence of CS to steadily decrease after that (Fig. 3.1). Since PP's cross-section grows linearly with  $Z^2$ , the values of  $\mu_m$  rose over the range of 9 to 20 MeV. The highest lead, zirconium, and barium concentrations were found in the S5 sample, which also had the highest  $\mu_m$  values.



**Figure 3.1:** Variation of mass attenuation coefficient ( $\mu_p$ ) values as a function of photon energy for given glasses



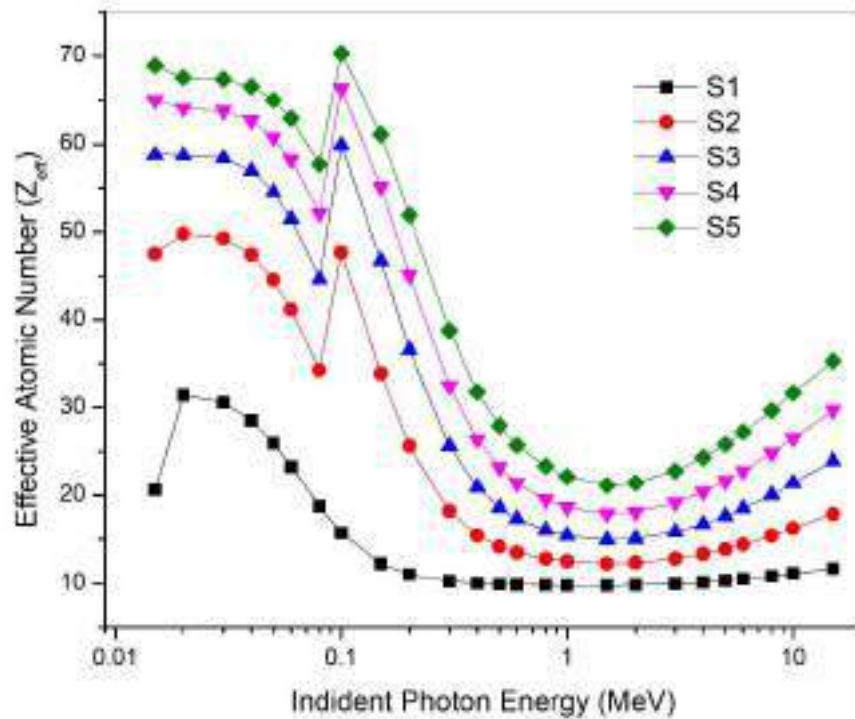
Given that the linear attenuation coefficient (LAC) is a density-dependent property, it is assumed that there is a correlation between density and the LAC values in this case, and subsequently, the amount of lead oxide. Figures 3.2 show the shifting LAC in relation to the incident photon energy, accordingly. In the graph, it can be shown that as photon energy increased, the LAC rapidly reduced, reaching as low as 0.05 MeV in all cases. The photoelectric effect predominates in the low-energy region, where the majority of photon-matter interactions take place, with cross-sectional changes proportional to  $Z$ . For medium-level energies above the energy level, Compton scattering becomes increasingly significant when considering the changes in chemical composition of the specimens. The cross section of Compton scattering has a linear relationship with atomic number  $Z$ , hence the samples' values decreased gradually and remained constant below 2 MeV. However, considerable differences in the linear attenuation coefficients were observed as the glass density changed progressively. At various energies, we saw an intriguing impact of lead oxide on the photon resistance of glass samples. Our findings show that the lead oxide content was highest in the S5 sample, which also exhibited the highest linear attenuation coefficients for all entering photon energies. This is explained by the fact that the S5 sample, which has a density of  $7.6003 \text{ g/cm}^3$ , contains the most lead oxide in the glass structure and has a higher value of LAC.



**Figure 3.2:** Variation of linear attenuation coefficient ( $\mu$ ) values as a function of photon energy for given glasses

Figure 3.3 show how the tested glasses effective atomic number ( $Z_{\text{eff}}$ ) values fluctuate as a function of incident photon energy. According to Figure 3.3, S5 have the highest effective atomic number values across all energies investigated. The enhanced lead oxide reinforcement, which raised the sample's total atomic number from S1 to S5, can be attributed to this. The changes in the glass structure between the reduced ( $\text{B}_2\text{O}_3$  and  $\text{SiO}_2$ ) and enlarged ( $\text{PbO}$ ) replacements led to a considerable change in the overall atomic number of the S1 - S5 sample. The absorption edge of B at about 0.03 MeV caused a sharp increase in  $Z_{\text{eff}}$  curves. This was because to PEA's dominance in the relevant energies. In the middle energies, where CS played a significant role, the  $Z_{\text{eff}}$  values were remarkably similar. The modification in the cross-section of PP with  $Z^2$  caused the  $Z_{\text{eff}}$  values to rise once more. It is clear that the glass sample's high lead

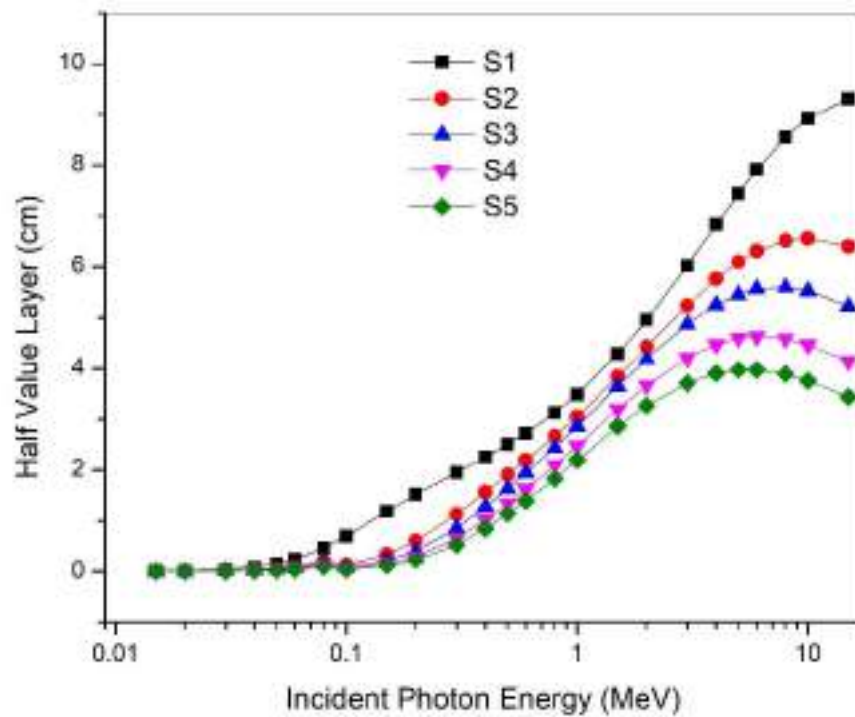
content is what caused it to have the highest  $Z_{\text{eff}}$  value. Present study demonstrates that the S5 sample exhibited the highest  $Z_{\text{eff}}$  values across the entire gamma-ray energy range.



**Figure 3.3:** Variation of effective atomic ( $Z_{\text{eff}}$ ) number values as a function of photon energy for given glass samples.

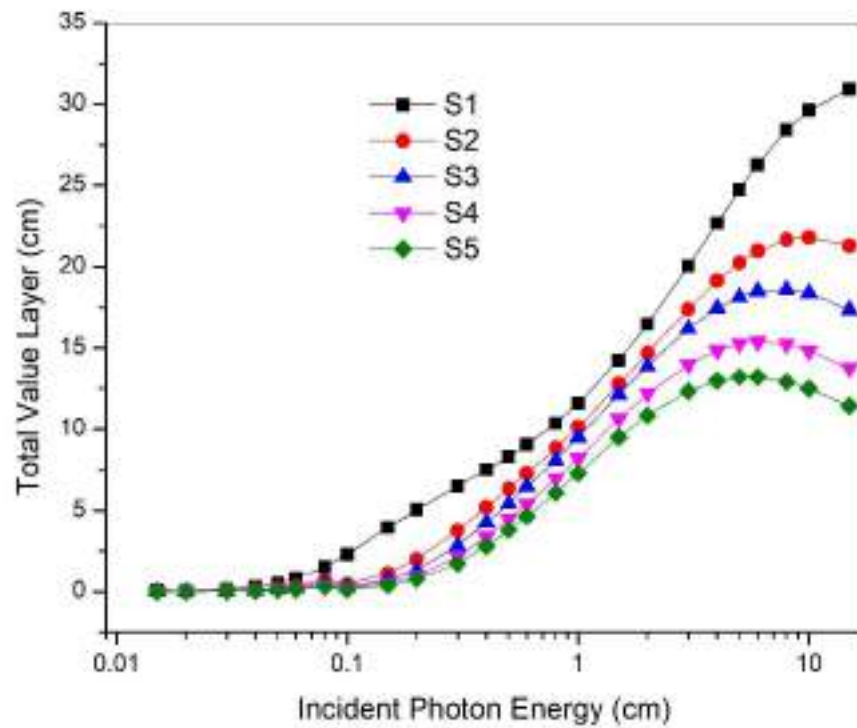
The half value layer term (HVL), which enables the calculation of the material thickness needed to reduce the initial gamma-ray intensity by half, is crucial in research on radiation shielding. This is due to the requirement that shielding requirements be predetermined depending on the kind and energy of the radiation utilized in radiation experiments. Therefore, a more thorough understanding of gamma-ray attenuation capabilities during the incident gamma-contact rays with the attenuator specimen should be used to establish the amount of the half value layer

necessary for each type of prospective shielding material. Figure 3.4 show the HVL fluctuation trend of the tested glass samples as a function of incident photon energy. According to what is to be predicted, the necessary half value layer expands with rising gamma-ray energy. The penetrating dominance of accompanying gamma-ray photons, which is caused by enhanced gamma-ray energy, typically produces this effect. The S5 sample, according to our observations, satisfies the sample thickness requirements down to the last detail. Because lead oxide contributes the most, the S5 sample exhibits better gamma-ray shielding properties, which is another convincing indication of this sample as gamma shielding material.



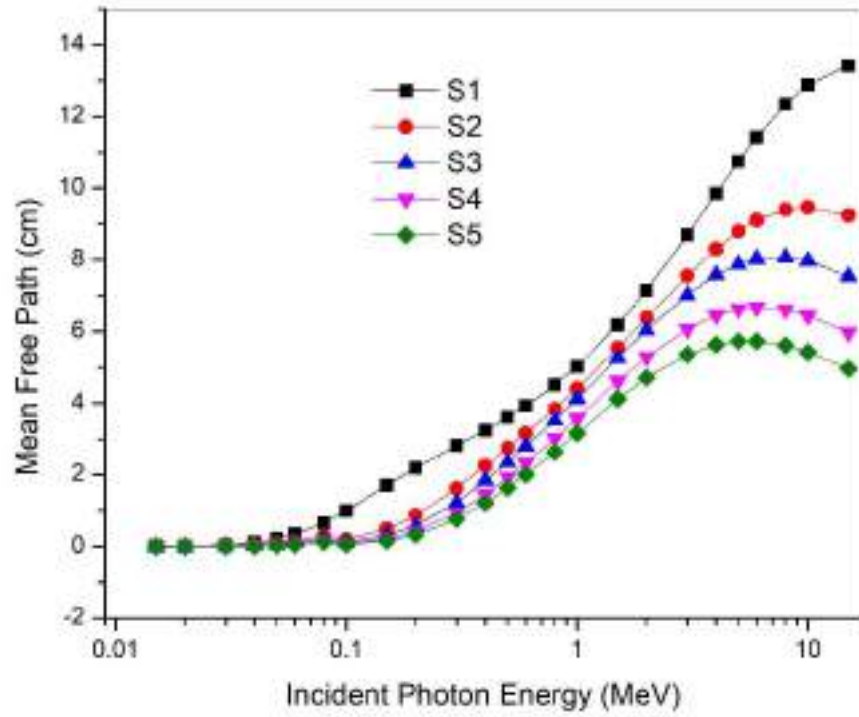
**Figure 3.4:** Half-value layer (HVL) against photon energy for investigated glass samples

The variation of TVL with photon energy in region 0.05 MeV – 15 MeV for glass samples is shown in Figure 3.5. TVL shows similar variations as HVL in in similar energy regions and both are alike mfp (Figure 3.6) variations as these quantities depend inversely to linear attenuation coefficient with difference of constant factor only. It is clear from figures that more are the gamma ray energies higher is the thickness required for shielding.



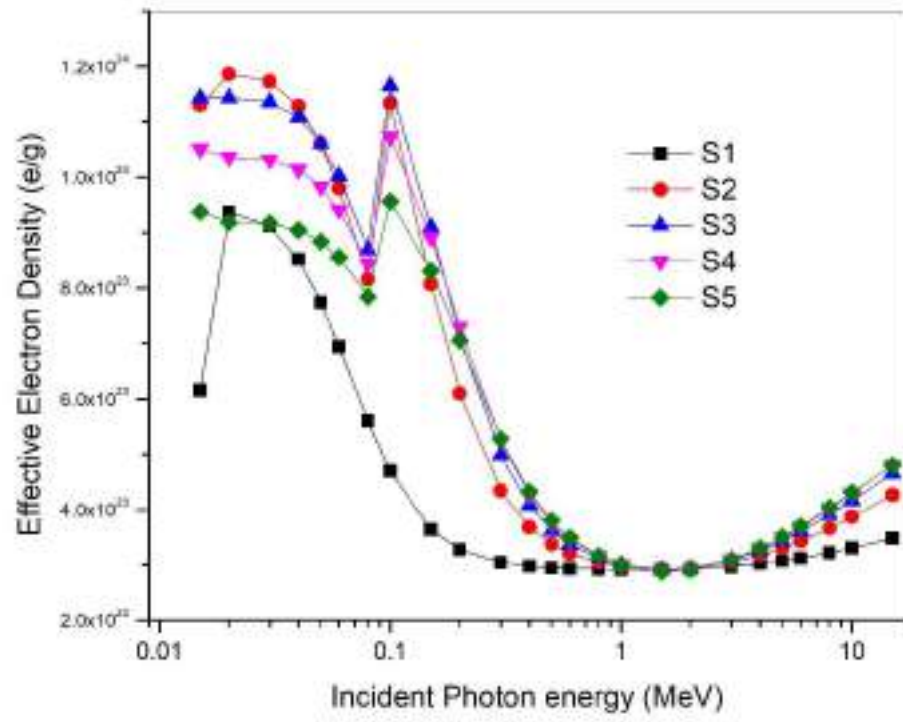
**Figure 3.5:** Half-value layer (TVL) against photon energy for investigated glass samples



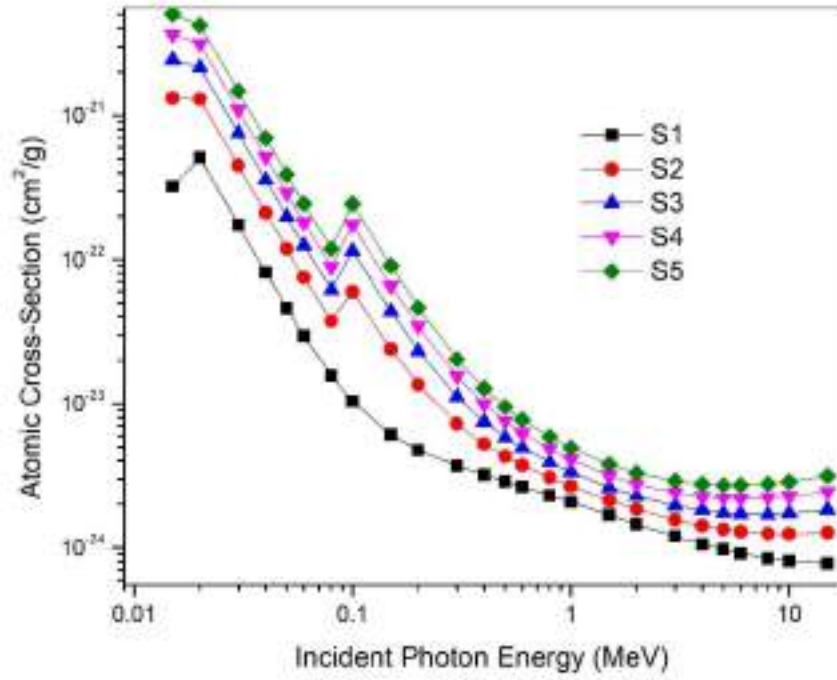


**Figure 3.6:** Mean free path (MFP) against photon energy for investigated glass samples

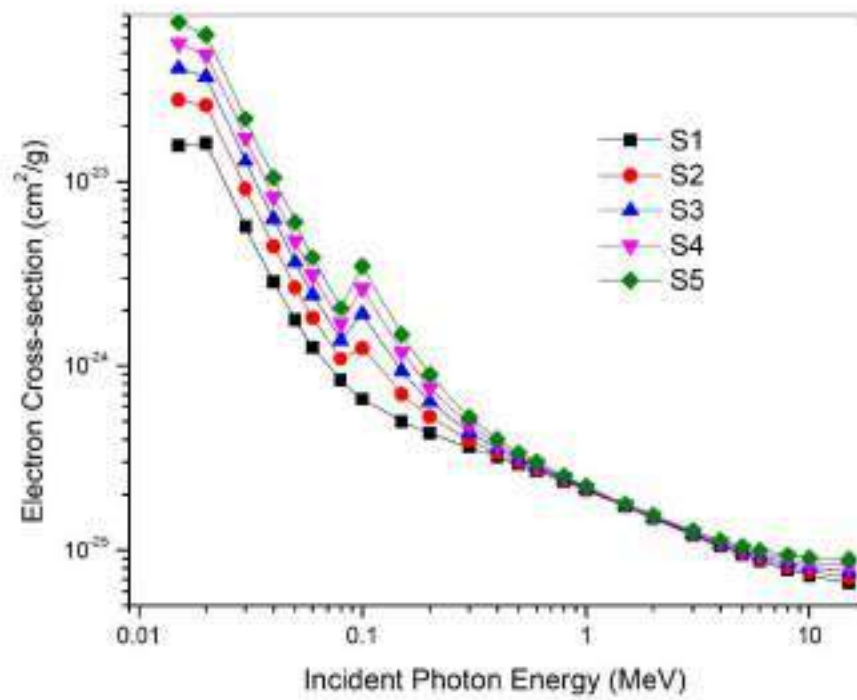
All produced glass samples were also assessed for their effective electron densities ( $N_{\text{eff}}$ ), which show the number of electrons per unit mass. Figure 3.7 shows in low photon energy region,  $N_{\text{eff}}$  altered in a non-monotonic pattern with photon energy until it reached a sharp jump close to the La absorption edge (0.0880 MeV). The PE process is to be responsible for this behavior. All of the samples under investigation showed a sharp decline in  $N_{\text{eff}}$  values in the photon energy range between 0.1 and 1 MeV; this tendency is connected to the CS process, which predominates in this range. An increase in the  $N_{\text{eff}}$  values was noticed in the energy range above 2 MeV and was attributed to the PP process, which dominates in this range. The S5 sample, which had the highest concentration of lead oxide, clearly had a considerable advantage in terms of gamma-ray attenuation.



**Figure 3.7:** Variation of electron density ( $N_{\text{eff}}$ ) number values as a function of photon energy for given glass samples

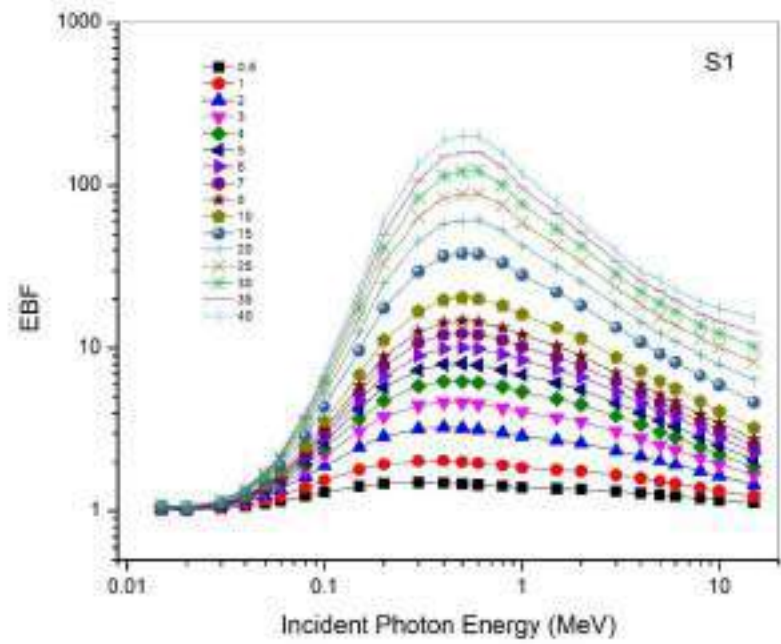


**Figure 3.8:** Variation of Atomic cross section values as a function of photon energy for given glass samples

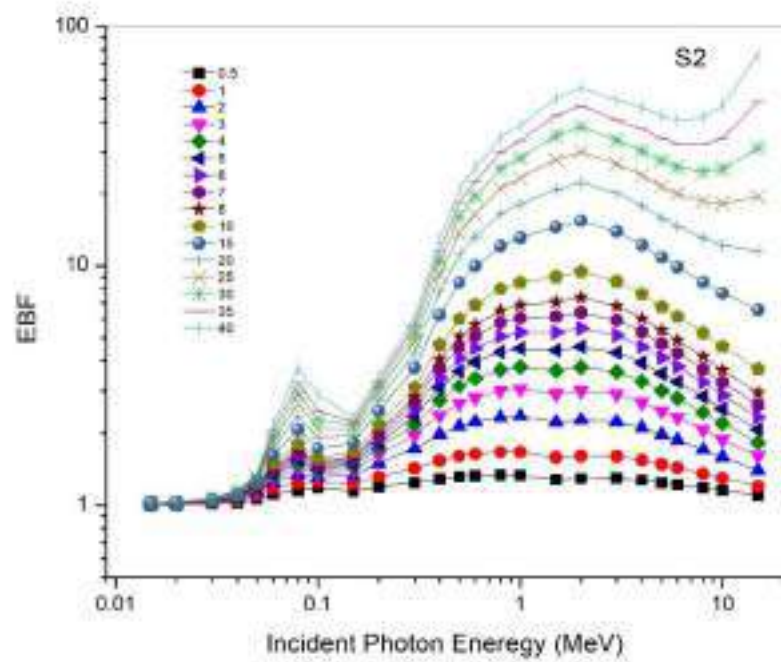


**Figure 3.8:** Variation of Electron cross section values as a function of photon energy for given glass samples

For a proper assessment of gamma attenuation of the prepared ceramic samples, the term "Build-up factor" is necessary and could impact the measurement's accuracy. Nuclear technology is necessary for usage in industry, medicine, agriculture, education, research, and military applications; hence gamma ray measurement is necessary. It is also important for the construction of radiation-protective buildings that safeguard human health. Un-collided photons and colliding photons are the two types of radiation that are produced when gamma radiation passes through a shielding material. As a result, the accumulation factor is a crucial statistic for gamma ray measurement. It is determined by dividing the total number of particles at a given position by the total number of particles that have not yet collided there. Figures 3.9-3.10, 3.11, 3.12 and 3.13 for S1, S2, S3, S4 and S5 glass samples, respectively, illustrate the fluctuation of the exposure buildup factor with incident photon energy in the range of 0.015 to 15.0 MeV at some of the penetration depths (0.5 - 40 mfp). The majority of gamma ray absorption occurs in the low- and high-energy regions. On the other hand, Compton scattering dominates as the primary mechanism of photon-matter interaction at intermediate energies. As a result, the Compton region has the highest EBF values in the low-energy region. At intermediate energies, photon scattering was not completely eliminated, but their energy was reduced, increasing the likelihood that photons would multiply in the material. The probability of photons engaging with the material in the 15-40 MFP range varied with  $Z^2$  after 3 MeV. As a result of secondary photons forming at deep penetration levels, EBF values were increased. The least EBF values were discovered for the BZT sample as the EBF values fell with increasing barium and zirconium insertions.

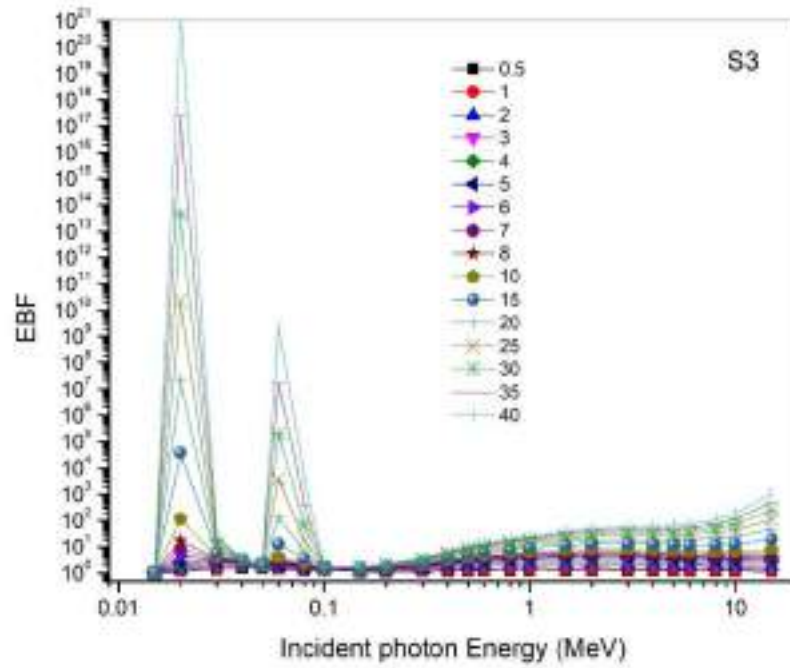


**Figure 3.9:** Variations of the exposure buildup factors (EBF) with photon energy for S1 glass sample as a function of mean free path.

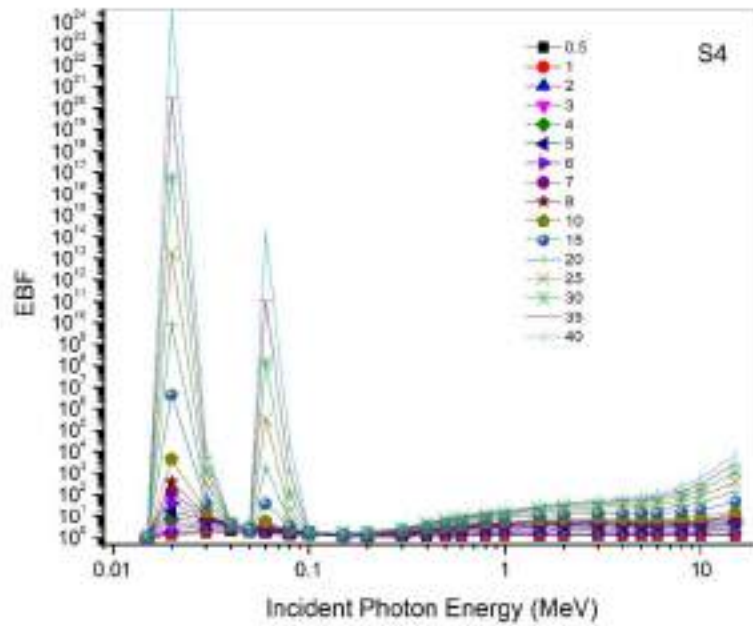


**Figure 3.10:** Variations of the exposure buildup factors (EBF) with photon energy for S2 glass sample as a function of mean free path

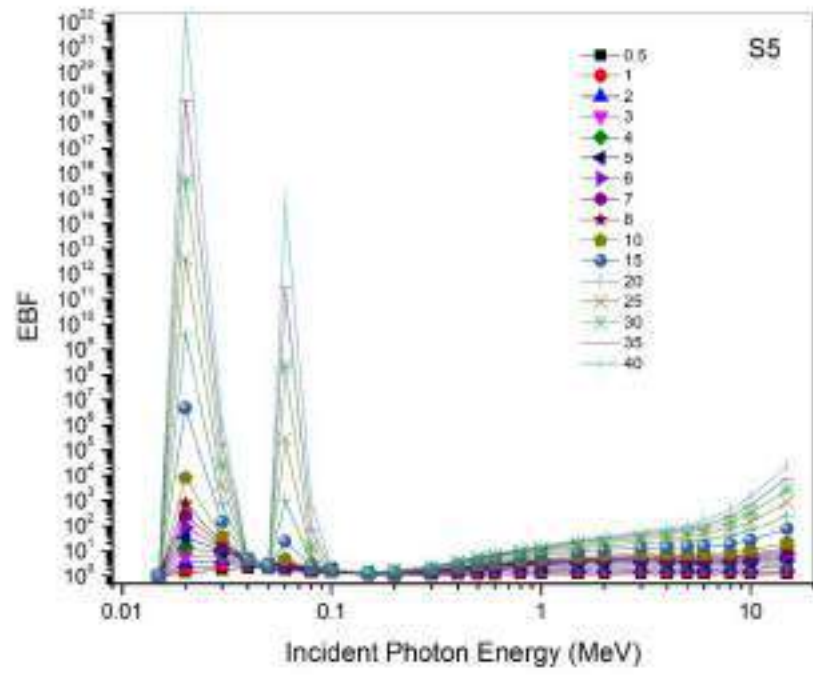




**Figure 3.11:** Variations of the exposure buildup factors (EBF) with photon energy for S3 glass sample as a function of mean free path



**Figure 3.12:** Variations of the exposure buildup factors (EBF) with photon energy for S4 glass sample as a function of mean free path



**Figure 3.13:** Variations of the exposure buildup factors (EBF) with photon energy for S5 glass sample as a function of mean free path

## CHAPTER 4

### CONCLUSIONS

In this study, the gamma-ray shielding parameters using WinXcom computer software have been investigated with change in lead doping in the glass structure. Accordingly, the influence of lead on the gamma-ray shielding properties of lead zirconium titanate glasses  $xPbO: 14TiO_2: 16ZrO_2: (40 - 0.5x)B_2O_3: (40 - 0.5x)SiO_2$ , ( $x = 0, 10, 20, 30, 40$ ) was examined using WinXcom software. Several significant radiation shielding parameters were evaluated. The ceramic density was increased from 5.5102 g/cm<sup>3</sup> to 7.6003 g/cm<sup>3</sup> with increasing lead content.

Results revealed the following points based on shielding parameter studies:

1. At each energy within the spectrum of interest in this research, MAC generally trends in the order that (S1) MAC < (S2) MAC < (S3) MAC < (S4) MAC < (S5) MAC.
2. The maximum and minimum values of LAC were obtained at 15 keV and 8 MeV, respectively with values of 30.93 and 0.074 cm<sup>-1</sup>; 111.54 and 0.108 cm<sup>-1</sup>; 175.19 and 0.133 cm<sup>-1</sup>; 249.21 and 0.167 cm<sup>-1</sup>; and 322.08 and 0.201 cm<sup>-1</sup> for S1 to S5, respectively.
3. The minimum and maximum values of HVL were obtained at 15 keV and 8 MeV, respectively with values of 0.022 and 8.55 cm; 0.006 and 6.52 cm; 0.004 and 5.60 cm; 0.003 and 4.58 cm; and 0.002 and 3.89 cm for S1 to S5, respectively.
4. The maximum and minimum values of  $Z_{eff}$  were obtained at 15 keV and 8 MeV, respectively with values of 20.64 and 10.81; 47.46 and 15.40; 58.75 and 20.06; 64.98 and 24.82; and 68.93 and 29.67 for S1 to S5, respectively.

5. The trend of variation of electron density ( $N_{\text{eff}}$ ) as a function of photon energy for BZT ceramic is  $S1 > S2 > S3 > S4 > S5$  for all photon energy range 0.015 MeV to 15 MeV.
6. It has been observed that the exposure buildup factor first increases for 0.5 MFP to 10 MFP and afterwards decreases for 15 MFP again increases for 20 MFP than fall at 25 MFP, rise at 30 to 35 MFP and finally fall at 40 MFP for all BZT, BLT and BLZT ceramic samples at 15 MeV.

Generally, increasing of lead oxide increment in the glass samples has a positive influence on their radiation shielding capability. One can conclude that all samples can attenuate gamma rays. Therefore, the investigated samples can be applied successfully in nuclear shielding applications. The total  $\mu_m$ ,  $Z_{\text{eff}}$  and  $N_{\text{eff}}$  of the ceramics decreases exponentially toward higher energy of gamma-rays. These results are good indications of the potential of the prepared glasses as a radiation shielding material.

As a result, these findings may deepen our understanding of the structural properties and gamma ray shielding capabilities of lead Zirconium titanate in various systems and offer a thorough viewpoint for the development of useful glasses with enhanced applications.

## REFERENCES

1. Ikegami, S., Ueda, I., & Nagata, T. (1971). Electromechanical properties of PbTiO<sub>3</sub> ceramics containing La and Mn. *The Journal of the Acoustical Society of America*, 50(4A), 1060-1066.
2. Takahashi, T. (1991). Lead titanate ceramics with large piezoelectric anisotropy and their applications. *Toshiba's Selected Papers on Science and Technology*; (Japan), 3(1).
3. Lines, M. E., & Glass, A. M. (2001). *Principles and applications of ferroelectrics and related materials*. Oxford university press.
4. Rahangdale, V. U., & Deshpande, V. K. (2020). Lead-zirconate-titanate based glass and glass-ceramics: Preparation, physical, dielectric and ferroelectric properties. *Materials Today: Proceedings*, 29, 866-871.
5. Rahangdale, V. U., & Deshpande, V. K. (2020). Lead-zirconate-titanate based glass and glass-ceramics: Preparation, physical, dielectric and ferroelectric properties. *Materials Today: Proceedings*, 29, 866-871.
6. McMillan, P. W. (1982). The crystallisation of glasses. *Journal of Non-Crystalline Solids*, 52(1-3), 67-76.
7. Rahangdale, V. U., & Deshpande, V. K. (2020). Lead-zirconate-titanate based glass and glass-ceramics: Preparation, physical, dielectric and ferroelectric properties. *Materials Today: Proceedings*, 29, 866-871.
8. Sahu, A. K., Kumar, D., & Parkash, O. (2006). Lead-strontium titanate glass ceramics: I-crystallization and microstructure. *Journal of materials science*, 41(7), 2075-2085.
9. Herczog, A. (1964). Microcrystalline BaTiO<sub>3</sub> by crystallization from glass. *Journal of the American Ceramic Society*, 47(3), 107-115.
10. Borrelli, N. F. (1967). Electro-optic Effect in Transparent Niobate Glass—Ceramic Systems. *Journal of Applied Physics*, 38(11), 4243-4247.
11. Layton, M. M., & Herczog, A. (1967). Nucleation and Crystallization of NaNbO<sub>3</sub> from Glasses in the Na<sub>2</sub>O-Nb<sub>2</sub>O<sub>5</sub>-SiO<sub>2</sub> System. *Journal of the American Ceramic Society*, 50(7), 369-375.



12. Borrelli, N. F., & Layton, M. M. (1969). Electrooptic properties of transparent ferroelectric glass—Ceramic systems. *IEEE Transactions on Electron Devices*, 16(6), 511-514.
13. Layton, M. M., & Herczog, A. (1969). STRUCTURE AND CRYSTALLISATION OF GLASSES OF LOW NETWORK-FORMER CONTENT. *Glass Technology*, 10(2), 50.
14. Rahangdale, V. U., & Deshpande, V. K. (2014). Study of physical properties of PbTiO<sub>3</sub> based glass-ceramic with variation of heat treatment duration. *Ferroelectrics*, 467(1), 85-98.
15. Ulrich, D. R. (1968). *High dielectric thick films for screened circuit capacitors* (No. LAR-10294).
16. Rahangdale, V. U., & Deshpande, V. K. (2020). Lead-zirconate-titanate based glass and glass-ceramics: Preparation, physical, dielectric and ferroelectric properties. *Materials Today: Proceedings*, 29, 866-871.
17. Tummala, R. R. (1976). Low-temperature and low-expansion glass-crystal composites by the formation of Perovskite lead titanate. *Journal of Materials Science*, 11, 125-128.
18. Ito, S., Kokubo, T., & Tashiro, M. (1978). Transparency of LiTaO<sub>3</sub>-SiO<sub>2</sub>-Al<sub>2</sub>O<sub>3</sub> glass-ceramics in relation to their microstructure. *Journal of Materials Science*, 13, 930-938.
19. HERCZOG, A. (1984). Barrier Layers in Semiconducting Barium Titanate Glass-Ceramics. *Journal of the American Ceramic Society*, 67(7), 484-490..
20. Mianxue, W. U., & Peinan, Z. (1986). Piezoelectricity, pyroelectricity and ferroelectricity in glass ceramics based on PbTiO<sub>3</sub>. *Journal of Non-Crystalline Solids*, 84(1-3), 344-351.
21. Banach, U., HÜbert, T., Fellmuth, B., & Hegenbarth, E. (1989). Low-temperature dielectric properties of SrTiO<sub>3</sub> alumino-borate glass-ceramics. *Ferroelectrics*, 100(1), 111-120.
22. Herczog, A. (1990). Phase Distribution and Transparency in Glass-Ceramics Based on a Study of the Sodium Niobate–Silica System. *Journal of the American Ceramic Society*, 73(9), 2743-2746.
23. Kusumoto, K., & Sekiya, T. (1993). Preparation of lead titanate particles by crystallization of glass. *Materials research bulletin*, 28(9), 885-891.

24. Shankar, J., & Deshpande, V. K. (2010). Study of lead titanate based glass ceramics with addition of BaO. *Integrated Ferroelectrics*, 119(1), 110-121.
25. Rema, K. P., & Kumar, V. (2008). Structure–Property Relationship in Mn-Doped (Pb<sub>0.94</sub>Sr<sub>0.06</sub>)(Zr<sub>0.53</sub>Ti<sub>0.47</sub>)O<sub>3</sub>. *Journal of the American Ceramic Society*, 91(1), 164-168.
26. Kumar, V., Achuthan, A. T., Sivanandan, K., Divya, P. V., & Rema, K. P. (2006). Sol–Gel Synthesis of PZT–Glass Nanocomposites Using a Simple System and Characterization. *International journal of applied ceramic technology*, 3(5), 345-352.
27. K.H. Lee, C.C. Chu (1996) Gamma irradiation sterilizing of biomaterial medical devices or products, with improved degradation and mechanical properties, US Patent 5485496 A
28. T. von Woedtke, W.D. Julich, V. Hartmann, M. Stieber, P.U. Abel (2002) Sterilization of enzyme glucose sensors: problems and concepts. *Biosens Bioelectron.* 17(5), 373– 382
29. W.C. Sung (2005) Effect of gamma irradiation on rice and its food products. *Radiat. Phys. Chem.* 73, 224–228
30. J.F. Diehl (2002) Food irradiation – past, present and future. *Radiat. Phys. Chem.* 63, 211–215
31. S. Matsunaga, T. Shuto, N. Kawahara, J. Suenaga, S. Inomori, H. Fujino (2011) Gamma knife surgery for brain metastases from colorectal cancer. *J. Neurosurg.* 114, 782–789
32. A. Wyszomirska (2012) Iodine-131 for therapy of thyroid diseases. Physical and Biological basis. In: *Nucl. Med. Rev.*, 15, 120–123
33. G. Quarta, L. Calcagnile, M. Vidale (2012) Integrating non-destructive ion beam analysis methods and AMS radiocarbon dating for the study of ancient bronze status. *Radiocarbon* 54, 801–812
34. S.K. Saha, C.W. Cheng, K.M. Barfoot, J.D. MacArthur, B.C. Robertson (1982) Bulk elemental analysis using  $\gamma$ -rays from inelastic scattering of neutrons produced by the  $^{13}\text{C}(\alpha, n)^{16}\text{O}$  reaction, *Nucl. Instrum. Methods*, 201, 465–471
35. H.S. Cho, J.E. Oh, S.I. Choi, H.M. Cho, Y.O. Park, D.K. Hong, M.S. Lee, Y.J. Yang, U.K. Je, D.S. Kim, T.H. Woo, B.S. Lee, H.K. Lee (2011) Performance

- evaluation of a gamma-ray imaging system for non-destructive testing of welded pipes, Nucl. Instrum. Methods Phys. Res., Sect. A, 652, 650–653.
36. A.E. Moura, C.C. Dantas, M.S. Nery, J.M. Barbosa, T.L. Rolim, E.A.O. Lima, S.B. Melo, V.A. Dos Santos (2015) Non-destructive evaluation of weld discontinuity in steel tubes by gamma ray CT. Nucl. Instrum. Methods Phys. Res., Sect. B 349, 155–162
  37. D.F. Jackson, D.J. Hawkes (1981) X-ray attenuation coefficients of elements and mixtures, Physics Reports, Volume 70, Issue 3, Pages 169-233
  38. J.H. Hubbell, (1982) Photon Mass Attenuation and Energy-Absorption Coefficients from 1KeV to 20 MeV. International Journal of Applied Radiation and Isotopes, 33, 1269-1290
  39. J. H. Hubbell, S. M. Seltzer (1995) Tables of X-Ray Mass Attenuation Coefficients and Mass Energy-Absorption Coefficients 1 keV to 20 MeV for Elements  $Z = 1$  to 92 and 48 Additional Substances of Dosimetric Interest, NISTIR 5632, (1995) Gaithersburg, MD 20899 pp. 1-120
  40. M.J. Berger, J.H. Hubbell (1987) "XCOM: Photon Cross Sections on a Personal Computer," National Bureau of Standards, Gaithersburg, MD. 87-3597
  41. C. T. Chantler (2000) Detailed Tabulation of Atomic Form Factors, Photoelectric Absorption and Scattering Cross Section, and Mass Attenuation Coefficients in the Vicinity of Absorption Edges in the Soft X-Ray ( $Z=30-36$ ,  $Z=60-89$ ,  $E=0.1$  keV–10 keV), Addressing Convergence Issues of Earlier Work, Journal of Physical and Chemical Reference Data, 29, 597
  42. J.F. Krocher, R.E. Browman (Eds.) (1984) Effects of Radiation on Materials and Components, Reinhold, New York
  43. M.J. Kreidl, J.R. Hensler, H.H. Hower (Ed.) (1958) Modern Materials, Vol. 1, Academic Press, New York, p. 217
  44. W.S. Rothwell (1958) Radiation Shielding Windows Glasses, Bull. PE-50, Corning Glass Works, Corning, NY
  45. L.M. Melnick, H.W. Safford, K.H. Sun, A.J. Silverman (1951) Neutron – absorbing glass: CdO–SiO<sub>2</sub>–B<sub>2</sub>O<sub>3</sub> system, Am. Ceram. Soc., 34, 82–6

46. A. Khanna, S.S. Bhatti, K.J. Singh and K.S. Thind (1996) Gamma-ray attenuation coefficients in some heavy metal oxide borate glasses at 662 keV, Nucl. Instrum. Meth. B, 114, 217
47. J. F. Krocher and R. E. Browman, Effects of radiation on materials and components, Reinhold, New York, 1984
48. S.R. Manonara, S.M. Hanagodimath, L. Gerward, and K.C. Mittal (2011) Exposure Buildup Factors for Heavy Metal Oxide Glass: A Radiation Shield. Journal of the Korean Physical Society, 59(2), 2039-2042
49. A. Khanna, S. S. Bhatti, K. J. Singh and K. S. Thind (1996) Nucl. Instrum. Methods Phys. Res. Sect. B 114, 217
50. N. Singh, K. J. Singh, K. Singh and H. Singh (2004) Comparative study of lead borate and bismuth lead borate glass systems as gamma-radiation shielding materials, Nucl. Instrum. Methods Phys. Res., Sect. B, 225, 305–309
51. H. Singh, K. Singh, G. Sharma, R. Nathuram and H. S. Sahota (2002) Photon Interaction Studies with Some Glasses and Building Materials, Nuclear Science and Engineering, Vol. 142, No. 3, pp. 342-348.
52. K. Singh, H. Singh, V. Sharma, R. Nathuram, A. Khanna, R. Kumar, S.S. Bhatti, H.S. Sahota (2002) Gamma ray attenuation coefficients in bismuth borate glasses, Nucl. Instrum. Methods Phys. Res. Sect. B, 194, 1–6.
53. H. Gill, G. Kaur, K. Singh, V. Kumar, and J. Singh (1998) Study of effective atomic numbers in some glasses and rocks, Radiation Physics and Chemistry, 51, 4–6, 671–672
54. S. R. Manohara, S. M. Hanagodimath and L. Gerward (2009) Photon interaction and energy absorption in glass: A transparent gamma ray shield, Journal of Nuclear Materials 393(3), 465-472
55. G S Sidhu, P S Singh, and G S Mudahar (1999) Computation of geometrical-progression (G-P) fitting parameters of plastic materials, Indian J. Phys. 73A(6), 811-819
56. S. Singh, S. S. Ghumman, C. Singh, K. S. Thind, and G. S. Mudahar (2010) Buildup of gamma ray photons in flyash concretes: a study, Annals of Nuclear Energy, vol. 37, no. 5, 681–684

57. G. S. Brar, K. Singh, M. Singh, and G. S. Mudahar(1994) Energy absorption buildup factor studies in water, air and concrete up to 100mfp using G-P fitting formula, *Radiation Physics and Chemistry*, vol. 43, no. 6, 623–627
58. V. P. Singh and N. M. Badiger (2012) Comprehensive study of energy absorption and exposure buildup factor for concrete shielding in photon energy range 0.015–15MeV upto 40 mfp penetration depth: dependency of density, chemical element, photon energy,” *International Journal of Nuclear Energy Science and Technology*, vol. 7, no. 1, 75–99
59. V. P. Singh and N. M. Badiger (2013) Photon energy absorption buildup factor of gaseous mixtures used in radiation detectors, *Radioprotection*, vol. 48, no. 1, 63–78.
60. M. Kurudirek, B. Doğan, M. Ingeç, N. Ekinci, and Y. Özdemir (2011) Gamma-ray energy absorption and exposure buildup factor studies in some human tissues with endometriosis, *Applied Radiation and Isotopes*, vol. 69, no. 2, 381–388
61. G. Sandeep and S. S. Gurdeep (2012) A comprehensive study on energy absorption and exposure buildup factors for some soils and ceramic materials, *Journal of Applied Physics*, vol. 2, no. 3, 24–30
62. S. Tejbir, K. Gurpreet, and S. S. Parjit (2013) Study of gamma ray exposure buildup factor for some ceramics with photon energy, penetration depth and chemical composition, *Journal of Ceramics*, vol. 2013, Article ID 721606.
63. E.Yilmaz, H.Baltas, E. Kiris, I. Ustabas, U. Cevik, andA.M. El-Khayatt (2011) Gamma ray and neutron shielding properties of some concrete materials, *Annals of Nuclear Energy*, vol. 38, no. 10, 2204–2212
64. Y. Harima, Y. Sakamoto, S. Tanaka and M. Kawai (1986) Validity of the geometric-progression formula in approximatingthe gamma ray buildup factors, *Nucl. Sci. Eng.*, 94, 24
65. Y. Harima, Y. Sakamoto, S. Tanaka, M. Kawai, T. Fujita, T. Ishikawa, M. Kinno, K. Hayashi, Y. Matsumoto and T. Nishimura (1986) Applicability of geometrical progression approximation (G-P method) of gamma-ray buildup factors, *Japan Atomic Energy Research Institute*, M 86, 071
66. J. Kaewkhao and P. Limsuwan (2010) Mass attenuation coefficients and effective atomic numbers in phosphate glass containing Bi<sub>2</sub>O<sub>3</sub>, PbO, and BaO at 662 keV, *Nucl. Instrum. Methods Phys. Res., Sect. A*, vol. 619, pp. 295–297



67. K.J. Singh, N. Singf, N., R.S. Kaundal, and K. Singh (2008) Gamma-ray shielding and structural properties of PbO-SiO<sub>2</sub> glasses, Nucl. Instrum. Methods Phys. Res., Sect. B, 2008, vol. 266, pp. 944–948
68. K. Kirdsiri, J. Kaewkhao, A. Pokaipisit, W. Chewpraditkul, and P. Limsuwan, (2009) Gamma-rays shielding properties of xPbO:(100–x)B<sub>2</sub>O<sub>3</sub> glasses system at 662 keV, Ann. Nucl. Energy, vol. 36, no. 9, pp. 1360–1365
69. K. Kirdsiri, J. Kaewkhao, N. Chanthima, and P. Limsuwan (2011) Comparative study of silicate glasses containing Bi<sub>2</sub>O<sub>3</sub>, PbO, and BaO: Radiation shielding and optical properties, Ann. Nucl. Energy, vol. 38, pp. 1438–1441
70. S. Glasstone and A. Sesonske (2004) Nuclear Reactor Engineering: Reactor Design Basics, New York: Springer-Verlag, 4th ed., vol. 1
71. A.I. Fawazi, A.A. El-Sayes, A.A. El-Latif and M. El-Desoky (2006) Borate glass with lead and nickel oxides for radiation attenuation, Abhath Al-Yarmouk, vol. 15, no. 2, pp. 195–205

**INFLUENCE OF LEAD ON THE PHOTON  
INTERACTION PARAMETERS OF LEAD-ZIRCONATE-  
TITANATE BASED GLASS  
PROJECT REPORT**

*Submitted in partial fulfillment of the  
requirements for the award of the degree of*

**MASTER OF SCIENCE**

**in**

**PHYSICS**

*By*

**Harshdeep Kaur  
Regn. No. 811-2019-812**



**DEPARTMENT OF PHYSICS  
SRI GURU TEG BAHADUR KHALSA COLLEGE, SRI  
ANANDPUR SAHIB  
(An Autonomous College)  
ANANDPUR SAHIB– 140118, PUNJAB (INDIA)**



**SRI GURU TEG BAHADUR KHALSA COLLEGE, SRI ANANDPUR SAHIB**  
(An Autonomous College)  
**ANANDPUR SAHIB-140118. PUNJAB (INDIA)**

---

## **CERTIFICATE**

It is certified that the work contained in the project report entitled “**INFLUENCE OF LEAD ON THE PHOTON INTERACTION PARAMETERS OF LEAD-ZIRCONATE-TITANATE BASED GLASS**” is an original contribution by me and has not been submitted in part or full for any other degree at this or other University/ Institute.

The assistance and help received during the course of the thesis work have been acknowledged.

**Harshdeep Kaur**

Regn. No. **811-2019-812**

I, the undersigned, Supervisor of **Harshdeep Kaur**, **Regn. No. 811-2019-812**, a candidate for the degree of **Master of Science**, agree that the project report entitled, “**INFLUENCE OF LEAD ON THE PHOTON INTERACTION PARAMETERS OF LEAD-ZIRCONATE-TITANATE BASED GLASS**”, may be submitted in partial fulfillment of the requirements for the award of degree.

This is to certify that the above statement made by the candidate is correct to the best of my knowledge.

**Supervisor**

**Dr. Amrit Singh**

Assistant Professor

Department of Physics

Sri Guru Teg Bahadur Khalsa College

Sri Anandpur Sahib

## ACKNOWLEDGEMENT

Firstly, I had like to express my gratitude to my supportive Dr. Amrit Singh Assistant Professor at Department of physics Sri Guru Teg Bahadur Khalsa College Sri Anandpur Sahib, who has resourcefully guided me throughout this research project. I'm extremely grateful for his motivating discussions while enable me to accomplish this task successfully. Without his active guidance, support and encouragement I would not have made headway in this project.

I also thankful to my Parents for their moral support and suggestions to improve the dissertation work. I'm also thankful to other faculty members in the department for their encouragement and fruitful academic discussions.

A special thanks to Ms. Monika Sharma Assistant Professor at Department of Physics for the help and their valuable suggestions whenever I needed out of their busy schedule. I'm also thankful to my classmates and my friends who was directly or indirectly help me to complete this project report.

Harshdeep Kaur

## ABSTRACT

The Gamma ray shielding parameters using WinXcom computer software have been investigated with change in lead doping in the glass structure. Accordingly the influence of lead on the Gamma ray shielding properties of lead Zirconium titanate glasses  $xPbO:14TiO_2:16ZrO_2:(40 - 0.5x)B_2O_3:(40 - 0.5x)SiO_2$ , ( $x = 0, 10, 20, 30, 40$ ) was examined using WinXcom computer software. Several significant radiation shielding parameters were evaluated. The ceramic density was increased from 5.5102 to 7.6003 g/cm<sup>3</sup> with increasing lead content.

At each energy within the spectrum of interest in this research MAC generally trends in the order that (S1)MAC < (S2)MAC < (S3)MAC < (S4)MAC < (S5)MAC. The maximum and minimum values of LAC were obtained at 15 KeV and 8MeV respectively, with values of 30.93 and 0.074 cm<sup>-1</sup> ; 111.54 and 0.108 cm<sup>-1</sup> ; 175.19 and 0.133 cm<sup>-1</sup> ; 249.21 and 0.167 cm<sup>-1</sup> ; 322.08 and 0.201 cm<sup>-1</sup> for S1 to S5 respectively. The minimum and maximum values of HVL were obtained at 15KeV and 8MeV respectively with values of 0.022 and 8.55 cm ; 0.066 and 6.52 cm : 0.004 and 5.60 cm : 0.003 and 4.58 cm : 0.002 and 3.89 cm for S1 to S5 respectively. The maximum and minimum values of Z effective were obtained at 15 KeV and 8 MeV respectively with values of 20.64 and 10.81; 47.46 and 15.40; 58.75 and 20.06; 64.98 and 24.82; 68.93 and 29.67 for S1 to S5 respectively. The trend of variation of electron density N effective as a function of photon energy for BZT ceramic is S1>S2>S3>S4>S5 for all photon energy range 0.015 MeV to 15 MeV.



## CONTENTS

CHAPTER	Page No.
<b>1. Introduction.</b>	<b>1-14</b>
1.1 Introduction.	
1.1.1 Photoelectric effect.	
1.1.2 Compton scattering.	
1.1.3 Pair production.	
1.1.4 Rayleigh scattering.	
1.1.5 Thomson scattering by nucleus.	
1.1.6 Delbruck scattering.	
1.1.7 Nuclear resonance scattering	
1.1.8 Photo disintegration of the nuclei	
1.2 Fundamental parameters related to Attenuation of Gamma rays	
1.2.1 Linear Attenuation coefficient of the material.	
1.2.2 Mass Attenuation coefficient.	
1.2.3 Mean free path	
1.2.4 Half value layer.	
1.2.5 Tenth value layer.	
1.2.6 Effective atomic number.	
1.2.7 Electron density.	
<b>2. Literature survey.</b>	<b>15-20</b>
<b>3. Results and discussions.</b>	<b>21-30</b>
3.1 Introduction.	
3.2 Shielding properties.	
<b>4. Conclusions.</b>	<b>31-32</b>
<b>5. References</b>	<b>33-39</b>

## LIST OF FIGURES

S. No.	Name of the Figure
--------	--------------------

<b>Fig.1.1</b>	Schematic representation of photoelectric absorption
<b>Fig.1.2</b>	Schematic representation of pair production.
<b>Fig.3.1</b>	Variation of mass Attenuation coefficient values as a function of photon energy for given glasses
<b>Fig.3.2</b>	Variation of linear Attenuation coefficient values as a function of photon energy for given glasses
<b>Fig.3.3</b>	Variation of effective atomic number as a function of photon energy for given glasses samples
<b>Fig.3.4</b>	Half value layer against photon energy for investigated Glass samples
<b>Fig.3.5</b>	Tenth value layer against photon energy for given glasses samples
<b>Fig.3.6</b>	Mean free path against photon energy for given glasses samples
<b>Fig.3.7</b>	Variation of electron density number values as a function of photon energy for given glasses samples
<b>Fig.3.8</b>	Variation of atomic cross section values as a function of photon energy for given glasses samples
<b>Fig.3.9</b>	Variation of electron cross section values as a function of photon energy for given glasses samples

## LIST OF TABLES

S. No.	Name of the Table
--------	-------------------

Table 3.1	Sample codes , densities and chemical composition of glass samples
-----------	--

# CHAPTER-1

## INTRODUCTION

### 1.1 Introduction

The study of interaction of gamma-rays with matter is of great importance in the field of science and technology due to its vast applications in the fields of medicine, engineering, bio-technology, electric power generation plants and in non-destructive spectroscopic analysis, etc.

Around 1920s, de-Broglie developed the theory of matter-wave duality which introduced the concept of photon. Radiation emission, in the form of photon is the release of discrete amount of energy by a system as it moves from one state to other. Energy of the photon is the function of its frequency  $\nu$  (or wavelength  $\lambda$ ) and can be expressed as  $E = h\nu$ , where  $h$  is Plank's constant. Nature of radiation mainly depends upon its origin. When nucleus makes transition from high energy state to low energy state gamma-rays are emitted. Characteristic X-rays have atomic origins which are emitted when an electron makes transition from high energy state to low energy state. Continuous X-rays or Bremsstrahlung radiations are emitted due to the accelerated motion of the charged particles. The manner of interaction of X-rays and gamma-rays with matter is entirely different from the interaction of energetic charged particles because X-rays and gamma-rays are uncharged and massless (rest mass=0). During the interaction of the gamma-ray photon with matter, it either disappears entirely or is scattered through a significant angle. But the charged particles slow down gradually because of continuous interaction with many absorber atoms. As a result, range and specific energy loss concepts can't be applied in the same way on X-rays and gamma-rays as can be done on charged particles.

Incident gamma ray photons may interact with atomic electrons, with nucleons, with electric field surrounding the nuclei or with meson field surrounding the nucleons. These interactions may lead to complete or partial absorption of the incident photons and there is possibility of the scattering also. The most prominent incident energy range of photons is 0.01 to 5 MeV in which mainly photoelectric absorption, Compton scattering and pair production takes place. Brief introduction to various possible interactions is given below (Evans, 1955);

### **1.1.1 Photoelectric effect**

The photoelectric effect is the most important interaction in the 1-100 keV energy range of incident gamma ray. In this process, energy of the incident gamma ray photon gets completely transferred to the bounded electron of the atom. The necessary condition for the photoelectric emission is that the energy of the incident photon should be greater than the binding energy of the electron under consideration. If the incident energy is comparable with the binding energy of the electron photoelectric effect takes place more readily.

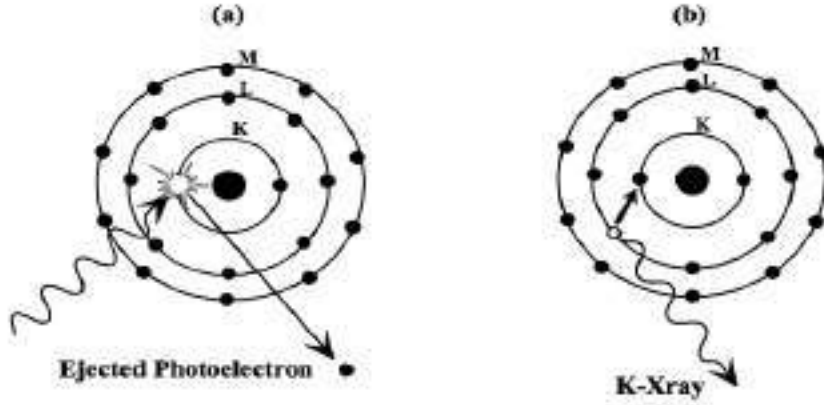
If  $E_\gamma$  is the energy of the incident gamma ray photon and  $E_b$  is the binding energy of the electron then kinetic energy of the ejected electron  $E_k$  is given as

$$E_k = E_\gamma - E_b \quad (1.01)$$

After the photoelectric emission of electron from the inner shell, the residual atom is in the ionized state with a vacancy in the inner shell. This vacancy gets filled by transition of the next higher shell electron with a lower binding energy as shown in Figure 1.1. This results in the shifting of the vacancy to the next higher shell, which in turn gets filled by electron from an even lower binding energy shell. So, we can say photoelectric effect triggers an electron cascade from outer to inner shell of the atom. These transitions of electrons from lower binding energy shells to high binding energy



shells appear as characteristic X-rays or Auger electrons. However, the probability of the characteristic X-ray emission is more for high atomic number (Z) targets.



**Figure 1.1: Schematic representation of photoelectric absorption**

K-shell has greatest contribution to the photoelectric effect while L, M and N shells have decreasing order of the importance. If the energy of the incident gamma ray photon is less than the binding energy of K shell electron then there will be interaction of the L, M or N shell electrons with gamma rays. So, there will be sharp decrease in the photoelectric cross-sections ( $\tau_{PE}$ ) with the decrease in the incident photon energy. The photoelectric cross-sections ( $\tau_{PE}$ ) or the photoelectric coefficient is defined as the probability of this interaction to take place.  $\tau_{PE}$  is a function of energy of the incident gamma rays ( $E_\gamma$ ), atomic number (Z) and atomic mass number (A) is given in equation 1.02,

$$\tau_{PE} \propto (N_t) \frac{Z^n}{E_\gamma^m} \quad (1.02)$$

The values of  $m$  and  $n$  lies from 3 to 5, which is a function of  $E_\gamma$ . The number of atoms/m<sup>3</sup> ( $N_t$ ) in the material through which the photon transverses and can be calculated mathematically as

$$N_t = \rho \frac{N_A}{A} \quad (1.03)$$

Such as,  $\rho$  is the bulk density,  $N_A$  is the Avogadro's number and  $A$  is atomic weight of the target (Tsoulfanidis, 1995).

### 1.1.2 Compton scattering

Compton scattering is the process in which the incident gamma ray photon interacts directly with the outermost shell electron of the target material. In Compton scattering incident gamma ray photon losses, a fraction of its energy contrary to photoelectric effect in which complete absorption of the photon takes place. Assuming the electron at rest before the collision, kinetic energy ( $K_e$ ) acquired by recoiled electron after the collision can be represented as (Dyson (2005))

$$K_e = E_{\gamma_i} - E_{\gamma_f} \quad (1.04)$$

Here  $E_{\gamma_i}$  and  $E_{\gamma_f}$  is the energy of the gamma photon before and after the interaction with the electron. To obtain expression for  $E_{\gamma_f}$ , laws of conservation of momentum can be applied and it is found that  $E_{\gamma_f}$  is the function of the scattering angle  $\theta$  as

$$E_{\gamma_f} = \frac{E_{\gamma_i}}{1 + (1 - \cos\theta) \frac{E_{\gamma_i}}{m_0 c^2}} \quad (1.05)$$

Equation 1.04 & 1.05 are used to obtain the kinetic energy  $K_e$  of the electron as

$$K_e = \frac{(1 - \cos\theta) \frac{E_{\gamma_i}}{m_0 c^2}}{1 + (1 - \cos\theta) \frac{E_{\gamma_i}}{m_0 c^2}} E_{\gamma_i} \quad (1.06)$$

Here  $m_0 c^2$  is the rest mass energy of the electron (0.511MeV). For  $\theta = \pi$  minimum energy is carried by the scattered photon, i.e.

$$E_{\gamma_f}^{min} = \frac{E_{\gamma_i}}{1 + 2 \frac{E_{\gamma_i}}{m_0 c^2}} \quad (1.07)$$

If  $\theta = 0^\circ$  there will be maximum energy taken by the scattered photon, i.e.,

$$E_{\gamma_f}^{max} = E_{\gamma_i} \quad (1.08)$$

From equation (1.07), it can be concluded that minimum energy of the scattered photon is greater than zero. So, in Compton scattering it is not possible that whole of the incident energy is carried by the ejected electron. From equation (1.08), we can say that there will be no interaction between the incident photon and the outer electron, as energy of the scattered photon remains unaffected.

Compton cross-section  $\sigma_C$  or Compton coefficient is defined as the probability of Compton interaction to take place per unit distance.  $\sigma_C$  is a complicated function of  $E_{\gamma_i}$ . Such that,

$$\sigma_C = NZ.f(E_{\gamma_i}) \quad (1.09)$$

Here  $f(E_{\gamma_i})$  is a function of  $E_{\gamma_i}$  and  $N$  is the atom density, which can be obtained using equation (1.03).

$$\sigma_C = \rho \frac{N_A}{A} Z.f(E_{\gamma_i}) \quad (1.10)$$

In most of the materials except Hydrogen, value of  $A \approx 2Z$  to  $2.6Z$ , so equation (1.10) can be modified as (Tsoufanidis, 1995)

$$\sigma_C \sim \rho \left( \frac{N_A}{2} \right).f(E_{\gamma_i}) \quad (1.11)$$

### 1.1.3 Pair production

Pair production is the third type of the interaction of highly energetic gamma ray with matter which becomes energetically possible if the incident gamma energy is more than twice of rest mass energy of the electron (1.02 MeV). In this type of interaction electron-positron pair appears on the cost of gamma ray photon. The

presence of the nucleus is must in this type of interaction; however it does not involve any change.

Kinetic energies  $K_e^-$  and  $K_e^+$  of electron and positron respectively can be obtained from the following equation using the law of conservation of mass and energy as (Tsoulfanidis (1995))

$$K_e^- + K_e^+ = E_\gamma - (mc^2)_{e^-} - (mc^2)_{e^+} = E_\gamma - 1.022\text{MeV} \quad (1.12)$$

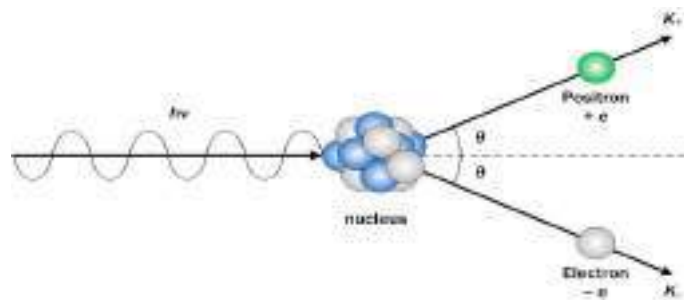
This energy is shared by electron and positron equally, so

$$K_e^- = K_e^+ = \frac{1}{2}(E_\gamma - 1.022\text{MeV}) \quad (1.13)$$

Pair production cross section ' $\kappa_{PP}$ ' or pair-production coefficient is the probability for pair production to occur which a complicated function is of  $E_\gamma$  and  $Z$  and can be written as

$$\kappa_{PP} = NZ^2 f(E_\gamma, Z) \quad (1.14)$$

It is important to note that  $\kappa_{PP}$  has threshold at 1.022 MeV and increases with  $E_\gamma$  and  $Z$ .



**Figure 1.2 Schematic representation of Pair-production**

#### 1.1.4 Rayleigh scattering

Rayleigh scattering is also known as coherent scattering in which the incident gamma ray photon interacts coherently with the all electrons of the absorber atom. In this scattering event, the energy is retained by the gamma ray photon after the interaction as a result target atom neither excites nor ionizes. Rayleigh scattering is

mainly due to the electric polarizability of the interacting atoms as a result this start oscillating with the same frequency of the incident radiation. The atoms behave like small radiating dipoles. Rayleigh scattering is most predominant at low incident photon energy, small scattering angles and high Z absorbers. So, in contrast to Compton scattering, Rayleigh scattering is negligible.

### **1.1.5 Thomson scattering by the nucleus**

Thomson scattering of the incident gamma ray is explained on the basis of classical electromagnetism in which nucleus is considered as a point charge. This involves scattering of the gamma rays by free electrons and nucleus as a whole (nuclear Thomson scattering). In this scattering process, there will be no change in the particle kinetic energy and the photon frequency before and after the scattering. However, this remains valid till the photon energy remains very- very small in contrast to the rest mass energy of the particle., i.e.,  $\nu \ll \frac{mc^2}{h}$ .

### **1.1.6 Delbruck scattering**

Delbruck scattering is also known as the elastic nuclear potential scattering in which there is coherent elastic scattering of photons in the Coulomb field of high Z nuclei. It is the deflection of highly energetic photons because of virtual electron pair formation in the coulomb field of nucleus. It is one of the two nonlinear effects of quantum electrodynamics (QED) in the Coulomb field investigated experimentally, which involves the splitting of single photon into two photons. However, this effect is quite small and cannot be detected in experiments done to measure it effectively. But these interactions are of good importance as it explain the inconsistencies between experimental and theoretical values of Compton scattering experiments on high Z elements.



### **1.1.7 Nuclear resonance scattering**

Nuclear resonance scattering depends upon the properties of the nuclear excited states. When there is resonance between the incident gamma ray photons and absorbing nuclei, then it gets excited to the higher energy levels. So, there will be absorption and re-emission of the photon by the nuclear energy levels of the resonant atom. This type of scattering occurs at energies near a resonance level, where the incident particle can easily form a compound nucleus and a similar particle may be emitted before any other competing emission or radiative process takes place in the compound nucleus.

### **1.1.8 Photo-disintegration of the nuclei**

Photo-disintegration or photo-transmutation is a process in which high energy gamma ray (nearly 8 MeV) is absorbed by an atomic nucleus. As a result, it gets excited and further decays immediately by emitting a subatomic particle like proton, neutron or alpha particle. This process is possible when the incident gamma ray photon has energy more than that of the separation energy of neutron or proton.

## **1.2 Fundamental parameters related to attenuation of gamma rays**

Attenuation is the removal of the incident photons from the collimated beam of monoenergetic photons during their passage through given target material. Linear attenuation coefficient, mass attenuation coefficient, effective atomic number and intensity ratios are the important fundamental parameters which describe the attenuation of the gamma rays through materials.

### **1.2.1 Linear attenuation coefficient of the materials**

Linear attenuation coefficient ( $\mu$ ) of a material is defined as a measure of the probability of interaction of the photons per unit linear path length in the absorber that leads to their elimination from the incident photon beam. Typically, it has the units of  $cm^{-1}$ . The number of removed photons  $n$  from the beam after traversing thickness  $x$  can be given as,

$$n = \mu N_o x \quad (1.15)$$

Here,  $N_o$  is the total number of incident photons.

Depending upon the energy of photon and atomic number of the target, incident photon interacts in different ways with matter. There are mainly three interaction mechanisms, i.e., photoelectric effect, Compton scattering and pair production with which a photon interacts with matter (explained in section 1.1).

The probability of a photon traversing a given amount of absorber without any kind of interaction is just the product of the probabilities of survival for each interaction. The probability of traversing a thickness  $x$  of absorber without a Compton collision is  $e^{-\sigma_C x}$  where  $\sigma_C$  is linear attenuation coefficient for the Compton process. Similarly, the probability of no photoelectric interaction is  $e^{-\tau_{PE} x}$ , where  $\tau_{PE}$  is the linear attenuation coefficient for the Photoelectric process and for probability of no pair-production collision is  $e^{-\kappa_{PP} x}$ , where  $\kappa_{PP}$  is the linear attenuation coefficient for the pair-production process. A collimated gamma-ray beam of initial intensity  $I_o$  after traversing a thickness  $x$  of absorber will have a residual or transmitted intensity  $I$  which is a function of incident gamma-ray energy, absorber composition and absorber thickness. Such that,

$$I = I_o(e^{-\sigma_C x} + e^{-\tau_{PE} x} + e^{-\kappa_{PP} x}) \quad (1.16)$$

$$= I_o e^{-(\sigma_C + \tau_{PE} + \kappa_{PP})x} \quad (1.17)$$

$$= I_o e^{-\mu x} \quad (1.18)$$

Where the quantity

$$\mu = \sigma_C + \tau_{PE} + \kappa_{PP} \quad (1.19)$$

is the total linear attenuation coefficient. The reciprocal of the attenuation coefficient has the units of length and is often known as mean free path, i.e., average distance a gamma ray travels in the absorber before interacting. Equation (1.19) establishes a linear relationship between the absorbance, density of an absorbing species and path length of the target and it is known as Beer-Lambert's law.

For the application of the Beer-Lambert law the target material must have uniform thickness and density. The linear relationship between absorption coefficient and thickness  $x$  of the material does not holds well, in case photons reaching the detector have unequal chances of absorption in the target material. This may happen due to the difference in the density or thickness of the target under study. Another reason behind it is the presence of impurity atoms in the target or some chemical change taking place in it, which causes non-uniformity in the density of the target.

Later, Silva et al. (2000) modified the general Beer-Lambert's law theoretically and proposed new method, i.e., Two Media Method for the measurement of the linear attenuation coefficient for materials having non-uniform thickness.

### **1.2.2 Mass attenuation coefficient**

When a collimated and monoenergetic beam of photons interact with the given thickness of the target material, the probability of interaction depends on the number of atoms per unit volume. This dependence can be normalised by defining linear attenuation coefficient per unit density of the target material, which is known as mass attenuation coefficient ( $\mu_m$ ) of the target. It can be calculated by dividing the linear

attenuation coefficient of the material under study by the density of the same material as;

$$\mu_m = \mu/\rho \quad (1.20)$$

Here  $\rho$  is the density of the target material in  $g/cm^3$ . So, the expression of Beer-Lambert's law becomes

$$I = I_0 e^{-\mu_m \rho x} \quad (1.21)$$

Here  $\rho x$  is the mass thickness of the material which is measured as mass per unit area.

In case of the compounds or homogenous mixtures, mass attenuation coefficient can be calculated by finding the weighted sum of the coefficients for the elements using simple rule as

$$\mu_m = \sum_i w_i \left( \frac{\mu}{\rho} \right)_i \quad (1.22)$$

In the above equation  $\left( \frac{\mu}{\rho} \right)_i$  is the mass attenuation coefficient for the  $i^{th}$  element and  $w_i$  is its weight fraction. For a chemical compound with formula  $(A_{x1}B_{x2}C_{x3} \dots \dots D_{xn})$  the weight fraction for the  $i^{th}$  element is given by

$$w_i = \frac{x_i A_i}{\sum_{i=1}^n x_i A_i} \quad (1.23)$$

Here,  $A_i$  is the atomic weight of the  $i^{th}$  element.

### 1.2.3 Mean Free Path

The mfp is defined as the average distance a gamma ray photon travels in the target absorbing material before any interaction with it. The  $\mu$  has the units  $cm^{-1}$ . Its reciprocal, possessing the units of length, represents the mfp. The mfp may also be defined as the thickness of the interacting substance which produces a gamma ray transmission as:

$$\frac{I}{I_0} = \frac{1}{e} = 0.37$$

In shielding process, considering samples of same thickness and targeted by the same gamma ray photon energy, the samples with lower mfp values are better gamma ray

shielders than high mfp value samples. Generally GP fitting parameters are utilized to calculate the gamma ray energy absorption buildup factor at various mean free path penetration depths for different incident photon energies.

#### 1.2.4 Half Value Layer

HVL or half value distance of an interacting target material is the width of material required at which the intensity of incident radiation narrow beam entering the target material is reduced to half of its original value. The HVL is given as:

$$HVL = \frac{\ln 2}{\mu} = \frac{0.693}{\mu} \quad (1.24)$$

The units of HVL are reciprocal of units of  $\mu$ . Normally, HVL is expressed in cm as the  $\mu$  is given in  $cm^{-1}$ . The lower value of HVL either indicates low photon energy or a better shielding material in terms of required thickness.

#### 1.2.5 Tenth Value Layer

The tenth value layer (TVL) of shielding is defined as a thickness of absorbing material that will reduce incident gamma radiation beam to tenth value of its initial intensity. Like HVL, the TVL thickness is also measured in units of distance i.e. mm or cm. The tenth value layer is given as:

$$TVL = \frac{\ln 10}{\mu} = \frac{2.303}{\mu} \quad (1.25)$$

#### 1.2.6 Effective atomic number

As attenuation of gamma photons is a function of the energy of incident photon, density and atomic number of the target element, so it is not possible to assign a single atomic number to a compound material for innumerable incident energies (Hine, 1952). However, for particular energy interaction of radiation with compound material is identical to the interaction of radiation with a single element whose atomic number is equivalent to the effective atomic number ( $Z_{eff}$ ) of the material.  $Z_{eff}$  can be obtained from atomic numbers of constituent elements, weighted according to the different partial photon interaction processes. Mathematically,  $Z_{eff}$  can be calculated from the following relation



$$Z_{eff} = \frac{\sigma_{t,a}}{\sigma_{t,el}} \quad (1.26)$$

Here  $\sigma_{t,a}$  is total atomic cross-section and  $\sigma_{t,el}$  is effective electronic cross-section. Total molecular cross-section can be obtained from mass attenuation coefficient according to following relation.

$$(\sigma_{t,m}) = \mu_m \left( \frac{M}{N_A} \right)$$

Where  $M = \sum_i n_i A_i$  is molecular weight of compound,  $n_i$  is total number of atoms in the molecule and  $A_i$  is the atomic weight of the  $i^{th}$  element.

Further, total atomic cross section can be calculated as

$$(\sigma_{t,a}) = \frac{1}{N_A} \sum_i f_i A_i (\mu_m)_i \quad (1.27)$$

Effective electronic cross-section is calculated by using the relation (Singh et al. (2002))

$$(\sigma_{t,el}) = \frac{1}{N} \sum_i \frac{f_i A_i}{Z_i} (\mu_m)_i \quad (1.28)$$

Here  $f_i = n_i / \sum_j n_j$  is fractional abundance and  $Z_i$  is atomic number of  $i^{th}$  constituent element,  $\sum_j n_j$  is the total number of atoms present in the molecular formula and  $N_A$  is Avogadro's number.

#### 1.2.4 Electron Density

The  $N_e$  is also a significant parameter for understanding and visualizing the incident radiation photon interactions probability with a particular absorbing substance. It is the more trustworthy parameter in comparison to the effective atomic number as it is directly associated with number of charged particles present in a unit mass of the material however its large values make the analysis process somewhat cumbersome. Higher is the value of  $N_e$  more is the probability of photon interaction and better is the sensing and shielding material.  $Z_{eff}$  offers similar information regarding mixed compositions as does the simple atomic number for single elements

$N_e$ , expressed as number of electrons in unit mass of the target interacting material. It exhibits the probability of incident photon interaction with target atom electrons. The higher  $N_e$  values mean that there are more chances of incident photon interaction with target shielding sample electrons. Thus  $Z_{eff}$  and  $N_e$  are the parameters which indicate the energy radiation incident photon interaction probabilities with various shielding materials. The  $N_e$  is closely related to the  $Z_{eff}$  and is given as:

$$N_e = \frac{\left(\frac{\mu}{\rho}\right)_{comp} Z_{eff}}{\sigma_a} \quad (1.29)$$

## CHAPTER – 2

### LITERATURE SURVEY

Lead titanate ( $\text{PbTiO}_3$ ) is a perovskite type ferroelectric material with high Curie temperature of  $490^\circ\text{C}$  which make them attractive for high-temperature and high-frequency piezoelectric applications [1–2]. Above  $T_c$ , the material has a simple cubic structure with lead atoms at the corners of the cubic unit cell, the titanium is at the body center position and oxygens are at the face-centered positions. Below  $T_c$ , the structure is tetragonal with the atoms distorted from the cubic arrangement by small relative displacements along the (polar) tetragonal  $c$  axis exhibiting a large tetragonality ( $c/a = 1.064$ ). It is reported in the literature that large ionic displacements in PT lead to a large spontaneous polarization of the order of  $453\text{ mC/cm}^2$  at room temperature [3]. However, it is difficult to sinter pure lead titanate ceramics because of its large lattice anisotropy of  $c/a = 1.063$ .  $\text{PbTiO}_3$  ceramics prepared by conventional route usually have microcracks and fracture on cooling below crystallization temperature ( $T_c$ ) as a result of the large spontaneous strain generated due to phase transition from cubic to tetragonal. This has constrained the applications of undoped lead titanate ceramics. The glass–ceramic route therefore offers the possibility of fabricating lead titanate without cracking. The other advantages of this method, such as no ageing or depoling problems and good stability at high temperature, high-pressure and in harsh environments can be achieved [4]. In this method, a glass medium consisting of glass network formers and ferroelectric constituents is prepared by conventional melt-quenching technique. Ferroelectric phase is then precipitated within the glass matrix during subsequent heat treatment [5–6]. The advantages of glass–ceramic processing over traditional ceramic route include

ease of forming complicated shapes free from porosity, voids and microcracks [7]. The amount of ferroelectric phase and its microstructure can be controlled by choosing a suitable initial glass composition and a heat treatment schedule [8]. Ferroelectric glass-ceramics with uniform fine-grained structure have attracted much attention and, in many applications, like transducers [9–24]. Composition of the glass, proper proportion of glass forming oxides like  $B_2O_3$  and  $SiO_2$  and glass preparation methods plays very important role to develop ferroelectric phases in the glass-ceramics [25]. The phase diagram of  $PbO-TiO_2-B_2O_3$  shows that the glass compositions  $PbO-B_2O_3$  and  $2PbO-B_2O_3$  is suitable for crystallization of  $PbTiO_3$  and the glass system,  $5PbO-B_2O_3-SiO_2$  for the crystallization of PZT [26].

Gamma radiations are used in a number of applications which include apparatus sterilization in medical field [27-28] protecting the food articles by irradiation [29-30] in diagnosing and treatment of cancer and some other medical conditions [31-32] element analysis [33-34] checking any flaws in welded materials [35-36] and in agriculture and engineering fields. At the same time these high energy and most penetrating radiation exposure for longer time period on any living being may also cause radiation sickness, mutation and cancer. Thus, for the effective use of gamma radiation in scientific, engineering, medical and agricultural applications, there is an urgent requirement to develop materials that can act as good radiation shield to avoid the unnecessary harmful effect on human body and environment. These shielding materials are may also be useful to protect reactor vessel from overheating due to continuous gamma ray absorption.

The study of absorption of gamma radiations in any material is valuable in formulating accurate semi-empirical formulations [37]. Understanding  $\mu_m$  has great significance as gamma ray absorption is dependent upon  $Z_{eff}$  and density of the

absorbing/shielding material. Using  $\mu_m$  various parameters like the mass energy-absorption coefficient, the total interaction cross-section, the  $Z_{eff}$ , and the  $N_e$  can be derived. Mass attenuation coefficients of many elements and compounds are available in tabulated form published by Hubbell [38] for photon energy range 1 keV-20 MeV. However, these tables consisted of only 40 elements and 45 compounds only. A new tabulation by Hubbel and Seltzer [39], consisted all elements from atomic number 1-92 and 48 additional compounds and substances. Berger and Hubbel [40] have further updated these values. Chantler [41] has recently provided wide ranging tabulated values of mass attenuation coefficients.

$Z_{eff}$  of any amalgamated and complex absorbing material is a very handy parameter in various technological and engineering applications. This parameter has a physical meaning and allows many characteristics of absorbing material to be envisaged by using it just as a number. However, the value of  $Z_{eff}$  during its measurement changes with different measurement techniques. After many efforts to formulate rules for finding  $Z_{eff}$  of any composite material, the available formulas have limited validity subject to the experimental conditions used in the particular work. As the technology advances there is a need to develop shielding materials that can work even in unforgiving gamma radiation exposure situations [42]. In the process many glass systems have been developed for nuclear engineering applications [43]. Glasses have been developed which accomplish the double task. Glasses are not only transparent to visible light but also protect us by absorbing high energy gamma radiations [44]. Cadmium and boron containing glasses are used to absorb slow neutrons [45]. In general, any absorbing glass material should be chemically, mechanically and optically inert to irradiation effects having radiation absorption cross section to be extra ordinary.



For using glasses as shielding materials, their effective atomic numbers and gamma attenuation coefficients study possess considerable importance. A. Khanna et al. [46] has done previous measurements in some heavy metal oxide borate glasses. This study is performed on lead alumino borophosphate glasses.

There is also a constant need to develop better and better absorbing materials which can act as a good radiation shield in extreme unfriendly environment [47]. In this regard, glasses are promising materials because of their homogeneity and range of composition. Typical applications of radiation shielding glasses are in hospital X-ray rooms, radiation therapy rooms, airport security X-ray screens, for materials testing, nuclear facilities, dental clinics, laboratories, X-ray and radiation protection spectacles. Glasses are also used in space technology for protecting human beings and equipment from harmful radiation such as gamma and cosmic rays. Glass has also been suggested for the containment of radioactive waste products [48]. In general, the Heavy Metal Oxide glasses based on for example PbO or  $Bi_2O_3$  [49-53], have potential applications in radiation shielding, since they have large absorption cross section for radiation and at the same time small irradiation effects on their mechanical and optical properties. HMO glasses are better shields and may be used as transparent radiation shielding materials [54].

The transmitted intensity of a gamma ray beam through a medium follows Lambert's Beer law ( $I = I_0 e^{-\mu t}$ ) where  $I$ ,  $I_0$  are transmitted and incident intensities of photons for thickness  $t$  of the medium having linear attenuation coefficient,  $\mu$  under three conditions: (i) monochromatic ray (ii) thin absorbing material, and (iii) narrow collimated beam. The law becomes invalid in case all these three conditions are not exactly fulfilled. The law can be made valid by using a correction factor, called as "buildup factor". The buildup factor is defined as the ratio of total value of specified

radiation quantity at any point to the contribution to that value from radiation reaching to the point without having undergone a collision. To evaluate the shielding and exposure of gamma radiations a comprehensive and reliable buildup factor data is very useful for analysis and control [55]. Buildup factors are shielding material and geometry dependent parameters which are applied to correct the attenuation calculations by including the contribution to the radiation field produced by the collided part of the incident beam. Many researchers have studied gamma ray buildup factors for concretes/flyash concretes [56], soil and ceramic [57,58], human tissues [59], gaseous mixture [60], building materials [61] and found that G-P fitting method is quite useful in valuation of energy absorption and exposure buildup factors. Geometrical-Progression (GP) fitting formula has been developed by Harima et al [62]. This formula can reproduce data over full range of distance, energy and atomic number. Harima et al [63] have demonstrated the applicability of G-P method to generate buildup factor data for a wide range of energy and distance.

The shielding properties of the glasses can be modified by change in the chemical compositions. Gamma ray shielding properties of the glasses have been carried out for phosphate glass [64], lead silicate [65] and lead borate and silicate glass [66-69]. In nuclear reactors and other facilities where neutron radiations also exist alongside gamma radiations, neutron absorbing glasses must also possess elements such as Li, H, C, B etc. In the nuclear reactors the energy of neutron ranges up to 8 MeV [70] and gamma ray in range of 0.10–10 MeV. Therefore, boron containing glass shielding materials are found to be a promising and potential shielding candidate. The gamma ray attenuation coefficient of borate glasses has been investigated for photon energy 1173 and 1332 keV [71]. There is no such study for gamma ray and neutron shielding

by the borophosphate glasses in the literature. This encouraged us to investigate the shielding efficiencies of gamma ray and neutron.

## CHAPTER-3

### RESULTS AND DISCUSSION

#### 3.1 Introduction

Present work is focused on theoretically exploring radiation shielding properties of lead zirconium titanate glasses viz.  $xPbO:14TiO_2:16ZrO_2:(40 - 0.5x)B_2O_3:(40 - 0.5x)SiO_2$ , ( $x = 0, 10, 20, 30, 40$ ). The radiation shielding parameters such as mass attenuation coefficient, linear attenuation coefficient, effective atomic number, electron density, half value layer and exposure buildup factor were obtained theoretically as preliminary data for preparing sample of required thickness.

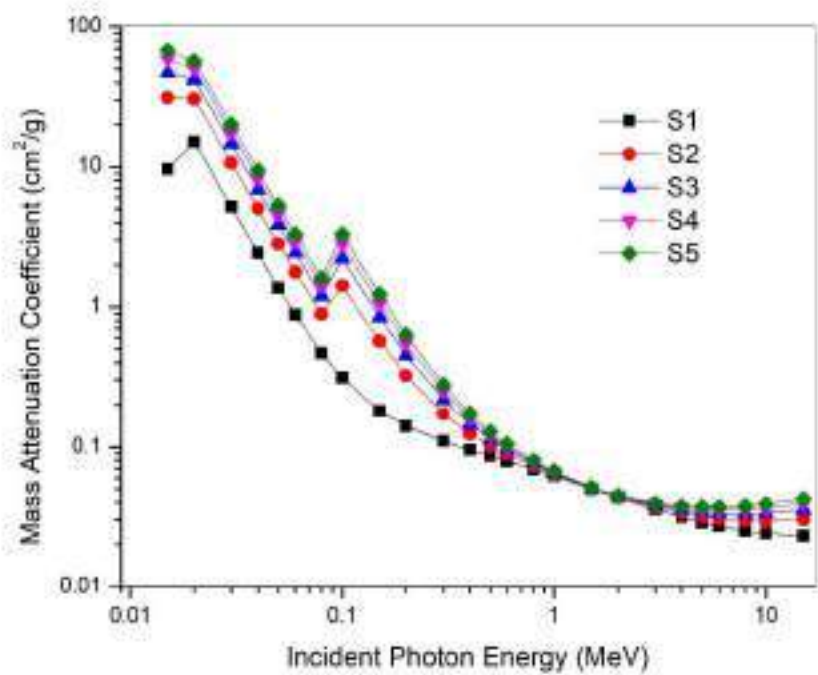
#### 3.2 Shielding Properties

In this study, the gamma-ray attenuation properties of lead zirconate titanate samples were investigated. The molar and elemental mass percentages and densities of the samples analyzed are listed in Table 1. According to Table 1, the density of the glasses increased from 5.5102 g/cm<sup>3</sup> to 7.6003 g/cm<sup>3</sup>. The sample with the highest structural lead oxide content, had the highest density.

**Table 3.1:** Sample codes, densities and chemical compositions of glasses

Sample Code	PbO	TiO <sub>2</sub>	ZrO <sub>2</sub>	B <sub>2</sub> O <sub>3</sub>	SiO <sub>2</sub>	Density (g/cm <sup>3</sup> )
S1	0	14	16	40	40	5.5102
S2	10	14	16	35	35	5.9216
S3	20	14	16	30	30	6.3217
S4	30	14	16	25	25	6.7105
S5	40	14	16	20	20	7.6003

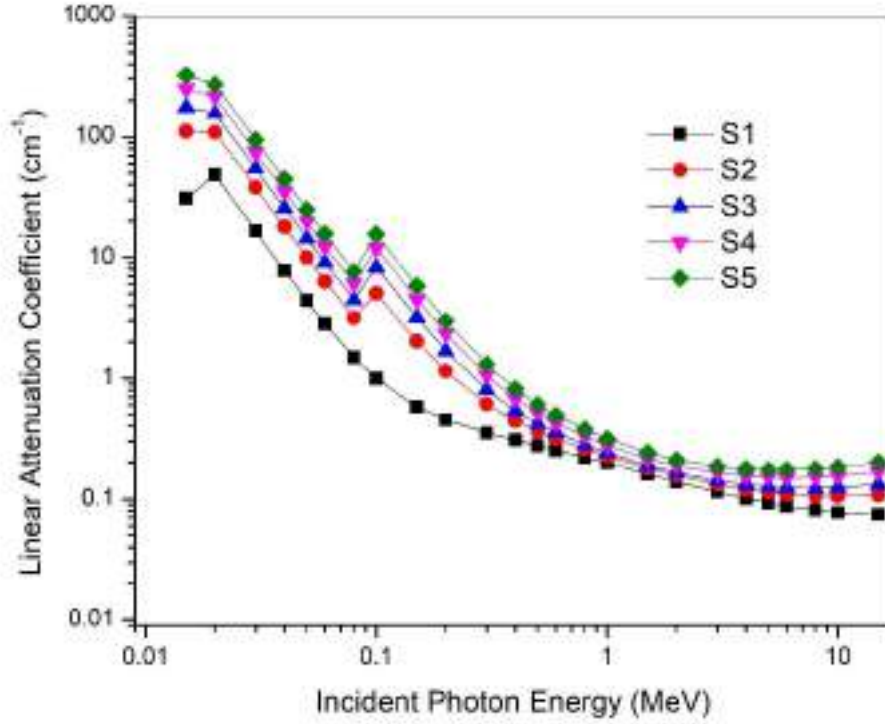
The WinXcom program's theoretical results were first used to obtain the  $\mu_m$  values in order to explore the gamma-ray attenuation properties of the selected glasses. Gamma energy was increased up to 15 MeV, and this caused a sharp fall in the  $\mu_m$  values (Fig. 3.1). Photoelectric absorption (PEA) was the reason for this decrease. The main influence on absorption in this sector regime came from the PEA. The  $\mu_m$  values changed more slowly after 1 MeV. This was caused by the strength of the linear Z-dependent Compton scattering (CS), which was present at this range of energy. Pair production (PP), which was the main mechanism above 5 MeV, caused the influence of CS to steadily decrease after that (Fig. 3.1). Since PP's cross-section grows linearly with  $Z^2$ , the values of  $\mu_m$  rose over the range of 9 to 20 MeV. The highest lead, zirconium, and barium concentrations were found in the S5 sample, which also had the highest  $\mu_m$  values.



**Figure 3.1:** Variation of mass attenuation coefficient ( $\mu_p$ ) values as a function of photon energy for given glasses



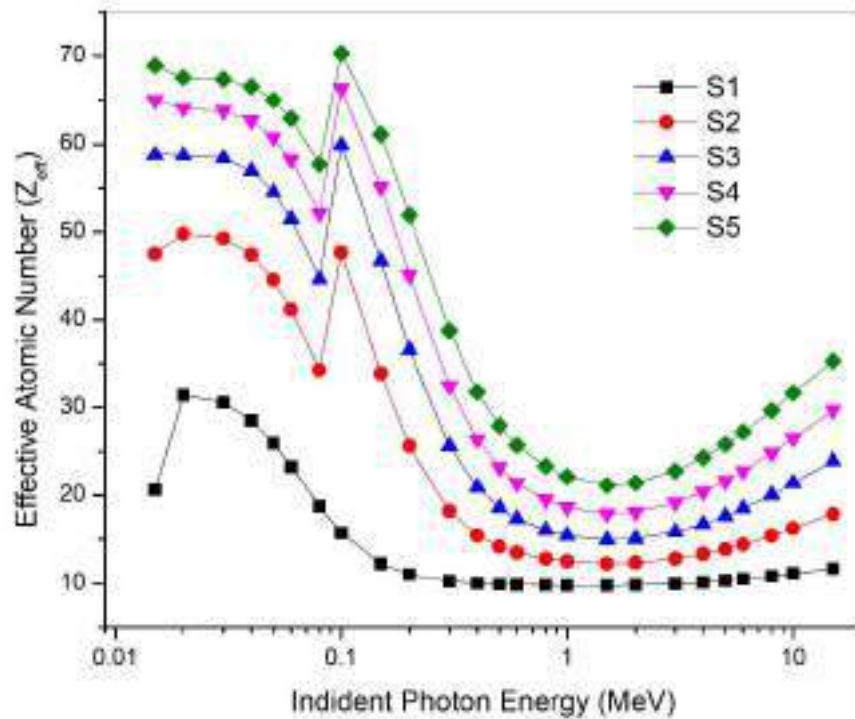
Given that the linear attenuation coefficient (LAC) is a density-dependent property, it is assumed that there is a correlation between density and the LAC values in this case, and subsequently, the amount of lead oxide. Figures 3.2 show the shifting LAC in relation to the incident photon energy, accordingly. In the graph, it can be shown that as photon energy increased, the LAC rapidly reduced, reaching as low as 0.05 MeV in all cases. The photoelectric effect predominates in the low-energy region, where the majority of photon-matter interactions take place, with cross-sectional changes proportional to  $Z$ . For medium-level energies above the energy level, Compton scattering becomes increasingly significant when considering the changes in chemical composition of the specimens. The cross section of Compton scattering has a linear relationship with atomic number  $Z$ , hence the samples' values decreased gradually and remained constant below 2 MeV. However, considerable differences in the linear attenuation coefficients were observed as the glass density changed progressively. At various energies, we saw an intriguing impact of lead oxide on the photon resistance of glass samples. Our findings show that the lead oxide content was highest in the S5 sample, which also exhibited the highest linear attenuation coefficients for all entering photon energies. This is explained by the fact that the S5 sample, which has a density of  $7.6003 \text{ g/cm}^3$ , contains the most lead oxide in the glass structure and has a higher value of LAC.



**Figure 3.2:** Variation of linear attenuation coefficient ( $\mu$ ) values as a function of photon energy for given glasses

Figure 3.3 show how the tested glasses effective atomic number ( $Z_{\text{eff}}$ ) values fluctuate as a function of incident photon energy. According to Figure 3.3, S5 have the highest effective atomic number values across all energies investigated. The enhanced lead oxide reinforcement, which raised the sample's total atomic number from S1 to S5, can be attributed to this. The changes in the glass structure between the reduced ( $\text{B}_2\text{O}_3$  and  $\text{SiO}_2$ ) and enlarged ( $\text{PbO}$ ) replacements led to a considerable change in the overall atomic number of the S1 - S5 sample. The absorption edge of B at about 0.03 MeV caused a sharp increase in  $Z_{\text{eff}}$  curves. This was because to PEA's dominance in the relevant energies. In the middle energies, where CS played a significant role, the  $Z_{\text{eff}}$  values were remarkably similar. The modification in the cross-section of PP with  $Z^2$  caused the  $Z_{\text{eff}}$  values to rise once more. It is clear that the glass sample's high lead

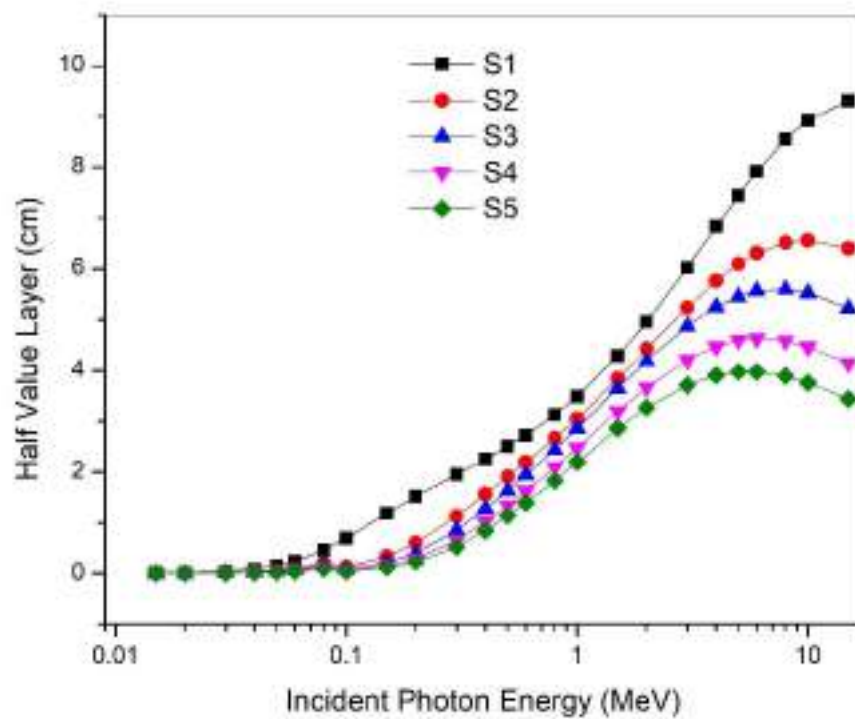
content is what caused it to have the highest  $Z_{\text{eff}}$  value. Present study demonstrates that the S5 sample exhibited the highest  $Z_{\text{eff}}$  values across the entire gamma-ray energy range.



**Figure 3.3:** Variation of effective atomic ( $Z_{\text{eff}}$ ) number values as a function of photon energy for given glass samples.

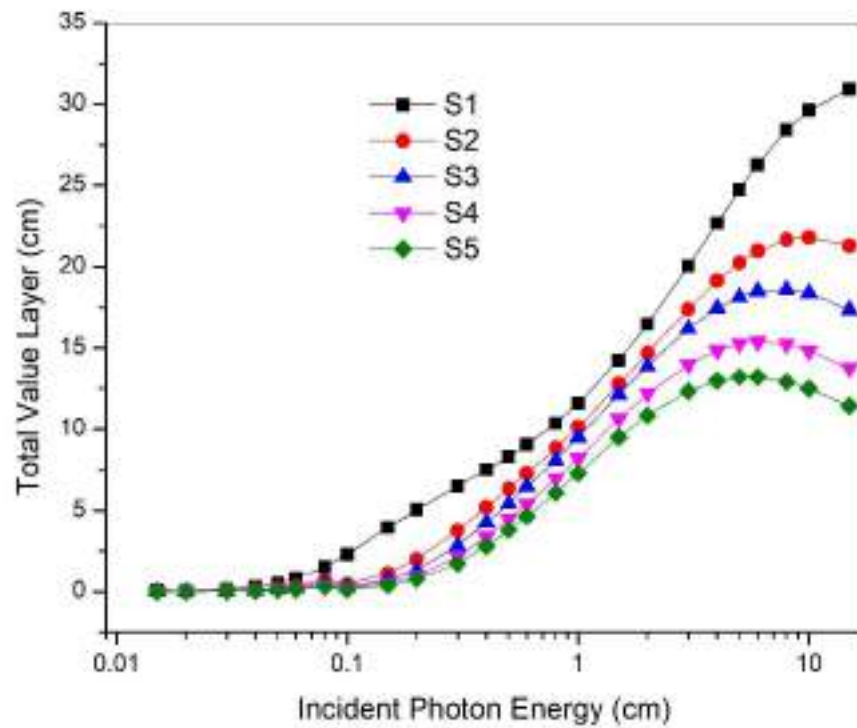
The half value layer term (HVL), which enables the calculation of the material thickness needed to reduce the initial gamma-ray intensity by half, is crucial in research on radiation shielding. This is due to the requirement that shielding requirements be predetermined depending on the kind and energy of the radiation utilized in radiation experiments. Therefore, a more thorough understanding of gamma-ray attenuation capabilities during the incident gamma-contact rays with the attenuator specimen should be used to establish the amount of the half value layer

necessary for each type of prospective shielding material. Figure 3.4 show the HVL fluctuation trend of the tested glass samples as a function of incident photon energy. According to what is to be predicted, the necessary half value layer expands with rising gamma-ray energy. The penetrating dominance of accompanying gamma-ray photons, which is caused by enhanced gamma-ray energy, typically produces this effect. The S5 sample, according to our observations, satisfies the sample thickness requirements down to the last detail. Because lead oxide contributes the most, the S5 sample exhibits better gamma-ray shielding properties, which is another convincing indication of this sample as gamma shielding material.



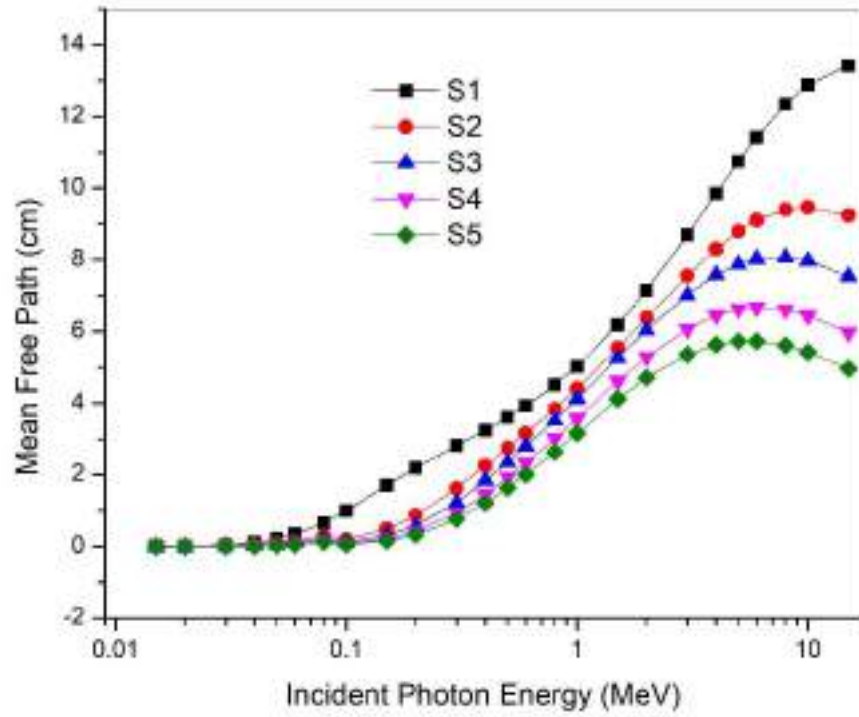
**Figure 3.4:** Half-value layer (HVL) against photon energy for investigated glass samples

The variation of TVL with photon energy in region 0.05 MeV – 15 MeV for glass samples is shown in Figure 3.5. TVL shows similar variations as HVL in similar energy regions and both are alike mfp (Figure 3.6) variations as these quantities depend inversely to linear attenuation coefficient with difference of constant factor only. It is clear from figures that more are the gamma ray energies higher is the thickness required for shielding.



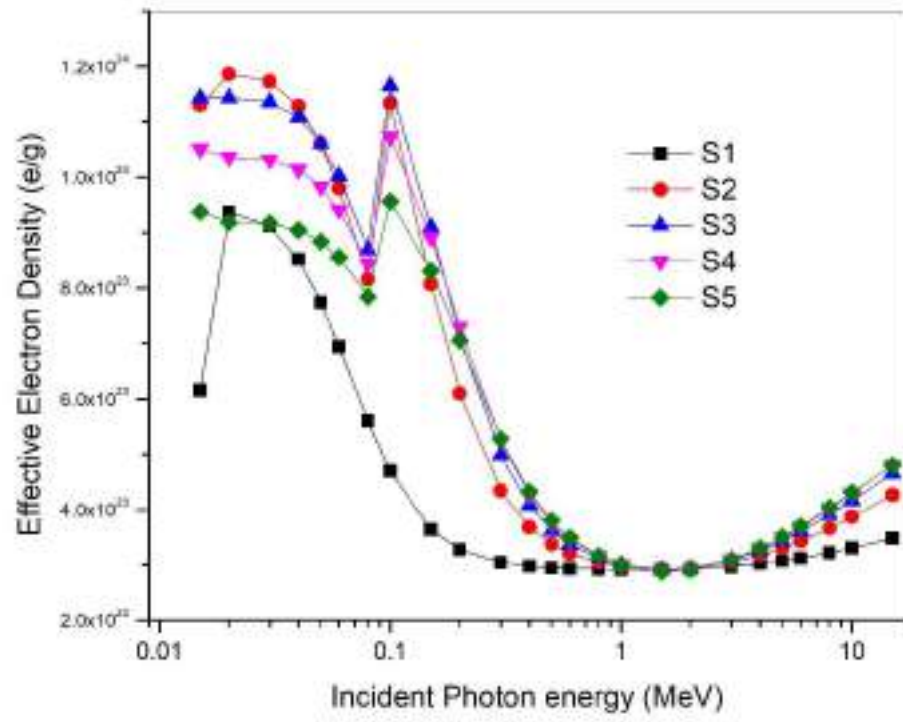
**Figure 3.5:** Half-value layer (TVL) against photon energy for investigated glass samples



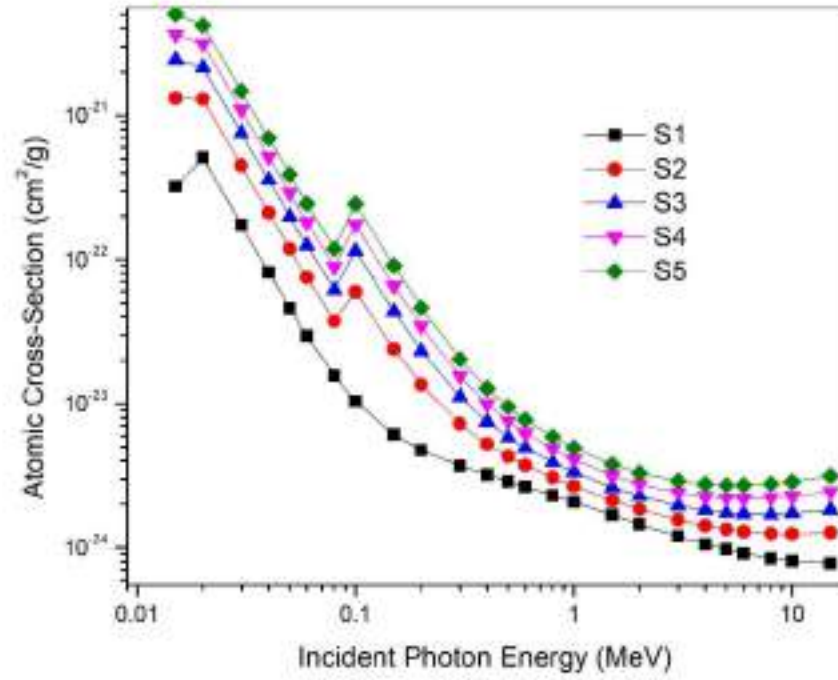


**Figure 3.6:** Mean free path (MFP) against photon energy for investigated glass samples

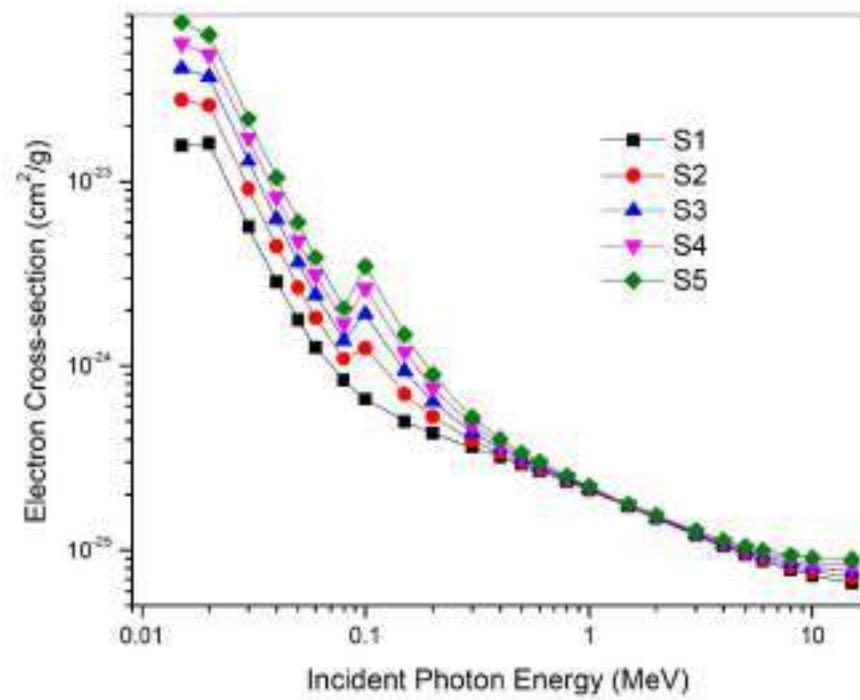
All produced glass samples were also assessed for their effective electron densities ( $N_{\text{eff}}$ ), which show the number of electrons per unit mass. Figure 3.7 shows in low photon energy region,  $N_{\text{eff}}$  altered in a non-monotonic pattern with photon energy until it reached a sharp jump close to the La absorption edge (0.0880 MeV). The PE process is to be responsible for this behavior. All of the samples under investigation showed a sharp decline in  $N_{\text{eff}}$  values in the photon energy range between 0.1 and 1 MeV; this tendency is connected to the CS process, which predominates in this range. An increase in the  $N_{\text{eff}}$  values was noticed in the energy range above 2 MeV and was attributed to the PP process, which dominates in this range. The S5 sample, which had the highest concentration of lead oxide, clearly had a considerable advantage in terms of gamma-ray attenuation.



**Figure 3.7:** Variation of electron density ( $N_{\text{eff}}$ ) number values as a function of photon energy for given glass samples



**Figure 3.8:** Variation of Atomic cross section values as a function of photon energy for given glass samples



**Figure 3.8:** Variation of Electron cross section values as a function of photon energy for given glass samples

## CHAPTER 4

### CONCLUSIONS

In this study, the gamma-ray shielding parameters using WinXcom computer software have been investigated with change in lead doping in the glass structure. Accordingly, the influence of lead on the gamma-ray shielding properties of lead zirconium titanate glasses  $xPbO: 14TiO_2: 16ZrO_2: (40 - 0.5x)B_2O_3: (40 - 0.5x)SiO_2$ , ( $x = 0, 10, 20, 30, 40$ ) was examined using WinXcom software. Several significant radiation shielding parameters were evaluated. The ceramic density was increased from 5.5102 g/cm<sup>3</sup> to 7.6003 g/cm<sup>3</sup> with increasing lead content.

Results revealed the following points based on shielding parameter studies:

1. At each energy within the spectrum of interest in this research, MAC generally trends in the order that (S1) MAC < (S2) MAC < (S3) MAC < (S4) MAC < (S5) MAC.
2. The maximum and minimum values of LAC were obtained at 15 keV and 8 MeV, respectively with values of 30.93 and 0.074 cm<sup>-1</sup>; 111.54 and 0.108 cm<sup>-1</sup>; 175.19 and 0.133 cm<sup>-1</sup>; 249.21 and 0.167 cm<sup>-1</sup>; and 322.08 and 0.201 cm<sup>-1</sup> for S1 to S5, respectively.
3. The minimum and maximum values of HVL were obtained at 15 keV and 8 MeV, respectively with values of 0.022 and 8.55 cm; 0.006 and 6.52 cm; 0.004 and 5.60 cm; 0.003 and 4.58 cm; and 0.002 and 3.89 cm for S1 to S5, respectively.
4. The maximum and minimum values of  $Z_{eff}$  were obtained at 15 keV and 8 MeV, respectively with values of 20.64 and 10.81; 47.46 and 15.40; 58.75 and 20.06; 64.98 and 24.82; and 68.93 and 29.67 for S1 to S5, respectively.

5. The trend of variation of electron density ( $N_{\text{eff}}$ ) as a function of photon energy for BZT ceramic is  $S1 > S2 > S3 > S4 > S5$  for all photon energy range 0.015 MeV to 15 MeV.

Generally, increasing of lead oxide increment in the glass samples has a positive influence on their radiation shielding capability. One can conclude that all samples can attenuate gamma rays. Therefore, the investigated samples can be applied successfully in nuclear shielding applications. The total  $\mu_m$ ,  $Z_{\text{eff}}$  and  $N_{\text{eff}}$  of the ceramics decreases exponentially toward higher energy of gamma-rays. These results are good indications of the potential of the prepared glasses as a radiation shielding material.

As a result, these findings may deepen our understanding of the structural properties and gamma ray shielding capabilities of lead Zirconium titanate in various systems and offer a thorough viewpoint for the development of useful glasses with enhanced applications.



## REFERENCES

1. Ikegami, S., Ueda, I., & Nagata, T. (1971). Electromechanical properties of PbTiO<sub>3</sub> ceramics containing La and Mn. *The Journal of the Acoustical Society of America*, 50(4A), 1060-1066.
2. Takahashi, T. (1991). Lead titanate ceramics with large piezoelectric anisotropy and their applications. *Toshiba's Selected Papers on Science and Technology*; (Japan), 3(1).
3. Lines, M. E., & Glass, A. M. (2001). *Principles and applications of ferroelectrics and related materials*. Oxford university press.
4. Rahangdale, V. U., & Deshpande, V. K. (2020). Lead-zirconate-titanate based glass and glass-ceramics: Preparation, physical, dielectric and ferroelectric properties. *Materials Today: Proceedings*, 29, 866-871.
5. Rahangdale, V. U., & Deshpande, V. K. (2020). Lead-zirconate-titanate based glass and glass-ceramics: Preparation, physical, dielectric and ferroelectric properties. *Materials Today: Proceedings*, 29, 866-871.
6. McMillan, P. W. (1982). The crystallisation of glasses. *Journal of Non-Crystalline Solids*, 52(1-3), 67-76.
7. Rahangdale, V. U., & Deshpande, V. K. (2020). Lead-zirconate-titanate based glass and glass-ceramics: Preparation, physical, dielectric and ferroelectric properties. *Materials Today: Proceedings*, 29, 866-871.
8. Sahu, A. K., Kumar, D., & Parkash, O. (2006). Lead-strontium titanate glass ceramics: I-crystallization and microstructure. *Journal of materials science*, 41(7), 2075-2085.
9. Herczog, A. (1964). Microcrystalline BaTiO<sub>3</sub> by crystallization from glass. *Journal of the American Ceramic Society*, 47(3), 107-115.
10. Borrelli, N. F. (1967). Electro-optic Effect in Transparent Niobate Glass—Ceramic Systems. *Journal of Applied Physics*, 38(11), 4243-4247.
11. Layton, M. M., & Herczog, A. (1967). Nucleation and Crystallization of NaNbO<sub>3</sub> from Glasses in the Na<sub>2</sub>O-Nb<sub>2</sub>O<sub>5</sub>-SiO<sub>2</sub> System. *Journal of the American Ceramic Society*, 50(7), 369-375.

12. Borrelli, N. F., & Layton, M. M. (1969). Electrooptic properties of transparent ferroelectric glass—Ceramic systems. *IEEE Transactions on Electron Devices*, 16(6), 511-514.
13. Layton, M. M., & Herczog, A. (1969). STRUCTURE AND CRYSTALLISATION OF GLASSES OF LOW NETWORK-FORMER CONTENT. *Glass Technology*, 10(2), 50.
14. Rahangdale, V. U., & Deshpande, V. K. (2014). Study of physical properties of PbTiO<sub>3</sub> based glass-ceramic with variation of heat treatment duration. *Ferroelectrics*, 467(1), 85-98.
15. Ulrich, D. R. (1968). *High dielectric thick films for screened circuit capacitors* (No. LAR-10294).
16. Rahangdale, V. U., & Deshpande, V. K. (2020). Lead-zirconate-titanate based glass and glass-ceramics: Preparation, physical, dielectric and ferroelectric properties. *Materials Today: Proceedings*, 29, 866-871.
17. Tummala, R. R. (1976). Low-temperature and low-expansion glass-crystal composites by the formation of Perovskite lead titanate. *Journal of Materials Science*, 11, 125-128.
18. Ito, S., Kokubo, T., & Tashiro, M. (1978). Transparency of LiTaO<sub>3</sub>-SiO<sub>2</sub>-Al<sub>2</sub>O<sub>3</sub> glass-ceramics in relation to their microstructure. *Journal of Materials Science*, 13, 930-938.
19. HERCZOG, A. (1984). Barrier Layers in Semiconducting Barium Titanate Glass-Ceramics. *Journal of the American Ceramic Society*, 67(7), 484-490..
20. Mianxue, W. U., & Peinan, Z. (1986). Piezoelectricity, pyroelectricity and ferroelectricity in glass ceramics based on PbTiO<sub>3</sub>. *Journal of Non-Crystalline Solids*, 84(1-3), 344-351.
21. Banach, U., HÜbert, T., Fellmuth, B., & Hegenbarth, E. (1989). Low-temperature dielectric properties of SrTiO<sub>3</sub> alumino-borate glass-ceramics. *Ferroelectrics*, 100(1), 111-120.
22. Herczog, A. (1990). Phase Distribution and Transparency in Glass-Ceramics Based on a Study of the Sodium Niobate–Silica System. *Journal of the American Ceramic Society*, 73(9), 2743-2746.
23. Kusumoto, K., & Sekiya, T. (1993). Preparation of lead titanate particles by crystallization of glass. *Materials research bulletin*, 28(9), 885-891.

24. Shankar, J., & Deshpande, V. K. (2010). Study of lead titanate based glass ceramics with addition of BaO. *Integrated Ferroelectrics*, 119(1), 110-121.
25. Rema, K. P., & Kumar, V. (2008). Structure–Property Relationship in Mn-Doped (Pb<sub>0.94</sub>Sr<sub>0.06</sub>)(Zr<sub>0.53</sub>Ti<sub>0.47</sub>)O<sub>3</sub>. *Journal of the American Ceramic Society*, 91(1), 164-168.
26. Kumar, V., Achuthan, A. T., Sivanandan, K., Divya, P. V., & Rema, K. P. (2006). Sol–Gel Synthesis of PZT–Glass Nanocomposites Using a Simple System and Characterization. *International journal of applied ceramic technology*, 3(5), 345-352.
27. K.H. Lee, C.C. Chu (1996) Gamma irradiation sterilizing of biomaterial medical devices or products, with improved degradation and mechanical properties, US Patent 5485496 A
28. T. von Woedtke, W.D. Julich, V. Hartmann, M. Stieber, P.U. Abel (2002) Sterilization of enzyme glucose sensors: problems and concepts. *Biosens Bioelectron.* 17(5), 373– 382
29. W.C. Sung (2005) Effect of gamma irradiation on rice and its food products. *Radiat. Phys. Chem.* 73, 224–228
30. J.F. Diehl (2002) Food irradiation – past, present and future. *Radiat. Phys. Chem.* 63, 211–215
31. S. Matsunaga, T. Shuto, N. Kawahara, J. Suenaga, S. Inomori, H. Fujino (2011) Gamma knife surgery for brain metastases from colorectal cancer. *J. Neurosurg.* 114, 782–789
32. A. Wyszomirska (2012) Iodine-131 for therapy of thyroid diseases. Physical and Biological basis. In: *Nucl. Med. Rev.*, 15, 120–123
33. G. Quarta, L. Calcagnile, M. Vidale (2012) Integrating non-destructive ion beam analysis methods and AMS radiocarbon dating for the study of ancient bronze status. *Radiocarbon* 54, 801–812
34. S.K. Saha, C.W. Cheng, K.M. Barfoot, J.D. MacArthur, B.C. Robertson (1982) Bulk elemental analysis using  $\gamma$ -rays from inelastic scattering of neutrons produced by the  $^{13}\text{C}(\alpha, n)^{16}\text{O}$  reaction, *Nucl. Instrum. Methods*, 201, 465–471
35. H.S. Cho, J.E. Oh, S.I. Choi, H.M. Cho, Y.O. Park, D.K. Hong, M.S. Lee, Y.J. Yang, U.K. Je, D.S. Kim, T.H. Woo, B.S. Lee, H.K. Lee (2011) Performance

- evaluation of a gamma-ray imaging system for non-destructive testing of welded pipes, Nucl. Instrum. Methods Phys. Res., Sect. A, 652, 650–653.
36. A.E. Moura, C.C. Dantas, M.S. Nery, J.M. Barbosa, T.L. Rolim, E.A.O. Lima, S.B. Melo, V.A. Dos Santos (2015) Non-destructive evaluation of weld discontinuity in steel tubes by gamma ray CT. Nucl. Instrum. Methods Phys. Res., Sect. B 349, 155–162
  37. D.F. Jackson, D.J. Hawkes (1981) X-ray attenuation coefficients of elements and mixtures, Physics Reports, Volume 70, Issue 3, Pages 169-233
  38. J.H. Hubbell, (1982) Photon Mass Attenuation and Energy-Absorption Coefficients from 1KeV to 20 MeV. International Journal of Applied Radiation and Isotopes, 33, 1269-1290
  39. J. H. Hubbell, S. M. Seltzer (1995) Tables of X-Ray Mass Attenuation Coefficients and Mass Energy-Absorption Coefficients 1 keV to 20 MeV for Elements  $Z = 1$  to 92 and 48 Additional Substances of Dosimetric Interest, NISTIR 5632, (1995) Gaithersburg, MD 20899 pp. 1-120
  40. M.J. Berger, J.H. Hubbell (1987) "XCOM: Photon Cross Sections on a Personal Computer," National Bureau of Standards, Gaithersburg, MD. 87-3597
  41. C. T. Chantler (2000) Detailed Tabulation of Atomic Form Factors, Photoelectric Absorption and Scattering Cross Section, and Mass Attenuation Coefficients in the Vicinity of Absorption Edges in the Soft X-Ray ( $Z=30-36$ ,  $Z=60-89$ ,  $E=0.1$  keV–10 keV), Addressing Convergence Issues of Earlier Work, Journal of Physical and Chemical Reference Data, 29, 597
  42. J.F. Krocher, R.E. Browman (Eds.) (1984) Effects of Radiation on Materials and Components, Reinhold, New York
  43. M.J. Kreidl, J.R. Hensler, H.H. Hower (Ed.) (1958) Modern Materials, Vol. 1, Academic Press, New York, p. 217
  44. W.S. Rothwell (1958) Radiation Shielding Windows Glasses, Bull. PE-50, Corning Glass Works, Corning, NY
  45. L.M. Melnick, H.W. Safford, K.H. Sun, A.J. Silverman (1951) Neutron – absorbing glass: CdO–SiO<sub>2</sub>–B<sub>2</sub>O<sub>3</sub> system, Am. Ceram. Soc., 34, 82–6

46. A. Khanna, S.S. Bhatti, K.J. Singh and K.S. Thind (1996) Gamma-ray attenuation coefficients in some heavy metal oxide borate glasses at 662 keV, Nucl. Instrum. Meth. B, 114, 217
47. J. F. Krocher and R. E. Browman, Effects of radiation on materials and components, Reinhold, New York, 1984
48. S.R. Manonara, S.M. Hanagodimath, L. Gerward, and K.C. Mittal (2011) Exposure Buildup Factors for Heavy Metal Oxide Glass: A Radiation Shield. Journal of the Korean Physical Society, 59(2), 2039-2042
49. A. Khanna, S. S. Bhatti, K. J. Singh and K. S. Thind (1996) Nucl. Instrum. Methods Phys. Res. Sect. B 114, 217
50. N. Singh, K. J. Singh, K. Singh and H. Singh (2004) Comparative study of lead borate and bismuth lead borate glass systems as gamma-radiation shielding materials, Nucl. Instrum. Methods Phys. Res., Sect. B, 225, 305–309
51. H. Singh, K. Singh, G. Sharma, R. Nathuram and H. S. Sahota (2002) Photon Interaction Studies with Some Glasses and Building Materials, Nuclear Science and Engineering, Vol. 142, No. 3, pp. 342-348.
52. K. Singh, H. Singh, V. Sharma, R. Nathuram, A. Khanna, R. Kumar, S.S. Bhatti, H.S. Sahota (2002) Gamma ray attenuation coefficients in bismuth borate glasses, Nucl. Instrum. Methods Phys. Res. Sect. B, 194, 1–6.
53. H. Gill, G. Kaur, K. Singh, V. Kumar, and J. Singh (1998) Study of effective atomic numbers in some glasses and rocks, Radiation Physics and Chemistry, 51, 4–6, 671–672
54. S. R. Manohara, S. M. Hanagodimath and L. Gerward (2009) Photon interaction and energy absorption in glass: A transparent gamma ray shield, Journal of Nuclear Materials 393(3), 465-472
55. G S Sidhu, P S Singh, and G S Mudahar (1999) Computation of geometrical-progression (G-P) fitting parameters of plastic materials, Indian J. Phys. 73A(6), 811-819
56. S. Singh, S. S. Ghumman, C. Singh, K. S. Thind, and G. S. Mudahar (2010) Buildup of gamma ray photons in flyash concretes: a study, Annals of Nuclear Energy, vol. 37, no. 5, 681–684



57. G. S. Brar, K. Singh, M. Singh, and G. S. Mudahar (1994) Energy absorption buildup factor studies in water, air and concrete up to 100mfp using G-P fitting formula, *Radiation Physics and Chemistry*, vol. 43, no. 6, 623–627
58. V. P. Singh and N. M. Badiger (2012) Comprehensive study of energy absorption and exposure buildup factor for concrete shielding in photon energy range 0.015–15MeV upto 40 mfp penetration depth: dependency of density, chemical element, photon energy,” *International Journal of Nuclear Energy Science and Technology*, vol. 7, no. 1, 75–99
59. V. P. Singh and N. M. Badiger (2013) Photon energy absorption buildup factor of gaseous mixtures used in radiation detectors, *Radioprotection*, vol. 48, no. 1, 63–78.
60. M. Kurudirek, B. Doğan, M. Ingeç, N. Ekinci, and Y. Özdemir (2011) Gamma-ray energy absorption and exposure buildup factor studies in some human tissues with endometriosis, *Applied Radiation and Isotopes*, vol. 69, no. 2, 381–388
61. G. Sandeep and S. S. Gurdeep (2012) A comprehensive study on energy absorption and exposure buildup factors for some soils and ceramic materials, *Journal of Applied Physics*, vol. 2, no. 3, 24–30
62. S. Tejbir, K. Gurpreet, and S. S. Parjit (2013) Study of gamma ray exposure buildup factor for some ceramics with photon energy, penetration depth and chemical composition, *Journal of Ceramics*, vol. 2013, Article ID 721606.
63. E. Yilmaz, H. Baltas, E. Kiris, I. Ustabas, U. Cevik, and A. M. El-Khayatt (2011) Gamma ray and neutron shielding properties of some concrete materials, *Annals of Nuclear Energy*, vol. 38, no. 10, 2204–2212
64. Y. Harima, Y. Sakamoto, S. Tanaka and M. Kawai (1986) Validity of the geometric-progression formula in approximating the gamma ray buildup factors, *Nucl. Sci. Eng.*, 94, 24
65. Y. Harima, Y. Sakamoto, S. Tanaka, M. Kawai, T. Fujita, T. Ishikawa, M. Kinno, K. Hayashi, Y. Matsumoto and T. Nishimura (1986) Applicability of geometrical progression approximation (G-P method) of gamma-ray buildup factors, *Japan Atomic Energy Research Institute*, M 86, 071
66. J. Kaewkhao and P. Limsuwan (2010) Mass attenuation coefficients and effective atomic numbers in phosphate glass containing Bi<sub>2</sub>O<sub>3</sub>, PbO, and BaO at 662 keV, *Nucl. Instrum. Methods Phys. Res., Sect. A*, vol. 619, pp. 295–297

67. K.J. Singh, N. Singf, N., R.S. Kaundal, and K. Singh (2008) Gamma-ray shielding and structural properties of PbO-SiO<sub>2</sub> glasses, Nucl. Instrum. Methods Phys. Res., Sect. B, 2008, vol. 266, pp. 944–948
68. K. Kirdsiri, J. Kaewkhao, A. Pokaipisit, W. Chewpraditkul, and P. Limsuwan, (2009) Gamma-rays shielding properties of xPbO:(100–x)B<sub>2</sub>O<sub>3</sub> glasses system at 662 keV, Ann. Nucl. Energy, vol. 36, no. 9, pp. 1360–1365
69. K. Kirdsiri, J. Kaewkhao, N. Chanthima, and P. Limsuwan (2011) Comparative study of silicate glasses containing Bi<sub>2</sub>O<sub>3</sub>, PbO, and BaO: Radiation shielding and optical properties, Ann. Nucl. Energy, vol. 38, pp. 1438–1441
70. S. Glasstone and A. Sesonske (2004) Nuclear Reactor Engineering: Reactor Design Basics, New York: Springer-Verlag, 4th ed., vol. 1
71. A.I. Fawazi, A.A. El-Sayes, A.A. El-Latif and M. El-Desoky (2006) Borate glass with lead and nickel oxides for radiation attenuation, Abhath Al-Yarmouk, vol. 15, no. 2, pp. 195–205

**"Assessing Uranium and Radon in Groundwater Using Integrated  
Fluorimeter and Rad7: A Case Study of Nalagarh City, District Solan,  
Himachal Pradesh, India."**

***PROJECT REPORT***

*Submitted in partial fulfillment of the  
requirements for the award of the degree of*

**MASTER OF SCIENCE**

**in**

**PHYSICS**

*By*

**Baljeet Singh**  
**(Regn. No. 8114-19-778)**



**DEPARTMENT OF PHYSICS**  
**SRI GURU TEG BAHADUR KHALSA COLLEGE, SRI ANANDPUR SAHIB**  
**(An Autonomous College)**  
**ANANDPUR SAHIB– 140118, PUNJAB (INDIA)**



**SRI GURU TEG BAHADUR KHALSA COLLEGE, SRI ANANDPUR SAHIB**  
(An Autonomous College)  
**ANANDPUR SAHIB-140118. PUNJAB (INDIA)**

## **CERTIFICATE**

It is certified that the work contained in the project report entitled "**Assessing Uranium and Radon in Groundwater Using Integrated Fluorimeter and Rad7: A Case Study of Nalagarh City, District Solan, Himachal Pradesh, India.**" is an original contribution by me and has not been submitted in part or full for any other degree at this or other University/ Institute.

The assistance and help received during the course of the thesis work have been acknowledged.

**Baljeet Singh**

Regn. No. 8114-19-778

I, the undersigned, Supervisor of Baljeet Singh, Regn. No. 8114-19-778, a candidate for the degree of **Master of Science**, agree that the project report entitled, "**Assessing Uranium and Radon in Groundwater Using Integrated Fluorimeter and Rad7: A Case Study of Nalagarh City, District Solan, Himachal Pradesh, India.**", may be submitted in partial fulfillment of the requirements for the award of degree.

This is to certify that the above statement made by the candidate is correct to the best of my knowledge.

**Dr. Vimal Mehta**  
**Assistant Professor**  
Department of Physics,  
Sri Guru Teg Bahadur Khalsa College  
Sri Anandpur Sahib  
**Supervisor**

**Dr. Randev Sandhu**  
**Head of department**  
Department of Physics,  
Sri Guru Teg Bahadur Khalsa College  
Sri Anandpur Sahib

**Prof. Amandeep Kaur**  
**Assistant Professor**  
Department of Physics,  
Sri Guru Teg Bahadur Khalsa College  
Sri Anandpur Sahib  
**Mentor**

## **Content**

<b>1. Abstract</b>	<b>1</b>
<b>2. Introduction</b>	<b>1-5</b>
<b>3. Research objectives</b>	<b>5-6</b>
• Properties and safe drinking water ingestion levels of Uranium	<b>5</b>
• Properties and safe drinking water ingestion levels of Radon	<b>5-6</b>
<b>4. Literature review</b>	<b>6-7</b>
• Uranium and Radon in ground water	<b>6</b>
• Research in India	<b>7</b>
<b>5. Methodology</b>	<b>8-23</b>
• Sample collection	<b>8-9</b>
• Location and pictures of sampling sites	<b>10-21</b>
• LED Fluorimeter	<b>21-22</b>
• Rad7	<b>23</b>
<b>6. Results and discussion</b>	<b>24-28</b>
<b>7. Conclusion</b>	<b>28</b>
<b>8. Acknowledgement</b>	<b>28</b>
<b>9. References</b>	<b>29-32</b>



# **"Assessing Uranium and Radon in Groundwater Using Integrated Fluorimeter and Rad7: A Case Study of Nalagarh City, District Solan, Himachal Pradesh, India."**

## **Abstract**

The research project focuses on the integration of two advanced tools for analysis, namely a LED fluorimeter and DurrIDGE Rad7, to conduct a steady analysis of groundwater in Nalagarh City, District Solan, Himachal Pradesh, India. The primary aims are to assess the concentrations of uranium and radon in the groundwater, highlighting critical concerns related to the presence of these naturally occurring radioactive materials. The LED fluorimeter provides high-precision measurements, for uranium, while Rad7 is very efficient and accurate to assess the radon levels. The study aims to define the distribution of uranium and radon in the groundwater of the Nalagarh city, to identify hotspots and to understanding the geological factors influencing their occurrence. By integrating these advance apparatus that is LED Fluorimeter for Uranium and Rad7 for Radon, the research work seeks to enhance the precision and reliability of groundwater assessments, contributing valuable insights for environmental and public health considerations in the Nalagarh region. The outcomes of this study is to ensure the safety of the environment, animals and the civilians of the city.

**Keywords:** - Uranium concentration, Radon contamination, LED Fluorimeter, DurrIDGE Rad7.

## **Introduction**

Availability of clean and safe drinking water is an essential aspect of public health, and the presence of contaminations in groundwater causes a major threat to water quality. In the Nalagarh City which is situated in District Solan, Himachal Pradesh, India, concerns arise in the uranium and radon contamination. These naturally occurring radioactive elements can contaminates groundwater, leading to potential health risks when consumed beyond permissible limits. As urbanization and industrial activities increasing drastically in Nalagarh and it gets more important now to monitor the contaminations such as Uranium and Radon

- **Uranium**

Uranium, a heavy metal with the atomic number 92, is a pivotal element in environmental research, especially concerning its occurrence in groundwater. This comprehensive overview aims to delve into the multifaceted aspects of uranium, encompassing its isotopes, oxidation states, water solubility, and geological behavior. This knowledge is fundamental for a

thorough environmental assessment and understanding the potential health risks associated with uranium contamination in groundwater.

### 1. Uranium Isotopes: Tracing Radioactive Signatures

Uranium presents a diverse array of isotopes, with Uranium-238 ( $^{238}\text{U}$ ) being the most abundant and naturally occurring. The decay series initiated by U-238 introduces isotopes such as Thorium-234 ( $^{234}\text{Th}$ ) and Radium-226 ( $^{226}\text{Ra}$ ), acting as distinctive signatures for tracking uranium behavior in environmental systems. Research studies by Tissot et al. (2015)[1] and Carvalho et al. (2023)[2] provide valuable insights into the isotopic composition of uranium in diverse geological settings.

### 2. Oxidation States: Chemical Flexibility Unveiled

Uranium showcases remarkable chemical versatility by adopting various oxidation states, ranging from +3 to +6. In natural environments, U(IV) and U(VI) are the most relevant states. The redox cycling between these states influences uranium's mobility and reactivity in subsurface environments. In-depth investigations by Nolan et al. (2023)[3] and Dang et al. (2023)[4] shed light on the dynamic behavior of uranium oxidation states.

### 3. Water Solubility: A Crucial Transport Mechanism

The solubility of uranium in water is a critical factor influencing its transport through aquifers. U(VI) species, particularly uranyl ions ( $\text{UO}_2^{2+}$ ), exhibit higher solubility. This characteristic significantly impacts the potential for uranium migration and contamination in groundwater. Noteworthy contributions by Chevreux et al. (2021)[5] and Smedley et al. (2023)[6] provide detailed insights into uranium solubility dynamics.

### 4. Geological Behaviour: Unraveling Weathering and Mobilization

Uranium's geological behaviour is intricately tied to weathering processes. The breakdown of uranium-rich minerals releases uranium into soil and water, contributing to its mobilization. Specific geological formations, such as sedimentary rocks or aquifer materials, can enhance uranium accumulation in groundwater. Pioneering work by Gomez et al. (2006)[7] and Sharma et al. (2022)[8] elucidate the geological factors influencing uranium mobility.

### 5. Health Implications: Chronic Exposure and Bioavailability

Chronic exposure to elevated uranium levels in drinking water poses health risks, including nephrotoxicity and an increased risk of cancer. The bioavailability of uranium in groundwater, influenced by its chemical speciation, contributes to potential health impacts on communities relying on contaminated water sources. Studies by Zamora et al. (1998)[9] and Zhang et al. (2022)[10] offer valuable insights into the health implications of uranium exposure.

## 6. Regulatory Measures and Monitoring: Safeguarding Water Quality

Given the potential health risks associated with uranium contamination, regulatory measures and monitoring programs play a pivotal role. Established guidelines and standards aim to limit uranium concentrations in drinking water, ensuring the safety of water supplies. The comprehensive work by Environmental Protection Agency (EPA) guidelines[11] and ongoing monitoring efforts by regional agencies contribute to the development of effective strategies for managing and mitigating uranium-related risks in groundwater.

- **Radon**

Radon, a noble gas with the symbol Rn and atomic number 86, is a key element in environmental studies, particularly concerning its presence in groundwater. This comprehensive overview aims to delve into the multifaceted aspects of radon, including its isotopes, oxidation states, water solubility, and geological behavior. This knowledge is crucial for a thorough environmental assessment and understanding the potential health risks associated with radon contamination in groundwater.

### 1. Radon Isotopes: Tracing Radioactive Signatures

Radon exists in multiple isotopic forms, with Radon-222 ( $^{222}\text{Rn}$ ) being the most prevalent and naturally occurring. The decay series initiated by  $^{222}\text{Rn}$  introduces isotopes such as Polonium-218 ( $^{218}\text{Po}$ ) and Lead-214 ( $^{214}\text{Pb}$ ), acting as distinctive signatures for tracking radon behavior in environmental systems. Research studies by Nunes et al. (2023)[12] and Monnin et al. (2002)[13] provide valuable insights into the isotopic composition of radon in diverse geological settings.

### 2. Oxidation States: Noble Gas Anomaly

As a noble gas, radon does not have conventional oxidation states in the same sense as metals. Its inert nature contributes to its mobility and stability in groundwater. Research by

Sicilia et al. (2022)[14] and Feng et al. (2022)[15] explores the unique chemical behavior and migration patterns of radon in different geological contexts.

### 3. Water Solubility: Gaseous Mobility in Aquifers

Radon's solubility in water is a critical factor influencing its transport through aquifers. Being a gas, radon dissolves in water to form  $^{222}\text{Rn}$ , and its solubility is influenced by factors such as temperature and pressure. Research contributions by Malvicini et al. (2004)[16] and Ye et al. (2019)[17] provide detailed insights into radon solubility dynamics in various hydrogeological conditions.

### 4. Geological Behavior: Influencing Transport and Accumulation

Radon's geological behavior is influenced by factors such as soil composition and aquifer characteristics. The breakdown of uranium-rich minerals contributes to the release of radon into soil and water, impacting its mobilization. Specific geological formations, such as karst aquifers or granitic bedrocks, can enhance radon accumulation in groundwater. Pioneering work by Veeger et al. (1998)[18] and Lupulescu et al. (2023)[19] elucidates the geological factors influencing radon mobility.

### 5. Health Implications: Inhalation Risks and Cancer Concerns

Ingesting water containing elevated radon levels can lead to health issues, especially lung cancer through inhalation. Research studies by Kang et al. (2019)[20] and Riudavets et al. (2022)[21] offer valuable insights into the health implications of radon exposure, emphasizing the importance of continuous monitoring and assessment.

### 6. Regulatory Measures and Monitoring: Ensuring Air and Water Safety

Given the potential health risks associated with radon, regulatory measures and monitoring programs play a pivotal role. Established guidelines aim to limit radon concentrations in both air and water, ensuring the safety of the environment and public health. The comprehensive work by Environmental Protection Agency (EPA) guidelines[22] and ongoing monitoring efforts by regional agencies contribute to the development of effective strategies for managing and mitigating radon-related risks in groundwater.

This introduction serves as a foundation for our research project, providing an extensive overview of uranium and radon in groundwater. As we assess their concentrations, this foundational knowledge will guide our exploration, contributing to a more profound understanding of these elements' dynamics in diverse environmental contexts.

## **Research Objectives:**

The main objective of this study is to contribute in the detailed understanding of uranium and radon in groundwater. Main goal is to characterize the distribution of Uranium and Radon and to explore the synergies between geochemical processes, optimizing analytical methodologies, and assessing the potential health and environmental consequences. Through these objectives, the research aims to inform groundwater management practices and contribute to the broader discourse on water resource sustainability.

As we are going into following sections, the methodology, results and findings, and discussions will everything, about the complexities surrounding uranium and radon in groundwater. The properties of Uranium and Radon and their MCL in consumable water are given as follow:

### **Properties and safe drinking water ingestion levels of Uranium**

Uranium, a heavy metal, is a ubiquitous component of the Earth's crust. Its radioactivity and chemical toxicity are of concern when present in groundwater. The most common uranium isotopes,  $^{238}\text{U}$  with a half life of 4.5 billion years and  $^{235}\text{U}$  with a half life of 700 million years, undergo radioactive  $\alpha$  decay, emitting  $\alpha$  particles. To understand Uranium's chemical behavior and its potential migration pathways in groundwater is crucial for accurate assessment.

- The World Health Organization (WHO)[23] sets a provisional guideline value of 15 micrograms per liter ( $\mu\text{g/L}$ ) for uranium in drinking water.
- The U.S. Environmental Protection Agency (EPA)[11] has a Maximum Contaminant Level (MCL) of 30  $\mu\text{g/L}$  for uranium in public water supplies.

### **▪ Properties and safe drinking water ingestion levels of Radon**

Radon, a colorless, odorless, and tasteless radioactive gas, is a decay product of uranium. Its primary isotopes are,  $^{222}\text{Rn}$  and  $^{220}\text{Rn}$ , causes health risks when inhaled or ingested. Radon is water-soluble, allowing it to enter groundwater, making its detection and measurement crucial for assessing the overall water quality. The DurrIDGE Rad7 is known for its sensitivity to radon, enhances the precision of radon concentration measurements in groundwater



- The World Health Organization (WHO)[23] sets a provisional guideline value of 11 Bq/L for Radon in drinking water.
- According to UNSEAR[24] safe Radon concentration value in water for consumption is between 4-40 Bq/L.

## **Literature Review**

Groundwater quality assessment is a critical part of environmental monitoring, especially in the regions prone to contamination by uranium and radon. In Nalagarh City, situated in District Solan, Himachal Pradesh, India, understanding the concentrations of these radioactive elements is essential for safeguarding public health. This literature review explores the existing knowledge, methodologies, and recent research which is related to the integration of LED fluorimeters and Rad7 instruments in groundwater analysis for uranium and radon concentration assessment.

### **Uranium and Radon in Groundwater:**

In India we get to see different types of geological settings and it encounters challenges related to groundwater contamination by uranium and radon. Uranium, a naturally occurring radioactive element, can infiltrate groundwater through weathering processes and it can potentially leading to severe health[25] issues upon ingestion without being aware to it. Radon, a radioactive gas is a by product of uranium decay it dissolves in groundwater which causes risks through inhalation. Managing and mitigating these risks makes it very important to understand the sources like its transport mechanisms, and concentrations of uranium and radon in groundwater.

Access to safe and clean drinking water is a critical aspect of public health. In Nalagarh City, situated in the picturesque district of Solan, Himachal Pradesh, India, concerns have arisen regarding the presence of uranium and radon in groundwater. This literature review provides a comprehensive exploration of past research, aiming to establish a foundational understanding of the dynamics and challenges associated with uranium and radon concentrations in the groundwater of Nalagarh City.

So on all those grounds, today, many researchers have done many research studies on assessment of Uranium and Radon concentration levels in groundwater and many still going on so hereby, there are few research studies done in India for the assessment of Uranium and Radon in groundwater;

## **Researches in India:**

Several studies in India have explored groundwater quality, uranium, and radon concentrations few of them are as follow:

1. **"Analysis of Uranium in drinking water samples using laser induced fluorimetry in some regions of Himachal Pradesh and Punjab"[26]**
2. **" A study on uranium and radon levels in drinking water sources of a mineralized zone of Himachal Pradesh "[27]**
3. **"A preliminary appraisal of radon concentration in groundwater from the high background radiation area (HBRA) of Coastal Kerala "[28]**
4. **" Measurement of uranium and radon concentration in drinking water samples and assessment of ingestion dose to local population in Jalandhar district of Punjab " [29]**
5. **"Radiological risk assessment to the public due to the presence of radon in water of Barnala district, Punjab, India. " [30]**
6. **"Radiation dose-dependent risk on individuals due to ingestion of uranium and radon concentration in drinking water samples of four districts of Haryana, India " [31]**
7. **" Quantification of radiological dose and chemical toxicity due to radon and uranium in drinking water in Bageshwar region of Indian Himalaya. "[32]**
8. **"Age-dependent ingestion and inhalation doses due to intake of uranium and radon in water samples of Shiwalik Himalayas of Jammu and Kashmir, India. "[33]**
9. **"Appraisal of age-dependent radiological risk caused by ingestion of Uranium in groundwater of Patiala District, Punjab"[34]**
10. **"Radon monitoring in groundwater samples from some areas of northern Rajasthan, India, using a Rad7 detector" [35]**
11. **"Uranium in groundwater in parts of India and world: A comprehensive review of sources, impact to the environment and human health, analytical techniques, and mitigation technologies "[36]**
12. **"Age-dependent ingestion doses to the public of Rupnagar and Una regions of India due to intake of uranium. " [37]**

## Methodology:

Nalagarh is a town in the Solan district of Himachal Pradesh, India. Geographically, it is situated at approximately 31.05°N latitude and 76.72°E longitude. The town is surrounded by the Shivalik Hills. Nalagarh is situated along the banks of Satluj river, which plays significant role in the region's geography and ecology. The specific land area covered by Nalagarh town is approximately 25 Km<sup>2</sup>. Thi figure represents the town's administrative boundaries and includes both developed and undeveloped areas within those limits. The city has 10708 people living there (according of 2011 census), that is 428 persons per Km<sup>2</sup>.

## Sample collection

23 ground water samples were collected across the city by using a grid on the map of the city. The sites are mentioned in the Figure 1a and Figure 1b given below. The exact latitude and longitude of the sites are obtained by using a application called GPS Map Camera.

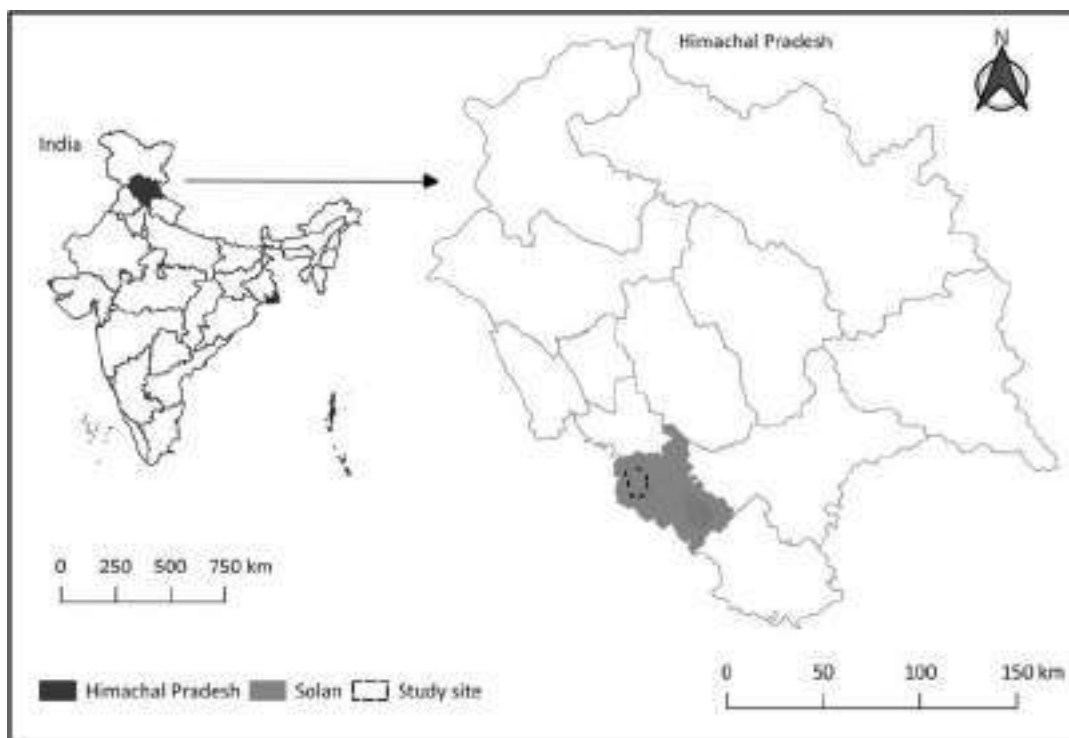


Fig 1a:- Study area site[38]

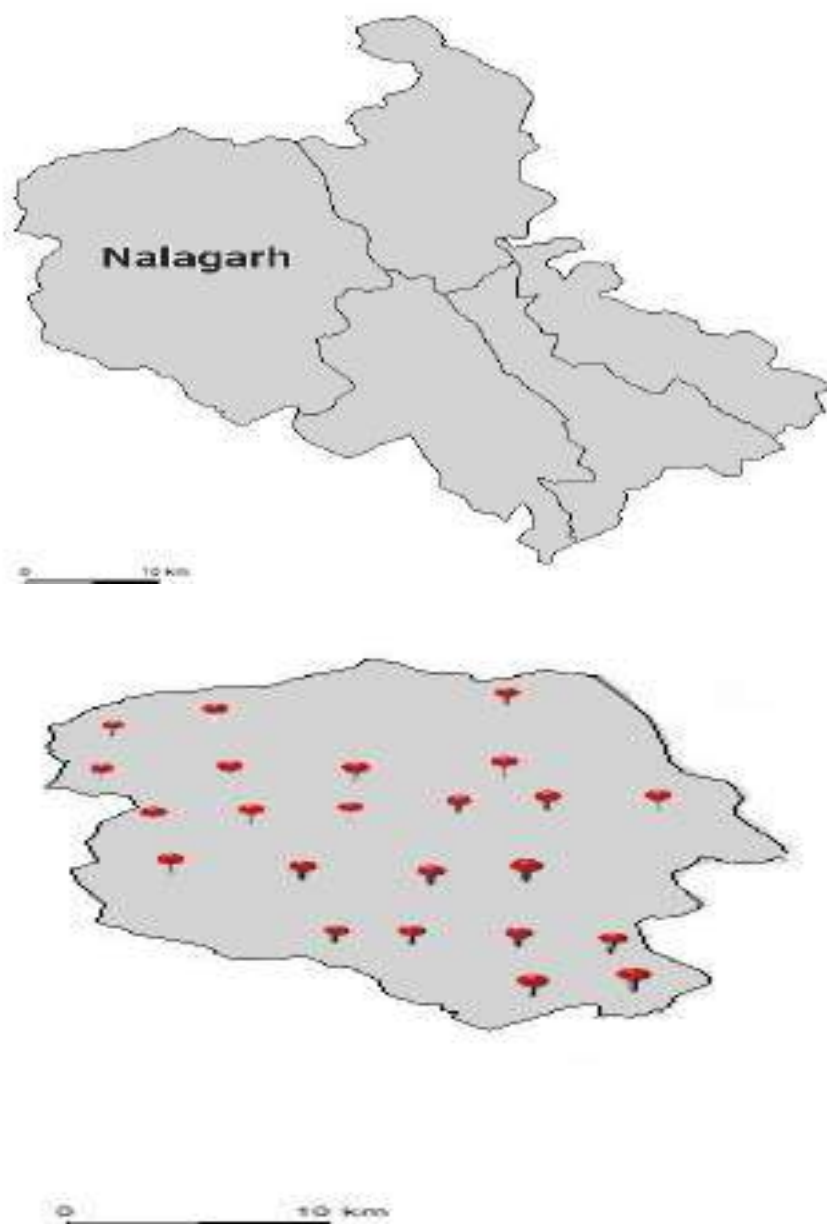


Fig. 1b:- Location of the sampling Sites.

High density polyethylene plastic bottles of 250ml were used to collect samples which were cleaned using dilute HCL (0.5N HCL) and were rinsed with deionised water before taking sample. Before collecting sample the water sources were run made to run for few minutes so that we can collect fresh water for sampling for better and accurate results. And then bottles are prewashed with source water 2-3 times before collecting sample. Samples are collected in that way so that there will be minimum or no air bubble left inside the bottles because it will affect the radon detection. Then uranium concentration in all 23 samples are measured by LED Fluorimeter and Randon concentration is measured by DurrIDGE Rad7.

## Location and Pictures of sampling sites

### Sample 1



Site of sample 1



Location of sample 1

### Sample 2



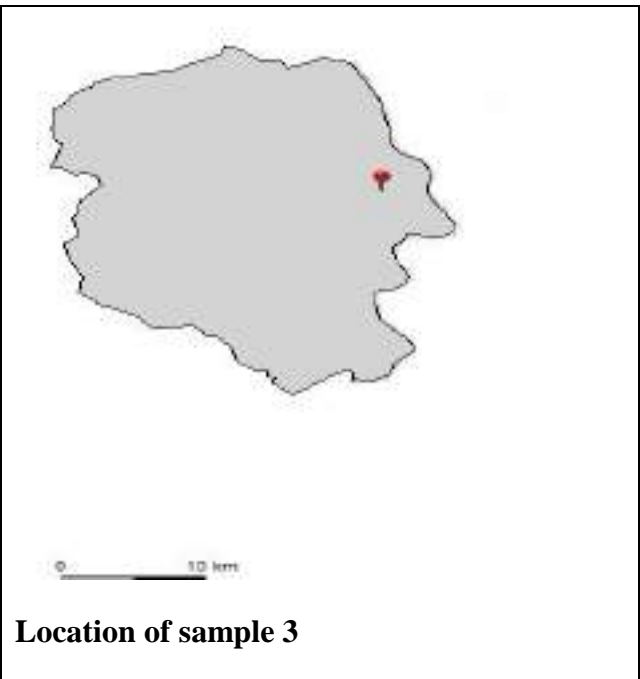
Site of sample 2



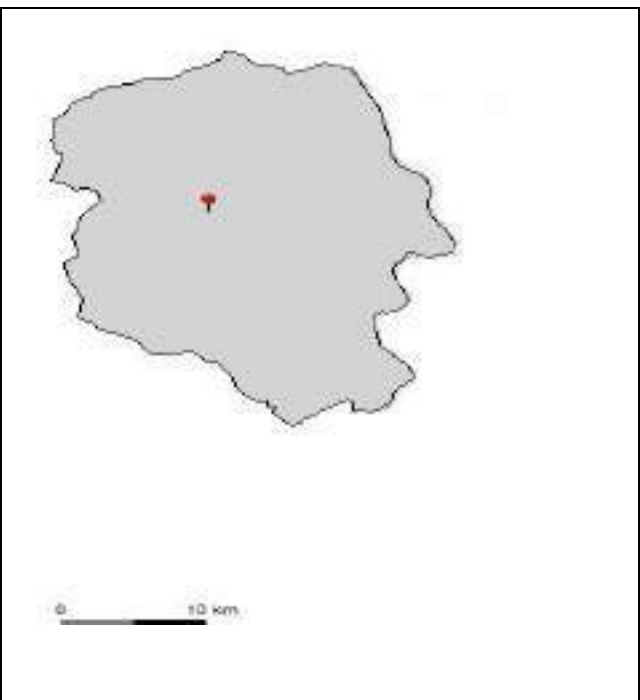
Location of sample 2



### Sample 3



### Sample 4



## Sample 5



Site of sample 5



0 10 km

Location of sample 5

## Sample 6



Site of sample 6



0 10 km

Site of sample 6

## Sample 7



Site of sample 7



Location sample 7

## Sample 8



Site of sample 8

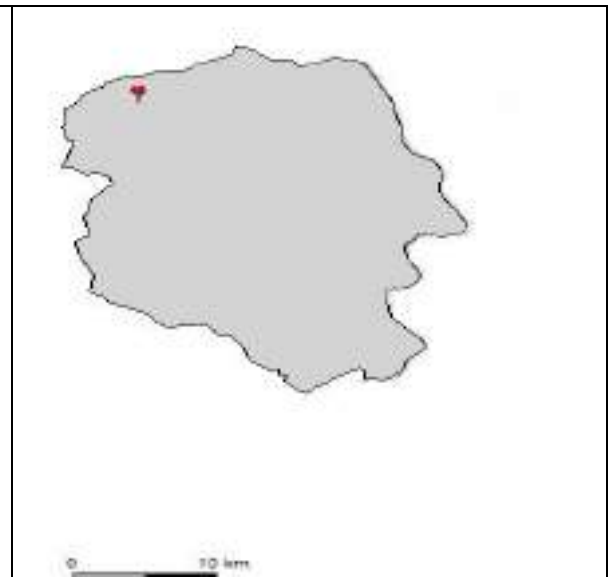


Location of sample 8

## Sample 9



Site of sample 9

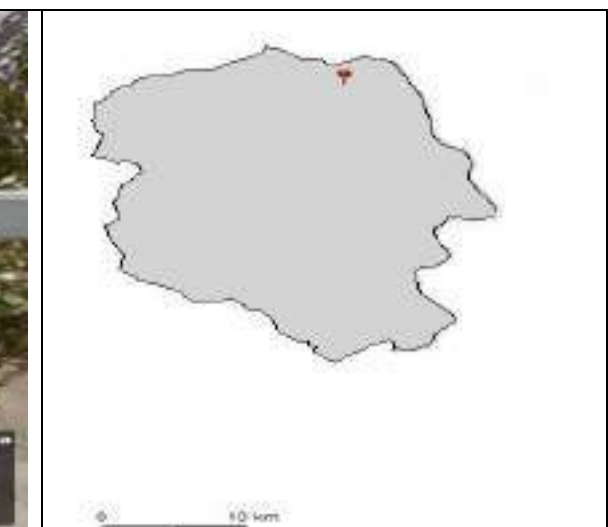


Location of sample 9

## Sample 10



Site of sample 10



Location of sample 10



## Sample 11



Site of sample 11



0 10 km

Location of sample 11

## Sample 12



Site of sample 12



0 10 km

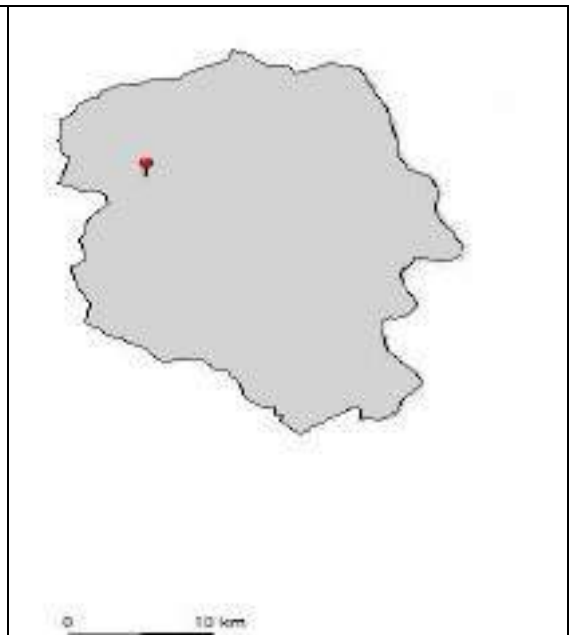
Location of sample 12



## Sample 13



Site of sample 13



Location of sample 13

## Sample 14



Site of sample 14

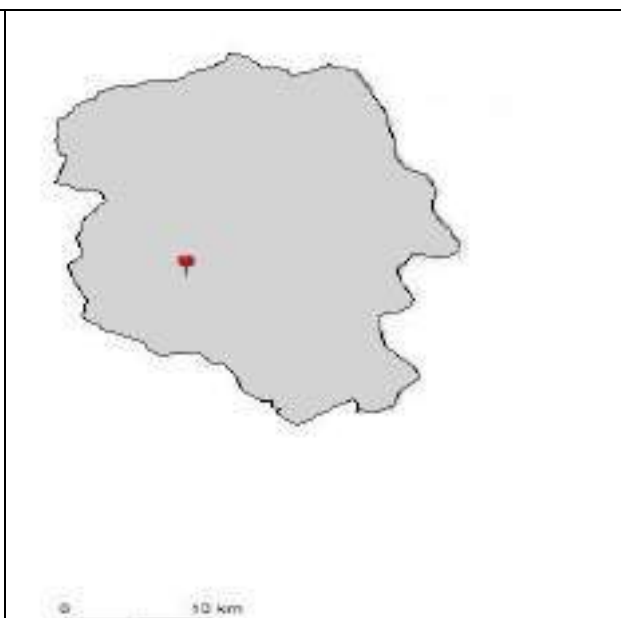


Location of sample 14

## Sample 15



Site of sample 15



Location of sample 15

## Sample 16



Site of sample 16



Location of sample 16

## Sample 17



Site of sample 17



Location of sample 17

## Sample 18



Site of sample 18



Location of sample 18

## Sample 19

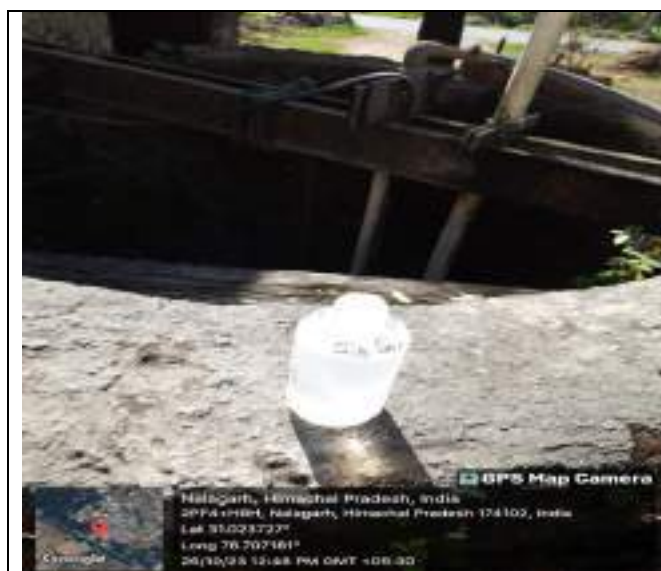


Site of sample 19

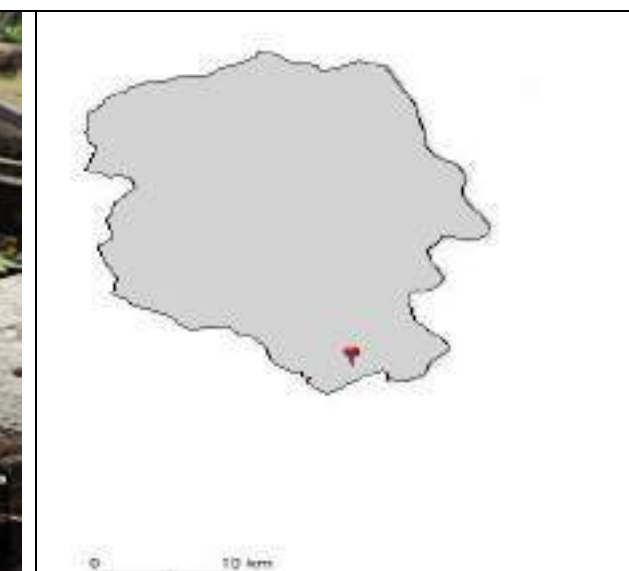


Location of Sample 19

## Sample 20



Site of sample 20



Location of sample 20



## Sample 21



Site of sample 21



0 50 km

Location of sample 21

## Sample 22



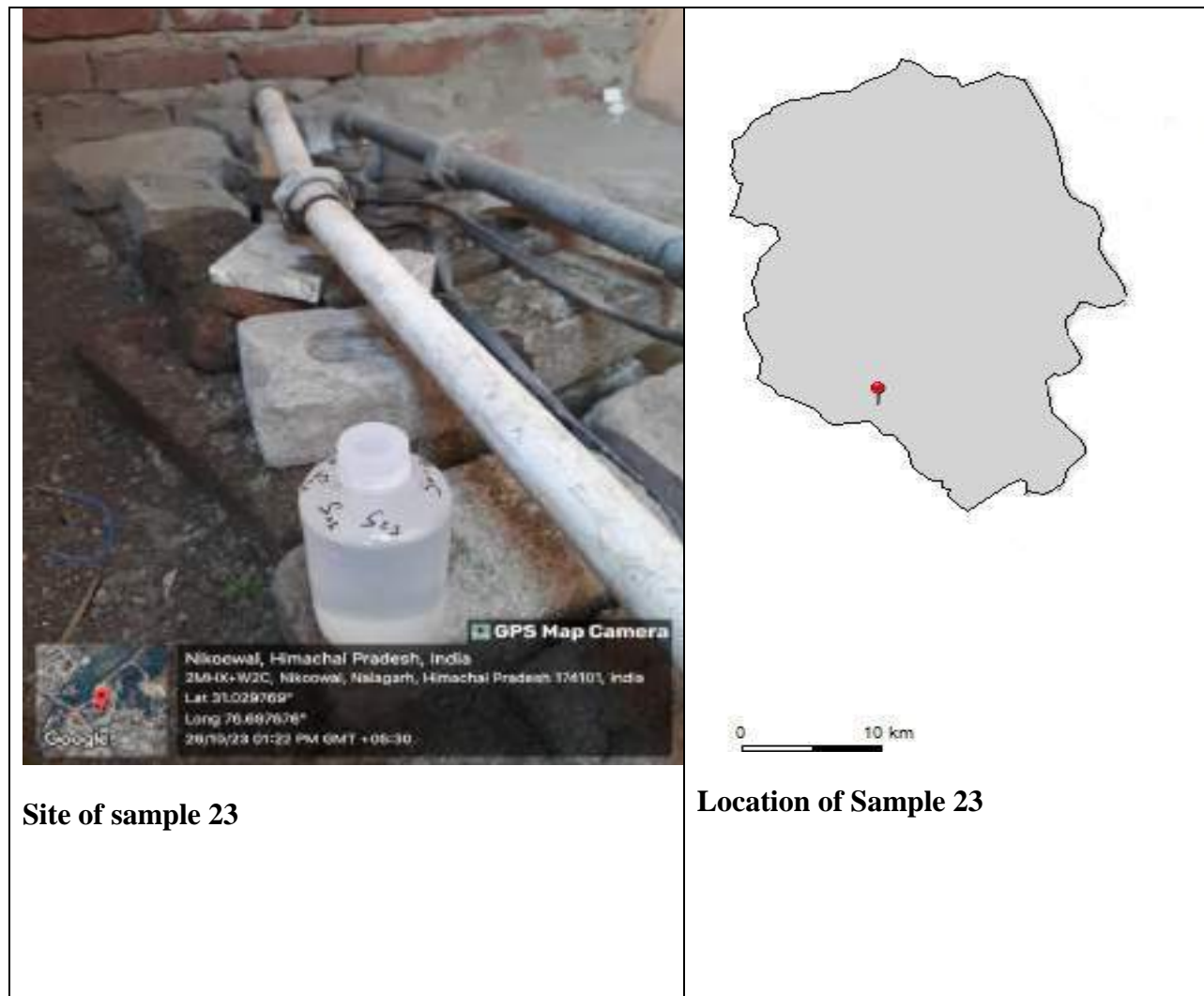
Site of sample 22



0 50 km

Location of sample 22

## Sample 23



Site of sample 23

Location of Sample 23

## LED Fluorimeter

A fluorimeter is a device used to measure the fluorescence emitted by a sample when exposed to specific wavelengths of light. LED fluorimeters use light-emitting diodes (LEDs) as the light source and it is the one of the quickest, highly sensitive and most reliable device. The LED Fluorimeter is capable to measure concentration in water sample from 0.5  $\mu\text{g/L}$  to 4000  $\mu\text{g/L}$ [39] with high accuracy, block diagram of LED fluorimeter is shown in Fig. 2. The working principle involves:



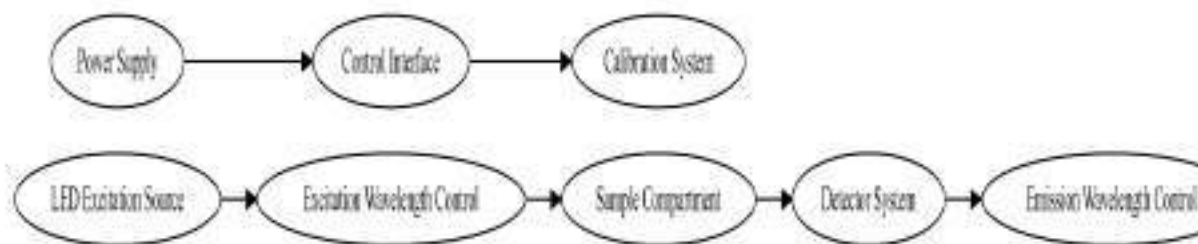


Fig. 2 Block diagram of LED fluorimeter.

**Excitation:** The LED emits light at a specific wavelength, known as the excitation wavelength. This light is directed towards the sample.

**Sample Interaction:** The sample absorbs the excitation light and then re-emits light at a longer wavelength, known as the emission wavelength. This phenomenon is called fluorescence.

**Detection:** A photodetector in the fluorimeter detects the emitted fluorescence. The intensity of the fluorescence is proportional to the concentration of the fluorescent substance in the sample.

**Signal Processing:** The detected fluorescence signal is processed and often displayed as a numerical value or a fluorescence spectrum

All the samples are first filtered through a filter paper of 45  $\mu\text{m}$ . Then pH of the water is measured by using a pH meter by Hanna instruments. We have three available specific modes in the device by which Uranium concentration can be measured first one is standard calibration mode, calibration mode and uncalibrated mode. And we are Utilizing the uncalibrated mode for measurement, we have employed the method specified by BARC in this study. The significant advantage of this approach lies in its ability to enhance the accuracy of uranium concentration measurements. Initially, the fluorescence of a background solution, composed of 5.0 mL of distilled water and 0.5 mL of buffer solution, is determined. Subsequently, the fluorescence of the sample solution (consisting of 5.0 mL of the sample and 0.5 mL of buffer solution) is recorded. Following this, increments of 50  $\mu\text{L}$  of a 500 ppb standard uranium solution are then added, and we get the corresponding counts of each stage for all 23 samples.

## Rad7

RAD7 H<sub>2</sub>O is a special attachment of RAD7 used for the measurement of radon concentration in water. The range of the Rad7 lies between 10 pCi/l to 4105 pCi/l [40], with a lower limit of detection below, 10 pCi/l. This portable and battery-operated equipment ensures expeditious measurements. The schematic diagram of RAD H<sub>2</sub>O is illustrated in Figure 3. Post a 20 minutes analysis, RAD H<sub>2</sub>O delivers results with sensitivity matching or surpassing that of liquid scintillation methods. Employing a closed-loop aeration scheme, RAD H<sub>2</sub>O maintains constant air and water volumes independent of the flow rate. The system achieves equilibrium

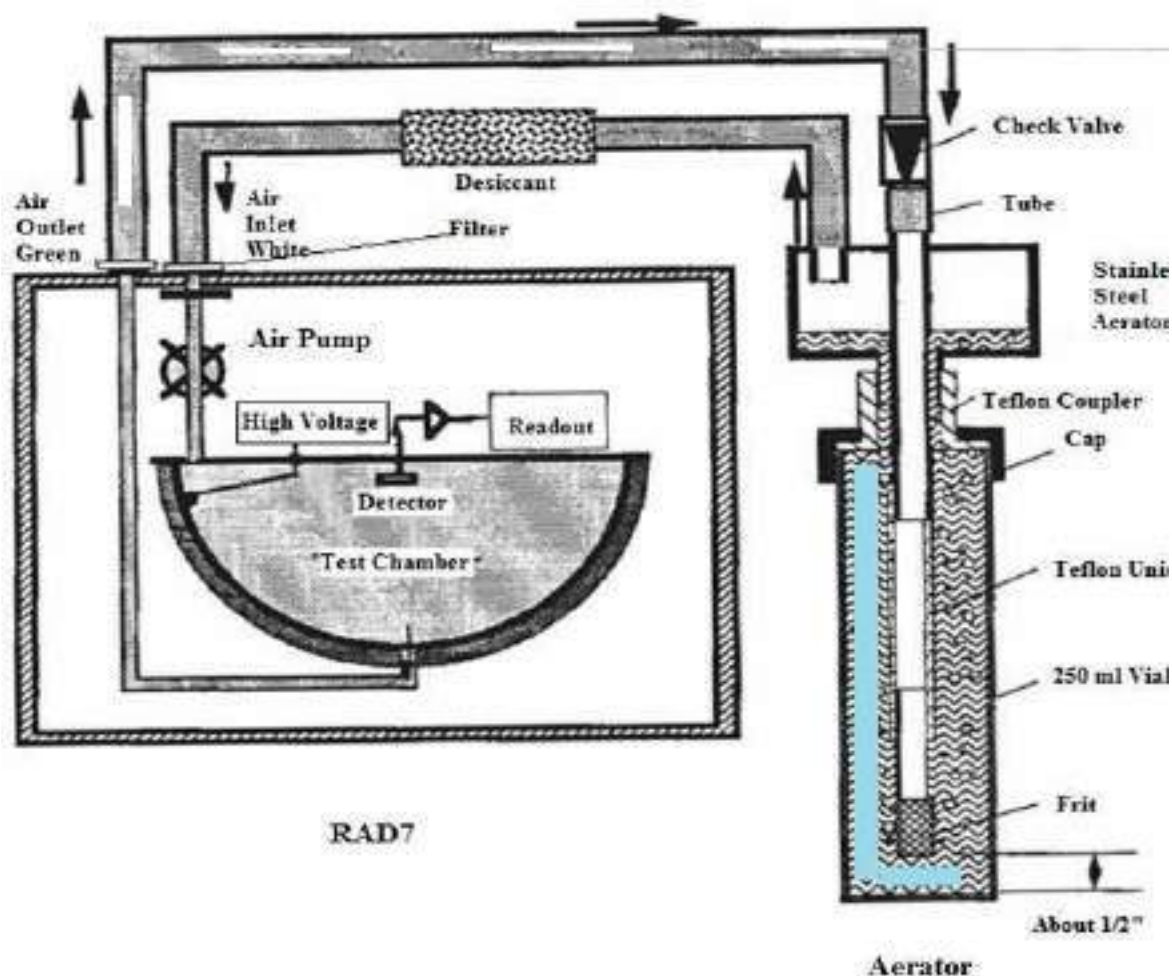


Fig. 3 Schematic diagram of RAD7-H<sub>2</sub>O [40]

within approximately 5 minutes, ceasing radon extraction thereafter. The extraction efficiency, representing the percentage of radon removed from the water to the air loop, is notably high at  $\approx 94\%$  for a 250ml sample. While the extraction efficiency may slightly vary with ambient temperature, it consistently exceeds 90%. The RAD7 detector transforms alpha radiation into an electric signal directly, possessing the capability to differentiate between aged and fresh radon, as well as radon emanating from thoron.

## Results and discussion

The results of uranium and radon analysis in water samples of the study are presented in Table 1. The values of uranium in all 23 samples were in the range  $1.65 \pm 0.26$   $\mu\text{g/L}$  to  $16.98 \pm 0.65$   $\mu\text{g/L}$  and the values of Radon were in the range  $2.64 \pm 0.4$  Bq/L to  $24.01 \pm 4.71$  Bq/L with an average value of Uranium is  $7.334 \pm 0.291$   $\mu\text{g/L}$  and average value of Radon is  $8.63 \pm 1.72$  Bq/L and when the values of Uranium concentration is compared with the allowed MCL proposed by WHO[23], we observed that 95% of the samples were below the value proposed by WHO[23] and only 5% of samples were higher than that of the value proposed by WHO[23]. The MCL value suggested by USEPA[11] is 30  $\mu\text{g/L}$  and values of all the samples was below than this value (suggested by USEPA). When the Radon concentration value is compared with value suggested by WHO[23] that is 11 Bq/L we found that approx. 74% of the samples were below the MCL value and the values of 16% of the samples higher then value suggested by WHO[23] and UNSCEAR[24] suggested the concentration value between 4-40 Bq/L when compared to this value 100% of the samples were below the suggested value. The Radon concentration values are when compared with European Commission recommendations for the protection of living beings against Radon exposure in drinking water supply (2001/928/Euratom)[41] which suggests the action level of 100 Bq/L for drinking water supply. The Radon concentration levels in some areas of Northern Rajasthan is  $0.5 \pm 0.3$  Bq/L to  $85.7 \pm 4.9$  Bq/L with an average of  $9.03 \pm 1.03$  Bq/ L which is reported by Rohit Mehra[35] . The Radon concentration in samples of Bathinda and Gurdaspur districts, Punjab lies between  $0.2 \pm 8.8$  Bq/ L reported by Walia, V[42]. The average Uranium concentration in tube wells of Patiala District, Punjab, India is 31.1987  $\mu\text{g/L}$  reported by Vimal Mehta[34].

Table 1. Values of Uranium and Radon of all 23 samples collected from Nalagarh

Sr. No.	Locations	Latitude	Longitude	pH	Source	Depth (ft)	Uranium conc. ( $\mu\text{g/L}$ )	Radon conc. ( $\text{Bq/L}$ )
S1	Nalagarh 4	31°02'35.3"N	76°42'52.0"E	7.2	OW	50	1.65 $\pm$ 0.26	3.03 $\pm$ 1.46
S2	Nalagarh 3	31°02'32.4"N	76°43'01.3"E	7.1	SP	170	10.1 $\pm$ 0.12	8.88 $\pm$ 1.08
S3	Nalagarh 5	31°02'31.3"N	76°43'27.2"E	7.5	SW	500	2.06 $\pm$ 0.22	10.34 $\pm$ 1.99
S4	New Nalagarh 1	31°02'32.4"N	76°42'03.1"E	6.8	OW	100	8.77 $\pm$ 1.01	11.41 $\pm$ 0.11
S5	New Nalagarh 3	31°02'34.0"N	76°41'52.9"E	7.4	SP	170	1.11 $\pm$ 0.51	12.19 $\pm$ 3.85
S6	New Nalagarh 2	31°02'31.1"N	76°41'37.9"E	6.5	SP	200	13.5 $\pm$ 0.44	13.47 $\pm$ 3.01
S7	Nalagarhh 2	31°02'47.5"N	76°42'08.9"E	6.9	SP	400	8.48 $\pm$ 0.40	7.48 $\pm$ 0.87
S8	Nalagarh 1	31°03'10.2"N	76°41'14.1"E	6.7	SP	100	12.41 $\pm$ 0.61	9.57 $\pm$ 0.58
S9	Nalagarh 6	31°02'31.3"N	76°43'27.2"E	6.8	OW	65	12.66 $\pm$ 0.39	11.46 $\pm$ 1.34
S10	Sabhowal	31°03'12.0"N	76°42'35.4"E	6.3	SP	220	16.98 $\pm$ 0.65	24.01 $\pm$ 4.71
S11	Salhewal	31°02'55.9"N	76°42'25.5"E	8	OW	80	7.82 $\pm$ 0.13	9.78 $\pm$ 4.38
S12	Nalagarh	31°02'47.1"N	76°42'13.1"E	7.8	SP	250	4.56 $\pm$ 0.21	16.49 $\pm$ 3.2
S13	Nalagarh	31°02'51.7"N	76°41'47.8"E	7.3	SP	120	9.23 $\pm$ 0.08	5.7 $\pm$ 1.44
S14	Nalagarh	31°02'08.1"N	76°41'23.3"E	7.5	OW	100	5.67 $\pm$ 0.18	9.53 $\pm$ 2.25
S15	New Nalagarh	31°02'11.7"N	76°41'45.1"E	7.2	SP	300	8.34 $\pm$ 0.24	2.75 $\pm$ 0.92
S16	Nalagarh	31°02'17.6"N	76°42'05.6"E	7.9	SP	350	3.78 $\pm$ 0.11	4.17 $\pm$ 1.01
S17	Nalagarh	31°02'10.0"N	76°42'31.2"E	7.7	SP	200	6.45 $\pm$ 0.2	4.06 $\pm$ 0.82
S18	Nalagarh	31°01'35.9"	76°42'41.8"E	8.2	OW	100	2.89 $\pm$ 0.09	2.64 $\pm$ 0.4
S19	Nalagarh	31°01'28.1"N	76°42'57.5"E	7.4	SP	200	9.01 $\pm$ 0.14	6.97 $\pm$ 0.7
S20	Nalagarh	31°01'25.4"N	76°42'25.9"E	7.6	OW	60	4.12 $\pm$ 0.23	5.41 $\pm$ 0.88
S21	Nalagarh	31°01'35.0"N	76°42'36.6"E	7.5	SP	120	6.89 $\pm$ 0.1	5.75 $\pm$ 1.48
S22	Nalagarh	31°01'36.5"N	76°42'12.0"E	8.2	HP	70	3.45 $\pm$ 0.17	7.74 $\pm$ 1.73
S23	Nalagarh	31°01'47.2"N	76°41'51.6"E	7.3	SP	140	8.76 $\pm$ 0.22	5.68 $\pm$ 1.41

\*OW=Open well, SP= Submersible motor pump, SW=Surface water, HP= Hand-pump

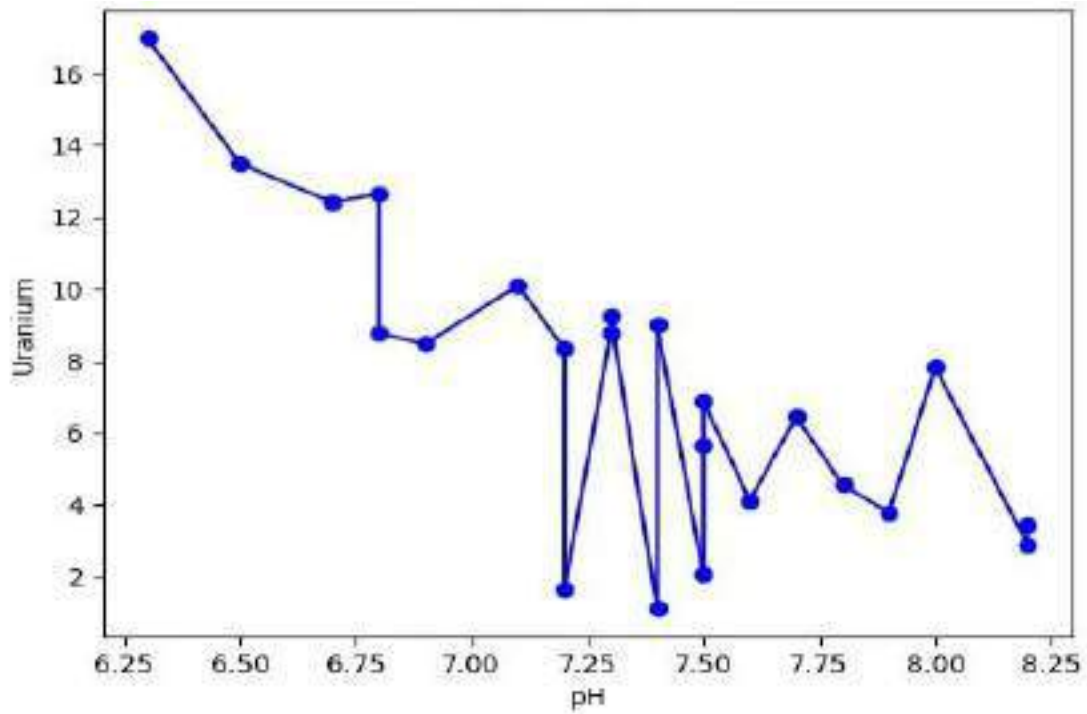


Fig. 4 Uranium concentration variation with pH of the collected samples, units for Uranium concentration in µg/L

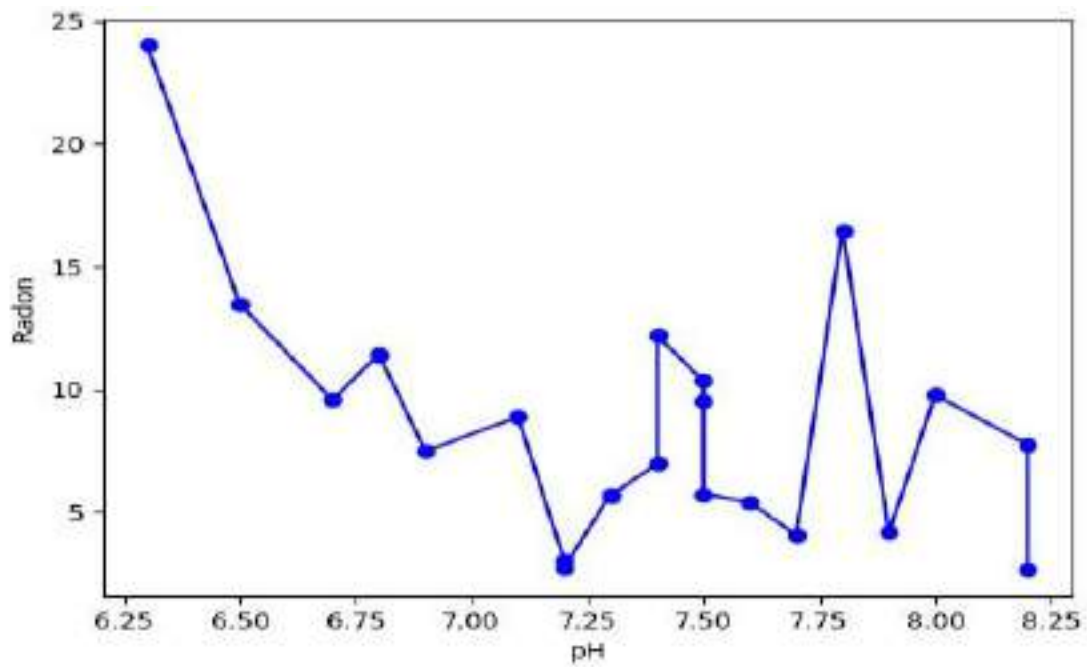


Fig. 5 Radon concentration variation with pH of collected samples, units of Radon concentration in Bq/L

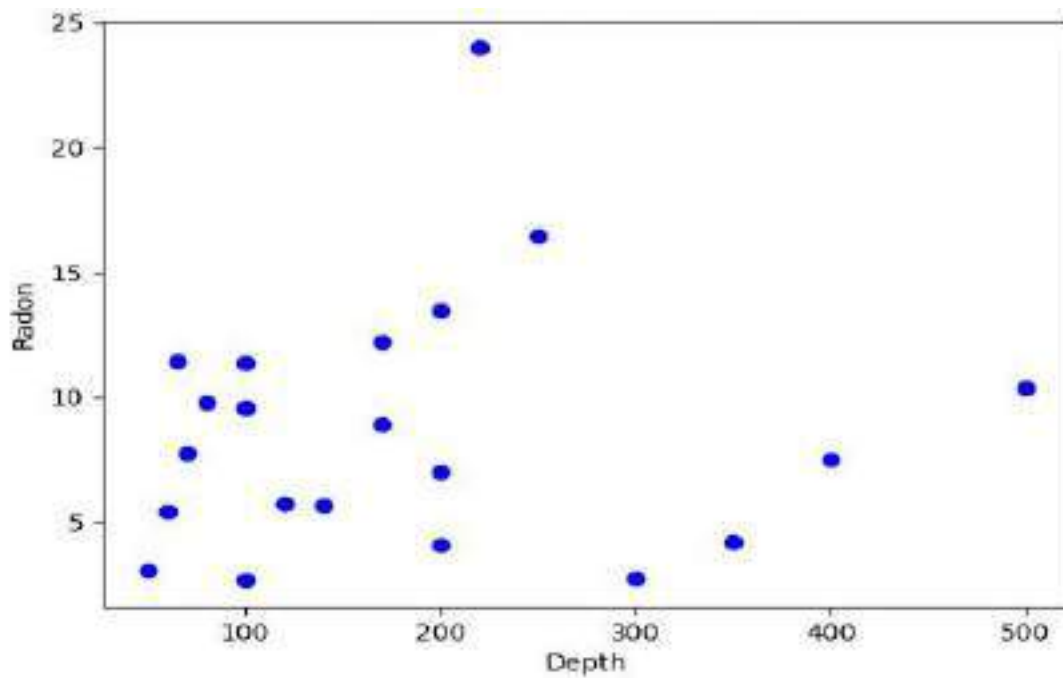


Fig. 6 Radon concentration Variation with Depth of the source, units of Radon concentration in Bq/L

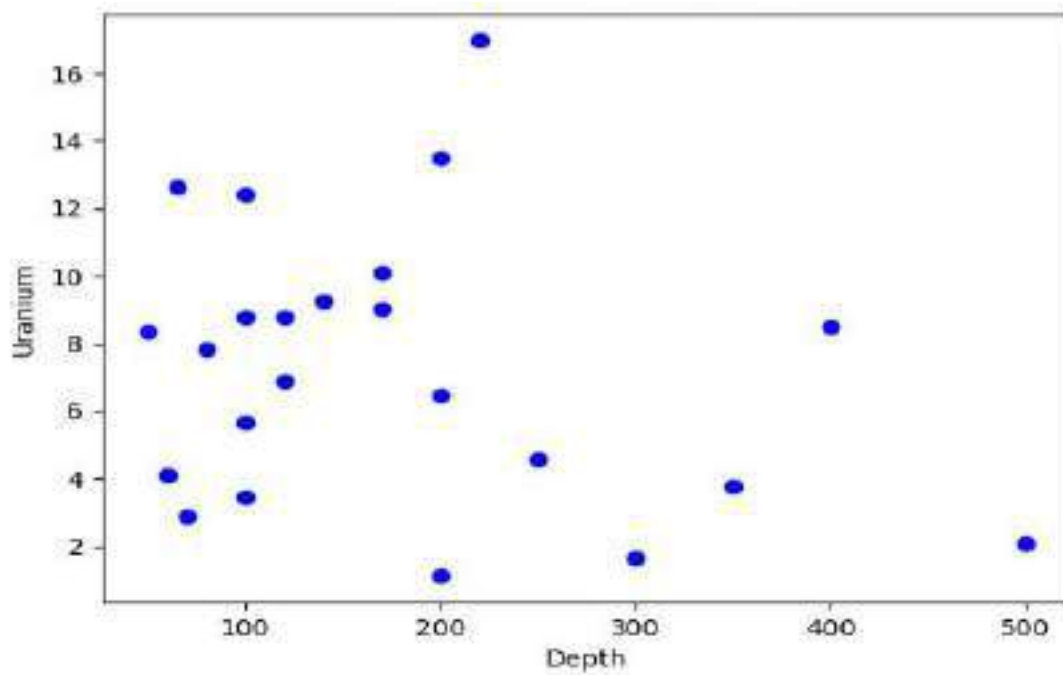


Fig. 7 Uranium concentration variation with depth of the source, , units for Uranium concentration in µg/L



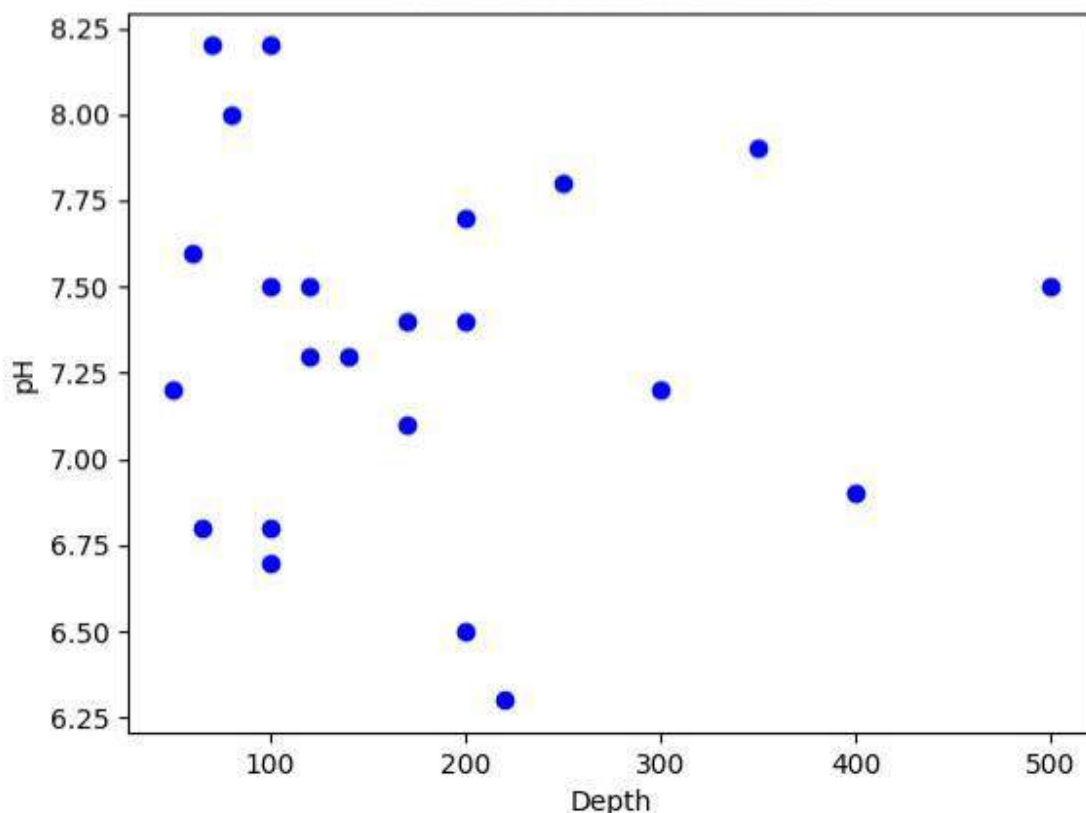


Fig. 8 pH variation with depth of the source, Units of depth in Feet (ft)

## Conclusion

Uranium concentration in all 23 samples were in the range  $1.65 \pm 0.26$   $\mu\text{g/L}$  to  $16.98 \pm 0.65$   $\mu\text{g/L}$  and the values of Radon were in the range  $2.64 \pm 0.4$  Bq/L to  $24.01 \pm 4.71$  Bq/L with an average value of Uranium is  $7.334 \pm 0.291$   $\mu\text{g/L}$  and average value of Radon is  $8.63 \pm 1.72$  Bq/. In Uranium concentration 95% of sample values are below than suggested value by and 5% were above than that. And according to USEPA suggested value all the 100% of sample values are below then the suggested value. The Radon concentration in all the samples were 74% under suggested value by the WHO and 16% were above than that and acc to UNSCEAR suggested value all the 100% of sample values are under MCL suggested by organisation.

## Acknowledgement

The authors extend heartfelt gratitude to the residents of Nalagarh for their invaluable cooperation during the field work. Special thanks are due to the Department of Physics at SGTB Khalsa College, Sri Anandpur Sahib, for providing essential resources and support. The authors acknowledge the guidance and support received from the Head of Department, Dr. Randev Sandhu, as well as the invaluable mentorship of the Supervisor, Dr. Vimal Mehta, and Professor Amandeep Kaur, which greatly contributed to the success of this research paper.

## References

1. Tissot, F. L., & Dauphas, N. (2015). Uranium isotopic compositions of the crust and ocean: Age corrections, U budget and global extent of modern anoxia. *Geochimica et Cosmochimica Acta*, 167, 113-143.
2. Carvalho, F. P., Fesenko, S., Harbottle, A. R., Lavrova, T., Mitchell, N. G., Payne, T. E., ... & Yankovich, T. L. (2023). The environmental behaviour of uranium.
3. Nolan, J., & Weber, K. A. (2015). Natural uranium contamination in major US aquifers linked to nitrate. *Environmental Science & Technology Letters*, 2(8), 215-220.
4. Deng, C., Liang, J., Sun, R., Wang, Y., Fu, P. X., Wang, B. W., ... & Huang, W. (2023). Accessing five oxidation states of uranium in a retained ligand framework. *Nature Communications*, 14(1), 4657.
5. Chevreux, P., Tissandier, L., Laplace, A., Vitova, T., Bahl, S., Le Guyadec, F., & Deloule, E. (2021). Uranium solubility and speciation in reductive soda-lime aluminosilicate glass melts. *Journal of Nuclear Materials*, 544, 152666.
6. Smedley, P. L., & Kinniburgh, D. G. (2023). Uranium in natural waters and the environment: Distribution, speciation and impact. *Applied Geochemistry*, 148, 105534.
7. Gómez, P., Garralón, A., Buil, B., Turrero, M. J., Sánchez, L., & De la Cruz, B. (2006). Modeling of geochemical processes related to uranium mobilization in the groundwater of a uranium mine. *Science of the Total Environment*, 366(1), 295-309.
8. Sharma, D. A., Keesari, T., Pant, D., Rishi, M. S., Sangwan, P., Thakur, N., & Sinha, U. K. (2022). Appraising the factors favouring uranium mobilization and associated health risk assessment in groundwaters of north-western India. *Ecotoxicology and Environmental Safety*, 229, 113086.
9. Zamora, M. L., Tracy, B. L., Zielinski, J. M., Meyerhof, D. P., & Moss, M. A. (1998). Chronic ingestion of uranium in drinking water: a study of kidney bioeffects in humans. *Toxicological Sciences*, 43(1), 68-77.
10. Zhang, L., Chu, J., Xia, B., Xiong, Z., Zhang, S., & Tang, W. (2022). Health effects of particulate uranium exposure. *Toxics*, 10(10), 575.
11. USEPA. (2000) National Primary Drinking Water Regulations; Radionuclides; Final Rule. *Fed Reg.* 65(236), 76708
12. Nunes, L. J., Curado, A., & Lopes, S. I. (2023). The Relationship between Radon and Geology: Sources, Transport and Indoor Accumulation. *Applied Sciences*, 13(13), 7460.

13. Monnin, M., & Seidel, J. L. (2002). Radon concentrations in karstic aquifers. *Geofísica Internacional*, 41(3), 265-270.
14. Sicilia, I., Aparicio, S., González, M., Anaya, J. J., & Frutos, B. (2022). Radon transport, accumulation patterns, and mitigation techniques applied to closed spaces. *Atmosphere*, 13(10), 1692.
15. Feng, X., Zhong, J., Yan, R., Zhou, Z., Tian, L., Zhao, J., & Yuan, Z. (2022). Groundwater radon precursor anomalies identification by EMD-LSTM model. *Water*, 14(1), 69.
16. Malvicini, A., ESPOSITO, P., & Depiesse, D. (2004). Influence of hydrogeological properties of rocky substratum, ventilation and meteorological conditions on environmental radioactivity in underground galleries. In *Proceedings of the 11th International Congress of the International Radiation Protection Association*, Madrid.
17. Ye, Y. J., Xia, X. Q., Dai, X. T., Huang, C. H., & Guo, Q. (2019). Effects of temperature, salinity, and pH on <sup>222</sup>Rn solubility in water. *Journal of Radioanalytical and Nuclear Chemistry*, 320, 369-375.
18. Veeger, A. I., & Ruderman, N. C. (1998). Hydrogeologic controls on radon-222 in a buried valley-fractured bedrock aquifer system. *Groundwater*, 36(4), 596-604.
19. Lupulescu, A., Baci, C., Dicu, T., Burghel, B. D., & Cucos, A. L. (2023). Determining the Geogenic Radon Potential in Different Layouts and Numbers of Points. *Atmosphere*, 14(4), 713.
20. Kang, J. K., Seo, S., & Jin, Y. W. (2019). Health effects of radon exposure. *Yonsei medical journal*, 60(7), 597-603.
21. Riudavets, M., Garcia de Herreros, M., Besse, B., & Mezquita, L. (2022). Radon and lung cancer: current trends and future perspectives. *Cancers*, 14(13), 3142.
22. United States Environmental Protection Agency. Radon in drinking water, Factsheet. EPA 815-F-99007. USEPA (1999)
23. WHO, 2003. Guidelines for Drinking Water Quality. Health Criteria and Other Supporting Information. World Health Organization (2003).
24. United Nations Scientific Committee on the effect of Atomic Radiation. The general assembly with scientific annex, United Nation. UNSCEAR (2000).

25. Ma, M., Wang, R., Xu, L., Xu, M., & Liu, S. (2020). Emerging health risks and underlying toxicological mechanisms of uranium contamination: Lessons from the past two decades. *Environment international*, 145, 106107.
26. Rani, A., & Singh, S. (2006). Analysis of uranium in drinking water samples using laser induced fluorimetry. *Health physics*, 91(2), 101-107.
27. Singh, P., Singh, P., Sahoo, B. K., & Bajwa, B. S. (2016). A study on uranium and radon levels in drinking water sources of a mineralized zone of Himachal Pradesh, India. *Journal of Radioanalytical and Nuclear Chemistry*, 309, 541-549.
28. Nandakumaran, P., & Vinayachandran, N. (2020). A preliminary appraisal of radon concentration in groundwater from the high background radiation area (HBRA) of Coastal Kerala. *Journal of the Geological Society of India*, 95, 491-496.
29. Kumar, M., Kaushal, A., Sahoo, B. K., Sarin, A., Mehra, R., Jakhu, R., ... & Sharma, N. (2019). Measurement of uranium and radon concentration in drinking water samples and assessment of ingestion dose to local population in Jalandhar district of Punjab, India. *Indoor and Built Environment*, 28(5), 611-618.
30. Rani, S., Kansal, S., Singla, A. K., & Mehra, R. (2021). Radiological risk assessment to the public due to the presence of radon in water of Barnala district, Punjab, India. *Environmental Geochemistry and Health*, 43(12), 5011-5024.
31. Panghal, A., Kumar, A., Kumar, S., Singh, J., Sharma, S., Singh, P., ... & Bajwa, B. S. (2017). Radiation dose-dependent risk on individuals due to ingestion of uranium and radon concentration in drinking water samples of four districts of Haryana, India. *Radiation effects and defects in solids*, 172(5-6), 441-455.
32. Kumar, A., Arora, T., Singh, P., Singh, K., Singh, D., Pathak, P. P., & Ramola, R. C. (2021). Quantification of radiological dose and chemical toxicity due to radon and uranium in drinking water in Bageshwar region of Indian Himalaya. *Groundwater for Sustainable Development*, 12, 10049
33. Kaur, M., Kumar, A., Mehra, R., & Mishra, R. (2019). Age-dependent ingestion and inhalation doses due to intake of uranium and radon in water samples of Shiwalik Himalayas of Jammu and Kashmir, India. *Environmental monitoring and assessment*, 191, 1-17.

34. Mehta, V., Kapil, C., Shikha, D., & Kanse, S. (2023). Appraisal of age-dependent radiological risk caused by ingestion of uranium in groundwater of Patiala district, Punjab. *Journal of Radioanalytical and Nuclear Chemistry*, 1-11.
35. Rani, A., Mehra, R., & Duggal, V. (2013). Radon monitoring in groundwater samples from some areas of Northern Rajasthan, India, using a RAD7 detector. *Radiation protection dosimetry*, 153(4), 496-501.
36. Balaram, V., Rani, A., & Rathore, D. P. S. (2022). Uranium in groundwater in parts of India and world: A comprehensive review of sources, impact to the environment and human health, analytical techniques, and mitigation technologies. *Geosystems and Geoenvironment*, 1(2), 100043.
37. Mehta, V., Kaur, J., Shikha, D., & Kanse, S. (2023). Age-dependent ingestion doses to the public of Rupnagar and Una regions of India due to intake of uranium. *Journal of Radioanalytical and Nuclear Chemistry*, 1-15.
38. Shaurabh Anand, Srinivas Vaidyanathan, Sindhu Radhakrishna The Role of Landscape Structure in Primate Crop Feeding: Insights from Rhesus Macaques (*Macaca mulatta*) in Northern India (2021)
39. Mehra, R., Gupta, D., & Jakhu, R. (2017). Risk assessment for natural uranium present in ground water of Mahendragarh district of Haryana. *J. Radiat. Nucl. Appl*, 2, 67-73.
40. DURRIDGE Radon Instrumentation. RAD H2O User Manual, Radon in Water Accessory. DURRIDGE Company (2011)
41. European Commission. Commission directive of defining requirements for the parameters for radioactivity for monitoring the quality of water for the Council Directive 98/83 of 3 November 1998 on the quality of water intended for human consumption. Draft V3.029/11/2005.
42. Virk, H. S., Walia, V., & Bajwa, B. S. (2001). Radon monitoring in underground water of Gurdaspur and Bathinda districts of Punjab, India.

**INTEGRATION OF FLUORIMETER AND RAD7 IN  
GROUNDWATER ANALYSIS FOR URANIUM AND  
RADON ASSESSMENT IN NALAGARH CITY,  
DISTRICT SOLAN, HIMACHAL PRADESH, INDIA**

**PROJECT REPORT**

*Submitted in partial fulfillment of the  
requirements for the award of the degree of*

**MASTER OF SCIENCE**

**in**

**PHYSICS**

*By*

**Hritik Sahore  
(Regn. No. 8114-2022-1796)**



**DEPARTMENT OF PHYSICS  
SRI GURU TEG BAHADUR KHALSA COLLEGE, SRI ANANDPUR  
SAHIB**

**(An Autonomous College)**

**ANANDPUR SAHIB- 140118, PUNJAB (INDIA)**





**SRI GURU TEG BAHADUR KHALSA COLLEGE, SRI ANANDPUR SAHIB**  
(An Autonomous College)  
**ANANDPUR SAHIB-140118. PUNJAB (INDIA)**

## **CERTIFICATE**

It is certified that the work contained in the project report entitled "INTEGRATION OF FLUORIMETER AND RAD7 IN GROUNDWATER ANALYSIS FOR URANIUM AND RADON ASSESSMENT IN NALAGARH CITY, DISTRICT SOLAN, HIMACHAL PRADESH, INDIA" is an original contribution by me and has not been submitted in part or full for any other degree at this or other University/ Institute.

The assistance and help received during the course of the thesis work have been acknowledged.

*Hritik Sahore*

**Hritik Sahore**

Regn. No. 8114-2022-1796

I, the undersigned, Supervisor of **Hritik Sahore**, Regn. No. 8114-2022-1796, a candidate for the degree of **Master of Science**, agree that the project report entitled, "INTEGRATION OF FLUORIMETER AND RAD7 IN GROUNDWATER ANALYSIS FOR URANIUM AND RADON ASSESSMENT IN NALAGARH CITY, DISTRICT SOLAN, HIMACHAL PRADESH, INDIA", may be submitted in partial fulfillment of the requirements for the award of degree.

This is to certify that the above statement made by the candidate is correct to the best of my knowledge.

*Vimal Mehta*  
**Dr. Vimal Mehta**  
Assistant Professor  
Department of Physics,  
Sri Guru Teg Bahadur Khalsa College  
Sri Anandpur Sahib  
Supervisor

*Rande Sandhu*  
**Dr. Rande Sandhu**  
Head of department  
Department of Physics,  
Sri Guru Teg Bahadur Khalsa College  
Sri Anandpur Sahib

*Amandeep Kaur*  
**Prof. Amandeep Kaur**  
Assistant Professor  
Department of Physics,  
Sri Guru Teg Bahadur Khalsa College  
Sri Anandpur Sahib  
Mentor

## **Content**

<b>1. Abstract</b>	<b>1</b>
<b>2. Introduction</b>	<b>1-5</b>
<b>3. Research objectives</b>	<b>5-6</b>
• Properties and safe drinking water ingestion levels of Uranium	<b>5</b>
• Properties and safe drinking water ingestion levels of Radon	<b>5-6</b>
<b>4. Literature review</b>	<b>6-7</b>
• Uranium and Radon in ground water	<b>6</b>
• Research in India	<b>7</b>
<b>5. Methodology</b>	<b>8-23</b>
• Sample collection	<b>8-9</b>
• Location and pictures of sampling sites	<b>10-21</b>
• LED Fluorimeter	<b>21-22</b>
• Rad7	<b>23</b>
<b>6. Results and discussion</b>	<b>24-28</b>
<b>7. Conclusion</b>	<b>28</b>
<b>8. Acknowledgement</b>	<b>28</b>
<b>9. References</b>	<b>29-32</b>

# **INTEGRATION OF FLUORIMETER AND RAD7 IN GROUNDWATER ANALYSIS FOR URANIUM AND RADON CONCENTRATION ASSESSMENT IN NALAGARH CITY, DISTRICT SOLAN, HIMACHAL PRADESH, INDIA**

## **Abstract**

The research project focuses on the integration of two advanced tools for analysis, namely a LED fluorimeter and Durrige Rad7, to conduct a steady analysis of groundwater in Nalagarh City, District Solan, Himachal Pradesh, India. The primary aims are to assess the concentrations of uranium and radon in the groundwater, highlighting critical concerns related to the presence of these naturally occurring radioactive materials. The LED fluorimeter provides high-precision measurements, for uranium, while Rad7 is very efficient and accurate to assess the radon levels. The study aims to define the distribution of uranium and radon in the groundwater of the Nalagarh city, to identify hotspots and to understanding the geological factors influencing their occurrence. By integrating these advance apparatus that is LED Fluorimeter for Uranium and Rad7 for Radon, the research work seeks to enhance the precision and reliability of groundwater assessments, contributing valuable insights for environmental and public health considerations in the Nalagarh region. The outcomes of this study is to ensure the safety of the environment, animals and the civilians of the city.

**Keywords:** - Uranium concentration, Radon contamination, LED Fluorimeter, Durrige Rad7.

## **Introduction**

Availability of clean and safe drinking water is an essential aspect of public health, and the presence of contaminations in groundwater causes a major threat to water quality. In the Nalagarh City which is situated in District Solan, Himachal Pradesh, India, concerns arise in the uranium and radon contamination. These naturally occurring radioactive elements can contaminates groundwater, leading to potential health risks when consumed beyond permissible limits. As urbanization and industrial activities increasing drastically in Nalagarh and it gets more important now to monitor the contaminations such as Uranium and Radon

- **Uranium**

Uranium, a heavy metal with the atomic number 92, is a pivotal element in environmental research, especially concerning its occurrence in groundwater. This comprehensive overview aims to delve into the multifaceted aspects of uranium, encompassing its isotopes, oxidation states, water solubility, and geological behavior. This knowledge is fundamental for a

thorough environmental assessment and understanding the potential health risks associated with uranium contamination in groundwater.

### 1. Uranium Isotopes: Tracing Radioactive Signatures

Uranium presents a diverse array of isotopes, with Uranium-238 ( $^{238}\text{U}$ ) being the most abundant and naturally occurring. The decay series initiated by U-238 introduces isotopes such as Thorium-234 ( $^{234}\text{Th}$ ) and Radium-226 ( $^{226}\text{Ra}$ ), acting as distinctive signatures for tracking uranium behavior in environmental systems. Research studies by Tissot et al. (2015)[1] and Carvalho et al. (2023)[2] provide valuable insights into the isotopic composition of uranium in diverse geological settings.

### 2. Oxidation States: Chemical Flexibility Unveiled

Uranium showcases remarkable chemical versatility by adopting various oxidation states, ranging from +3 to +6. In natural environments, U(IV) and U(VI) are the most relevant states. The redox cycling between these states influences uranium's mobility and reactivity in subsurface environments. In-depth investigations by Nolan et al. (2023)[3] and Dang et al. (2023)[4] shed light on the dynamic behavior of uranium oxidation states.

### 3. Water Solubility: A Crucial Transport Mechanism

The solubility of uranium in water is a critical factor influencing its transport through aquifers. U(VI) species, particularly uranyl ions ( $\text{UO}_2^{2+}$ ), exhibit higher solubility. This characteristic significantly impacts the potential for uranium migration and contamination in groundwater. Noteworthy contributions by Chevreux et al. (2021)[5] and Smedley et al. (2023)[6] provide detailed insights into uranium solubility dynamics.

### 4. Geological Behaviour: Unraveling Weathering and Mobilization

Uranium's geological behaviour is intricately tied to weathering processes. The breakdown of uranium-rich minerals releases uranium into soil and water, contributing to its mobilization. Specific geological formations, such as sedimentary rocks or aquifer materials, can enhance uranium accumulation in groundwater. Pioneering work by Gomez et al. (2006)[7] and Sharma et al. (2022)[8] elucidate the geological factors influencing uranium mobility.

### 5. Health Implications: Chronic Exposure and Bioavailability

Chronic exposure to elevated uranium levels in drinking water poses health risks, including nephrotoxicity and an increased risk of cancer. The bioavailability of uranium in groundwater, influenced by its chemical speciation, contributes to potential health impacts on communities relying on contaminated water sources. Studies by Zamora et al. (1998)[9] and Zhang et al. (2022)[10] offer valuable insights into the health implications of uranium exposure.

## 6. Regulatory Measures and Monitoring: Safeguarding Water Quality

Given the potential health risks associated with uranium contamination, regulatory measures and monitoring programs play a pivotal role. Established guidelines and standards aim to limit uranium concentrations in drinking water, ensuring the safety of water supplies. The comprehensive work by Environmental Protection Agency (EPA) guidelines[11] and ongoing monitoring efforts by regional agencies contribute to the development of effective strategies for managing and mitigating uranium-related risks in groundwater.

- **Radon**

Radon, a noble gas with the symbol Rn and atomic number 86, is a key element in environmental studies, particularly concerning its presence in groundwater. This comprehensive overview aims to delve into the multifaceted aspects of radon, including its isotopes, oxidation states, water solubility, and geological behavior. This knowledge is crucial for a thorough environmental assessment and understanding the potential health risks associated with radon contamination in groundwater.

### 1. Radon Isotopes: Tracing Radioactive Signatures

Radon exists in multiple isotopic forms, with Radon-222 ( $^{222}\text{Rn}$ ) being the most prevalent and naturally occurring. The decay series initiated by  $^{222}\text{Rn}$  introduces isotopes such as Polonium-218 ( $^{218}\text{Po}$ ) and Lead-214 ( $^{214}\text{Pb}$ ), acting as distinctive signatures for tracking radon behavior in environmental systems. Research studies by Nunes et al. (2023)[12] and Monnin et al. (2002)[13] provide valuable insights into the isotopic composition of radon in diverse geological settings.

### 2. Oxidation States: Noble Gas Anomaly

As a noble gas, radon does not have conventional oxidation states in the same sense as metals. Its inert nature contributes to its mobility and stability in groundwater. Research by



Sicilia et al. (2022)[14] and Feng et al. (2022)[15] explores the unique chemical behavior and migration patterns of radon in different geological contexts.

### 3. Water Solubility: Gaseous Mobility in Aquifers

Radon's solubility in water is a critical factor influencing its transport through aquifers. Being a gas, radon dissolves in water to form  $^{222}\text{Rn}$ , and its solubility is influenced by factors such as temperature and pressure. Research contributions by Malvicini et al. (2004)[16] and Ye et al. (2019)[17] provide detailed insights into radon solubility dynamics in various hydrogeological conditions.

### 4. Geological Behavior: Influencing Transport and Accumulation

Radon's geological behavior is influenced by factors such as soil composition and aquifer characteristics. The breakdown of uranium-rich minerals contributes to the release of radon into soil and water, impacting its mobilization. Specific geological formations, such as karst aquifers or granitic bedrocks, can enhance radon accumulation in groundwater. Pioneering work by Veeger et al. (1998)[18] and Lupulescu et al. (2023)[19] elucidates the geological factors influencing radon mobility.

### 5. Health Implications: Inhalation Risks and Cancer Concerns

Ingesting water containing elevated radon levels can lead to health issues, especially lung cancer through inhalation. Research studies by Kang et al. (2019)[20] and Riudavets et al. (2022)[21] offer valuable insights into the health implications of radon exposure, emphasizing the importance of continuous monitoring and assessment.

### 6. Regulatory Measures and Monitoring: Ensuring Air and Water Safety

Given the potential health risks associated with radon, regulatory measures and monitoring programs play a pivotal role. Established guidelines aim to limit radon concentrations in both air and water, ensuring the safety of the environment and public health. The comprehensive work by Environmental Protection Agency (EPA) guidelines[22] and ongoing monitoring efforts by regional agencies contribute to the development of effective strategies for managing and mitigating radon-related risks in groundwater.



This introduction serves as a foundation for our research project, providing an extensive overview of uranium and radon in groundwater. As we assess their concentrations, this foundational knowledge will guide our exploration, contributing to a more profound understanding of these elements' dynamics in diverse environmental contexts.

## **Research Objectives:**

The main objective of this study is to contribute in the detailed understanding of uranium and radon in groundwater. Main goal is to characterize the distribution of Uranium and Radon and to explore the synergies between geochemical processes, optimizing analytical methodologies, and assessing the potential health and environmental consequences. Through these objectives, the research aims to inform groundwater management practices and contribute to the broader discourse on water resource sustainability.

As we are going into following sections, the methodology, results and findings, and discussions will everything, about the complexities surrounding uranium and radon in groundwater. The properties of Uranium and Radon and their MCL in consumable water are given as follow:

### **Properties and safe drinking water ingestion levels of Uranium**

Uranium, a heavy metal, is a ubiquitous component of the Earth's crust. Its radioactivity and chemical toxicity are of concern when present in groundwater. The most common uranium isotopes,  $^{238}\text{U}$  with a half life of 4.5 billion years and  $^{235}\text{U}$  with a half life of 700 million years, undergo radioactive  $\alpha$  decay, emitting  $\alpha$  particles. To understand Uranium's chemical behavior and its potential migration pathways in groundwater is crucial for accurate assessment.

- The World Health Organization (WHO)[23] sets a provisional guideline value of 15 micrograms per liter ( $\mu\text{g/L}$ ) for uranium in drinking water.
- The U.S. Environmental Protection Agency (EPA)[11] has a Maximum Contaminant Level (MCL) of 30  $\mu\text{g/L}$  for uranium in public water supplies.

### **Properties and safe drinking water ingestion levels of Radon**

Radon, a colorless, odorless, and tasteless radioactive gas, is a decay product of uranium. Its primary isotopes are,  $^{222}\text{Rn}$  and  $^{220}\text{Rn}$ , causes health risks when inhaled or ingested. Radon is water-soluble, allowing it to enter groundwater, making its detection and measurement crucial for assessing the overall water quality. The DurrIDGE Rad7 is known for its sensitivity to radon, enhances the precision of radon concentration measurements in groundwater

- The World Health Organization (WHO)[23] sets a provisional guideline value of 11 Bq/L for Radon in drinking water.
- According to UNSEAR[24] safe Radon concentration value in water for consumption is between 4-40 Bq/L.

## **Literature Review**

Groundwater quality assessment is a critical part of environmental monitoring, especially in the regions prone to contamination by uranium and radon. In Nalagarh City, situated in District Solan, Himachal Pradesh, India, understanding the concentrations of these radioactive elements is essential for safeguarding public health. This literature review explores the existing knowledge, methodologies, and recent research which is related to the integration of LED fluorimeters and Rad7 instruments in groundwater analysis for uranium and radon concentration assessment.

### **Uranium and Radon in Groundwater:**

In India we get to see different types of geological settings and it encounters challenges related to groundwater contamination by uranium and radon. Uranium, a naturally occurring radioactive element, can infiltrate groundwater through weathering processes and it can potentially leading to severe health[25] issues upon ingestion without being aware to it. Radon, a radioactive gas is a by product of uranium decay it dissolves in groundwater which causes risks through inhalation. Managing and mitigating these risks makes it very important to understand the sources like its transport mechanisms, and concentrations of uranium and radon in groundwater.

Access to safe and clean drinking water is a critical aspect of public health. In Nalagarh City, situated in the picturesque district of Solan, Himachal Pradesh, India, concerns have arisen regarding the presence of uranium and radon in groundwater. This literature review provides a comprehensive exploration of past research, aiming to establish a foundational understanding of the dynamics and challenges associated with uranium and radon concentrations in the groundwater of Nalagarh City.

So on all those grounds, today, many researchers have done many research studies on assessment of Uranium and Radon concentration levels in groundwater and many still going on so hereby, there are few research studies done in India for the assessment of Uranium and Radon in groundwater;

## **Researches in India:**

Several studies in India have explored groundwater quality, uranium, and radon concentrations few of them are as follow:

1. "Analysis of Uranium in drinking water samples using laser induced flurimetry in some regions if Himachal Pradesh and Punjab"[26]
2. " A study on uranium and radon levels in drinking water sources of a mineralized zone of Himachal Pradesh "[27]
3. "A preliminary appraisal of radon concentration in groundwater from the high background radiation area (HBRA) of Coastal Kerala "[28]
4. " Measurement of uranium and radon concentration in drinking water samples and assessment of ingestion dose to local population in Jalandhar district of Punjab " [29]
5. "Radiological risk assessment to the public due to the presence of radon in water of Barnala district, Punjab, India. " [30]
6. "Radiation dose-dependent risk on individuals due to ingestion of uranium and radon concentration in drinking water samples of four districts of Haryana, India " [31]
7. " Quantification of radiological dose and chemical toxicity due to radon and uranium in drinking water in Bageshwar region of Indian Himalaya. "[32]
8. "Age-dependent ingestion and inhalation doses due to intake of uranium and radon in water samples of Shiwalik Himalayas of Jammu and Kashmir, India. "[33]
9. "Appraisal of age-dependent radiological risk caused by ingestion of Uranium in groundwater of Patiala District, Punjab"[34]
10. "Radon monitoring in groundwater samples from some areas of northern Rajasthan, India, using a Rad7 detector" [35]
11. "Uranium in groundwater in parts of India and world: A comprehensive review of sources, impact to the environment and human health, analytical techniques, and mitigation technologies "[36]
12. "Age-dependent ingestion doses to the public of Rupnagar and Una regions of India due to intake of uranium. " [37]

## Methodology:

Nalagarh is a town in the Solan district of Himachal Pradesh, India. Geographically, it is situated at approximately 31.05°N latitude and 76.72°E longitude. The town is surrounded by the Shivalik Hills. Nalagarh is situated along the banks of Satluj river, which plays significant role in the region's geography and ecology. The specific land area covered by Nalagarh town is approximately 25 Km<sup>2</sup>. Thi figure represents the town's administrative boundaries and includes both developed and undeveloped areas within those limits. The city has 10708 people living there (according of 2011 census), that is 428 persons per Km<sup>2</sup>.

## Sample collection

23 ground water samples were collected across the city by using a grid on the map of the city. The sites are mentioned in the Figure 1a and Figure 1b given below. The exact latitude and longitude of the sites are obtained by using a application called GPS Map Camera.

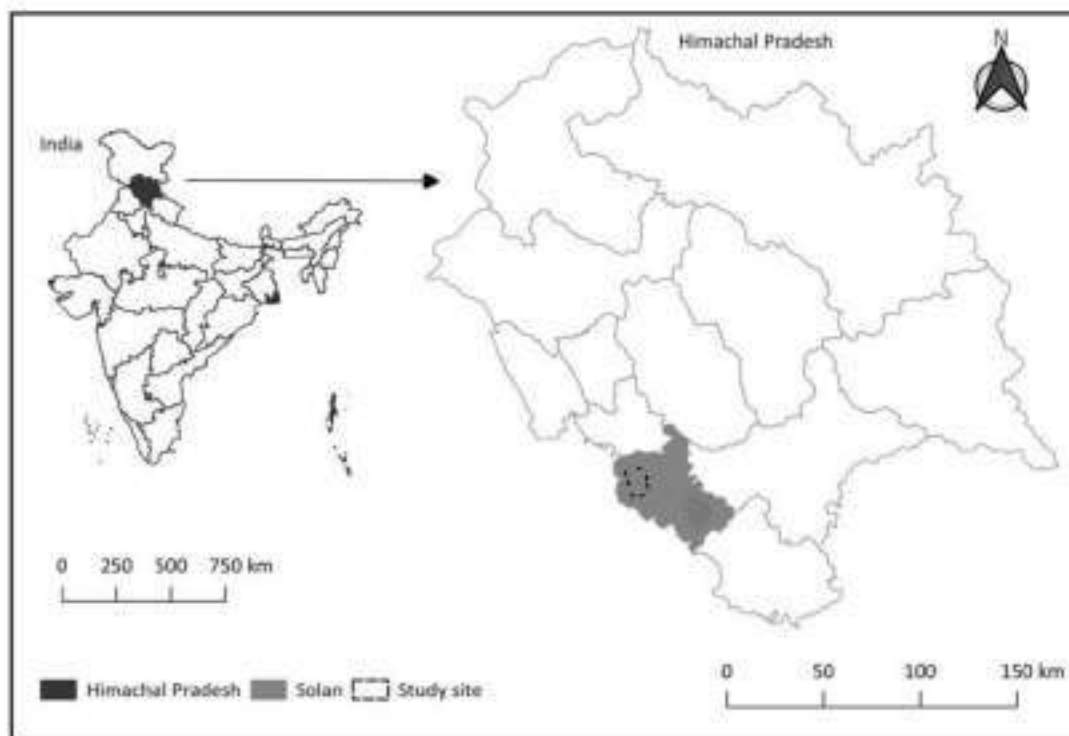


Fig 1a:- Study area site[38]

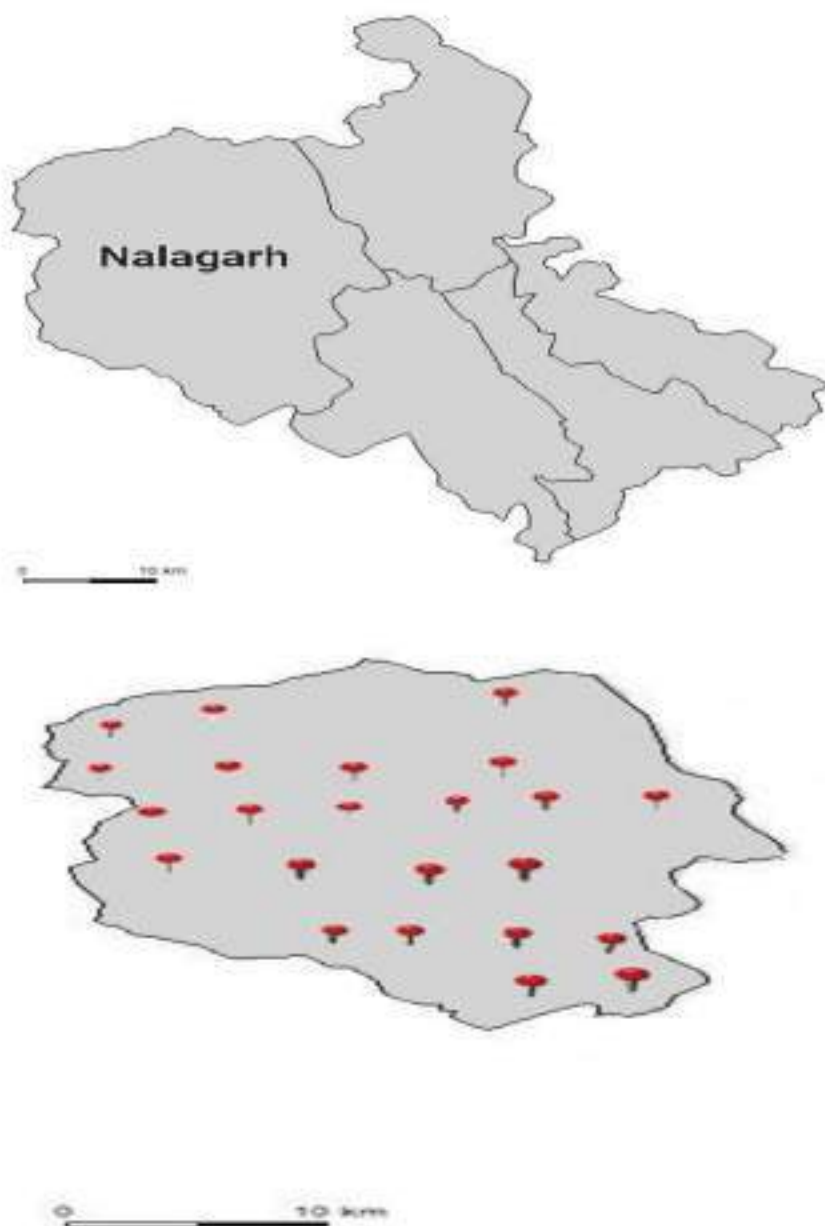


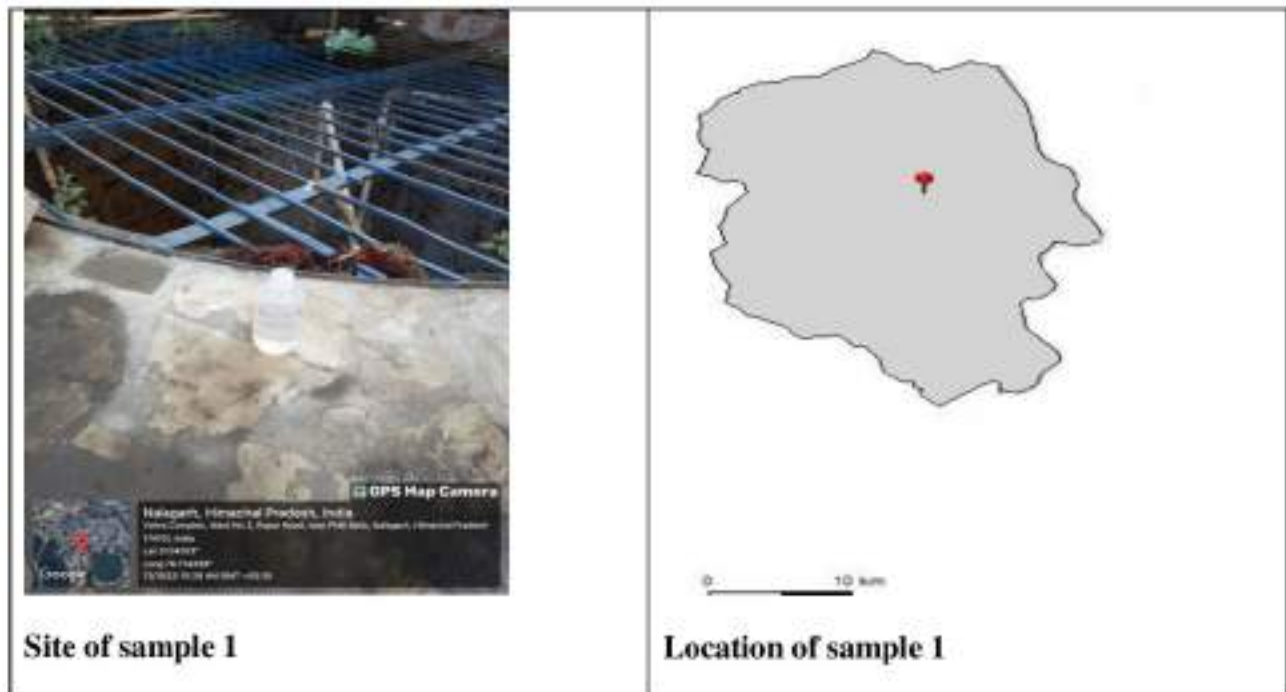
Fig. 1b:- Location of the sampling Sites.

High density polyethylene plastic bottles of 250ml were used to collect samples which were cleaned using dilute HCL (0.5N HCL) and were rinsed with deionised water before taking sample. Before collecting sample the water sources were run made to run for few minutes so that we can collect fresh water for sampling for better and accurate results. And then bottles are prewashed with source water 2-3 times before collecting sample. Samples are collected in that way so that there will be minimum or no air bubble left inside the bottles because it will affect the radon detection. Then uranium concentration in all 23 samples are measured by LED Fluorimeter and Randon concentration is measured by DurrIDGE Rad7.

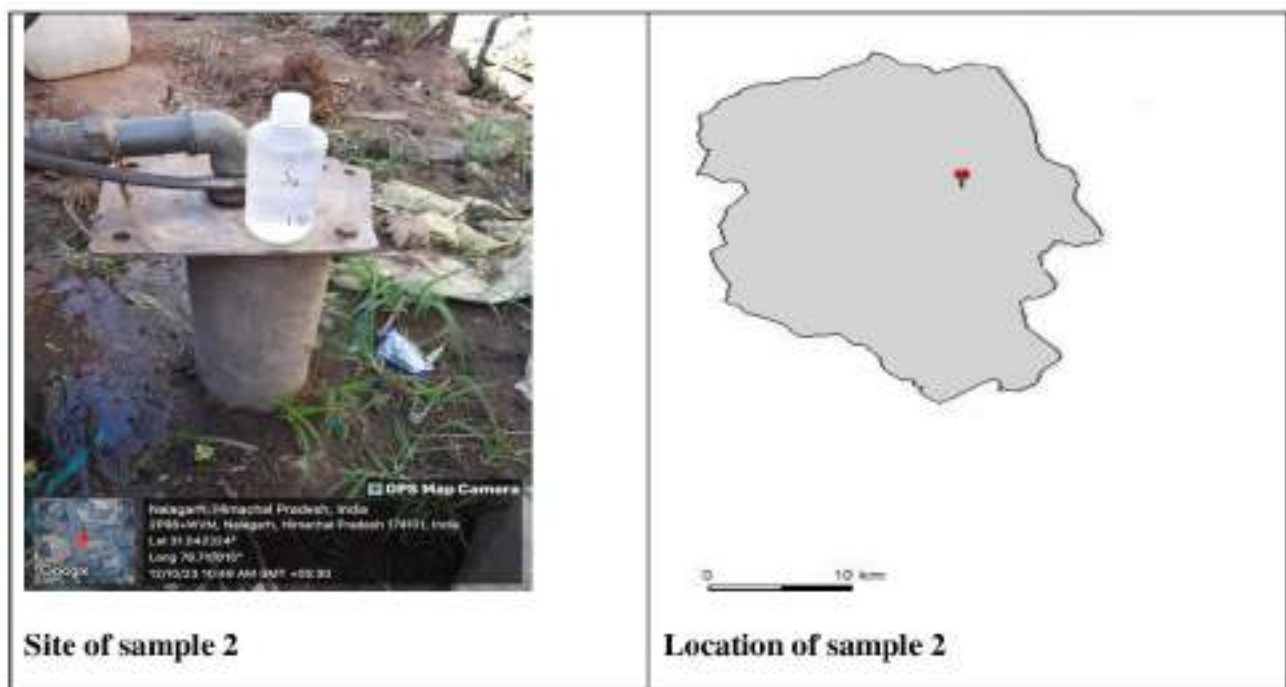


## Location and Pictures of sampling sites

### Sample 1



### Sample 2





### Sample 3



Site of Sample 3



0 10 km

Location of sample 3

### Sample 4



Location of sample 4



0 10 km

Site of sample 4

## Sample 5



Site of sample 5



0 10 km

Location of sample 5

## Sample 6



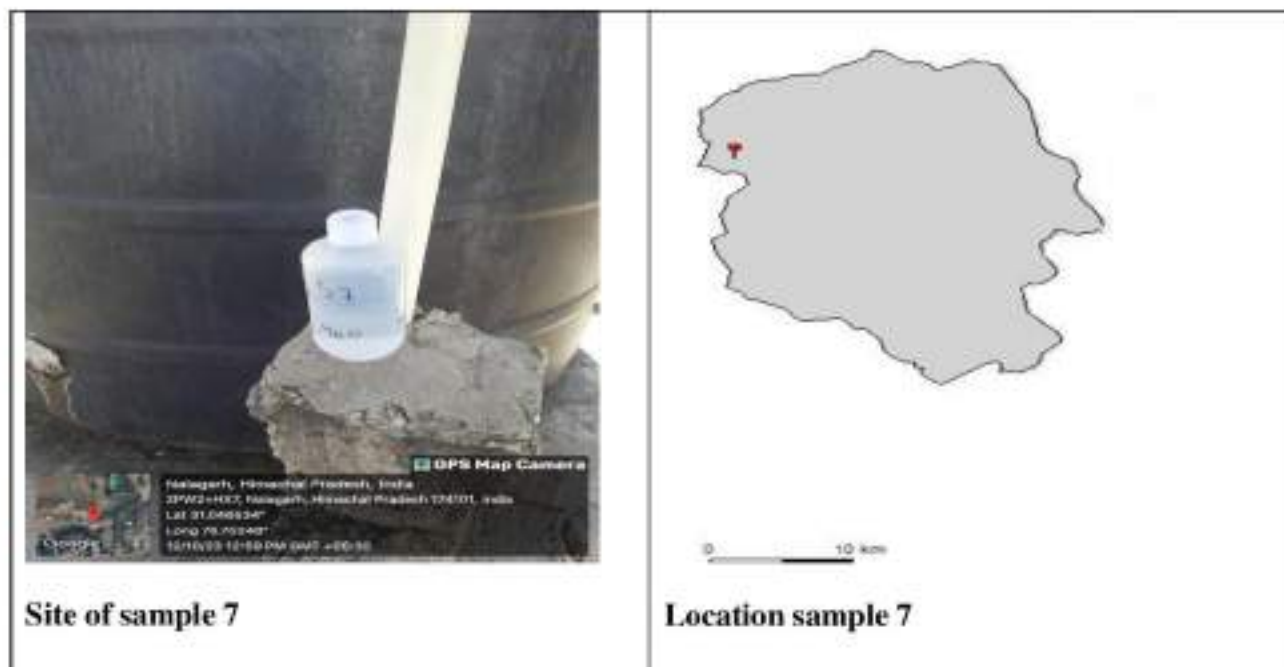
Site of sample 6



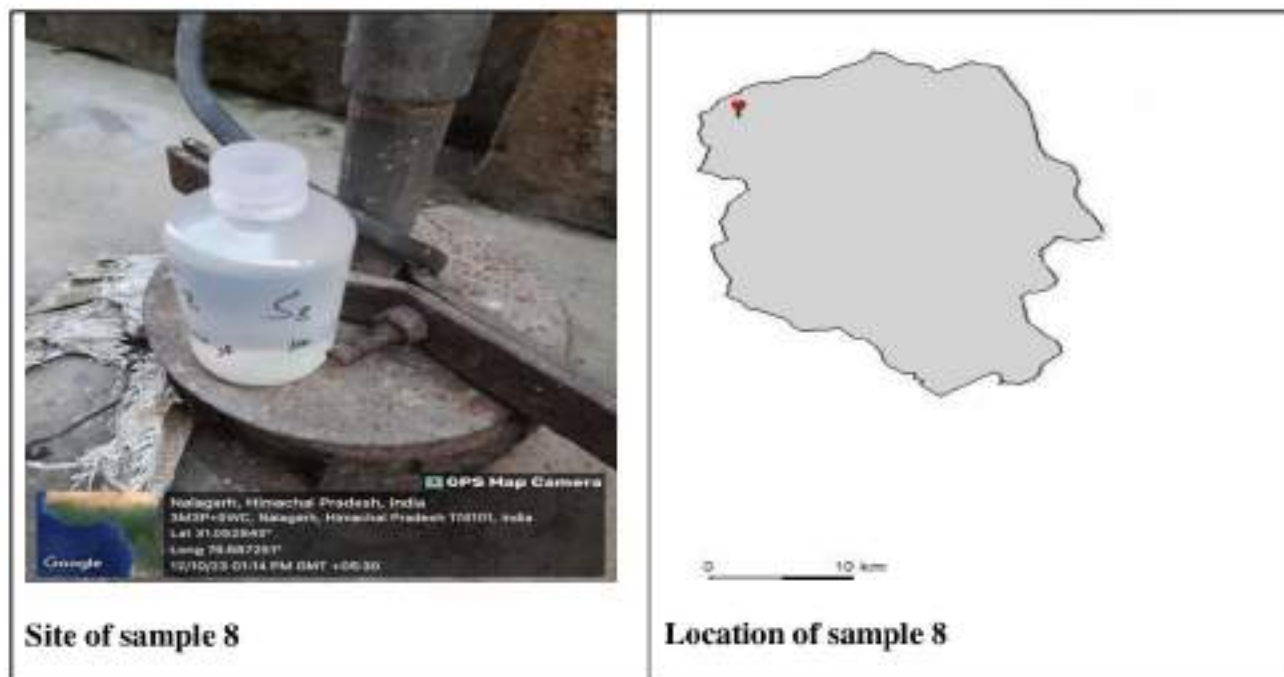
0 10 km

Site of sample 6

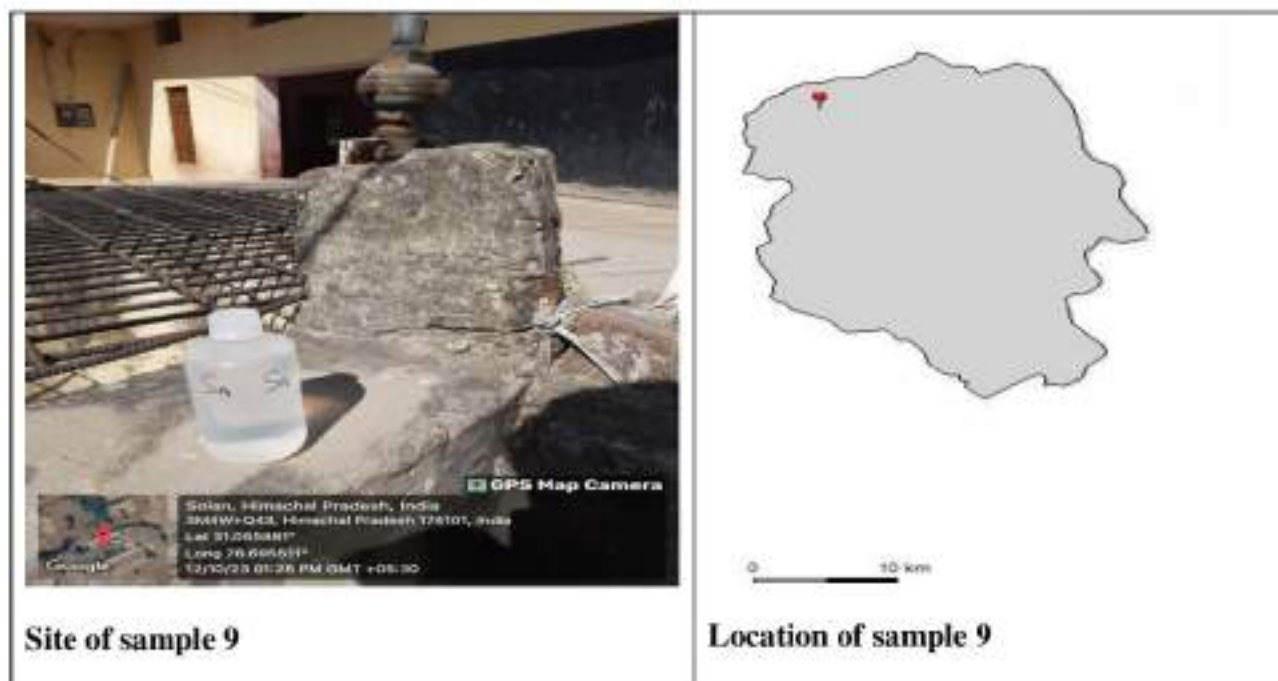
## Sample 7



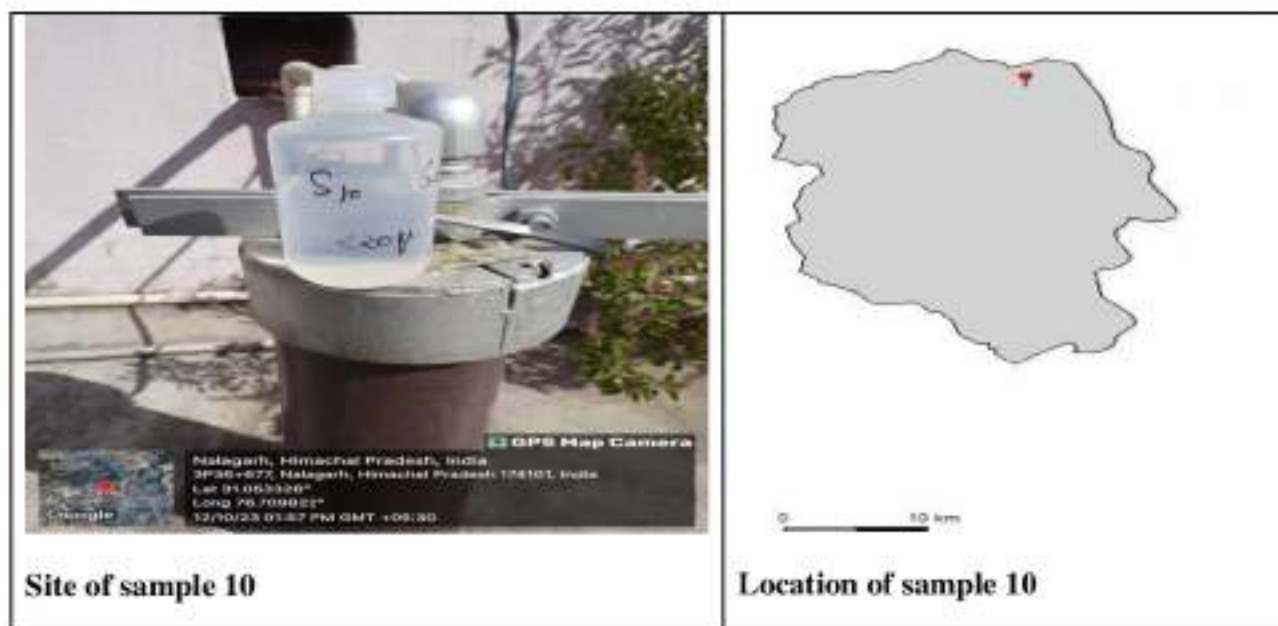
## Sample 8



## Sample 9



## Sample 10





## Sample 11



Site of sample 11



0 10 km

Location of sample 11

## Sample 12



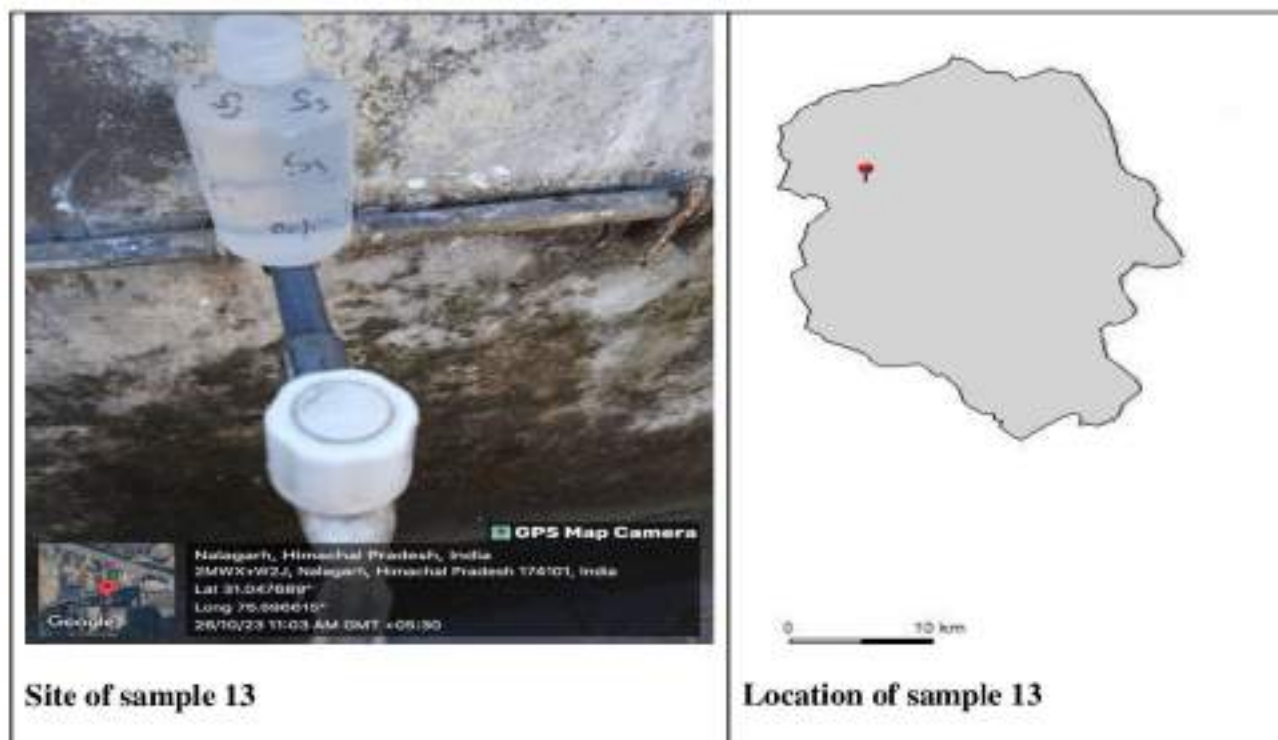
Site of sample 12



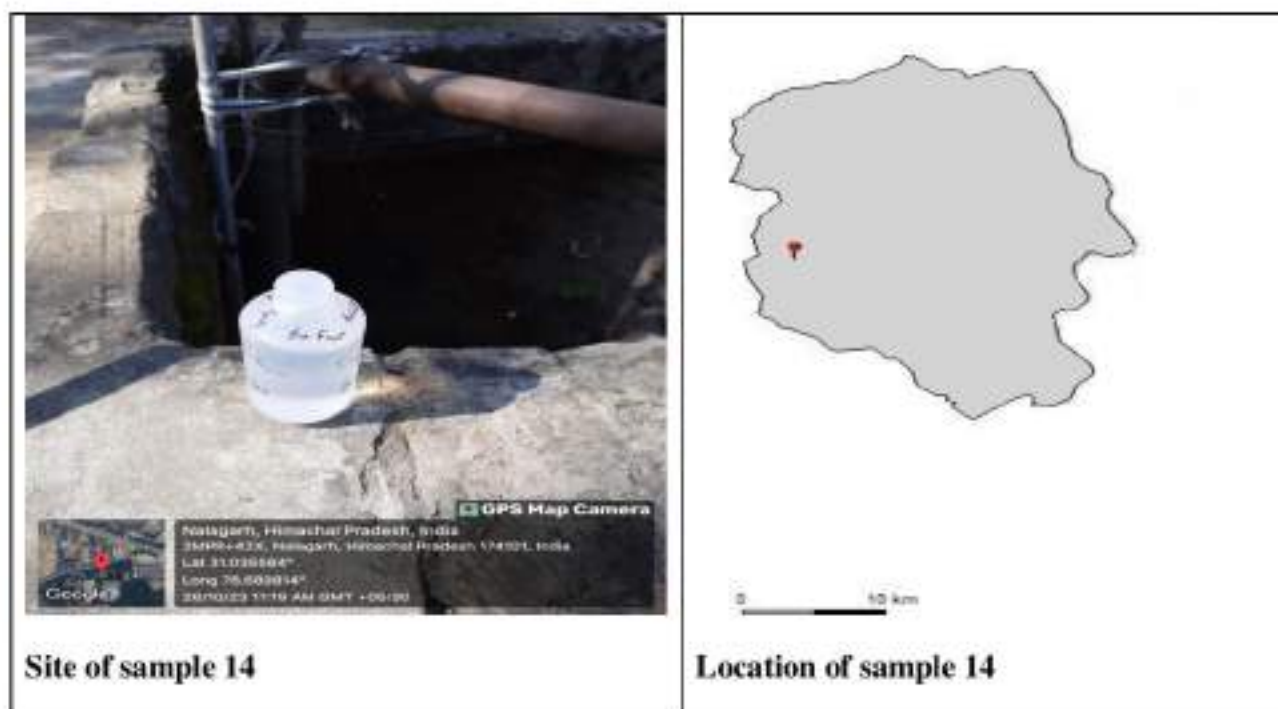
0 10 km

Location of sample 12

## Sample 13

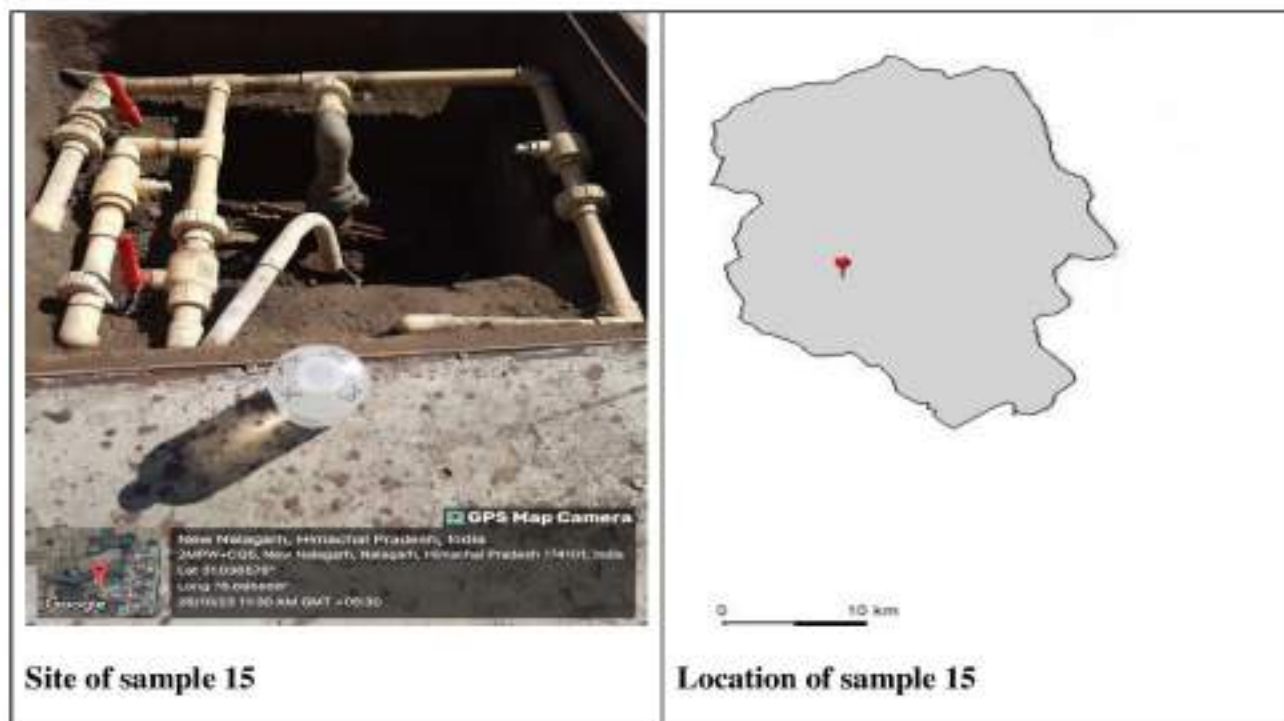


## Sample 14

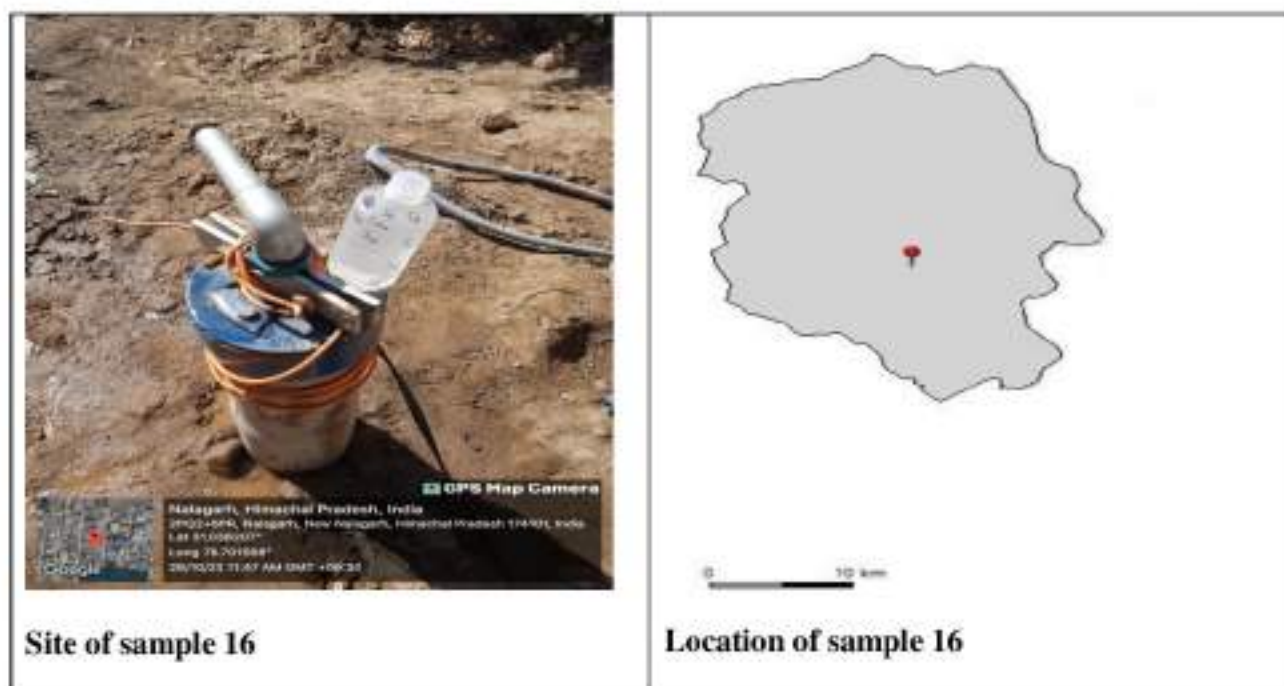




## Sample 15



## Sample 16



## Sample 17



Site of sample 17



Location of sample 17

## Sample 18

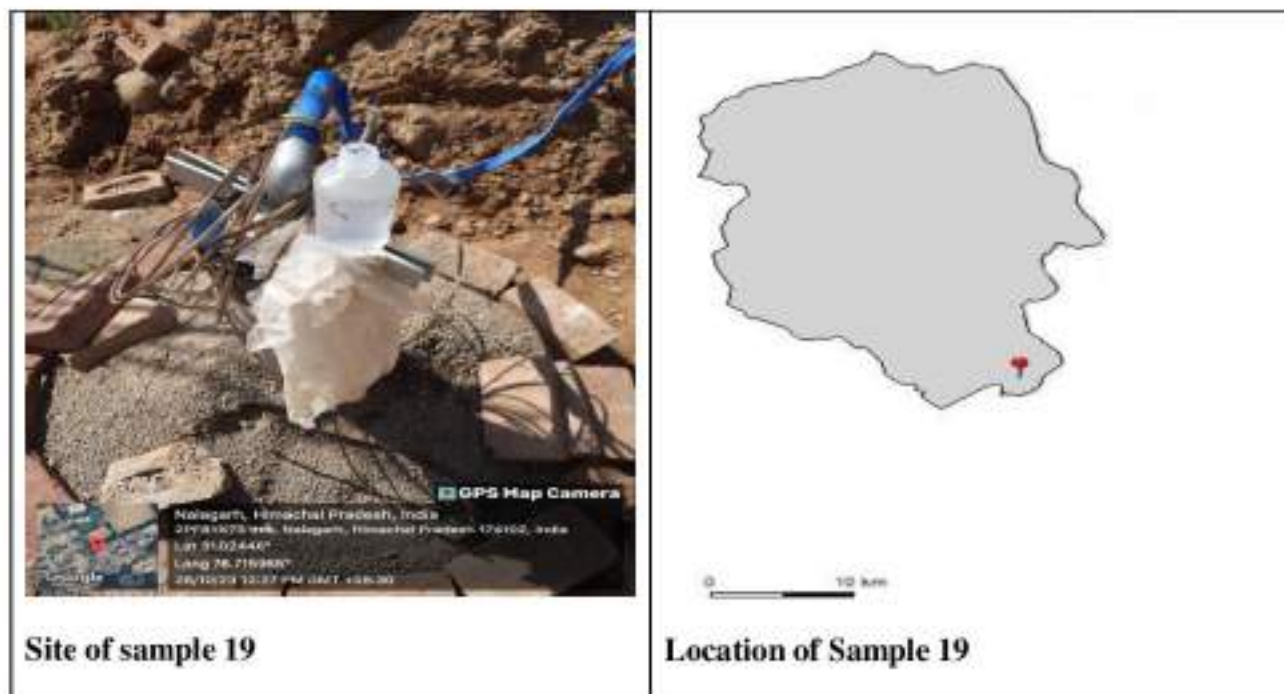


Site of sample 18



Location of sample 18

## Sample 19

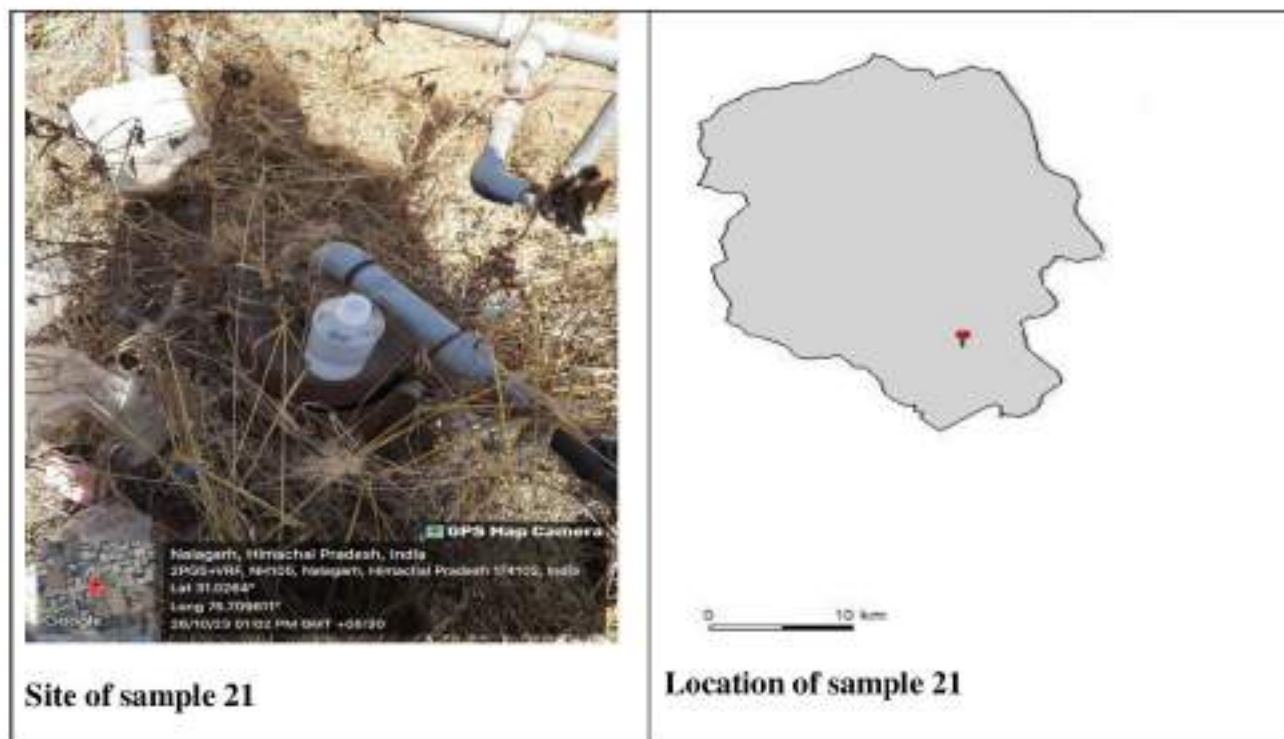


## Sample 20

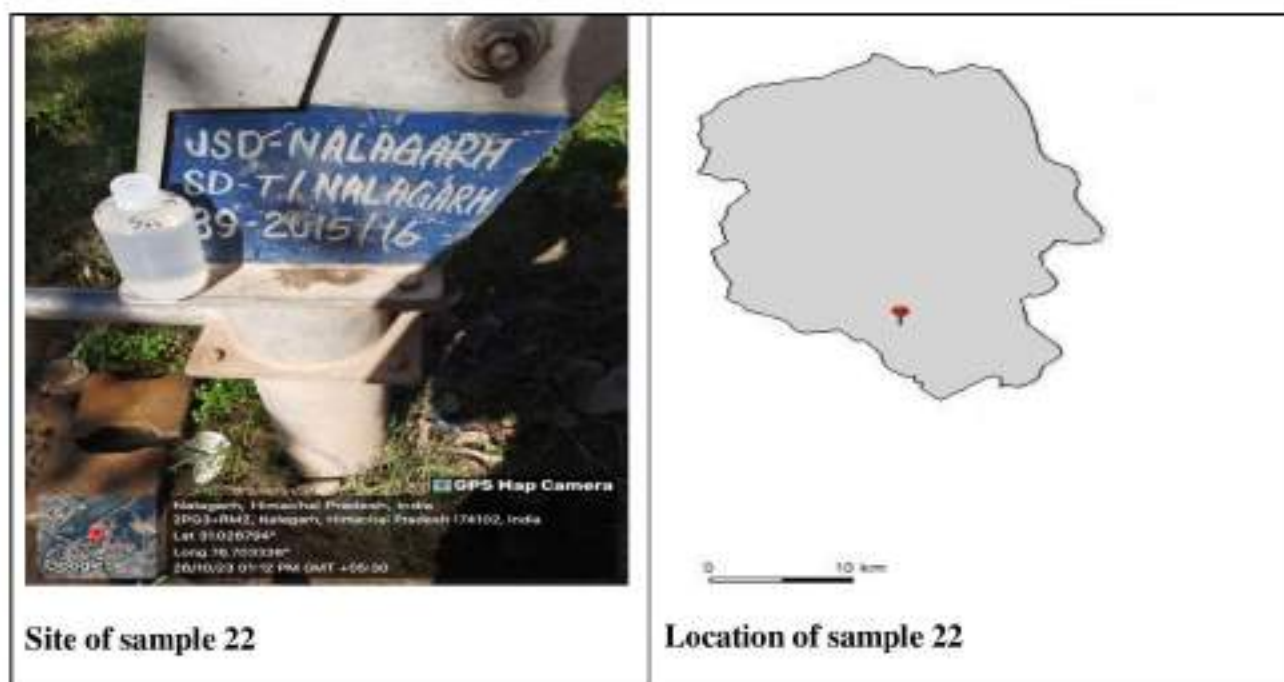




## Sample 21



## Sample 22



## Sample 23



## LED Fluorimeter

A fluorimeter is a device used to measure the fluorescence emitted by a sample when exposed to specific wavelengths of light. LED fluorimeters use light-emitting diodes (LEDs) as the light source and it is the one of the quickest, highly sensitive and most reliable device. The LED Fluorimeter is capable to measure concentration in water sample from 0.5  $\mu\text{g/L}$  to 4000  $\mu\text{g/L}$ [39] with high accuracy, block diagram of LED fluorimeter is shown in Fig. 2. The working principle involves:

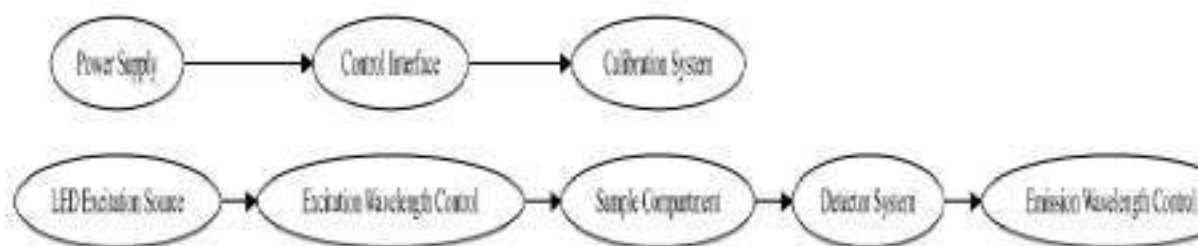


Fig. 2 Block diagram of LED fluorimeter.

**Excitation:** The LED emits light at a specific wavelength, known as the excitation wavelength. This light is directed towards the sample.

**Sample Interaction:** The sample absorbs the excitation light and then re-emits light at a longer wavelength, known as the emission wavelength. This phenomenon is called fluorescence.

**Detection:** A photodetector in the fluorimeter detects the emitted fluorescence. The intensity of the fluorescence is proportional to the concentration of the fluorescent substance in the sample.

**Signal Processing:** The detected fluorescence signal is processed and often displayed as a numerical value or a fluorescence spectrum

All the samples are first filtered through a filter paper of 45  $\mu\text{m}$ . Then pH of the water is measured by using a pH meter by Hanna instruments. We have three available specific modes in the device by which Uranium concentration can be measured first one is standard calibration mode, calibration mode and uncalibrated mode. And we are Utilizing the uncalibrated mode for measurement, we have employed the method specified by BARC in this study. The significant advantage of this approach lies in its ability to enhance the accuracy of uranium concentration measurements. Initially, the fluorescence of a background solution, composed of 5.0 mL of distilled water and 0.5 mL of buffer solution, is determined. Subsequently, the fluorescence of the sample solution (consisting of 5.0 mL of the sample and 0.5 mL of buffer solution) is recorded. Following this, increments of 50  $\mu\text{L}$  of a 500 ppb standard uranium solution are then added, and we get the corresponding counts of each stage for all 23 samples.



## Rad7

RAD7 H2O is a special attachment of RAD7 used for the measurement of radon concentration in water. The range of the Rad7 lies between 10 pCi/l to 4105 pCi/l [40], with a lower limit of detection below, 10 pCi/l. This portable and battery-operated equipment ensures expeditious measurements. The schematic diagram of RAD H2O is illustrated in Figure 3. Post a 20 minutes analysis, RAD H2O delivers results with sensitivity matching or surpassing that of liquid scintillation methods. Employing a closed-loop aeration scheme, RAD H2O maintains constant air and water volumes independent of the flow rate. The system achieves equilibrium

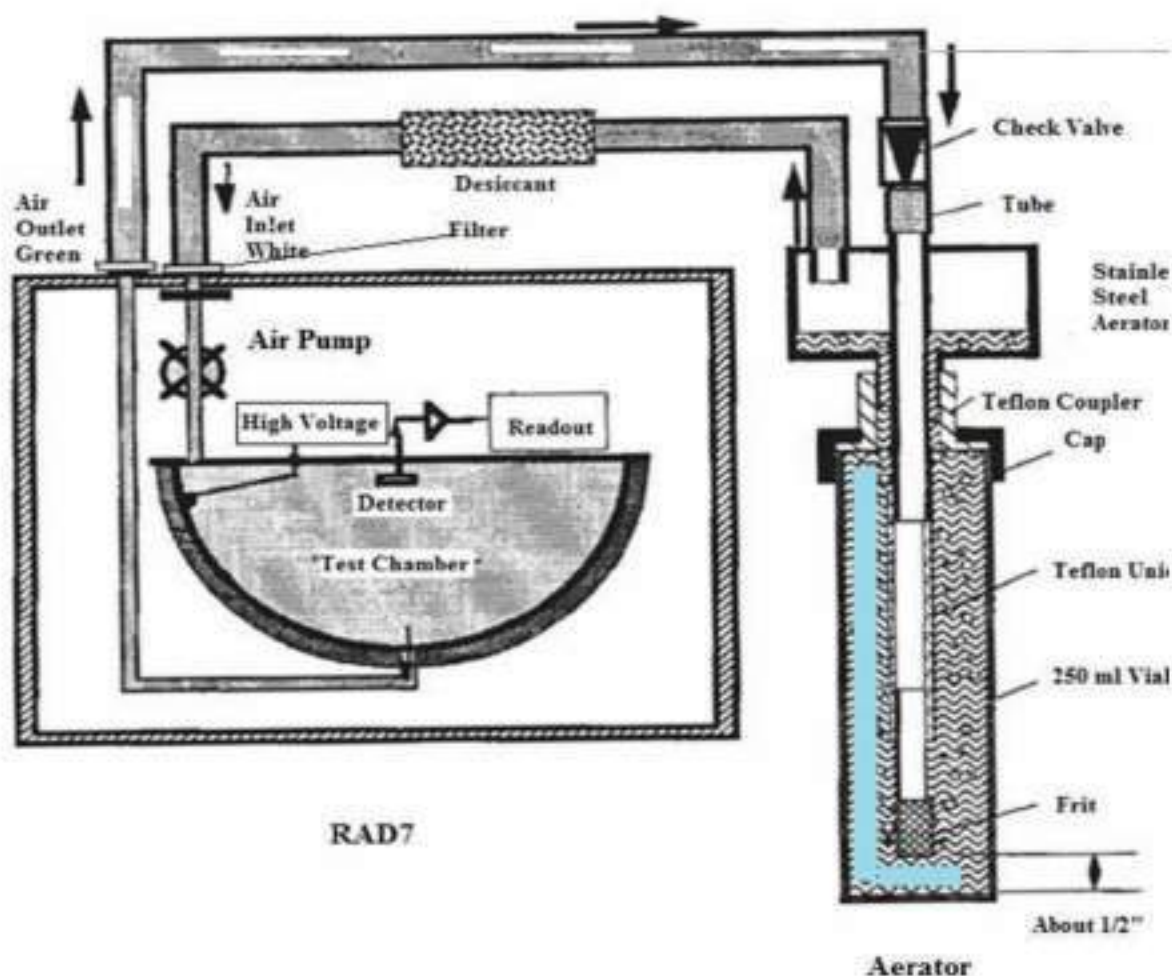


Fig. 3 Schematic diagram of RAD7-H2O [40]

within approximately 5 minutes, ceasing radon extraction thereafter. The extraction efficiency, representing the percentage of radon removed from the water to the air loop, is notably high at  $\approx 94\%$  for a 250ml sample. While the extraction efficiency may slightly vary with ambient temperature, it consistently exceeds 90%. The RAD7 detector transforms alpha radiation into an electric signal directly, possessing the capability to differentiate between aged and fresh radon, as well as radon emanating from thoron.

## Results and discussion

The results of uranium and radon analysis in water samples of the study are presented in Table 1. The values of uranium in all 23 samples were in the range  $1.65 \pm 0.26 \mu\text{g/L}$  to  $16.98 \pm 0.65 \mu\text{g/L}$  and the values of Radon were in the range  $2.64 \pm 0.4 \text{ Bq/L}$  to  $24.01 \pm 4.71 \text{ Bq/L}$  with an average value of Uranium is  $7.334 \pm 0.291 \mu\text{g/L}$  and average value of Radon is  $8.63 \pm 1.72 \text{ Bq/L}$  and when the values of Uranium concentration is compared with the allowed MCL proposed by WHO[23], we observed that 95% of the samples were below the value proposed by WHO[23] and only 5% of samples were higher than that of the value proposed by WHO[23]. The MCL value suggested by USEPA[11] is  $30 \mu\text{g/L}$  and values of all the samples was below than this value (suggested by USEPA). When the Radon concentration value is compared with value suggested by WHO[23] that is  $11 \text{ Bq/L}$  we found that approx. 74% of the samples were below the MCL value and the values of 16% of the samples higher then value suggested by WHO[23] and UNSCEAR[24] suggested the concentration value between  $4\text{--}40 \text{ Bq/L}$  when compared to this value 100% of the samples were below the suggested value. The Radon concentration values are when compared with European Commission recommendations for the protection of living beings against Radon exposure in drinking water supply (2001/928/Euratom)[41] which suggests the action level of  $100 \text{ Bq/L}$  for drinking water supply. The Radon concentration levels in some areas of Northern Rajasthan is  $0.5 \pm 0.3 \text{ Bq/L}$  to  $85.7 \pm 4.9 \text{ Bq/L}$  with an average of  $9.03 \pm 1.03 \text{ Bq/L}$  which is reported by Rohit Mehra[35]. The Radon concentration in samples of Bathinda and Gurdaspur districts, Punjab lies between  $0.2 \pm 8.8 \text{ Bq/L}$  reported by Walia, V[42]. The average Uranium concentration in tube wells of Patiala District, Punjab, India is  $31.1987 \mu\text{g/L}$  reported by Vimal Mehta[34].

Table 1. Values of Uranium and Radon of all 23 samples collected from Nalagarh

Sr. No.	Locations	Latitude	Longitude	pH	Source	Depth (ft)	Uranium conc. ( $\mu\text{g/L}$ )	Radon conc. ( $\text{Bq/L}$ )
S1	Nalagarh 4	31°02'35.3"N	76°42'52.0"E	7.2	OW	50	1.65±0.26	3.03±1.46
S2	Nalagarh 3	31°02'32.4"N	76°43'01.3"E	7.1	SP	170	10.1±0.12	8.88±1.08
S3	Nalagarh 5	31°02'31.3"N	76°43'27.2"E	7.5	SW	500	2.06±0.22	10.34±1.99
S4	New Nalagarh 1	31°02'32.4"N	76°42'03.1"E	6.8	OW	100	8.77±1.01	11.41±0.11
S5	New Nalagarh 3	31°02'34.0"N	76°41'52.9"E	7.4	SP	170	1.11±0.51	12.19±3.85
S6	New Nalagarh 2	31°02'31.1"N	76°41'37.9"E	6.5	SP	200	13.5±0.44	13.47±3.01
S7	Nalagarhh 2	31°02'47.5"N	76°42'08.9"E	6.9	SP	400	8.48±0.40	7.48±0.87
S8	Nalagarh 1	31°03'10.2"N	76°41'14.1"E	6.7	SP	100	12.41±0.61	9.57±0.58
S9	Nalagarh 6	31°02'31.3"N	76°43'27.2"E	6.8	OW	65	12.66±0.39	11.46±1.34
S10	Sabhowal	31°03'12.0"N	76°42'35.4"E	6.3	SP	220	16.98±0.65	24.01±4.71
S11	Salhewal	31°02'55.9"N	76°42'25.5"E	8	OW	80	7.82±0.13	9.78±4.38
S12	Nalagarh	31°02'47.1"N	76°42'13.1"E	7.8	SP	250	4.56±0.21	16.49±3.2
S13	Nalagarh	31°02'51.7"N	76°41'47.8"E	7.3	SP	120	9.23±0.08	5.7±1.44
S14	Nalagarh	31°02'08.1"N	76°41'23.3"E	7.5	OW	100	5.67±0.18	9.53±2.25
S15	New Nalagarh	31°02'11.7"N	76°41'45.1"E	7.2	SP	300	8.34±0.24	2.75±0.92
S16	Nalagarh	31°02'17.6"N	76°42'05.6"E	7.9	SP	350	3.78±0.11	4.17±1.01
S17	Nalagarh	31°02'10.0"N	76°42'31.2"E	7.7	SP	200	6.45±0.2	4.06±0.82
S18	Nalagarh	31°01'35.9"	76°42'41.8"E	8.2	OW	100	2.89±0.09	2.64±0.4
S19	Nalagarh	31°01'28.1"N	76°42'57.5"E	7.4	SP	200	9.01±0.14	6.97±0.7
S20	Nalagarh	31°01'25.4"N	76°42'25.9"E	7.6	OW	60	4.12±0.23	5.41±0.88
S21	Nalagarh	31°01'35.0"N	76°42'36.6"E	7.5	SP	120	6.89±0.1	5.75±1.48
S22	Nalagarh	31°01'36.5"N	76°42'12.0"E	8.2	HP	70	3.45±0.17	7.74±1.73
S23	Nalagarh	31°01'47.2"N	76°41'51.6"E	7.3	SP	140	8.76±0.22	5.68±1.41

\*OW=Open well, SP= Submersible motor pump, SW=Surface water, HP= Hand-pump

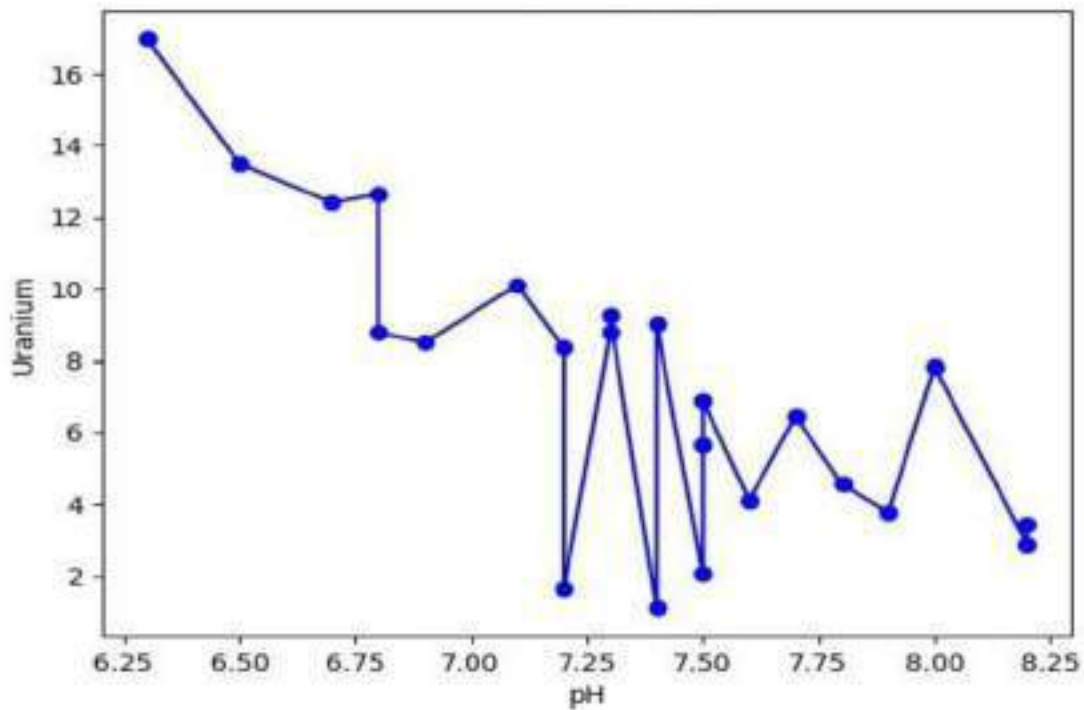


Fig. 4 Uranium concentration variation with pH of the collected samples, units for Uranium concentration in µg/L

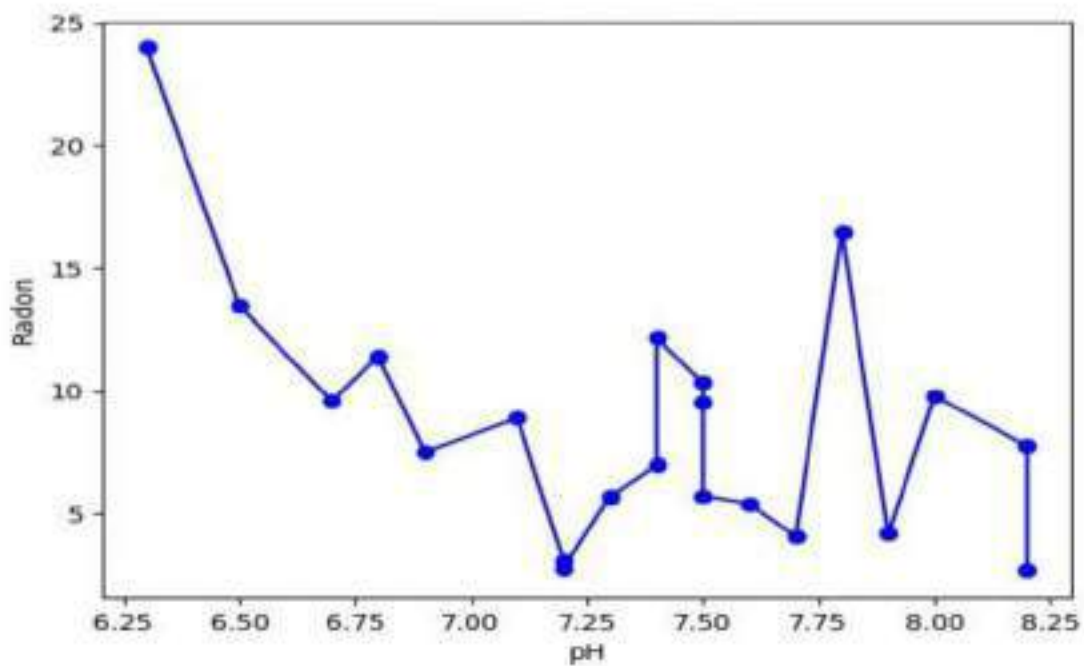


Fig. 5 Radon concentration variation with pH of collected samples, units of Radon concentration in Bq/L

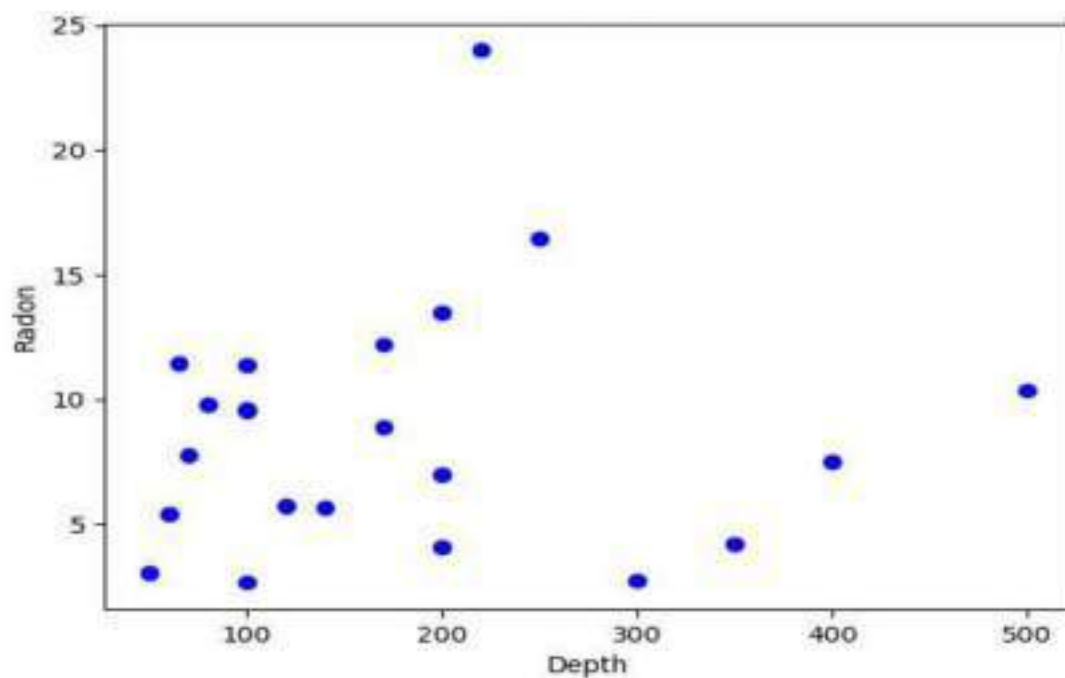


Fig. 6 Radon concentration Variation with Depth of the source, units of Radon concentration in Bq/L

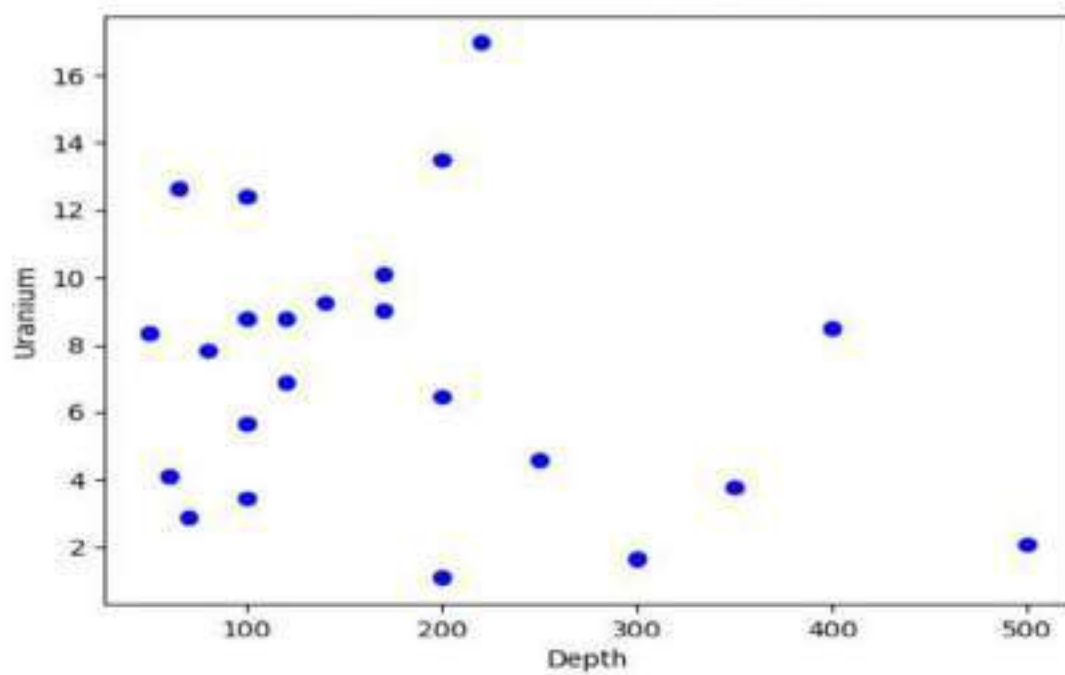


Fig. 7 Uranium concentration variation with depth of the source, , units for Uranium concentration in  $\mu\text{g/L}$



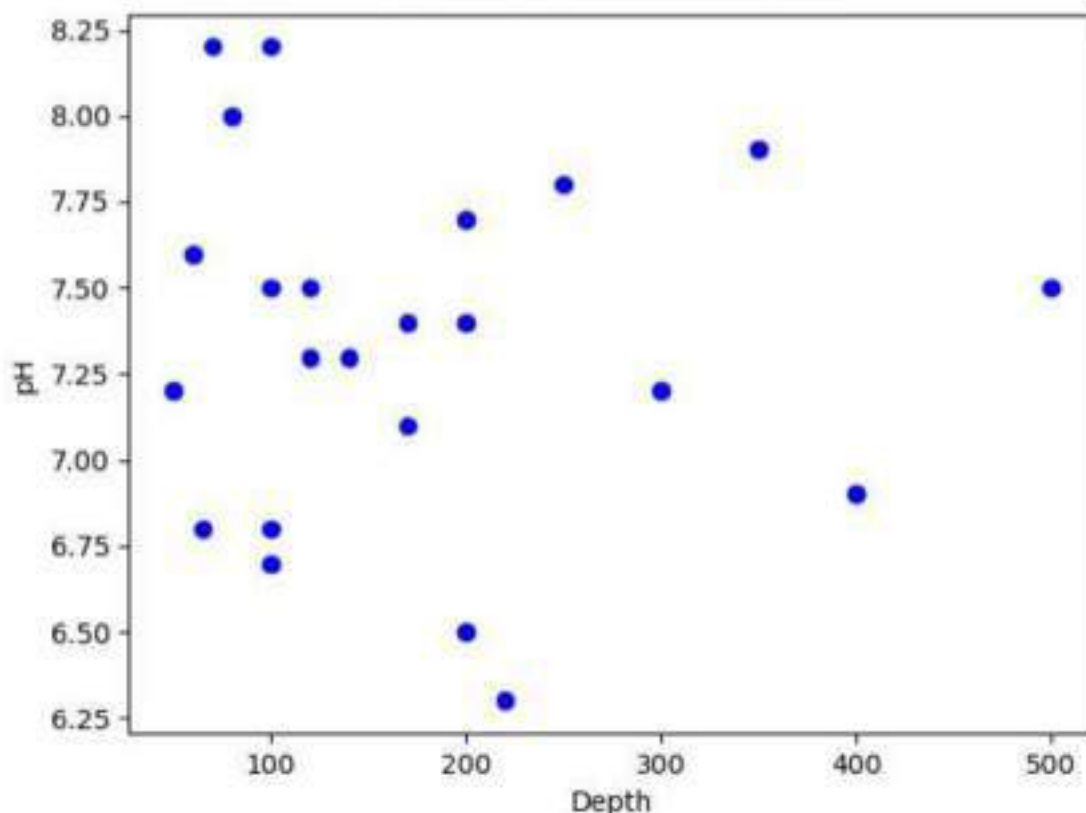


Fig. 8 pH variation with depth of the source, Units of depth in Feet (ft)

## Conclusion

Uranium concentration in all 23 samples were in the range  $1.65 \pm 0.26 \mu\text{g/L}$  to  $16.98 \pm 0.65 \mu\text{g/L}$  and the values of Radon were in the range  $2.64 \pm 0.4 \text{ Bq/L}$  to  $24.01 \pm 4.71 \text{ Bq/L}$  with an average value of Uranium is  $7.334 \pm 0.291 \mu\text{g/L}$  and average value of Radon is  $8.63 \pm 1.72 \text{ Bq/L}$ . In Uranium concentration 95% of sample values are below than suggested value by and 5% were above than that. And according to USEPA suggested value all the 100% of sample values are below then the suggested value. The Radon concentration in all the samples were 74% under suggested value by the WHO and 16% were above than that and acc to UNSCEAR suggested value all the 100% of sample values are under MCL suggested by organisation.

## Acknowledgement

The authors extend heartfelt gratitude to the residents of Nalagarh for their invaluable cooperation during the field work. Special thanks are due to the Department of Physics at SGTB Khalsa College, Sri Anandpur Sahib, for providing essential resources and support. The authors acknowledge the guidance and support received from the Head of Department, Dr. Randev Sandhu, as well as the invaluable mentorship of the Supervisor, Dr. Vimal Mehta, and Professor Amandeep Kaur, which greatly contributed to the success of this research paper.



## References

1. Tissot, F. L., & Dauphas, N. (2015). Uranium isotopic compositions of the crust and ocean: Age corrections, U budget and global extent of modern anoxia. *Geochimica et Cosmochimica Acta*, 167, 113-143.
2. Carvalho, F. P., Fesenko, S., Harbottle, A. R., Lavrova, T., Mitchell, N. G., Payne, T. E., ... & Yankovich, T. L. (2023). The environmental behaviour of uranium.
3. Nolan, J., & Weber, K. A. (2015). Natural uranium contamination in major US aquifers linked to nitrate. *Environmental Science & Technology Letters*, 2(8), 215-220.
4. Deng, C., Liang, J., Sun, R., Wang, Y., Fu, P. X., Wang, B. W., ... & Huang, W. (2023). Accessing five oxidation states of uranium in a retained ligand framework. *Nature Communications*, 14(1), 4657.
5. Chevreux, P., Tissandier, L., Laplace, A., Vitova, T., Bahl, S., Le Guyadec, F., & Deloule, E. (2021). Uranium solubility and speciation in reductive soda-lime aluminosilicate glass melts. *Journal of Nuclear Materials*, 544, 152666.
6. Smedley, P. L., & Kinniburgh, D. G. (2023). Uranium in natural waters and the environment: Distribution, speciation and impact. *Applied Geochemistry*, 148, 105534.
7. Gómez, P., Garralón, A., Buil, B., Turrero, M. J., Sánchez, L., & De la Cruz, B. (2006). Modeling of geochemical processes related to uranium mobilization in the groundwater of a uranium mine. *Science of the Total Environment*, 366(1), 295-309.
8. Sharma, D. A., Keesari, T., Pant, D., Rishi, M. S., Sangwan, P., Thakur, N., & Sinha, U. K. (2022). Appraising the factors favouring uranium mobilization and associated health risk assessment in groundwaters of north-western India. *Ecotoxicology and Environmental Safety*, 229, 113086.
9. Zamora, M. L., Tracy, B. L., Zielinski, J. M., Meyerhof, D. P., & Moss, M. A. (1998). Chronic ingestion of uranium in drinking water: a study of kidney bioeffects in humans. *Toxicological Sciences*, 43(1), 68-77.
10. Zhang, L., Chu, J., Xia, B., Xiong, Z., Zhang, S., & Tang, W. (2022). Health effects of particulate uranium exposure. *Toxics*, 10(10), 575.
11. USEPA. (2000) National Primary Drinking Water Regulations; Radionuclides; Final Rule. *Fed Reg.* 65(236), 76708
12. Nunes, L. J., Curado, A., & Lopes, S. I. (2023). The Relationship between Radon and Geology: Sources, Transport and Indoor Accumulation. *Applied Sciences*, 13(13), 7460.

13. Monnin, M., & Seidel, J. L. (2002). Radon concentrations in karstic aquifers. *Geofísica Internacional*, 41(3), 265-270.
14. Sicilia, I., Aparicio, S., González, M., Anaya, J. J., & Frutos, B. (2022). Radon transport, accumulation patterns, and mitigation techniques applied to closed spaces. *Atmosphere*, 13(10), 1692.
15. Feng, X., Zhong, J., Yan, R., Zhou, Z., Tian, L., Zhao, J., & Yuan, Z. (2022). Groundwater radon precursor anomalies identification by EMD-LSTM model. *Water*, 14(1), 69.
16. Malvicini, A., ESPOSITO, P., & Depiesse, D. (2004). Influence of hydrogeological properties of rocky substratum, ventilation and meteorological conditions on environmental radioactivity in underground galleries. In *Proceedings of the 11th International Congress of the International Radiation Protection Association*, Madrid.
17. Ye, Y. J., Xia, X. Q., Dai, X. T., Huang, C. H., & Guo, Q. (2019). Effects of temperature, salinity, and pH on <sup>222</sup>Rn solubility in water. *Journal of Radioanalytical and Nuclear Chemistry*, 320, 369-375.
18. Veeger, A. I., & Ruderman, N. C. (1998). Hydrogeologic controls on radon-222 in a buried valley-fractured bedrock aquifer system. *Groundwater*, 36(4), 596-604.
19. Lupulescu, A., Baciuc, C., Dicu, T., Burghel, B. D., & Cucos, A. L. (2023). Determining the Geogenic Radon Potential in Different Layouts and Numbers of Points. *Atmosphere*, 14(4), 713.
20. Kang, J. K., Seo, S., & Jin, Y. W. (2019). Health effects of radon exposure. *Yonsei medical journal*, 60(7), 597-603.
21. Riudavets, M., Garcia de Herreros, M., Besse, B., & Mezquita, L. (2022). Radon and lung cancer: current trends and future perspectives. *Cancers*, 14(13), 3142.
22. United States Environmental Protection Agency. Radon in drinking water, Factsheet. EPA 815-F-99007. USEPA (1999)
23. WHO, 2003. Guidelines for Drinking Water Quality. Health Criteria and Other Supporting Information. World Health Organization (2003).
24. United Nations Scientific Committee on the effect of Atomic Radiation. The general assembly with scientific annex, United Nation. UNSCEAR (2000).

25. Ma, M., Wang, R., Xu, L., Xu, M., & Liu, S. (2020). Emerging health risks and underlying toxicological mechanisms of uranium contamination: Lessons from the past two decades. *Environment international*, 145, 106107.
26. Rani, A., & Singh, S. (2006). Analysis of uranium in drinking water samples using laser induced fluorimetry. *Health physics*, 91(2), 101-107.
27. Singh, P., Singh, P., Sahoo, B. K., & Bajwa, B. S. (2016). A study on uranium and radon levels in drinking water sources of a mineralized zone of Himachal Pradesh, India. *Journal of Radioanalytical and Nuclear Chemistry*, 309, 541-549.
28. Nandakumaran, P., & Vinayachandran, N. (2020). A preliminary appraisal of radon concentration in groundwater from the high background radiation area (HBRA) of Coastal Kerala. *Journal of the Geological Society of India*, 95, 491-496.
29. Kumar, M., Kaushal, A., Sahoo, B. K., Sarin, A., Mehra, R., Jakhu, R., ... & Sharma, N. (2019). Measurement of uranium and radon concentration in drinking water samples and assessment of ingestion dose to local population in Jalandhar district of Punjab, India. *Indoor and Built Environment*, 28(5), 611-618.
30. Rani, S., Kansal, S., Singla, A. K., & Mehra, R. (2021). Radiological risk assessment to the public due to the presence of radon in water of Barnala district, Punjab, India. *Environmental Geochemistry and Health*, 43(12), 5011-5024.
31. Panghal, A., Kumar, A., Kumar, S., Singh, J., Sharma, S., Singh, P., ... & Bajwa, B. S. (2017). Radiation dose-dependent risk on individuals due to ingestion of uranium and radon concentration in drinking water samples of four districts of Haryana, India. *Radiation effects and defects in solids*, 172(5-6), 441-455.
32. Kumar, A., Arora, T., Singh, P., Singh, K., Singh, D., Pathak, P. P., & Ramola, R. C. (2021). Quantification of radiological dose and chemical toxicity due to radon and uranium in drinking water in Bageshwar region of Indian Himalaya. *Groundwater for Sustainable Development*, 12, 10049.
33. Kaur, M., Kumar, A., Mehra, R., & Mishra, R. (2019). Age-dependent ingestion and inhalation doses due to intake of uranium and radon in water samples of Shiwalik Himalayas of Jammu and Kashmir, India. *Environmental monitoring and assessment*, 191, 1-17.

34. Mehta, V., Kapil, C., Shikha, D., & Kanse, S. (2023). Appraisal of age-dependent radiological risk caused by ingestion of uranium in groundwater of Patiala district, Punjab. *Journal of Radioanalytical and Nuclear Chemistry*, 1-11.
35. Rani, A., Mehra, R., & Duggal, V. (2013). Radon monitoring in groundwater samples from some areas of Northern Rajasthan, India, using a RAD7 detector. *Radiation protection dosimetry*, 153(4), 496-501.
36. Balaram, V., Rani, A., & Rathore, D. P. S. (2022). Uranium in groundwater in parts of India and world: A comprehensive review of sources, impact to the environment and human health, analytical techniques, and mitigation technologies. *Geosystems and Geoenvironment*, 1(2), 100043.
37. Mehta, V., Kaur, J., Shikha, D., & Kanse, S. (2023). Age-dependent ingestion doses to the public of Rupnagar and Una regions of India due to intake of uranium. *Journal of Radioanalytical and Nuclear Chemistry*, 1-15.
38. Shaurabh Anand, Srinivas Vaidyanathan, Sindhu Radhakrishna The Role of Landscape Structure in Primate Crop Feeding: Insights from Rhesus Macaques (*Macaca mulatta*) in Northern India (2021)
39. Mehra, R., Gupta, D., & Jakhu, R. (2017). Risk assessment for natural uranium present in ground water of Mahendragarh district of Haryana. *J. Radiat. Nucl. Appl*, 2, 67-73.
40. DURRIDGE Radon Instrumentation. RAD H2O User Manual, Radon in Water Accessory. DURRIDGE Company (2011)
41. European Commission. Commission directive of defining requirements for the parameters for radioactivity for monitoring the quality of water for the Council Directive 98/83 of 3 November 1998 on the quality of water intended for human consumption. Draft V3.029/11/2005.
42. Virk, H. S., Walia, V., & Bajwa, B. S. (2001). Radon monitoring in underground water of Gurdaspur and Bathinda districts of Punjab, India.

# **Synthesis and characterization of lead Selenide Thin Film & Powder**

## **PROJECT REPORT**

*Submitted in partial fulfillment of the  
requirements for the award of the degree of*

### **MASTER OF SCIENCE**

**In**

**PHYSICS**

**By**

**Shruti Pathak  
(Reg. No.8114-19-515)**



**DEPARTMENT OF PHYSICS  
SRI GURU TEG BAHADUR KHALSA COLLEGE, SRI ANANDPUR SAHIB  
(An Autonomous College)  
ANANDPUR SAHIB- 140118, PUNJAB (INDIA)**





SRI GURU TEG BAHADUR KHALSA COLLEGE, SRI ANANDPUR SAHIB  
(An Autonomous College)  
ANANDPUR SAHIB-140118. PUNJAB (INDIA)

## CERTIFICATE

It is certified that the work contained in the project report entitled "**SYNTHESIS AND CHARACTERIZATION OF LEAD SELENIDE (PbSe) THIN FILM AND POWDER**" is an original contribution by me and has not been submitted in part or full for any other degree at this or other University/Institute.

The assistance and help received during the course of the thesis work have been acknowledged.

**Shruti Pathak**

**Reg. No. 8114-19-515**

I, the undersigned, Supervisor of **Shruti Pathak, Regn. No.8114-19-515**, a candidate for the degree of Master of Science, agree that the project report entitled, "**Synthesis and characterization of lead Selenide (PbSe) thin Film**", may be submitted in partial fulfillment of the requirements for the award of degree.

This is to certify that the above statement made by the candidate is correct to the best of my knowledge.

**Dr. Deep Shikha**

Assistant Professor

Department of Physics

Sri Guru Teg Bahadur Khalsa College

Sri Anandpur Sahib



## CERTIFICATE

This is certify that the "Project Report" entitled "**SYNTHESIS AND CHARCTERIZATION OF LEAD SELENIDE (PbSe) THIN FILM AND POWDER**" submitted by Shruti Pathak, (Regn. No. 8114-19-515) to Department of Physics, Sri Guru Teg Bahadur Khalsa College, Sri Anandpur Sahib in partial fullfillment of the requirements for the award of degree of MASTER OF SCIENCE IN PHYSICS and has been approved by the Department Research Committee (DRC) after the viva voice examination of the candidate.



Dr. Deep Shikha  
Supervisor



Dr. Randev Singh  
Chairman (DRC)

## ACKNOWLEDGEMENT

*First of all, I would like to thank Almighty for giving me opportunity and guidance to achieve my goals then I would like to acknowledge my parents for their unwavering support and understanding during the course of this project, their motivation and belief in my abilities have been a constant source of inspiration.*

*I wish to thank the Principal **Dr. Jasvir Singh** of my college for permitting me to use all the facilities available in the institution for my project work. I would like to thank to Head of the Physics Department **Dr. Randev Singh**, the teacher faculty for their support in completing the work successfully.*

*I am grateful to my Guide **Dr. Deep Shikha** for her encouragement, guidance and supervision of my project work during the semester. I'm extremely grateful for her motivating discussions while enable me to accomplish this task successfully. Without her active guidance, support and encouragement I would not have made headway in this project.*

*A special thanks to Prof. Kajal assistant professor at Sri Guru Teg Bahadur Khalsa College Sri Anandpur Sahib for the help and her valuable suggestions whenever I needed out of her busy schedule. I'm also thankful to my classmates and my friends who was directly or indirectly helped me to complete this project report.*

*Shruti Pathak*

**Shruti Pathak**

## CONTENT

S. No.	Title	Page No.
1.	Abstract	7
2.	Introduction	8-9
3.	Thin Film Deposition	9-17
3.1	Thin film	9-10
3.2	Growth of Film and Nucleation	10
3.3	Deposition Technique	11-16
3.4	Why Chemical Bath Deposition used?	16-17
4.	Characterization Techniques	17-21
4.1	X-Ray Diffraction	17-18
4.2	Scanning Electron Microscopy(SEM)	18-20
4.3	Transmission Electron Microscopy(TEM)	20-21
5.	Synthesis and Characterization of PbSe Thin film and Powder	21-23
5.1	Experiment	22-23
6.	Result	24-27
7.	Conclusion	28
8.	Reference	29-30

## **FIGURES TABLE**

<b>S.No.</b>	<b>Title</b>	<b>Page NO.</b>
1.	Crystal Structure of lead Selenide (PbSe)	8
2.	Powder form of Lead Selenide (PbSe)	9
3.	Experimental setup of Chemical Bath Deposition Technique	17
4.	Ray Diagram of XRD	18
5.	Schematic Diagram of Scanning electron Microscope	20
6.	Schematic Diagram of Transmission Electron Microscope	21
7.	Experimental arrangement of deposition of PbSe Thin film by CBD Method	24
8.	Lead Selenide (PbSe) Thin Film by CBD Method	25
9.	Lead Selenide (PbSe) Powder	25
10.	XRD Spectra of Lead Selenide Thin Film	27
11.	XRD Spectra of Lead Selenide Powder	27
12.	Size and Strain graph of PbSe Thin Film	28
13.	Size and Strain graph of PbSe powder	28

## **ABSTRACT**

Thin films are everywhere in modern world with many of technologies depend upon daily life. The films are considered as backbone for advanced application in various field such as telecommunication devices, energy storage device, optical devices and so on. Thin films are deposited by physical deposition and chemical deposition. The thin film of lead Selenide (PbSe) was prepared by chemical bath deposition. Chemical bath deposition includes principle of chemical vapour depositions. The structural properties of thin films were studied by X-Ray diffraction (XRD) technique. The crystal size and strain values are calculating from data of X-Ray Diffraction.

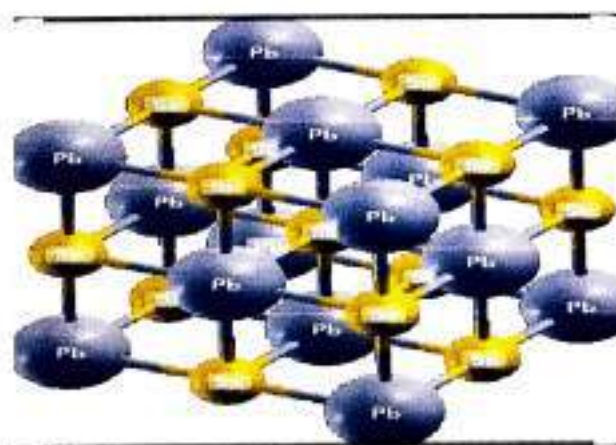
- The peaks from XRD pattern of (PbSe) indicate its cubic structure.
- Crystallite size of (PbSe) thin film and powder form was measured and found to be ~60.5nm and ~75.9nm respectively.
- From W-H plot we calculate the crystallite size and strain value.

## Introduction

Nowadays, most of technologies are used for minimizing the material into nano size as well as nano thickness. Research on nano crystalline materials is due to their distinctive properties and future applications in semiconductor devices. They are used for study of semiconductor communication, integrated circuit, photoconductors, light emitting diode etc. lead Selenide (PbSe) belongs to group IV-VI compound semiconductor. Due to their properties search groups have shown great interest in study and development of material by various deposition techniques such as electrodeposition, spray pyrolysis atomic layer deposition, spin coating method, sputtering, chemical bath deposition, SILAR method etc. Chemical bath deposition is presently attracting considerable attention, as it does not require advanced instrumentation.

Lead Selenide is an organic compound with formula PbSe. PbSe. It is most important ore and most important compound of lead. It is also known as essential element which means it is essential for life of some species, including human.

Molecular formula:	PbSe
Molecular mass:	286.16g/mol
Melting point:	1078 °C
Crystal structure:	cubic



**Fig. 1 : crystal structure of lead Selenide (PbSe)**

**Application of lead Selenide:** -Lead Selenide is semiconductor material. It is oldest and common detection element material in various infrared detectors. It has been extensively used in optoelectronic devices working in infrared region. Lead Selenide find application in following:[2,2]



- Infrared detectors
- Gas analysis
- Industrial process and Quality Control
- Defense Applications



**Fig.2: Powder form of Lead Selenide**

### **Literature review:**

Several studies have explored the synthesis and characterization of lead selenide (PbSe) thin films using various deposition techniques.

**Saloniemi et al. [3]** investigated the electrodeposition of PbSe thin films, focusing on the influence of deposition parameters such as deposition potential, source material concentrations, and current density. **Hankare et al. [4]** demonstrated a straightforward chemical bath deposition method capable of producing uniform, brownish-red PbSe thin films on glass substrates. **Thanikaikan et al. [5]** utilized X-ray diffraction analysis to explain the crystal structure of PbSe thin films. **Hone et al. [6]** investigated the impact of deposition temperature on the structural, morphological, and optical properties of PbSe thin films synthesized via the chemical bath deposition method. This research revealed that films deposited at lower temperatures exhibited an amorphous nature, while increasing deposition temperature led to improved crystallinity.

### **References:**

1. Saloniemi, H., Kanninen, T., Ritala, M., Leskelä, M., & Lappalainen, R. (1998). Electrodeposition of lead selenide thin films. *Journal of materials chemistry*, 8(3), 651-654.
2. Hankare, P. P., Delekar, S. D., Bhuse, V. M., Garadkar, K. M., Sabane, S. D., & Gavali, L. V. (2003). Synthesis and characterization of chemically deposited lead selenide thin films. *Materials chemistry and physics*, 82(3), 505-508.
3. Thanikaikarasan, S., Mahalingam, T., Dhanasekaran, V., Kathalingam, A., & Rhee, J. K. (2012). Growth and characterization of lead selenide thin films. *Journal of Materials Science: Materials in Electronics*, 23, 1562-1568.

4. Hone, F. G., & Ampong, E. K. (2016). Effect of deposition temperature on the structural, morphological and optical band gap of lead selenide thin films synthesized by chemical bath deposition method. *Materials Chemistry and Physics*, 183, 320-325.

### **3. Thin film deposition**

#### **3.1 Thin film**

Thin film deposition is a process of depositing thin film coating on glass substrate. Whenever growth of material is only in two dimensions that third dimension is negligible to other dimensions, is called thin films.

Thin film is a layer of material ranging from nanometer to several micrometers in thickness. Thin film deposition is an important manufacturing step in production of solid state and optoelectronic device. Thin films have directly or indirectly advanced in area of search in solid state physics which based on phenomena of thickness, geometry and structure of thin film. Thin films are used because their properties are different than bulk material. There are different properties of thin film such as optical, magnetic, electrical, thermal, chemical, mechanical properties. The properties of thin films are more affected by surface to volume ratio.

There are several methods used for deposition of thin film. Thin film deposition is mainly classified by physical and chemical methods. lead Selenide thin film is prepared by both physical and chemical deposition. In physical deposition process electromechanical and thermodynamic methods are used to produce thin film. Physical deposition system requires low-pressure vapor environment to function properly. In chemical deposition technique, a fluid precursor undergoes chemical change at solid surface and leaving solid layer. Among all these chemical bath deposition methods was chosen for preparation of thin film because physical methods are costly and required advanced instrumentation.

Any thin film deposition method process involves three main steps:

1. Production of appropriate atomic, molecular species.
2. Transport of these species to substrate.
3. Condensation on substrate[7]

#### **3.2 GROWTH OF THIN FILM AND NUCLEATION**

The phenomenon of formation of a stable nucleus is called Nucleation. The initial process that occurs in the formation of a crystal from a solution, a liquid, or a vapor, in which a small number of ions, atoms, or molecules becomes arranged in a pattern characteristic of a crystalline solid, forming a site upon which additional particles are deposited as the crystal grows. There are two stages in the crystallization process: nucleation and growth.

In the first nucleation stage, a small nucleus containing the newly forming crystal is created. Nucleation occurs relatively slowly as the initial crystal components must impinge on each other in correct orientation and placement for them to adhere and form the crystal. After successful formation of a stable nucleus, a growth stage ensues in which free particles (atoms or molecules) adsorb onto the nucleus and propagate its crystalline structure outwards from the nucleating site. This process is significantly faster than nucleation. The reason behind such rapid growth is that crystals contain dissociations and other defects, which act as a catalyst for the addition of particles to the existing crystalline structure. By contrast, perfect crystals (lacking defects) would grow exceedingly slowly. Most often, the properties of the film are affected by the underlying properties of the substrate and can vary drastically depending on the thickness of the film and the deposition technique employed for deposition.[8]

There are three major steps required in thin film growth and nucleation. The first step involves the creation of deposition species, i.e., the substrates and the target material, followed by the transportation from the target to the substrate using any deposition technique and the final stage involves the growth of the target on the substrate to form the thin film. A nucleus can grow in the two modes named parallel and perpendicular depending on the configuration of the substrates and target, and the two scenarios can be experienced in a single deposition. Parallel growth occurs on the substrate by surface diffusion of the absorbed atoms while perpendicular growth is because of direct impingement of the incident species. However, the rate of parallel growth is sometimes called lateral growth, at this stage is much higher than perpendicular growth and the grown nuclei are called islands.

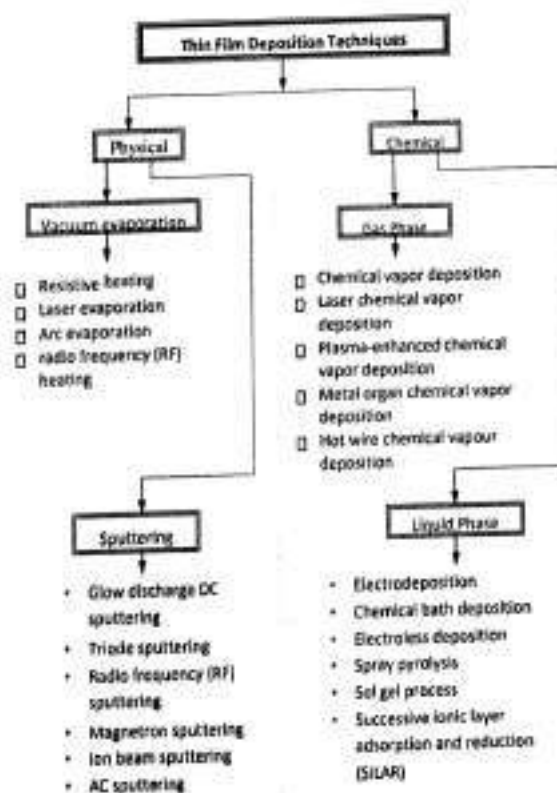
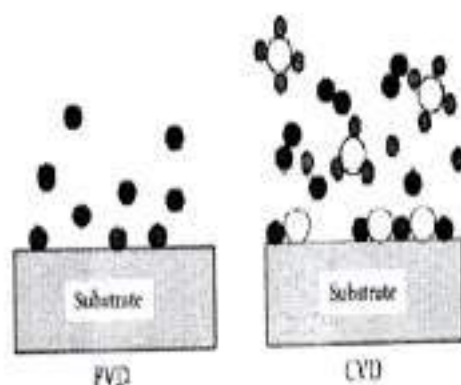
### 3.3 Deposition techniques

Thin films have distinct advantages over bulk material. Most of deposition techniques are used for formation of thin films. A deposition technique is considered as an integral key for creation of thin film new materials due to increasing demand from industries for versatile and multi-dynamics materials. The deposition techniques all properties of thin film and can also be modify the existing properties. Combination of different techniques can also be used to form a hybrid deposition with each contributing to outcome of thin film. In the present time thin films can be fabricated in various methods.

There are several types of thin film deposition techniques. The subset of deposition techniques are physical vapour deposition (PVD) and chemical vapour deposition (CVD). The distinguishing between PVD and CVD is in vapour. In PVD, the vapour is made up of atom and molecule simply in condense on substrate, and for CVD the vapour undergoes chemical reaction on substrate which resulted into thin film. Physical

deposition system requires low-pressure vapor environment to function properly. In chemical deposition technique, a fluid precursor undergoes chemical change at solid surface and leaving solid layer.[4],[5]

In PVD uses physical processes and use pure source material while in CVD uses chemical process and mixed source material.





### 3.3.1 ELECTRODEPOSITION:

Electrodeposition is widely utilized in making metallic coating. This technique is very old process which involve coating a thin layer of metal on top of different metal. It can be understood as extraordinary electrolysis resulting in deposition of solid material on electrode. This process involves saturated solution of charged development species through arrangement when external electric field is applied. Reduction of charge development species at growth and deposition surface which also such as electrode. This process is also known as electroplating.

### 3.3.2 ELECTROLESS DEPOSITION

In electroless deposition film of metal may deposit directly without any electrode potential being involved by suitable compound in solution. This is also called chemical reduction plating. In electroless deposition film can be grown on glass substrate by dipping them in appropriate solution of metal salt and reducing agent without any electric field. Deposition may occur by homogenous chemical reaction; reduction of metal ion in solution by reducing of metal ion in solution by reducing agent. There are three types of reaction take place:

- Non catalytic reaction where types of substrates used.
- Catalytic reactions were used where film formation takes place on metallic substrates.
- Catalytic reaction using activator where deposition takes place with help of activate non catalytic surface.

### 3.3.3 CHEMICAL BATH DEPOSITION

It is also called solution growth technique. CBD is method of deposition of thin film and nanoparticles is based on formation of solid phase from liquid solution. This technique is easy. In CBD two steps are involved in formation of phase from precursors solution as formation of nucleation particle growth. The necessary step precursors solution as formation of nucleation particle growth. The necessary step is that molecules cluster form undergoes rapid decomposition and particles combine to form film on substrate. Formation of film also depends on deposition condition such as bath temp, stirring rate, pH, concentration of solution. Growth may occur through ion concentration of material. This technique is mostly used to prepare Chalcogenide (Sulphur, selenium etc.) film as well as metal oxide film.[17]

### 3.3.4 SOL GEL METHOD:

This technique is broadly used for synthesis of oxide material. Sol gel processing is high purity and uniform nanostructure achievable at low temperature. In this method molecule precursors are dissolved in water or alcohol and converted to gel by heating and stirring by hydrolysis. The gel we obtained from hydrolysis process is wet, it should be dried. After drying we get powdered. The Sol gel method can be used in the process of making ceramics as molding material and used as intermediate by thin film of metal oxides in

various application. A sol gel process involves formation of sol in liquid and then connecting sol particles to form porous network by drying liquid possible to obtained powder thin films.[12, 13]

### **3.3.5 SPRAY PYROLYSIS METHOD:**

Spray coating technique may be one of the most useful coverings surfaces. In this method thin film is deposited by spraying solution on heated surfaces where constituent react to form chemical compound. Spray pyrolysis equipment consist of atomizer, precursor sol. Substrate heater and temperature controller. This technique involves spraying a metal salt solution onto a heated surface. Spray pyrolysis is a process in which nanostructure is obtained when a solution contained a precursor is spray using nano porous nebulizer on hot substrate in furnace. It is an aerosol process that atomizes a solution and heats the droplet to produce solid particles. Pyrolysis means decomposition of chemical compound under action of heat at higher temperature

- Transform liquid precursor or sol precursor into ionized droplets.
- Making solvent to evaporate
- Allowing solute to condense
- Making solute decompose and react
- Sintering the solid particles

### **3.3.6 SILAR METHOD:**

SILAR is successive ionic layer absorption and reaction. This is one of the most suitable for preparing semiconductor material. In Silar method thin films are obtained by immersing substrate into separately placed cationic and anionic precursor and rinsing between every immersion with ion exchanged bath. Rinsing time in ion exchange bath is critical for ionic layers formation.

- Immersion of substrate in cationic
- Immersion of substrate in distilled water
- Immersion of substrate in anionic
- Immersion of substrate in distilled water

### **3.3.7 SPIN COATING TECHNIQUE:**

This method has ability to quickly and easily product very uniform films

- Deposition
- Spin up
- Spin off
- Evaporation



Initially solution is cast on to substrate using pipette, whether substrate is already spinning after deposition, the centrifugal motion will spread the solution across suitable. Most of the solutions are expelled from substrate. The fluid now begins to thin film will change color due to interference effect, when color stops changing, this will indicate that film is mostly dry, fluid out of flow stops and thinning is dominated by evaporation of solvent.

### **3.3.8 ELECTRO BEAM EVAPORATION:**

In electron beam evaporation where intensive beam of electrons is generated from filament and steered through both electric and magnetic fields to hit target and vaporize it under vacuum environment. Thin film prepared by electron beam evaporation is good quality and purity. Large categories of materials can be prepared by electron beam evaporation technique. The electron system only heats the target source material, not the entire container resulting in lower degree of contamination from the container by concentrating energy on target rather than entire vacuum chamber, it helps reduce the possibility of heat damage substrate. Electron beam evaporation used in variety of application ranging from high performance aerospace and automobiles industries [14-16]

### **3.3.9 SPUTTERING:**

Sputtering is usually understood as sputter deposition. It is a physical vapors deposition process. It is the process of directing high energy ions to target in vacuum and remove target atoms. The deposition of these emitted atoms on surface is called sputter deposition. The requirement for sputtering deposition is ion beam and potential low pressure (less than 5m torr), good vacuum. Sputtering is a process in which particles are ejected from solid target materials due to bombarding of target by energetic particles. The kinetic energy of incident particles should be greater than thermal energy. [17, 18]

### **3.3.10 PULSED LASER DEPOSITION:**

It is a powerful method to grow thin films and multi layers complex material. It is technique where high power laser beam focused inside vacuum chamber to strike target of desired composition material is then vaporized from target as deposited as thin film on substrate such as silicon wafer facing target. The process can occur in ultra-high vacuum or in presence of background gas such as oxygen which is commonly used when depositing oxide to fully oxygenated deposited films. The process of Pulse laser deposition can schematically be divided into four stages:

- Laser analysis of target material and creation of plasma.
- Dynamics of plasma under vacuum.
- Deposition of material on substrate.

- Nucleation and growth of film on substrate surface [9]

### 3.3.11 CATHODIC ARC DEPOSITION (ARC-PVD):

This is a physical vapor deposition technique in which an electric arc is used to vaporize material from a cathode target. The vaporized materials are then condensed on a substrate and form a thin film. This technique is being done to deposit metallic, ceramics, and composite films.

### 3.3.12 ELECTRO HYDRODYNAMICS DEPOSITION (ELECTRO SPRAY DEPOSITION):

This is a relatively new process of film deposition. The liquid can be deposited either in the form of nanoparticles solution or simply a solution and it is fed to small capillary nozzle (usually metallic) which is connected to high power sources. The substrate on which the film will be deposited is connected to the ground terminal of the power source. Through the influence of electric field, the liquid comes out of the nozzles and takes a conical shape (Taylor cone) and at the apex of the cone a thin jet emanates which disintegrates into very fine and small positively charged droplets. The droplets keep getting smaller and smaller and finally get deposited on the substrate as a uniform thin layer.

## 3.4 Why chemical bath deposition?

This is chemical liquid phase method. Chemical bath deposition is one of the most suitable methods to get uniform, good reproducibility thin film. It is one of the cheapest methods to deposit thin film. As it does not depend upon expensive equipment and scalable technique that can be employed for large area batch processing or continuous deposition.

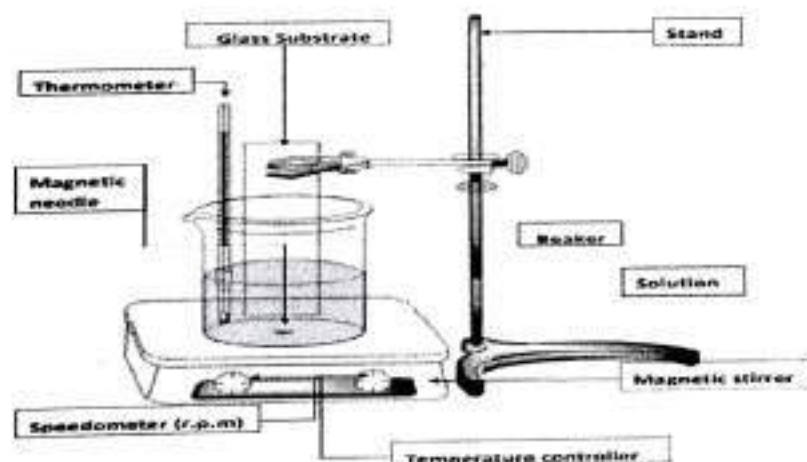


Fig.3 Experimental Setup of Chemical Bath Deposition technique

The major advantage of chemical bath deposition is that requires only solution container and substrate mounting device. The substrate is stirred with help of magnetic stirrer. Water or paraffin bath with constant stirring are used to heat the chemical bath to desired temperature. In some case stirring is continuous from room temperature the beaker containing precursor. Solution and deionized water are alternately placed. Films produced by chemical bath deposition are used in semiconductor, photovoltaic cells and supercapacitor and there is increasing interest in using chemical bath deposition to create nanoparticles thin films.

### **Advantages of chemical bath deposition method**

This method is presently attracting considered attention as it does not require an instrumentation like vacuum system other expensive equipment simple equipment like water bath with temperature indicator, magnetic stirrer, solution breaks used in this method. The starting chemical are commonly available and cheap with this method, large number of depositions of thin film can done with number of cycles. It is low cost efficient methods and easy to scale up industrial purpose. They have advantages:

- low cost
- simplicity
- Uniformity
- controlled growth

#### **USES:**

- I. Chemical bath deposition is used to deposit buffer layer in photovoltaic cells because chemical bath deposition does not damage substrate.
- II. Chemical bath deposition has possible application in antireflection, optical fiber, total reflector, LED, solar cells etc.
- III. Use in field of nanomaterials because properties of nanostructure of chemical bath deposition films can be precisely controlled because of uniform thickness, composition.

### **4. Characterization techniques**

Thin films are widely used in the electronic, optical and magnetic devices. In order to study different properties of these semiconducting materials in form of thin films. Various characterization techniques are used. These techniques include thickness measured structural morphology by X-Ray diffraction, surface morphology by scanning electron microscopy, optical absorption and transmission by UV visible spectrophotometer, electrical resistivity measurement etc.

## 4.1 X-RAY DIFFRACTION (XRD)

XRD is well known technique to obtain the information of composition, phase and crystalline orientation of material. It gives information about crystal structure, chemical composition and physical properties of material and thin film. This technique based on observing the scattering intensity of an X-Ray beam hitting a sample as a function of incident and scattered angle and, wavelength of energy. Interaction of incident ray with sample produce constructive when condition satisfy Bragg's law

$$n\lambda = 2d \sin \theta$$

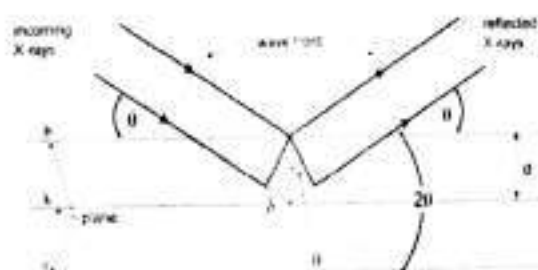


Fig.4 : Ray Diagram of XRD

$n$  = integer

$d$  = interplanar spacing

$\lambda$  = wavelength

$\theta$  = diffraction angle

It measures average spacing between layer of atoms, find structure of unknown materials. The different phase can be analyzed by X-Ray analysis. It determines the orientation of single crystal or grain. X ray is generated in a cathode ray tube by heating filament to produce electron accelerating electron toward target by applying voltage and bombarding target material with electron have sufficient energy to dislodge inner shell electron of target material. Characteristics of X- Ray spectra are produced. As sample and detector are rotated intensity of reflected X-Ray is recorded when geometry of incident X-Ray satisfies Bragg equation, constructive interface occurs and peak in intensity occur.[20]

### Application of X-Ray diffraction:

- Analysis of phase change under other special conditions such as temperature, humidity.
- Analysis of physical properties such crystallite size, orientations.

- Determination of unit cell dimension.
- Measurement of sample purity.

## 4.2 SEM (SCANNING ELECTRON MICROSCOPY)

A scanning electron microscope is type of electron microscope that produces image of sample by scanning it with focused beam electrons. The electron interacts with atoms in sample, producing various signals that can be detected and contain information about the samples surface topography and composition. The electron beam is generally scanned in roaster scan pattern, and the beams position is combined with detected signal to produce image.

- SEM can achieve resolution better than 1 nanometer. It provides precise control over the degree of magnification because it uses electromagnets rather than lenses.
- The SEM allowed researchers to study a much variety of specimens.
- Scanning electron microscopes have development new areas of study in the medical and physical science communities.
- Specimen can observe in high vacuum, in low vacuum, in wet condition and at a wide range of elevated temperature.

When beam of electrons strikes the surface and specimen and interact with the atoms of sample signals in the form of secondary electrons, back scattered electron and characteristics X-rays are generated that contain information about the sample's surface topography, composition, etc. The SEM can produce a high-resolution images of sample surface, revealing detail about 1-5 nm in its primary detection mode i.e. secondary electron imaging.

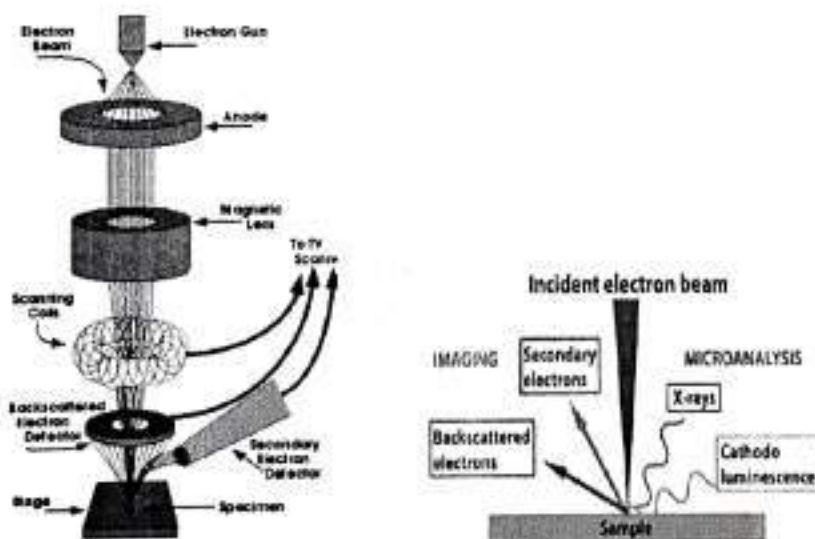


Fig.5: schematic diagram of scanning electron microscope



When electron beam hits the surface of sample, it penetrates the sample to depth of few microns depending on the accelerating voltage and the density of the sample. The three types of signals produced by SEM include secondary electrons, backscattered electrons and characteristic X-rays. Secondary electrons are electrons that interact with top surface of the sample. Backscattered electrons are generated from elastic and inelastic collision between electron and the atoms within the sample. The energy of the characteristic X-ray can be captured by Electron-dispersive X-rays spectrometer to qualitatively analyze the chemical character of the sample. The spatial resolution of SEM depends on size of electron spot, which in turn depends on both the wavelength of electrons and electron-optical system that produce the scanning beam. The resolution is also limited by size of interaction volume, volume of specimen material that interacts with electron beam.[21, 22]

### 4.3 Transmission electron microscopy (TEM)

Transmission electron microscopy is good complementary technique to XRD for evaluating the crystallography of materials using high electron beam ( $>200\text{keV}$ ). A high energy beam of electron is shone through a very thin sample, and interaction between electron and the atoms can be used to observe feature such as crystal structure. TEM can be used to study the growth of layer, their composition and defect. It is one of the most powerful microscopes with respect to its magnification and resolution, it is applied in wide range of applications can be utilized in variety of different scientific, educational and industrial fields. The TEM operates on the same basic principle as light microscope but uses electrons instead of light. Because wavelength of electron is much smaller than that of light. TEM can reveal finest details of internal structure.

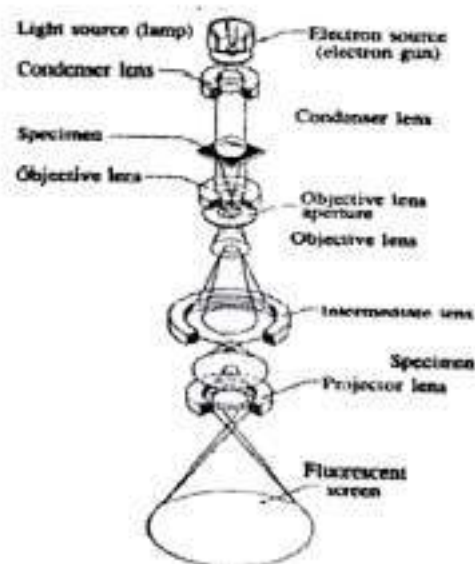


Fig.6: schematic diagram of transmission electron microscopy

In transmission electron microscope the electron gun, fires a beam of electrons. The gun accelerates the electrons to extremely high-speed using electromagnetic coils and high voltage. The electron beam is focused into a thin, small beam by condenser lens has a high aperture that eliminates high angle electrons. The beam then strikes the specimen and part are transmitted depending upon thickness and electron transparency of specimen. The objective lens focuses the portion of the beam that is emitted from sample into an image. Another component of TEM is vacuum system. The transmitted portion is focused by objective lens into an image on phosphorous screen or charged coupled device (CCD) camera. The darker area of image represents those area of sample that fewer electrons are transmitted through while the lighter area of image represent those areas of sample that more electrons were transmitted through. The image produced by TEM, called micrograph.[23,29]

## **5. Synthesis and characterization of lead Selenide PbSe thin Film and PbSe powder**

### **Introduction**

Research on nanocrystalline materials is due to their distinctive properties and future applications in semiconductor devices. They are used for study of semiconductor communication, integrated circuit, photoconductors, light emitting diode etc. lead Selenide (PbSe) belongs to group IV-VI compound semiconductor with its smaller band gap. PbSe also low -toxicity and cost-effective materials. These properties indicate uses of PbSe in solar cells, IR detector material, photothermal conversion of solar energy. For these reasons many search groups have shown great interest in study and development of material by various deposition techniques such as electrodeposition, spray pyrolysis atomic layer deposition, spin coating method, sputtering, chemical bath deposition, SILAR method etc. Chemical bath deposition is presently attracting considerable attention, does not require advanced instrumentation. It is relatively inexpensive, easy to handle, large area deposition, capable of good quality thin film. The characteristics of chemical bath deposited PbSe thin film depend upon growth conditions.[25]

### **5.1: Experiment:**

With help of chemical bath deposition (CBD) method thin film of polycrystalline lead Sulphide deposited on the glass slab. The glass substrate degreased in hydrochloric acid solution (200ml deionized water and 100ml HCl) for 24 hours and then cleaned in chromic acid solution. Finally rinsed in deionized water and dry in air. Cleaning of glass slab due to remove hydrocarbons and other particle from glass slab. The chemicals used are lead acetate , sodium selenosulphate , sodium hydroxide and ammonia. Sodium

selenosulphate was prepared by refluxing amount of 9gm of selenium powder with approximately 15gm of sodium sulphate in 250ml of distilled water for 6 hours at  $80^{\circ}\text{C}$ .

The mixture of the bath was prepared by mixing of appropriate amount of lead acetate and 10ml (0.5M) of NaOH in 100 ml beaker. Initially, the solution looked milky turbid due the formation of  $\text{Pb}(\text{OH})_2$  it later change into a colorless solution after the addition of a sufficient amount of ammonia. Sodium selenosulphate was added to obtain a final volume of 70ml. chemically cleaned substrate vertically immersed into the solution with the help of substrate holder. The reaction mixture was continuously stirred with a magnetic stirrer and maintained at a temperature of  $90^{\circ}\text{C}$  for the deposition of thin film. The prepared solution was initially clear and colorless but turned to dark grey after a few minutes later, a mirror like thin film began to deposit onto the side of the beaker and the substrate confirming the formation of PbSe. There after substrate coated PbSe was removed and dried in air and then dried in oven.



Fig.7 : Experimental arrangement of deposition of PbSe thin film by chemical bath deposition method.



## Result and Discussion



Fig.8 : Lead Selenide (PbSe) thin film by chemical bath deposition

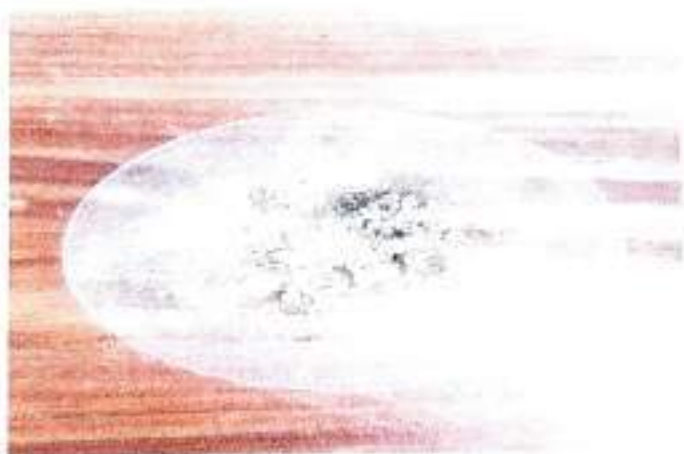


Fig.9: Lead Selenide (PbSe) powder



## X-ray Diffraction

X-Ray diffraction is the powerful and non-destructive technique for characterizing crystal material. Structural characterization was carried out with the help of XRD. XRD pattern of PbSe thin film deposited by chemical bath deposition. The XRD pattern were collected with XPERT-PRO diffraction pattern. The intensity of diffracted x-rays measured as function of diffraction angle. The intensities of the spots provide information about the atomic basis. The sharpness and shape of spots are related to the perfection of crystal. The structure of material can be obtained from plot between intensity vs diffraction angle. The diffraction peaks provide the information about lattice plane and crystal structure. In fig (4.4) and (4.5) shows XRD spectra of lead Selenide thin film and powder form of PbSe. All the diffraction peaks (111), (200), (220), (311) are matched to standard data. So, it is confirmed that formation of PbSe takes place cubic structure.[26]

The Full Width Half Maximum (FWHM) ( $\beta$ ) can be related to strain ( $\epsilon$ ) and crystallite size (D) as:

$$\beta(\cos\theta)/\lambda = 1/D + \epsilon(\sin\theta)/\lambda$$

The plot of  $\beta(\cos\theta)/\lambda$  vs  $\sin\theta/\lambda$  are shown in Fig. 4.6. The reciprocal of the intercept on y axis in these graphs provides particle size, and the slope of graph will give strain value. The plot of  $\beta(\cos\theta)/\lambda$  vs  $\sin\theta/\lambda$ , known as W-H plot. Williamson and Hall proposed this method for obtaining size and grain. The size and strain graph of lead Selenide thin film and powder form are shown in fig (4.6) and (4.7) respectively. From these graphs we find the particle size and strain value.[27]

Dislocation density denotes the number of dislocation line per unit volume of crystal, which is size of crystal defects possessed by a crystal. In other words, the dislocation value will illustrate the degree of crystallinity of nanoparticles.

$$\delta = 1/D^2$$

small dislocation density had high degree of crystallite. [11]

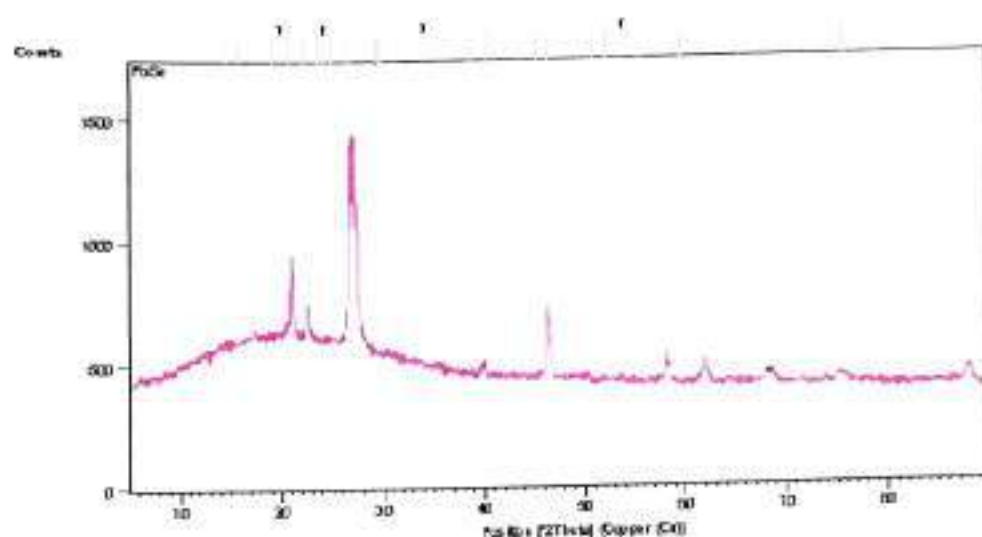


Fig.10: XRD Spectra of lead selenide thin film

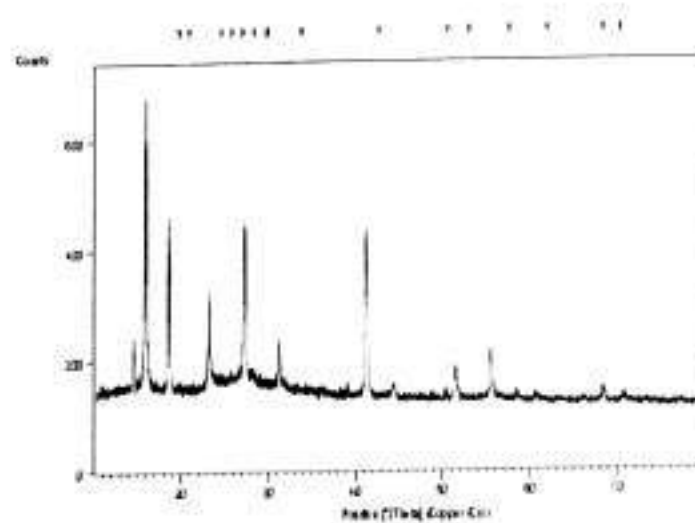


Fig.11 : XRD Spectra of Lead Selenide Powder.

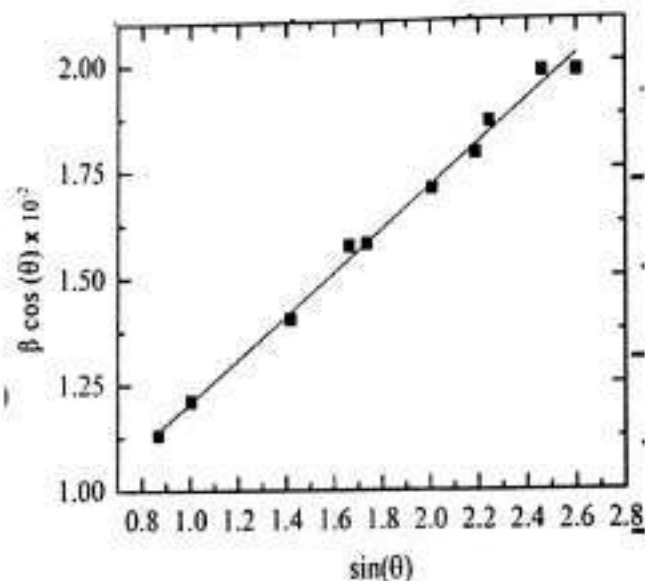


Fig.12 : Size and Strain graph of PbSe thin film

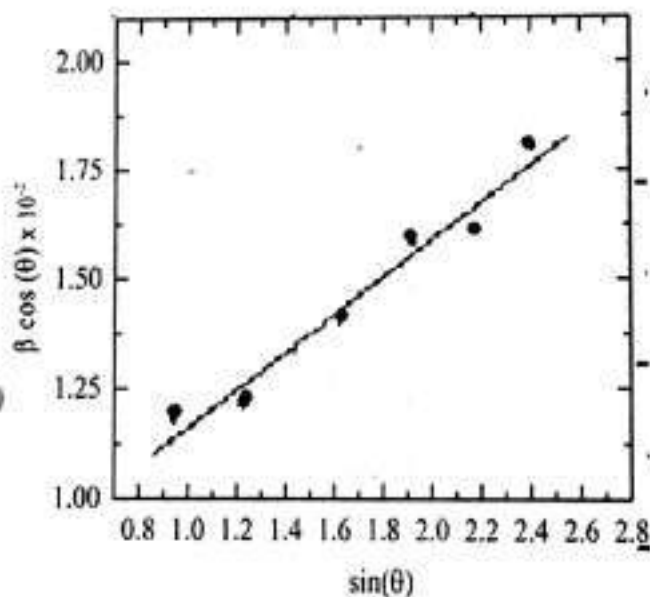


Fig.13 : Size and Strain graph of PbSe powder

Type of Material	Particle Size (nm)	Strain ( $\epsilon$ )	Dislocation Density ( $m^{-2}$ )
PbSe thin film	60.5	$6 \times 10^{-4}$	$2.45 \times 10^{-14}$
PbSe powder	75.9	$1 \times 10^{-2}$	$1.12 \times 10^{-14}$

## CONCLUSION

In this, PbSe Thin films can be successfully deposited by chemical bath deposition method. Structural characterization was carried out with the help of XRD. The XRD pattern were collected with XPERT-PRO diffraction pattern.

- XRD confirms the cubic structure of lead Selenide.
- The particle size of PbSe thin film ~60.5nm and particle size of PbSe powder is 75.9 nm
- The strain value for PbSe thin film and powder forms are found to be  $6 \times 10^{-4}$  and  $1 \times 10^{-2}$  respectively.
- The Dislocation density of PbSe thin film and powder form are found to be  $2.45 \times 10^{-14}$  and  $1.12 \times 10^{-14}$ .
- The confinement effect resulting from decrease in crystal size in grown nanocrystalline sample is responsible for blue shift.
- Lead Selenide thin film have many applications in solar cell and photovoltaic cells.
- Size of particle of thin film and powder are different due to surface area to volume ration increase. The confinement effect resulting from decrease in crystal size in grown nanocrystalline sample is responsible for blue shift.

## REFERENCE

1. Okimura H., Matsumae T. and Makable R., Thin Solid Films, **71**, 53-599 (1908).
2. Loferski J. J., Physics., **27**, 777 (1956).
3. Saloniemi, H., Kanninen, T., Ritala, M., Leskelä, M., & Lappalainen, R. (1998). Electrodeposition of lead selenide thin films. *Journal of materials chemistry*, *8*(3), 651-654.
4. Hankare, P. P., Delekar, S. D., Bhuse, V. M., Garadkar, K. M., Sabane, S. D., & Gavali, L. V. (2003). Synthesis and characterization of chemically deposited lead selenide thin films. *Materials chemistry and physics*, *82*(3), 505-508.
5. Thanikaikarasan, S., Mahalingam, T., Dhanasekaran, V., Kathalingam, A., & Rhee, J. K. (2012). Growth and characterization of lead selenide thin films. *Journal of Materials Science: Materials in Electronics*, *23*, 1562-1568.
6. Hone, F. G., & Ampong, F. K. (2016). Effect of deposition temperature on the structural, morphological and optical band gap of lead selenide thin films synthesized by chemical bath deposition method. *Materials Chemistry and Physics*, *183*, 320-325.
7. A. Gaiduk, P. Gaiduk, A. Larsen, Thin Solid Films. 516, 3791 (2008).
8. Ohring, Milton (2002). Materials Science of Thin Film: Deposition and Structure (2<sup>nd</sup> edition).
9. [www.electropedia.org](http://www.electropedia.org), retrieved 17Nov2023.
10. Hadanu R, Idris S and Sutapa I W 2015 Indones. J. Chem. 15 86-92
11. Grozdanov I., Najdoski M. and Dey S.K., A simple solution growth technique for PbSe thin films. *Mater. Lett.*, **38**, 28-32 (1999).
12. Klein, L.C. and Garvey, G.J., "Kinetics of the Sol-Gel Transition" *Journal of Non-Crystalline Solids*, Vol. 38, p.45 (1980)
13. J. F. Ziegler, J. P. Biersack, U. Littmark (1984). *The Stopping and Range of Ions in Solids*, "vol. 1 of series Stopping and Ranges of Ions in Matter. Pergamon Press, New York.
14. T. Schenkel; Briere, M.; Schmidt-Böcking, H.; Bethge, K.; Schneider, D.; et al. (1997). "Electronic Sputtering of Thin Conductors by Neutralization of Slow Highly Charged Ions". *Physical Review Letters*, **78** (12): 2481.
15. Robbie, K.; Brett, M. J. (1997). "Sculptured thin films and glancing angle deposition: Growth mechanics and applications". *Journal of Vacuum Science & Technology A: Vacuum, Surfaces, and Films*, **15** (3). American Vacuum Society: 1460-1465.
16. Harsha, K. S. S., "Principles of Physical Vapor Deposition of Thin Films", Elsevier, Great Britain (2006), p. 400.
17. T. Schenkel; Briere, M.; Schmidt-Böcking, H.; Bethge, K.; Schneider, D.; et al. (1997). "Electronic Sputtering of Thin Conductors by Neutralization of Slow Highly Charged Ions". *Physical Review Letters*, **78** (12): 2481.



18. Rumianowski R.T., Dygdala R.S., Jung W. and Bala W., Growth of PbSe thin film on Si substrate by pulsed laser deposition method, *J.Cryst. Growth*, **252**,230-235(2003).
19. McMullan, D. (1988). "Von Ardenne and the scanning electron microscope". *Proc Roy Microsc Soc.* **23**: 283-288.
20. von Ardenne, Manfred. "Improvements in electron microscopes", published 1939-08-15.
21. Wells OC (1957) The construction of a scanning electron microscope and its application to the study of fibres. PhD Dissertation, Cambridge University.
22. ultraviolet microscope. (2010). In Encyclopædia Britannica. Retrieved November 20, 2010, from [Encyclopædia Britannica Online](#)
23. Hawkes, P., ed. (1985). *The beginnings of Electron Microscopy*. Academic Press.
24. Champness, P. E. (2001). *Electron Diffraction in the Transmission Electron Microscope*. Garland Science.
25. Brinker, C. J.; G. W. Scherer (1990). *Sol-Gel Science: The Physics and Chemistry of Sol-Gel Processing*. Academic Press.
26. W.H.Hall (Acta Metall. 1, 22-31 (1953)).
27. McMullan, D. (1988). "Von Ardenne and the scanning electron microscope". *Proc Roy Microsc Soc.* **23**: 283-288.

**COULOMB CORRECTED BETHE-HEITLER THEORY  
FOR EXTERNAL BREMSSTRAHLUNG  
CALCULATIONS: FORTRAN CODE  
PROJECT REPORT**

*Submitted in partial fulfillment of the  
requirements for the award of the degree of*

**MASTER OF SCIENCE**

**in**

**PHYSICS**

*By*

**Bhawana**

**Regn. No. 8114-19-771**



**DEPARTMENT OF PHYSICS  
SRI GURU TEG BAHADUR KHALSA COLLEGE, SRI  
ANANDPUR SAHIB  
(An Autonomous College)  
ANANDPUR SAHIB- 140118, PUNJAB (INDIA)**



SRI GURU TEG BAHADUR KHALSA COLLEGE, SRI ANANDPUR SAHIB  
(An Autonomous College)  
ANANDPUR SAHIB-140118. PUNJAB (INDIA)

---

## CERTIFICATE

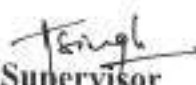
It is certified that the work contained in the project report entitled "**COULOMB CORRECTED BETHE-HEITLER THEORY FOR EXTERNAL BREMSSTRAHLUNG CALCULATIONS: FORTRAN CODE**" is an original contribution by me and has not been submitted in part or full for any other degree at this or other University/ Institute.

The assistance and help received during the course of the thesis work have been acknowledged.

Bhawana  
Regn. No. **8114-19-771**

I, the undersigned, Supervisor of Bhawana, Regn. No. **8114-19-771**, a candidate for the degree of **Master of Science**, agree that the project report entitled, "**COULOMB CORRECTED BETHE-HEITLER THEORY FOR EXTERNAL BREMSSTRAHLUNG CALCULATIONS: FORTRAN CODE**", may be submitted in partial fulfillment of the requirements for the award of degree.


This is to certify that the above statement made by the candidate is correct to the best of my knowledge.

  
**Supervisor**  
Dr. Amrit Singh  
Assistant Professor  
Department of Physics  
Sri Guru Teg Bahadur Khalsa College  
Sri Anandpur Sahib

### CERTIFICATE II

This is to certify that the "Project report" entitled " **COULOMB CORRECTED BETHE-HEITLER THEORY FOR EXTERNAL BREMSSTRAHLUNG CALCULATIONS: FORTRAN CODE**" submitted by **Bhawana** (Regn. No. 8114-19-771) to Department of Physics, Sri Gurur Teg Bahadur Khalsa College, Sri Anandpur Sahib in partial fulfillment of the requirements for the award of degree of **MASTER OF SCIENCE IN PHYSICS** and has been approved by the Department Research committee (DRC) after the viva-voce examination of the candidate.

  
Dr. Amrit Singh  
Supervisor

  
Dr. Randev Singh  
Chairman DRC

## ACKNOWLEDGEMENT

Firstly, I would like to express my gratitude to my Supervisor, Dr. Amrit Singh Assistant Professor at Department of physics Sri Guru Teg Bahadur Khalsa College Sri Anandpur Sahib, who has resourcefully guided me throughout this research project. I'm extremely grateful for his motivating discussions while enable me to accomplish this task successfully. Without his active guidance, support and encouragement I would not have made headway in this project.

I also thankful to my Parents for their moral support and suggestions to improve the dissertation work. I'm also thankful to other faculty members in the department for their encouragement and fruitful academic discussions.

A special thanks to Ms. Neha Assistant Professor at Department of Physics for the help and their valuable suggestions whenever I needed out of their busy schedule. I'm also thankful to my classmates and my friends who was directly or indirectly help me to complete this project report.

Bhawana



## ABSTRACT

Theoretical investigation of bremsstrahlung processes was started on the basis of classical electrodynamics. The initial attempts were made in 1923 by Kramers to develop the bremsstrahlung theory on the basis of semi-classical calculation by using correspondence principle. The first Quantum mechanical cross-section formulae for the elementary processes of bremsstrahlung were derived in 1931 by Sommerfeld in the non-relativistic dipole approximation including retardation for non-relativistic electrons without taking accounts the nuclear screening effects. Elbert and Goth give the multiplicative coulomb correction factor ( $F_{Elbert}$ ) for Bethe-Heitler OB cross-section ( $\sigma_{BH}(k)$ ).

In the present investigation a FORTRAN code has been created to find the external bremsstrahlung cross section using Bethe-Heitler theory and also a code is made for the Coulomb correction proposed by the Elbert. The results obtained from these codes are in good agreement with the results available in literature.

## CONTENTS

CHAPTER	Page No.
1. Introduction and Literature Survey	1-13
1.1 General Introduction	
1.2 Description of ordinary bremsstrahlung	
1.3 Theoretical aspect of ordinary bremsstrahlung	
1.4 Bremsstrahlung in material medium	
2. Fortran Code	14-18
3. Results and discussions.	19-21
4. References	22-24

## LIST OF FIGURES

S. No.	Name of the Figure
--------	--------------------

Fig.3.1	The plots of number of photons of energy $k$ per $m_0c^2$ per unit total photon yield for Al target
---------	--

Fig.3.2	The plots of number of photons of energy $k$ per $m_0c^2$ per unit total photon yield for BP target
---------	--

## CHAPTER 1

### INTRODUCTION AND LITERATURE SURVEY

#### 1.1 General Introduction

Rontgen (1895, 1896) discovered X-rays, but the study of two different components, the characteristic line spectrum and the continuous spectrum started in early 1905s. For the continuous spectrum Sommerfeld (1931) proposed the name *bremsstrahlung* (braking radiation) with the approval of Rontgen himself. *Bremsstrahlung* is the fundamental processes, in which the photon emission occurs due to the scattering of an electron from an atom. *Bremsstrahlung* plays an important role in all branches of physics: atomic and nuclear physics, solid state physics, and plasma physics and in the field of astrophysics. It has a wide range of application in many areas of experimental and theoretical physics research.

Until the 1970s, *bremsstrahlung* was considered in the domain of the acceleration of electron in the static screened coulomb field of the target nuclei. In early 1970s, several people consider the dynamic response of the target atom that can be polarized by the incident electron and the photon emission occurs. Therefore, the new mechanism of photon emission polarization *bremsstrahlung* was introduced. The total *bremsstrahlung* (BS) amplitude is the sum of ordinary *bremsstrahlung* (OB) and polarization *bremsstrahlung* (PB) amplitudes. Ordinary *bremsstrahlung* is the process by which the photon is emitted by the electron decelerating in the static field of the target atom. Polarization *bremsstrahlung* is the process by which the photon is emitted by the target as a result of its

polarization by incident electron. During the collision of the incident electron and the atom, the internal structure of the atom is deformed or polarized and an electric dipole moment is induced. Being time-dependent, it becomes a source of continuous electromagnetic radiation called polarization bremsstrahlung. It is more complicated than the ordinary bremsstrahlung since in addition to the electron-photon interaction one has to consider the dynamic response of the target atom created by the action of the two fields created by the incident electron and the emitted photon. The polarization bremsstrahlung plays important role particularly at lower and medium photon energy and its contribution in the total bremsstrahlung spectra must be taken into account, while comparing the theoretical and experimental results.

A beam of mono-energetic electron passes through the material medium suffers elastic and inelastic scattering, multiple scattering. The electron loses energy through the excitation and ionization of the absorbing atoms of the material media. The scattering of electrons through the finite angle always accompanied by the emission of electromagnetic radiation termed as bremsstrahlung. The behavior of the continuous beta particles is same as that of the mono-energetic electrons except for the continuous nature of the beta particles whose energy spread over from zero to maximum end point energy of the beta radioactive source. The continuous spectrum of beta particles or electrons produces electromagnetic radiation photon on suffering deflection through acceleration or retardation from the coulomb field of the nuclei in material medium. However, there exist an important difference between the mono-energetic electron and continuous beta particles of radioactive beta source. In case of beta radioactive source an electromagnetic radiation is emitted along with the



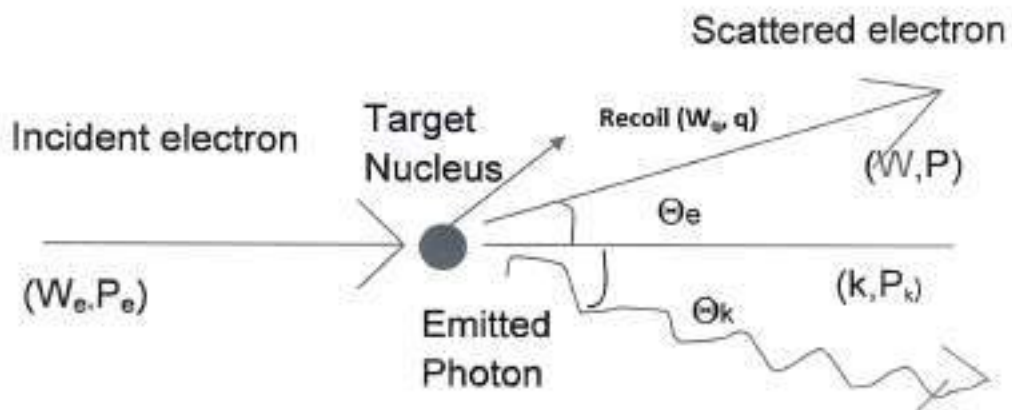
originated electrons or continuous beta particles interaction with the coulomb field of the daughter nucleus. This electromagnetic radiation is termed as internal bremsstrahlung and it is dependent purely on the characteristic of beta emitter. However, the emission of electromagnetic radiation photon due to the interaction of the continuous beta particles with the static coulomb field of target nuclei is termed as ordinary bremsstrahlung. The mode of production of ordinary bremsstrahlung is relatively different from the production of the internal or inner bremsstrahlung due to electron capture. Historically, the first measurement of the ordinary bremsstrahlung produced by the continuous beta particles of the beta emitter was reported by Gray (1911, 1912) Chadwick (1912) and Hess and Lawson [5]. Later, Gray (1922) measured the ordinary bremsstrahlung spectra in targets of iron, lead and paper produce by the absorption of continuous beta particles of beta emitter. The phenomenon of internal bremsstrahlung was first discovered by Aston in (1927) in beta decay of radioactive source. The experimental evidence of internal bremsstrahlung was given by Bramston in 1930. Later, the detail experimental studies have been carried out by Sahel and Kipper (1936), Gray and Hinds (1936) and Dorset (1936).

## 1.2 Description of ordinary bremsstrahlung

In classical electrodynamics an accelerated charged particle passed through the static field of the target nucleus emits a photon this termed as ordinary bremsstrahlung. The ordinary bremsstrahlung amplitude is proportional to the acceleration produced by nucleus ' $Ze$ ', on a particle of charge ' $Ze$ ' and mass ' $m$ '. Therefore, the bremsstrahlung intensity which is given by the square of amplitude will vary as the square of the  $Z^2/m^2$ . The bremsstrahlung intensity is directly proportional to the square of atomic number of the target element or absorbing

material and varies inversely as the square of the mass of the projectile. Therefore, the bremsstrahlung intensity is more for the light particle like electron and it is relatively small for the heavy particle like proton, alpha particles etc.

The following diagram shows the processes of production of ordinary bremsstrahlung depicts the production of photon by the interaction of the incident charged particle electron with the interaction of the nucleus of the target atom –



Here  $w_e$  and  $W$  are the total energies of the incident and scattered electron.  $P_e$  and  $P$  are the momentum of the incident and scattered electron. Where,  $W_q$  and  $q$  be the total energy and momentum of the recoil atom.  $k$  and  $P_k$  be the energy and momentum of the emitted photon.

Now, according to the conservation laws of energy and momentum we have,

$$W_e = W + k + W_q$$

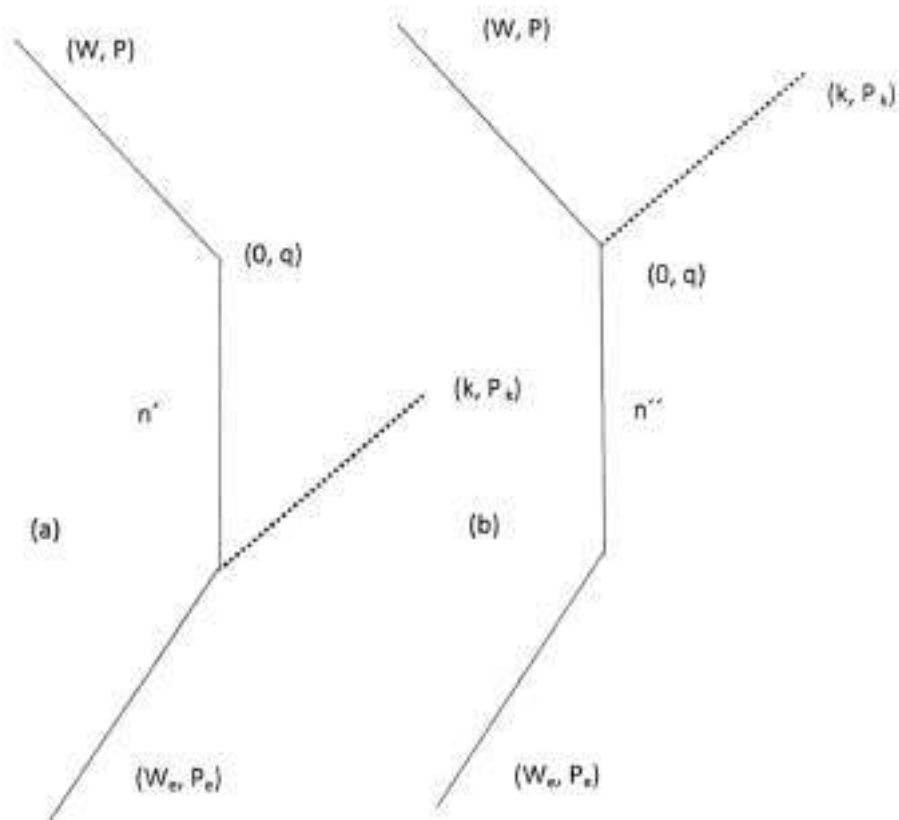
$$P_e = P + k + q$$

Therefore, in individual interaction of the incident electron with the target nucleus, the incident electron losses energy from 0 up to maximum amount of its total kinetic energy  $T_e = W_e - 1$ . The maximum photon energy  $k_{max}$  at the short wavelength limit of continuous X-ray spectrum is given by

$$k_{max} = T_e = W_e - 1$$

This relation was experimentally established by Duane and Hunt's in 1915 and is known as Duane and Hunt's law.

The Feynman diagram representation of the processes of OB looks approximately as shown given below



The two possible intermediate states can occur firstly, the photon is emitted and then the electron is scattered afterwards, or the sequence is reversed. In one of the case the intermediate states is a virtual state, since photon cannot be emitted at least violating one of the conservation law.

### 1.3 Theoretical aspect of ordinary bremsstrahlung

Theoretical investigation of bremsstrahlung processes was started on the basis of classical electrodynamics. The initial attempts were made in 1923 by Kramer's to develop the bremsstrahlung theory on the basis of semi-classical calculation by using correspondence principle. The first Quantum mechanical cross-section formulae for the elementary processes of bremsstrahlung were derived in 1931 by Sommerfeld in the non-relativistic dipole approximation including retardation for non-relativistic electrons without taking accounts the nuclear screening effects. For the relativistic case, by using the Dirac theory Bethe and Heitler (1934), Saunter (1934) and Reach (1934) obtained independently an analytical expression for the OB cross-section by using the first order Born approximation. They neglecting the coulomb field effects on the wave function of incident and scattering electrons on the nucleus. Elbert (1939) and Goth (1941) give the multiplicative coulomb correction factor ( $F_{Elwert}$ ) for Bethe-Heitler OB cross-section ( $\sigma_{BH}(k)$ ). Tseng and Pratt (1971) developed a quantum theory for the bremsstrahlung for relativistic electrons by using screened self-consistent field wave function. Pratt et al. (1977) published extensive tables of OB cross-section for  $Z$  values between 2 and 92 and incident electron energy between 1 and 2000 keV. Berger and Seltzer (1986) calculated the contribution of electron-electron bremsstrahlung given by Pratt et al. (1977). There have been extensive reviews on

the theory of OB Pratt and Feng (1985), Pratt (1995), Seltzer and Berger (1985) and Haug and Nakel ([23-27].

The expression for ordinary bremsstrahlung cross-section in Born's approximation is known as Bethe-Heitler formula. This was first derived simultaneously and independently by Bethe and Heitler (1934), Sauter (1934) and Racah (1934). They obtained the OB cross-section ( $\sigma_{BH}(W_e, k, Z)$ ) is given below -

$$\sigma_{BH}(W_e, k, Z) = \frac{Z^2 r_0^2}{137} \frac{dk}{k} \frac{p}{p_e} \left[ \frac{4}{3} - 2W_e W \frac{p_e^2 + p^2}{p_e^2 p^2} + \frac{E_e W}{p_e^2} + \frac{E_e W_e}{p^2} - \frac{E_e E}{p_e p} + L(A+B) \right]$$

Where

$$A = \frac{8}{3} \frac{W_e W}{p_e p} + \frac{k^2 (W_e W^2 + p_e^2 p^2)}{p_e^3}$$

$$B = \frac{k}{2p_e p} \left( \frac{W_e W + p_e^2}{p_e^2} E_e - \frac{W_e W + p^2}{p^2} E + \frac{2kW_e W}{p_e^2 p^2} \right)$$

$r_0$  = classical radius of electron

$$= 2.818 \times 10^{-3}$$

$$W_e = W + k$$

$$p_e = \sqrt{W_e^2 - 1}$$

$$p = \sqrt{W^2 - 1}$$

$$E_e = \ln \frac{W_e + p_e}{W_e - p_e}$$



$$E = \ln \frac{W + p}{W - p}$$

$$L = \ln \frac{p_e^2 + p_e p - W_e k}{p_e^2 - p_e p - W_e k}$$

$W_e, W$  = initial and final total energy of electron

$p_e, p$  = initial and final momentum of electron

In the non relativistic limit following approximations have been used

- (i) Non screened :  $137Z^{-1/3} \gg (W_e W/k)$
- (ii) Born's approximation :  $(2\pi\alpha ZW_e / p_e); (2\pi\alpha ZW / p) \ll 1$
- (iii) Non relativistic :  $\frac{p_e}{W_e} \ll 1$

The total OB cross-section follows as the limit of equation is given by

$$\sigma(W_e, k, Z) = \frac{Zr_0}{137} \frac{16}{3} \frac{dk}{k} \frac{1}{p_e^2} \ln \left( \frac{p_e + p}{p_e - p} \right)$$

The multiplicative coulomb correction factor ( $F_{Elwert}$ ) for Bethe-Heitler OB cross-

section ( $\sigma_{BH}(k)$ ) is given by

$$F_{Elwert} = \frac{W / p [1 - \exp(-2\pi\alpha ZW_e / p_e)]}{W_e / p_e [1 - \exp(-2\pi\alpha ZW / p)]}$$

This correction factor was derived on the basis of a comparison between the non-relativistic Born-approximation and non-relativistic calculations. For electron energies roughly below 100 keV, Elwert factor give accurate result within 10 %.

## 1.4 Bremsstrahlung in material medium

The various theories OB or BS spectra discussed in the previous sections are applicable to thin target only, in which the monoenergetic electron has only a single radioactive interaction. In the case of thick target, processes such as electron scattering, excitation and ionization that compete with bremsstrahlung are required to be taken into account. In this case an electron loses a significant part of its energy while coming to rest in a target. For continuous Beta particles Bethe and Heitler (1934) gave an expression for the bremsstrahlung spectral distribution  $n(k, W_e', Z)$  in a sufficiently thick target to absorb an electron of energy  $W_e'$  with  $N$  atoms per unit volume. At lower photon energies in thick targets, the correction due to absorption of BS photons in the target and electron backscattering from the target can not be neglected. Seaman and Quarles (2001) have reported that the correction for the self absorption of BS photons in the target and electron backscattering are required for  $n(W_e', k, Z)$  in case of low energy thick target bremsstrahlung. The BS spectral distribution  $[n_{cor}(W_e', k, Z)]$  after absorption correction and electron backscattering correction in thick target is given by

$$n_{cor}(W_e', k, Z) = RN \int_{k+k}^{W_e'} \frac{d\sigma(W_e', k, Z) / dk}{(-dW_e' / dx)} dW_e' \times \exp(-\mu x)$$

Here  $d\sigma(W_e', k, Z) / dk$  is the singly differential cross section taken from the different theoretical models Bethe and Heitler (1934) and Abdormal and Pratt (1999). And  $-dW_e' / dx$  is the total energy loss per unit path length of an electron

in a target material taken from the tabulations given by Berger and Seltzer (2000). Where  $\exp(-\mu x)$  is the absorption factor,  $\mu$  is the mass attenuation coefficient for the given target element taken from the tabulations given by Chandler *et al* (2008) and ' $x$ ' is the optimum thickness of the target which is equal to the range of the beta particle in a target. ' $R$ ' is the electron backscattering factor given by Seaman and Quarles (2001)

$$R = \frac{1 - \eta(W_e, Z)}{1 - \eta(W_e, Z) \frac{k^2}{W_e^2}}$$

Here,  $W_e = 0.4W_{\max}$ ,  $W_{\max}$  is the end point energy of beta particles and  $\eta(W_e, Z)$  is the total backscattering factor. The BS spectral distribution in a thick target obtained on complete absorption of beta particles of a end point energy  $W_{\max}$  is expressed as number of photons of energy  $k$  per unit  $m_e c^2$  per beta disintegration for continuous beta particle is given by  $S(k, Z)$

$$S(k, Z) = \int_{1+k}^{W_{\max}} n_{cor}(W_e', k, Z) P(W_e') dW_e'$$

Here  $P(W_e') dW_e'$  is the beta spectrum of the beta source under study.

The BS photon yield  $T$  for the target, with  $k_{\min}$  and  $k_{\max}$  as the lower and upper limit of photon energy of the BS spectrum respectively is given by

$$T = \int_{k_{\min}}^{k_{\max}} S(k, Z) dk$$

Computer programs are written to calculate the BS spectral distribution in terms of the number of photons of energy  $k$  per unit  $m_0c^2$  per beta disintegration, i.e.  $S(k,Z)$  by using Eqns. ( ) from various theories. The total photon yields  $T$  were obtained for different targets from graphical integration of the BS spectra from the plots of  $S(k,Z)$  versus photon energy  $k$  between  $k_{min}$  and  $k_{max}$ . The experimental and theoretical results were compared in terms of the number of photons of energy  $k$  per  $m_0c^2$  per unit total photon yield. This method makes the results independent of source strength and removes the uncertainties associated with its measurements.

## 1.5 Z-dependence of bremsstrahlung spectra

The bremsstrahlung spectral photon energy distribution depends upon the fundamental cross-section for interaction of an electron with an atom of the target material. The study of dependence of bremsstrahlung spectral photon distribution on the atomic number of the target atom at various electron energies and photon energies is important to know the  $Z$ -dependence of spectral shape of bremsstrahlung. Bremsstrahlung cross-section is proportional to the square of the atomic number of the target atom. For the continuous beta particles the bremsstrahlung intensity is proportional to the atomic number  $Z$  of the target element. The theories which describe the bremsstrahlung processes are adequate to explain the bremsstrahlung cross-section at various electron energies. The  $Z$ -dependence of ordinary bremsstrahlung (OB) spectra has been reported by Hipper et al. (1981) and Seaman and Quarles (1982) for monoenergetic electron. For continuous beta particles Wu (1941) and Evans (1955) reported that the bremsstrahlung intensity is linearly dependent on the



atomic number of the target element ( $Z$ ). The  $Z$ -dependence of the spectral shape of OB spectra for continuous beta particles as a function of photon energy region above 30 keV has been reported by Dhaliwal (2002, 2003, 2005). However, in literature the  $Z$ -dependence of the spectral shape of total bremsstrahlung spectra (BS) and OB spectra for continuous beta particles has not been reported so far particularly in the photon energy region of 5-30 keV. So, there is need to study the  $Z$ -dependence of the spectral shape of BS and OB spectra produced by continuous beta particles, particularly in the photon energy region of 5-30 keV.

In order to investigate the  $Z$ -dependence of the spectral shape of the OB, the  $S(k,Z)$  number of photons of energy  $k$  per unit  $m_0c^2$  per beta disintegration at the photon energy  $k$  can be expressed as a function of  $Z$  and is reported by Dhaliwal (2003) i.e.

$$S(k,Z) = K(k)Z^n$$

Where ' $n$ ' is the index of the  $Z$ -dependence of a photon energy  $k$  per unit  $m_0c^2$  per beta disintegration and  $K(k)$  is the proportionality factor, which is independent of  $Z$  at particular photon energy  $k$ . Knowledge of the index ' $n$ ' is essential for evaluating the  $Z$ -dependence of the spectral shape of OB. Dhaliwal (2002, 2003, 2005) has been study the  $Z$ -dependence of spectral shape of OB produced by continuous beta particles in thick metallic targets and compared their experimental results with the theoretical results obtained from Tseng and Pratt (1971) and Bethe and Heitler (1934) theories which describes OB only. By using the above relation, in the present measurements of bremsstrahlung efforts were made to check the  $Z$ -dependence of the



spectral shape of OB and total bremsstrahlung (BS) spectra which includes the contribution of PB into OB as a function of photon energy in the region 5-30 keV. Theoretical and experimental BS spectral distributions were required for the determination of the Z-dependence index and the proportionality factor K (k) defined at different photon energies. These spectral photon distributions were calculated on the basis of the continuous slowing down approximation given by Seltzer and Berger (1986). In these approximations the rate at which the electron loses energy has two components (i) the average energy loss per unit path length, due to inelastic collision with the bound electron of the medium resulting in ionization and excitation and (ii) the average energy loss per unit path length due to the emission of the bremsstrahlung in the coulomb electric field of the atomic nucleus. The BS spectral photon distribution as a function of the photon energy k has been studied through the Z-dependence index of the bremsstrahlung production by using different beta emitter ( $^{204}\text{Tl}$ ,  $^{90}\text{Sr}$ ,  $^{147}\text{Pm}$ , and  $^{45}\text{Ca}$ ) in the different thick target elements (Al, Ti, Cu, Sn and Pb).

## CHAPTER-2

### FORTRAN CODE

- 2.1 Program for the calculation of Bethe Heitler ordinary bremsstrahlung cross-section

```
WRITE(*,*)'ATOMIC NO. OF THE ATOM'
```

```
READ(*,*)Z
```

```
WRITE(*,*)'INITIAL TOTAL ELECTRON ENERGY'
```

```
READ(*,*)W
```

```
WRITE(*,*)'PHOTON ENERGY'
```

```
READ(*,*)N
```

```
DO 10 K=1,N
```

```
S=W-K
```

```
T=SQRT(S*S-1)
```

```
P=SQRT(W*W-1)
```

```
E1=2.0*ALOG(S+T)
```

```
F=2.0*ALOG(W+P)
```

```
G=2.0*ALOG((W*S+P*T-1)/K)
```

```
A=T/P/K
```

$$B=1.3333-(2.0*W*S*((T*T+P*P)/(P*P)/(T*T)))+(S/P**3)*F+(W/T**3)*E1-((F*E1)/P/T)$$

$$C=(2.6666*W*S/P/T+(K**2/P**3/T**3)*(W**2*S**2+P**2*T**2))*G$$

$$D1=(K/2/P/T)*G$$

$$A1=((W*S+P*P)/P**3)*F$$

$$B1=((W*S+T*T)/T**3)*E1$$

$$C2=(2*K*W*S)/(T*T)/(P*P)$$

$$D=D1*(A1-B1+C2)$$

$$Y1=0.058046*A*(B+C+D)$$

$$Y=Z*Z*Y1$$

$$FMOD=(P/T)*((1-EXP(-860.8*Z/P))/(1-EXP(-860.8*Z/T)))$$

$$C1=(1+0.0000133*Z*Z*(3-W))$$

$$Q=T+P$$

$$R=P-T$$

$$S1=Q/R$$

$$S2=(0.5516)*A\text{LOG}(S1)$$

$$SP1=(0.5516)*(2*A\text{LOG}(Q/R)+A\text{LOG}((Q*Q+0.798*Z)/(R*R+0.798*Z)))$$

$$SP2=(0.5516)*(R*R/(R*R+0.798*Z)-Q*Q/(Q*Q+0.798*Z))$$

$$SP=SP1+SP2$$

FAT=SP-S2

CR= C1\*FMOD\*Y

YT=CR+FAT

CRT= YT\*511.0034E-026

WRITE(5,\*) K , CRT

10 CONTINUE

STOP

END

2.2 Program for the calculation of Elwert Correction factor for ordinary bremsstrahlung cross-section

REAL K1,W,L,S,PI,PE,EI,EE,A1,A2,B1,B2,B3,S1,S2,S3,S4,S5,S6

WRITE(\*,\*)'ATOMIC NUMBER OF THE ATOM'

READ(\*,\*)Z

WRITE(\*,\*)'INITIAL TOTAL ELECTRON IN MC2'

READ(\*,\*)W

WRITE(\*,\*)'PHOTON ENERGY'

READ(\*,\*)N

DO 10 K=1,N

K1=K/511.0034

S=W-K1

PI=SQRT(W\*W-1)

PE=SQRT(S\*S-1)

EI=ALOG((W+PI)/(W-PI))

EE=ALOG((S+PE)/(S-PE))

F1=(2.0\*3.142\*Z\*W)/(137.0\*PI)

F2=(2.0\*3.142\*Z\*S)/(137.0\*PE)

F3=S/PE

F4=W/PI

F5=(2.0\*3.142\*Z\*137)/PI

F6=(2.0\*3.142\*Z\*137)/PE

FMOD=(PI\*(1-EXP(-F5)))/(PE\*(1-EXP(-F6)))

FELWERT=(F3\*(1-EXP(-F1)))/(F4\*(1-EXP(-F2)))

C=1+((Z/137)\*\*2)\*((2-(1-W))/4)



CFMOD=C\*FMOD

WRITE(\*,\*)K,FELWERT,CFMOD

10 CONTINUE

STOP

END

## CHAPTER 3

### RESULTS AND DISCUSSION

The results of experimentally measured BS spectra for the targets of Al and Pb produced by  $^{90}\text{Sr}$  beta particles, were compared with the theoretical external bremsstrahlung spectral photon distributions obtained from Bethe-Heitler theory and Elwert corrected (non-relativistic) Bethe-Heitler theory (EBH) which describes the ordinary bremsstrahlung. The plots of number of photons of energy  $k$  per  $m_e c^2$  per unit total photon yield for Al and Pb targets are shown in the in Figs. 3.1 and 3.2.

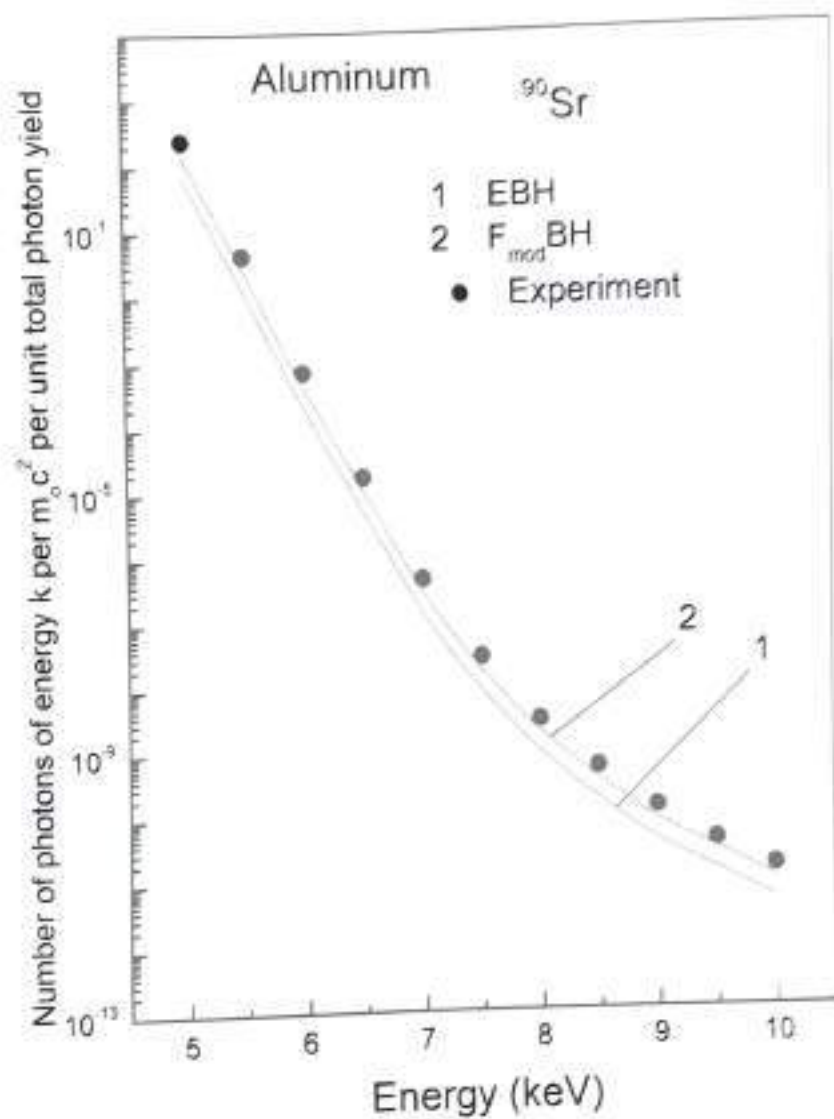
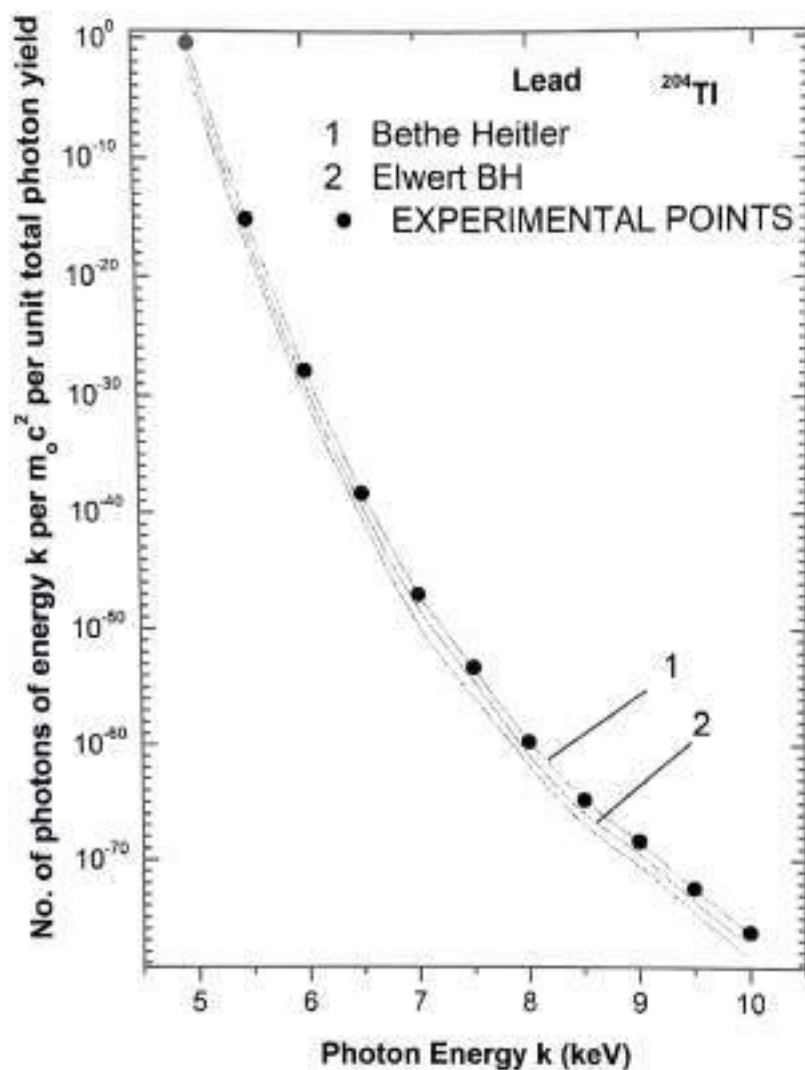


Figure 3.1: The plots of number of photons of energy  $k$  per  $m.c.$  per unit total photon yield for Al target



**Figure 3.2:** The plots of number of photons of energy  $k$  per  $m_e c^2$  per unit total photon yield for Pb target

It is clear from the plots that the experimental BS spectral distributions for Al and Pb target materials are in agreement with the theoretical BS spectral distributions obtained from Elwert corrected (non-relativistic) Bethe-Heitler theory (EBH), within 10 %.

## REFERENCES

- Aston, G. H. 1929 The Amount of Energy Emitted in the  $\gamma$ -Ray Form by Radium E
- Bethe, H. and Heitler, W. 1934. On the stopping of fast particles and on the creation of positive electrons. *Proc. Roy. Soc. Lond. A* 146: 83–112
- Berger, M. and Seltzer, S. 2000. U.S. National Aeronautics and Space Administration Report No. NASA-SP3012 (1964). Current tabulation on the Web: Program ESTAR, <http://physics.nist.gov/PhysRefData/Star/Text/ESTAR.html> (2000).
- Chadwick J. 1912. The  $\gamma$  rays excited by the  $\beta$  rays of radium *Phil. Mag. Series 6*. 24: 1941-5990
- Chantler C T, Olsen K, Dragoset R A, Chang J, Kishore A R, Kotochigova S A, Zucker, D. S. (2005), X-Ray Form Factor, Attenuation and Scattering Tables (Version 2.1). [Online] Available: <http://Physics.nist.gov/ffast> [2008, June] National Institute of Standards and Technology, Gaithersburg, MD.
- Droste, G. F. V. 1938 über Versuche eines Nachweises von  $\alpha$ -Strahlen während der Bestrahlung von Thorium und Uran mit Radium + Beryllium-Neutronen. *Zeitschrift für Physik A Hadrons and Nuclei*. 110: 84-94
- Dhaliwal, A. 2002. Z-dependence of spectral shape of external bremsstrahlung produced by beta particles of  $^{147}\text{Pm}$  and  $^{32}\text{P}$ . *Nucl. Instr. and Meth. B*. 198: 32-36
- Dhaliwal, A. 2003. Study of the Z-dependence of spectral shape of external bremsstrahlung produced by beta particles. *J. Phys. B: At. Mol. Opt. Phys.* 36: 2229-2237
- Dhaliwal, A. S. 2003. Bremsstrahlung spectra produced by  $^{89}\text{Sr}$  beta particles in thick targets *X-ray spectrum*. 32: 367–372
- Dhaliwal, A. 2005. Z-dependence of spectral photon energy distributions of thick target bremsstrahlung. *Nucl. Instr. and Meth. B*. 234: 194-202
- Elwert, G. 1939. Verschärfte Berechnung von Intensität und Polarisation im kontinuierlichen Röntgenspektrum . 178–208
- Elwert, G. and Haug, E. 1969. Calculation of Bremsstrahlung Cross Sections with Sommerfeld–Maue Eigenfunctions. *Phys. Rev.* 183: 90–105
- Gray, J. A. 1911 Secondary gamma -Rays Produced by beta -Rays. *Proc. R. Soc. Lond.* 85:131-139
- Gray, J. A. 1912 The Nature of the gamma -Rays Excited by beta S-Rays *Proc. R. Soc. Lond.* 86:513-529



- Gray, J. A. and Hinds, J. F. 1936. The Gamma-Rays of Radium E. *Phys. Rev.* 49: 477
- Hippler R, Saeed K, McGregor I, Kleinpoppen, H. 1981. Z dependence of bremsstrahlung radiation from free atoms. *Phys. Rev. Lett.* 46 :1622
- Kramers, H. 1923. On the theory of X-ray absorption and the continuous X-ray spectrum. *Phila. Mag.* 46: 836
- Koch, H. and Motz, J. 1959. Bremsstrahlung cross-section formulas and related data. *Rev. Mod. Phys.* 31: 920-955
- Pratt R, Tseng H, Lee C, Kissel L, MacCallum C, Riley, M. 1977. Bremsstrahlung energy spectra from electrons of kinetic energy 1keV to 2000keV incident on neutral atoms  $2 \leq Z \leq 92$ . *At. Data Nucl. Data Tables.* 20: 175-209
- Pratt, R. H. and Feng, I. J. 1985. Electron-atom bremsstrahlung. In Crasemann, B. (Ed), Atomic inner shell physics. Plenum Press, New York, pp. 533-580 (Chapter 12)
- Pratt R, David Shaffer C, Avdonina N. B, Xiao-Min Tong, Florescu, V. 1995. New developments in the theory of bremsstrahlung. *Nucl. Instr. Meth. B* 99: 156-159
- Röntgen, W. 1895. Eine neue Art von Strahlen, Sitzungsberichten der Würzburger Physik-medie, Gesellschaft, Stahl, Würzburg.
- Röntgen, W. 1896. On a new kind of rays. *Nature.* 53:1369 London
- Williams, S. and Quarles, C. 2008. Absolute bremsstrahlung yields at  $135^\circ$  from 53 keV electron on gold film targets. *Phys. Rev. A* 78: 062704
- Semaan, M. and Quarles, C. 1981. Bremsstrahlung spectrum from low-energy electron bombardment of rare gas atoms. *Phys. Rev. A* 24: 2280
- Semaan, M. and Quarles, C. 1982. Z dependence of atomic-field bremsstrahlung. *Phys. Rev. A* 26 :3152
- Semaan, M. and Quarles, C. 2001. A model for low energy thick-target bremsstrahlung produced in a scanning electron microscope. *X-ray Spectrom.* 30:37-43
- Sommerfeld, A. 1931. The deflection and slowing down of electron., *Ann. Phys.* 11: 257-330
- Sauter, F. 1931. Über den atomaren Photoeffekt in der K-Schale nach der relativistischen Wellenmechanik Diracs. *Ann. Phys.* 11: 454-488
- Seltzer, S. and Berger, M. 1985. Bremsstrahlung spectra from electron interactions with screened atomic nuclei and orbital electrons. *Nucl. Instrum. Methods Phys. Res. B* 12: 95-134

Seltzer, S. and Berger, M. 1986. Bremsstrahlung Energy Spectra from Electrons with Kinetic Energy 1 keV-10 GeV Incident on Screened Nuclei and Orbital Electrons of Neutral Atoms with  $Z = 1-100$ . *At. Data Nucl. Data Tables*. 35: 345-418

Tseng, H. and Pratt, R. 1971. Exact screened calculations of atomic-field bremsstrahlung. *Phys. Rev. A*. 3: 100-115

Tseng, H. and Pratt, R. 1974. Electron bremsstrahlung from neutral atoms. *Phys. Rev. Lett.* 33: 516-518

Tsyтович, V. N. Ojringel, I. M. (Eds.) 1993. Polarizational bremsstrahlung. Plenum, NY.

Zon, B. 1977. Bremsstrahlung in collisions between electron and atoms. *Soviet Physics JETP*. 46: 65-68

**PREPARATION OF TRANSITION METAL OXIDE DOPED  
BOROSILICATE BASED BIOACTIVE GLASS**

**PROJECT REPORT**

*Submitted in partial fulfillment of the  
requirements for the award of the degree of*

**MASTER OF SCIENCE**

**in**

**PHYSICS**

*By*

**Dalvir Kaur  
(Reg. 8114-19-1024)**



**DEPARTMENT OF PHYSICS  
SRI GURU TEG BAHADUR KHALSA COLLEGE, SRI ANANDPUR SAHIB  
(An Autonomous College)  
ANANDPUR SAHIB- 140118, PUNJAB (INDIA)**



**SRI GURU TEG BAHADUR KHALSA COLLEGE, SRI ANANDPUR SAHIB**  
(An Autonomous College)  
ANANDPUR SAHIB-140118. PUNJAB (INDIA)

**CERTIFICATE**

It is certificate that the work contained in the project report entitled “ **PREPARATION OF TRANSITION METAL OXIDE DOPED BOROSILICATE BASED BIOACTIVE GLASSES** ” is an original contribution by me and has not been submitted in part or full for any other degree at this or other University/ Institute.

The assistance and help received during the course of the thesis work have been acknowledged.

*Dalvir Kaur*  
**Dalvir Kaur**

Regn. No. 8114-19-1024

I, the undersigned, Supervisor of **Dalvir Kaur**, Reg. No. 8114-19-1024, a candidate for the degree of **Master of Science**, agree that the project report entitled, “**PREPARATION OF TRANSITION METAL OXIDE DOPED BOROSILICATE BASED BIOACTIVE GLASSES**”, may be submitted in partial fulfilment of the requirements for the award of degree.

This is to certify that the above statement made by the candidate is correct to the best of my knowledge.

*Randev Singh*

**Supervisor**

**Dr. Randev Singh**

**HOD and Associate Professor**

**Sri Guru Teg Bahadur Khalsa College**

**Sri Anandpur Sahib**

*Devinder Singh*

**Supervisor**

**Dr. Devinder Singh**

**Assistant Professor**


**Sri Guru Teg Bahadur Khalsa College**

**Sri Anandpur Sahib**

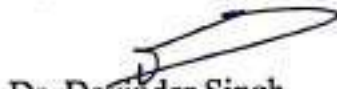


## CERTIFICATE

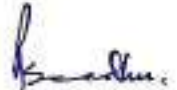
This is to certify that the "Project Report" entitled "**PREPARATION OF TRANSITION METAL OXIDE DOPED BOROSILICATE BASED BIOACTIVE GLASSES**" submitted by **Dalvir Kaur** (Reg. No. 8114-19-1024) to Department of Physics, Sri Guru Teg Bahadur Khalsa College, Sri Anandpur Sahib in partial fulfilment of the requirements for the award of degree of **MASTER OF SCIENCE IN PHYSICS** and has been approved by the Department Research Committee (DRC) after the viva-voce examination of the candidate.



Dr. Randev Singh  
Supervisor



Dr. Devinder Singh  
Supervisor



Dr. Randev Singh  
Chairman DRC



## ACKNOWLEDGEMENT

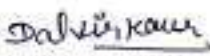
First of all, I would like to thank Almighty for giving me opportunity and guidance to achieve my goals then I would like to acknowledge my Parents of their unwavering support and understanding during the course of this project. Their motivation and belief in my abilities have been a constant source of inspiration.

I would like to thank my talented and supportive supervisor Dr. Randev Singh HOD and Associate Professor and Dr. Devinder Singh Assistant Professor at Department of Physics Sri Guru Teg Bahadur Khalsa College Sri Anandpur Sahib, who have resourcefully guided me throughout this research project. I'm extremely grateful for their motivating discussions which enabled me to accomplish this task successfully. Without their active guidance, support and encouragement I would not have made headway in this project.

A special thanks to Prof. Prabhjot Kaur Assistant Professor at Sri Guru Teg Bahadur Khalsa College Sri Anandpur Sahib for the help and her valuable suggestions whenever I needed out of her busy schedule. I'm also thankful to other faculty members in the department for their encouragement and fruitful academic discussions.

I'm also thankful to my classmates and my friends who have directly or indirectly helped me to complete this project report.

Anandpur Sahib

  
Dalvir Kaur

## CONTENTS

Title	Page No.
Abstract	7
Chapter-1 Introduction	8-9
Chapter-2 Bioactive glasses (Review)	10
2.1 Types of Bioactive glasses	10-11
2.2 Method of Synthesis Bioactive glasses	11-13
Chapter-3 Experimental	14-25
3.1 Preparation of Borosilicate Bioactive glasses	14-17
3.2 Transition metal doped Borosilicate Bioactive glasses	18-19
3.3 Copper Oxide doped Borosilicate Bioactive glass	19-20
3.4 Titanium dioxide doped Borosilicate Bioactive glass	21-22
3.5 Zinc Oxide doped Borosilicate Bioactive glass	22-25
Chapter-4 Characterization	26-31
4.1 X-Ray Diffraction	26-29
4.2 Archimedes Principle	29-31
4.3 Result & Discussion of XRD	32-35
Conclusion	36
References	37-39

## FIGURES TABLE

### Figure No.

- |     |   |
|-----|---|
| 1.  | Melt-quenching Method                             |
| 2.  | Sol-gel method                                    |
| 3.  | Preparation of Borosilicate Bioactive Glass       |
| 4.  | Borosilicate Bioactive Glass                      |
| 5.  | Schematic representation of Bragg equation        |
| 6.  | Basic scheme of an X-ray diffraction              |
| 7.  | Schematic representation of XRD working principle |
| 8.  | Apparatus of Archimedes Principle                 |
| 9.  | Spectra of Borosilicate Bioactive Glass           |
| 10. | Spectra of Copper doped Bioactive Glass           |
| 11. | Spectra of Titanium doped Bioactive Glass         |
| 12. | Spectra of Zinc doped Bioactive Glass             |
| 13. | XRD Spectra of Bioactive Glass                    |

## ABSTRACT

Borosilicate bioactive glasses are a class of material known for their exceptional bioactivity, biocompatibility and versatile properties that make them highly suitable for various biomedical applications. These glasses combine the beneficial characteristics of borate and silicate glasses, offering a unique balance of degradation rates and bioactivity. The incorporation of boron into silicate network enhances the material ability to form hydroxyapatite layers in physiological environment, crucial for bone bonding and regeneration. Borosilicate bioactive glasses are utilized in bone engineering, dental applications and wound healing due to their ability to promote osteogenesis, angiogenesis and antibacterial effects. Recent advancement in the field focus on optimizing their composition and structure to improve their mechanical properties and functional performance, thereby expanding their potential in clinical applications. Research continues to explore the compositional variables and the resultant biological responses to develop next-generation bioactive glasses with tailored functionalities for specific medical needs.



## Chapter-1

### Introduction

The Transition of glass into bioactive glass marks a significant revolution in both the glass and biomaterial fields. Centuries of scientific exploration and technological advancements have led to this momentous development. As the time is progressed, extensive research and the industrial revolution propelled glass production forward, enabling mass manufacturing and refining techniques. In the mid 20<sup>th</sup> century, the emergence of biomaterial led to investigations into materials compatibility with the human body.

In 1960, Larry Hench, a young scientist, merged these fields by introducing bioactive glass. Bioactive glass is great revolution in field of glass and biomaterial. The composition of bioactive glasses is resembled with the composition of human body such as calcium, magnesium and phosphorous etc. Bioactive glasses form hydroxyapatite layer, so it used as a implant device on the place of damage bones. Bioactive glasses are non- crystalline ceramic. These glasses have ability to form a strong bond with living tissue. They are used in field of dentistry. Also bioactive glasses are employed in various medical applications, including dental filling and implants. Over the years, their versatility has expanded to supporting cell growth, tissue regeneration, cancerous tissue replacement (especially bones), drug delivery systems and spinal cord repair.

Borosilicate bioactive glasses are composed primarily of silicon dioxide and boron oxide, along with other oxides such as calcium oxide and sodium oxide. The inclusion of boron in the glass matrix distinguishes these materials from traditional silicate bioactive glasses, influencing their physical and chemical properties.

These glasses can bond with bone and soft tissue when implanted in the body. They are also a mineral similar to the inorganic component of bone, on their surface in physiological environments. The porous structure of borosilicate bioactive glasses allows for the incorporation and controlled release of therapeutic agents, making them suitable for drug delivery systems. Their bioactive properties help in the healing of soft tissues and skin wounds, promoting faster recovery and reducing the risk of infection.

Ongoing research is focused on optimizing the composition and properties of borosilicate bioactive glasses to enhance their performance and broaden their range of

applications. This includes developing new formulations with improved mechanical properties, controlled degradation rates and tailored biological responses.

In conclusion, borosilicate bioactive glasses represent versatile and promising material in the field of biomedicine, offering significant benefit for bone regeneration, dental care, drug delivery and wound healing. Their development continues to advance, driven by the need for more effective and innovation medical solutions.



## CHAPTER-2

### BIOACTIVE GLASSES (REVIEW)

Bioactive glasses are a remarkable type of material capable of bonding with living tissue, making them highly valuable for biomedical applications. They can stimulate bone growth and are commonly used in bone graft, dental implants, and tissue engineering. Their composition enables the release of ions that encourage cell proliferation and tissue regeneration.

Further, bioactivity glasses form a chemical connection with bone and can replace by it. These characteristics make them highly useful in the medical field. Bioactive glasses can bond with both hard and soft tissues [1], whether in vivo or in vitro, by forming a surface layer of hydroxycarbonate apatite through the transfer of ionic species from the bulk material [2].

Bioactive glasses interact with bone through inorganic chemical and biochemical processes triggered by the dissolution products of the glass. Efforts to restore the physiological functions of damaged body parts have a long driven research into discovering and designing new biomaterial for this purpose biologically and chemically, bioactive glasses possess many properties ideal for scaffolding[3][4]. Their high reactivity is a significant advantage in periodontal repair and bone augmentation. When they come in contact with physiological fluids, they form an appetite-like layer on the surface, resembling the inorganic components of bone [5][6]. Additionally, cancer involves the uncontrolled growth of abnormal cells. The aim of treatment is to kill as many cancerous cells as possible while minimizing damage to normal cells. Today, incorporating radionuclide's such as yttrium into bioactive glass could revolutionize cancer therapy [7].

#### 2.1 Types of Bioactive Glasses:

Bioactive glasses are a group of surface-reactive glass-ceramic biomaterials with applications in medical and dental fields. They are known for their ability to bond with bone and soft tissues, and they can stimulate cellular activity and bone regeneration. Here are the primary types of bioactive glasses:

1. **45S5 Bioactive Glass:** The most widely studied and used type, often referred to as bioglass. It has a composition of 45%  $\text{SiO}_2$ , 24.5%  $\text{Na}_2\text{O}$ , 24.5%  $\text{CaO}$  and 6%  $\text{P}_2\text{O}_5$  by weight. It is used in bone grafting, dental applications, and as a coating for implants.
2. **S53P4 Bioactive Glass:** Known for its antimicrobial properties, S53P4 contains 53%  $\text{SiO}_2$ , 23%  $\text{Na}_2\text{O}$ , 20%  $\text{CaO}$ , and 4%  $\text{P}_2\text{O}_5$  by weight. It is used in orthopedic and dental applications, particularly where infection control is critical.
3. **58S Bioactive Glass:** Contains 60%  $\text{SiO}_2$ , 36%  $\text{CaO}$ , and 4%  $\text{P}_2\text{O}_5$ . It is used in bone tissue engineering and regenerative medicine due to its high bioactivity and ability to support bone cell growth.
4. **13-93 Bioactive Glass:** Composed of 53%  $\text{SiO}_2$ , 6%  $\text{Na}_2\text{O}$ , 12%  $\text{K}_2\text{O}$ , 5%  $\text{MgO}$ , 20%  $\text{CaO}$ , and 4%  $\text{P}_2\text{O}_5$ . It has good mechanical properties and bioactivity, making it suitable for load-bearing applications.
5. **Biosilicate Glasses:** These are silicate-based glasses with compositions that can vary, but typically includes oxides like  $\text{SiO}_2$ ,  $\text{CaO}$ ,  $\text{Na}_2\text{O}$ , and sometimes  $\text{Al}_2\text{O}_3$ . They are used in dental applications and bone regeneration.
6. **Phosphate-based Bioactive Glasses:** These glasses have a borate network and can dissolve more rapidly in bodily fluids, releasing ions that can stimulate cellular responses. They are used in soft tissue engineering and as a component in composite materials for bone repair.
7. **Borate-based Bioactive Glasses:** These glasses have a borate network instead of a silicate network, making them more soluble in bodily fluids. This property can be useful in applications requiring rapid resorption and ion release to stimulate tissue repair.

Each type of bioactive glass has specific properties tailored to different medical and dental applications, based on their composition and bioactivity.



## 2.2 Methods of Synthesis Of Bioactive Glasses:

The Bioactive Glasses mainly produced by two techniques are Melt-Quenching Method and the Sol- gel Method. The first bioactive glass itself made by Professor Larry Hench in the 1970 was made through melt-quenched method. And the after 20 years later same glass is prepared by sol-gel method.

### 2.2.1 Melt-Quenching Method:

In melt-quenching method, the mixed composition of the bioactive glass is heated at higher temperature usually above  $500^{\circ}\text{C}$ . In the melt-quenching method, glass is obtained by mixing, homogenizing, calcining and fusing glass precursors in a platinum crucible, the melt is quenched in cold water to obtain a glass frit or cast/quenched in graphite mold to obtain bulk glass [8][9][10]. Important factor to remember while melting a glass are viscosity, thermal expansion and crystallization characteristics.

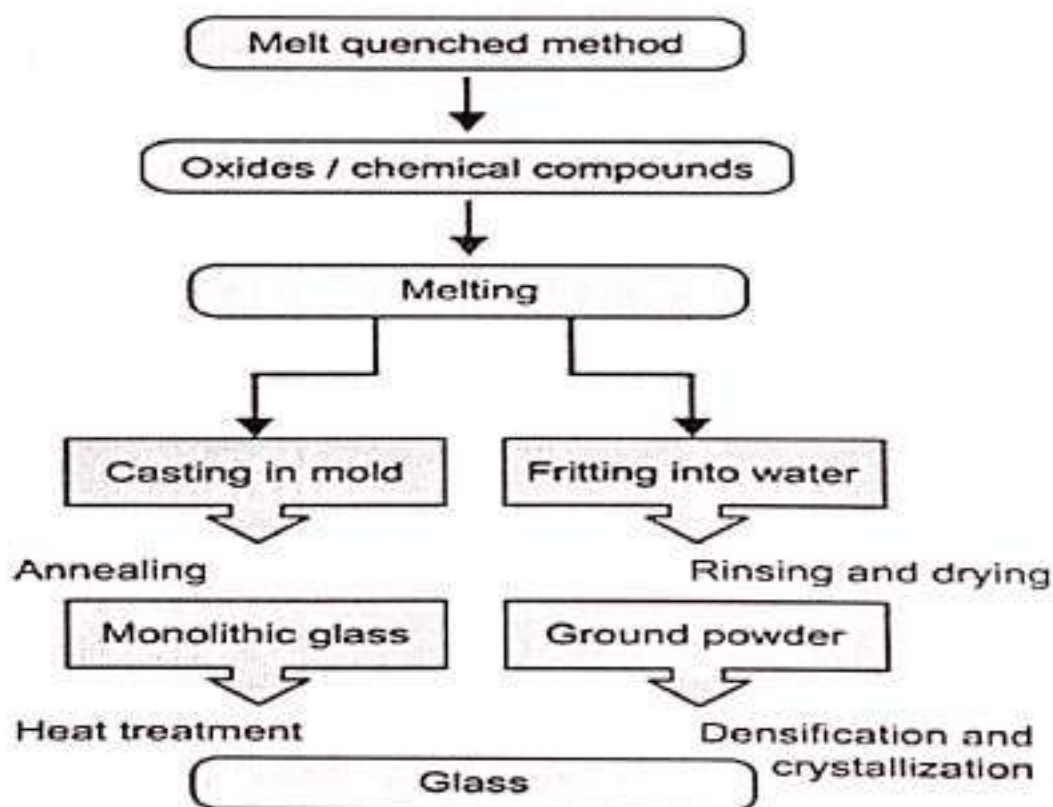


Fig. 1: Melt – Quenching Method

### 2.2.2 Sol-Gel Method:

Sol-gel glasses are made by a chemical based process at much lower temperature than the traditional processing method [11][12]. The Sol-gel method in order to increase the specific surface area and thus the surface reactivity and degradability of material [13]. And

the sol-gel method also provided the control over homogeneity and purity. The preparation of gel glasses by a sol-gel method composed of several steps. First, the alkoxide or organometallic precursors are mixed to form the low-viscosity sol, followed by hydrolysis of liquid alkoxide precursors with de-ionized water [14][15]. While the aging of a gel for several hours at 25-80°C, decreases the porosity and increases in the strength. This is then dried and aged for a long period of time usually weeks, then followed by calcinations to obtain glass granules. These glasses have high porosity.

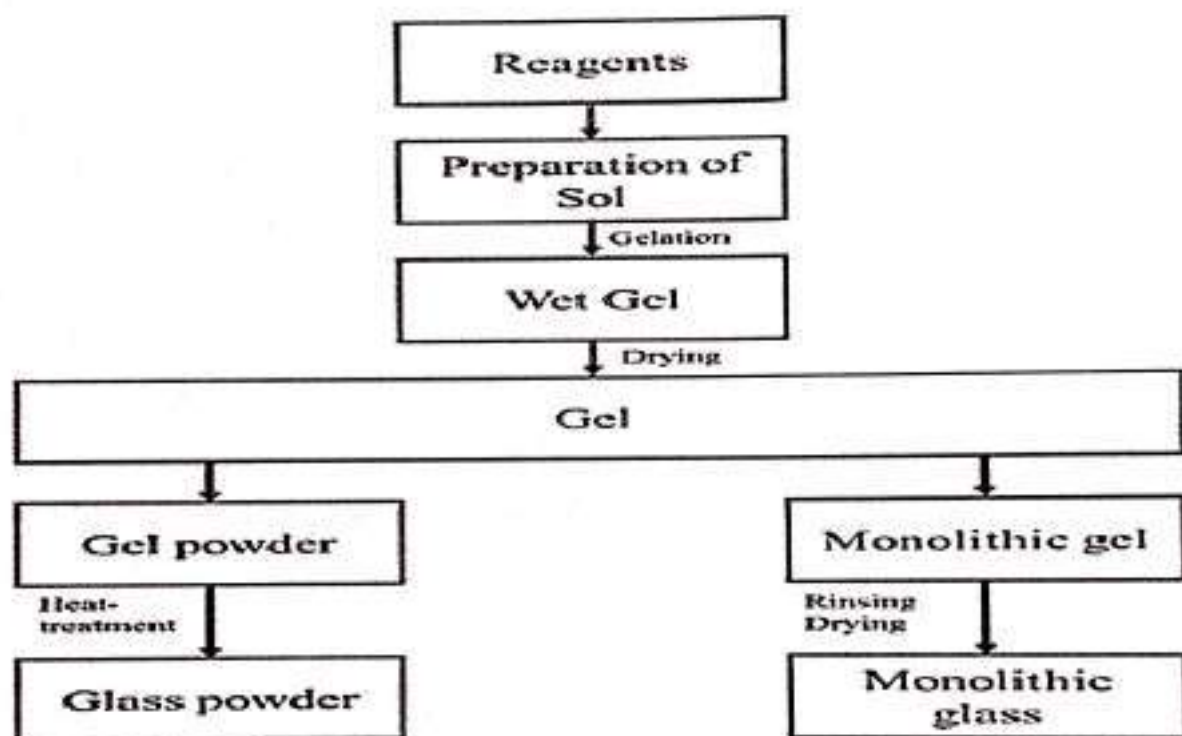


Fig. 2: Sol – gel Method



## **CHAPTER-3**

### **EXPERIMENTAL**

Borosilicate Bioactive glasses are a type of biomaterial that have gained attention for their ability to bond with living tissues, making them suitable for medical applications such as bone regeneration and wound healing. These glasses release ions that promote tissue growth and integrate with surrounding biological environment. They offer promising prospects in various field of medicine, including orthopedics and dentistry.

It composed of primarily of silicon oxide ( $\text{SiO}_2$ ), Boron oxide ( $\text{B}_2\text{O}_3$ ), Sodium oxide ( $\text{Na}_2\text{O}$ ) and Calcium oxide ( $\text{CaO}$ ). It exhibits excellent biocompatibility and bioactivity. These glasses possess unique properties that make them highly attractive for biomedical applications. When in contact with bodily fluids, they form a hydroxyapatite layer on their surface, mimicking the natural mineral phase of bone tissue. This process, known as bioactivity facilitates the integration of the glass with living tissue, promoting cell attachment, proliferation and ultimately, tissue regeneration. The controlled release of ions such as silicon, calcium and further form the glass enhance its bioactivity, stimulating specific cellular responses favorable for tissue repair.

Borosilicate Bioactive glasses have shown promise in various medical fields including orthopedics, dentistry and wound healing. Their biocompatibility, tunable degradation rates and ability to promote tissue regeneration make them valuable candidates for application ranging from bone scaffolds delivery system. Continued research and development in this area holds the potential to advance medical treatment and improve patient outcomes.

#### **3.1 Preparation of Borosilicate Bioactive Glasses:**

Borosilicate Bioactive glasses are prepared by melt-quenching technique. Melt-quenching technique is the most common technique for the production of the Bioactive glasses. The procedure includes melting oxides of Silica, Borate, Calcium, Magnesium and Sodium. [25%  $\text{B}_2\text{O}_3$ , 25% $\text{SiO}_2$ , 25% $\text{CaO}$ , 15% $\text{Na}_2\text{O}$ , 10% $\text{MgO}$ ] at  $1100^\circ\text{C}$  in a crucible and quenched in graphite mold.

Firstly these chemical [25 $\text{SiO}_2$ -25 $\text{B}_2\text{O}_3$ -25 $\text{CaO}$ -15 $\text{Na}_2\text{O}$ -10 $\text{MgO}$ ] is grinded by a ball. Mill a powder of mixture. Then this powder is added in the crucible and these crucible is place in the furnace. Set the function of furnace from  $S_1$  to  $S_8$ . The mixture is melted in



furnace and the melted material is poured into molds of graphite to make the desired shape of glass. At 400°C the glass is kept at 24 hours for slow cooling. For the slowing cooling the glass is placed in the muffle furnace and set the temperature 400°C and then form an amorphous glass. This glass can then be further processed into various forms like powders or scaffolds for biomedical applications.

The composition can vary depending on the specific properties desired for the application. This process is cooled annealing to remove the internal stress from the glasses. The borosilicate bioactive glasses has been tissue engineering due to its bioactivity to enable efficient formation of hydroxyapatite (HA), as well to enhance bone regeneration with bioactive ions released.

Borosilicate bioactive glasses are a class of bioactive material used in biomedical material applications, particularly for bone regeneration and tissue engineering. They are characterized their ability to bond with bone and other tissues, leading to their use in implants, coating, scaffolds. Also by adjusting the composition and processing parameters, the properties of borosilicate bioactive glasses can be tailored to specific biomedical applications. Also by carefully selecting and processing the raw materials, it is possible to tailor the composition and characteristics of bioactive glass to meet specific biomedical needs. Through continued research and optimization, borosilicate bioactive glasses will continued to play a crucible role in advancing medical treatment and improving patient outcomes.

The synthesis of bioactive glass via melting and quenching is a complex process with multiple crucial steps, each essential for achieving the desired properties for biomedical applications. This method is extensively used because it can produce a material with enhanced bioactivity, making it suitable for bone grafts, dental implants and other medical devices. The melt quenching technique is a widely used method for producing glass and amorphous materials. Also choose the raw materials based on the desired composition of the glass or amorphous material. Heat the selected material in a furnace to a temperature above their melting points. This forms a homogenous liquid. Rapidly cool the molten material by pouring it onto a cold surface or into a cold liquid. The rapid cooling prevents the formation of a crystalline structure, resulting in an amorphous or glassy state. Also to relieve the internal stresses and prevent cracking, the quenched material may be subjected to an

annealing process. This involves heating the material to a lower temperature and then slowly cooling it.

**Table 1:** Details of chemical composition of the glasses in mol%

Sr. No.	Sample name	B <sub>2</sub> O <sub>3</sub>	SiO <sub>2</sub>	Na <sub>2</sub> O	CaO	MgO	CuO	TiO <sub>2</sub>	ZnO
1.	Borosilicate Bioactive glass	25	25	15	25	10	0	0	0
2.	Copper doped Borosilicate glass	25	25	15	25	9	1	0	0
3.	Titanium doped Borosilicate glass	25	25	15	25	9	0	1	0
4.	Zinc doped Borosilicate glass	25	25	15	25	9	0	0	1





Fig. 3: Preparation of Borosilicate Bioactive Glasses



### 3.2 Transition Metal Doped Borosilicate Bioactive Glasses

Transition metal ions vital roles as micronutrients in all living organisms, functioning as cofactors in proteins to facilitate their biological activities, regulate their functions and stabilize their structures [16]. In tissue engineering, the involvement of transition metal ions is crucial for triggering diverse biological processes. For instance, metal like nickel and cobalt have been identified as activators of hypoxia-inducible factor, leading to notable enhancement in blood vessel formation within tissue engineering contexts. Recent studies have documented the creation of bioactive glass doped with  $\text{Co}^{2+}$  ions, mimicking hypoxic environments [17]. The functional role of transition metal ions in biological systems can be broken down broadly into non-catalytic functions, redox catalysis and non-redox catalysis. Copper and Manganese have been developed due to their favorable effect on bone and tissue regeneration.

Copper is known to play an important role in angiogenesis as a significant amount of Cu is found in human endothelial cells when undergoing angiogenesis. Also Manganese is another transition metal cation that is an essential key cofactor for Metallo-enzymes, DNA polymerases and Kinesin. The transition metal-doped borosilicate bioactive glasses have garnered significant attention in the field of biomaterials due to their potential applications in bone regeneration and tissue engineering. These glasses are typically composed of a borosilicate glass matrix doped with transition metal such as copper, zinc, cobalt or manganese. The incorporation of these transition metals into the glass structure imparts unique properties to the material, making it suitable for biomedical purposes.

One of the key advantages of transition metal-doped borosilicate bioactive glasses is their enhanced bioactivity. The presence of transition metals can accelerate the formation of a hydroxyapatite layer on the glass surface when in contact with bodily fluids. The hydroxyapatite layer mimics the composition of natural bone mineral, promoting the adhesion of bone cells and facilitating the integration of the biomaterial with the surrounding tissue.

Moreover, these glasses can exhibit antimicrobial properties, particularly when doped with metals like copper or silver. This antimicrobial activity is beneficial for preventing infection at the implantation site, thereby improving the success rate of medical procedures involving the use of these biomaterials.



Overall, transition metal-doped borosilicate bioactive glasses hold great promise for various biomedical applications, including bone grafts, dental implants and controlled drug delivery systems, contributing to advancements in regeneration medicine and tissue engineering.

Therefore, Conducting through experimental investigation is crucible for designing glasses containing transition metal ions with controlled dissolution behavior. These studies are essential for comprehensively understanding the influence of transition metal ions on the structure and their effects on the bioactivity of bioactive glasses.

Transition metal-doped borosilicate bioactive glasses represent a promising field of study with significant potential in medical applications. Their ability to combine the bioactivity of borosilicate glasses with the unique properties of transition metals open new avenues for enhancing the performance and functionality of bioactive materials. Ongoing research is focused on optimizing the material for clinical use and understanding their interaction with biological systems.

### **3.2.1 Copper Oxide (CuO) doped Borosilicate Bioactive Glass**

Copper Oxide doped Borosilicate bioactive glasses are material that contains copper oxide (CuO) as a doping in borosilicate glass.  $25\text{B}_2\text{O}_3\text{-}25\text{SiO}_2\text{-}25\text{CaO-}15\text{Na}_2\text{O-}9\text{MgO-}1\text{CuO}$ . These glasses are designed to have specific biomedical applications due to their bioactive properties. Copper Oxide doping can enhance certain properties like antimicrobial activity or bioactivity making these glasses potentially useful in various medical applications such as bone regeneration or wound healing.

Copper is essential as a micronutrient for the human body, playing a crucible role in maintaining bodily homeostasis. From regeneration point of view, copper is required for the repair of several tissues and organs such as bone and skin. Previously, it has been confirmed that broken bone heal faster when copper is present [18]. Copper is a improve cell proliferation, stimulating new vessel formation as well as inhibiting bacterial growth [19].

Among the most promising strategies developed for tissue engineering in the integration of copper into the structure of bioactive glasses with time, copper containing glasses and glass-ceramics have expanded beyond bone repair applications, finding utility in diverse realms of science and medicine, including cancer therapy. This advancement opens new horizons for biomedical scientists, particularly those specializing in photo thermal-



enhanced chemotherapy [20]. However, the number of in vitro and in vivo studies on cancer therapy restricted and more research conducted in the future to fully disclose the real potential of these constructs in cancer theranostics.

Copper is acknowledged as a crucial metal for the healthy growth and development of human skeleton. Earlier research has elucidated its capacity to induce osteogenic differentiation in mesenchymal stem cell. These biological phenomena could be useful for accelerating the bone healing process. Angiogenesis, the emergence of new blood vessels from existing ones, stands as a crucial factor for the successful regeneration of living tissues. It plays vital roles in delivering nutrients and oxygen while eliminating cellular and tissue waste products.

Copper is known to act as both an antibacterial particles and a surface agent against various bacterial strains [21]. Several well defined mechanisms elucidate how copper can eliminate bacteria, including causing damage to the outer plasma membrane, leading to subsequent disruption of membrane integrity, transport protein activity and ion permeability [22]. Several parameters could affect the antibacterial property of copper, including size, shape, concentration and types of microorganism. While low concentration of copper is essential for regulating critical bodily functions such as homeostasis and bone formation, an excessive amount of this element can generate free radicals, leading to toxicity or inflammation [23]. Also the melt quenching route is maybe the most common technique used for glass production, not only in the biomedical field [24]. Cu-doped melt derived bioactive glasses can be obtained by following two different strategies.

The first copper is incorporated into the glass network by introducing a suitable precursor into the initial batch of reagents, which will then be melted at elevated temperatures and in second, the melt quenching method is employed to create the fundamental copper free glass, which is subsequently doped using ion exchange techniques. These procedures typically involve immersing glass powder in a copper-containing aqueous solution for a specific duration.

The sample starts melt at 700°C. Coupled melt at 1000°C. Kept at 1000°C for 1 hour to make bubble free liquid. Then sample poured at 1100°C and then they are added in graphite mold. Set the temperature of muffle furnace at 400°C and then put the mold in that furnace for the 24 hours for slow cooling.



### 3.2.2 Titanium dioxide (TiO<sub>2</sub>) doped Borosilicate Bioactive Glass

Titanium dioxide doped borosilicate bioactive glasses are material used in biomedical applications. (25 B<sub>2</sub>O<sub>3</sub>-25SiO<sub>2</sub>-25CaO-15Na<sub>2</sub>O-9MgO-1TiO<sub>2</sub>), the titanium dioxide as the applications are particularly in bone tissue engineering. The addition of titanium dioxide enhances the bioactivity and mechanical properties of the glass, making it suitable for implants and scaffolds in bone regeneration. These glasses have the potential to promote the bone growth and integration with surrounding tissue due to their bioactive properties.

Titanium has gained importance recently for its broad range of applications in the biomedical field [25]. The current study focuses on incorporating titanium dioxide into borosilicate glass to create composition that feature a regulated degradation rate and improved biological reactivity. This development aims to produce a material ideal for applications in bone tissue engineering, leveraging titanium widespread use in dental and orthopedic setting. Titanium is acting on both active as well as inert material depending on the host composition.

The glasses with the composition 25B<sub>2</sub>O<sub>3</sub>-25 SiO<sub>2</sub>-25CaO-15Na<sub>2</sub>O-9MgO-1TiO<sub>2</sub> were prepared by melt quenching technique. It has been previously shown by titanium dioxide is cytocompatible and has no significant effect on cell viability [26]. TiO<sub>2</sub> can also increases osteoblast differentiation and promote HA formation by the contact with body fluid [35]. As a result, TiO<sub>2</sub> in directly stimulated angiogenesis by developing new blood vessel which help bone formation and bone repair. In the recent studies have shown that increasing the amount of TiO<sub>2</sub> incorporated in the glass can influence its role as a network modifying oxide in a glass which will consequently influence its solubility [27] and facilitate the modification of the degradation rate .

Numerous investigations into titanium and its alloy indicates their potential biomedical applications due to their capability to directly integrate with the bone tissue [28]. Titanium, extensively studied, serves as a biomedical substance in medical equipment. For example, it can fashion into pure metals, alloy and foams for the acetabular cup component in hip joint replacement. Moreover, titanium coating is frequently applied to medical implants. Based on contemporary understanding of bioactive glass compositions, the proposition in that integrating TiO<sub>2</sub> into the glass and reduce dissolution rates. TiO<sub>2</sub> glass composition exhibit higher mechanical properties than bioglass based compositions [29].



Also  $\text{TiO}_2$  has a tendency to absorb water at surface, resulting in the formation of  $\text{Ti-OH}$  groups. Titanium is widely used as a biomaterial for several dental and orthopedics clinical purpose. In present work, titanium dioxide was incorporated into borosilicate glass to produce composition with controlled degradation rate and enhanced biological response which is suitable material for bone tissue engineering applications. In this context, the present study aims at producing different  $\text{TiO}_2$  doped borosilicate bioglass and also to investigate their bioactivity, cytocompatibility using cell proliferation assays, protein expression studies. When the addition of the  $\text{TiO}_2$  then the decreases the dissolution rate to the glass. Also the addition of  $\text{TiO}_2$  into the glass matrix introduced several advantageous characteristics, making it a promising material for use in various medical device and tissue engineering scaffolds. Bioactivity refers to the ability of a material to form a strong bond with living tissue, promoting osseointegration and facilitating the regeneration of bone.

Moreover,  $\text{TiO}_2$  doped borosilicate glasses exhibit excellent mechanical properties including high strength and fracture toughness. The biocompatibility of  $\text{TiO}_2$  doped borosilicate glasses is another crucial aspect that makes the suitable for biomedical use. In the titanium doped borosilicate bioactive glass, the sample tap start to melt at  $700^\circ\text{C}$ . Coupled melted at  $1000^\circ\text{C}$ . Kept at  $1000^\circ\text{C}$  for 1 hour to make bubble free liquid. The sample is poured as  $1100^\circ\text{C}$  and then set the temperature of muffle furnace at  $400^\circ\text{C}$ , so that they sample is poured at the graphite mold and they put in the furnace for 24 hr. for slow cooling.

### **3.2.3 Zinc oxide ( $\text{ZnO}$ ) doped Borosilicate Bioactive glass**

Zinc oxide doped borosilicate bioactive glasses are a type of material used in biomedical applications, particularly in bone tissue engineering and repair. The addition of zinc oxide enhances the mechanical and biological properties of the glass, making it suitable for use in implants and scaffolds for bone regeneration. These glasses have attracted interest due to their ability to promote bone formation and integration with surrounding tissue.

Zinc is an essential trace element in the human body and has a stimulatory effect on bone formation. The proper amount of zinc can increases the alkaline phosphate activity and DNA content in bone tissue. Also zinc has been introduced into inorganic bone repairing material to promote the proliferation of osteoblasts. Zinc is recognized for its significant role in the metabolism of bones. Also zinc possesses stimulatory effect on bone formation, ability to promote the expression and maintenance of osteoblastic phenotypes in vitro. Despite the established roles of zinc in bone metabolism, the practical use of zinc containing biomaterial



in clinical setting on various factors, particularly safety concerns related to zinc levels. Additionally, the impact of zinc on the degradation and bioactivity of borosilicate bioactive glass is stimulated body fluid, as well as its effect on human bone, marrow-derived stem cells, there is currently no research on properties of zinc doped borosilicate bioactive glass either in laboratory setting or in living organism.

This study aimed to test the hypothesis that scaffolds made from zinc doped borosilicate bioactive glass could promote osteogenesis, making them promising for bone tissue engineering. The study objectives included creating porous 3D scaffold using borosilicate bioactive glass doped with varying level of zinc and assessing the effect on zinc doping on degradation and bioactivity of the glass. Additionally, the in vitro response of human bone marrow derived stem cell to the bioactive glass zinc scaffolds was examined. Moreover, the impact of introducing zinc into the glass on bone formation in osseous defects was systematically investigated using a rodent calvarias defects model in vivo.

Zinc, when added to silicate and borosilicate glasses, enhances their thermal and mechanical properties. In phosphate glasses, zinc enhances chemical durability in water. Additionally, research has shown that zinc, an essential trace element, stimulates bone formations both in laboratory setting and in living organism. Moreover, the controlled release of zinc from implanted material encourages bone growth around the implants, expediting patient recovery [30]. Zinc in the bioactive glass materials has been proposed to stimulate bone cell proliferation and differentiation, and to improve the bone bonding ability to bioglass.

The addition of zinc can contribute to antibacterial properties enhance haemostatic ability and also improve vascularization [31]. Also zinc is crucial for preserving the stability of cell walls and promoting the synthesis of DNA, RNA and proteins. Additionally, it supports the multiplication of fibroblasts, aiding in the process of wound healing [33]. Zinc can regulate thrombotic factor and improve coagulation, demonstrating homeostatic properties [44]. Regardless of the zinc concentration within the bioglass produced via conventional melt quenching, it exhibited toxicity towards human osteoblast cells in biological evaluations.

So we can say that, zinc oxide doped borosilicate bioactive glasses offer several advantages including enhanced bioactivity, improved mechanical properties, controlled degradation rates and potentially antimicrobial properties due to the presence of zinc ions.

Additionally, they make exhibit better biocompatibility and promote osthogenesis, making them promising materials for bone tissue engineering applications. Also the procedure for making zinc oxide doped borosilicate bioactive glass, the sample is melt at  $700^{\circ}\text{C}$ . Coupled melted at  $1100^{\circ}\text{C}$ . Kept at  $1000^{\circ}\text{C}$  for the 1 hr. to make bubble free liquid. Also set the temperature of muffle furnace at  $400^{\circ}\text{C}$  so that the sample is poured at the graphite mold so that the glass make proper shape and the mold is put in the furnace for 24 hr. to slow cooling.



SAMPLE -1



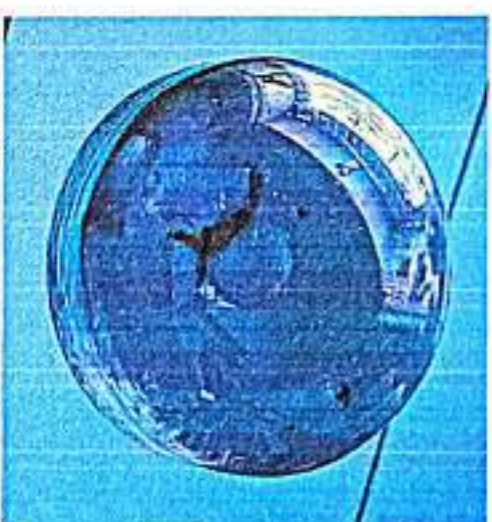
$25\text{B}_2\text{O}_3$ - $25\text{SiO}_2$ - $25\text{CaO}$ - $15\text{Na}_2\text{O}$ - $10\text{MgO}$

SAMPLE-3



$25\text{B}_2\text{O}_3$ - $25\text{SiO}_2$ - $25\text{CaO}$ - $15\text{Na}_2\text{O}$ - $9\text{MgO}$ - $1\text{TiO}_2$

SAMPLE-2



$25\text{B}_2\text{O}_3$ - $25\text{SiO}_2$ - $25\text{CaO}$ - $15\text{Na}_2\text{O}$ - $9\text{MgO}$ - $1\text{CuO}$

SAMPLE -4



$25\text{B}_2\text{O}_3$ - $25\text{SiO}_2$ - $25\text{CaO}$ - $15\text{Na}_2\text{O}$ - $9\text{MgO}$ - $1\text{ZnO}$

Fig. 4: Borosilicate Bioactive glasses

## CHAPTER-4

### CHARACTERIZATION

#### 4.1 X-RAY DIFFRACTION

X-ray diffraction (XRD) is a versatile non-destructive analytical technique used to analyze physical properties such as phase composition, crystal structure and orientation of powder, solid and liquid samples.

Many materials are made up of tiny crystallites. The chemical composition and structural type of these crystals is called their 'phase'. Materials can be single-phase or multiphase mixtures and may contain crystalline and non-crystalline components. In an X-ray diffractometer, different crystalline phases give different diffraction patterns. Phase identification can be performed by comparing X-ray diffraction patterns obtained from unknown samples to patterns in reference databases. This process is like matching fingerprints in a crime scene investigation.

The X-rays produced by the source illuminate the sample. It is then diffracted by the sample phase and enters the detector. By moving the tube or sample and detector to change the diffraction angle ( $2\theta$ , the angle between the incident and diffracted beams), the intensity is measured, and diffraction data are recorded. Depending on the geometry of the diffractometer and the type of sample, the angle between the incident beam and the sample can be either fixed or variable and is usually paired with the diffracted beam angle.

According to Braggs law,

$$n\lambda = 2d \sin \theta$$

Where,  $n$  = An integer (1, 2, 3, -----) which represent to serial order of diffracted beams

$d$  = distance between planes of constituent particles in crystal

$\lambda$  = wavelength of x-ray

$\theta$  = angle between incident x-rays and plane of crystal



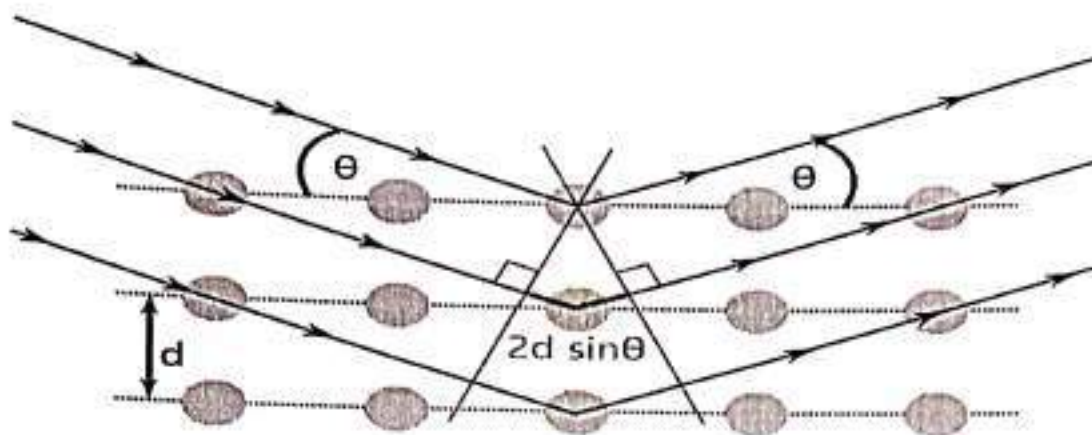


Fig. 5: Schematic representation of Bragg equation

### XRD Instrumentation and Working:

The instrument is called an X-Ray diffractometer. In the diffractometer, an X-ray beam of single wavelength is used to examine the specimen. By continuously changing the incident angle of the X-ray beam, a specimen of diffraction intensity versus the angle between incident and diffraction beam is recorded. The X-rays produced by the source illuminate the sample. It is then diffracted by the sample phase and then enters in the detector.

The main components of diffractometer are,

- X-ray Tube: The source of X- Rays.
- Incident-beam optics : to condition the X – ray beam before it hits the sample
- Goniometer : the platform that holds and moves the sample, optics, detector and tube
- Sample holder
- Receiving – side optics : to condition the X-ray beam after it has encountered the sample
- Detector : to count the number of X-rays scattered by the sample

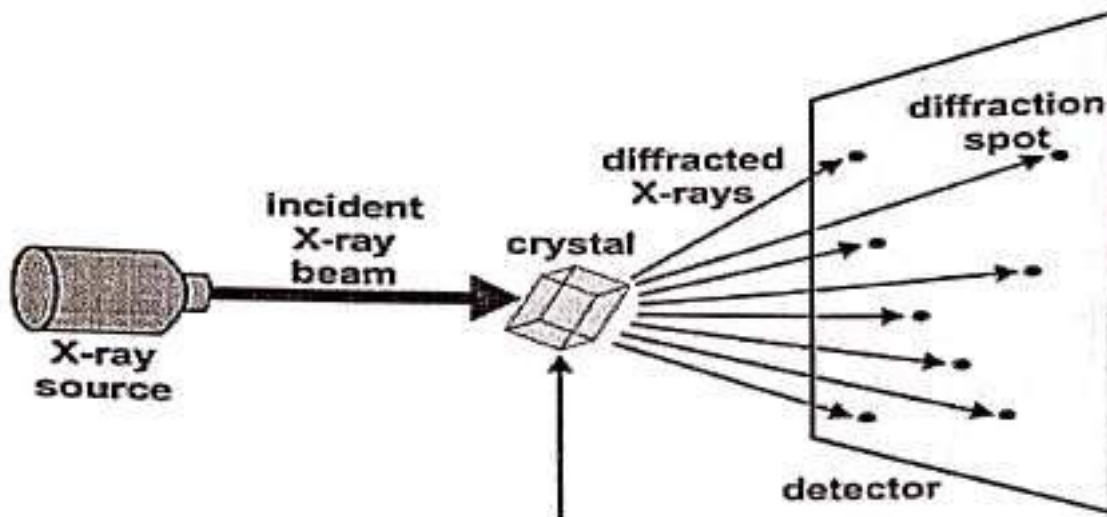


Fig. 6: Basic scheme of an X-ray diffraction

X-rays are a type of electromagnetic radiation, when a monochromatic x-ray scatters from a substance with a structure on this scale, it causes interferences. This interference creates a pattern of lower and higher intensities due to constructive and destructive interference (Bragg's law). If there is a crystalline substance then a three-dimensional pattern is created like the spacing's of planes in the crystal lattice, this process is called constructive interference. By collecting the entire diffracted x-rays one can analyze the samples' structure. The way the X-ray reveals the atomic structure of the crystals is based on Bragg's law. The schematic representations of the XRD are shown in fig.

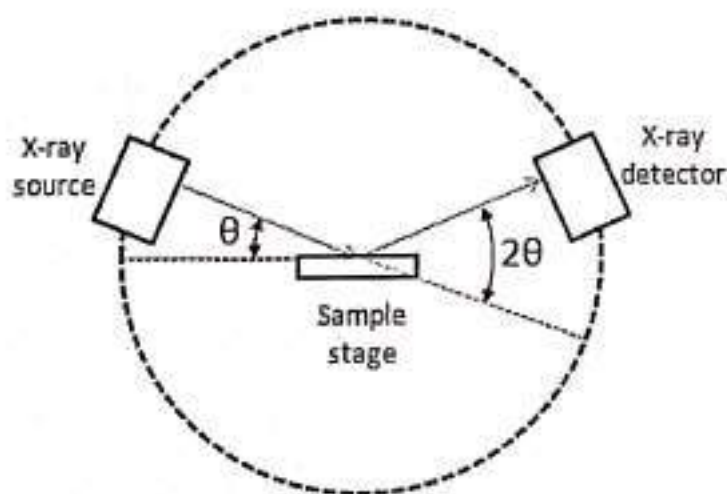


Fig. 7: Schematic representation of XRD working principle

### **Applications of XRD:**

1. Measurement of sample purity.
2. Determination of unit cell dimensions.
3. Characterization of crystalline materials and determine structural properties including.
4. Determine atomic arrangement.
5. Lattice parameters- Strain, Grain size, Epitaxial, Phase composition, preferred orientation.

### **4.2 ARCHIMEDES PRINCIPLE**

“The upward buoyant force that is exerted on a body immersed in a fluid, whether partially or fully submerged, is equal to the weight of the fluid that the body displaces and acts in the upward direction at the center of mass of the displaced fluid”.

The value of thrust force is given by the Archimedes law which Archimedes of Syracuse of Greece discovered. When an object is partially or fully immersed in a liquid, the apparent loss of weight is equal to the weight of the liquid displaced by it.

#### **Archimedes Formula:**

In simple form, the Archimedes law states that the buoyant force on an object is equal to the weight of the fluid displaced by the object. Mathematically written as:

$$F_b = \rho \times g \times V$$

Where,  $F_b$  is the buoyant force,  $\rho$  is the density of the fluid,  $V$  is the submerged volume, and  $g$  is the acceleration due to gravity.

#### **Archimedes principle derivation:**

We know that the density is defined as

$$\text{Density} = \text{Mass/volume}$$

Therefore, the mass of the displaced liquid can be written as follows:

$$\text{Mass} = \text{Density Volume}$$

Now, the weight of the displaced liquid can be calculated as follows:



Weight = Mass  $\times$  Acceleration due to gravity

Weight = Mass  $\times$  g = density  $\times$  V  $\times$  g

From Archimedes' principle, we know that the apparent loss of weight is equal to the weight of the water displaced therefore the thrust force is given by the following equation:

Thrust force = density  $\times$  V  $\times$  g

Where  $\rho$  is the density of the liquid, V is the volume of liquid displaced and g is the acceleration due to gravity.

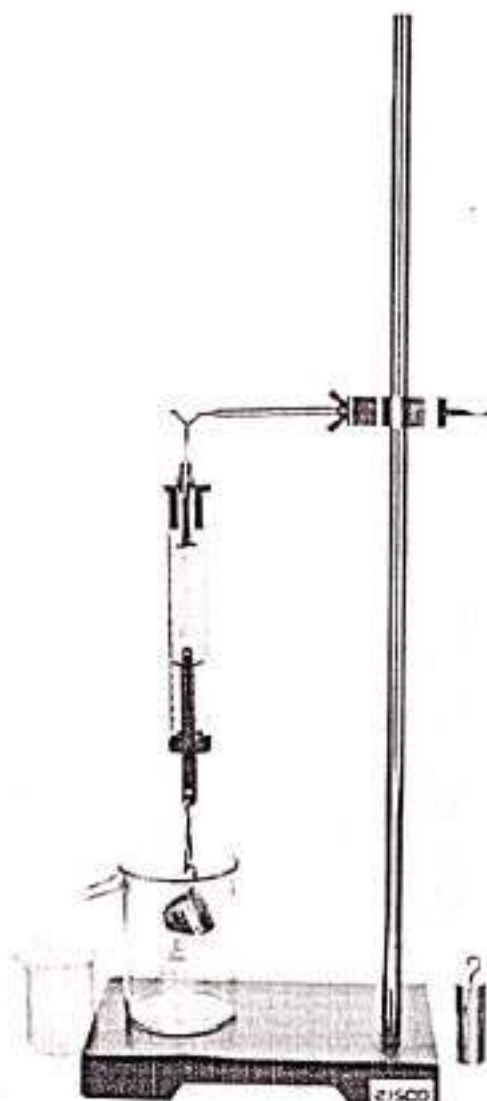


Fig. 10: Apparatus of Archimedes principle

**Applications:**

1. Ship design and floating vessels
2. Hydrometer
3. Hot air balloons
4. Determine volume and density
5. Submarine Buoyancy control
6. Icebergs
7. Swimming and floating

### 4.3 RESULT & DISCUSSION OF XRD

Borosilicate Bioactive glasses are a type of biomaterial that have gained attention for their ability to bond with living tissues, making them suitable for medical applications such as bone regeneration and wound healing. These glasses release ions that promote tissue growth and integrate with surrounding biological environment. They offer promising prospects in various field of medicine, including orthopedics and dentistry.

Copper oxide (CuO) doped borosilicate bioactive glasses have shown significant promise in biomedical applications due to their combined bioactivity, antibacterial properties and ability to promote bone regeneration.

Titanium dioxide (TiO<sub>2</sub>) doped borosilicate bioactive glasses are a type of advanced material studied for their potential applications in biomedical field, particularly in bone regeneration and repair.

Zinc oxide (ZnO) doped borosilicate bioactive glasses are type of material designed for use in biomedical applications, particularly in the field of bone regeneration and repair. Also Zn has inherent antibacterial properties and also play role in bone metabolism.

X-ray diffraction study of borosilicate bioactive glasses shows that a fully amorphous glass structure is obtained.

Fig. 11: SPECTRA OF BOROSILICATE BIOACTIVE GLASS

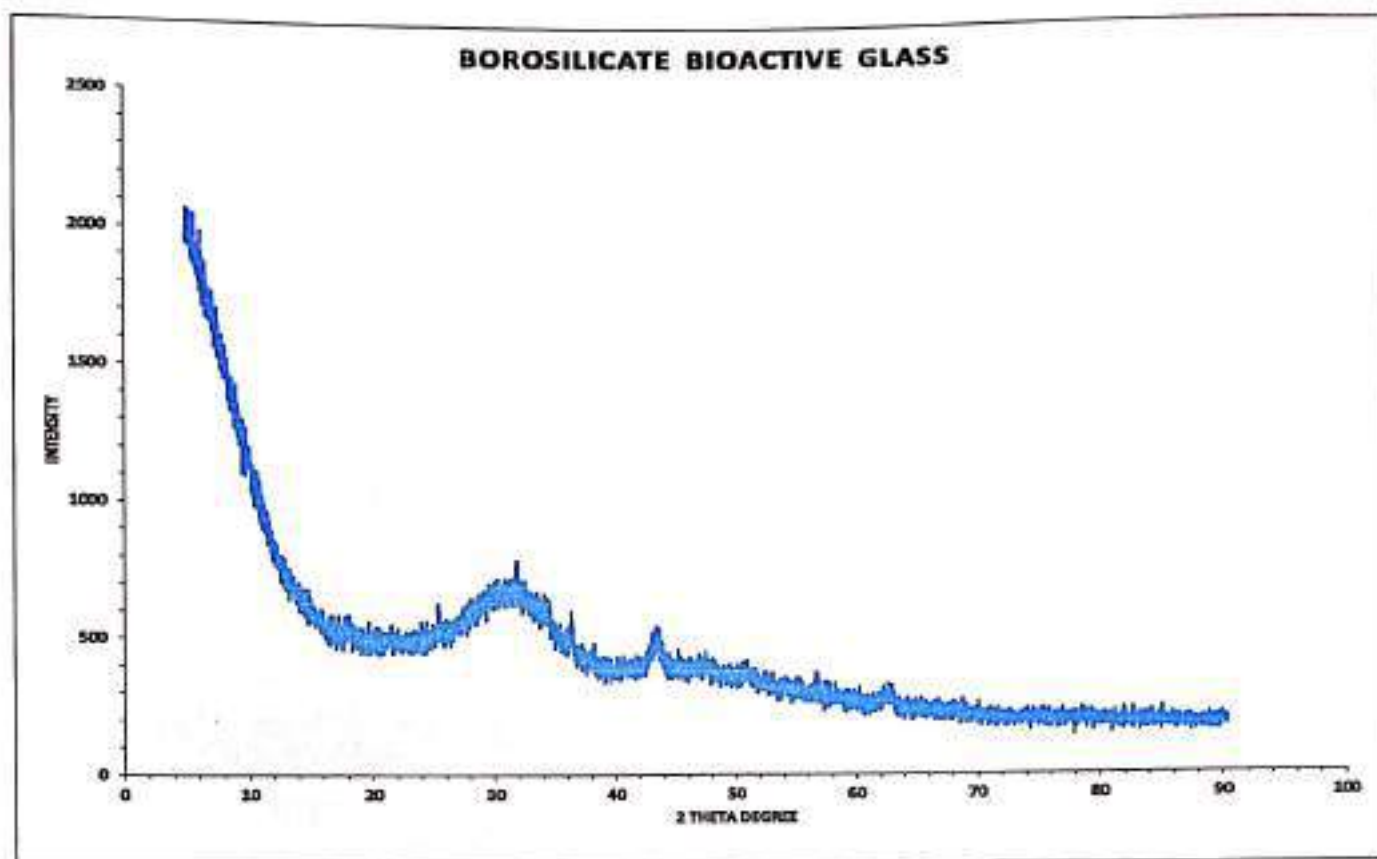


Fig. 12: SPECTRA OF COPPER DOPED BIOACTIVE GLASS

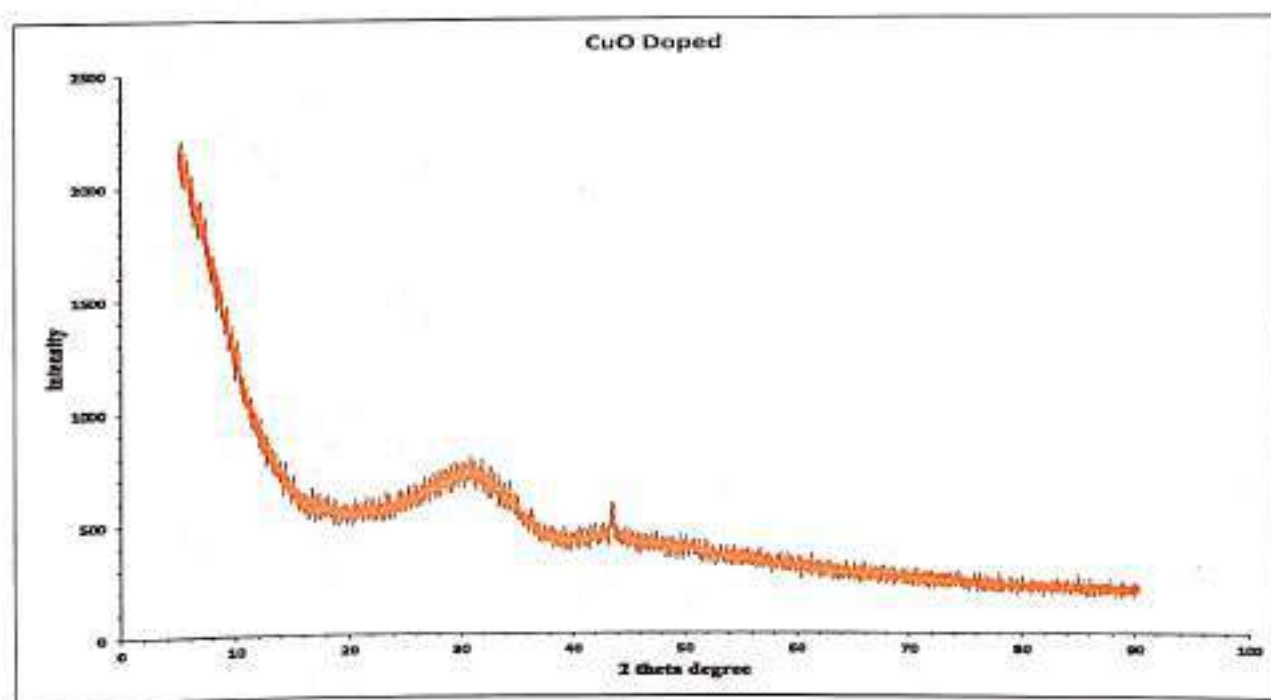


Fig. 13: SPECTRA OF TITANIUM DIOXIDE BIOACTIVE GLASS

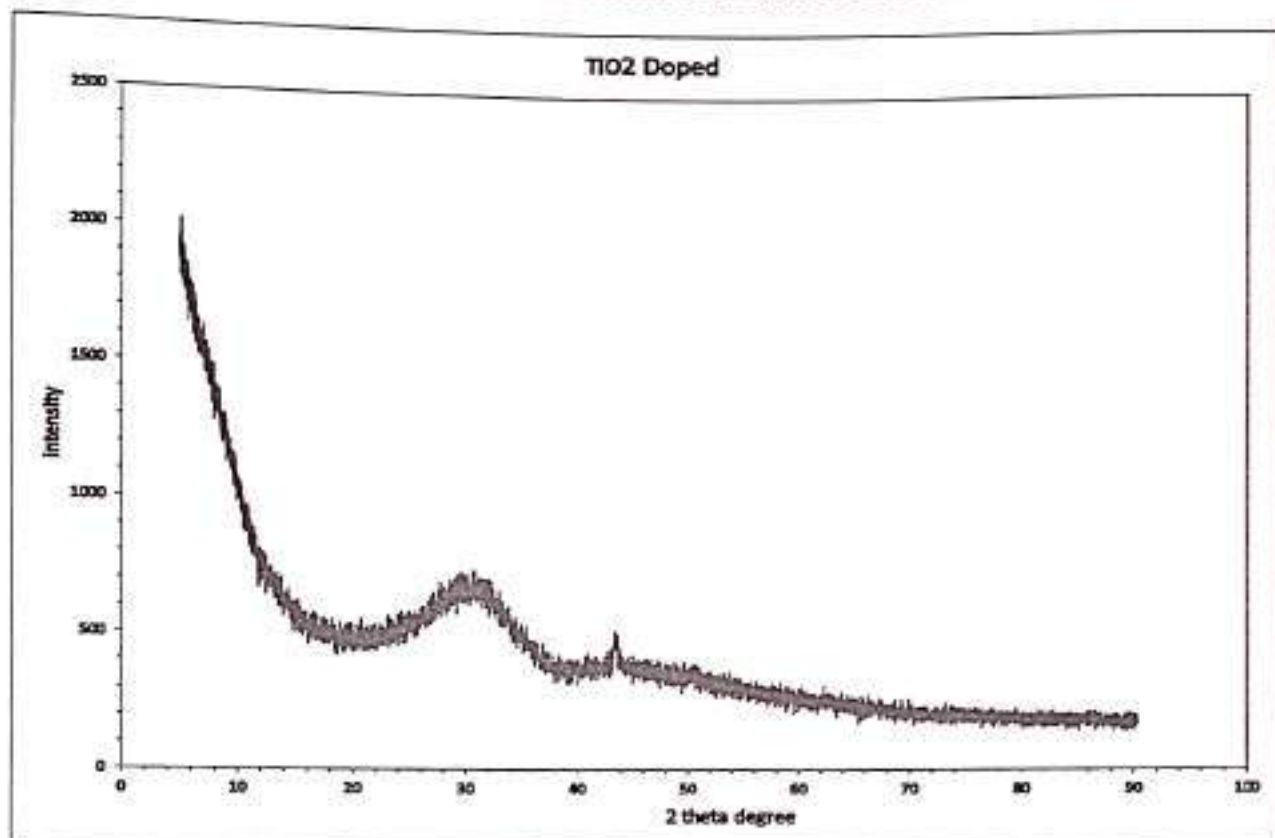


Fig. 14: SPECTRA OF ZINC DOPED BIOACTIVE GLASS

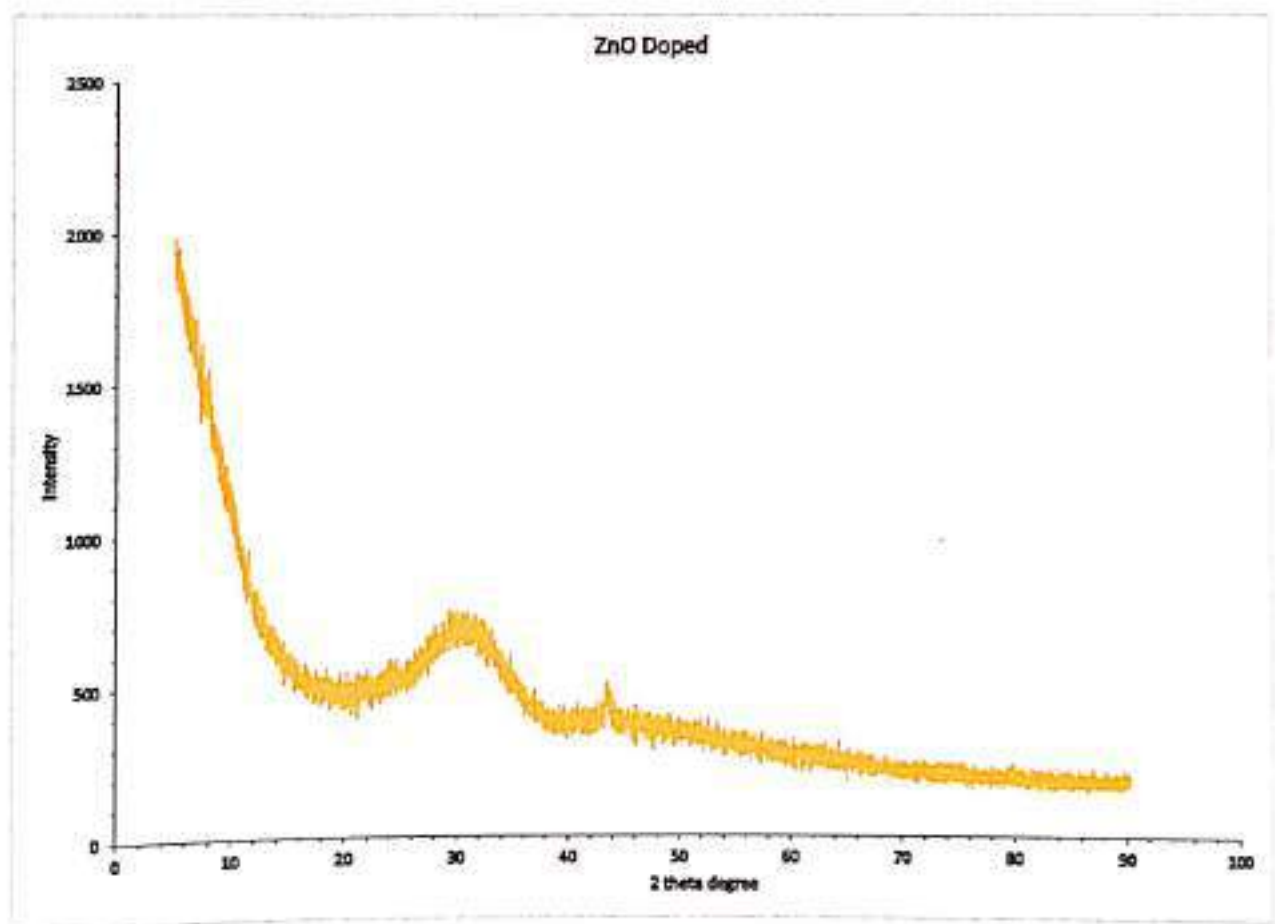
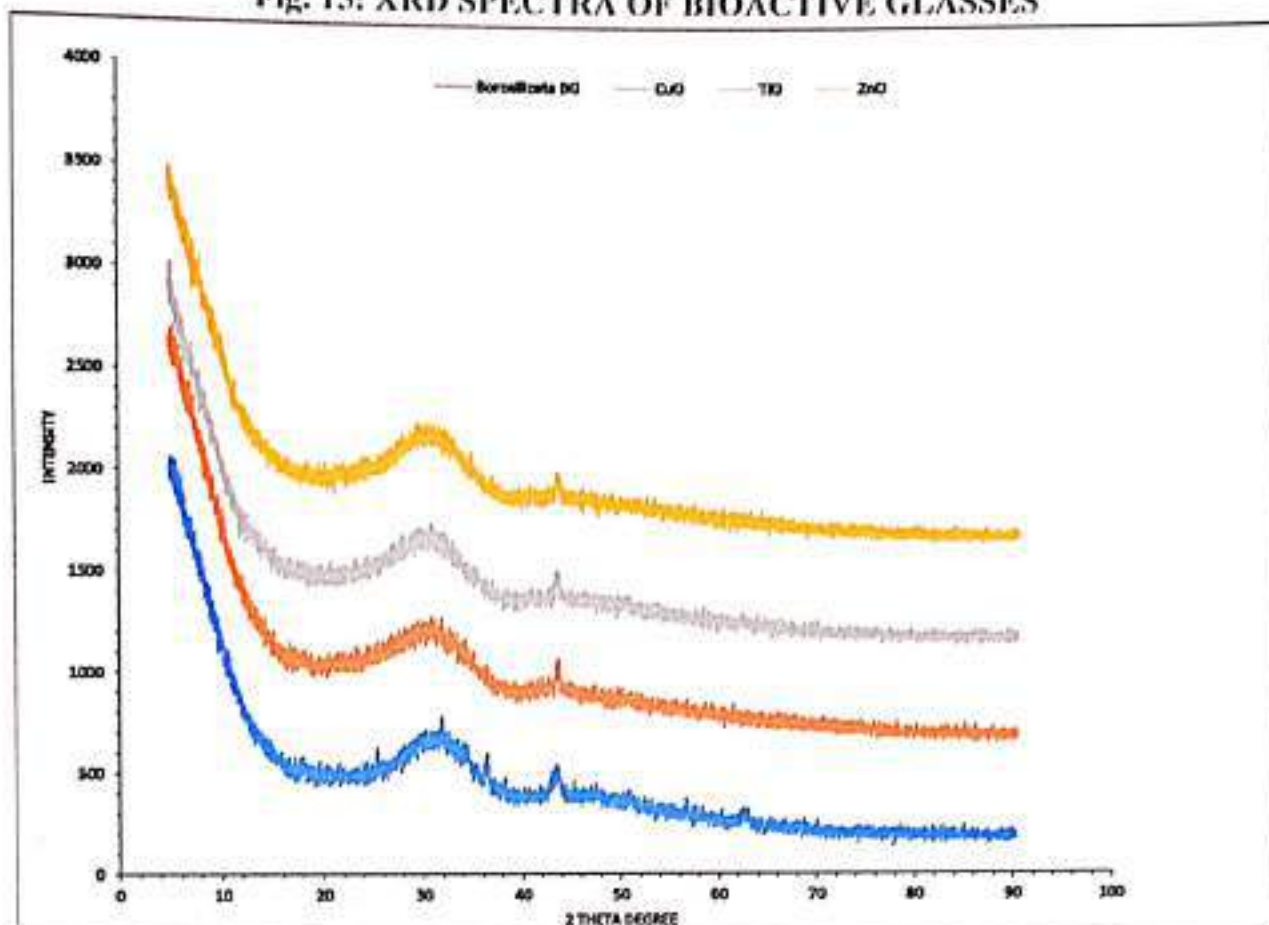




Fig. 15: XRD SPECTRA OF BIOACTIVE GLASSES



## CONCLUSION

The Borosilicate bioactive glasses are prepared by melt-quenching technique. Borosilicate bioactive glasses represent a promising class of materials for advancing medical treatments and improving patient outcomes.

Copper oxide-doped borosilicate bioactive glasses offer a multifunctional approach of biomedical materials, combining bioactivity, antibacterial properties and support of bone regeneration. The potential applications in orthopedics, dentistry and wound care make them a valuable addition to the field of biomaterial.

Titanium dioxide doped borosilicate bioactive glasses represent a promising class of materials for biomedical applications offering a combination of mechanical strength, biocompatibility and enhanced bioactivity.

Zinc oxide-doped borosilicate bioactive glasses offer a multifaceted approach to improving bone healing and regeneration. They combine the inherent benefits of borosilicate bioactive glasses with the additional advantages provided by zinc oxide, making them highly promising for wide range of medical applications including bone graft, tissue engineering scaffolds and coating implants.

## REFERENCES

1. M.N. Rahaman, D.E. Day, B.S. Bal, Q. Eu, S.B. Jung, L.F. Bonewald, A.P. Tomsia "Bioactive glass in Tissue engineering". *Acta Biomaterial* 7(6) ,2355-2373, (2011).
2. Williams DF, " The Williams dictionary of biomaterial", Liverpool university press (1999).
3. D. Allcos and M. vallet – Regi, " Sol-gel silical Based Biomaterial and Bone Tissue Regeneration ", *Acta Biomater*, 6, 2874-2888 [2010].
4. J.J. Jones " Review of Bioactive glass : from Hench to Hybrids," *Acta Biomater*, 9, 4457-4486 (2013).
5. L.L. Hench, R.J. Spliter, T.K. Greenlee and W.C. Allen, " Bonding Mechanism at the interface of ceramic prosthetic materials," *J. Biomed. Matter Res*; 2 ,117-141 (1971).
6. M. Vallet- Regi, C.V. Ragel and A.J. Salinas " Glass with Medical applications," *Eur. J. Inorg. Chem.*, 1029-1042 (2003).
7. Y. Lin, J.C. Mauro, G.Kaur, "Bioactive glasses for cancer therapy", woodhead publishing series in Biomaterial, 273-312 (2019).
8. Jones, J.R, " Review of bioactive glass"; from Hench to hybrid. *Acta Biomater*, 9, 4457-4486 (2013).
9. Hench, L.L; " Bioceramics" ; *J. Am. Ceram. Soc*; 81, 1705-1728 (2005).
10. Hench, L.L; " Bioceramics ; from concept to clinic". *J. Am. Ceram. Sac*;74, 1487-1510 (1991).
11. Liu, J. Mia O, X., "Sol-gel Derived Bioglass as coating material for porous Alumina Scaffolds", *Ceramics international*, 309(7): 1781-5, (2004).
12. Li, N, Jie, Q, Zhu, S, Wang, R, "Preparation and Characterization of Macroporous Sol-Gel processing" , *ceramics international*, 31(5): 641-6, (2005).
13. Li, R, Clark , A, Hench, L, L, "An Investigation of Bioactive glass powders by Sol-gel processing", *Journal of Applied Biomaterial*, 2(4): 231-9, (1991).
14. Vallet – Regi, M, "ceramics for medical applications", *Journal of chemical society, Dalton Transactions*, (2), 97-108, (2001).
15. Iler, R.K., "The Colloid Chemistry of Silica and Silicate", *Soil science*, 80-86, (1955).
16. E. wu et al. "Hypoxiamimicking mesoporous bioactive glass scaffolds with controllable cobalt ion release for bone tissue engineering", *Biomaterial* (2012).



17. H. Ri Co et al. "Effect on bone loss of manganese alone or with copper supplement in ovariectomized rats": a morphometric and densitometric study, *Eur. J. Obstet. Gynecol. Reprod. Biol.* (2000).
18. L. Wang, G Li, L. Ren, X. Kong, Y. Wang, X. Han, W. Jiang, K. Dai, K. Yang, Y. Hao, " Nano-copper-bearing stainless steel promotes fracture healing by accelerating the callus evolution process", *Int. J. Nanomedicine*, 12, pp. 8443-8457, (2017).
19. J. P. Rodriguez, S. Rios, M. Gonzalez J. Cell. " Modulation of the proliferation and differentiation of human mesenchymal stem cell by copper", *Biochem*; 85, pp. 92-100, (2002).
20. L. Chang, Y.Liu, C.Wu, " Copper-doped Mesoporous bioactive glass for photothermal enhanced chemotherapy", *J. Biomed. Nanotechnology*, 14, pp. 786-794, (2018).
21. M. Vincent, R.E. Duval, P. Hartemann, M. Engles – Deutsch, "Contact killing and antimicrobial property of copper", *J. Appl. Microbiol*; 124, pp. 1032-1046, (2018).
22. C. E. Santo, D. Quaranta, G. Grass, " Antimicrobial effect of Monovalent copper ion, room atmospheric applications", *Microbiologyopen*, 1, pp. 46-52, (2012).
23. A. P. Ingle, N. Duran, M. Rai, " Bioactivity, mechanism of action and cytotoxicity of copper based nanoparticles", *Appl. Microbiol. Bioechnol*; 98, pp. 1001- 1009, (2014).
24. L. Hupa, "1-melt derived bioactive glasses", in: H. O. Ylanen (Ed.) *Bioactive glasses*, woodhead pub; pp. 3-28, (2011).
25. S. Rafique, M. Idress, A. Nasim, H. Akbar, A. Athar, " Transition metal complexes as potential therapeutic agents", *Mol. Biol.* 5, pp. 38-45, (2010).
26. J. Y. Wang, B. H. Wicklund, R. B. Gustilo, D. T. Tsulayama, "Titanium, Chromium and Cobalt ions modulated the release of bone-associated cytokines by human nano-cytes/ macrophages in vitro", *biomaterials* 17, 2233-2240, (1996).
27. M. Hashimoto, S. Kitaoka, H. Kanetaka, "Effect of surface change of  $TiO_2$  particles on hydroxyapatite formation in simulate body fluid", *Adv. Powder Technol.* 27, 2409-2415, (2016).
28. L. M. Placek, T. J. Keenan, Y. Li, C. Yatongchai, D. Pradhan, D. Boyd, et al, investigating "The effect if  $TiO_2$  on the st. and biocompatibility of bioactive glass", *J. Biomed. Matter, Res. BAppl. Biomater.* 104, 1703-1712, (2016).
29. Yamaguchi, M, Yamaguchi, R. and Suketa, "Stimulatory effect of zinc on bone formation in tissue culture", *Biochem. Pharmacol.* 35(5) : 773-777, (1987).

30. Ito A, Kawamura H, Ossuka M, Ikeuchi M, Ohgushi H, Ishikawa K, et al. "zinc-releasing calcium phosphate for stimulating bone formation", *matter sci. eng C*; 22: 21-5, (2002).
31. S. Pourshahrestani, E-Zeimiran, N.A. Kadri, N. Gargiulo, S. Samuel, S.V. Naveen, T. Kamarul, M.R.Towler, " Gallium-Containing mesoporous bioactive glass with patent hemostatic activity and antibacterial efficacy", *J. Mater. Chem. B*; 4, pp. 71-86, (2016).
32. B.R. Marriage-arcari, "The role of zinc in wound healing", *wound care Canada*, 14, pp. 18-21, (2016).
33. S. Tubek, P. Grzanka, I. Tubek, "Role of Zinc in hemostasis": a review *Biol. Trace Elem. Res.* 121, pp. 1-8, (2008).



# **Synthesis and characterization of lead Selenide Thin Film & Powder**

## **PROJECT REPORT**

*Submitted in partial fulfillment of the  
requirements for the award of the degree of*

**MASTER OF SCIENCE**

**In**

**PHYSICS**

**By**

**Nirupama**  
**(Reg. No. 8114-2022-1795)**



**DEPARTMENT OF PHYSICS**  
**SRI GURU TEG BAHADUR KHALSA COLLEGE, SRI ANANDPUR SAHIB**  
**(An Autonomous College)**  
**ANANDPUR SAHIB- 140118, PUNJAB (INDIA)**



SRI GURU TEG BAHADUR KHALSA COLLEGE, SRI ANANDPUR SAHIB  
(An Autonomous College)  
ANANDPUR SAHIB-140118. PUNJAB (INDIA)

## CERTIFICATE

It is certified that the work contained in the project report entitled **"SYNTHESIS AND CHARACTERIZATION OF LEAD SELENIDE (PbSe) THIN FILM AND POWDER"** is an original contribution by me and has not been submitted in part or full for any other degree at this or other University/Institute.

The assistance and help received during the course of the thesis work have been acknowledged.

  
Nirupama

Reg. No. 8114-2022-1795

I, the undersigned, Supervisor of Nirupama, Regn. No.8114-2022-1795, a candidate for the degree of Master of Science, agree that the project report entitled, **"Synthesis and characterization of lead Selenide (PbSe) thin Film"**, may be submitted in partial fulfillment of the requirements for the award of degree.

This is to certify that the above statement made by the candidate is correct to the best of my knowledge.

  
Supervisor

Dr. Deep Shikha  
Assistant Professor

Department of Physics

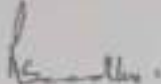
Sri Guru Teg Bahadur Khalsa College

Sri Anandpur Sahib

## CERTIFICATE

This is certify that the "Project Report" entitled "**SYNTHESIS AND CHARCTERIZATION OF LEAD SELENIDE (PbSe) THIN FILM AND POWDER**" submitted by Nirupama, (Regn. No. 8114-2022-1795) to Department of Physics, Sri Guru Teg Bahadur Khalsa College, Sri Anandpur Sahib in partial fullfillment of the requirements for the award of degree of MASTER OF SCIENCE IN PHYSICS and has been approved by the Department Research Committee (DRC) after the viva voice examination of the candidate.

  
Dr. Deep Shikha  
Supervisor

  
Dr. Randev Singh  
Chairman (DRC)

## ACKNOWLEDGEMENT

*First of all, I would like to thank Almighty for giving me opportunity and guidance to achieve my goals then I would like to acknowledge my parents for their unwavering support and understanding during the course of this project, their motivation and belief in my abilities have been a constant source of inspiration.*

*I wish to thank the Principal **Dr. Jasvir Singh** of my college for permitting me to use all the facilities available in the institution for my project work. I would like to thank to Head of the Physics Department **Dr. Randev Singh**, the teacher faculty for their support in completing the work successfully.*

*I am grateful to my Guide **Dr. Deep Shikha** for her encouragement, guidance and supervision of my project work during the semester. I'm extremely grateful for her motivating discussions while enable me to accomplish this task successfully. Without her active guidance, support and encouragement I would not have made headway in this project.*

*A special thanks to Prof. Kajal assistant professor at Sri Guru Teg Bahadur Khalsa College Sri Anandpur Sahib for the help and her valuable suggestions whenever I needed out of her busy schedule. I'm also thankful to my classmates and my friends who was directly or indirectly helped me to complete this project report.*



**Nirupama**

## CONTENT

S. No.	Title	Page No.
1.	Abstract	7
2.	Introduction	8-9
3.	Thin Film Deposition	9-17
3.1	Thin film	9-10
3.2	Growth of Film and Nucleation	10
3.3	Deposition Technique	11-16
3.4	Why Chemical Bath Deposition used?	16-17
4.	Characterization Techniques	17-21
4.1	X-Ray Diffraction	17-18
4.2	Scanning Electron Microscopy(SEM)	18-20
4.3	Transmission Electron Microscopy(TEM)	20-21
5.	Synthesis and Characterization of PbSe Thin film and Powder	21-23
5.1	Experiment	21-23
6.	Result	23-26
7.	Conclusion	27
8.	Reference	28-29



## FIGURES TABLE

S.No.	Title	Page NO.
1.	Crystal Structure of lead Selenide (PbSe)	8
2.	Powder form of Lead Selenide (PbSe)	9
3.	Experimental setup of Chemical Bath Deposition Technique	17
4.	Ray Diagram of XRD	18
5.	Schematic Diagram of Scanning electron Microscope	20
6.	Schematic Diagram of Transmission Electron Microscope	21
7.	Experimental arrangement of deposition of PbSe Thin film by CBD Method	24
8.	Lead Selenide (PbSe) Thin Film by CBD Method	25
9.	Lead Selenide (PbSe) Powder	25
10.	XRD Spectra of Lead Selenide Thin Film	27
11.	XRD Spectra of Lead Selenide Powder	27
12.	Size and Strain graph of PbSe Thin Film	28
13.	Size and Strain graph of PbSe powder	28

## ABSTRACT

Thin films are everywhere in modern world with many of technologies depend upon daily life. The films are considered as backbone for advanced application in various field such as telecommunication devices, energy storage device, optical devices and so on. Thin films are deposited by physical deposition and chemical deposition. The thin film of lead Selenide (PbSe) was prepared by chemical bath deposition. Chemical bath deposition includes principle of chemical vapour depositions. The structural properties of thin films were studied by X-Ray diffraction (XRD) technique. The crystal size and strain values are calculating from data of X-Ray Diffraction.

- The peaks from XRD pattern of (PbSe) indicate its cubic structure.
- Crystallite size of (PbSe) thin film and powder form was measured and found to be ~60.5nm and ~75.9nm respectively.
- From W-H plot we calculate the crystallite size and strain value.

## Introduction

Nowadays, most of technologies are used for minimizing the material into nano size as well as nano thickness. Research on nano crystalline materials is due to their distinctive properties and future applications in semiconductor devices. They are used for study of semiconductor communication, integrated circuit, photoconductors, light emitting diode etc. lead Selenide ( $\text{PbSe}$ ) belongs to group IV-VI compound semiconductor. Due to their properties search groups have shown great interest in study and development of material by various deposition techniques such as electrodeposition, spray pyrolysis atomic layer deposition, spin coating method, sputtering, chemical bath deposition, SILAR method etc. Chemical bath deposition is presently attracting considerable attention, as it does not require advanced instrumentation.

Lead Selenide is an organic compound with formula  $\text{PbSe}$ . It is most important ore and most important compound of lead. It is also known as essential element which means it is essential for life of some species, including human.

Molecular formula:	$\text{PbSe}$
Molecular mass:	286.16g/mol
Melting point:	1078 °C
Crystal structure:	cubic

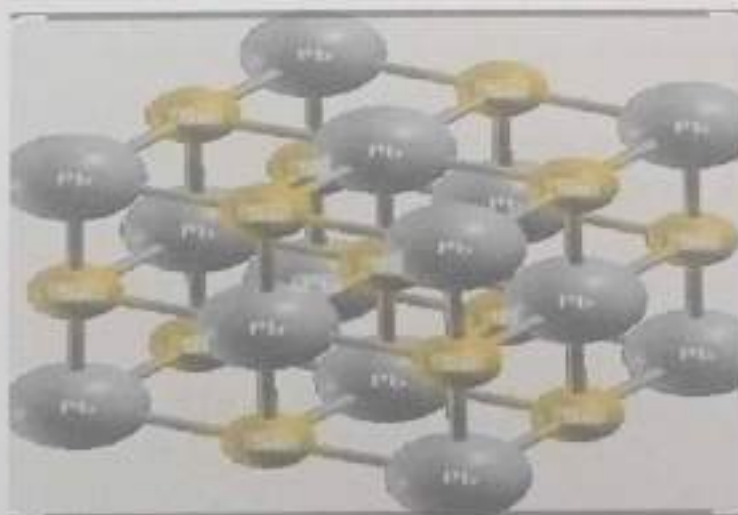


Fig. 1 : crystal structure of lead Selenide ( $\text{PbSe}$ )

**Application of lead Selenide:** -Lead Selenide is semiconductor material. It is oldest and common detection element material in various infrared detectors. It has been extensively used in optoelectronic devices working in infrared region. Lead Selenide find application in following [1,2]

- Infrared detectors
- Gas analysis
- Industrial process and Quality Control
- Defense Applications



**Fig.2: Powder form of Lead Selenide**

### Literature review:

Several studies have explored the synthesis and characterization of lead selenide (PbSe) thin films using various deposition techniques.

**Saloniemi et al. [3]** investigated the electrodeposition of PbSe thin films, focusing on the influence of deposition parameters such as deposition potential, source material concentrations, and current density. **Hankare et al. [4]** demonstrated a straightforward chemical bath deposition method capable of producing uniform, brownish-red PbSe thin films on glass substrates. **Thanikaikan et al. [5]** utilized X-ray diffraction analysis to explain the crystal structure of PbSe thin films. **Hone et al. [6]** investigated the impact of deposition temperature on the structural, morphological, and optical properties of PbSe thin films synthesized via the chemical bath deposition method. This research revealed that films deposited at lower temperatures exhibited an amorphous nature, while increasing deposition temperature led to improved crystallinity.

### References:

1. Saloniemi, H., Kanninen, T., Ritala, M., Leskelä, M., & Lappalainen, R. (1998). Electrodeposition of lead selenide thin films. *Journal of materials chemistry*, 8(3), 651-654.
2. Hankare, P. P., Delekar, S. D., Bhuse, V. M., Garadkar, K. M., Sabane, S. D., & Gavali, L. V. (2003). Synthesis and characterization of chemically deposited lead selenide thin films. *Materials chemistry and physics*, 82(3), 505-508.
3. Thanikaikarasan, S., Mahalingam, T., Dhanasekaran, V., Kathalingam, A., & Rhee, J. K. (2012). Growth and characterization of lead selenide thin films. *Journal of Materials Science: Materials in Electronics*, 23, 1562-1568.



4. Hone, F. G., & Ampong, F. K. (2016). Effect of deposition temperature on the structural, morphological and optical band gap of lead selenide thin films synthesized by chemical bath deposition method. *Materials Chemistry and Physics*, 183, 320-325.

### **3. Thin film deposition**

#### **3.1 Thin film**

Thin film deposition is a process of depositing thin film coating on glass substrate. Whenever growth of material is only in two dimensions that third dimension is negligible to other dimensions, is called thin films. Thin film is a layer of material ranging from nanometer to several micrometers in thickness. Thin film deposition is an important manufacturing step in production of solid state and optoelectronic device. Thin films have directly or indirectly advanced in area of search in solid state physics which based on phenomena of thickness, geometry and structure of thin film. Thin films are used because their properties are different than bulk material. There are different properties of thin film such as optical, magnetic, electrical, thermal, chemical, mechanical properties. The properties of thin films are more affected by surface to volume ratio.

There are several methods used for deposition of thin film. Thin film deposition is mainly classified by physical and chemical methods. lead Selenide thin film is prepared by both physical and chemical deposition. In physical deposition process electromechanical and thermodynamic methods are used to produce thin film. Physical deposition system requires low-pressure vapor environment to function properly. In chemical deposition technique, a fluid precursor undergoes chemical change at solid surface and leaving solid layer. Among all these chemical bath deposition methods was chosen for preparation of thin film because physical methods are costly and required advanced instrumentation.

Any thin film deposition method process involves three main steps:

1. Production of appropriate atomic, molecular species.
2. Transport of these species to substrate.
3. Condensation on substrate[7]

#### **3.2 GROWTH OF THIN FILM AND NUCLEATION**

The phenomenon of formation of a stable nucleus is called Nucleation. The initial process that occurs in the formation of a crystal from a solution, a liquid, or a vapor, in which a small number of ions, atoms, or molecules becomes arranged in a pattern characteristic of a crystalline solid, forming a site upon which additional particles are deposited as the crystal grows. There are two stages in the crystallization process: nucleation and growth.



In the first nucleation stage, a small nucleus containing the newly forming crystal is created. Nucleation occurs relatively slowly as the initial crystal components must impinge on each other in correct orientation and placement for them to adhere and form the crystal. After successful formation of a stable nucleus, a growth stage ensues in which free particles (atoms or molecules) adsorb onto the nucleus and propagate its crystalline structure outwards from the nucleating site. This process is significantly faster than nucleation. The reason behind such rapid growth is that crystals contain dissociations and other defects, which act as a catalyst for the addition of particles to the existing crystalline structure. By contrast, perfect crystals (lacking defects) would grow exceedingly slowly. Most often, the properties of the film are affected by the underlying properties of the substrate and can vary drastically depending on the thickness of the film and the deposition technique employed for deposition.[3]

There are three major steps required in thin film growth and nucleation. The first step involves the creation of deposition species, i.e., the substrates and the target material, followed by the transportation from the target to the substrate using any deposition technique and the final stage involves the growth of the target on the substrate to form the thin film. A nucleus can grow in the two modes named parallel and perpendicular depending on the configuration of the substrates and target, and the two scenarios can be experienced in a single deposition. Parallel growth occurs on the substrate by surface diffusion of the absorbed atoms while perpendicular growth is because of direct impingement of the incident species. However, the rate of parallel growth is sometimes called lateral growth, at this stage is much higher than perpendicular growth and the grown nuclei are called islands.

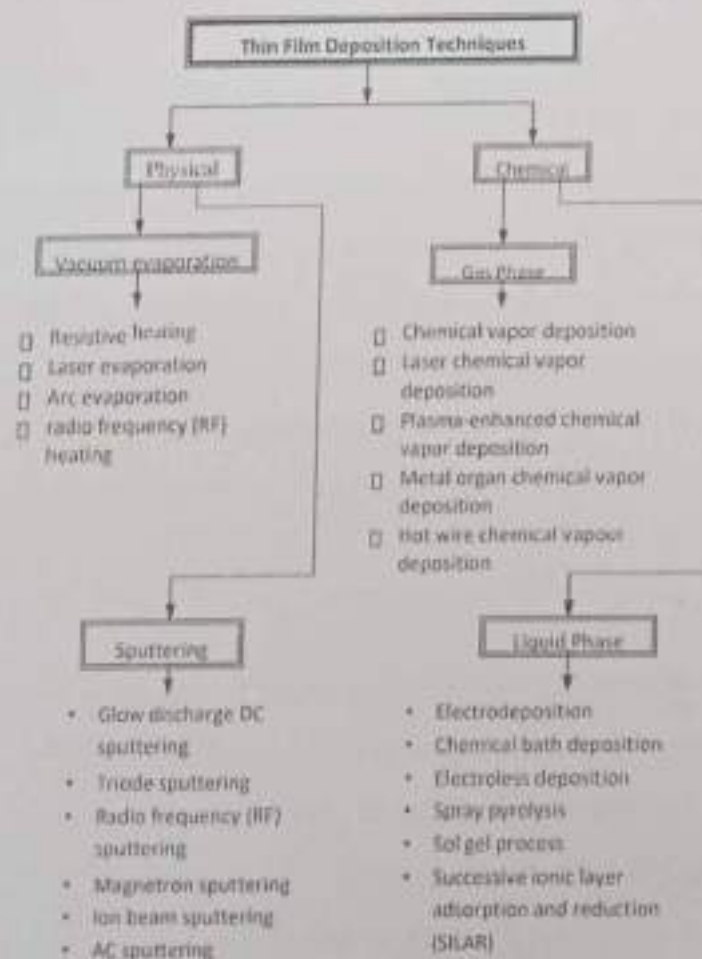
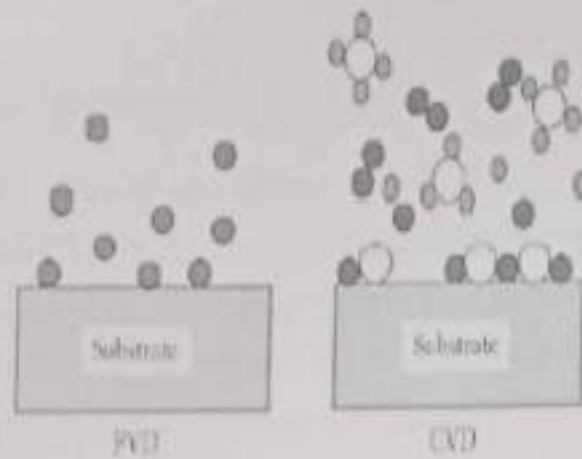
### 3.3 Deposition techniques

Thin films have distinct advantages over bulk material. Most of deposition techniques are used for formation of thin films. A deposition technique is considered as integral key for creation of thin film new materials due to increasing demand from industries for versatile and multi-dynamics materials. The deposition techniques all properties of thin film and can also be modify the existing properties. Combination of different techniques can also be used to form a hybrid deposition with each contributing to outcome of thin film. In the present time thin films can be fabricated in various method.

There are several types of thin film deposition techniques. The subset of deposition techniques are physical vapour deposition (PVD) and chemical vapour deposition (CVD). The distinguishing between PVD and CVD is in vapour. In PVD, the vapour is made up of atom and molecule simply in condense on substrate, and for CVD the vapour undergoes chemical reaction on substrate which resulted into thin film. Physical

deposition system requires low-pressure vapor environment to function properly. In chemical deposition technique, a fluid precursor undergoes chemical change at solid surface and leaving solid layer.[7],[8]

In PVD uses physical processes and use pure source material while in CVD uses chemical process and mixed source material.



### 3.3.1 ELECTRODEPOSITION:

Electrodeposition is widely utilized in making metallic coating. This technique is very old process which involve coating a thin layer of metal on top of different metal. It can be understood as extraordinary electrolysis resulting in deposition of solid material on electrode. This process involves saturated solution of charged development species through arrangement when external electric field is applied. Reduction of charge development species at growth and deposition surface which also such as electrode. This process is also known as electroplating.

### 3.3.2 ELECTROLESS DEPOSITION

In electroless deposition film of metal may deposit directly without any electrode potential being involved by suitable compound in solution. This is also called chemical reduction plating. In electroless deposition film can be grown on glass substrate by dipping them in appropriate solution of metal salt and reducing agent without any electric field. Deposition may occur by homogenous chemical reaction; reduction of metal ion in solution by reducing of metal ion in solution by reducing agent. There are three types of reaction take place:

- Non catalytic reaction where types of substrates used.
- Catalytic reactions were used where film formation takes place on metallic substrates.
- Catalytic reaction using activator where deposition takes place with help of activate non catalytic surface.

### 3.3.3 CHEMICAL BATH DEPOSITION

It is also called solution growth technique. CBD is method of deposition of thin film and nanoparticles is based on formation of solid phase from liquid solution. This technique is easy. In CBD two steps are involved in formation of phase from precursors solution as formation of nucleation particle growth. The necessary step precursors solution as formation of nucleation particle growth. The necessary step is that molecules cluster form undergoes rapid decomposition and particles combine to form film on substrate. Formation of film also depends on deposition condition such as bath temp, stirring rate, pH, concentration of solution. Growth may occur through ion concentration of material. This technique is mostly used to prepare Chalcogenide (Sulphur, selenium etc.) film as well as metal oxide film.[1]

### 3.3.4 SOL GEL METHOD:

This technique is broadly used for synthesis of oxide material. Sol gel processing is high purity and uniform nanostructure achievable at low temperature. In this method molecule precursors are dissolved in water or alcohol and converted to gel by heating and stirring by hydrolysis. The gel we obtained from hydrolysis process is wet, it should be dried. After drying we get powdered. The Sol gel method can be used in the process of making ceramics as molding material and used as intermediate by thin film of metal oxides in



Various application. A sol gel process involves formation of sol in liquid and then connecting sol particles to form porous network by drying liquid possible to obtained powder thin films.[12,13]

### **3.3.5 SPRAY PYROLYSIS METHOD:**

Spray coating technique may be one of the most useful coverings surfaces. In this method thin film is deposited by spraying solution on heated surfaces where constituent react to form chemical compound. Spray pyrolysis equipment consist of atomizer, precursor sol. Substrate heater and temperature controller. This technique involves spraying a metal salt solution onto a heated surface. Spray pyrolysis is a process in which nanostructure is obtained when a solution contained a precursor is spray using nano porous nebulizer on hot substrate in furnace. It is an aerosol process that atomizes a solution and heats the droplet to produce solid particles. Pyrolysis means decomposition of chemical compound under action of heat at higher temperature

- Transform liquid precursor or sol precursor into ionized droplets.
- Making solvent to evaporate
- Allowing solute to condense
- Making solute decompose and react
- Sintering the solid particles

### **3.3.6 SILAR METHOD:**

SILAR is successive ionic layer absorption and reaction. This is one of the most suitable for preparing semiconductor material. In Silar method thin films are obtained by immersing substrate into separately placed cationic and anionic precursor and rinsing between every immersion with ion exchanged bath. Rinsing time in ion exchange bath is critical for ionic layers formation.

- Immersion of substrate in cationic
- Immersion of substrate in distilled water
- Immersion of substrate in anionic
- Immersion of substrate in distilled water

### **3.3.7 SPIN COATING TECHNIQUE:**

This method has ability to quickly and easily product very uniform films

- Deposition
- Spin up
- Spin off
- Evaporation

Initially solution is cast on to substrate using pipette, whether substrate is already spinning after deposition, the centrifugal motion will spread the solution across suitable. Most of the solutions are expelled from substrate. The fluid now begins to thin film will change color due to interference effect, when color stops changing, this will indicate that film is mostly dry, fluid out of flow stops and thinning is dominated by evaporation of solvent.

### 3.3.8 ELECTRO BEAM EVAPORATION:

In electron beam evaporation where intensive beam of electrons is generated from filament and steered through both electric and magnetic fields to hit target and vaporize it under vacuum environment. Thin film prepared by electron beam evaporation is good quality and purity. Large categories of materials can be prepared by electron beam evaporation technique. The electron system only heats the target source material, not the entire container resulting in lower degree of contamination from the container by concentrating energy on target rather than entire vacuum chamber, it helps reduce the possibility of heat damage substrate. Electron beam evaporation used in variety of application ranging from high performance aerospace and automobiles industries. [[4-16]

### 3.3.9 SPUTTERING:

Sputtering is usually understood as sputter deposition. It is a physical vapors deposition process. It is the process of directing high energy ions to target in vacuum and remove target atoms. The deposition of these emitted atoms on surface is called sputter deposition. The requirement for sputtering deposition is ion beam and potential low pressure (less than 5m torr), good vacuum. Sputtering is a process in which particles are ejected from solid target materials due to bombarding of target by energetic particles. The kinetic energy of incident particles should be greater than thermal energy. [[7,18]

### 3.3.10 PULSED LASER DEPOSITION:

It is a powerful method to grow thin films and multi layers complex material. It is technique where high power laser beam focused inside vacuum chamber to strike target of desired composition material is then vaporized from target as deposited as thin film on substrate such as silicon wafer facing target. The process can occur in ultra-high vacuum or in presence of background gas such as oxygen which is commonly used when depositing oxide to fully oxygenated deposited films. The process of Pulse laser deposition can schematically be divided into four stages:

- Laser analysis of target material and creation of plasma.
- Dynamics of plasma under vacuum.
- Deposition of material on substrate.



- Nucleation and growth of film on substrate surface.[7]

### 3.3.11 CATHODIC ARC DEPOSITION (ARC-PVD):

This is a physical vapor deposition technique in which an electric arc is used to vaporize material from a cathode target. The vaporized materials are then condensed on a substrate and form a thin film. This technique is being done to deposit metallic, ceramics, and composite films.

### 3.3.12 ELECTRO HYDRODYNAMICS DEPOSITION (ELECTRO SPRAY DEPOSITION):

This is a relatively new process of film deposition. The liquid can be deposited either in the form of nanoparticles solution or simply a solution and it is fed to small capillary nozzle (usually metallic) which is connected to high power sources. The substrate on which the film will be deposited is connected to the ground terminal of the power source. Through the influence of electric field, the liquid comes out of the nozzles and takes a conical shape (Taylor cone) and at the apex of the cone a thin jet emanates which disintegrates into very fine and small positively charged droplets. The droplets keep getting smaller and smaller and finally get deposited on the substrate as a uniform thin layer.

### 3.4 Why chemical bath deposition?

This is chemical liquid phase method. Chemical bath deposition is one of the most suitable methods to get uniform, good reproducibility thin film. It is one of the cheapest methods to deposit thin film. As it does not depend upon expensive equipment and scalable technique that can be employed for large area batch processing or continuous deposition.

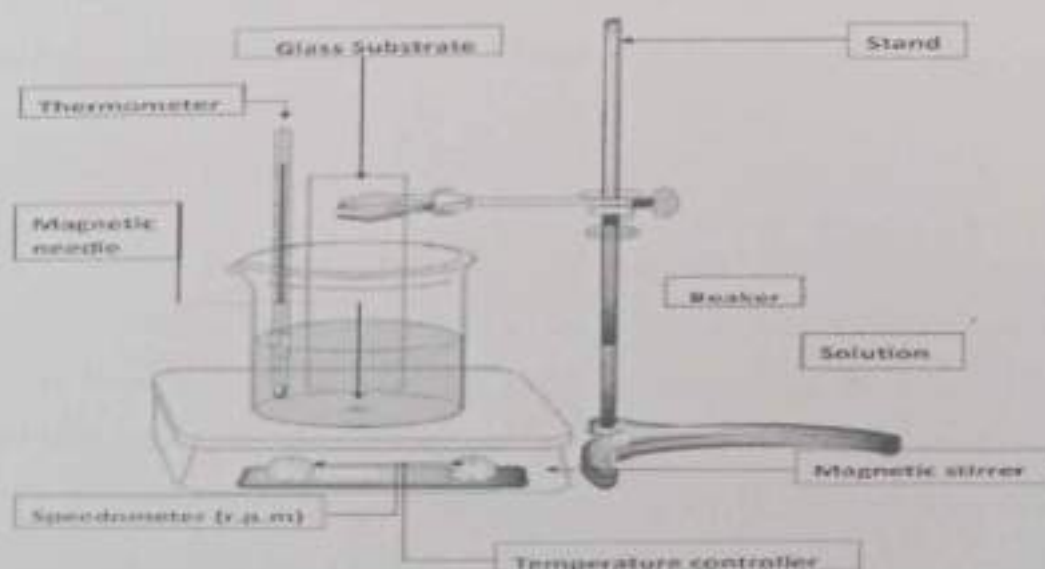


Fig.3 Experimental Setup of Chemical Bath Deposition technique

The major advantage of chemical bath deposition is that requires only solution container and substrate mounting device. The substrate is stirred with help of magnetic stirrer. Water or paraffin bath with constant stirring are used to heat the chemical bath to desired temperature. In some case stirring is continuous from room temperature the beaker containing precursor. Solution and deionized water are alternately placed. Films produced by chemical bath deposition are used in semiconductor, photovoltaic cells and supercapacitor and there is increasing interest in using chemical bath deposition to create nanoparticles thin films.

### **Advantages of chemical bath deposition method**

This method is presently attracting considered attention as it does not require an instrumentation like vacuum system other expensive equipment simple equipment like water bath with temperature indicator, magnetic stirrer, solution breaks used in this method. The starting chemical are commonly available and cheap with this method, large number of depositions of thin film can done with number of cycles. It is low cost efficient methods and easy to scale up industrial purpose. They have advantages:

- low cost
- simplicity
- Uniformity
- controlled growth

#### **USES:**

- I. Chemical bath deposition is used to deposit buffer layer in photovoltaic cells because chemical bath deposition does not damage substrate.
- II. Chemical bath deposition has possible application in antireflection, optical fiber, total reflector, LED, solar cells etc.
- III. Use in field of nanomaterials because properties of nanostructure of chemical bath deposition films can be precisely controlled because of uniform thickness, composition.

### **4. Characterization techniques**

Thin films are widely used in the electronic, optical and magnetic devices. In order to study different properties of these semiconducting materials in form of thin films. Various characterization techniques are used. These techniques include thickness measured structural morphology by X-Ray diffraction, surface morphology by scanning electron microscopy, optical absorption and transmission by UV visible spectrophotometer, electrical resistivity measurement etc.

## 4.1 X-RAY DIFFRACTION (XRD)

XRD is well known technique to obtain the information of composition, phase and crystalline orientation of material. It gives information about crystal structure, chemical composition and physical properties of material and thin film. This technique based on observing the scattering intensity of an X-Ray beam hitting a sample as a function of incident and scattered angle and, wavelength of energy. Interaction of incident ray with sample produce constructive when condition satisfy Bragg's law

$$n\lambda = 2d \sin \theta$$



Fig.4 : Ray Diagram of XRD

$n$  = integer

$d$  = interplanar spacing

$\lambda$  = wavelength

$\theta$  = diffraction angle

It measures average spacing between layer of atoms, find structure of unknown materials. The different phase can be analyzed by X-Ray analysis. It determines the orientation of single crystal or grain. X ray is generated in a cathode ray tube by heating filament to produce electron accelerating electron toward target by applying voltage and bombarding target material with electron have sufficient energy to dislodge inner shell electron of target material. Characteristics of X- Ray spectra are produced. As sample and detector are rotated intensity of reflected X-Ray is recorded when geometry of incident X-Ray satisfies. Bragg equation, constructive interface occurs and peak in intensity occur.[20]

### Application of X-Ray diffraction:

- Analysis of phase change under other special conditions such as temperature, humidity.
- Analysis of physical properties such crystallite size, orientations.



- Determination of unit cell dimension.
- Measurement of sample purity.

## 4.2 SEM (SCANNING ELECTRON MICROSCOPY)

A scanning electron microscope is type of electron microscope that produces image of sample by scanning it with focused beam electrons. The electron interacts with atoms in sample, producing various signals that can be detected and contain information about the samples surface topography and composition. The electron beam is generally scanned in roaster scan pattern, and the beams position is combined with detected signal to produce image.

- SEM can achieve resolution better than 1 nanometer. It provides precise control over the degree of magnification because it uses electromagnets rather than lenses.
- The SEM allowed researchers to study a much variety of specimens.
- Scanning electron microscopes have development new areas of study in the medical and physical science communities.
- Specimen can observe in high vacuum, in low vacuum, in wet condition and at a wide range of elevated temperature.

When beam of electrons strikes the surface and specimen and interact with the atoms of sample signals in the form of secondary electrons, back scattered electron and characteristics X-rays are generated that contain information about the sample's surface topography, composition, etc. The SEM can produce a high-resolution images of sample surface, revealing detail about 1-5 nm in its primary detection mode i.e. secondary electron imaging.

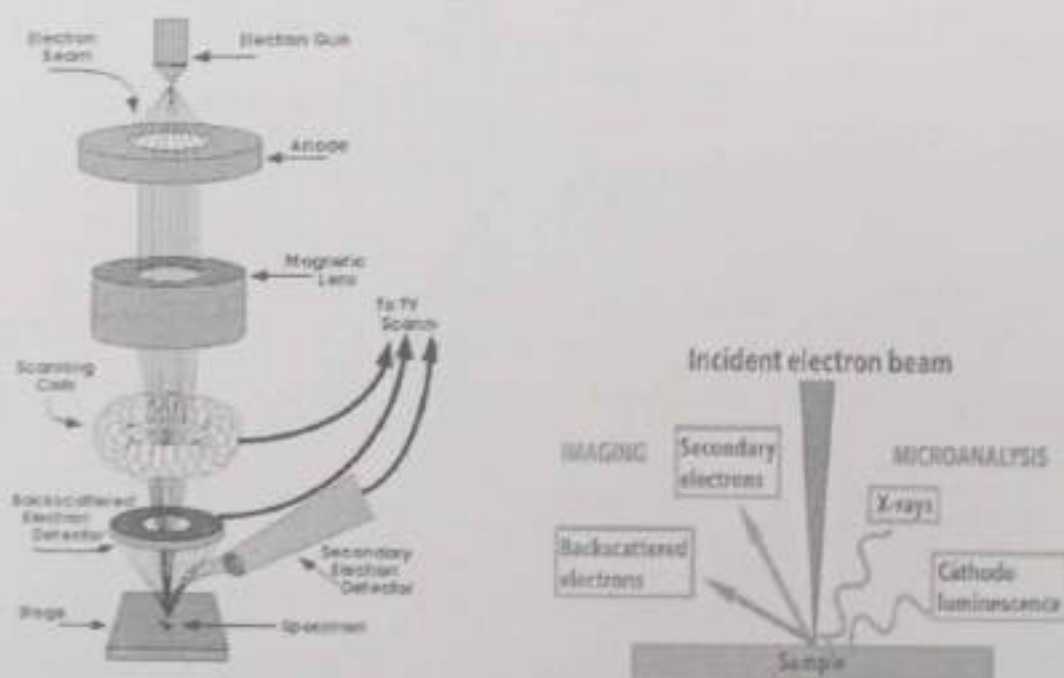


Fig.5: schematic diagram of scanning electron microscope

When electron beam hits the surface of sample, it penetrates the sample to depth of few microns depending on the accelerating voltage and the density of the sample. The three types of signals produced by SEM include secondary electrons, backscattered electrons and characteristic X-rays. Secondary electrons are electrons that interact with top surface of the sample. Backscattered electrons are generated from elastic and inelastic collision between electron and the atoms within the sample. The energy of the characteristic X-ray can be captured by Electron-dispersive X-rays spectrometer to qualitatively analyze the chemical character of the sample. The spatial resolution of SEM depends on size of electron spot, which in turn depends on both the wavelength of electrons and electron-optical system that produce the scanning beam. The resolution is also limited by size of interaction volume, volume of specimen material that interacts with electron beam.[21, 22]

### 4.3 Transmission electron microscopy (TEM)

Transmission electron microscopy is good complementary technique to XRD for evaluating the crystallography of materials using high electron beam ( $>200\text{keV}$ ). A high energy beam of electron is shone through a very thin sample, and interaction between electron and the atoms can be used to observe feature such as crystal structure. TEM can be used to study the growth of layer, their composition and defect. It is one of the most powerful microscopes with respect to its magnification and resolution, it is applied in wide range of applications can be utilized in variety of different scientific, educational and industrial fields. The TEM operates on the same basic principle as light microscope but uses electrons instead of light. Because wavelength of electron is much smaller than that of light. TEM can reveal finest details of internal structure.

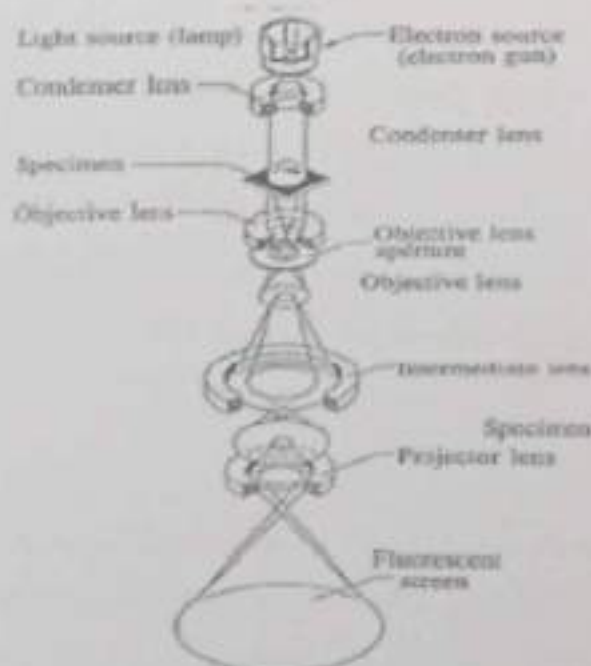


Fig.6: schematic diagram of transmission electron microscopy



In transmission electron microscope the electron gun, fires a beam of electrons. The gun accelerates the electrons to extremely high-speed using electromagnetic coils and high voltage. The electron beam is focused into a thin, small beam by condenser lens has a high aperture that eliminates high angle electrons. The beam then strikes the specimen and part are transmitted depending upon thickness and electron transparency of specimen. The objective lens focuses the portion of the beam that is emitted from sample into an image. Another component of TEM is vacuum system. The transmitted portion is focused by objective lens into an image on phosphorous screen or charged coupled device (CCD) camera. The darker area of image represents those area of sample that fewer electrons are transmitted through while the lighter area of image represent those areas of sample that more electrons were transmitted through. The image produced by TEM, called micrograph.[23,24]

## **5. Synthesis and characterization of lead Selenide PbSe thin Film and PbSe powder**

### **Introduction**

Research on nanocrystalline materials is due to their distinctive properties and future applications in semiconductor devices. They are used for study of semiconductor communication, integrated circuit, photoconductors, light emitting diode etc. lead Selenide (PbSe) belongs to group IV-VI compound semiconductor with its smaller band gap. PbSe also low -toxicity and cost-effective materials. These properties indicate uses of PbSe in solar cells, IR detector material, photothermal conversion of solar energy. For these reasons many search groups have shown great interest in study and development of material by various deposition techniques such as electrodeposition, spray pyrolysis atomic layer deposition, spin coating method, sputtering, chemical bath deposition, SILAR method etc. Chemical bath deposition is presently attracting considerable attention, does not require advanced instrumentation. It is relatively inexpensive, easy to handle, large area deposition, capable of good quality thin film. The characteristics of chemical bath deposited PbSe thin film depend upon growth conditions.[25]

### **5.1: Experiment:**

With help of chemical bath deposition (CBD) method thin film of polycrystalline lead Sulphide deposited on the glass slab. The glass substrate degreased in hydrochloric acid solution (200ml deionized water and 100ml HCl) for 24 hours and then cleaned in chromic acid solution. Finally rinsed in deionized water and dry in air. Cleaning of glass slab due to remove hydrocarbons and other particle from glass slab. The chemicals used are lead acetate , sodium selenosulphate , sodium hydroxide and ammonia. Sodium

selenosulphate was prepared by refluxing amount of 9gm of selenium powder with approximately 15gm of sodium sulphate in 250ml of distilled water for 6 hours at  $80^{\circ}\text{C}$ .

The mixture of the bath was prepared by mixing of appropriate amount of lead acetate and 10ml (0.5M) of NaOH in 100 ml beaker. Initially, the solution looked milky turbid due the formation of  $\text{Pb}(\text{OH})_2$  it later change into a colorless solution after the addition of a sufficient amount of ammonia. Sodium selenosulphate was added to obtain a final volume of 70ml. chemically cleaned substrate vertically immersed into the solution with the help of substrate holder. The reaction mixture was continuously stirred with a magnetic stirrer and maintained at a temperature of  $90^{\circ}\text{C}$  for the deposition of thin film. The prepared solution was initially clear and colorless but turned to dark grey after a few minutes later, a mirror like thin film began to deposit onto the side of the beaker and the substrate confirming the formation of PbSe. There after substrate coated PbSe was removed and dried in air and then dried in oven.



Fig.7 : Experimental arrangement of deposition of PbSe thin film by chemical bath deposition method.

## Result and Discussion



Fig.8 : Lead Selenide (PbSe) thin film by chemical bath deposition



Fig.9: Lead Selenide (PbSe) powder



## X-ray Diffraction

X-Ray diffraction is the powerful and non-destructive technique for characterizing crystal material. Structural characterization was carried out with the help of XRD. XRD pattern of PbSe thin film deposited by chemical bath deposition. The XRD pattern were collected with XPERT-PRO diffraction pattern. The intensity of diffracted x-rays measured as function of diffraction angle. The intensities of the spots provide information about the atomic basis. The sharpness and shape of spots are related to the perfection of crystal. The structure of material can be obtained from plot between intensity vs diffraction angle. The diffraction peaks provide the information about lattice plane and crystal structure. In fig (4.4) and (4.5) shows XRD spectra of lead Selenide thin film and powder form of PbSe. All the diffraction peaks (111), (200), (220), (311) are matched to standard data. So, it is confirmed that formation of PbSe takes place cubic structure.[26]

The Full Width Half Maximum (FWHM) ( $\beta$ ) can be related to strain ( $\epsilon$ ) and crystallite size (D) as:

$$\beta(\cos\theta)/\lambda = 1/D + \epsilon(\sin\theta)/\lambda$$

The plot of  $\beta(\cos\theta)/\lambda$  vs  $\sin\theta/\lambda$  are shown in Fig. 4.6. The reciprocal of the intercept on y axis in these graphs provides particle size, and the slope of graph will give strain value. The plot of  $\beta(\cos\theta)/\lambda$  vs  $\sin\theta/\lambda$  known as W-H plot. Williamson and Hall proposed this method for obtaining size and grain. The size and strain graph of lead Selenide thin film and powder form are shown in fig (4.6) and (4.7) respectively. From these graphs we find the particle size and strain value.[27]

Dislocation density denotes the number of dislocation line per unit volume of crystal, which is size of crystal defects possessed by a crystal. In other words, the dislocation value will illustrate the degree of crystallinity of nanoparticles.

$$\delta = 1/D^2$$

small dislocation density had high degree of crystallite.

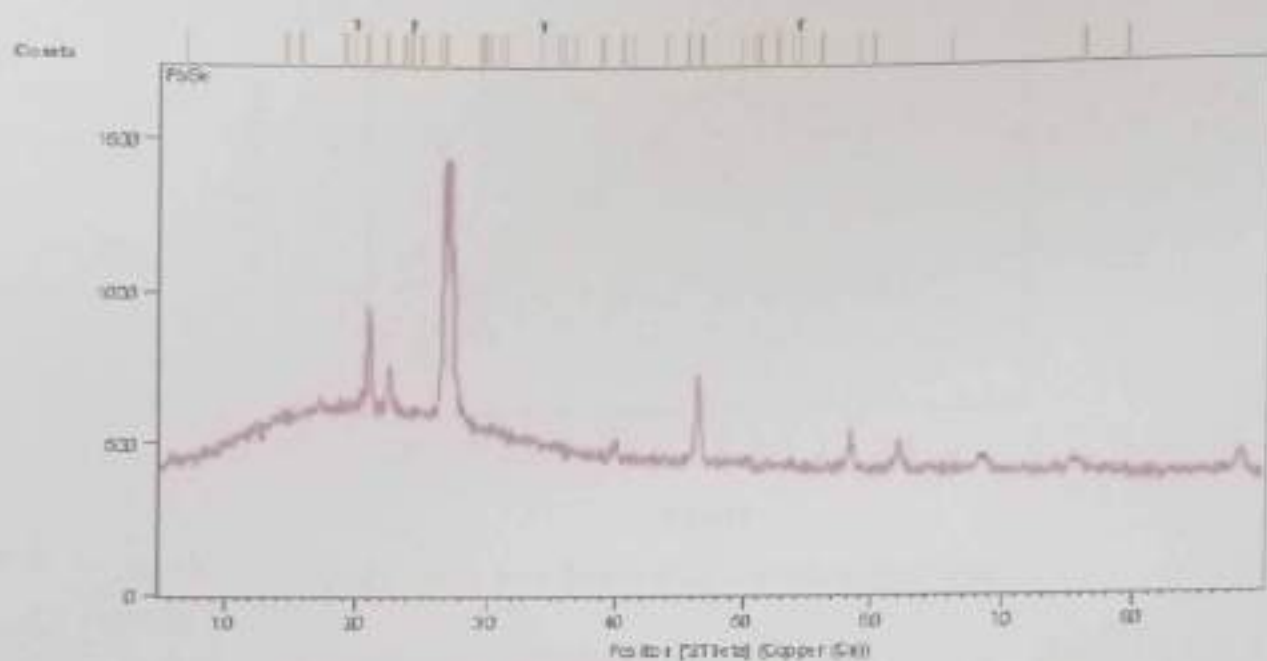


Fig.10: XRD Spectra of lead selenide thin film

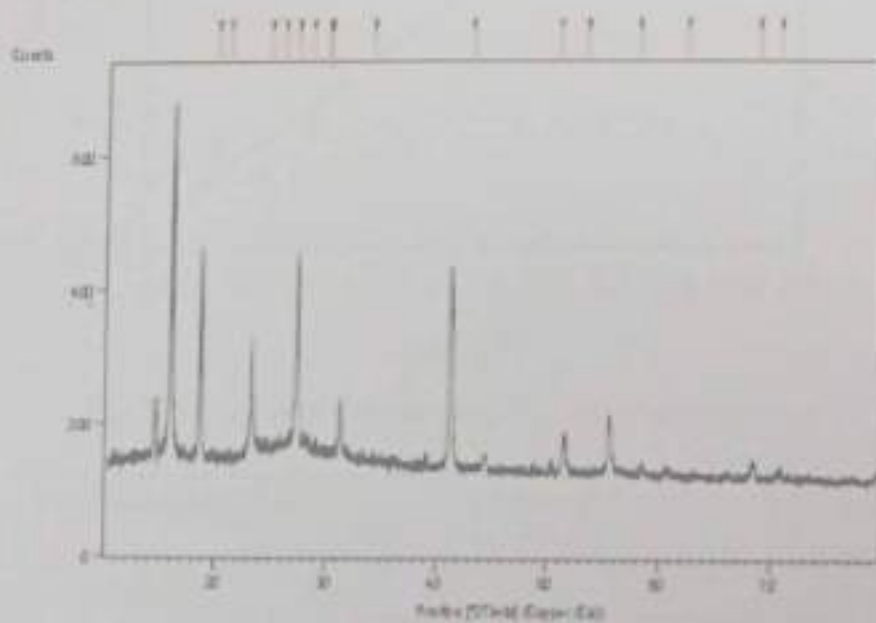


Fig.11 : XRD Spectra of Lead Selenide Powder.



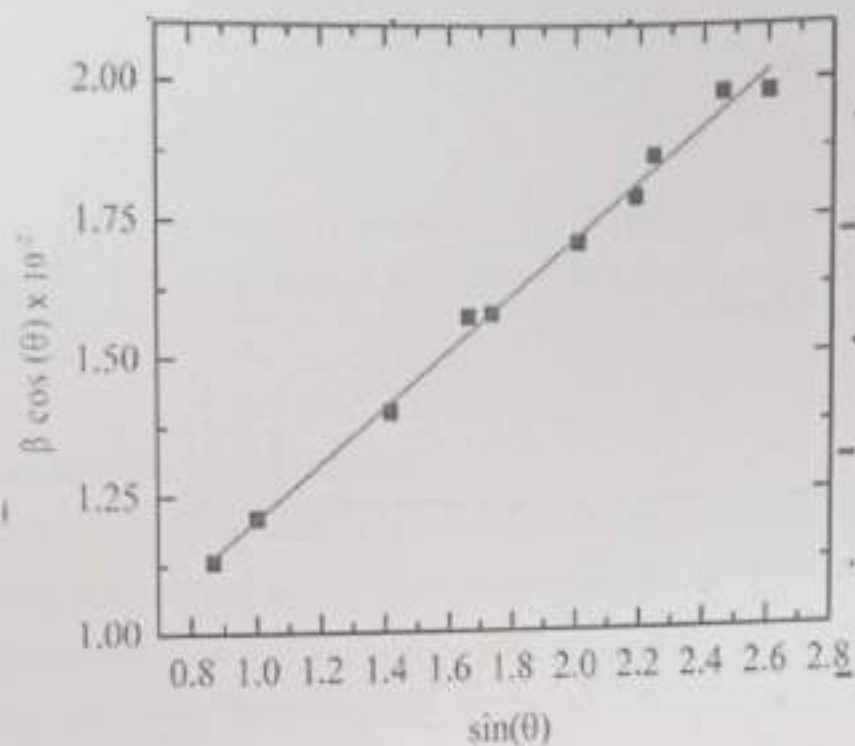


Fig.12 : Size and Strain graph of PbSe thin film

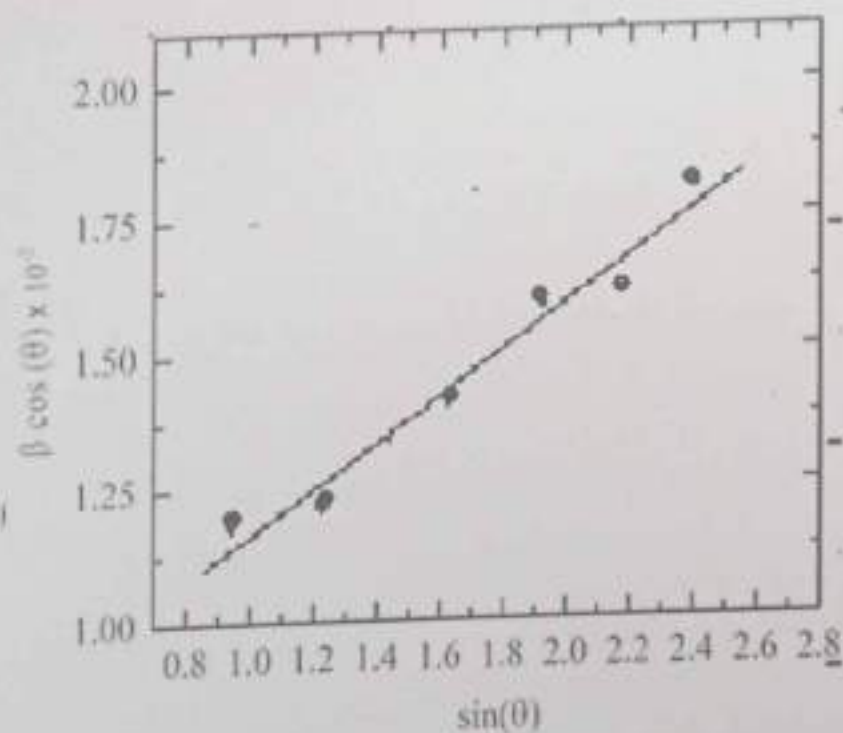


Fig.13 : Size and Strain graph of PbSe powder

Type of Material	Particle Size (nm)	Strain ( $\epsilon$ )	Dislocation Density ( $m^{-2}$ )
PbSe thin film	60.5	$6 \times 10^{-4}$	$2.45 \times 10^{-14}$
PbSe powder	75.9	$1 \times 10^{-2}$	$1.12 \times 10^{-14}$

## CONCLUSION

In this, PbSe Thin films can be successfully deposited by chemical bath deposition method. Structural characterization was carried out with the help of XRD. The XRD pattern were collected with XPERT-PRO diffraction pattern.

- XRD confirms the cubic structure of lead Selenide.
- The particle size of PbSe thin film ~60.5nm and particle size of PbSe powder is 75.9 nm
- The strain value for PbSe thin film and powder forms are found to be  $6 \times 10^{-4}$  and  $1 \times 10^{-2}$  respectively.
- The Dislocation density of PbSe thin film and powder form are found to be  $2.45 \times 10^{-14}$  and  $1.12 \times 10^{-14}$ .
- The confinement effect resulting from decrease in crystal size in grown nanocrystalline sample is responsible for blue shift.
- Lead Selenide thin film have many applications in solar cell and photovoltaic cells.
- Size of particle of thin film and powder are different due to surface area to volume ration increase. The confinement effect resulting from decrease in crystal size in grown nanocrystalline sample is responsible for blue shift.

## REFERENCE

1. Okimura H., Matsumae T. and Makable R., Thin Solid Films, **71**, 53-599 (1908).
2. Loferski J. J., Physics., **27**, 777 (1956).
3. Saloniemi, H., Kanninen, T., Ritala, M., Leskeli, M., & Lappalainen, R. (1998). Electrodeposition of lead selenide thin films. *Journal of materials chemistry*, *8*(3), 651-654.
4. Hankare, P. P., Delekar, S. D., Bhuse, V. M., Garadkar, K. M., Sabane, S. D., & Gavali, L. V. (2003). Synthesis and characterization of chemically deposited lead selenide thin films. *Materials chemistry and physics*, *82*(3), 505-508.
5. Thanikaikarasan, S., Mahalingam, T., Dhanasekaran, V., Kathalingam, A., & Rhee, J. K. (2012). Growth and characterization of lead selenide thin films. *Journal of Materials Science: Materials in Electronics*, *23*, 1562-1568.
6. Hone, F. G., & Ampong, F. K. (2016). Effect of deposition temperature on the structural, morphological and optical band gap of lead selenide thin films synthesized by chemical bath deposition method. *Materials Chemistry and Physics*, *183*, 320-325.
7. A. Gaiduk, P. Gaiduk, A. Larsen, Thin Solid Films. 516, 3791 (2008).
8. Ohring, Milton (2002). Materials Science of Thin Film: Deposition and Structure (2<sup>nd</sup> edition).
9. [www.electropedia.org](http://www.electropedia.org). retrieved 17Nov2023.
10. Hadanu R, Idris S and Sutapa I W 2015 Indones. J. Chem. 15 86-92
11. Grozdanov I., Najdoski M. and Dey S.K., A simple solution growth technique for PbSe thin films, Mater. Lett., **38**, 28-32 (1999).
12. Klein, L.C. and Garvey, G.J., "Kinetics of the Sol-Gel Transition" Journal of Non-Crystalline Solids, Vol. 38, p.45 (1980)
13. J. F. Ziegler, J. P. Biersack, U. Littmark (1984). *The Stopping and Range of Ions in Solids*, vol. 1 of series *Stopping and Ranges of Ions in Matter*. Pergamon Press, New York.
14. T. Schenkel; Briere, M.; Schmidt-Böcking, H.; Bethge, K.; Schneider, D.; et al. (1997). "Electronic Sputtering of Thin Conductors by Neutralization of Slow Highly Charged Ions". *Physical Review Letters*. **78** (12): 2481.
15. Robbie, K.; Brett, M. J. (1997). "Sculptured thin films and glancing angle deposition: Growth mechanics and applications". *Journal of Vacuum Science & Technology A: Vacuum, Surfaces, and Films*. **15** (3). American Vacuum Society: 1460-1465.
16. Harsha, K. S. S, "Principles of Physical Vapor Deposition of Thin Films", Elsevier, Great Britain (2006), p. 400.
17. T. Schenkel; Briere, M.; Schmidt-Böcking, H.; Bethge, K.; Schneider, D.; et al. (1997). "Electronic Sputtering of Thin Conductors by Neutralization of Slow Highly Charged Ions". *Physical Review Letters*. **78** (12): 2481.

18. Rumianowski R.T., Dygdala R.S., Jung W. and Bala W., Growth of PbSe thin film on Si substrate by pulsed laser deposition method, *J.Cryt. Growth*, **252**,230-235(2003).
19. McMullan, D. (1988). "Von Ardenne and the scanning electron microscope", *Proc Roy Microsc Soc.* **23**: 283–288.
20. von Ardenne, Manfred, "Improvements in electron microscopes", published 1939-08-15.
21. Wells OC (1957) The construction of a scanning electron microscope and its application to the study of fibres. PhD Dissertation, Cambridge University.
22. ultraviolet microscope. (2010). In *Encyclopædia Britannica*. Retrieved November 20, 2010, from [Encyclopædia Britannica Online](#)
23. Hawkes, P., ed. (1985). *The beginnings of Electron Microscopy*. Academic Press.
24. Champness, P. E. (2001). *Electron Diffraction in the Transmission Electron Microscope*. Garland Science.
25. Brinker, C. J.; G. W. Scherer (1990). *Sol-Gel Science: The Physics and Chemistry of Sol-Gel Processing*. Academic Press.
26. W.H.Hall (*Acta Metall.* 1, 22-31 (1953)).
27. McMullan, D. (1988). "Von Ardenne and the scanning electron microscope", *Proc Roy Microsc Soc.* **23**: 283–288.



# **CHARACTERIZATION OF TRANSITION METAL DOPED BOROSILICATE BASED BIOACTIVE GLASSES**

## **PROJECT REPORT**

*Submitted in partial fulfilment of the  
requirements for the award of the degree of*

## **MASTER OF SCIENCE**

*in*

## **PHYSICS**

*By*

**Amandeep Kaur**  
**(Reg. No. 8114-19-535)**



**DEPARTMENT OF PHYSICS**

**SRI GURU TEG BAHADUR KHALSA COLLEGE, SRI ANANDPUR SAHIB**

**(An Autonomous College)**

**ANANDPUR SAHIB- 140118, PUNJAB (INDIA)**





**SRI GURU TEG BAHADUR KHALSA COLLEGE, SRI ANANDPUR SAHIB**

(An Autonomous College)

**ANANDPUR SAHIB-140118. PUNJAB (INDIA)**

## **CERTIFICATE**

It is certified that the work contained in the project report entitled **"CHARACTERIZATION OF TRANSITION METAL DOPED BOROSILICATE BASED BIOACTIVE GLASSES"** is an original contribution by me and has not been submitted in part or full for any other degree at this or other University/Institute.

The assistance and help received during the course of the thesis work have been acknowledged.

*Amandeep Kaur*

**Amandeep Kaur**

**Reg. No. 8114-19-535**

I, the undersigned, Supervisor of **Amandeep Kaur, Regn. No. 8114-19-535**, a candidate for the degree of Master of Science, agree that the project report entitled, **"CHARACTERIZATION OF TRANSITION METAL DOPED BOROSILICATE BASED BIOACTIVE GLASSES"**, may be submitted in partial fulfilment of the requirements for the award of degree.

This is to certify that the above statement made by the candidate is correct to the best of my knowledge.

*Dr. Randev Singh*

**Supervisor**

**Dr. Randev Singh**

**HOD & Associate Professor**

**Department of Physics**

**Sri Guru Teg Bahadur Khalsa College**

**Sri Anandpur Sahib**

*Dr. Devinder Singh*

**Supervisor**

**Dr. Devinder Singh**

**Assistant Professor**

**Department of Physics**

**Sri Guru Teg Bahadur Khalsa College**

**Sri Anandpur Sahib**

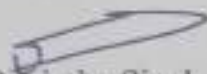
## CERTIFICATE

This is to certify that the "Project Report" entitled "CHARACTERIZATION OF TRANSITION METAL DOPED BOROSILICATE BASED BIOACTIVE GLASSES" submitted by **Amandeep Kaur** (Reg. No. 8114-19-535) to Department of Physics, Sri Guru Teg Bahadur Khalsa College, Sri Anandpur Sahib in partial fulfilment of the requirements for the award of degree of **MASTER OF SCIENCE IN PHYSICS** and has been approved by Department Research Committee (DRC) after the viva-voce examination of the candidate.



Dr. Randev Singh

Supervisor



Dr. Devinder Singh

Supervisor



Dr. Randev Singh

Chairman DRC

## ACKNOWLEDGEMENT

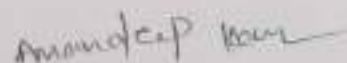
First of all, I would like to thank Almighty for giving me opportunity and guidance to achieve my goals then I would like to acknowledge my Parents for their unwavering support and understanding during the course of this project. Their motivation and belief in my abilities have been a constant source of inspiration.

I would like to thank my talented and supportive supervisors Dr. Randev Singh HOD and Associate Professor and Dr. Devinder Singh Assistant Professor at Department of Physics Sri Guru Teg Bahadur Khalsa College Sri Anandpur Sahib, who have resourcefully guided me throughout this research project. I'm extremely grateful for their motivating discussions which enabled me to accomplish this task successfully. Without their active guidance, support and encouragement I would not have made headway in this project.

A special thanks to Prof. Prabhjot Kaur, Assistant Professor at Sri Guru Teg Bahadur Khalsa College Sri Anandpur Sahib for the help and her valuable suggestions whenever I needed out of her busy schedule. I'm also thankful to other faculty members in the department for their encouragement and fruitful academic discussions.

I'm also thankful to my classmates and my friends who was directly or indirectly help me to complete this project report.

Anandpur Sahib

  
Amandeep Kaur

# CONTENTS

Title	Page No.
Abstract	7
Chapter-1 Introduction	8-9
Chapter-2 Bioactive Glasses	10-14
2.1. Bioactive glass	10
2.2. Types of Bioactive glass	10-12
2.3. Method of Synthesis of Bioactive glass	12-14
Chapter-3 Borosilicate Bioactive glasses	15-19
3.1. Borosilicate Bioactive glass	15
3.2. Transition metal doped Bioactive glass	16
3.2.1. Copper doped Borosilicate Bioactive glass	16-17
3.2.2. Titanium doped Borosilicate Bioactive glass	17-18
3.2.3. Zinc doped Borosilicate Bioactive glass	18-19
Chapter-4 Characterization Techniques	20-24
4.1. X-Ray Diffraction	20-23
4.2. Archimedes Principle	23-24
Chapter-5 Experimental Work	25-35
5.1.1. Preparation of Borosilicate Bioactive glass	25-26
5.1.2. Preparation of Copper doped Borosilicate glass	27
5.1.3. Preparation of Titanium doped Borosilicate glass	27-28
5.1.4. Preparation of Zinc doped Borosilicate glass	28-29
5.1.5. Archimedes Principle	30-31
5.2. Result and Discussion	31
5.2.1. Archimedes Principle	31-32
5.2.2. X-Ray Diffraction	32-35
Conclusion	36
References	37-39

## FIGURES TABLE

Figure No.	
1.	Schematic representation of Melt-quench method
2.	Schematic representation of Sol-gel glass synthesis
3.	Bragg's law reflection
4.	Schematic representation of X-ray diffraction
5.	Schematic representation of X-ray diffractometer
6.	The equilibrium of forces on an object hanging from scale while submerged
7.	Muffle furnace for melting glass
8.	Borosilicate Bioactive Glasses
9.	Apparatus of Archimedes Principle
10.	Density graph of Borosilicate Bioactive glasses
11.	XRD spectra of Borosilicate Bioactive glass
12.	XRD spectra of Copper doped Borosilicate glass
13.	XRD spectra of Titanium doped Borosilicate glass
14.	XRD spectra of Zinc doped Borosilicate glass
15.	XRD spectra Borosilicate Bioactive glasses



## ABSTRACT

Borosilicate Bioactive forms a strong bond with bones. These glasses are synthesised through two processes, melt- quenching method and sol- gel method. Borosilicate and transition metal doped borosilicate bioactive glasses have garnered significant interest for their applications in biomedical fields, particularly in bone regeneration and tissue engineering. Borosilicate glasses, known for their superior chemical durability and thermal stability, serve as an excellent base material for developing bioactive glasses. The incorporation of transition metals such as cobalt, copper, zinc, titanium and iron into the borosilicate matrix can enhance the bioactivity, mechanical properties, and antimicrobial effects of the glass. These doped bioactive glasses exhibit improved apatite-forming ability when immersed in simulated body fluid (SBF), promoting osteointegration and supporting bone tissue growth. Additionally, the transition metal ions can impart beneficial biological properties, such as antibacterial activity and angiogenesis stimulation, which are crucial for successful implant integration and healing.

This reviews the synthesis methods, structural characteristics, and biomedical applications of borosilicate and transition metal doped borosilicate bioactive glasses, highlighting their potential.

## CHAPTER -1

### INTRODUCTION

Bioactive glass is a great revolution in the field of glass and biomaterials. Many years ago, glasses were used for the particular purpose. As time progressed, extensive research and industrial revolution propelled glass production forward, enabling mass manufacturing and refining techniques. In 1960 a young scientist named Larry Hench successfully combined both the fields and introduced a special type of glass which was biomaterial biocompatible and bioactive. The name of the glass is "BIOACTIVE GLASS" changed the entire journey of biomaterials. The composition of bioactive glass is resembled with the composition of human bone such as calcium, magnesium and phosphorous etc. Bioactive glass forms a hydroxyapatite layer, so it is used as a implant device on the place of damage bones. Bioactive glasses are non - crystalline ceramic. These glasses have ability to form a strong bond with living tissues. Bioactive glass is used in the field of dentistry. Bioactive glass represents a significant advancement in biomaterials, offering a versatile and effective solution for a range of medical and dental challenges. Its ability to bond living tissues and support regeneration makes it is invaluable tool in modern medicine.

Borosilicate bioactive glass has composition of  $(25\text{B}_2\text{O}_3 - 25\text{SiO}_2 - 25\text{CaO} - 15\text{Na}_2\text{O} - 10\text{MgO})$ . Borosilicate bioactive glasses are synthesised with the melt-quenching method. These glasses have ability to interact with body fluid which trigger the series of chemical reactions that ultimately lead to the formation of hydroxyapatite layer.

Doping of transition metal ions are enhance the properties of bioactive glasses. Copper doped bioactive glass has ability to heal the broken bones faster. Titanium enhances the strength of bioactive glass. Zinc doping enhances the antimicrobial properties of bioactive glass. It can introduce new electronic state within gap, affecting colour and light absorption characteristics. These metals can introduce a new functionality, such as antimicrobial activity, improved mechanical strength and enhanced bioactivity. Transition metal doped glasses serve as scaffolds that support cell growth and tissue regeneration. The controlled degradation and ion release properties allow these glasses to be used as drug delivery systems, providing localized therapeutic effects. Achieving a uniform distribution of transition metal dopants remains a technical challenge.

Borosilicate bioactive glasses can firmly bond with bones, support soft – tissue infiltration and promote bone growth. Release of bioactive elements, such as Ca, P, B, Si, and Na. Bioactive glass application found beyond dentistry such as ability to support cell growth, tissue regeneration and replacement of cancerous tissues, bioactive glass in drug delivery, and spinal cord repair. Ongoing research is focussed on optimizing the composition and properties of borosilicate bioactive glasses to enhance their performance and broaden the range of applications.

Future challenges for bioactive glasses include enhancing mechanical properties, developing reliable bioactive coating, refining manufacturing processes, achieving rapid degradability and ensuring multiple property performances while maintaining biocompatibility and bioactivity. Developing bioactive glass with multifunctional properties such as antibacterial activity, drug delivery capability, or the ability to respond to environment stimuli, is an exciting challenge area of research.



## CHAPTER – 2

### BIOACTIVE GLASSES

#### 2.1. DEFINITION OF BIOACTIVE GLASS

Bioactive glass is a type of glass that is capable of forming a strong bond with living tissues such as bone. Bioactive glass has ability to form bond with mineralised bone tissue in the physiological body environment [1]. Bioactive glass are based on the sodium oxide, calcium oxide, phosphorous oxide, silicon oxide. Bioactive glass can be developed, showing composition dependent promising properties such as bone forming capability, antibacterial properties, degradability and wound healing [2]. Bioactive glass is a non-crystalline ceramic. The first bioactive glass was silicate – based glass 45S5 by Larry Hench and co-workers [3]. Bioactive glass comprises three oxides; Network formers, Network modifiers, and intermediate oxides. Network former build the glass network and linked to each other, e.g. Silicon dioxide, phosphorous penta-oxide, boron trioxide. Network modifiers break the glass network by linking to the non-bridging oxygen at the end, e.g., sodium oxide, calcium oxide, magnesium oxide, potassium oxide. Intermediate oxide either network former or modifier [4][5].

Bioactive glass is used as drug carrier, proposed a system with an amino group – modified MBAG system for the delivery of alendronate. When bioactive glass interacts with the body, it establishes a robust chemical bond with the bone promoting the growth of new bone tissue. Bioactive toothpaste called Sensodyne, repair and protect the teeth [6]. Yttrium in bioactive glasses generate a revolutionary era for cancer therapy. Brach therapy uses bioglass microspheres as drug carriers to convey beta radiation emission into cancerous tissue via injection [7]. Bioactive glass is used in bone grafts for its osteoconductive and osteoinductive properties.

#### 2.2 TYPES OF BIOACTIVE GLASS

There are several types of bioactive glass each with unique composition tailored for specific biomedical applications. Common types include:

1. Silicate – Based Bioactive glass
2. Borate – Based Bioactive glass
3. Phosphate – Based Bioactive glass

4. Borosilicate Bioactive glass
5. Copper doped Bioactive glass
6. Titanium doped Bioactive glass
7. Zinc doped Bioactive glass
8. Silver doped Bioactive glass

**1. Silicate – Based Bioactive glass:** The term “silica based” refers to the presence of silica in glass composition. Silica, being main component, is essential for the glass bioactive behaviour, facilitating interactions with living tissues. Silica’s role in the ion exchange mechanism between glass and biological environment is critical, as it initiate the formation of hydroxyapatite, a mineral closely resembling bone structure. silica based bioactive glass is widely used in orthopaedic and dental applications like it enhance dental restoration and provide antimicrobial benefits.

**2. Borate - based Bioactive glass:** Borate glasses typically contain boron trioxide as a significant component. Boron is known to stimulate bone formation. These materials are known for their ability to interact with biological tissues and support bone regeneration. Borate based bioactive glasses form hydroxyapatite layer on their surface when it contacts with bodily fluid. These glasses have ability to release ions such as boron, calcium and phosphate, which enhance bone healing and antimicrobial activity. These glasses typically degrade faster than silicate-based glass.

**3. Phosphate – based Bioactive glass:** Phosphate-based bioactive glasses are primarily composed of phosphorous pentoxide. The release of phosphate ion can influence cellular behaviour. These glasses generally tolerated by body, reducing risk of inflammation. The bioactive bonding of Phosphate – based bioactive glass is particularly advantageous in orthopaedic applications. Phosphate harmlessly dissolves in the body.

**4. Borosilicate Bioactive glass:** It composed primarily  $\text{SiO}_2$ ,  $\text{B}_2\text{O}_3$ ,  $\text{Na}_2\text{O}$ ,  $\text{CaO}$ , it exhibit excellent biocompatibility and bioactivity.

**5. Copper doped Bioactive glass:** These bioactive glasses made with doping of copper. Copper increases healing process of broken bones.

**6. Titanium doped Bioactive glass:** Doping of titanium in bioactive glass improve its mechanical strength, making it more robust, and it is better suited for load bearing applications.



7. **Zinc doped Bioactive glass:** Zinc doped bioactive glasses have improved antibacterial properties. This can help in reducing risk of infection.

8. **Silver doped Bioactive glass:** Silver doped bioactive glass stands at the intersection of material science, medicine, and biotechnology.

## 2.3.METHOD OF SYNTHESIS OF BIOACTIVE GLASS

Bioactive glasses are mainly produced by two techniques, Sol - Gel [8] and Melt Quenching method [9]. The first bioactive glass is prepared by melt quenching method [10] and after 20 years later same glass is prepared by sol-gel method [11].

### 2.3.1. MELT – QUENCHING METHOD

Melt quenching is widely used technique for the preparation of bioactive glass. In this method, mixed composition of bioactive glass is heated at a higher temperature usually above  $500^{\circ}\text{C}$ . Important factors while melting a glass are viscosity, thermal expansion and crystallisation characteristics. The mixed precursors are heated in a crucible and then the resulting melt is pour into graphite moulds [12] or into cold water bath for rapid cooling (quench) of melt. Batch particle size and their mixing in proper proportion are the other factors to provide homogeneity in glass structure [13]. The quenched glass may be subjected to an annealing process to relieve internal stresses.

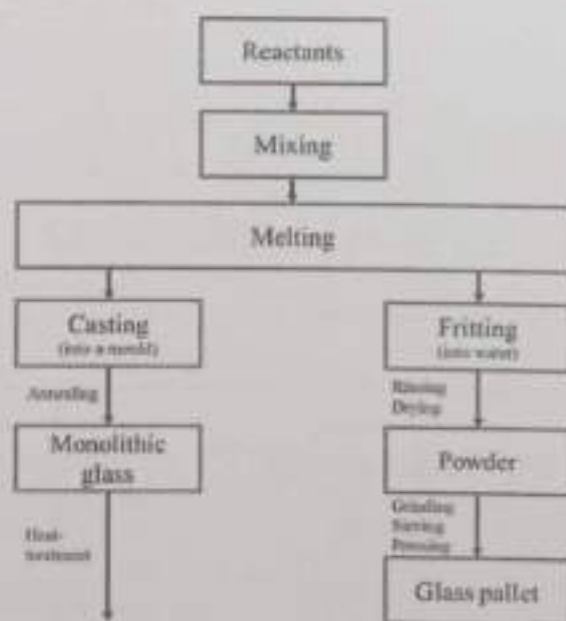


Fig.1: Schematic representation of melt quench method [14]

### 2.3.2. SOL – GEL METHOD

The sol – gel method also known as “sol – gel process” is a versatile and widely used technique for preparing bioactive glass. Sol – Gel synthesis mainly involves hydrolysis and polycondensation. Sol – Gel glasses are made by a chemical – based process at much lower temperature [15-18]. Sol -Gel method used to increase the surface area and degradability of material [19]. The precursors for glass are metal alkoxide i.e. tetraethyl orthosilicate for silicon and nitric acid as a catalyst, along with triethyl phosphate. The precursor is stirred for hydrolysis and condensation resulting in clear sol [20][21]. This is then dried and aged for a long period of time usually weeks, then followed by calcination to obtain glass granules. These glasses have high porosity. The molecular level mixing of precursors ensures a homogeneity distribution of elements within glass. The porous structure of sol-gel derived bioactive glasses makes them suitable carriers for controlled drug release.

This technique ensures the high degree of homogeneity at the molecular level. It enables the production of glasses with controlled porosity, which is beneficial for applications such as bone regeneration where porosity influences bioactivity and cell integration. The physical differences between the two synthesis routes are that the sol-gel glasses tend to have nano porosity whereas melt – derived glasses are dense in nature.

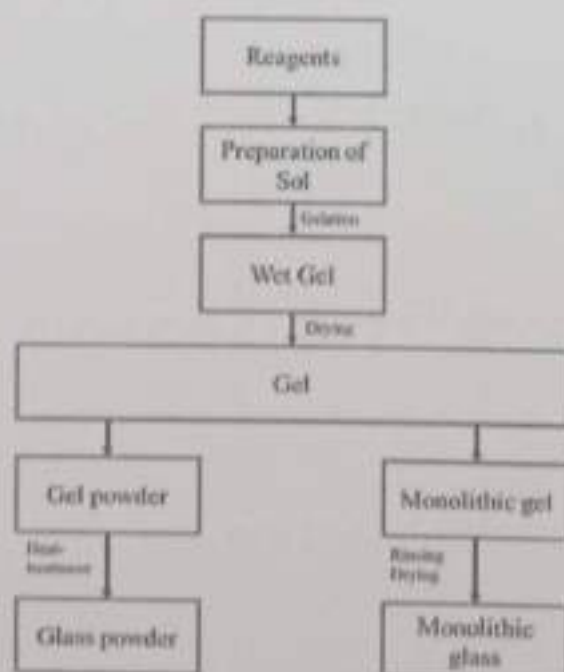


Fig.2: Schematic representation of sol – gel glass synthesis

The surface area of sol – gel derived glasses are higher than melt – derived glasses, which results in greater dissolution rate, and hence higher cellular response. However sol- gel made scaffolds have lower strength than melt – quenched glasses and thus inappropriate to use in hard tissue engineering.

### 2.3.3. MICROWAVE SYNTHESIS

Recently ultrasonic assisted synthesis and microwave assisted synthesis are gaining attention as they can help to reaction in short time and can modify the reaction environment to produce nano phase powders. It is rapid and low-cost powder synthesis methods for powders. For synthesis, the precursors were dissolved in de- ionized water and transferred to the ultrasonic irradiation. The irradiation time was varied to obtain the optimum synthesis condition. Microwave operation was performed in a second batch of powders after the ultrasonic irradiation. The obtained amorphous powder was washed with deionised water and filtered. After drying for 24 hours in an oven at 80°C the powders were calcined at 700°C for the development of bioglass.

## CHAPTER – 3

### BOROSILICATE BIOACTIVE GLASSES

#### 3.1.BOROSILICATE BIOACTIVE GLASS

Borosilicate bioactive glass is a specialised type of glass with unique properties that make it valuable in medical and dental applications. It composed primarily of silicon dioxide, boron trioxide, sodium oxide and calcium oxide, it exhibits excellent biocompatibility and bioactivity. Borosilicate bioactive glass interact with bodily fluids, triggering a series of chemical reactions that ultimately lead to the formation of a layer of hydroxy-apatite on its surface. Hydroxyapatite is a mineral found in natural bone and its presence on the surface of the glass promotes the integration of material with surrounding bone tissue.

Borosilicate bioactive glass serve as templates for new bone formation. Additionally, in dentistry, it is used in restorative materials and dental implants to facilitate osteointegration, the process by which implants fuse with surrounding bone. Borosilicate bioactive glass typically exhibit lower thermal expansion, excellent chemical resistance, high dielectric strength and higher softening temperature compared to other commercial glasses. Recently, they have also been explored for immobilizing nuclear wastes and as materials capable of demonstrating bioactivity.

Borosilicate bioactive glasses have emerged as promising materials for bone repair. Compared with silicate bioactive glasses, they exhibit superior bioactivities and faster degradation rates owing to their lower Si content[22]. Borosilicate bioactive glass can firmly bond with bones, support soft tissue infiltration, and promote bone growth and osteoconductivity. However, degradation of borosilicate bioactive glass is characterized by rapid degradation at the initial stage and slow degradation at later stage, which easily lead to the local enrichment of multiple bioactive components at the beginning and weak bone regeneration ability later on. These glasses offer a promising solution for enhancing bone repair and regeneration with its biocompatibility. The unique properties of borosilicate bioactive glasses, such as their bioactivity, biocompatibility, and ability to release therapeutic ions, make them versatile materials for a wide range of biomedical applications. The ongoing research and development in this field continue to expand their potential uses in medical science.



### **3.2.TRANSITION METALDOPED BOROSILICATE GLASS**

Transition metal ions play a crucial role in micronutrients in all living organisms and are vital for bone metabolism [24]. Transition metals like cobalt and nickel are recognised for their ability to stimulate the hypoxia inducible factor , thereby significantly enhancing blood vessel formation in tissue engineering applications .

The functional roles of transition metal ions in biological systems can be categorised broadly into non – catalytic functions, redox catalysis and non – redox catalysis [26]. The iron(Fe) effectively enhances bone metabolism especially osteoblastic, proliferation, differentiation and calcification [27].Manganese is essential for metalloenzymes,DNA polymerases and kinesis [28]. Manganese is known to influence bone remodelling and its deficiency causes reduction of organic matrix synthesis and retards endochondral ontogenesis, increasing the possibility of bone abnormalities such as decrease of bone thickness and length [29]. Transition metal doped bioactive glasses often exhibit antimicrobial properties. Copper and silver posses' inherent antimicrobial activity. These metals inhibit the growth of bacteria and other pathogens, reducing the risk of infections associate with medical implants. Transition metal doping can inhibit specific therapeutic properties to bioactive glasses e.g. cobalt and copper ions have been shown to stimulate angiogenesis, the formation of new blood vessels, which is crucial for tissue regeneration and wound healing processes. Doping can enhance the mechanical properties of bioactive glass such as hardness, strength and fracture toughness.

Silver-doped bioactive glasses exhibit strong antibacterial properties due to the release of silver ions, which can disrupt bacterial cell membranes and interface with their metabolic processes. This makes then ideal for applications where infection control is critical, such as wound dressings and coatings for medical implants. Strontium-doped bioactive glasses can promote bone formation and reduce bone resorption, making them beneficial for treating osteoporosis and other bone related diseases.

#### **3.2.1.COPPER-DOPED BOROSILICATE BIOACTIVE GLASS**

Copper is known to promote angiogenesis in other words a new blood vessel formation, through stimulation of endothelial [30].Copper is one of the most used therapeutic metallic elements in biomedicine. Copper can modulate the physio – chemical properties of bioactive glasses and improve therapeutic potential. Copper has ability to act as an enzymatic



cofactor, it directly impacts cellular functions as well as tissue biosynthesis. Healing process of broken bones occurs faster in the presence of copper.

Copper containing bioactive glass have been found as potent materials for enhancing the healing process of both hard and soft tissues. It causes no adverse effect on glass bioactivity. Copper is reported as an effector in improving ALP activity, collagen type - I secretion. Copper could significantly promote the expression and biogenesis of ANG in endothelial cells, thereby triggering angiogenesis. Copper is known to act as both antibacterial particle and surface agent against various bacterial strains. Oxidative stress and DNA degradation are two actions of copper for killing bacteria. Size, shape, concentration and type of microorganisms effect the antibacterial property of copper. Copper exhibit other antimicrobial properties including antifungal and antiviral activities which may be interested for designing and developing a new class of glasses in the future.

Copper doped borosilicate bioactive glass exhibit superior osteogenic properties, fastening bone regeneration and integration. They enhance the expression of genes associated with osteogenesis while suppressing osteoclast activity, thereby promoting bone formation and inhibiting bone resorption. Copper's ability to modulate the immune system response further contributes to the biocompatibility of bioactive glass implants.

Copper ions possess strong antibacterial properties, making copper-doped bioactive glasses effective in preventing and treating infections. This is particularly valuable in applications involving implants and wound healing. Copper ions exhibit antioxidant properties, which can help in reducing inflammation and oxidative stress in the body, further supporting tissue healing and regeneration. Research in this field focuses on optimizing the composition and processing conditions of these glasses to maximize their therapeutic benefits. Studies also explore the synergistic effects of combining copper with other therapeutic ions.

### **3.2.2. TITANIUM-DOPED BOROSILICATE BIOACTIVE GLASS**

Titanium has broad range of applications in the biomedical field[31]. It has antitumor properties. Titanium is widely used as a biomaterials for several dental and orthopedic clinical purpose. Titanium dioxide was added to borosilicate bioactive glass to create a composition with a regulated degradation rate and tailored biological response, making it a suitable material for bonding in tissue engineering applications. Depending on the host composition, titanium serves as both an active and inert material. Titanium dioxide can also increase osteoblast differentiation and promote HA formation by contact with body fluid

[32][33].Titanium dioxide indirectly stimulates angiogenesis by developing new blood vessels which help bone formation and bone repair.

It has tendency to absorb water at a surface resulting in the formation of Ti – OH groups. The basic Ti – OH groups are reported to induce apatite nucleation and crystallisation in SBF. Titanium reduces dissolution rates. Titanium dioxide in general are known to have good hem compatibility and non- toxicity. Titanium doping can improve the mechanical properties of the glass, making it more robust and better suited for load bearing applications. Integration with surrounding tissues. While the antimicrobial properties of titanium help in preventing infections.

Similar to other bioactive glasses, titanium containing bioactive glass exhibit bioactivity by forming a hydroxyapatite layer on its surface when exposed to bodily fluids. The bioactivity promotes the integration of the glass with surrounding tissues, facilitating bone bonding and regeneration. These glasses can be used in orthopaedic and dental applications to repair and regenerate bone tissues. It can serve as coating material for metallic implants to improve their integration with bone and reduce the risk of infection. Due to its bioactivity and mechanical strength, it is suitable for use as a scaffold material in tissue engineering.

### **3.2.3. ZINC-DOPED BIOACTIVE GLASS**

Zinc is an essential mineral that plays an important role in the formation of blood vessels, maturation and bacterial resistance. The presence of zinc ion has been discovered to enhance the binding of calcium to bone proteins and boost alkaline phosphatase activity[34].

Zinc in the body has significant impact on the anabolic process of bone formation, even at low concentrations. Administering zinc ion supplementation to enhance physiological process could potentially expedite healing time and alleviate discomfort in patients suffering from traumatic injuries to skeletal tissues.

Zinc has antibacterial activity against both gram – negative and gram – positive bacteria. This effect stem from the cations increasing the pH of the surrounding and from the intracellular incursion of zinc ions, causing disruption of the cell membrane. Zinc plays an important role in human body, especially for the growth of bone tissue, although it is present only in trace amount. Zinc has been known to encourage attachment, proliferation of osteoblast and increase ALP expression in vitro as well as inhibit osteoclastic cell.

Zinc known to retard the nucleation rate of apatite formation during initial phase of SBF immersion. Zinc is a highly selective inhibitor of orthoclastic bone resorption in vitro. The effect of zinc on the degradation and bioactivity of borosilicate bioactive glass in simulated body fluid (SBF) and the response of human bone marrow derived stem cells. Zinc doped borosilicate bioactive glass scaffolds could stimulate osteogenesis, which would be great interest for the applications in bone tissue engineering. Zinc acts as a cofactor in several transcription factors and enzymes [35]. While the role of zinc as an essential mineral has long been known, recent research presented the need for the future development of localised Zinc based therapy for enhance anabolic effects.



## CHAPTER – 4

### CHARACTERIZATION TECHNIQUES

Characterization techniques in physics refer to a variety of methods used to analyse the properties and behaviour of materials, systems or particles. These techniques are crucial in understanding the fundamental aspects of physical phenomena and are widely applied in research and industrial setting. These techniques include thickness measured structural morphology by X – Ray diffraction, density find by Archimedes principle and surface morphology by UV- Visible spectrophotometer, electrical resistivity measurement.

#### 4.1. X-RAY DIFFRACTION

X- Ray diffraction is a well -known technique to obtain the information of composition, phase crystalline orientation of material. It gives information about crystal structure, chemical composition and physical properties of material. It detects crystalline material having crystal domains greater than 3-5 nm. It is used to check the monophasic nature of samples. It helps to identify the presence of different phases. Diffraction pattern is obtained by measuring the intensity of scattered waves as a function of scattering angle.

X-Ray is a form of radiation having range wavelength from 0.01 – 0.7 nm which is comparable with the spacing's between lattice planes in the crystal. Spacing between atoms in metals ranges from 0.2-0.3 nm. When an incident beam of X-Rays interacts with target atom, X-Ray photons are scattered in different directions. Scattering is elastic when there is no change in energy between incident ray and scattered ray so interference is constructive and peaks have high intensity. If scattering is inelastic then interference is destructive. In the case of fine particles, with reduction in the size of the particles, XRD lines get broadened, which indicates clearly that particle size has been reduced. Information of the particle size is obtained from the full width at half maximum(FWHMs) of the diffraction peaks.

X-Ray diffraction is based on the Braggs law. This law gives the relationship between wavelength, interplanar spacing and diffraction angle.

$$n\lambda = 2d \sin \theta$$

Where  $n$  = An integer (1,2,3,...)which represents the serial order of diffracted beams

$d$  = distance between planes of the constituent particles in a crystal

$\lambda$  = wavelength of x-rays

$\theta$  = angle between incident x-rays and plane of crystal

$2\theta$  = angle between diffracted x-rays and projection of x-rays

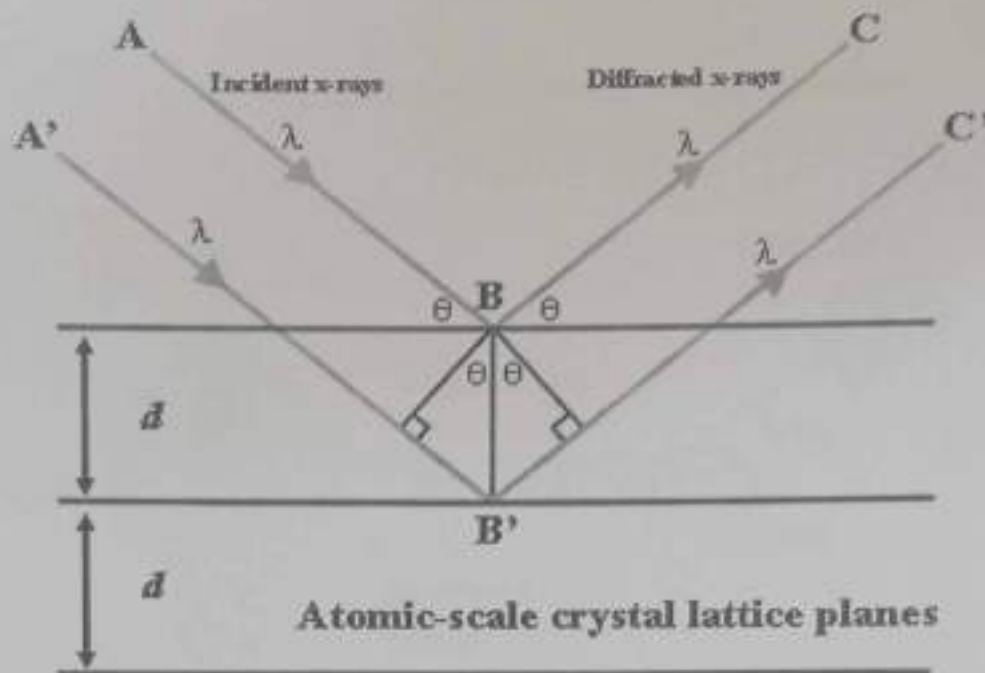


Fig.3: Bragg's law reflection

- **XRD instrumentation and working**

The instrument is called X-Ray Diffractometer. In the diffractometer, an X-ray beam of a single wavelength is used to examine the specimens. By continuously changing the incident angle of the X-Ray beam, a spectrum of diffraction intensity versus the angle between incident and diffraction beam is recorded.

The main components of diffractometer are:

- X-Ray tube: source of X-RAYS
- Incident- beam- optics: to condition the X-ray before it hits the sample
- Goniometer: the platform that holds and moves the sample, optics
- Sample holder
- Receiving – side optics: to condition the X-ray beam after it has encountered the sample
- Detector: to count the number of X-rays scattered by the sample





Fig.4:Schematic representation of x-ray diffraction

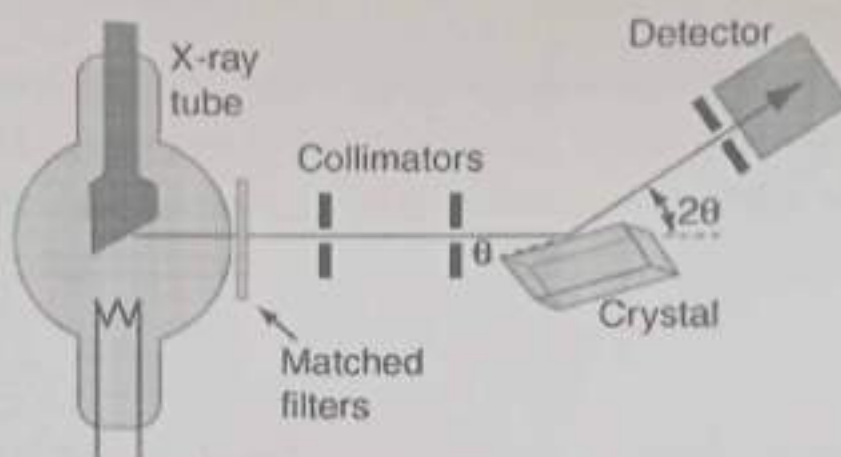


Fig.5:Schematic representation of x-ray diffractometer

X-ray source and detector with its associated optics lie on the circumference of focussing circle and sample stage at the centre of the circle. The angle between the incident x-ray and crystal plane is  $\theta$  and the angle between the projection of x-ray and the detector is  $2\theta$ . For the XRD analysis, fine powder sample can be mounted on the sample holder. When the beam of x-ray is incident on the sample, X-rays are scattered by each atom of the sample. If the scattered beams are in phase, these interfere constructively and one gets intensity maximum at that angle. The atomic planes from where the X-ray are scattered are referred to as "reflecting planes"

### Applications

- Phase identification
- Crystal structure determination
- Radial distribution function
- Crystal size

- Defect studies
- Crystallographic structures
- Quantitative phase analysis
- Residual stress analysis
- High temperature and in-situ studies

## 4.2. ARCHIMEDES' PRINCIPLE

Archimedes' principle states that "The upward buoyant force that is exerted on a body immersed in a fluid, whether partially or fully submerged, is equal to the weight of the fluid that the body displaces and acts in the upward direction at the centre of mass of the displaced fluid".

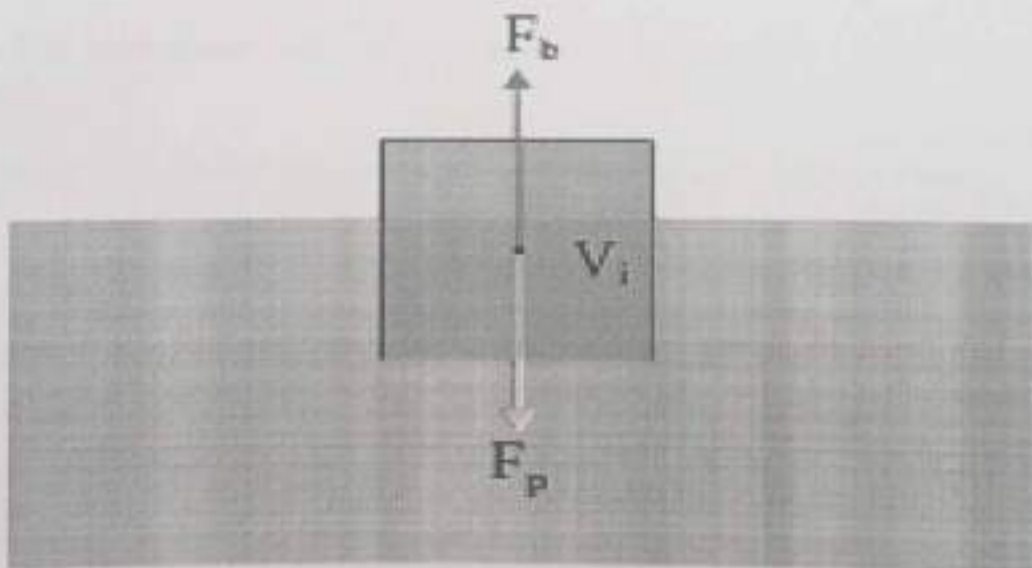


Fig.6: The equilibrium of forces on an object hanging from scale while submerged

### FORMULA

In simple form, the Archimedes law states that the buoyant force on an object is equal to the weight of the fluid displaced by the object. Mathematically written as

$$F_b = \rho \times g \times V$$

Where  $\rho$  is density and  $g$  is the acceleration due to gravity,  $V$  is the submerged volume and  $F_b$  is buoyant force.

We know that the density is defined as

$$\text{Density} = \text{Mass} / \text{Volume}$$

Therefore the mass of the displaced liquid can be written as follows:

$$\text{Mass} = \text{Density} \times \text{Volume}$$

Thrust force is given by the formula

$$\text{Thrust force} = \rho g V$$

This equation is called the law of buoyancy.

So with this technique we can find the density of irregular body by following formula:

$$\text{Density of irregular body} = \text{weight in air} / \text{weight in air} - \text{weight in liquid}$$

### Applications

- **Ships and submarine design:** By calculating the volume of water displaced by the hull, engineers ensure that the ship will float and remain stable under various loading conditions. Submarines adjust their buoyancy by taking in or expelling water from ballast tanks to dive or surface.
- **Hydrometers:** These instruments measure the density or specific gravity of liquids. A hydrometer floats in the liquid, and the level to which it sinks correlates with the liquid's density.
- **Hot air balloons:** They rise because of hot air inside the balloon is less dense than cooler air outside. The buoyant force acting on the balloon is equal to the weight of air displaced by the balloon.

## CHAPTER – 5

### EXPERIMENTAL WORK

#### 5.1.1 PREPARATION OF BOROSILICATE BIOACTIVE GLASS

Borosilicate bioactive glass is prepared by melt – quenching method. Melt – quenching technique is most common technique for the production of bioactive glass. The procedure includes melting oxides of silica, borate, magnesium and sodium ( $25 \text{ B}_2\text{O}_3$ - $25\% \text{ SiO}_2$ - $25 \text{ CaO}$ - $15\text{Na}_2\text{O}$ -  $10\text{MgO}$ ) at  $1100^\circ \text{C}$  in a crucible and quenched in a graphite mold.

First the mixture of ( $25\text{B}_2\text{O}_3 - 25 \text{ SiO}_2 - 25\text{CaO} - 15 \text{ Na}_2\text{O} - 10 \text{ MgO}$ ) is grinded in mortar and pestle to form the powder of mixture. Then powder is taken in a crucible and crucible is placed in the furnace. Set the function of furnace from  $S_1$  to  $S_8$ . Set the temperature of furnace about  $1100^\circ \text{C}$ . The mixture is melted about 5-7 hours in the furnace. The melted mixture is poured into molds of graphite to make the desired shape of glass. Molds of graphite are used for the quenching. Molds of graphite in which mixture is poured, are placed into the muffle furnace where the set temperature is  $400^\circ \text{C}$ . In muffle furnace the mixture is cooled slowly to make the glass amorphous. This process is called annealing. { }.

The synthesis of Bioactive glass through melting and quenching is a sophisticated process that involve several steps, each step is crucial to achieving the desire properties of biomedical applications. This method is widely employed due to its ability to produce a material with enhanced bioactivity, makes it suitable for used in bone grafts, dental implants, and in other medical devices.

Procedure:

1. Raw Material Selection: The synthesis begins with careful selection of raw materials, including  $\text{SiO}_2$ ,  $\text{B}_2\text{O}_3$ ,  $\text{CaO}$ ,  $\text{MgO}$ ,  $\text{Na}_2\text{O}$ , and sometimes additional trace elements. The choice of these compounds is pivotal in achieving a glass composition.
2. Weighing and Mixing: Accurate weighing and precise mixing of the raw materials are crucial to achieving a desired glass composition. The proportions are carefully controlled to ensure the optimal balance of structural integrity, bioactivity and other essential properties.



3. **Melting Process:** The mixed raw materials are then subjected to a high temperature melting process, typically carried out in specialized furnace. The temperature is precisely controlled to allow for the complete homogenization of the components. During the melting phase in furnace, the mixture transforms to a molten glass, a crucial step in the synthesis.
4. **Quenching:** Following the melting process, the molten glass undergoes rapid cooling. Quenching is sudden cooling of glass; it can be done by graphite mold or water. Rapid cooling is critical step that imparts unique characteristics of bioactive glass.
5. **Amorphous Structure Formation:** Quenching prevents the formation of large crystalline structure in glass, resulting in an amorphous structure.
6. **Annealing:** Glass annealing is the heat treatment process where glass is slowly cooled to relieve internal stresses and increase its strength and durability. The slow cooling process allows the glass to reach a state equilibrium, minimizing internal tensions. This treatment is done in the muffle furnace at lower temperature. Annealed glass less prone to breaking.
7. **Shaping:** Shaping and sizing glass typically involve processes like cutting, grinding, and polishing. Shaping can also be done in the molds, where the molten glass is poured for quenching. This method varies based on the type of glass and desired outcome.

**Table1:**Details of chemical composition of the glasses in mol%.

Sr. No.	Sample name	B <sub>2</sub> O <sub>3</sub>	SiO <sub>2</sub>	Na <sub>2</sub> O	CaO	MgO	CuO	TiO <sub>2</sub>	ZnO
1.	Borosilicate Bioactive glass	25	25	15	25	10	0	0	0
2.	Copper doped Borosilicate glass	25	25	15	25	9	1	0	0
3.	Titanium doped Borosilicate glass	25	25	15	25	9	0	1	0
4.	Zinc doped Borosilicate glass	25	25	15	25	9	0	0	1

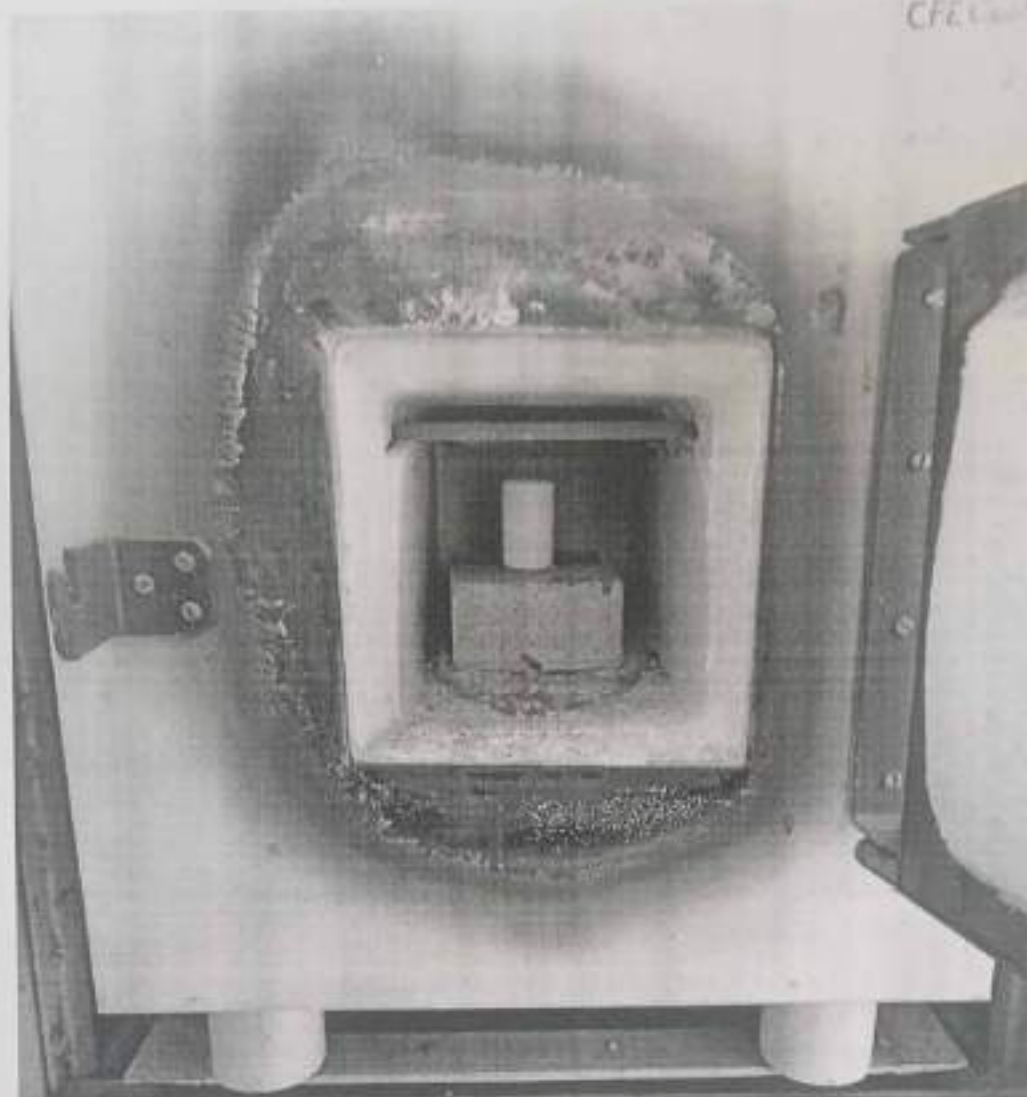


### 5.1.2 PREPARATION OF COPPER DOPED BOROSILICATE BIOACTIVE GLASS

Doping in bioactive glass is typically done to enhance their properties and functionality for biomedical applications. Copper ions have well known antimicrobial properties. Copper play significant role in angiogenesis, the formation of new blood cells. Copper doped borosilicate bioactive glass is makes with the melt quenching method. First the mixture of  $(25 \text{ B}_2\text{O}_3 - 25\text{SiO}_2 - 25\text{CaO} - 15\text{Na}_2\text{O} - 9 \text{ MgO} - 1\text{CuO})$  is grinded in mortar and pestle to form the fine powder of mixture. There is a doping of 1% CuO to enhance the antimicrobial properties of borosilicate bioactive glasses. The crucible is filled by mixture of copped doped bioactive glass. Set the functions from  $S_1$  to  $S_8$ , where the temperature is set at  $1100^\circ\text{C}$  to  $1200^\circ\text{C}$  to melt the mixture. Melted mixture is poured into the graphite molds to obtain the desired shape glass. Mold is placed in to the muffle furnace where the temperature is set to about  $400^\circ\text{C}$  for quenching of glass. A blue coloured copper doped borosilicate bioactive glass is obtained.

### 5.1.3. TITANIUM DOPED BOROSILICATE BIOACTIVE GLASS

Titanium has broad range of applications in the biomedical field. Titanium doping can improve the mechanical properties of the glass, making it more robust and better suited for load bearing applications. First the mixture of  $(25 \text{ B}_2\text{O}_3 - 25\text{SiO}_2 - 25\text{CaO} - 15\text{Na}_2\text{O} - 9 \text{ MgO} - 1\text{TiO}_2)$  is grinded in the mortar and pestle to form the fine powder to mixture. 1% $\text{TiO}_2$  doped in borosilicate bioactive glass to enhance the strength of glass for bearing a load. Mixture is taken in a crucible which is made up of quartz, pyrax, etc. The melting point of crucible should be greater than the melting point of mixture so that when the mixture is melted there no probability of impurity addition. And the mixture is free from impurities. Melt the mixture at  $1100^\circ\text{C}$ , pour the melted mixture into the graphite Mold for quenching of glass. Set the muffle furnace at  $400^\circ\text{C}$  and placed the mold into it. leave it for the 24 hours for annealing. A light yellowish coloured titanium doped borosilicate bioactive glass is formed.



**Fig.7:**Muffle furnace for melting glass by melt quench method

#### **5.1.4. PREPRATION OF ZINC DOPED BOROSILICATE BIOACTIVE GLASS**

The presence of zinc ions has been discovered to enhance the binding of calcium to bone proteins and boost alkaline phosphate activity. Zinc doped borosilicate bioactive glass is made with the melt quenching method. First the mixture of (25 B<sub>2</sub>O<sub>3</sub> – 25SiO<sub>2</sub> – 25CaO – 15Na<sub>2</sub>O – 9 MgO – 1ZnO) is grinded in the ball mill to form the fine powder. Take the mixture in crucible and placed it in the furnace for melting at 1100°C to 1200°C. Poured the mixture into the graphite mold for quenching. Placed the graphite mold in the muffle furnace for annealing process by setting the temperature 400°C. A transparent zinc doped borosilicate bioactive glass is formed with improved properties.

SAMPLE -1



$25\text{B}_2\text{O}_3\text{-}25\text{SiO}_2\text{-}25\text{CaO-}15\text{Na}_2\text{O-}10\text{MgO}$

SAMPLE-3



$25\text{B}_2\text{O}_3\text{-}25\text{SiO}_2\text{-}25\text{CaO-}15\text{Na}_2\text{O-}9\text{MgO-}1\text{TiO}_2$

SAMPLE-2



$25\text{B}_2\text{O}_3\text{-}25\text{SiO}_2\text{-}25\text{CaO-}15\text{Na}_2\text{O-}9\text{MgO-}1\text{CuO}$

SAMPLE -4



$25\text{B}_2\text{O}_3\text{-}25\text{SiO}_2\text{-}25\text{CaO-}15\text{Na}_2\text{O-}9\text{MgO-}1\text{ZnO}$

Fig. 8: Borosilicate Bioactive glasses

### 5.1.5. ARCHIMEDES PRINCIPLE

Archimedes' principle states that the buoyant force on an object equals the weight of the fluid it displaces. Specific gravity is the ratio of density of an object to the fluid. We can determine the density of an object from this principle in the following way: if we measure the weight of the object when immersed in liquid in a fluid  $W_i$  and the weight outside in air  $W_o$  the difference in these forces equal to buoyant force.



Fig.9: Apparatus of Archimedes principle for finding density of glass

For finding the density of glass, first find the weight of glass in air and then for finding the volume of glass immersed it in the benzene solution. Sample is totally immersed in the benzene solution so that accurate weight of glass in solution can be obtained.



Formula Used:

$$\text{Density} = \frac{\text{weight in air}}{\text{weight in air} - \text{weight in benzene}} \times 0.879 \text{ g/m}^3$$

The table given below gives the density of each glass which is calculated by Archimedes principle:

## 5.2. RESULT AND DISCUSSION

### 5.2.1 Archimedes Principle

Table2:

Sr. No.	Type of glass	Weight in air (g)	Weight in Benzene(g)	Density of Benzene(g/m <sup>3</sup> )	Density of glass (g/m <sup>3</sup> )
1.	Borosilicate bioactive glass	5.572	3.560	0.879	2.434
2.	Copper doped borosilicate glass	7.989	5.214	0.879	2.530
3.	Titanium doped borosilicate glass	6.315	4.065	0.879	2.466
4.	Zinc doped borosilicate glass	7.612	4.942	0.879	2.505



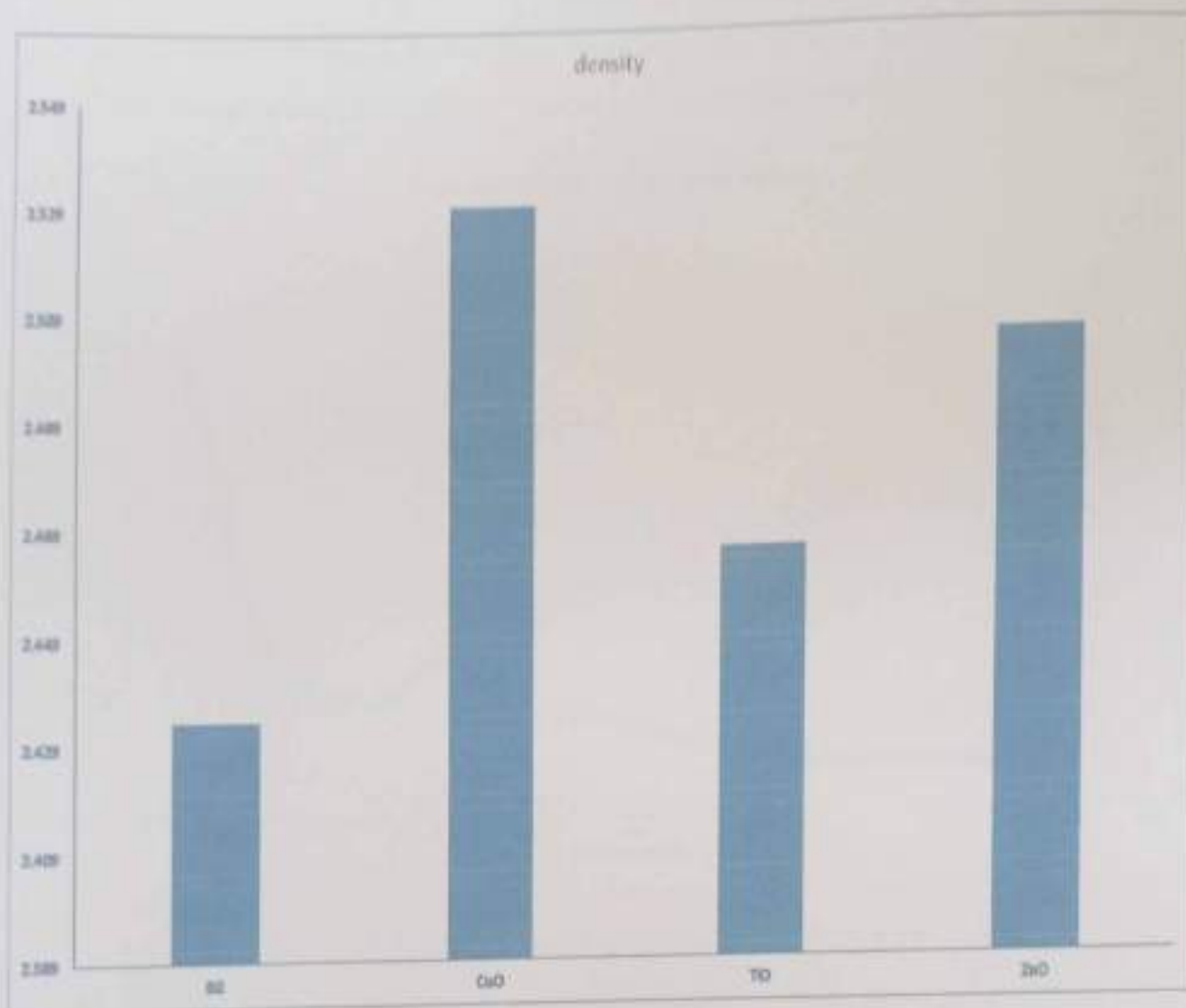


Fig.10: density graph of Borosilicate Bioactive glasses

**Result:** Density of borosilicate bioactive glass is  $2.434\text{g/m}^3$ . By the doping of transition metals in borosilicate bioactive the density of glasses increases.

### 5.2.2. X – RAY DIFFRACTION

Borosilicate bioactive glass interact with body fluid, triggering a series of chemical reactions that ultimately lead to the formation of a layer of hydroxyapatite on its surface.

Doping of copper in Borosilicate bioactive glass enhance its ability to act as an enzymatic cofactor, which directly impacts cellular functions as well as tissue biosynthesis. Copper increases the healing process of broken bones.

Doping of  $\text{TiO}_2$  in borosilicate bioactive glass improve the mechanical properties of glass, making it more robust and it is better suited for load bearing applications.

Zinc doping in borosilicate bioactive glass increase its antibacterial properties. This can help in reducing the risk of infection when the glass used in medical implants or wound dressings.

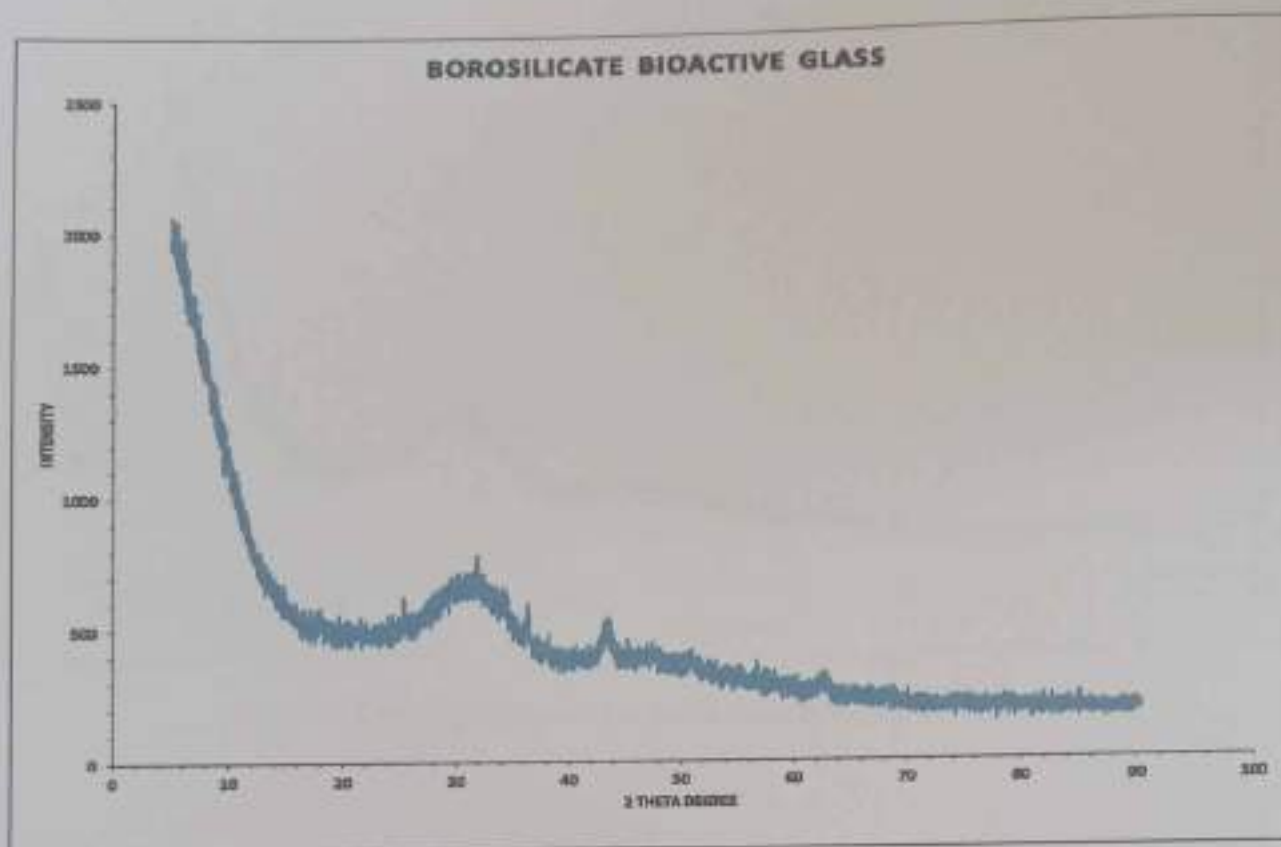


Fig. 11: XRD Spectra of borosilicate bioactive glass

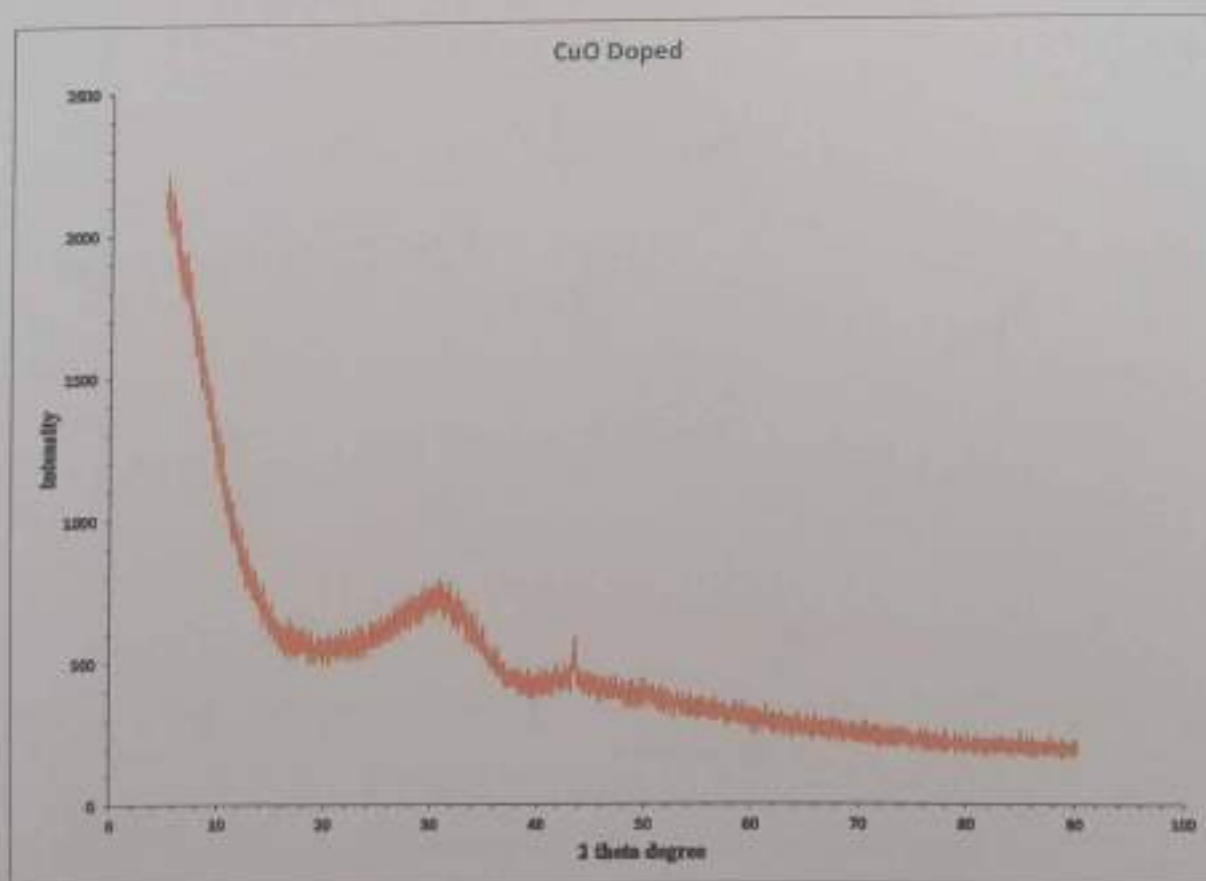


Fig. 12: XRD Spectra of copper doped bioactive glass

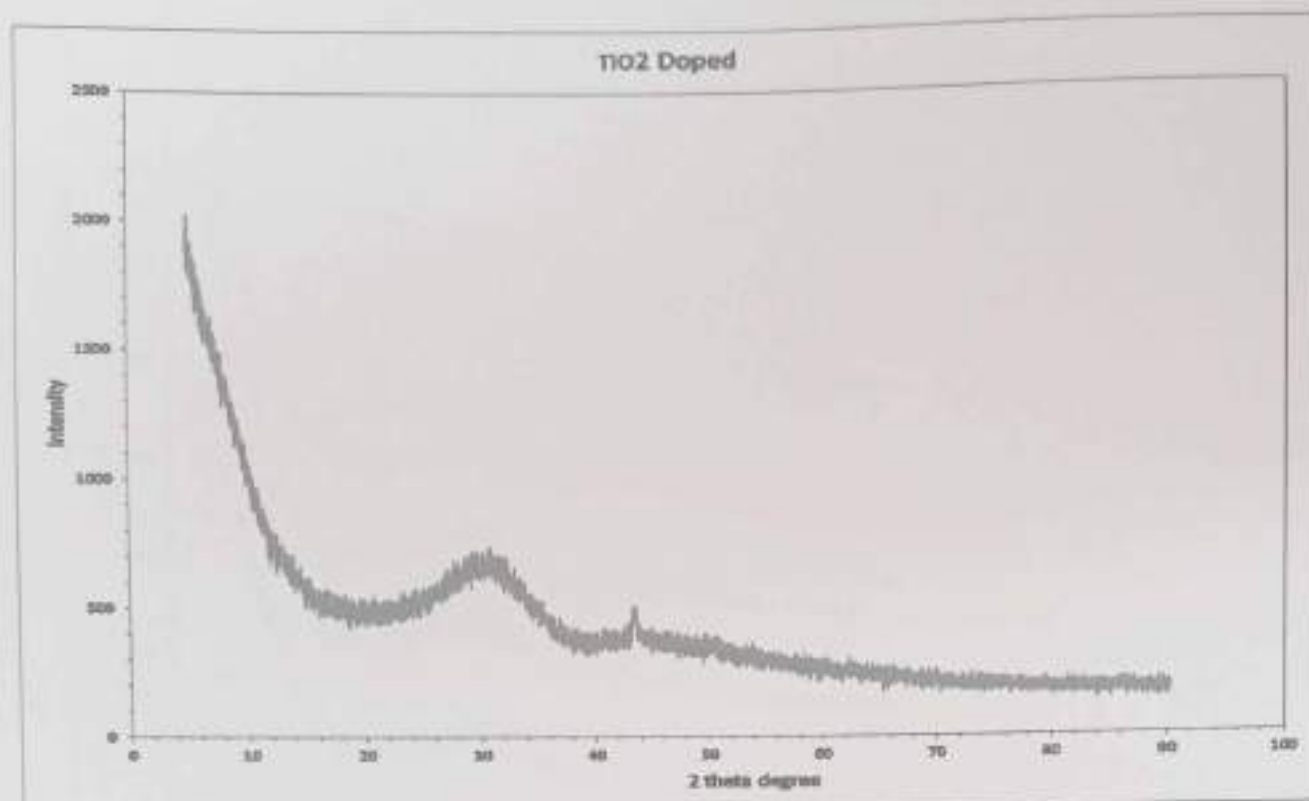


Fig. 13:XRD Spectra of titanium doped bioactive glass

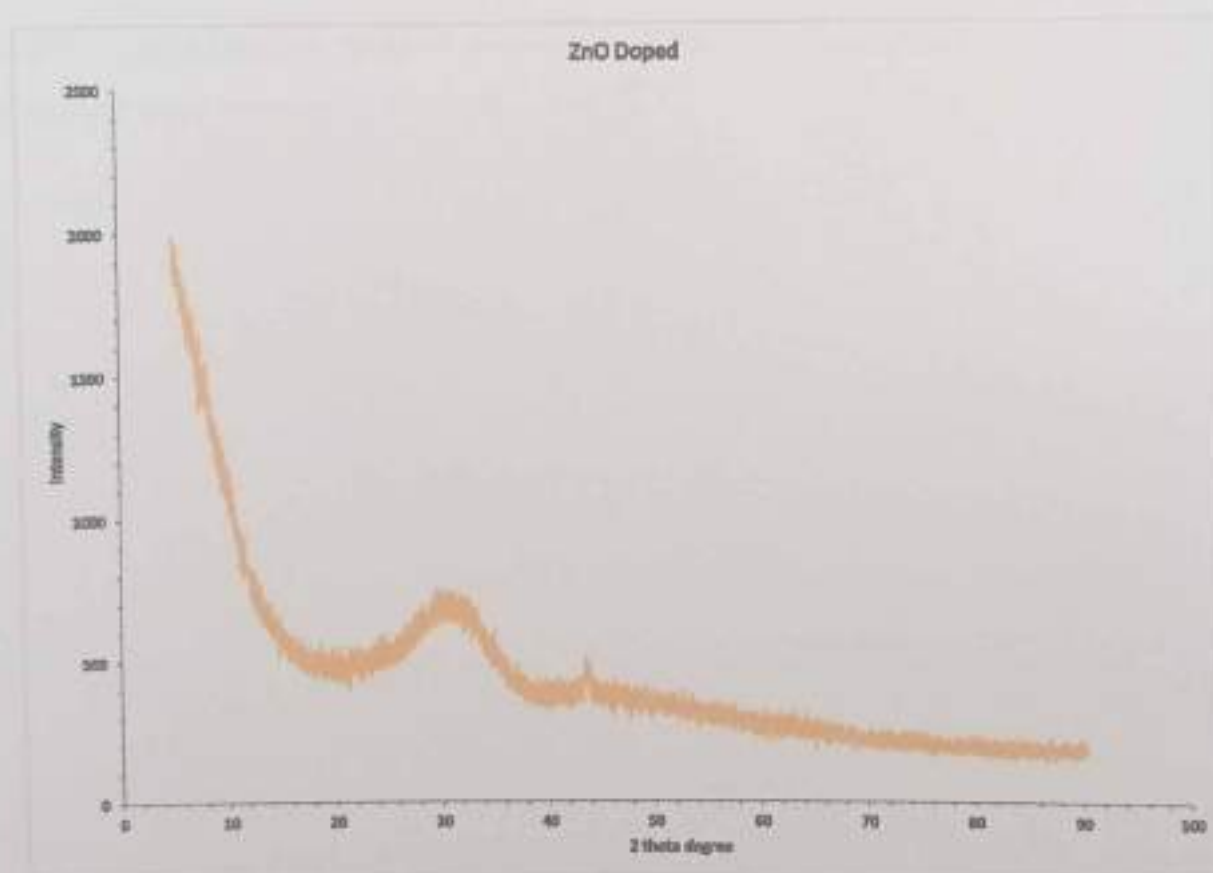


Fig. 14:XRD Spectra of Zinc doped bioactive glass

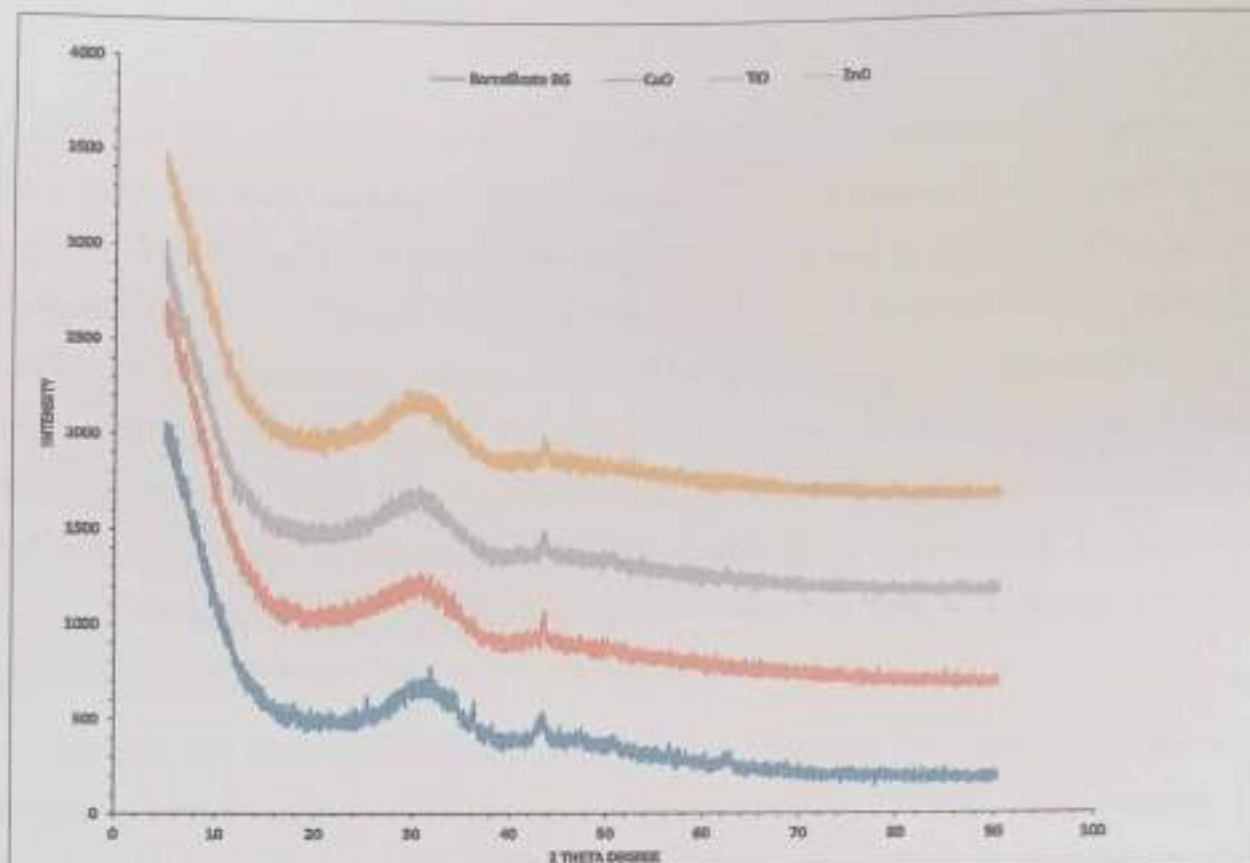


Fig. 15:XRD spectra of Bioactive glasses

**Result:** X-ray diffraction study of Borosilicate Bioactive glasses shows that a fully amorphous glass structure is obtained.

## CONCLUSION

Borosilicate bioactive glass made with melt-quenching technique, have properties to make a bond with bones and lead to the formation of hydroxyapatite layer. Transition metal doped borosilicate bioactive glasses have enhanced mechanical properties such as strength, hardness, and fracture toughness. Doping of copper in Borosilicate bioactive glass enhance its ability to act as an enzymatic cofactor, which directly impacts cellular functions as well as tissue biosynthesis. Copper increases the healing process of broken bones. Doping of  $\text{TiO}_2$  in borosilicate bioactive glass improve the mechanical properties of glass, making it more robust and it is better suited for load bearing applications. Zinc doping in borosilicate bioactive glass increase its antibacterial properties. This can help in reducing the risk of infection when the glass used in medical implants or wound dressings.

Density of Borosilicate bioactive glasses is measured by Archimedes Principle. Borosilicate bioactive glass have density  $2.434\text{g/m}^3$ . Transition metal doping borosilicate bioactive glass have more density than base glass. Copper doped borosilicate bioactive glass have much more density than zinc and titanium doped bioactive glass. X-ray diffraction study shows that borosilicate bioactive glass has amorphous structure.



## REFERENCES

1. Jones, J.R. Reprint of: Review of bioactive glass: From Hench to hybrids. *Acta Biomaterials*. 23, S53 – S82, (2015).
2. Gerhard, L.-C. Boccaccini, "A.R. Bioactive Glass and Glass – Ceramic Scaffolds for Bone Tissue Engineering". *Materials*, 3, 3867-3910, (2010).
3. Jones, J.R. Reprint of: Review of bioactive glass: From Hench to hybrids. *Acta Biomaterials*, Vol. 23, No. 1, 23, S53 – S82, (2015).
4. Kargozar, S. F. Baino, S. Hamzehlou, R. G. Hill, and M. Mozafari. "Bioactive Glasses entering the mainstream". *Drug Discovery*, Vol. 23, No. 10, pp. 1700-1704, (2018).
5. Fernandes, H.R., A. Rebelo, D. Brazete, G.E. Stan, and J.M.F. Ferreira. "Bioactive glasses and glass ceramics for healthcare applications in bone regeneration and tissue engineering". *Materials (Basel)*, Vol. 11, No. 12, id. 2530, (2018).
6. Ratner B.D., Hoffman A.S., Schoen F.J., Lemons J.E. *Biomaterials Science: "An Introduction to Materials in Medicine"*. Academic press; Cambridge, MA, USA, (2004).
7. Y. Lin, J. C. Mauro, G. Kaur "Bioactive glass for Cancer therapy". *Woodhead Publishing Series in Biomaterials*, 273-31 (2019).
8. Ben- Arfa, B.A.E.; Neto, A.S.; Palama, I.E.; Salvado, I.M.M.; Pullar, R.C.; Ferreira, J.M.F. "Robocasting of  $\text{Cu}^{2+}$  and  $\text{La}^{3+}$  doped sol – gel glass scaffolds with greatly enhanced mechanical properties: Compressive Strength up to 14 MPa". *Acta Biomater.* 87, 265 – 272, (2019).
9. Hench L.L. "Bioceramics: From Concept to Clinic". *J. Am. Ceram. Soc.* 81, 1705 – 1728, 2005.
10. Hench L.L. "The Story of Bioglass". *Journal of Material Science. Materials in medicine*, Vol. 17, No. 11, pp 967- 978, Nov (2006).
11. Li, R. Clark, A.E. Hench L.L. "An Investigation of Bioactive glass Powders by Sol – Gel Processing". *J. Appl. Biomater.* 2, 231 – 239, (1991).
12. Hench L.L. Bioceramics: "From Concept to Clinic". *J. Am. Ceram. Soc.* 74, 1487- 1510, (1991).
13. Hulbert, S.F. Young, F.A. Mathews, R.S. Klawitter, J.J. Talbert C.D. Stelling, F.H. "Potential of Ceramic Materials as Permanently implantable Skeletal Prostheses", *J. Biomed Mater. Res.* 4: 433 – 456, (1970).

14. <https://www.intechopen.com/books/advanced-techniques-in-bone-regeneration/doped-bioactive-glass-materials-in-bone-regeneration>. Access 18.04.2017.
15. Liu, J. Miao X. "Sol – Gel Derived BIOGLASS as a Coating material for porous Alumina Scaffolds", *ceramics International*, 30(7):1781-1805, (2004).
16. Li, N.Jie, Q. Zhu, S. Wang, R. "Preparation and characterisation of Mesoporous Sol-Gel Bioglass", *Ceramic International*, 31(5) : 641-6, (2005).
17. Xia, W. Chang J. "Well – ordered Mesoporous Bioactive Glasses (MBG) ; A Promising Bioactive Drug Delivery system", *Journal of Control Release*, 110(3): 522-30,(2006).
18. Balamurugan, A. Sockalingum, G. Michel. J. Faure, J., Banchet, V. Wortham, C. et al. " Synthesis and Characterisation of Sol gel Derived Bioactive glass for Biomedical Applications", *Materials Letter*, 60(29) : 3752-7, (2006).
19. Li, R. Clark, A. Hench, L.L. " An investigation of Bioactive glasspowdersby sol-gel processing", *Journal of Applied Biomaterials*, 2(4) ; 231-9, (1991).
20. Oki, A. B. Parveen, S. Hossain, S. Adenji, and H. Donative. "Preparation and in Vitro bioactivity of Zinc Containing Sol-Gel derived bioglass materials". *Journal of Biomedical Materials Research. Part A*, Vol. 69, No. 2, pp.216-221, (2004).
21. Baino, F. and C. Vitale- Borovaron. "Three dimensional glass derived scaffolds for bone tissue engineering; Current trends and forecasts for the future". *Journal of Biomedical Materials. Research. Part A*, Vol. 97, No.4, pp. 514-535, (2011).
22. C. Wu et al. "Hypoxia – mimicking mesoporous bioactive glass scaffolds with controllable cobalt ion release for bone tissue engineering", *Biomaterials* (2012).
23. H. Rico et al. "Effects on bone loss of Mg alone or with copper supplement in ovariectomised rats; a morphometric and densitometric study". *Eur J. Obstet. Gynecol. Reprod. Biol.* (2000).
24. S.P. Singh et al. "Enhanced in vivo biocompatibility of magnesia- contained Bioactive glasses" *J. Aust. Ceram. Soc.* (2018).
25. M. Daziadek et al. "A simple way of modulating in vitro angiogenic response using Cu and Co – doped Bioactive glasses". *Mater. Lett.* (2018).
26. Lacefield, W. Hench, L.L. "The Bonding of Bioglass to a Cobalt-Chromium Surgical Implant Alloy", *Biomaterials*, 7(2):104-8, (1986).
27. C. Wu et al. "Copper Containing mesoporous bioactive glass scaffolds with multifunctional properties of angiogenesis capacity, osteostimulation and antibacterial", *Biomaterials* (2013).

28. B.R. Mc Auslan, W. Reilly, "Endothelial cell phagokinesis in response to specific metal ions", *Exp. Cell Res.* 130(1) 147-157,( 1980 Nov 1).
29. G.F. Hu, "Copper stimulates proliferation of human endothelial cell under culture", *J.Cell. Biochem.* 69(3).326-335. (1998).
30. E.A. Abou Neel, J.C. Knowles, "physical and Biocompatibility studies of novel titanium dioxide doped phosphate-based glasses for bone tissue engineering applications", *J. Mater. Sci. Mater. Med.* 19. 377-386, (2018).
31. M. Hashimoto, S. Kitakaoka, "Effect of Surface Charge of  $TiO_2$  particles on hydroxyapatite formation in simulated body fluid", *Adv. Powder Technol.* 27 ,2409-2415, (2016).
32. A.L. Raines, R. Olivares- Navarrete, M. Wieland, D.L. Coachron, Z. Schwartz, B.D. Boyan, "Regulation of angiogenesis during osseointegration by titanium surface microstructure and energy", *Biomaterials* 31, 4909-4917, (2010).
33. Ishakawa, K. Miyamoto, Y. Yuasa, T. Ito, A.Nagayama, M. Suzuki, K. "Fabrication of Zn containi8ng apatite cement and its initial evaluation using human osteoblastic cells". *Biomaterials*, 22, 423-428, (2002).
34. Wey, A.; Cunningham, C.; Hraha, J.; Breitbart, E.; Cattel, J.; Ippolito, J.; Clark, D.; Lin, H.N.; Benevenia, J.; o' Conner, J.P.; et al." Local  $ZnCl_2$  Accelerates fracture healing" , *J. Ortho. Res.* 32,834-841, (2014).
35. L.L. Hench et al. "Bonding mechanism at the interface of ceramic prosthetic materials". *J. Biomed. Mater. Res.* (1971).



**INVESTIGATING RADON CONCENTRATION IN GROUNDWATER  
USING RAD7: A CASE STUDY OF BADDI CITY, DISTRICT SOLAN,  
HIMACHAL PRADESH, INDIA**

***PROJECT REPORT***

Submitted in partial fulfillment of the  
requirements for the award of the degree of

**MASTER OF SCIENCE**

**in**

**PHYSICS**

*By*

**Dharamveer Singh**  
(Reg.No.8114-2022-1793)



**DEPARTMENT OF PHYSICS**  
**SRI GURU TEG BAHADUR KHALSA COLLEGE, SRI ANANDPUR SAHIB**  
(An Autonomous College)  
**ANANDPUR SAHIB-140118, PUNJAB (INDIA)**



## CERTIFICATE

It is certified that the work contained in the project report entitled "**Investigating Radon Concentration in Groundwater Using RAD7: A Case Study of Baddi City, District Solan, Himachal Pradesh, India**" is an original contribution by me and has not been submitted in part or full for any other degree at this or other University/Institute.

The assistance and help received during the course of the thesis work have been acknowledged.

*Dharamveer Singh*  
**Dharamveer Singh**  
Regn.No. **8114-2022-1793**

I, the undersigned, Supervisor of **Dharamveer Singh**, Reg.No **8114-2022-1793**, a candidate for the degree of **Master of Science**, agree that the project report entitled, "**Investigating Radon Concentration In Groundwater Using RAD7: A Case Study of Baddi City, District Solan, Himachal Pradesh, India**", may be submitted in partial fulfillment of the requirements for the award of degree.

This is to certify that the above statement made by the candidate is correct to the best of my knowledge.


*Vimal Mehta*  
**Supervisor**  
Dr. Vimal Mehta  
Assistant Professor  
Department of Physics  
Sri Guru Teg Bahadur Khalsa College  
Sri Anandpur Sahib



## CERTIFICATE

This is to certify that the "Project report" entitled **"INVESTIGATING RADON CONCENTRATION IN GROUNDWATER USING RAD7: A CASE STUDY OF BADDI CITY, DISTRICT SOLAN, HIMACHAL PRADESH, INDIA"** submitted by **DHARAMVEER SINGH (Regn. No. 8114-2022-1793)** to Department of Physics, Sri Guru Teg Bahadur Khalsa College, Sri Anandpur Sahib in partial fulfillment of the requirements for the award of degree of **MASTER OF SCIENCE IN PHYSICS** and has been approved by the Department Research committee (DRC) after the viva-voce examination of the candidate.

  
Dr. Vimal Mehta  
Supervisor

  
Dr. Randev Singh  
Chairman DRC

## ACKNOWLEDGEMENT

Firstly, I would like to express my gratitude to my Supervisor, Dr. Vimal Mehta Assistant Professor at Department of physics Sri Guru Teg Bahadur Khalsa College Sri Anandpur Sahib, who has resourcefully guided me throughout this research project. I'm extremely grateful for his motivating discussions while enable me to accomplish this task successfully. Without his active guidance, support and encouragement I would not have made headway in this project.

I also thankful to my Parents for their moral support and suggestions to improve the dissertation work. I'm also thankful to other faculty members in the department for their encouragement and fruitful academic discussions.

A special thank to Ms. Seema Assistant Professor at Department of Physics for the help and their valuable suggestions whenever I needed out of their busy schedule. I'm also thankful to my classmates and my friends who were directly or indirectly help me to complete this project report.

Dharamveer Singh

## ABSTRACT

The detection of Radon in groundwater presents a significant environmental issue due to its potential health hazards. This investigation is centered on Baddi City in the Solan District of Himachal Pradesh, India, where industrial activities increase the risk of groundwater contamination. The aim is to evaluate Radon concentrations in groundwater utilizing the RAD7 method. Water samples from various locations in Baddi City were collected and analyzed using the RAD7 device to determine Radon levels. This methodology integrated RAD7 usage to comprehensively analyze groundwater quality concerning radioactive elements. Additionally, the study examined the health risks associated with consuming this contaminated water. The results underscore the necessity for regular monitoring and remediation strategies to mitigate Radon risks in groundwater. This study serves as a critical reference for environmental scientists and policymakers, emphasizing the importance of employing integrated technological approaches for accurate groundwater contamination assessment and effective environmental health policies. In conclusion, it offers valuable insights into Baddi City's groundwater quality and stresses the need for ongoing research and monitoring to safeguard public health and groundwater sustainability. The integrated use of RAD7 emerges as a dependable method for assessing Radon in groundwater, paving the way for future studies in similar industrial areas. Results indicated varying Radon concentrations across different sampling points, with some locations exceeding safe limits set by international health agencies.

**Keywords:** - Radon contamination, DurrIDGE RAD7.

## **CONTENT**

<b>CHAPTER</b>	<b>Page No.</b>
<b>1. Introduction</b>	<b>7-8</b>
<b>2. Research Objectives</b>	<b>9</b>
<b>3. Literature Review</b>	<b>10-12</b>
<b>4. Methodology</b>	<b>13-29</b>
• Sample collection	<b>13-15</b>
• Location and pictures of sampling sites	<b>15-28</b>
• RAD7	<b>28-29</b>
<b>5. Results and Discussion</b>	<b>30-32</b>
<b>6. Conclusion</b>	<b>33</b>
<b>7. References</b>	<b>34-35</b>

## LIST OF FIGURES

S. No.	Name of the Figure
Fig.1	Study area site (Baddi City)
Fig.2	Location of the sampling sites
Fig.3	RAD7
Fig.4	Schematic diagram of RAD7-H2O
Fig.5	Radon concentration variation with Depth of the Source
Fig.6	Radon concentration variation with pH of the Collected Samples
Fig.7	pH variation with depth of the Source



## INTRODUCTION

The quality of groundwater is crucial for environmental well-being, especially in areas where it's the main drinking water source. Elements like Radon can have significant implications for both human health and the ecosystem. In Baddi City, situated in the picturesque Solan district of Himachal Pradesh, India, it's vital to grasp the levels of Radon in groundwater. This research project is focused on conducting a comprehensive assessment of Radon concentrations in Baddi City's groundwater, utilizing data obtained from the RAD7 Radon analyzer. Radon is a noble gas with the chemical symbol Rn and atomic number 86. It is colorless, odorless, and tasteless. Radon occurs naturally as a decay product of uranium and thorium in soil, rocks, and groundwater. Due to its radioactive nature, Radon poses health risks when inhaled. It is the second leading cause of lung cancer after smoking. This knowledge is crucial for a thorough environmental assessment and understanding the potential health risks associated with Radon contamination in groundwater.

### • RADON

#### 1. Radon Isotopes: Tracing Radioactive Signatures

The Radon Isotopes  $\text{Rn}^{219}$  (Actinon),  $\text{Rn}^{220}$  (Thoron), and  $\text{Rn}^{222}$  (Radon) occur in nature. Despite their rather short half-lives, because they are continuously generated from their mothers  $\text{Ra}^{223}$ ,  $\text{Ra}^{224}$ , and  $\text{Ra}^{226}$ , which are in secular equilibrium with long-lived isotopes  $\text{U}^{235}$ ,  $\text{U}^{238}$ , and  $\text{Th}^{232}$ , and are in turn continuously formed from these long-lived isotopes [1] Radon -222 ( $^{222}\text{Rn}$ ) being the most prevalent and naturally occurring.

#### 2. Oxidation States: Noble Gas Anomaly

As a noble gas, Radon does not have conventional oxidation states in the same sense as metals. Its inert nature contributes to its mobility and stability in groundwater. Research by Sicilia et al. [2] and Feng et al. [3] explores the unique chemical behavior and migration patterns of Radon in different geological contexts.

#### 3. Water Solubility: Gaseous Mobility in Aquifers

Radon's solubility in water is a critical factor influencing its transport through aquifers. Being a gas, Radon dissolves in water to form  $^{222}\text{Rn}$ , and its solubility is influenced by

factors such as temperature and pressure. Research contributions by Malvicini et al. [4] and Ye et al. [5] provide detailed insights into Radon solubility dynamics in various hydro geological conditions.

#### 4. Geological Behavior: Influencing Transport and Accumulation

Radon's geological behavior is influenced by factors such as soil composition and aquifer characteristics. The emanation of Radon depends upon the source term uranium concentration, the nature of the host mineralogy, the permeability of the host rock and soil and the characteristics of the transporting medium. Weather can have a profound effect upon the concentration of Radon in soil gas but often the variation due to the geological substrate is greater. Radon is not a problem unless it collects in buildings and underground structures. [6]

#### 5. Health Implications: Inhalation Risks and Cancer Concerns

Ingesting water containing elevated Radon levels can lead to health issues, especially lung cancer through inhalation. Extrapolation from cohort studies on miners suggested that Radon is the second leading cause of lung cancer death after tobacco smoke. The majority of studies on the relationship between Radon and other types of cancers showed weak or no association. Low levels of Radon can be found in drinking water; however, Radon released during water usage adds small quantities to indoor Radon concentration. [7]

#### 6. Regulatory Measures and Monitoring: Ensuring Air and Water Safety

Given the potential health risks associated with Radon, regulatory measures and monitoring programs play a pivotal role. Established guidelines aim to limit Radon concentrations in both air and water, ensuring the safety of the environment and public health. The comprehensive work by Environmental Protection Agency (EPA) guidelines [8] and ongoing monitoring efforts by regional agencies contribute to the development of effective strategies for managing and mitigating Radon-related risks in groundwater.

This introduction serves as a foundation for our research project, providing an extensive overview of Radon in groundwater. As we assess their concentration, this foundational knowledge will guide our exploration, contributing to a more profound understanding of these elements' dynamics in diverse environmental contexts.

## RESEARCH OBJECTIVES

This study is all about getting a deeper understanding of how Radon is present in our groundwater. We're looking to figure out how they're distributed, how different earthy chemical processes affect them, and how we can better analyze them. Plus, we want to know what kind of impact they could have on our health and the environment. By digging into these details, we hope to offer some insights that can help manage our groundwater better and add to the ongoing conversation about keeping our water resources sustainable for the future. In the sections that follow, we'll dive into the methods we used, what we discovered, and our thoughts on the whole issue, focusing on the tricky bits about Radon in groundwater. The properties of Radon and their MCL in consumable water are given as follow:

### • Properties and safe drinking water ingestion levels of Radon

Radon, a colorless, odorless, and tasteless radioactive gas, is a decay product of uranium. Its primary isotopes are,  $^{222}\text{Rn}$  and  $^{220}\text{Rn}$ , causes health risks when inhaled or ingested. Radon is water-soluble, allowing it to enter groundwater, making its detection and measurement crucial for assessing the overall water quality. The DurrIDGE RAD7 is known for its sensitivity to Radon, enhances the precision of Radon concentration measurements in groundwater

- The World Health Organization (WHO) [9] sets a provisional guideline value of 11 Bq/L for Radon in drinking water.
- According to UNSCEAR [10] safe Radon concentration value in water for consumption is between 4-40 Bq/L.

## LITERATURE REVIEW

Assessing groundwater quality plays a crucial role in environmental monitoring, particularly in regions susceptible to Radon contamination. In Baddi City, located in Solan district, Himachal Pradesh, India, understanding the level of this radioactive element is vital for public health protection. This literature review investigates existing knowledge, methodologies, and recent research related to RAD7 instruments for assessing Radon concentration in groundwater.

### Radon in Groundwater:

In India, diverse geological conditions pose challenges related to groundwater contamination by Radon. Radon, a radioactive gas produced during uranium decay, dissolves in groundwater, posing risks through inhalation. Understanding the sources, transport mechanisms, and concentrations of Radon is crucial for managing and mitigating these risks.

Ensuring access to safe and clean drinking water is vital for public health. In Baddi City, located in the scenic district of Solan, Himachal Pradesh, India, there are growing concerns about Radon contamination in groundwater.

This literature review aims to establish a foundational understanding of the dynamics and challenges related to Radon concentration in Baddi City's groundwater. Numerous researchers have conducted studies on assessing Radon concentration in Indian groundwater. Some ongoing research focuses on understanding the sources, transport mechanisms, and health risks associated with this element.

Several studies in India have explored groundwater quality, Radon concentration few of them are as follow:

Singh et al. collected drinking water samples from Hamirpur and Kangra districts of Himachal Pradesh and adjoining areas of Jammu and Kashmir, India and found concentration of,  $^{238}\text{U}$  and  $^{222}\text{Rn}$  in these samples in the range of  $0.26 \pm 0.1$  to  $29.5 \pm 2.5$  ug/L and  $0.86 \pm 0.12$  to  $7.62 \pm 0.64$  Bq/l. respectively. The measured values of  $^{238}\text{U}$  and  $^{222}\text{Rn}$  concentration are within the safe limits as recommended by WHO and USEPA. [11]

P. Nandakumaran et al. do comparative study of the radon concentrations in groundwater in the high and normal background radiation areas in the coastal tract has been taken up using analytical data of 24 ground water samples collected from tube wells of ranging in depth from 6.0 to 300.0 m. The radon concentration in the samples ranged from 0.88 to 25.80 Bq/L. [12]

Manish Kumar et al. found concentration of Uranium and radon in the range of  $1.53 \pm 0.06$  mg/m<sup>3</sup> to  $50.2 \pm 0.08$  mg/m<sup>3</sup> with a geometric mean value of 14.85 mg/m<sup>3</sup> and  $0.34 \pm 0.07$  kBq/m<sup>3</sup> to  $3.84 \pm 0.48$  kBq/m<sup>3</sup> with a geometric mean value of 1.46 kBq/m<sup>3</sup> respectively in the drinking water samples which collected from Jalandhar district of Punjab. [13]

Supriya Rani et al. emphasize the risks associated with radon gas. In Barnala, Punjab, India, scintillation detectors were employed to assess radon isotopes in drinking water. Concentrations varied from  $0.17 \pm 0.01$  to  $9.84 \pm 0.59$  BqL<sup>-1</sup>, with an average of  $3.37 \pm 0.29$  BqL<sup>-1</sup>. These findings remained below the WHO limit of 100 BqL<sup>-1</sup>, suggesting negligible health risks from radon in water. [14]

Panghal and Kumar et al. Collected drinking water samples from various locations of four districts of Haryana, India. The uranium (<sup>238</sup>U) and radon (<sup>222</sup>Rn) concentrations in water samples have been found to vary from 1.07 to 40.25 µg/L with an average of 17.91 µg/L and  $16.06 \pm 0.97$  to  $57.35 \pm 1.28$  Bq/L with an average of  $32.98 \pm 2.45$  Bq/L, respectively. [15]

Ankur Kumar et al. give result that revealed radon activity in water samples from Bageshwar region varies from 3.4 to 101.3 Bq/L with a mean value of  $34.4 \pm 3.8$  Bq/L while the uranium concentration in water samples ranges from 0.1 to 28.4 µg/L with the mean value of 1.6 µg/L. [16]

Manpreet Kaur et al. collected water samples used by the inhabitants, of the villages of the Shiwalik Himalayas of Jammu and Kashmir, India. Measured the concentration of Uranium and Radon and reported all values of doses were below the proposed limit of 100 µSv/ year for all age categories except for infants due to the high-dose conversion factor. [17]

Asha Rani et al. found varying radon concentrations in groundwater samples from northern Rajasthan, India. Levels ranged from  $0.5 \pm 0.3$  Bq/L (Chimanpura) to  $85.7 \pm 4.9$  Bq/L (Khandela), averaging  $9.03 \pm 1.03$  Bq/L. 89% of samples fell below the US EPA's maximum



contamination level (MCL) of 11 Bq/L. Only 11% exceeded this limit, with 5% surpassing the UNSCEAR's suggested range of 4-40 Bq/L for human consumption. [18]

## METHODOLOGY

Baddi is a town in the Solan district of Himachal Pradesh, India. Geographically, it is situated at approximately 30.928°N latitude and 76.796°E longitude. Baddi lies on the border of Himachal Pradesh, Punjab, and Haryana states in the Shivalik Hills. The specific land area covered by Baddi town is approximately 38.57 Km<sup>2</sup>. This figure represents the town's administrative boundaries and includes both developed and undeveloped areas within those limits. The city has 29,911 people living there (according of 2011 census), that is 775.45 persons per Km<sup>2</sup>.

### Sample collection

27 ground water samples were collected across the city by using a grid on the map of the city. The sites are mentioned in the Figure 1a and Figure 1b given below. The exact latitude and longitude of the sites are obtained by using a application called GPS Map Camera.

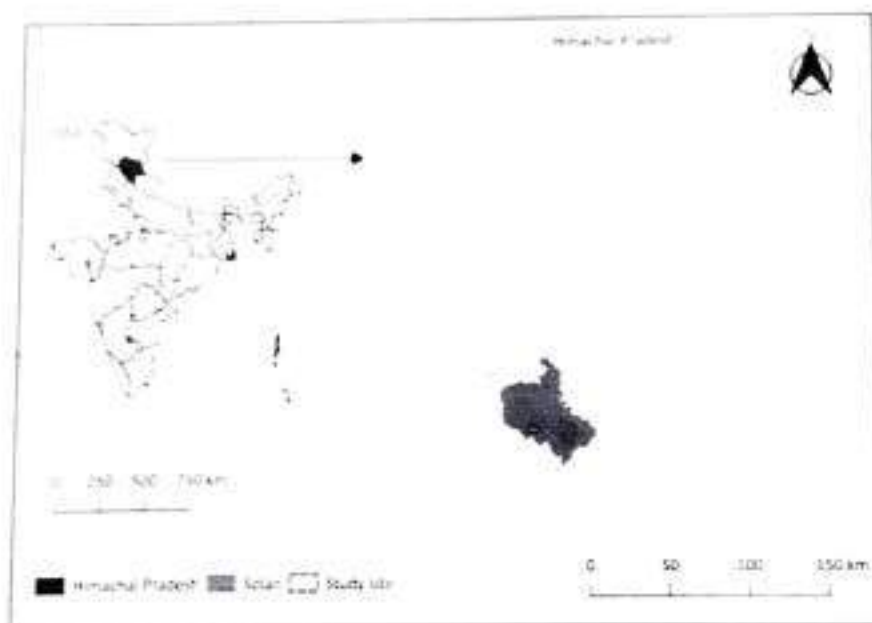


Fig.1: Study area site (Baddi City)

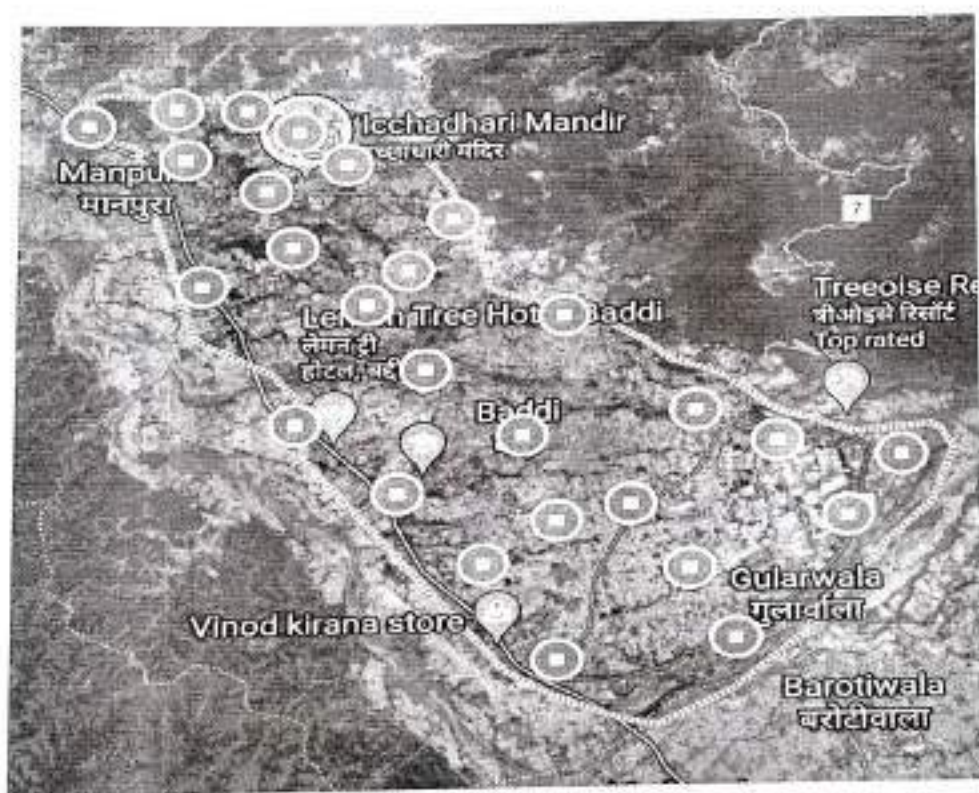


Fig.2: Location of the sampling sites

High density polyethylene plastic bottles of 250ml were used to collect samples which were cleaned using dilute HCL (0.5N HCL) and were rinsed with deionised water before taking sample. Before collecting sample the water sources were run made to run for few minutes so that we can collect fresh water for sampling for better and accurate results. And then bottles are prewashed with source water 2-3 times before collecting sample. Samples are collected in



that way so that there will be minimum or no air bubble left inside the bottles because it will affect the Radon detection. Then Radon concentration is measured by DurrIDGE RAD7.

## Location and Pictures of sampling sites

### Sample 1



Site of sample 1



Location of sample 1

### Sample 2



Site of sample 2



Location of sample 2

### Sample 3



Site of Sample 3



Location of sample 3

### Sample 4



Location of sample 4



Site of sample 4



## Sample 5



Site of sample 5



Location of sample 5

## Sample 6

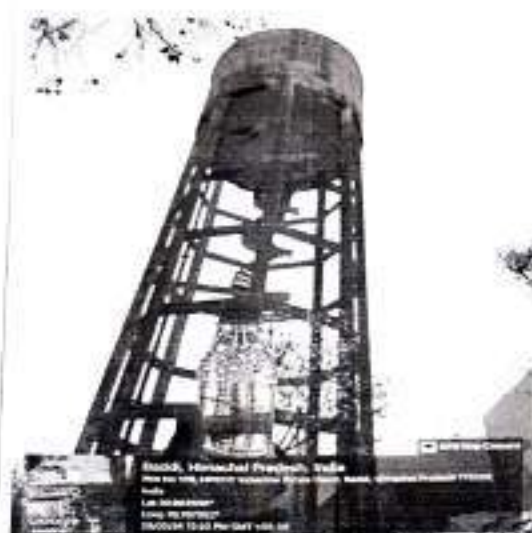


Site of sample 6



Site of sample 6

## Sample 7



Site of sample 7



Location sample 7

## Sample 8



Site of sample 8



Location of sample 8



## Sample 9



Site of sample 9



Location of sample 9

## Sample 10



Site of sample 10



Location of sample 10

## Sample 11



Site of sample 11



Location of sample 11

## Sample 12



Site of sample 12



Location of sample 12



### Sample 13



Site of sample 13



Location of sample 13

### Sample 14



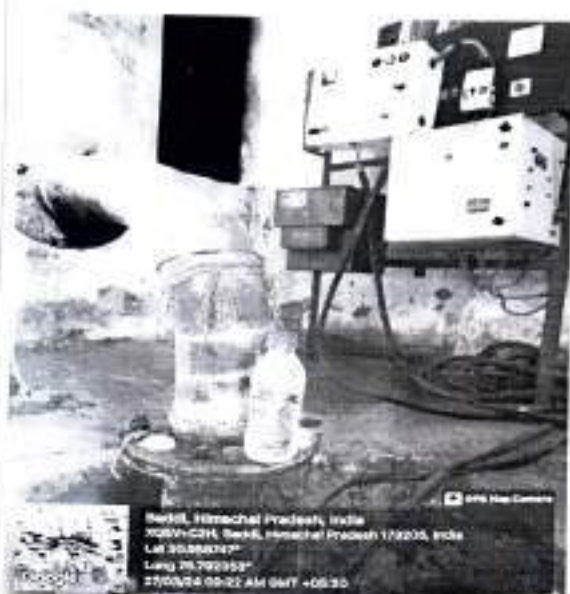
Site of sample 14



Location of sample 14



## Sample 15



Site of sample 15



Location of sample 15

## Sample 16



Site of sample 16



Location of sample 16

## Sample 17



Site of sample 17



Location of sample 17

## Sample 18



Site of sample 18



Location of sample 18



## Sample 19



Site of sample 19



Location of Sample 19

## Sample 20



Site of sample 20



Location of sample 20

## Sample 21



Site of sample 21



Location of sample 21

## Sample 22



Site of sample 22



Location of sample 22



## Sample 23



Site of sample 23



Location of sample 23

## Sample 24



Site of sample 24



Location of sample 24



## Sample 25



Site of sample 25



Location of sample 25

## Sample 26



Site of sample 26



Location of sample 26

## Sample 27



Site of sample 27



Location of sample 27

## RAD7

RAD7 H<sub>2</sub>O is a special attachment of RAD7 used for the measurement of Radon concentration in water. The range of the RAD7 lies between 10 pCi/l to 4105 pCi/l [19], with a lower limit of detection below, 10 pCi/l. This portable and battery-operated equipment ensures expeditious measurements. The schematic diagram of RAD H<sub>2</sub>O is illustrated in Figure 4. Post a 20 minutes analysis, RAD H<sub>2</sub>O delivers results with sensitivity matching or surpassing that of liquid scintillation methods. Employing a closed-loop aeration scheme, RAD H<sub>2</sub>O maintains constant air and water volumes independent of the flow rate. The system achieves equilibrium.



Fig.3: RAD7

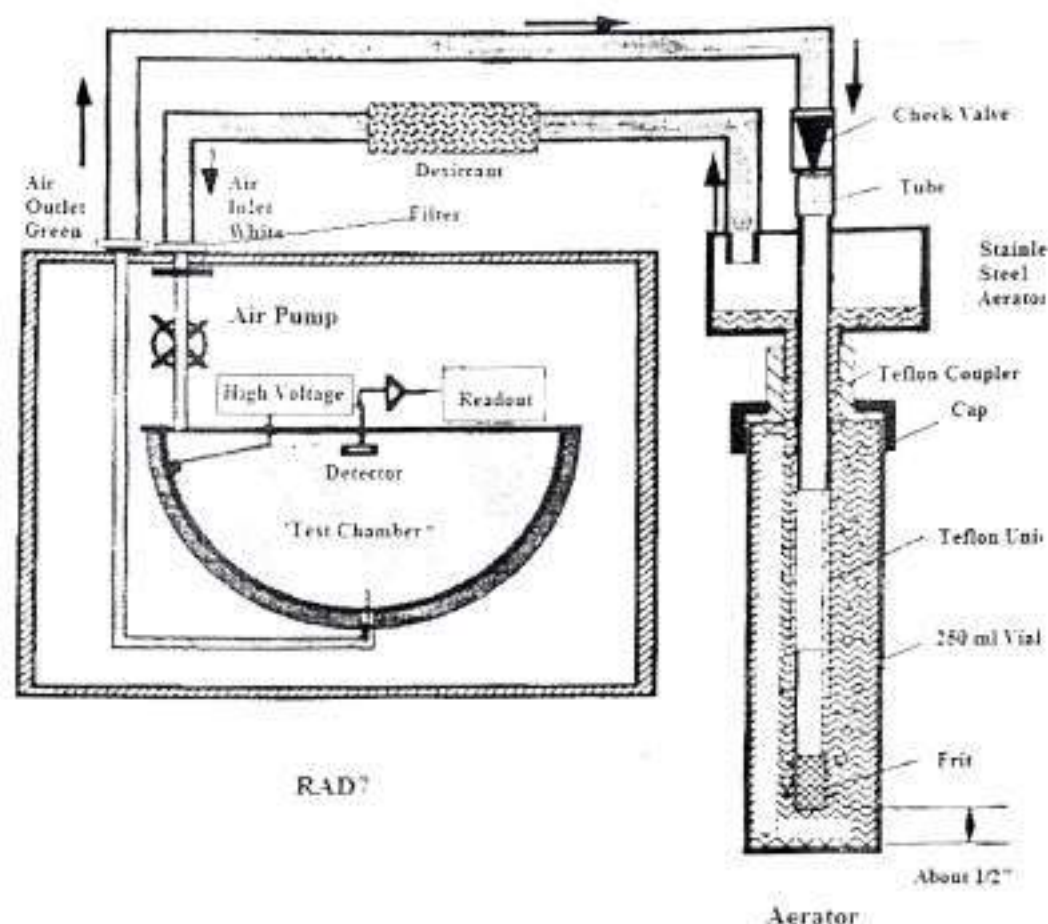


Fig.4: Schematic diagram of RAD7-H<sub>2</sub>O [19]

Within approximately 5 minutes, ceasing Radon extraction thereafter. The extraction efficiency, representing the percentage of Radon removed from the water to the air loop, is notably high at  $\approx 94\%$  for a 250ml sample. While the extraction efficiency may slightly vary with ambient temperature, it consistently exceeds 90%. The RAD7 detector transforms alpha radiation into an electric signal directly, possessing the capability to differentiate between aged and fresh Radon, as well as Radon emanating from thoron.



## RESULT AND DISCUSSION

The results of Radon analysis in water samples of the study are presented in Table 1. The values of Radon were in the range  $1.10 \pm 0.09$  Bq/L to  $20.4 \pm 1.79$  Bq/L with an average value of Radon is  $7.89 \pm 1.398$  Bq/L. When the Radon concentration value is compared with value suggested by WHO [9] that is 11 Bq/L we found that approx. 77.77% of the samples were below the MCL value and the values of 22.22% of the samples higher than value suggested by WHO [9] and UNSCEAR [10] suggested the concentration value between 4-40 Bq/L when compared to this value 100% of the samples were below the suggested value.

Table 1. Values of Radon of all 27 samples collected from Baddi

Sr. No.	Locations	Latitude	Longitude	pH	Source	Depth (ft)	Radon conc. (Bq/L)
S1	Baddi 1	30.997003°	76.740966°	7.1	SP	150	3.18±0.92
S2	Baddi 2	30.992714°	76.752163°	7.3	SP	120	6.78±0.86
S3	Baddi 3	30.999112°	76.751084°	8.2	SP	180	5.68±0.57
S4	Baddi 4	30.99944°	76.759802°	8.0	HP	60	1.10±0.09
S5	Baddi 5	30.991918°	76.771099°	7.4	SP	250	17.99±3.49
S6	Baddi 6	30.998159°	76.770941°	7.8	OW	30	11.14±1.04
S7	Baddi 7	30.983496°	76.787992°	7.9	SP	280	9.13 ± 0.43
S8	Manakpur	30.979075°	76.777813°	7.8	SP	180	7.22±0.54
S9	Baddi 8	30.981045°	76.764085°	7.3	SP	328	5.91±5.92
S10	Baddi 9	30.973685°	76.773492°	7.7	SP	180	18.53±4.75
S11	Baddi 10	30.97626°	76.754175°	7.5	SP	110	8.67±0.73
S12	Baddi 11	30.988558°	76.760791°	7.3	SP	180	5.13±1.4
S13	Baddi 12	30.972039°	76.797588°	7.4	SP	150	15.92±2.8
S14	Baddi 13	30.961835°	76.813607°	7.8	SP	250	20.4±1.79
S15	Baddi 14	30.958747°	76.792353°	7.6	SP	247	6.30±1.4
S16	Baddi 15	30.964406°	76.7818°	8.3	SP	140	4.60±0.24
S17	Baddi 16	30.958992°	76.765344°	8.0	SP	210	9.72±2.11
S18	Baddi 17	30.952098°	76.778555°	7.6	SP	150	11.4±1.86
S19	Baddi 18	30.942281°	76.785767°	7.3	SP	210	2.6±0.23
S20	Baddi 19	30.946045°	76.796202°	6.9	SP	190	2.07±0.39
S21	Baddi 20	30.947951°	76.8048°	7.5	OW	50	3.92±0.72
S22	Baddi 21	30.956222°	76.82182°	7.8	SP	150	3.06±0.30
S23	Baddi 22	30.954236°	76.836816°	8.1	OW	30	2.20±0.19
S24	Baddi 23	30.94563°	76.830415°	7.9	SP	250	9.99±2.9
S25	Baddi 24	30.931238°	76.817067°	7.8	SP	180	6.54±0.38
S26	Baddi 25	30.937713°	76.810812°	7.6	SP	240	5.42±0.17
S27	Baddi 26	30.928822°	76.795828°	7.9	SP	280	8.45±1.54

OW=Open well, SP= Submersible motor pump, SW=Surface water, HP= Hand-pump

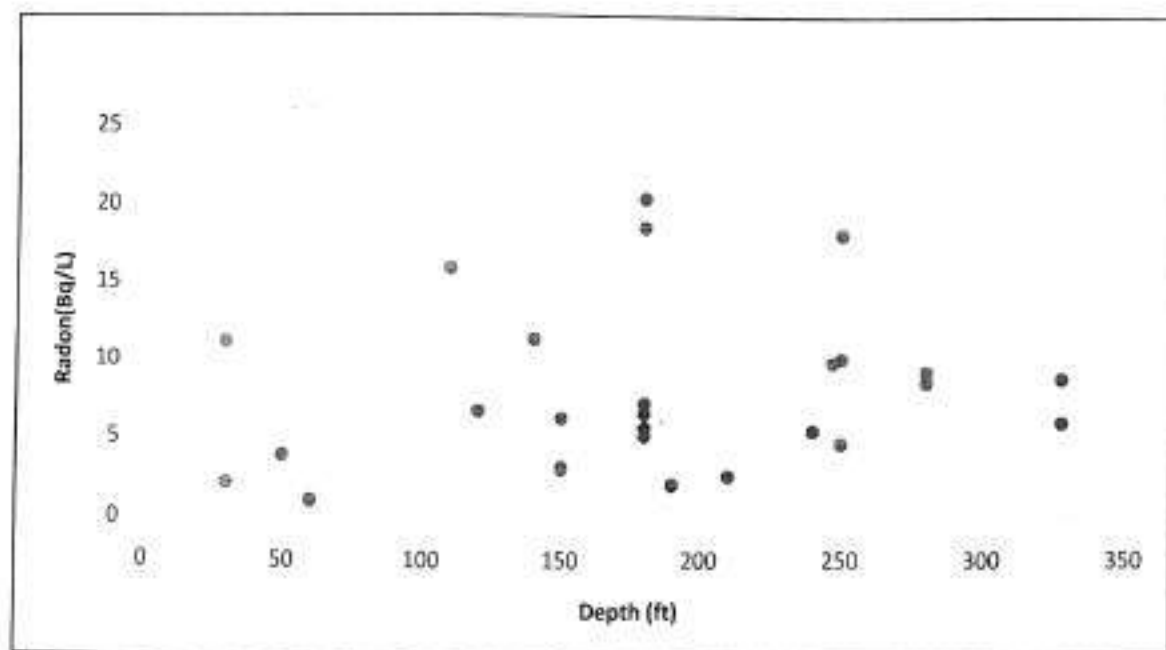


Fig.5: Radon concentration variation with Depth of the source

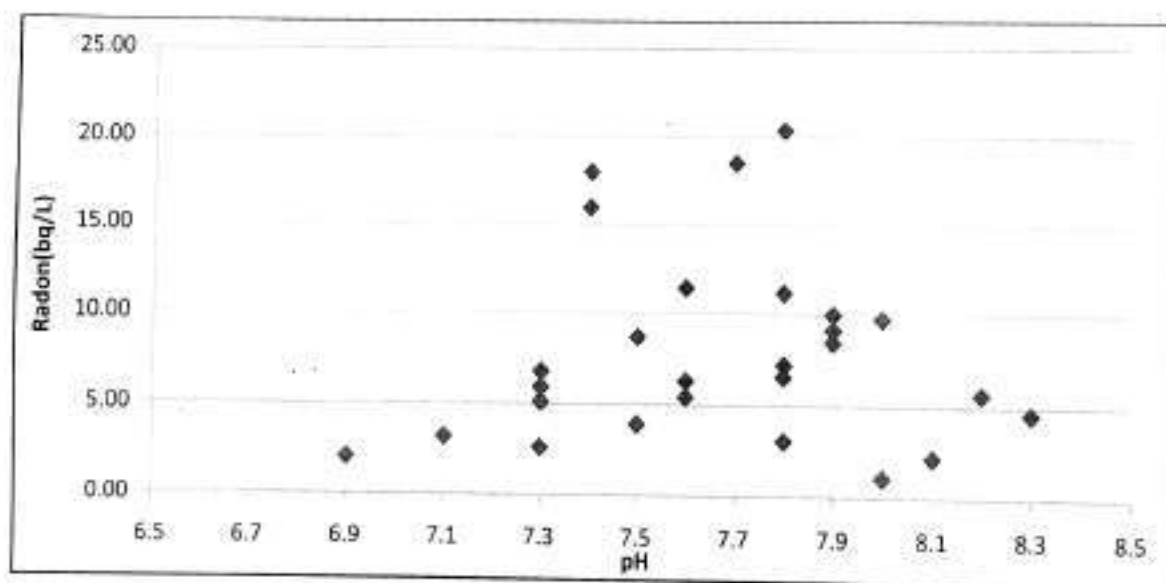


Fig.6: Radon concentration variation with pH of collected samples



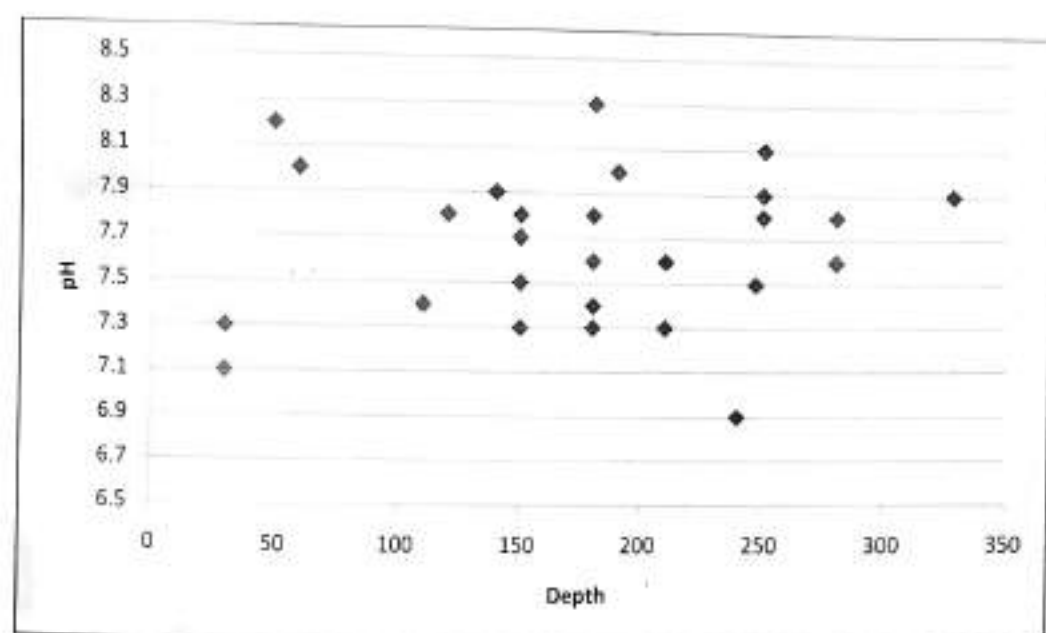


Fig.7: pH variation with depth of the source

## CONCLUSION

The Radon concentrations spanned from  $1.10 \pm 0.09$  Bq/L to  $20.4 \pm 1.79$  Bq/L. The average Radon concentration stood at  $7.89 \pm 1.398$  Bq/L.

In terms of Radon concentration, approximately 77.77% of the samples were found to be below WHO's suggested MCL of 11 Bq/L, while 22.22% exceeded this threshold. However, all samples remained within the concentration range of 4–40 Bq/L recommended by the United Nations Scientific Committee on the Effects of Atomic Radiation (UNSCEAR).

## REFERENCES

- [1]. Radon Weigel, F. (Muenchen Univ. (Germany, F.R.). Inst. FuerAnorganischeChemie) 1978.
- [2]. Sicilia, I., Aparicio, S., González, M., Anaya, J. J., &Frutos, B. (2022). Radon transport, Accumulation patterns, and mitigation techniques applied to closed spaces. *Atmosphere*, 13(10), 1692.
- [3]. Feng, X., Zhong, J., Yan, R., Zhou, Z., Tian, L., Zhao, J., & Yuan, Z. (2022). Groundwater Radon precursor anomalies identification by EMD-LSTM model. *Water*, 14(1), 69.
- [4]. Malvicini, A., ESPOSITO, P., &Depiesse, D. (2004). Influence of hydrogeological Properties of rocky substratum, ventilation and meteorological conditions on Environmental radioactivity in underground galleries. In *Proceedings of the 11<sup>th</sup> International Congress of the International Radiation Protection Association*, Madrid
- [5]. Ye, Y. J., Xia, X. Q., Dai, X. T., Huang, C. H., &Guo, Q. (2019). Effects of temperature, Salinity, and pH on 222 Rn solubility in water. *Journal of Radioanalytical and Nuclear Chemistry*, 320, 369-375.
- [6]. Behaviour of Radon in the geological environment: a review TK Ball, DG Cameron, TB Colman, PD Roberts *Quarterly Journal of Engineering Geology and Hydrogeology* 24 (2), 169-182, 1991
- [7]. Health effects of Radon : a review of the literature Mustafa Al-Zoughool, Daniel Krewski *International journal of radiation biology* 85 (1), 57-69, 2009
- [8]. United States Environmental Protection Agency. Radon in drinking water, Factsheet. EPA 815-F-99007, USEPA (1999)
- [9]. WHO, 2003. Guidelines for Drinking Water Quality. Health Criteria and Other Supporting Information. World Health Organization (2003).
- [10]. United Nations Scientific Committee on the effect of Atomic Radiation. The general Assembly with scientific annex, United Nation. UNSCEAR (2000).
- [11]. Singh, P., Singh, P., Sahoo, B. K., &Bajwa, B. S. (2016). A study on uranium and Radon Levels in drinking water sources of a mineralized zone of Himachal Pradesh, India. *Journal of Radioanalytical and Nuclear Chemistry*, 309, 541-549.
- [12]. Nandakumaran, P., &Vinayachandran, N. (2020). A preliminary appraisal of Radon Concentration in groundwater from the high background radiation area (HBRA) of Coastal Kerala. *Journal of the Geological Society of India*, 95, 491-496.

- [13]. Kumar, M., Kaushal, A., Sahoo, B. K., Sarin, A., Mehra, R., Jakhu, R., ... & Sharma, N. (2019). Measurement of uranium and Radon concentration in drinking water samples and Assessment of ingestion dose to local population in Jalandhar district of Punjab, India. *Indoor and Built Environment*, 28(5), 611-618.
- [14]. Rani, S., Kansal, S., Singla, A. K., & Mehra, R. (2021). Radiological risk assessment to the public due to the presence of Radon in water of Barnala district, Punjab, India. *Environmental Geochemistry and Health*, 43(12), 5011-5024.
- [15]. Panghal, A., Kumar, A., Kumar, S., Singh, J., Sharma, S., Singh, P., ... & Bajwa, B. S. (2017). Radiation dose-dependent risk on individuals due to ingestion of uranium and Radon concentration in drinking water samples of four districts of Haryana, India. *Radiation effects and defects in solids*, 172(5-6), 441-455.
- [16]. Kumar, A., Arora, T., Singh, P., Singh, K., Singh, D., Pathak, P. P., & Ramola, R. C. (2021). Quantification of radiological dose and chemical toxicity due to Radon and uranium in drinking water in Bageshwar region of Indian Himalaya. *Groundwater for Sustainable Development*, 12, 10049.
- [17]. Kaur, M., Kumar, A., Mehra, R., & Mishra, R. (2019). Age-dependent ingestion and inhalation doses due to intake of uranium and Radon in water samples of Shiwalik Himalayas of Jammu and Kashmir, India. *Environmental monitoring and assessment*, 191, 1-17.
- [18]. Rani, A., Mehra, R., & Duggal, V. (2013). Radon monitoring in groundwater samples from some areas of Northern Rajasthan, India, using a RAD7 detector. *Radiation Protection dosimetry*, 153(4), 496-501.
- [19]. DURRIDGE Radon Instrumentation. RAD H2O User Manual, Radon in Water Accessory. DURRIDGE Company (2011).

**ASSESSING URANIUM IN GROUNDWATER USING LED  
FLUORIMETER: A CASE STUDY OF BADDI CITY, DISTRICT SOLAN,  
HIMACHAL PARDESH, INDIA**

***PROJECT REPORT***

Submitted in partial fulfillment of the  
requirements for the award of the degree of

**MASTER OF SCIENCE**

**in**

**PHYSICS**

***By***

**Umesh Chauhan**  
(Reg. No. 811-2019-777)



**DEPARTMENT OF PHYSICS**  
**SRI GURU TEG BAHADUR KHALSA COLLEGE, SRI ANANDPUR SAHIB**  
(An Autonomous College)  
**ANANDPUR SAHIB– 140118, PUNJAB (INDIA)**





SRI GURU TEG BAHADUR KHALSA COLLEGE, SRI ANANDPUR SAHIB  
(An Autonomous College)  
ANANDPUR SAHIB-140118. PUNJAB (INDIA)

## CERTIFICATE

It is certified that the work contained in the project report entitled "Assessing Uranium in Groundwater Using LED Fluorimeter: A Case Study of Baddi City, District Solan, Himachal Pradesh, India" is an original contribution by me and has not been submitted in part or full for any other degree at this or other University/ Institute.

The assistance and help received during the course of the thesis work have been acknowledged.

*Umesh Chauhan*

**Umesh Chauhan**

Regn. No. **811-2019-777**

I, the undersigned, Supervisor of **Umesh Chauhan**, Reg. No. **811-2019-777**, a candidate for the degree of **Master of Science**, agree that the project report entitled, "Assessing Uranium in Groundwater Using LED Fluorimeter: A Case Study of Baddi City, District Solan, Himachal Pradesh, India", may be submitted in partial fulfillment of the requirements for the award of degree.

This is to certify that the above statement made by the candidate is correct to the best of my knowledge.

*Vimal Mehta*

**Supervisor**

**Dr. Vimal Mehta**

**Assistant Professor**

**Department of Physics**

**Sri Guru Teg Bahadur Khalsa College**

**Sri Anandpur Sahib**

## CERTIFICATE

This is to certify that the "Project report" entitled **"ASSESSING URANIUM IN GROUNDWATER USING LED FLUORIMETER: A CASE STUDY OF BADDI CITY, DISTRICT SOLAN, HIMACHAL PRADESH, INDIA"** submitted by **UMESH CHAUHAN** (Reg. No. 811-2019-777) to Department of Physics, Sri Guru Teg Bahadur Khalsa College, Sri Anandpur Sahib in partial fulfillment of the requirements for the award of degree of **MASTER OF SCIENCE IN PHYSICS** and has been approved by the Department Research committee (DRC) after the viva-voce examination of the candidate.

  
Dr. Vimal Mehta  
Supervisor

  
Dr. Randev Singh  
Chairman DRC

## ACKNOWLEDGEMENT

Firstly, I would like to express my gratitude to my Supervisor, Dr. Vimal Mehta Assistant Professor at Department of physics Sri Guru Teg Bahadur Khalsa College Sri Anandpur Sahib, who has resourcefully guided me throughout this research project. I'm extremely grateful for his motivating discussions while enable me to accomplish this task successfully. Without his active guidance, support and encouragement I would not have made headway in this project.

I also thankful to my Parents for their moral support and suggestions to improve the dissertation work. I'm also thankful to other faculty members in the department for their encouragement and fruitful academic discussions.

A special thanks to Ms. Seema Assistant Professor at Department of Physics for the help and their valuable suggestions whenever I needed out of their busy schedule. I'm also thankful to my classmates and my friends who was directly or indirectly help me to complete this project report.

umesh Chauhan

## ABSTRACT

The presence of Uranium in groundwater is a significant environmental concern due to their radiological health implications. This study focuses on Baddi City, District Solan, Himachal Pradesh, India, where industrial activities raise the potential for contamination of groundwater resources. The objective is to assess the concentrations of Uranium in the groundwater using an approach involving a LED Fluorimeter. Groundwater samples from various locations within Baddi City were collected and analyzed. The LED Fluorimeter was employed to measure the concentration of Uranium. The methodology used for this device to provide a comprehensive analysis of the groundwater quality concerning this radioactive element. Furthermore, the research delved into the potential health risks associated with the consumption of this contaminated groundwater. The findings highlighted the need for regular monitoring and the implementation of remediation strategies to mitigate the risks posed by Uranium in groundwater. This case study serves as a crucial reference for environmental scientists and policymakers. It underscores the importance of employing integrated technological approaches for the accurate assessment of groundwater contamination and the formulation of effective environmental health policies. In conclusion, the study provides valuable insights into the status of groundwater quality in Baddi City and emphasizes the necessity for continued research and monitoring to protect public health and ensure the sustainability of groundwater resources. The use of a LED Fluorimeter emerges as a reliable method for the assessment of Uranium in groundwater, paving the way for future studies in similar industrial regions. The results indicated varying concentration of Uranium across different sampling points. Some locations showed elevated levels of this contaminant, surpassing the safe limits as prescribed by international health agencies.

**Keywords:** - Uranium concentration, LED Fluorimeter.

## Content

CHAPTER	Page No.
1. Introduction	7-8
2. Research Objectives	9
3. Literature Review	10-12
4. Methodology	13-30
• Sample collection	13-14
• Location and pictures of sampling sites	15-28
• LED Fluorimeter	28-30
5. Results and Discussion	31-33
6. Conclusion	34
7. References	35-37



## LIST OF FIGURES

S. No.	Name of the Figure
--------	--------------------

- 
- |       |  |
|-------|--|
| Fig.1 | Study area site (Baddi City)                                     |
| Fig.2 | Location of the sampling sites                                   |
| Fig.3 | LED Fluorimeter  |
| Fig.4 | Block diagram of LED Fluorimeter                                 |
| Fig.5 | Uranium concentration variation with Depth of the Source         |
| Fig.6 | Uranium concentration variation with pH of the Collected Samples |
| Fig.7 | pH variation with depth of the Source                            |

# INTRODUCTION

Groundwater quality is a critical aspect of environmental health, particularly in regions where it serves as a primary source of drinking water. The presence of certain elements, such as Uranium can significantly impact both human health and the ecosystem. In the case of Baddi City, located in the picturesque district of Solan, Himachal Pradesh, India, understanding the levels of Uranium in groundwater is essential. This research project aims to comprehensively assess Uranium concentration in Baddi City's groundwater.

## • Uranium

Uranium is a silvery-white metallic chemical element in the periodic table, with atomic number 92. It is assigned the chemical symbol U. Uranium has the highest atomic weight of all naturally occurring elements. Uranium radioactively decays, usually by emitting an alpha particle. The half-life of this decay varies between 159,200 and 4.5 billion years for different isotopes. Uranium was discovered as a chemical element in a pitchblende specimen by Martin Heinrich Klaproth who published the results of his work in 1789. Henri Becquerel (1896), discovered the Radioactivity of Uranium. That's why the measuring of Uranium in ground water and drinking water is important.

## Nuclear Properties:-

Uranium, as it occurs in nature, consists of a mixture of the three isotopes  $^{238}\text{U}$ ,  $^{235}\text{U}$ , and  $\text{U}^{234}$ . From these Uranium-238( $^{238}\text{U}$ ) is most abundant and natural occurring [1]. The decay series initiated by U-238 introduces isotopes such as Thorium-234 ( $^{234}\text{Th}$ ) and Radium-226 ( $^{226}\text{Ra}$ ), acting as distinctive signatures for tracking Uranium behavior in environmental systems. Research studies by Tissot et al. [2] and Carvalho et al. [3] provide valuable insights into the isotopic composition of Uranium in diverse geological settings.

## 1. Occurrence in Nature

The most important oxidation states of Uranium in natural environments are +4 and +6. There are 200 minerals that contain Uranium as an essential component [4-5]. Of these, The U (VI) minerals constitute the largest portion. The redox cycling between +4 and +6 states influences uranium's mobility and reactivity in subsurface environments.

## 2. Water Solubility: A Crucial Transport Mechanism

In groundwater systems U (VI) is reduced to U (IV) if an Effective reductant is present, such as H<sub>2</sub>S. Other reducing agents may be fossil Plants, methane, and transported humic material [1] U (VI) species, particularly uranyl ions (UO<sub>2</sub><sup>2+</sup>), exhibit higher solubility. This characteristic significantly impacts the potential for Uranium migration and contamination in groundwater. Noteworthy contributions by Chevreux et al. [6] and Smedley et al. [7] provide detailed insights into Uranium solubility dynamics.

## 3. Geological Behaviour: Unraveling Weathering and Mobilization

Subsurface water interacts with crystalline rocks formed at a high temperature, the mineral composition of these rocks and Uranium species therein are thermodynamically unstable. Therefore, reactions directed toward the establishment of equilibrium proceed in the water-rock system [8]. The breakdown of uranium-rich minerals releases Uranium into soil and water, contributing to its mobilization. Specific geological formations, such as sedimentary rocks or aquifer materials, can enhance Uranium accumulation in groundwater. Pioneering work by Gomez et al. [9] and Sharma et al. [10] elucidate the geological factors influencing Uranium mobility.

## 4. Health Implications: Chronic Exposure and Bioavailability

The bioavailability of Uranium in groundwater, influenced by its chemical speciation, contributes to potential health impacts on communities relying on contaminated water sources. Chronic exposure to Uranium occurs predominantly via ingestion of food and water, and results in kidney disease and potential toxicity in bones [11-13].

## 5. Regulatory Measures and Monitoring: Safeguarding Water Quality

Given the potential health risks associated with Uranium contamination, regulatory measures and monitoring programs play a pivotal role. Established guidelines and standards aim to limit Uranium concentrations in drinking water, ensuring the safety of water supplies. The comprehensive work by United States Environmental Protection Agency (USEPA) guidelines [14] and ongoing monitoring efforts by regional agencies contribute to the development of effective strategies for managing and mitigating uranium-related risks in groundwater.

This introduction serves as a foundation for our research project, providing an extensive overview of Uranium in groundwater.

## RESEARCH OBJECTIVE

This study is all about getting a deeper understanding of how Uranium is present in our groundwater. We're looking to figure out how they're distributed, how different earthy chemical processes affect them, and how we can better analyze them. Plus, we want to know what kind of impact they could have on our health and the environment. By digging into these details, we hope to offer some insights that can help manage our groundwater better and add to the ongoing conversation about keeping our water resources sustainable for the future. In the sections that follow, we'll dive into the methods we used, what we discovered, and our thoughts on the whole issue, focusing on the tricky bits about Uranium in groundwater. The properties of Uranium and their MCL in consumable water are given as follow:

### Properties and safe drinking water ingestion levels of Uranium

Uranium, a heavy element, is widely distributed throughout the Earth's crust. When it is found in groundwater, its radioactivity and chemical toxicity are cause for concern. The two most common Uranium isotopes,  $^{238}\text{U}$  (half life 4.5 billion years) and  $^{235}\text{U}$  (half life 700 million years), undergo radioactive alpha decay, producing  $\alpha$  particles. Understanding Uranium's chemical behavior and probable migration paths in groundwater is critical for a correct assessment.

- The World Health Organization (WHO) [15] sets a provisional guideline value of 30 micrograms per liter ( $\mu\text{g/L}$ ) for Uranium in drinking water.
- The U.S. Environmental Protection Agency (USEPA) [14] has a Maximum Contaminant Level (MCL) of 30 microgram per liter ( $\mu\text{g/L}$ ) for Uranium in public water supplies.



## LITERATURE REVIEW

Assessing groundwater quality plays a crucial role in environmental monitoring, particularly in regions susceptible to Uranium contamination. In Baddi City, located in Solan district, Himachal Pradesh, India, understanding the level of this radioactive element is vital for public health protection. This literature review investigates existing knowledge, methodologies, and recent research related to LED Fluorimeter instrument for assessing Uranium concentrations in groundwater.

### Uranium in Groundwater:

In India, diverse geological conditions pose challenges related to groundwater contamination by Uranium. Uranium, a naturally occurring radioactive element, can infiltrate groundwater through weathering processes, potentially causing severe health issues upon ingestion [16].

Understanding the sources, transport mechanisms, and concentrations of Uranium is crucial for managing and mitigating these risks. Ensuring access to safe and clean drinking water is vital for public health. In Baddi City, located in the scenic district of Solan, Himachal Pradesh, India, there are growing concerns about Uranium contamination in groundwater.

This literature review aims to establish a foundational understanding of the dynamics and challenges related to Uranium concentration in Baddi City's groundwater. Numerous researchers have conducted studies on assessing Uranium concentration in Indian groundwater. Some ongoing research focuses on understanding the sources, transport mechanisms, and health risks associated with these elements.

Several studies in India have explored groundwater quality, uranium concentration few of them are as follow:

Asha Rani et al. reported that Uranium concentration in the water samples from Punjab varies from  $1.3 \pm 0.16$  to  $98.25 \pm 2.06$   $\mu\text{g/L}$  with a mean value of  $19.84 \pm 0.87$   $\mu\text{g/L}$ . The uranium concentration in most of the drinking water samples from Punjab exceeds the safe limit recommended by the World Health Organization. However, the uranium concentration in water samples from Himachal Pradesh is well within the recommended levels. [17]

Singh et al. collected drinking water samples from Hamirpur and Kangra districts of Himachal Pradesh and adjoining areas of Jammu and Kashmir, India and found concentration of,  $^{238}\text{U}$  and  $^{222}\text{Rn}$  in these samples in the range of  $0.26 \pm 0.1$  to  $29.5 \pm 2.5$   $\mu\text{g/L}$  and  $0.86 \pm 0.12$  to  $7.62 \pm 0.64$



Bq/L respectively. The measured values of  $^{238}\text{U}$  and  $^{222}\text{Rn}$  concentration are within the safe limits as recommended by WHO and USEPA. [18]

Manish Kumar et al. found concentration of Uranium and radon in the range of  $1.53 \pm 0.06 \text{ mg/m}^3$  to  $50.2 \pm 0.08 \text{ mg/m}^3$  with a geometric mean value of  $14.85 \text{ mg/m}^3$  and  $0.34 \pm 0.07 \text{ kBq/m}^3$  to  $3.84 \pm 0.48 \text{ kBq/m}^3$  with a geometric mean value of  $1.46 \text{ kBq/m}^3$  respectively in the drinking water samples which collected from Jalandhar district of Punjab. [19]

Panghal and Kumar et al. Collected drinking water samples from various locations of four districts of Haryana, India. The uranium ( $^{238}\text{U}$ ) and radon ( $^{222}\text{Rn}$ ) concentrations in water samples have been found to vary from 1.07 to 40.25  $\mu\text{g/L}$  with an average of 17.91  $\mu\text{g/L}$  and  $16.06 \pm 0.97$  to  $57.35 \pm 1.28 \text{ Bq/L}$  with an average of  $32.98 \pm 2.45 \text{ Bq/L}$ , respectively. [20]

Ankur Kumar et al. give result that revealed radon activity in spring-water samples varies from 3.4 to 101.3 Bq/L with a mean value of  $34.4 \pm 3.8 \text{ Bq/L}$  while the uranium concentration in water samples ranges from 0.1 to 28.4  $\mu\text{g/L}$  with the mean value of 1.6  $\mu\text{g/L}$ . [21]

Manpreet Kaur et al. collected water samples used by the inhabitants, of the villages of the Shiwalik Himalayas of Jammu and Kashmir, India. Measured the concentration of Uranium and Radon and reported all values of doses were below the proposed limit of 100  $\mu\text{Sv/year}$  for all age categories except for infants due to the high-dose conversion factor. [22]

Mehta et al. study uranium concentration in groundwater samples collected from various sources in the Patiala district, Punjab. Results reveal that 78% of locations have uranium concentration below the WHO limit 30  $\mu\text{g/L}$ , while 22% exceed the safe limit. The uranium concentration in the groundwater ranges from 5.59 to 57.53  $\mu\text{g/L}$ , with an average concentration of 24.57  $\mu\text{g/L}$ . [23]

V. Balram et al. Calculate concentration of Uranium in groundwater from shallow aquifers in various states such as Punjab, Rajasthan, Karnataka Telangana, and Madhya Pradesh of India which varies from 0 to 1443 ng/ml, exceeding the permissible levels by WHO for drinking water (30 ng/ml), at several places. [24]

Mehta et al. study water samples from Rupnagar, Punjab, and Una, Himachal Pradesh, and found that physicochemical parameters such as pH, electrical conductivity, and total dissolved solids in collected water samples to calculate the water quality index, indicating good water quality in both regions. The study also analyzed uranium concentration in groundwater at varying depths, revealing no significantly high values. [25]

R.M.Coyte et al. present compiled data on groundwater uranium from 16 Indian states and new data from 324 wells in the states of Rajasthan and Gujarat that show a high prevalence of uranium concentrations above the World Health Organization provisional guideline value of 30  $\mu\text{g/L}$  across India.[26]

## METHODOLOGY

Baddi is a town in the Solan district of Himachal Pradesh, India. Geographically, it is situated at approximately  $30.928^{\circ}\text{N}$  latitude and  $76.796^{\circ}\text{E}$  longitude. Baddi lies on the border of Himachal Pradesh, Punjab, and Haryana states in the Shivalik Hills. The specific land area covered by Baddi town is approximately  $38.57 \text{ Km}^2$ . This figure represents the town's administrative boundaries and includes both developed and undeveloped areas within those limits. The city has 29,911 people living there (according of 2011 census), that is 775.45 persons per  $\text{Km}^2$ .

### Sample collection

27 ground water samples were collected across the city by using a grid on the map of the city. The sites are mentioned in the Figure 1a and Figure 1b given below. The exact latitude and longitude of the sites are obtained by using a application called GPS Map Camera.

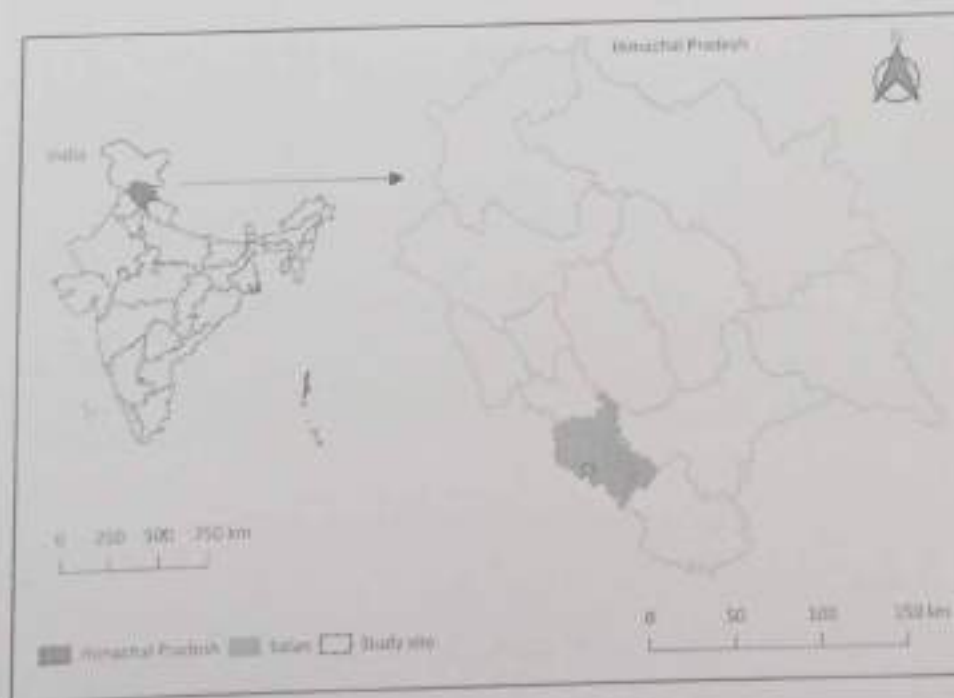


Fig. 1: Study area site (Baddi City)



Fig.2: Location of the sampling Sites

High density polyethylene plastic bottles of 250ml were used to collect samples which were cleaned using dilute HCL (0.5N HCL) and were rinsed with deionised water before taking sample. Before collecting sample the water sources were run made to run for few minutes so that we can collect fresh water for sampling for better and accurate results. And then bottles are prewashed with source water 2-3 times before collecting sample. Then Uranium concentration in all 27 samples is measured by LED Fluorimeter.



- Location and Pictures of sampling sites

### Sample 1



Site of sample 1



Location of sample 1

### Sample 2



Site of sample 2



Location of sample 2





## Sample 5



Site of sample 5



Location of sample 5

## Sample 6



Site of sample 6



Site of sample 6

## Sample 7



Site of sample 7

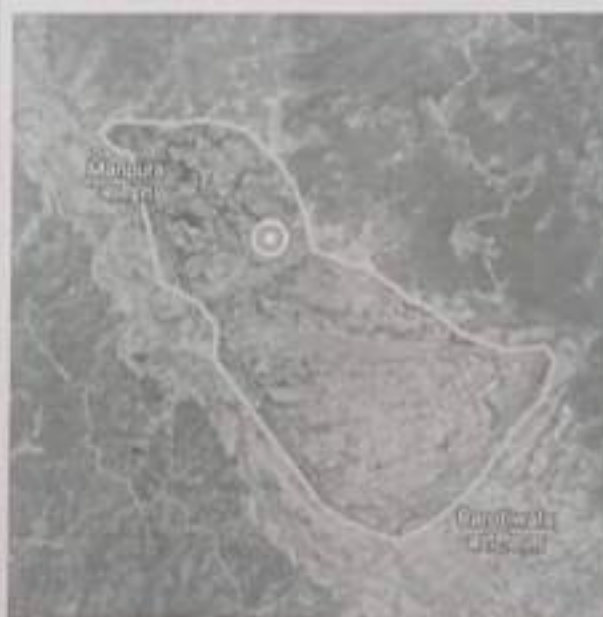


Location sample 7

## Sample 8



Site of sample 8



Location of sample 8



## Sample 9



Site of sample 9

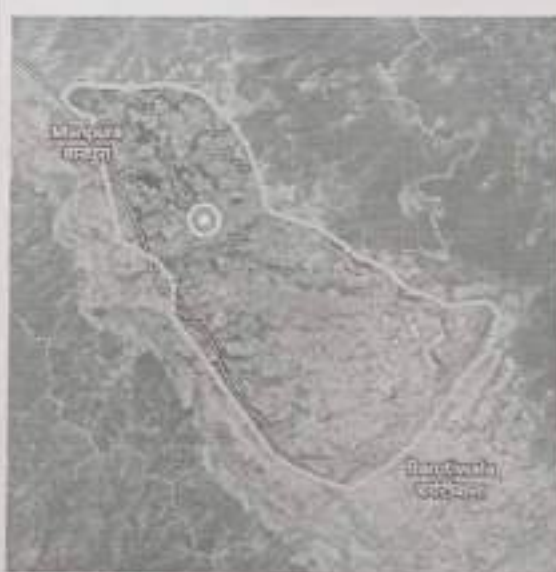


Location of sample 9

## Sample 10



Site of sample 10



Location of sample 10





## Sample 13



Site of sample 13



Location of sample 13

## Sample 14



Site of sample 14



Location of sample 14

## Sample 15



Site of sample 15



Location of sample 15

## Sample 16



Site of sample 16



Location of sample 16





## Sample 19



Site of sample 19



Location of Sample 19

## Sample 20



Site of sample 20



Location of sample 20

## Sample 21



Site of sample 21



Location of sample 21

## Sample 22



Site of sample 22



Location of sample 22



### Sample 23



Site of sample 23



Location of sample 23

### Sample 24



Site of sample 24



Location of sample 24



## Sample 27



Site of sample 27



Location of sample 27

- **LED Fluorimeter**

A Fluorimeter is instrumental in quantifying the fluorescence emitted by a sample upon exposure to specific light wavelengths. LED Fluorimeter distinguishes themselves by utilizing light-emitting diodes (LEDs) as their primary light source, boasting remarkable speed, sensitivity, and dependability. Notably, the LED Fluorimeter excels in its capacity to accurately measure concentrations in water samples spanning from 0.5  $\mu\text{g/L}$  to 1000  $\mu\text{g/L}$ , [27] demonstrating exceptional precision across a wide range. This capability is particularly significant for various applications requiring precise measurements in environmental, biological, or chemical analyses.

Accompanying this functionality is a comprehensive block diagram depicted in Figure 2, elucidating the operational framework of the LED Fluorimeter. This visual aid provides insight into the intricate mechanisms governing its operation, facilitating a deeper understanding of its sophisticated design and functionality. Through the visualization of its components and processes, users can grasp the device's inner workings, enhancing comprehension and enabling effective utilization. Thus, the LED Fluorimeter emerges not

only as a pinnacle of measurement accuracy but also as an exemplar of clarity and accessibility in scientific instrumentation.



Fig.3: LED Fluorimeter

The working principle involves:

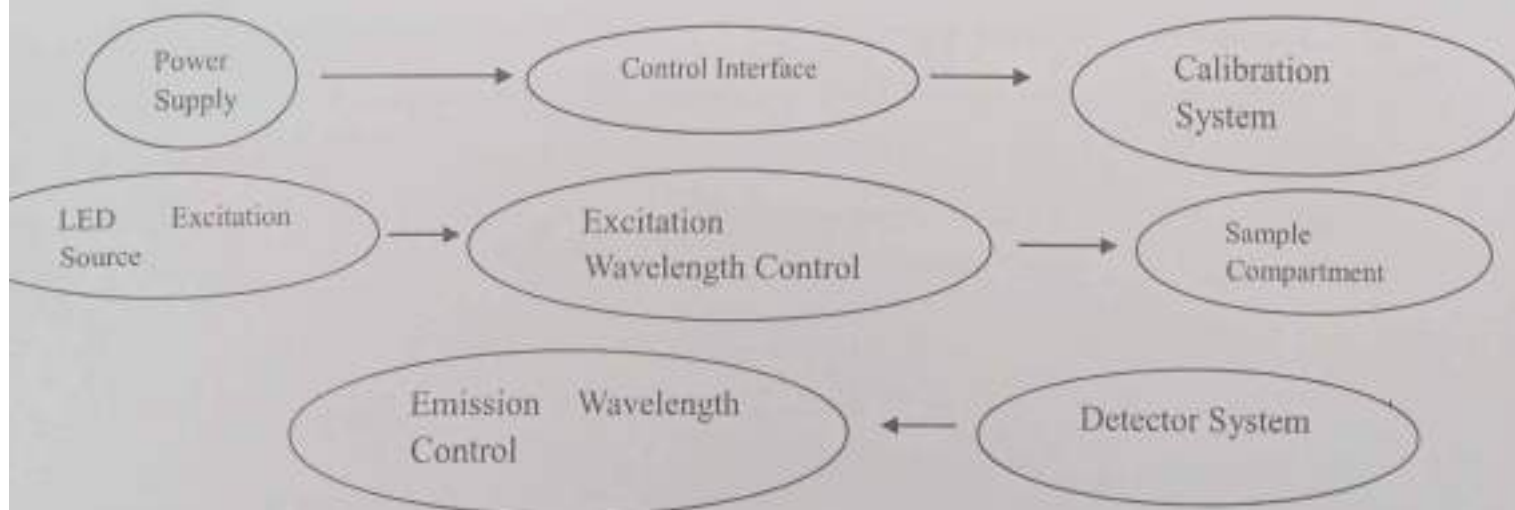


Fig.4: Block diagram of LED Fluorimeter



**Excitation:** The LED emits light at a specific wavelength, known as the excitation wavelength. This light is directed towards the sample.

**Sample Interaction:** The sample absorbs the excitation light and then re-emits light at a longer wavelength, known as the emission wavelength. This phenomenon is called fluorescence.

**Detection:** A photo detector in the Fluorimeter detects the emitted fluorescence. The intensity of the fluorescence is proportional to the concentration of the fluorescent substance in the sample.

**Signal Processing:** The detected fluorescence signal is processed and often displayed as a numerical value or a fluorescence spectrum

All the samples are first filtered through a filter paper of 45  $\mu\text{m}$ . Then pH of the water is measured by using a pH meter. We have three available specific modes in the device by which Uranium concentration can be measured first one is standard calibration mode, calibration mode and uncalibrated mode. And we are Utilizing the uncalibrated mode for measurement; we have employed the method specified by BARC in this study. The significant advantage of this approach lies in its ability to enhance the accuracy of Uranium concentration measurements. Initially, the fluorescence of a background solution, composed of 5.0 mL of distilled water and 0.5 mL of buffer solution, is determined. Subsequently, the fluorescence of the sample solution (consisting of 5.0 mL of the sample and 0.5 mL of buffer solution) is recorded. Following this, increments of 50  $\mu\text{L}$  of a 500 ppb standard Uranium solution are then added and we get the corresponding counts of each stage for all 27 samples.



## RESULT AND DISCUSSION

The results of Uranium analysis in water samples of the study are presented in Table 1. The values of Uranium in all 27 samples were in the range  $3.01 \pm 0.21 \mu\text{g/L}$  to  $19.22 \pm 0.87 \mu\text{g/L}$  with an average value of Uranium is  $7.089 \pm 0.45 \mu\text{g/L}$  and when the values of Uranium concentration is compared with the allowed MCL proposed by WHO [15], we observed that all samples were below the value proposed by WHO [15]. The MCL value suggested by USEPA [14] is  $30 \mu\text{g/L}$  and values of all the samples was below than this value (suggested by USEPA).

Table.1: Values of Uranium and Radon of all 27 samples collected from Baddi

Sr. No.	Locations	Latitude	Longitude	pH	Source	Depth (ft)	Uranium conc. ( $\mu\text{g/L}$ )
S1	Baddi 1	$30.997003^\circ$	$76.740966^\circ$	7.1	SP	150	$3.91 \pm 0.42$
S2	Baddi 2	$30.992714^\circ$	$76.752163^\circ$	7.3	SP	120	$19.22 \pm 0.87$
S3	Baddi 3	$30.999112^\circ$	$76.751084^\circ$	8.2	SP	180	$5.75 \pm 0.39$
S4	Baddi 4	$30.99944^\circ$	$76.759802^\circ$	8.0	HP	60	$7.43 \pm 0.50$
S5	Baddi 5	$30.991918^\circ$	$76.771099^\circ$	7.4	SP	250	$8.69 \pm 0.58$
S6	Baddi 6	$30.998159^\circ$	$76.770941^\circ$	7.8	OW	30	$5.53 \pm 0.29$
S7	Baddi 7	$30.983496^\circ$	$76.787992^\circ$	7.9	SP	280	$6.80 \pm 0.26$
S8	Manakpur	$30.979075^\circ$	$76.777813^\circ$	7.8	SP	180	$9.20 \pm 0.51$
S9	Baddi 8	$30.981045^\circ$	$76.764085^\circ$	7.3	SP	328	$8.12 \pm 0.56$
S10	Baddi 9	$30.973685^\circ$	$76.773492^\circ$	7.7	SP	180	$11.38 \pm 0.67$
S11	Baddi 10	$30.97626^\circ$	$76.754175^\circ$	7.5	SP	110	$8.31 \pm 0.55$
S12	Baddi 11	$30.988558^\circ$	$76.760791^\circ$	7.3	SP	180	$11.97 \pm 0.61$
S13	Baddi 12	$30.972039^\circ$	$76.797588^\circ$	7.4	SP	150	$8.23 \pm 0.56$
S14	Baddi 13	$30.961835^\circ$	$76.813607^\circ$	7.8	SP	250	$8.32 \pm 0.59$
S15	Baddi 14	$30.958747^\circ$	$76.792353^\circ$	7.6	SP	247	$7.12 \pm 0.43$
S16	Baddi 15	$30.964406^\circ$	$76.7818^\circ$	8.3	SP	140	$6.11 \pm 0.43$
S17	Baddi 16	$30.958992^\circ$	$76.765344^\circ$	8.0	SP	210	$9.44 \pm 0.37$
S18	Baddi 17	$30.952098^\circ$	$76.778555^\circ$	7.6	SP	150	$5.99 \pm 0.34$
S19	Baddi 18	$30.942281^\circ$	$76.785767^\circ$	7.3	SP	210	$5.24 \pm 0.32$
S20	Baddi 19	$30.946045^\circ$	$76.796202^\circ$	6.9	SP	190	$5.98 \pm 0.38$
S21	Baddi 20	$30.947951^\circ$	$76.8048^\circ$	7.5	OW	50	$11.63 \pm 0.51$
S22	Baddi 21	$30.956222^\circ$	$76.82182^\circ$	7.8	SP	150	$7.51 \pm 0.34$
S23	Baddi 22	$30.954236^\circ$	$76.836816^\circ$	8.1	OW	30	$3.43 \pm 0.27$
S24	Baddi 23	$30.94563^\circ$	$76.830415^\circ$	7.9	SP	250	$4.94 \pm 0.37$
S25	Baddi 24	$30.931238^\circ$	$76.817067^\circ$	7.8	SP	180	$6.15 \pm 0.48$
S26	Baddi 25	$30.937713^\circ$	$76.810812^\circ$	7.6	SP	240	$3.38 \pm 0.4$
S27	Baddi 26	$30.928822^\circ$	$76.795828^\circ$	7.9	SP	280	$3.01 \pm 0.21$

\*OW=Open well, SP= Submersible motor pump, SW=Surface water, HP= Hand-pump

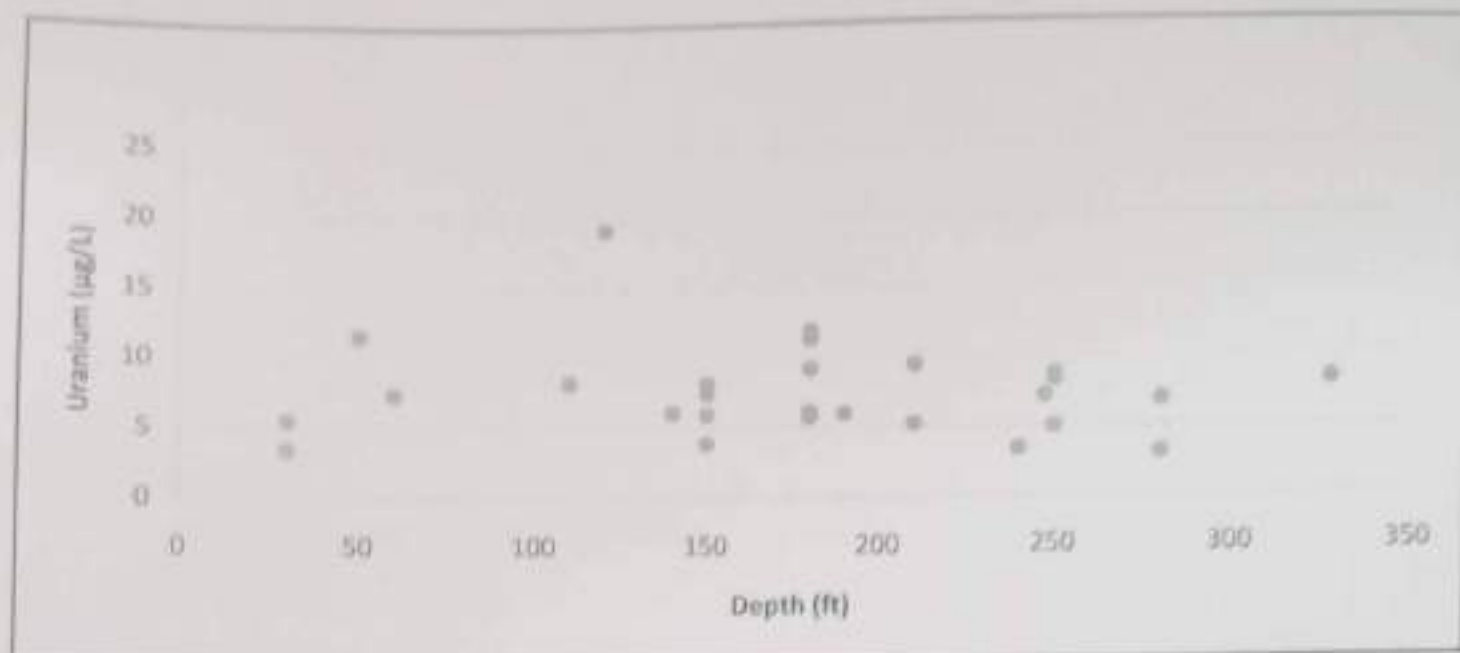


Fig.5: Uranium concentration variation with Depth of the source

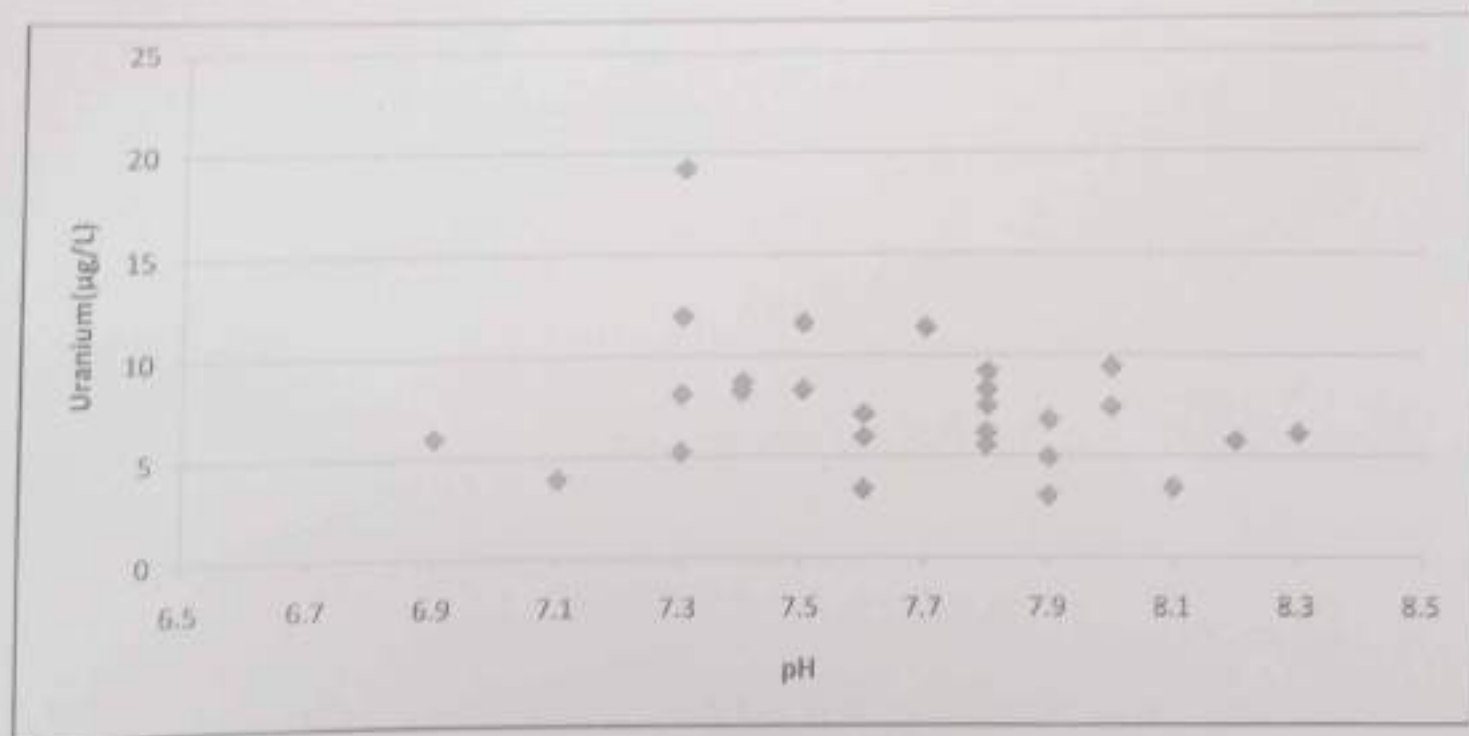


Fig.6: Uranium concentration variation with pH of the collected samples

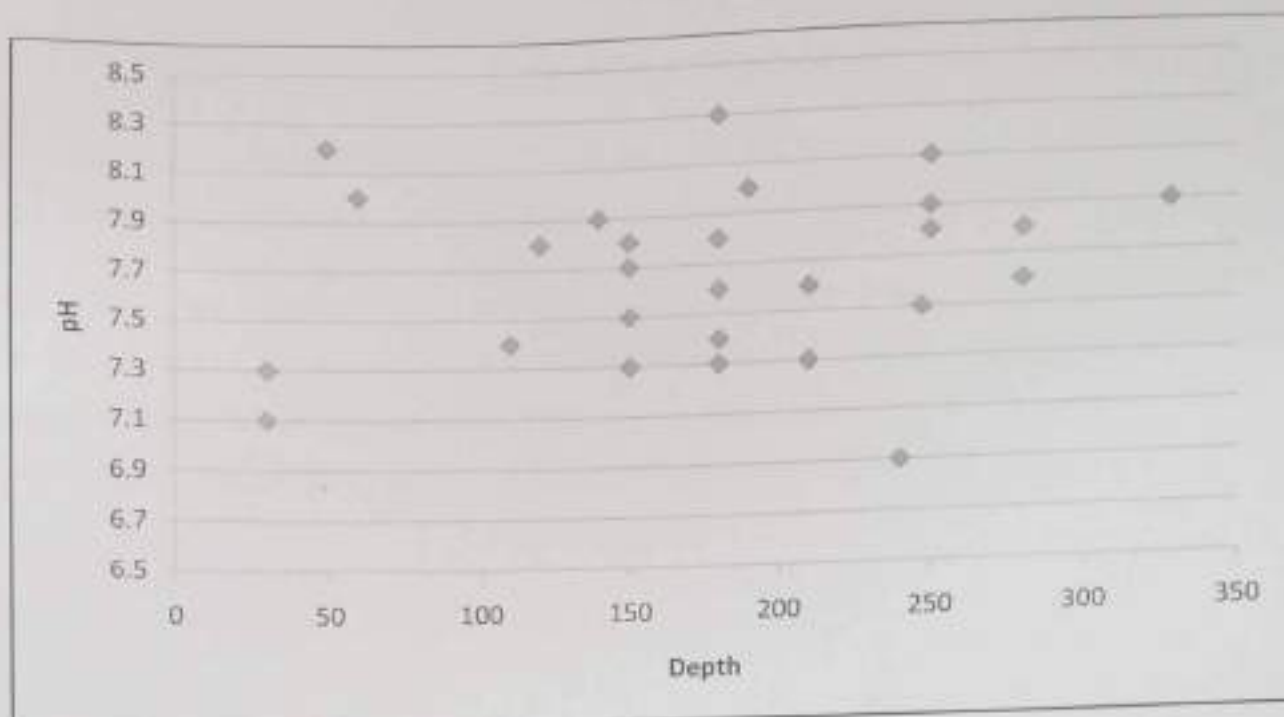


Fig.7: pH variation with depth of the source

## CONCLUSION

The Uranium concentrations in the 27 samples ranged from  $3.01 \pm 0.21$   $\mu\text{g/L}$  to  $19.22 \pm 0.87$   $\mu\text{g/L}$ . The average Uranium concentration was calculated at  $7.089 \pm 0.45$   $\mu\text{g/L}$ .

Upon comparing Uranium levels with the Maximum Contaminant Level (MCL) proposed by the World Health Organization (WHO), it was observed that all samples fell below WHO specified threshold. Additionally, all samples remained below the MCL value of 30  $\mu\text{g/L}$  set by the United States Environmental Protection Agency (USEPA).

## REFERENCES

- [1]. Ingmar Grenthe, JanuszDroz'dz'yn'ski, Takeo Fujino, Edgar Buck, Thomas E. Albrecht-Schmitt, and Stephen F. Wolf. (URANIUM\*).
- [2]. Tisso Aluminosilicatet, F. L., & Dauphas, N. (2015). Uranium isotopic compositions of the crust and ocean: Age corrections, U budget and global extent of modern anoxia. *Geochimica et Cosmochimica Acta*, 167, 113-1433.
- [3]. Carvalho, F. P., Fesenko, S., Harbottle, A. R., Lavrova, T., Mitchell, N. G., Payne, T. E., & Yankovich, T. L. (2023). The environmental behaviour of uranium.
- [4]. The crystal chemistry of Uranium (Peter C Burns, R Finch, 1999).
- [5]. Systematics and paragenesis of Uranium minerals (Robert Finch, Takashi Murakami, 1999)
- [6]. Chevreux, P., Tissandier, L., Laplace, A., Vitova, T., Bahl, S., Le Guyadec, F., & Deloule, E. (2021). Uranium solubility and speciation in reductive soda-lime glass melts. *Journal of Nuclear Materials*, 544, 152666
- [7]. Smedley, P. L., & Kinniburgh, D. G. (2023). Uranium in natural waters and the environment: Distribution, speciation and impact. *Applied Geochemistry*, 148, 105534
- [8]. Behavior of Uranium under conditions of interaction of rocks and ores with subsurface water. Bl Omel'yanenko, VA Petrov, VV Poluektov, *Geology of Ore Deposits* 49, 378-391, 2007.
- [9]. Gómez, P., Garralón, A., Buil, B., Turrero, M. J., Sánchez, L., & De la Cruz, B. (2006). Modeling of geochemical processes related to Uranium mobilization in the groundwater of a Uranium mine. *Science of the Total Environment*, 366(1), 295-309.
- [10]. Sharma, D. A., Keesari, T., Pant, D., Rishi, M. S., Sangwan, P., Thakur, N., & Sinha, U.K. (2022). Appraising the factors favouring Uranium mobilization and associated health risk assessment in groundwaters of north-western India. *Ecotoxicology and Environmental Safety*, 229, 113086.
- [11]. Health effects of uranium: new research findings Doug Brugge, Virginia Buchner Walter de Gruyter 26 (4), 231-249, 2011.
- [12]. Bone as a possible target of chemical toxicity of natural Uranium in drinking water PäiviKurtio, Hannu Komulainen, AilaLeino, LainaSalonen, AnssiAuvinen, HeikkiSaha *Environmental health perspectives* 113 (1), 68-72, 2005.



- [13]. Zamora, M. L., Tracy, B. L., Zielinski, J. M., Meyerhof, D. P., & Moss, M. A. (1998). Chronic ingestion of Uranium in drinking water: a study of kidney bioeffects in humans. *Toxicological Sciences*, 43(1), 68-77.
- [14]. USEPA. (2000) National Primary Drinking Water Regulations; Radionuclides; Final Rule. *Fed Reg.* 65(236), 76708.
- [15]. WHO. 2003. Guidelines for drinking water quality. Health Criteria and other supporting information. World Health Organization (2003).
- [16]. Ma, M., Wang, R., Xu, L., Xu, M., & Liu, S. (2020). Emerging health risks and underlying toxicological mechanisms of Uranium contamination: Lessons from the past two decades. *Environment international*, 145, 106107.
- [17]. Rani, A., & Singh, S. (2006). Analysis of Uranium in drinking water samples using laser Induced fluorimetry. *Health physics*, 91(2), 101-107.
- [18]. Singh, P., Singh, P., Sahoo, B. K., & Bajwa, B. S. (2016). A study on Uranium and radon Levels in drinking water sources of a mineralized zone of Himachal Pradesh, India. *Journal of Radioanalytical and Nuclear Chemistry*, 309, 541-549.
- [19]. Kumar, M., Kaushal, A., Sahoo, B. K., Sarin, A., Mehra, R., Jakhu, R., ... & Sharma, N. (2019). Measurement of Uranium and radon concentration in drinking water samples and assessment of ingestion dose to local population in Jalandhar district of Punjab, India. *Indoor and Built Environment*, 28(5), 611-618.
- [20]. Panghal, A., Kumar, A., Kumar, S., Singh, J., Sharma, S., Singh, P., ... & Bajwa, B. S. (2017). Radiation dose-dependent risk on individuals due to ingestion of Uranium and radon concentration in drinking water samples of four districts of Haryana, India. *Radiation effects and defects in solids*, 172(5-6), 441-455.
- [21]. Kumar, A., Arora, T., Singh, P., Singh, K., Singh, D., Pathak, P. P., & Ramola, R. C. (2021). Quantification of radiological dose and chemical toxicity due to radon and Uranium in drinking water in Bageshwar region of Indian Himalaya. *Groundwater for Sustainable Development*, 12, 10049.
- [22]. Kaur, M., Kumar, A., Mehra, R., & Mishra, R. (2019). Age-dependent ingestion and inhalation doses due to intake of Uranium and radon in water samples of Shiwalik Himalayas of Jammu and Kashmir, India. *Environmental monitoring and assessment*, 191, 1-17.
- [23]. Mehta, V., Kapil, C., Shikha, D., & Kanse, S. (2023). Appraisal of age-dependent radiological risk caused by ingestion of Uranium in groundwater of Patiala district, Punjab. *Journal of Radio analytical and Nuclear Chemistry*, 1-11.

- [24]. Balaram, V., Rani, A., & Rathore, D. P. S. (2022). Uranium in groundwater in parts of India and world: A comprehensive review of sources, impact to the environment and Human health, analytical techniques, and mitigation technologies. *Geosystems and Geoenvironment*, 1(2), 100043.
- [25]. Mehta, V., Kaur, J., Shikha, D., & Kanse, S. (2023). Age-dependent ingestion doses to the public of Rupnagar and Una regions of India due to intake of uranium. *Journal of Radioanalytical and Nuclear Chemistry*, 1-15.
- [26]. Rachel M Coyte, Ratan C Jain, Sudhir K Srivastava, Kailash C Sharma, Abedalrazq Khalil, Lin Ma, Avner Vengosh (2018). Large-scale uranium contamination of groundwater resources in India. *Environ. Sci. Technol. Lett.* 2018, 5, 6, 341–347
- [27]. Mehra, R., Gupta, D., & Jakhu, R. (2017). Risk assessment for natural Uranium present in ground water of Mahendragarh district of Haryana. *J. Radiat. Nucl. Appl.*, 2, 67-73.

**BETHE-HEITLER THEORY FOR EXTERNAL  
BREMSSTRAHLUNG CALCULATIONS: FORTRAN  
CODE**

**PROJECT REPORT**

*Submitted in partial fulfillment of the  
requirements for the award of the degree of*

**MASTER OF SCIENCE**

**in**

**PHYSICS**

*By*

**Anshu Sharma**

**Regn. No. 8114-2021-1308**



**DEPARTMENT OF PHYSICS  
SRI GURU TEG BAHADUR KHALSA COLLEGE, SRI  
ANANDPUR SAHIB  
(An Autonomous College)  
ANANDPUR SAHIB– 140118, PUNJAB (INDIA)**



**SRI GURU TEG BAHADUR KHALSA COLLEGE, SRI ANANDPUR SAHIB**  
(An Autonomous College)  
**ANANDPUR SAHIB-140118. PUNJAB (INDIA)**

---

---

## **CERTIFICATE**

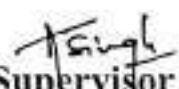
It is certified that the work contained in the project report entitled "**BETHE-HEITLER THEORY FOR EXTERNAL BREMSSTRAHLUNG CALCULATIONS: FORTRAN CODE**" is an original contribution by me and has not been submitted in part or full for any other degree at this or other University/ Institute.

The assistance and help received during the course of the thesis work have been acknowledged.

**Anshu Sharma**  
Regn. No. **8114-2021-1308**

I, the undersigned, Supervisor of **Anshu Sharma, Regn. No. 8114-2021-1308**, a candidate for the degree of **Master of Science**, agree that the project report entitled, "**BETHE-HEITLER THEORY FOR EXTERNAL BREMSSTRAHLUNG CALCULATIONS: FORTRAN CODE**", may be submitted in partial fulfillment of the requirements for the award of degree.

This is to certify that the above statement made by the candidate is correct to the best of my knowledge.

  
**Supervisor**  
Dr. Amrit Singh  
Assistant Professor  
Department of Physics  
Sri Guru Teg Bahadur Khalsa College  
Sri Anandpur Sahib



### CERTIFICATE

This is to certify that the "Project report" entitled "**BETHE-HEITLER THEORY FOR EXTERNAL BREMSSTRAHLUNG CALCULATIONS: FORTRAN CODE**" submitted by **Anshu Sharma** (Regn. No. **8114-2021-1308**) to Department of Physics, Sri Gurur Teg Bahadur Khalsa College, Sri Anandpur Sahib in partial fulfillment of the requirements for the award of degree of **MASTER OF SCIENCE IN PHYSICS** and has been approved by the Department Research committee (DRC) after the viva-voce examination of the candidate.

  
Dr. Anrit Singh  
Supervisor

  
Dr. Randev Singh  
Chairman DRC



## ACKNOWLEDGEMENT

Firstly, I would like to express my gratitude to my Supervisor, Dr. Amrit Singh Assistant Professor at Department of physics Sri Guru Teg Bahadur Khalsa College Sri Anandpur Sahib, who has resourcefully guided me throughout this research project. I'm extremely grateful for his motivating discussions while enable me to accomplish this task successfully. Without his active guidance, support and encouragement I would not have made headway in this project.

I also thankful to my Parents for their moral support and suggestions to improve the dissertation work. I'm also thankful to other faculty members in the department for their encouragement and fruitful academic discussions.

A special thanks to Ms. Monika Sharma Assistant Professor at Department of Physics for the help and their valuable suggestions whenever I needed out of their busy schedule. I'm also thankful to my classmates and my friends who was directly or indirectly help me to complete this project report.

Anshu Sharma

## ABSTRACT

Theoretical investigation of bremsstrahlung processes was started on the basis of classical electrodynamics. The initial attempts were made in 1923 by Kramers to develop the bremsstrahlung theory on the basis of semi-classical calculation by using correspondence principle. The first Quantum mechanical cross-section formulae for the elementary processes of bremsstrahlung were derived in 1931 by Sommerfeld in the non-relativistic dipole approximation including retardation for non-relativistic electrons without taking accounts the nuclear screening effects. Elwert and Guth give the multiplicative coulomb correction factor ( $F_{Elwert}$ ) for Bethe-Heitler OB cross-section ( $\sigma_{BH}(k)$ ).

In the present investigation a FORTRAN code has been created to find the external bremsstrahlung cross section using Bethe-Heitler theory and also a code is made for the Coulomb correction proposed by the Elwert. The results obtained from these codes are in good agreement with the results available in literature.

## CONTENTS

CHAPTER	Page No.
1. Introduction and Literature Survey	1-13
1.1 General Introduction	
1.2 Description of ordinary bremsstrahlung	
1.3 Theoretical aspect of ordinary bremsstrahlung	
1.4 Bremsstrahlung in material medium	
2. Fortran Code	14-18
3. Results and discussions.	19-21
4. References	22-24

## LIST OF FIGURES

S. No.	Name of the Figure
--------	--------------------

- |         |  |
|---------|--|
| Fig.3.1 | The plots of number of photons of energy $k$ per $m_0c^2$ per unit<br>total photon yield for Al target |
| Fig.3.2 | The plots of number of photons of energy $k$ per $m_0c^2$ per unit<br>total photon yield for Pb target |

## CHAPTER 1

### INTRODUCTION AND LITERATURE SURVEY

#### 1.1 General Introduction

Rontgen (1895, 1896) discovered X-rays, but the study of two different components, the characteristic line spectrum and the continuous spectrum started in early 1905s. For the continuous spectrum Sommerfeld (1931) proposed the name *bremsstrahlung* (braking radiation) with the approval of Rontgen himself. *Bremsstrahlung* is the fundamental processes, in which the photon emission occurs due to the scattering of an electron from an atom. *Bremsstrahlung* plays an important role in all braches of physics: atomic and nuclear physics, solid state physics, and plasma physics and in the field of astrophysics. It has a wide range of application in many areas of experimental and theoretical physics research.

Until the 1970s, *bremsstrahlung* was considered in the domain of the acceleration of electron in the static screened coulomb field of the target nuclei. In early 1970s, several people consider the dynamic response of the target atom that can be polarized by the incident electron and the photon emission occurs. Therefore, the new mechanism of photon emission polarization *bremsstrahlung* was introduced. The total *bremsstrahlung* (BS) amplitude is the sum of ordinary *bremsstrahlung* (OB) and polarization *bremsstrahlung* (PB) amplitudes. Ordinary *bremsstrahlung* is the process by which the photon is emitted by the electron decelerating in the static field of the target atom. Polarization *bremsstrahlung* is the process by which the photon is emitted by the target as a result of its



polarization by incident electron. During the collision of the incident electron and the atom, the internal structure of the atom is deformed or polarized and an electric dipole moment is induced. Being time-dependent, it becomes a source of continuous electromagnetic radiation called polarization bremsstrahlung. It is more complicated than the ordinary bremsstrahlung since in addition to the electron-photon interaction one has to consider the dynamic response of the target atom created by the action of the two fields created by the incident electron and the emitted photon. The polarization bremsstrahlung plays important role particularly at lower and medium photon energy and its contribution in the total bremsstrahlung spectra must be taken into account, while comparing the theoretical and experimental results.

A beam of mono-energetic electron passes through the material medium suffers elastic and inelastic scattering, multiple scattering. The electron loses energy through the excitation and ionization of the absorbing atoms of the material media. The scattering of electrons through the finite angle always accompanied by the emission of electromagnetic radiation termed as bremsstrahlung. The behavior of the continuous beta particles is same as that of the mono-energetic electrons except for the continuous nature of the beta particles whose energy spread over from zero to maximum end point energy of the beta radioactive source. The continuous spectrum of beta particles or electrons produces electromagnetic radiation photon on suffering deflection through acceleration or retardation from the coulomb field of the nuclei in material medium. However, there exist an important difference between the mono-energetic electron and continuous beta particles of radioactive beta source. In case of beta radioactive source an electromagnetic radiation is emitted along with the

originated electrons or continuous beta particles interaction with the coulomb field of the daughter nucleus. This electromagnetic radiation is termed as internal bremsstrahlung and it is dependent purely on the characteristic of beta emitter. However, the emission of electromagnetic radiation photon due to the interaction of the continuous beta particles with the static coulomb field of target nuclei is termed as ordinary bremsstrahlung. The mode of production of ordinary bremsstrahlung is relatively different from the production of the internal or inner bremsstrahlung due to electron capture. Historically, the first measurement of the ordinary bremsstrahlung produced by the continuous beta particles of the beta emitter was reported by Gray (1911, 1912) Chadwick (1912) and Hess and Lawson [5]. Later, Gray (1922) measured the ordinary bremsstrahlung spectra in targets of iron, lead and paper produce by the absorption of continuous beta particles of beta emitter. The phenomenon of internal bremsstrahlung was first discovered by Aston in (1927) in beta decay of radioactive source. The experimental evidence of internal bremsstrahlung was given by Bramson in 1930. Later, the detail experimental studies have been carried out by Stahel and Kipfer (1936), Gray and Hinds (1936) and Droste (1936).

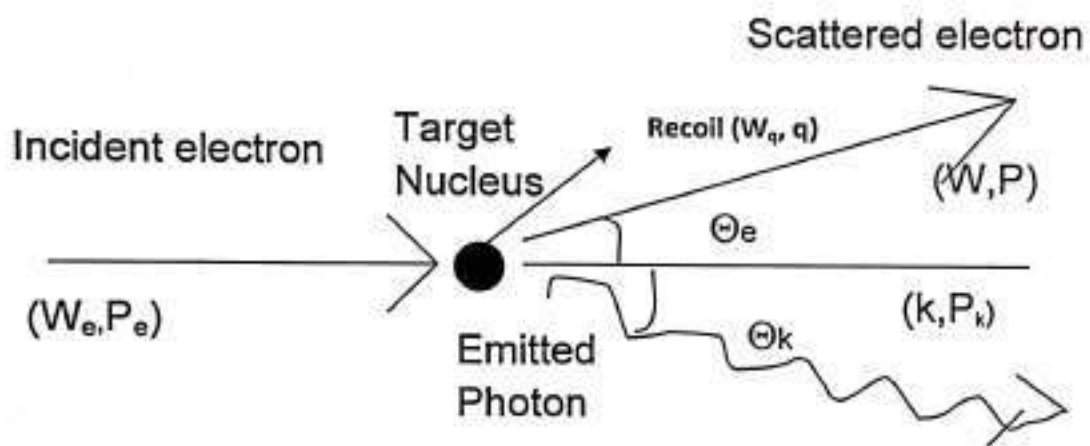
## 1.2 Description of ordinary bremsstrahlung

In classical electrodynamics an accelerated charged particle passed through the static field of the target nucleus emits a photon this termed as ordinary bremsstrahlung. The ordinary bremsstrahlung amplitude is proportional to the acceleration produced by nucleus ' $Ze$ ', on a particle of charge ' $Ze$ ' and mass ' $m$ '. Therefore, the bremsstrahlung intensity which is given by the square of amplitude will vary as the square of the  $Z^2/m^2$ . The bremsstrahlung intensity is directly proportional to the square of atomic number of the target element or absorbing



material and varies inversely as the square of the mass of the projectile. Therefore, the bremsstrahlung intensity is more for the light particle like electron and it is relatively small for the heavy particle like proton, alpha particles etc.

The following diagram shows the processes of production of ordinary bremsstrahlung depicts the production of photon by the interaction of the incident charged particle electron with the interaction of the nucleus of the target atom –



Here  $W_e$  and  $W$  are the total energies of the incident and scattered electron.  $P_e$  and  $P$  are the momentum of the incident and scattered electron. Where,  $W_q$  and  $q$  be the total energy and momentum of the recoil atom.  $k$  and  $P_k$  be the energy and momentum of the emitted photon.

Now, according to the conservation laws of energy and momentum we have,

$$W_e = W + k + W_q$$

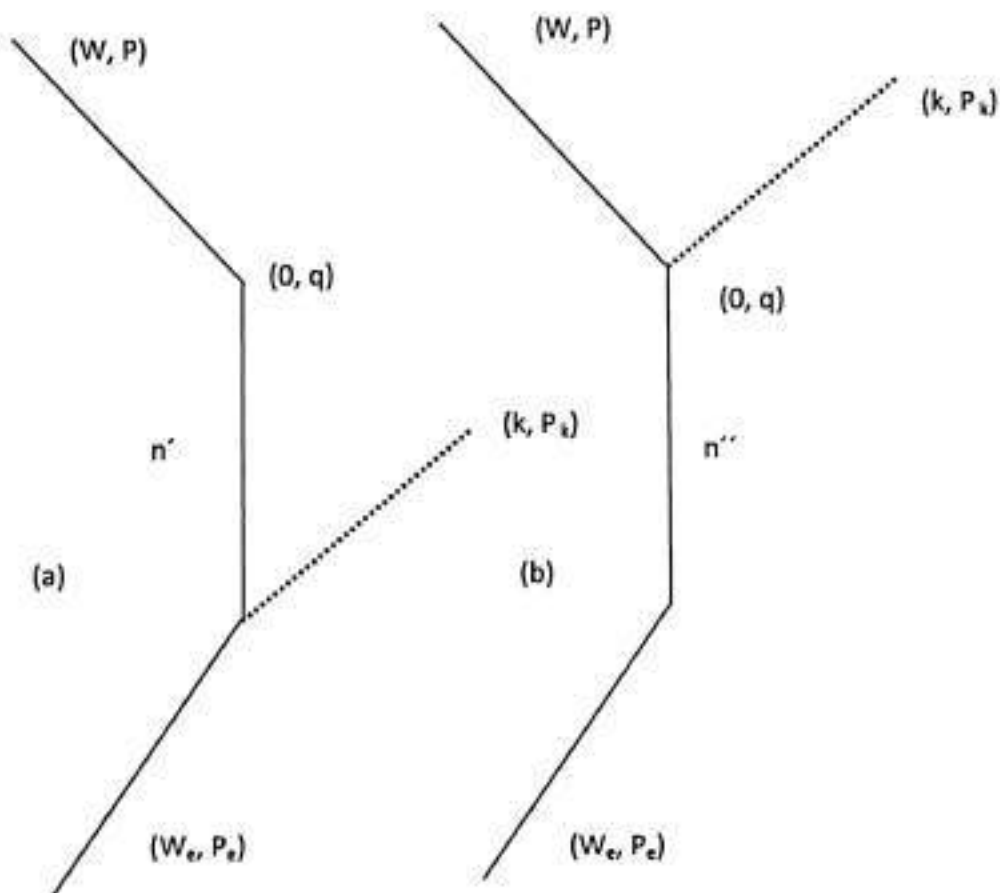
$$P_e = P + k + q$$

Therefore, in individual interaction of the incident electron with the target nucleus, the incident electron losses energy from 0 up to maximum amount of its total kinetic energy  $T_e = W_e - 1$ . The maximum photon energy  $k_{max}$  at the short wavelength limit of continuous X-ray spectrum is given by

$$k_{max} = T_e = W_e - 1$$

This relation was experimentally established by Duane and Hunt's in 1915 and is known as Duane and Hunt's law.

The Feynman diagram representation of the processes of OB looks approximately as shown given below



The two possible intermediate states can occur firstly, the photon is emitted and then the electron is scattered afterwards, or the sequence is reversed. In one of the case the intermediate states is a virtual state, since photon cannot be emitted at least violating one of the conservation law.

### 1.3 Theoretical aspect of ordinary bremsstrahlung

Theoretical investigation of bremsstrahlung processes was started on the basis of classical electrodynamics. The initial attempts were made in 1923 by Kramers to develop the bremsstrahlung theory on the basis of semi-classical calculation by using correspondence principle. The first Quantum mechanical cross-section formulae for the elementary processes of bremsstrahlung were derived in 1931 by Sommerfeld in the non-relativistic dipole approximation including retardation for non-relativistic electrons without taking accounts the nuclear screening effects. For the relativistic case, by using the Dirac theory Bethe and Heitler (1934), Sauter (1934) and Racah (1934) obtained independently an analytical expression for the OB cross-section by using the first order Born approximation. They neglecting the coulomb field effects on the wave function of incident and scattering electrons on the nucleus. Elwert (1939) and Guth (1941) give the multiplicative coulomb correction factor ( $F_{Elwert}$ ) for Bethe-Heitler OB cross-section ( $\sigma_{BH}(k)$ ). Tseng and Pratt (1971) developed a quantum theory for the bremsstrahlung for relativistic electrons by using screened self-consistent field wave function. Pratt et al. (1977) published extensive tables of OB cross-section for  $Z$  values between 2 and 92 and incident electron energy between 1 and 2000 keV. Berger and Seltzer (1986) calculated the contribution of electron-electron bremsstrahlung given by Pratt et al. (1977). There have been extensive reviews on



the theory of OB Pratt and Feng (1985), Pratt (1995), Seltzer and Berger (1985) and Haug and Nakel ().[23-27].

The expression for ordinary bremsstrahlung cross-section in Born's approximation is known as Bethe-Heitler formula. This was first derived simultaneously and independently by Bethe and Heitler (1934), Sauter (1934) and Racah (1934). They obtained the OB cross-section ( $\sigma_{BH}(W_e, k, Z)$ ) is given below –

$$\sigma_{BH}(W_e, k, Z) = \frac{Z^2 r_e^2}{137} \frac{dk}{k} \frac{p}{p_e} \left[ \frac{4}{3} - 2W_e W \frac{p_e^2 + p^2}{p_e^2 p^2} + \frac{E_e W}{p_e^3} + \frac{E_e W_e}{p^3} - \frac{E_e E}{p_e p} + L(A+B) \right]$$

Where

$$A = \frac{8}{3} \frac{W_e W}{p_e p} + \frac{k^2 (W_e W^2 + p_e^2 p^2)}{p_e^3}$$

$$B = \frac{k}{2p_e p} \left( \frac{W_e W + p_e^2}{p_e^3} E_e - \frac{W_e W + p^2}{p^3} E + \frac{2kW_e W}{p_e^2 p^2} \right)$$

$r_e$  = classical radius of electron

$$= 2.818 \times 10^{-3}$$

$$W_e = W + k$$

$$p_e = \sqrt{W_e^2 - 1}$$

$$p = \sqrt{W^2 - 1}$$

$$E_e = \ln \frac{W_e + p_e}{W_e - p_e}$$

$$E = \ln \frac{W + p}{W - p}$$

$$L = \ln \frac{p_e^2 + p_e p - W_e k}{p_e^2 - p_e p - W_e k}$$

$W_e, W$  = initial and final total energy of electron

$p_e, p$  = initial and final momentum of electron

In the non relativistic limit following approximations have been used

- (i) Non screened :  $137Z^{-1/3} \gg (W_e W / k)$
- (ii) Born's approximation :  $(2\pi\alpha Z W_e / p_e); (2\pi\alpha Z W / p) \ll 1$
- (iii) Non relativistic :  $\frac{p_e}{W_e} \ll 1$

The total OB cross-section follows as the limit of equation is given by

$$\sigma(W_e, k, Z) = \frac{Z r_e}{137} \frac{16}{3} \frac{dk}{k} \frac{1}{p_e^2} \ln \left( \frac{p_e + p}{p_e - p} \right)$$

The multiplicative coulomb correction factor ( $F_{Elwert}$ ) for Bethe-Heitler OB cross-

section ( $\sigma_{BH}(k)$ ) is given by

$$F_{Elwert} = \frac{W / p [1 - \exp(-2\pi\alpha Z W_e / p_e)]}{W_e / p_e [1 - \exp(-2\pi\alpha Z W / p)]}$$

This correction factor was derived on the basis of a comparison between the non-relativistic Born-approximation and non-relativistic calculations. For electron energies roughly below 100 keV, Elwert factor give accurate result within 10 %.

## 1.4 Bremsstrahlung in material medium

The various theories OB or BS spectra discussed in the previous sections are applicable to thin target only, in which the monoenergetic electron has only a single radiative interaction. In the case of thick target, processes such as electron scattering, excitation and ionization that compete with bremsstrahlung are required to be taken into account. In this case an electron loses a significant part of its energy while coming to rest in a target. For continuous Beta particles Bethe and Heitler (1934) gave an expression for the bremsstrahlung spectral distribution  $n(k, W_e', Z)$  in a sufficiently thick target to absorb an electron of energy  $W_e'$  with  $N$  atoms per unit volume. At lower photon energies in thick targets, the correction due to absorption of BS photons in the target and electron backscattering from the target can not be neglected. Semaan and Quarles (2001) have reported that the correction for the self absorption of BS photons in the target and electron backscattering are required for  $n(W_e', k, Z)$  in case of low energy thick target bremsstrahlung. The BS spectral distribution  $[n_{cor}(W_e', k, Z)]$  after absorption correction and electron backscattering correction in thick target is given by

$$n_{cor}(W_e', k, Z) = RN \int_{1+k}^{W_e'} \frac{d\sigma(W_e, k, Z) / dk}{(-dW_e / dx)} dW_e \times \exp(-\mu x)$$

Here  $d\sigma(W_e, k, Z) / dk$  is the singly differential cross section taken from the different theoretical models Bethe and Heitler (1934) and Avdonina and Pratt (1999). And  $-dW_e / dx$  is the total energy loss per unit path length of an electron



in a target material taken from the tabulations given by Berger and Seltzer (2000). Where  $\exp(-\mu x)$  is the absorption factor,  $\mu$  is the mass attenuation coefficient for the given target element taken from the tabulations given by Chantler *et al* (2008) and 'x' is the optimum thickness of the target which is equal to the range of the beta particle in a target. 'R' is the electron backscattering factor given by Semaan and Quarles (2001)

$$R = \frac{1 - \eta(W_e, Z)}{1 - \eta(W_e, Z) \frac{k^2}{W_e^2}}$$

Here,  $W_e = 0.4 W_{\max}$ ,  $W_{\max}$  is the end point energy of beta particles and  $\eta(W_e, Z)$  is the total backscattering factor. The BS spectral distribution in a thick target obtained on complete absorption of beta particles of a end point energy  $W_{\max}$  is expressed as number of photons of energy k per unit  $m_e c^2$  per beta disintegration for continuous beta particle is given by  $S(k, Z)$

$$S(k, Z) = \int_{1+k}^{W_{\max}} n_{cor}(W_e', k, Z) P(W_e') dW_e'$$

Here  $P(W_e') dW_e'$  is the beta spectrum of the beta source under study.

The BS photon yield T for the target, with  $k_{\min}$  and  $k_{\max}$  as the lower and upper limit of photon energy of the BS spectrum respectively is given by

$$T = \int_{k_{\min}}^{k_{\max}} S(k, Z) dk$$

Computer programs are written to calculate the BS spectral distribution in terms of the number of photons of energy  $k$  per unit  $m_0c^2$  per beta disintegration, i.e.  $S(k,Z)$  by using Eqns. () from various theories. The total photon yields  $T$  were obtained for different targets from graphical integration of the BS spectra from the plots of  $S(k,Z)$  versus photon energy  $k$  between  $k_{\min}$  and  $k_{\max}$ . The experimental and theoretical results were compared in terms of the number of photons of energy  $k$  per  $m_0c^2$  per unit total photon yield. This method makes the results independent of source strength and removes the uncertainties associated with its measurements.

### 1.5 Z-dependence of bremsstrahlung spectra

The bremsstrahlung spectral photon energy distribution depends upon the fundamental cross-section for interaction of an electron with an atom of the target material. The study of dependence of bremsstrahlung spectral photon distribution on the atomic number of the target atom at various electron energies and photon energies is important to know the Z-dependence of spectral shape of bremsstrahlung. Bremsstrahlung cross-section is proportional to the square of the atomic number of the target atom. For the continuous beta particles the bremsstrahlung intensity is proportional to the atomic number  $Z$  of the target element. The theories which describe the bremsstrahlung processes are adequate to explain the bremsstrahlung cross-section at various electron energies. The Z-dependence of ordinary bremsstrahlung (OB) spectra has been reported by Hippler et al. (1981) and Seeman and Quarles (1982) for monoenergetic electron. For continuous beta particles Wu (1941) and Evans (1955) reported that the bremsstrahlung intensity is linearly dependent on the



atomic number of the target element ( $Z$ ). The  $Z$ -dependence of the spectral shape of OB spectra for continuous beta particles as a function of photon energy region above 30 keV has been reported by Dhaliwal (2002, 2003, 2005). However, in literature the  $Z$ -dependence of the spectral shape of total bremsstrahlung spectra (BS) and OB spectra for continuous beta particles has not been reported so far particularly in the photon energy region of 5-30 keV. So, there is need to study the  $Z$ -dependence of the spectral shape of BS and OB spectra produced by continuous beta particles, particularly in the photon energy region of 5-30 keV.

In order to investigate the  $Z$ -dependence of the spectral shape of the OB, the  $S(k, Z)$  number of photons of energy  $k$  per unit  $m_0 c^2$  per beta disintegration at the photon energy  $k$  can be expressed as a function of  $Z$  and is reported by Dhaliwal (2003) i.e.

$$S(k, Z) = K(k)Z^n$$

Where ' $n$ ' is the index of the  $Z$ -dependence of a photon energy  $k$  per unit  $m_0 c^2$  per beta disintegration and  $K(k)$  is the proportionality factor, which is independent of  $Z$  at particular photon energy  $k$ . Knowledge of the index ' $n$ ' is essential for evaluating the  $Z$ -dependence of the spectral shape of OB. Dhaliwal (2002, 2003, 2005) has been study the  $Z$ -dependence of spectral shape of OB produced by continuous beta particles in thick metallic targets and compared their experimental results with the theoretical results obtained from Tseng and Pratt (1971) and Bethe and Heitler (1934) theories which describes OB only. By using the above relation, in the present measurements of bremsstrahlung efforts were made to check the  $Z$ -dependence of the

spectral shape of OB and total bremsstrahlung (BS) spectra which includes the contribution of PB into OB as a function of photon energy in the region 5-30 keV. Theoretical and experimental BS spectral distributions were required for the determination of the Z-dependence index and the proportionality factor K (k) defined at different photon energies. These spectral photon distributions were calculated on the basis of the continuous slowing down approximation given by Seltzer and Berger (1986). In these approximations the rate at which the electron loses energy has two components (i) the average energy loss per unit path length, due to inelastic collision with the bound electron of the medium resulting in ionization and excitation and (ii) the average energy loss per unit path length due to the emission of the bremsstrahlung in the coulomb electric field of the atomic nucleus. The BS spectral photon distribution as a function of the photon energy k has been studied through the Z-dependence index of the bremsstrahlung production by using different beta emitter ( $^{204}\text{Tl}$ ,  $^{90}\text{Sr}$ ,  $^{147}\text{Pm}$ , and  $^{45}\text{Ca}$ ) in the different thick target elements (Al, Ti, Cu, Sn and Pb).

## CHAPTER-2

### FORTRAN CODE

#### 2.1 Program for the calculation of Bethe Heitler ordinary bremsstrahlung cross-section

```
WRITE(*,*)'ATOMIC NO. OF THE ATOM'
```

```
READ(*,*)Z
```

```
WRITE(*,*)'INITIAL TOTAL ELECTRON ENERGY'
```

```
READ(*,*)W
```

```
WRITE(*,*)'PHOTON ENERGY'
```

```
READ(*,*)N
```

```
DO 10 K=1,N
```

```
S=W-K
```

```
T=SQRT(S*S-1)
```

```
P=SQRT(W*W-1)
```

```
E1=2.0*ALOG(S+T)
```

```
F=2.0*ALOG(W+P)
```

```
G=2.0*ALOG((W*S+P*T-1)/K)
```

```
A=T/P/K
```

$$B=1.3333-(2.0*W*S*((T*T+P*P)/(P*P)/(T*T)))+(S/P**3)*F+(W/T**3)*E1-((F*E1)/P/T)$$

$$C=(2.6666*W*S/P/T+(K**2/P**3/T**3)*(W**2*S**2+P**2*T**2))*G$$

$$D1=(K/2/P/T)*G$$

$$A1=((W*S+P*P)/P**3)*F$$

$$B1=((W*S+T*T)/T**3)*E1$$

$$C2=(2*K*W*S)/(T*T)/(P*P)$$

$$D=D1*(A1-B1+C2)$$

$$Y1=0.058046*A*(B+C+D)$$

$$Y=Z*Z*Y1$$

$$FMOD=(P/T)*((1-EXP(-860.8*Z/P))/(1-EXP(-860.8*Z/T)))$$

$$C1=(1+0.0000133*Z*Z*(3-W))$$

$$Q=T+P$$

$$R=P-T$$

$$S1=Q/R$$

$$S2=(0.5516)*ALOG(S1)$$

$$SP1=(0.5516)*(2*ALOG(Q/R)+ALOG((Q*Q+0.798*Z)/(R*R+0.798*Z)))$$

$$SP2=(0.5516)*(R*R/(R*R+0.798*Z)-Q*Q/(Q*Q+0.798*Z))$$

$$SP=SP1+SP2$$

FAT=SP-S2

CR= C1\*FMOD\*Y

YT=CR+FAT

CRT= YT\*511.0034E-026

WRITE(5,\*) K , CRT

10 CONTINUE

STOP

END



**2.2 Program for the calculation of Elwert Correction factor for ordinary bremsstrahlung cross-section**

REAL K1,W,L,S,PI,PE,EI,EE,A1,A2,B1,B2,B3,S1,S2,S3,S4,S5,S6

WRITE(\*,\*)'ATOMIC NUMBER OF THE ATOM'

READ(\*,\*)Z

WRITE(\*,\*)'INITIAL TOTAL ELECTRON IN MC2'

READ(\*,\*)W

WRITE(\*,\*)'PHOTON ENERGY'

READ(\*,\*)N

DO 10 K=1,N

K1=K/511.0034

S=W-K1

PI=SQRT(W\*W-1)

PE=SQRT(S\*S-1)

EI=ALOG((W+PI)/(W-PI))

EE=ALOG((S+PE)/(S-PE))

F1=(2.0\*3.142\*Z\*W)/(137.0\*PI)

F2=(2.0\*3.142\*Z\*S)/(137.0\*PE)

F3=S/PE

F4=W/PI

F5=(2.0\*3.142\*Z\*137)/PI

F6=(2.0\*3.142\*Z\*137)/PE

FMOD=(PI\*(1-EXP(-F5)))/(PE\*(1-EXP(-F6)))

FELWERT=(F3\*(1-EXP(-F1)))/(F4\*(1-EXP(-F2)))

C=1+((Z/137)\*\*2)\*((2-(1-W))/4)

CFMOD=C\*FMOD

WRITE(\*,\*)K,FELWERT,CFMOD

10 CONTINUE

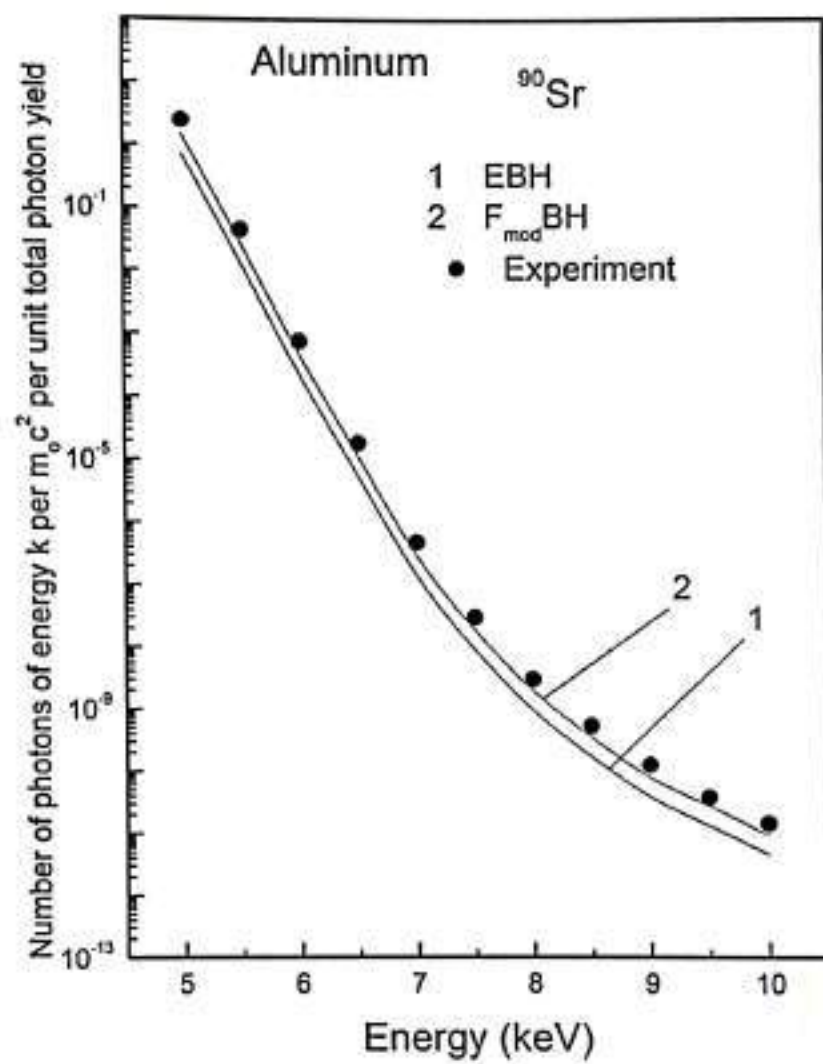
STOP

END

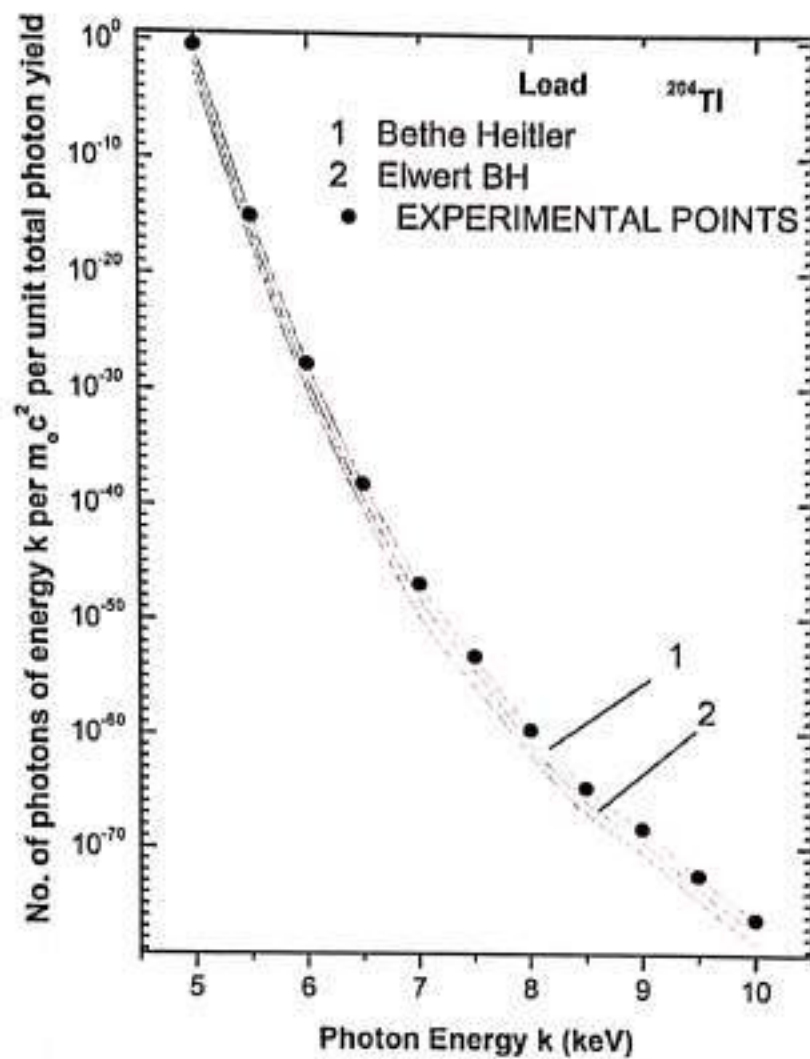
## CHAPTER 3

### RESULTS AND DISCUSSION

The results of experimentally measured BS spectra for the targets of Al and Pb produced by  $^{90}\text{Sr}$  beta particles, were compared with the theoretical external bremsstrahlung spectral photon distributions obtained from Bethe-Heitler theory and Elwert corrected (non-relativistic) Bethe-Heitler theory (EBH) which describes the ordinary bremsstrahlung. The plots of number of photons of energy  $k$  per  $m_0c^2$  per unit total photon yield for Al and Pb targets are shown in the in Figs. 3.1 and 3.2.



**Figure 3.1:** The plots of number of photons of energy  $k$  per  $m_0 c^2$  per unit total photon yield for Al target



**Figure 3.2:** The plots of number of photons of energy  $k$  per  $m_e c^2$  per unit total photon yield for Pb target

It is clear from the plots that the experimental BS spectral distributions for Al and Pb target materials are in agreement with the theoretical BS spectral distributions obtained from Elwert corrected (non-relativistic) Bethe-Heitler theory (EBH), within 10 %.



## REFERENCES

- Aston, G. H. 1929 The Amount of Energy Emitted in the  $\gamma$ -Ray Form by Radium B
- Bethe, H. and Heitler, W. 1934. On the stopping of fast particles and on the creation of positive electrons. *Proc. Roy. Soc. Lond. A* 146: 83-112
- Berger, M. and Seltzer, S. 2000. U.S. National Aeronautics and Space Administration Report No. NASA-SP3012 (1964). Current tabulation on the Web: Program ESTAR, <http://physics.nist.gov/PhysRefData/Star/Text/ESTAR.html> (2000).
- Chadwick J. 1912. The  $\gamma$  rays excited by the  $\beta$  rays of radium *Phil. Mag. Series 6*. 24: 1941-5990
- Chantler C T, Olsen K, Dragoset R A, Chang J, Kishore A R, Kotochigova S A, Zucker, D. S. (2005), X-Ray Form Factor, Attenuation and Scattering Tables (Version 2.1). [Online] Available: <http://Physics.nist.gov/ffast> [2008, June] National Institute of Standards and Technology, Gaithersburg, MD.
- Droste, G. F. V. 1938 über Versuche eines Nachweises von  $\alpha$ -Strahlen während der Bestrahlung von Thorium und Uran mit Radium + Beryllium-Neutronen. *Zeitschrift für Physik A Hadrons and Nuclei*. 110: 84-94
- Dhaliwal, A. 2002. Z-dependence of spectral shape of external bremsstrahlung produced by beta particles of  $^{147}\text{Pm}$  and  $^{32}\text{P}$ . *Nucl. Instr. and Meth. B*. 198: 32-36
- Dhaliwal, A. 2003. Study of the Z-dependence of spectral shape of external bremsstrahlung produced by beta particles. *J. Phys. B: At. Mol. Opt. Phys.* 36: 2229-2237
- Dhaliwal, A. S. 2003. Bremsstrahlung spectra produced by  $^{89}\text{Sr}$  beta particles in thick targets *X-ray spectrum*. 32: 367-372
- Dhaliwal, A. 2005. Z-dependence of spectral photon energy distributions of thick target bremsstrahlung. *Nucl. Instr. and Meth. B*. 234: 194-202
- Elwert, G. 1939. Verschärfte Berechnung von Intensität und Polarisation im kontinuierlichen Röntgenspektrum . 178-208
- Elwert, G. and Haug, E. 1969. Calculation of Bremsstrahlung Cross Sections with Sommerfeld-Maue Eigenfunctions. *Phys. Rev.* 183: 90-105
- Gray, J. A. 1911 Secondary gamma -Rays Produced by beta -Rays. *Proc. R. Soc. Lond.* 85:131-139
- Gray, J. A. 1912 The Nature of the gamma -Rays Excited by beta  $\beta$ -Rays *Proc. R. Soc. Lond.* 86:513-529

- Gray, J. A. and Hinds, J. F. 1936. The Gamma-Rays of Radium E. *Phys. Rev.* 49: 477
- Hippler R, Saeed K, McGregor I, Kleinpoppen, H. 1981. Z dependence of bremsstrahlung radiation from free atoms. *Phys. Rev. Lett.* 46 :1622
- Kramers, H. 1923. On the theory of X-ray absorption and the continuous X-ray spectrum. *Phila. Mag.* 46: 836
- Koch, H. and Motz, J. 1959. Bremsstrahlung cross-section formulas and related data. *Rev. Mod. Phys.* 31: 920-955
- Pratt R, Tseng H, Lee C, Kissel L, MacCallum C, Riley, M. 1977. Bremsstrahlung energy spectra from electrons of kinetic energy 1keV to 2000keV incident on neutral atoms  $2 \leq Z \leq 92$ . *At. Data Nucl. Data Tables.* 20: 175-209
- Pratt, R. H. and Feng, I. J. 1985. Electron-atom bremsstrahlung. In Crasemann, B. (Ed), Atomic inner shell physics. Plenum Press, New York, pp. 533-580 (Chapter 12)
- Pratt R, David Shaffer C, Avdonina N. B, Xiao-Min Tong, Florescu, V. 1995. New developments in the theory of bremsstrahlung. *Nucl. Instr. Meth. B* 99: 156-159
- Röntgen, W. 1895. Eine neue Art von Strahlen, Sitzungsberichten der Würzburger Physik-medie, Gesellschaft, Stahel, Würzburg.
- Röntgen, W. 1896. On a new kind of rays. *Nature.* 53:1369 London
- Williams, S. and Quarles, C. 2008. Absolute bremsstrahlung yields at 135° from 53 keV electron on gold film targets. *Phys. Rev. A* 78: 062704
- Semaan, M. and Quarles, C. 1981. Bremsstrahlung spectrum from low-energy electron bombardment of rare gas atoms. *Phys. Rev. A* 24: 2280
- Semaan, M. and Quarles, C. 1982. Z dependence of atomic-field bremsstrahlung. *Phys. Rev. A* 26 :3152
- Semaan, M. and Quarles, C. 2001. A model for low energy thick-target bremsstrahlung produced in a scanning electron microscope. *X-ray Spectrom.* 30:37-43
- Sommerfeld, A. 1931. The deflection and slowing down of electron., *Ann. Phys.* 11: 257-330
- Sauter, F. 1931. Über den atomaren Photoeffekt in der K-Schale nach der relativistischen Wellenmechanik Diracs. *Ann. Phys.* 11: 454-488
- Seltzer, S. and Berger, M. 1985. Bremsstrahlung spectra from electron interactions with screened atomic nuclei and orbital electrons. *Nucl. Instrum. Methods Phys. Res. B.* 12: 95-134



Seltzer, S. and Berger, M. 1986. Bremsstrahlung Energy Spectra from Electrons with Kinetic Energy 1 keV-10 GeV Incident on Screened Nuclei and Orbital Electrons of Neutral Atoms with  $Z = 1-100$ . *At. Data Nucl. Data Tables*. 35: 345-418

Tseng, H. and Pratt, R. 1971. Exact screened calculations of atomic-field bremsstrahlung. *Phys. Rev. A*. 3: 100-115

Tseng, H. and Pratt, R. 1974. Electron bremsstrahlung from neutral atoms. *Phys. Rev. Lett.* 33: 516-518

Tsyтович, V. N. Ojringel, I. M. (Eds.) 1993. Polarizational bremsstrahlung. Plenum, NY.

Zon, B. 1977. Bremsstrahlung in collisions between electron and atoms, *Soviet Physics JETP*. 46: 65-68

## SGTB KHALSA COLLEGE ANANDPUR SAHIB

### PG DEPARTMENT OF POLITICAL SCIENCE

#### LOK SABHA ELECTIONS 2024: Before Elections Survey of Sri Anandpur Sahib Constituency

The PG Department of Political Science conducted a survey on “LOK SABHA ELECTIONS 2024: Before Elections Survey of Sri Anandpur Sahib Constituency” on 19<sup>th</sup> Feb. 2024 with collaboration of Gram Panchyat Takhtgarh (Tehsil Sri Anandpur Sahib, Dist. Rupnagar). The students PG and UG classes of M.A.I, M.A.II and B.A.III conducted this survey under the guidance of the teachers. The objective of this survey was to understand the political knowledge and interests among voters. The students conducted the survey and submitted their report about the findings of their survey. The college principal Dr. Jasvir Singh appreciated the students for their contribution and efforts. The organizer of the survey was Dr. Sunita Rani and it was conducted under the guidance of Dr. Virpal Singh and Prof. Amandeep Kaur.



Department Of Punjabi  
Session:2023-24  
Post Graduate Course  
Project Details

Sr.No.	Class	Class Roll No.	University Roll No.	Students Name	Project Name
1	M.A.Punjabi-II, Sem-III	222303	5103	Kiranjeet Kaur	Punjabi Suffi Kav te Bir Kav Hoyea Khoj Kara]
2	M.A.Punjabi-II, Sem-III	222304	5104	Mandeep Kaur	Punjabi Suffi Kav te Bir Kav Hoyea Khoj Kara]
3	M.A.Punjabi-II, Sem-III	222305	5105	Neha devi	Punjabi Suffi Kav te Bir Kav Hoyea Khoj Kara]
4	M.A.Punjabi-II, Sem-III	222306	5106	Sakshi Sharma	Punjabi Suffi Kav te Bir Kav Hoyea Khoj Kara]
5	M.A.Punjabi-II, Sem-III	222307	5107	Shifali	Punjabi Suffi Kav te Bir Kav Hoyea Khoj Kara]
6	M.A.Punjabi-II, Sem-III	222308	5108	Randeep Kaur	Punjabi Suffi Kav te Bir Kav Hoyea Khoj Kara]
7	M.A.Punjabi-II, Sem-III	222309	5109	Ravita Rani	Punjabi Suffi Kav te Bir Kav Hoyea Khoj Kara]
8	M.A.Punjabi-II, Sem-III	222310	5110	Ramandeep Kaur	Punjabi Suffi Kav te Bir Kav Hoyea Khoj Kara]

  
 Head  
 P.G. Department of Punjabi  
 SGTB Khalsa College  
 In Amritsar Sarai



9	M.A.Punjabi-II, Sem-III	222311	5111	Gurpreet Kaur	Punjabi Suffi Kav te Bir Kav Hoyea Khoj Kara)
10	M.A.Punjabi-II, Sem-III	222315	5112	Kulwinder Kaur	Punjabi Suffi Kav te Bir Kav Hoyea Khoj Kara)
11	M.A.Punjabi-II, Sem-III	222316	5113	Gurmeet Kaur	Punjabi Suffi Kav te Bir Kav Hoyea Khoj Kara)
12	M.A.Punjabi-II, Sem-III	222317	5114	Poonam	Punjabi Suffi Kav te Bir Kav Hoyea Khoj Kara)
13	M.A.Punjabi-II, Sem-III	222323	5115	Shivani	Punjabi Suffi Kav te Bir Kav Hoyea Khoj Kara)
14	M.A.Punjabi-II, Sem-III	222313	5118	Harmandeep Singh	Punjabi Suffi Kav te Bir Kav Hoyea Khoj Kara)

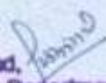
Head,  
P.G. Department of Punjabi  
SGTB Khalsa College  
Sri Anandpur Sahib

Department Of Punjabi  
Session:2023-24  
Post Graduate Course  
Project Details

Sr No.	Class	Class Roll No.	University Roll No	Students Name	Project Name
1	M.A.Punjabi-II, Sem-III	222303	5103	Kiranjeet Kaur	Madhkali Punjabi Vartak te Hoyea Khoj Kara
2	M.A.Punjabi-II, Sem-III	222304	5104	Mandeep Kaur	Madhkali Punjabi Vartak te Hoyea Khoj Kara
3	M.A.Punjabi-II, Sem-III	222305	5105	Neha devi	Madhkali Punjabi Vartak te Hoyea Khoj Kara
4	M.A.Punjabi-II, Sem-III	222306	5106	Sakshi Sharma	Madhkali Punjabi Vartak te Hoyea Khoj Kara
5	M.A.Punjabi-II, Sem-III	222307	5107	Shifali	Madhkali Punjabi Vartak te Hoyea Khoj Kara
6	M.A.Punjabi-II, Sem-III	222308	5108	Randeep Kaur	Madhkali Punjabi Vartak te Hoyea Khoj Kara
7	M.A.Punjabi-II, Sem-III	222309	5109	Ravita Rani	Madhkali Punjabi Vartak te Hoyea Khoj Kara
8	M.A.Punjabi-II, Sem-III	222310	5110	Ramandeep Kaur	Madhkali Punjabi Vartak te Hoyea Khoj Kara
9	M.A.Punjabi-II, Sem-III	222311	5111	Gurpreet Kaur	Madhkali Punjabi Vartak te Hoyea Khoj Kara
10	M.A.Punjabi-II, Sem-III	222315	5112	Kulwinder Kaur	Madhkali Punjabi Vartak te Hoyea Khoj Kara
11	M.A.Punjabi-II, Sem-III	222316	5113	Gurmeet Kaur	Madhkali Punjabi Vartak te Hoyea Khoj Kara
12	M.A.Punjabi-II, Sem-III	222317	5114	Poonam	Madhkali Punjabi Vartak te Hoyea Khoj Kara

Head,  
P.G. Department of Punjabi  
SGTB Khalsa College  
Amritsar, Punjab

13	M.A.Punjabi-II, Sem-III	222323	5115	Shivani	Madhkali Punjabi Vartak te Hoyea Khoj KaraJ
14	M.A.Punjabi-II, Sem-III	222313	5118	Harmandeep Singh	Madhkali Punjabi Vartak te Hoyea Khoj KaraJ

Head,   
P G Department of Punjabi  
SGTB Khalsa College  
Sri Anandpur Sahib

# ਸ੍ਰੀ ਗੁਰੂ ਤੇਗ ਬਹਾਦਰ ਖਾਲਸਾ, ਸੀ ਅਨੰਦਪੁਰ ਸਾਹਿਬ

(AN AUTONOMOUS COLLEGE)  
Affiliated to Punjabi University Patiala



(2023-24)

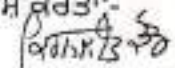
ਪ੍ਰੋਜੈਕਟ ਫਾਈਲ

ਵਿਸ਼ਾ:- ਮੱਧਕਾਲੀ ਪੰਜਾਬੀ ਵਾਰਤਕ ਉੱਤੇ ਹੋਇਆ ਖੋਜ ਕਾਰਜ।



ਪ੍ਰਾਪਤ ਕਰਤਾ:-

ਪ੍ਰੋ. ਸੁਖਵਿੰਦਰ ਸਿੰਘ

ਪੇਸ਼ ਕਰਤਾ:-  
  
ਕਿਰਨਜੀਤ ਬੈਰ

ਐਮ.ਏ ਪੰਜਾਬੀ,  
ਸਮੇਸਟਰ-III

ਫੋਨ ਨੰ.-222303



ਸ੍ਰੀ ਗੁਰੂ ਤੇਗ ਬਹਾਦਰ ਖਾਲਸਾ, ਸੀ ਅਨੰਦਪੁਰ ਸਾਹਿਬ

(AN AUTONOMOUS COLLEGE)  
Affiliated to Punjabi University Patiala



(2023-24)

ਪ੍ਰੋਜੈਕਟ ਫਾਈਲ

ਵਿਸ਼ਾ:- ਮੱਧਕਾਲੀ ਪੰਜਾਬੀ ਵਾਰਤਕ ਉੱਤੇ ਹੋਇਆ ਖੋਜ ਕਾਰਜ।

ਪ੍ਰਾਪਤ ਕਰਤਾ:-

ਪ੍ਰੋ. ਸੁਖਵਿੰਦਰ ਸਿੰਘ

ਪੇਸ਼ ਕਰਤਾ:-  
ਮਾਏਪਾ ਕੌਰ  
ਮਨਦੀਪ ਕੌਰ

ਐਮ.ਏ ਪੰਜਾਬੀ,  
ਸਮੈਸਟਰ-III

ਚੈਲ ਨੰ.-222304



ਸ੍ਰੀ ਗੁਰੂ ਤੇਗ ਬਹਾਦਰ ਖਾਲਸਾ, ਸੀ ਅਨੰਦਪੁਰ ਸਾਹਿਬ

(AN AUTONOMOUS COLLEGE)  
Affiliated to Punjabi University Patiala



(2023-24)

ਪ੍ਰੋਜੈਕਟ ਫਾਈਲ

ਵਿਸ਼ਾ:- ਮੱਧਕਾਲੀ ਪੰਜਾਬੀ ਵਾਰਤਕ ਉੱਤੇ ਹੋਇਆ ਖੋਜ ਕਾਰਜ।

ਪ੍ਰਾਪਤ ਕਰਤਾ:-

ਪ੍ਰੋ.ਸੁਖਵਿੰਦਰ ਸਿੰਘ

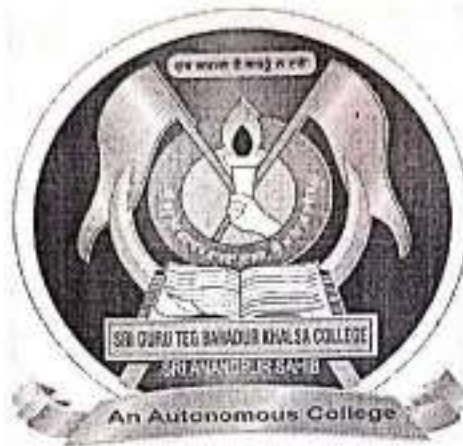
ਪੇਸ਼ ਕਰਤਾ:-  
ਨੇਹਾ ਦੇਵੀ

ਐਮ.ਏ ਪੰਜਾਬੀ,  
ਸਮੇਸਟਰ-III

ਰੋਲ ਨੰ.-222305

ਸ੍ਰੀ ਗੁਰੂ ਤੇਗ ਬਹਾਦਰ ਖਾਲਸਾ, ਸੀ ਅਨੰਦਪੁਰ ਸਾਹਿਬ

(AN AUTONOMOUS COLLEGE)  
Affiliated to Punjabi University Patiala



(2023-24)

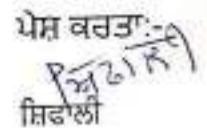
ਪ੍ਰੋਜੈਕਟ ਫਾਈਲ

ਵਿਸ਼ਾ:- ਮੱਧਕਾਲੀ ਪੰਜਾਬੀ ਵਾਰਤਕ ਉੱਤੇ ਹੋਇਆ ਖੋਜ ਕਾਰਜ।



ਪ੍ਰਾਪਤ ਕਰਤਾ:-

ਪ੍ਰੋ. ਸੁਖਵਿੰਦਰ ਸਿੰਘ

ਪੇਸ਼ ਕਰਤਾ:-  
  
ਸਿਫਾਲੀ

ਐਮ.ਏ ਪੰਜਾਬੀ,  
ਸਮੇਸਟਰ-III

ਰੋਲ ਨੰ.-222307

ਸ੍ਰੀ ਗੁਰੂ ਤੇਗ ਬਹਾਦਰ ਖਾਲਸਾ, ਸੀ ਅਨੰਦਪੁਰ ਸਾਹਿਬ


(AN AUTONOMOUS COLLEGE)  
Affiliated to Punjabi University Patiala



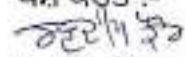
(2023-24)

ਪ੍ਰੋਜੈਕਟ ਫਾਈਲ

ਵਿਸ਼ਾ:- ਮੱਧਕਾਲੀ ਪੰਜਾਬੀ ਵਾਰਤਕ ਉੱਤੇ ਹੋਇਆ ਖੋਜ ਕਾਰਜ।

  
ਪ੍ਰਾਪਤ ਕਰਤਾ:-

ਪ੍ਰੋ. ਸੁਖਵਿੰਦਰ ਸਿੰਘ

ਪੇਸ਼ ਕਰਤਾ:-  
  
ਰਣਦੀਪ ਕੌਰ

ਐੱਮ.ਏ ਪੰਜਾਬੀ,  
ਸਮੇਸਟਰ-III

ਚੈਲ ਨੰ.-222308

ਸ੍ਰੀ ਗੁਰੂ ਤੇਗ ਬਹਾਦਰ ਖਾਲਸਾ, ਸੀ ਅਨੰਦਪੁਰ ਸਾਹਿਬ

(AN AUTONOMOUS COLLEGE)  
Affiliated to Punjabi University Patiala



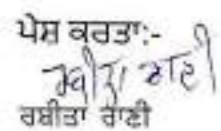
(2023-24)

ਪ੍ਰੋਜੈਕਟ ਫਾਈਲ

ਵਿਸ਼ਾ:- ਮੱਧਕਾਲੀ ਪੰਜਾਬੀ ਵਾਰਤਕ ਉੱਤੇ ਹੋਇਆ ਖੋਜ ਕਾਰਜ।

  
ਪ੍ਰਾਪਤ ਕਰਤਾ:-

ਪ੍ਰੋ. ਸੁਖਵਿੰਦਰ ਸਿੰਘ

ਪੇਸ਼ ਕਰਤਾ:-  
  
ਰਬੀਤਾ ਰਾਣੀ

ਐਮ.ਏ ਪੰਜਾਬੀ,  
ਸਮੈਸਟਰ-III

ਰੋਲ ਨੰ.-222309

# ਸ੍ਰੀ ਗੁਰੂ ਤੇਗ ਬਹਾਦਰ ਖਾਲਸਾ, ਸੀ ਅਨੰਦਪੁਰ ਸਾਹਿਬ

(AN AUTONOMOUS COLLEGE)  
Affiliated to Punjabi University Patiala



(2023-24)

ਪ੍ਰੋਜੈਕਟ ਫਾਈਲ

ਵਿਸ਼ਾ:- ਮੱਧਕਾਲੀ ਪੰਜਾਬੀ ਵਾਰਤਕ ਉੱਤੇ ਹੋਇਆ ਖੋਜ ਕਾਰਜ।

  
ਪ੍ਰਾਪਤ ਕਰਤਾ:-

ਪ੍ਰੋ. ਸੁਖਵਿੰਦਰ ਸਿੰਘ

ਪੇਸ਼ ਕਰਤਾ:-  
ਡਾ. ਅਮਰਿੰਦਰ ਕੌਰ  
ਚਮਨਦੀਪ ਕੌਰ

ਐਮ.ਏ ਪੰਜਾਬੀ,  
ਸਮੇਸਟਰ-III

ਰੋਲ ਨੰ.-222310



# ਸ੍ਰੀ ਗੁਰੂ ਤੇਗ ਬਹਾਦਰ ਖਾਲਸਾ, ਸੀ ਅਨੰਦਪੁਰ ਸਾਹਿਬ

(AN AUTONOMOUS COLLEGE)  
Affiliated to Punjabi University Patiala



(2023-24)

ਪ੍ਰੋਜੈਕਟ ਫਾਈਲ

ਵਿਸ਼ਾ:- ਮੱਧਕਾਲੀ ਪੰਜਾਬੀ ਵਾਰਤਕ ਉੱਤੇ ਹੋਇਆ ਖੋਜ ਕਾਰਜ।



ਪ੍ਰਾਪਤ ਕਰਤਾ:-

ਪ੍ਰੋ. ਸੁਖਵਿੰਦਰ ਸਿੰਘ

ਪੇਸ਼ ਕਰਤਾ:-

ਗੁਰਪ੍ਰੀਤ ਸੈਣੀ

ਐਮ.ਏ ਪੰਜਾਬੀ,  
ਸਮੇਸਟਰ-III

ਰੋਲ ਨੰ.-222311

ਸ੍ਰੀ ਗੁਰੂ ਤੇਗ ਬਹਾਦਰ ਖਾਲਸਾ, ਸੀ ਅਨੰਦਪੁਰ ਸਾਹਿਬ


(AN AUTONOMOUS COLLEGE)  
Affiliated to Punjabi University Patiala



(2023-24)

ਪ੍ਰੋਜੈਕਟ ਫਾਈਲ

ਵਿਸ਼ਾ:- ਮੱਧਕਾਲੀ ਪੰਜਾਬੀ ਵਾਰਤਕ ਉੱਤੇ ਹੋਇਆ ਖੋਜ ਕਾਰਜ।

  
ਪ੍ਰਮਾਤ ਕਰਤਾ:-

ਪ੍ਰੋ. ਸੁਖਵਿੰਦਰ ਸਿੰਘ

ਪੇਸ਼ ਕਰਤਾ:-

  
ਹਰਮਨਦੀਪ ਸਿੰਘ

ਐੱਮ.ਏ ਪੰਜਾਬੀ,  
ਸਮੇਸਟਰ-III

ਰੋਲ ਨੰ.-222313

ਸ੍ਰੀ ਗੁਰੂ ਤੇਗ ਬਹਾਦਰ ਖਾਲਸਾ, ਸੀ ਅਨੰਦਪੁਰ ਸਾਹਿਬ

(AN AUTONOMOUS COLLEGE)  
Affiliated to Punjabi University Patiala



(2023-24)

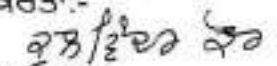
ਪ੍ਰੋਜੈਕਟ ਫਾਈਲ

ਵਿਸ਼ਾ:- ਮੱਧਕਾਲੀ ਪੰਜਾਬੀ ਵਾਰਤਕ ਉੱਤੇ ਹੋਇਆ ਖੋਜ ਕਾਰਜ।

  
ਪ੍ਰਾਪਤ ਕਰਤਾ:-

ਪ੍ਰੋ. ਸੁਖਵਿੰਦਰ ਸਿੰਘ

ਪੇਸ਼ ਕਰਤਾ:-

  
ਕੁਲਵਿੰਦਰ ਕੌਰ

ਐਮ.ਏ ਪੰਜਾਬੀ,  
ਸਮੈਸਟਰ-III

ਰੋਲ ਨੰ.-222315

ਸ੍ਰੀ ਗੁਰੂ ਤੇਗ ਬਹਾਦਰ ਖਾਲਸਾ, ਸੀ ਅਨੰਦਪੁਰ ਸਾਹਿਬ

(AN AUTONOMOUS COLLEGE)  
Affiliated to Punjabi University Patiala



(2023-24)

ਪ੍ਰੋਜੈਕਟ ਫਾਈਲ

ਵਿਸ਼ਾ:- ਮੱਧਕਾਲੀ ਪੰਜਾਬੀ ਵਾਰਤਕ ਉੱਤੇ ਹੋਇਆ ਖੋਜ ਕਾਰਜ।

ਪ੍ਰਾਪਤ ਕਰਤਾ:-

ਪ੍ਰੋ. ਸੁਖਵਿੰਦਰ ਸਿੰਘ

ਪੇਸ਼ ਕਰਤਾ:-

*Lymanat Kaur*  
ਗੁਰਮੀਤ ਕੌਰ

ਐੱਮ.ਏ ਪੰਜਾਬੀ,  
ਸਮੇਸਟਰ-III

ਰੋਲ ਨੰ.-222316

ਸ੍ਰੀ ਗੁਰੂ ਤੇਗ ਬਹਾਦਰ ਖਾਲਸਾ, ਸੀ ਅਨੰਦਪੁਰ ਸਾਹਿਬ


(AN AUTONOMOUS COLLEGE)  
Affiliated to Punjabi University Patiala



(2023-24)

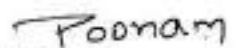
ਪ੍ਰੋਜੈਕਟ ਫਾਈਲ

ਵਿਸ਼ਾ:- ਮੱਧਕਾਲੀ ਪੰਜਾਬੀ ਵਾਰਤਕ ਉੱਤੇ ਹੋਇਆ ਖੋਜ ਕਾਰਜ।

  
ਪ੍ਰਾਪਤ ਕਰਤਾ:-

ਪ੍ਰੋ. ਸੁਖਵਿੰਦਰ ਸਿੰਘ

ਪੇਸ਼ ਕਰਤਾ:-

  
ਪੂਨਮ

ਐਮ.ਏ ਪੰਜਾਬੀ,  
ਸਮੇਸਟਰ-III

ਰੋਲ ਨੰ.-222317



ਸ੍ਰੀ ਗੁਰੂ ਤੇਗ ਬਹਾਦਰ ਖਾਲਸਾ, ਸੀ ਅਨੰਦਪੁਰ ਸਾਹਿਬ

(AN AUTONOMOUS COLLEGE)  
Affiliated to Punjabi University Patiala



(2023-24)

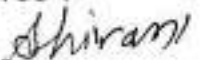
ਪ੍ਰੋਜੈਕਟ ਫਾਈਲ

ਵਿਸ਼ਾ:- ਮੱਧਕਾਲੀ ਪੰਜਾਬੀ ਵਾਰਤਕ ਉੱਤੇ ਹੋਇਆ ਖੋਜ ਕਾਰਜ।

  
ਪ੍ਰਾਪਤ ਕਰਤਾ:-

ਪ੍ਰੋ. ਸੁਖਵਿੰਦਰ ਸਿੰਘ

ਪੇਸ਼ ਕਰਤਾ:-

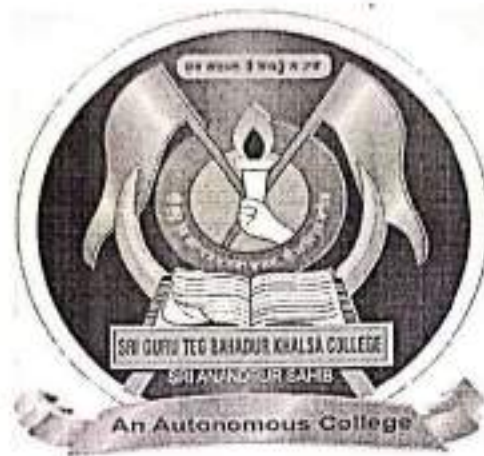
  
ਸ਼ਿਵਾਨੀ

ਐੱਮ.ਏ ਪੰਜਾਬੀ,  
ਸਮੈਸਟਰ-III

ਰੋਲ ਨੰ.-222323

ਸ੍ਰੀ ਗੁਰੂ ਤੇਗ ਬਹਾਦਰ ਖਾਲਸਾ, ਸੀ ਅਨੰਦਪੁਰ ਸਾਹਿਬ

(AN AUTONOMOUS COLLEGE)  
Affiliated to Punjabi University Patiala



(2023-24)

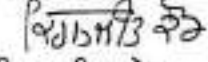
ਪ੍ਰੋਜੈਕਟ ਫਾਈਲ

ਵਿਸ਼ਾ:- ਪੰਜਾਬੀ ਸੂਫੀ ਅਤੇ ਵੀਰ ਕਾਵਿ ਉੱਤੇ ਹੋਇਆ ਖੋਜ ਕਾਰਜ।

ਪ੍ਰਾਪਤ ਕਰਤਾ:-

  
ਭਾ.ਗੁਰਪ੍ਰੀਤ ਕੌਰ

ਪੇਸ਼ ਕਰਤਾ:-

  
ਕਿਰਨਜੀਤ ਕੌਰ

ਐਮ.ਏ ਪੰਜਾਬੀ,  
ਸਮੇਸਟਰ-III

ਫੋਨ ਨੰ.-222303

ਸ੍ਰੀ ਗੁਰੂ ਤੇਗ ਬਹਾਦਰ ਖਾਲਸਾ, ਸੀ ਅਨੰਦਪੁਰ ਸਾਹਿਬ

(AN AUTONOMOUS COLLEGE)  
Affiliated to Punjabi University Patiala



(2023-24)

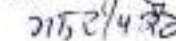
ਪ੍ਰੋਜੈਕਟ ਫਾਈਲ

ਵਿਸ਼ਾ:- ਪੰਜਾਬੀ ਸੂਫੀ ਅਤੇ ਵੀਰ ਕਾਵਿ ਉੱਤੇ ਹੋਇਆ ਖੋਜ ਕਾਰਜ।

ਪ੍ਰਾਪਤ ਕਰਤਾ:-

  
ਡਾ. ਗੁਰਪ੍ਰੀਤ ਕੌਰ

ਪੇਸ਼ ਕਰਤਾ:-

  
ਮਨਦੀਪ ਕੌਰ

ਐਮ.ਏ ਪੰਜਾਬੀ,  
ਸੈਸਟਰ-III

ਰੋਲ ਨੰ.-222304

ਸ੍ਰੀ ਗੁਰੂ ਤੇਗ ਬਹਾਦਰ ਖਾਲਸਾ, ਸੀ ਅਨੰਦਪੁਰ ਸਾਹਿਬ

(AN AUTONOMOUS COLLEGE)  
Affiliated to Punjabi University Patiala



(2023-24)

ਪ੍ਰੋਜੈਕਟ ਫਾਈਲ

ਵਿਸ਼ਾ:- ਪੰਜਾਬੀ ਸੂਫੀ ਅਤੇ ਵੀਰ ਕਾਵਿ ਉੱਤੇ ਹੋਇਆ ਖੋਜ ਕਾਰਜ।

ਪ੍ਰਾਪਤ ਕਰਤਾ:-

ਡਾ. ਗੁਰਪ੍ਰੀਤ ਕੌਰ

ਪੇਸ਼ ਕਰਤਾ:-

ਰਮਨਦੀਪ ਕੌਰ  
ਰਮਨਦੀਪ ਕੌਰ

ਐਮ.ਏ ਪੰਜਾਬੀ,  
ਸਮੇਸਟਰ-III

ਰੋਲ ਨੰ.-222310

ਸ੍ਰੀ ਗੁਰੂ ਤੇਗ ਬਹਾਦਰ ਖਾਲਸਾ, ਸੀ ਅਨੰਦਪੁਰ ਸਾਹਿਬ

(AN AUTONOMOUS COLLEGE)  
Affiliated to Punjabi University Patiala



(2023-24)

ਪ੍ਰੋਜੈਕਟ ਫਾਈਲ

ਵਿਸ਼ਾ:- ਪੰਜਾਬੀ ਸੂਫੀ ਅਤੇ ਵੀਰ ਕਾਵਿ ਉੱਤੇ ਹੋਇਆ ਖੋਜ ਕਾਰਜ।

ਪ੍ਰਾਪਤ ਕਰਤਾ:-

ਡਾ. ਗੁਰਪ੍ਰੀਤ ਕੌਰ

ਪੇਸ਼ ਕਰਤਾ:-

ਗੁਰਪ੍ਰੀਤ ਸੈਣੀ

ਐਮ.ਏ ਪੰਜਾਬੀ,  
ਸਮੇਸਟਰ-III

ਚੈਲ ਨੰ.-222311



ਸ੍ਰੀ ਗੁਰੂ ਤੇਗ ਬਹਾਦਰ ਖਾਲਸਾ, ਸੀ ਅਨੰਦਪੁਰ ਸਾਹਿਬ

(AN AUTONOMOUS COLLEGE)  
Affiliated to Punjabi University Patiala



(2023-24)

ਪ੍ਰੋਜੈਕਟ ਫਾਈਲ

ਵਿਸ਼ਾ:- ਪੰਜਾਬੀ ਸੂਫੀ ਅਤੇ ਵੀਰ ਕਾਵਿ ਉੱਤੇ ਹੋਇਆ ਖੋਜ ਕਾਰਜ।

ਪ੍ਰਾਪਤ ਕਰਤਾ:-

ਡਾ. ਗੁਰਪ੍ਰੀਤ ਕੌਰ

ਪੇਸ਼ ਕਰਤਾ:-

ਨੇਹਾ ਦੇਵੀ

ਐੱਮ.ਏ ਪੰਜਾਬੀ,  
ਸਮੈਸਟਰ-III

ਰੋਲ ਨੰ.-222305

ਸ੍ਰੀ ਗੁਰੂ ਤੇਗ ਬਹਾਦਰ ਖਾਲਸਾ, ਸੀ ਅਨੰਦਪੁਰ ਸਾਹਿਬ

(AN AUTONOMOUS COLLEGE)  
Affiliated to Punjabi University Patiala



(2023-24)

ਪ੍ਰੋਜੈਕਟ ਫਾਈਲ

ਵਿਸ਼ਾ:- ਪੰਜਾਬੀ ਸੂਫੀ ਅਤੇ ਵੀਰ ਕਾਵਿ ਉੱਤੇ ਹੋਇਆ ਖੋਜ ਕਾਰਜ।

ਪ੍ਰਾਪਤ ਕਰਤਾ:-

*lib*  
ਡਾ. ਗੁਰਪ੍ਰੀਤ ਕੌਰ

ਪੇਸ਼ ਕਰਤਾ:-  
*ਸ਼ਿਵਾਨੀ*  
ਸ਼ਿਵਾਨੀ

ਐਮ.ਏ ਪੰਜਾਬੀ,  
ਸਮੇਸਟਰ-III

ਰੋਲ ਨੰ.-222307

ਸ੍ਰੀ ਗੁਰੂ ਤੇਗ ਬਹਾਦਰ ਖਾਲਸਾ, ਸੀ ਅਨੰਦਪੁਰ ਸਾਹਿਬ

(AN AUTONOMOUS COLLEGE)  
Affiliated to Punjabi University Patiala



(2023-24)

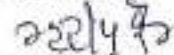
ਪ੍ਰੋਜੈਕਟ ਫਾਈਲ

ਵਿਸ਼ਾ:- ਪੰਜਾਬੀ ਸੂਫੀ ਅਤੇ ਵੀਰ ਕਾਵਿ ਉੱਤੇ ਹੋਇਆ ਖੋਜ ਕਾਰਜ।

ਪ੍ਰਾਪਤ ਕਰਤਾ:-

  
ਡਾ. ਗੁਰਪ੍ਰੀਤ ਕੌਰ

ਪੇਸ਼ ਕਰਤਾ:-

  
ਰਣਦੀਪ ਕੌਰ

ਐਮ.ਏ ਪੰਜਾਬੀ,  
ਸਸੇਸਟਰ-III

ਰੋਲ ਨੰ.-222308

ਸ੍ਰੀ ਗੁਰੂ ਤੇਗ ਬਹਾਦਰ ਖਾਲਸਾ, ਸੀ ਅਨੰਦਪੁਰ ਸਾਹਿਬ

(AN AUTONOMOUS COLLEGE)  
Affiliated to Punjabi University Patiala



(2023-24)

ਪ੍ਰੋਜੈਕਟ ਫਾਈਲ

ਵਿਸ਼ਾ:- ਪੰਜਾਬੀ ਸੂਫੀ ਅਤੇ ਵੀਰ ਕਾਵਿ ਉੱਤੇ ਹੋਇਆ ਖੋਜ ਕਾਰਜ।

ਪ੍ਰਾਪਤ ਕਰਤਾ:-

ਡਾ. ਗੁਰਪ੍ਰੀਤ ਕੌਰ

ਪੇਸ਼ ਕਰਤਾ:-

ਸ਼੍ਰੀਮਤੀ ਰਾਣੀ  
ਰਬੀਤਾ ਰਾਣੀ

ਐਮ.ਏ ਪੰਜਾਬੀ,  
ਸਮੇਸਟਰ-III

ਫੋਲ ਨੰ.-222309

ਸ੍ਰੀ ਗੁਰੂ ਤੇਗ ਬਹਾਦਰ ਖਾਲਸਾ, ਸੀ ਅਨੰਦਪੁਰ ਸਾਹਿਬ

(AN AUTONOMOUS COLLEGE)  
Affiliated to Punjabi University Patiala



(2023-24)

ਪ੍ਰੋਜੈਕਟ ਫਾਈਲ

ਵਿਸ਼ਾ:- ਪੰਜਾਬੀ ਸੂਫੀ ਅਤੇ ਵੀਰ ਕਾਵਿ ਉੱਤੇ ਹੋਇਆ ਖੋਜ ਕਾਰਜ।

ਪ੍ਰਾਪਤ ਕਰਤਾ:-  
*hbw*  
ਡਾ.ਗੁਰਪ੍ਰੀਤ ਕੌਰ

ਪੇਸ਼ ਕਰਤਾ:-  
*Harmandeep Singh*  
ਹਰਮਨਦੀਪ ਸਿੰਘ

ਐਮ.ਏ ਪੰਜਾਬੀ,  
ਸੈਮੇਸਟਰ-III

ਰੋਲ ਨੰ.-222313



ਸ੍ਰੀ ਗੁਰੂ ਤੇਗ ਬਹਾਦਰ ਖਾਲਸਾ, ਸੀ ਅਨੰਦਪੁਰ ਸਾਹਿਬ

(AN AUTONOMOUS COLLEGE)  
Affiliated to Punjabi University Patiala



(2023-24)

ਪ੍ਰੋਜੈਕਟ ਫਾਈਲ

ਵਿਸ਼ਾ:- ਪੰਜਾਬੀ ਸੂਫੀ ਅਤੇ ਵੀਰ ਕਾਵਿ ਉੱਤੇ ਹੋਇਆ ਖੋਜ ਕਾਰਜ।

ਪ੍ਰਾਪਤ ਕਰਤਾ:-

  
ਡਾ. ਗੁਰਪ੍ਰੀਤ ਕੌਰ

ਪੇਸ਼ ਕਰਤਾ:-

ਕੁਲਵਿਦ ਕੌਰ  
ਕੁਲਵਿਦ ਕੌਰ

ਐਮ.ਏ ਪੰਜਾਬੀ,  
ਸਮੈਸਟਰ-III

ਰੋਲ ਨੰ.-222315

ਸ੍ਰੀ ਗੁਰੂ ਤੇਗ ਬਹਾਦਰ ਖਾਲਸਾ, ਸੀ ਅਨੰਦਪੁਰ ਸਾਹਿਬ

(AN AUTONOMOUS COLLEGE)  
Affiliated to Punjabi University Patiala



(2023-24)

ਪ੍ਰੋਜੈਕਟ ਫਾਈਲ

ਵਿਸ਼ਾ:- ਪੰਜਾਬੀ ਸੂਫੀ ਅਤੇ ਵੀਰ ਕਾਵਿ ਉੱਤੇ ਹੋਇਆ ਖੋਜ ਕਾਰਜ।

ਪ੍ਰਾਪਤ ਕਰਤਾ:-

ਡਾ. ਗੁਰਪ੍ਰੀਤ ਕੌਰ

ਪੇਸ਼ ਕਰਤਾ:-

Gurmeet Kaur  
ਗੁਰਮੀਤ ਕੌਰ

ਐਮ.ਏ ਪੰਜਾਬੀ,  
ਸਮੇਸਟਰ-III

ਰੋਲ ਨੰ.-222316

ਸ੍ਰੀ ਗੁਰੂ ਤੇਗ ਬਹਾਦਰ ਖਾਲਸਾ, ਸੀ ਅਨੰਦਪੁਰ ਸਾਹਿਬ

(AN AUTONOMOUS COLLEGE)  
Affiliated to Punjabi University Patiala



(2023-24)

ਪ੍ਰੋਜੈਕਟ ਫਾਈਲ

ਵਿਸ਼ਾ:- ਪੰਜਾਬੀ ਸੂਫੀ ਅਤੇ ਵੀਰ ਕਾਵਿ ਉੱਤੇ ਹੋਇਆ ਖੋਜ ਕਾਰਜ।

ਪ੍ਰਾਪਤ ਕਰਤਾ:-

ਡਾ. ਗੁਰਪ੍ਰੀਤ ਕੌਰ

ਪੇਸ਼ ਕਰਤਾ:-

Poonam  
ਪੂਨਮ

ਐਮ.ਏ ਪੰਜਾਬੀ,  
ਸਮੇਸਟਰ-III

ਰੋਲ ਨੰ.-222317

ਸ੍ਰੀ ਗੁਰੂ ਤੇਗ ਬਹਾਦਰ ਖਾਲਸਾ, ਸੀ ਅਨੰਦਪੁਰ ਸਾਹਿਬ

(AN AUTONOMOUS COLLEGE)  
Affiliated to Punjabi University Patiala



(2023-24)

ਪ੍ਰੋਜੈਕਟ ਫਾਈਲ

ਵਿਸ਼ਾ:- ਪੰਜਾਬੀ ਸੂਫੀ ਅਤੇ ਵੀਰ ਕਾਵਿ ਉੱਤੇ ਹੋਇਆ ਖੋਜ ਕਾਰਜ।

ਪ੍ਰਾਪਤ ਕਰਤਾ:-

  
ਡਾ. ਗੁਰਪ੍ਰੀਤ ਕੌਰ

ਪੇਸ਼ ਕਰਤਾ:-

  
ਸ਼ਿਵਾਨੀ

ਐਮ.ਏ ਪੰਜਾਬੀ,  
ਸਮੇਸਟਰ-III

ਚੇਲ ਨੰ.-222323




Session → 2023-24  
B.Sc. (Hons.) Agriculture Sem - VII  
 Detail of students undertaking Internship

Sr. No	Name	University Roll No.
1	RAVNEET KAUR	551
2	MANDEEP KAUR	552
3	DALJEET KAUR	553
4	SIMRANDEEP KAUR	554
5	JASMEEN KAUR	555
6	NANCY SHARMA	556
7	POOJA RANI	557
8	JASVIR KAUR	558
9	AKANKSHA DEVI	560
10	VISHALI CHANDEL	561
11	SIMRAN	562
12	NAINA SHARMA	563
13	KOMAL SHARMA	564
14	RITIKA	565
15	PRIYANKA	566
16	SHILPA KUMARI	567
17	RISHIKA KAUSHAL	568
18	SANDEEP KAUR	569
19	RIYA	570
20	TANJOT SINGH	572
21	RATINDER SINGH	573
22	JASHMEET SINGH	574
23	NARAYAN SHARMA	580
24	MOHIT KUMAR	581
25	ARYAN AERY	582
26	VARUN	583
27	ABHISHEK BHARDWAJ	584
28	GURPREET SINGH	585
29	NITISH THAKUR	586
30	SHAMA SAINI	587
31	ANSHUL SHARMA	588
32	AJAY KUMAR	589
33	Shivam Banyal	590



34	PAWAN KUMAR	591
35	PARWINDER KUMAR	592
36	SOURAV DHIMAN	593
37	HARMAN SAINI	596
38	HARDEEP KUMAR	598
39	HARPREET SINGH	599
40	AJAY KUMAR	600
41	RAMAN	601
42	KANCHAN RANA	602
43	NIKHIL CHAUDHARY	604
44	HARSH RANA	594

  
 Head,  
 Department of Agriculture  
 SGTB Khimri College  
 Sri Anandpur Sahib


NO. RMU/ADMN/ 11673

DATED: 01/12/2023

TO WHOM IT MAY CONCERN

It is to certify that **Ms. Ravneet Kaur D/o Sh. Balwinder Singh**, Roll No. 200801 student of B.Sc. Agriculture (Hons.), Sri Guru Teg Bhadur Khalsa Collage, Sri Anandpur Sahib, Ropar (PB.) has undergone in-plant training in Quality Assurance and Production Section at Verka Mohali Dairy.

During the training period from 01.11.2023 to 30.11.2023 her performance has been adjudged as 'Good'.

  
IN-CHARGE (ADMN)  
VERKA MOHALI DAIRY





An ISO 9001:2015 Fax/Phone : 0172-2273247 Plant GST No  
E Mail : Mohali.agro@markfedpunjab.com 03AAAAAT3454G2Z5  
Website : [www.markfedpunjab.com](http://www.markfedpunjab.com)  
MARKFED AGRO CHEMICALS  
7 & 8-B, INDL. ESTATE, S.A.S.NAGAR, 160055,  
DISTT. S.A.S.NAGAR (PUNJAB)

No.MACM/EST/2023/ 1605

Dated: 2/12/2023

**TO WHOM SO EVER IT MAY CONCERN**

It is certified that Mandeep Kaur D/o Sh. Sher Singh of BSc Agriculture (Hons.) Roll No. 200812 of Shri Guru Teg Bahadur Khalsa College, Sri Anandpur Sahib has successfully completed her Industrial training w.e.f 03.11.2023 to 02-12.2023 in Markfed Agro Chemicals, Mohali.

Her work and conduct during training period is found satisfactory. We wish her all the success for her future.

(S.S. Bajwa )  
Supdt.

Markfed Agro Chemicals,  
S.A.S Nagar (Mohali)

**Sarbjit Singh Bajwa**  
Superintendent  
Markfed Agro Chemical  
Mohali.

An ISO 9001:2015 Fax/Phone: 0172-2273247

E Mail : Mohali.agro@markfedpunjab.com

Website : [www.markfedpunjab.com](http://www.markfedpunjab.com)

Plant GST No  
03AAAAT3454G225



MARKFED AGRO CHEMICALS  
7 & 8-B, INDL. ESTATE, S.A.S.NAGAR, 160055,  
DISTT. S.A.S.NAGAR (PUNJAB)


No. MACM/EST/2023/ 1604

Dated: 2/12/2023

**TO WHOM SO EVER IT MAY CONCERN**

It is certified that Daljeet Kaur D/o Sh. Jaswant Singh of BSc Agriculture (Hons.) Roll No. 200813 of Shri Guru Teg Bahadur Khalsa College, Sri Anandpur Sahib has successfully completed her Industrial training w.e.f 03.11.2023 to 02-12.2023 in Markfed Agro Chemicals, Mohali.

Her work and conduct during training period is found satisfactory. We wish her all the success for her future.

  
(S.S. Bajwa )  
Supdt.

Markfed Agro Chemicals,  
S.A.S Nagar (Mohali)

Sarbjit Singh Bajwa  
Superintendent  
Markfed Agro Chemical  
Mohali.


NO. RMU/ADMN/ 11677

DATED: 01/12/2023

**TO WHOM IT MAY CONCERN**

It is to certify that **Ms. Simrandeep Kaur D/o Sh. Jagtar Singh**, Roll No. 200814 student of B.Sc. Agriculture (Hons.), Sri Guru Teg Bhadur Khalsa Collage, Sri Anandpur Sahib, Ropar (PB.) has undergone in-plant training in Quality Assurance and Production Section at Verka Mohali Dairy.

During the training period from **01.11.2023** to **30.11.2023** her performance has been adjudged as 'Good'.

  
**IN-CHARGE (ADMN)**  
**VERKA MOHALI DAIRY**





NFL/Mktg/STL-R&D Farm/Nangal/ 762

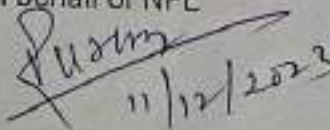
Dated: 11.12.2023

**CERTIFICATE OF TRAINING**

This is to certify that Miss Jasmeen Kaur student of B.Sc. (Hons) Agriculture of Sri Guru Teg Bahadur Khalsa College, Anandpur Sahib, (Pb) has undergone Training programme at **National Fertilizers Limited**, Naya Nangal for project work entitled on Package practices of Paddy Crop, Soil testing and R & D work at Farm. The project has been completed by the student in our company at Soil Testing Lab, Naya Nangal (Punjab) from **01.11.2023 to 30.11.2023**.

She took keen interest in her training and her conduct and performance was **excellent**. We wish her all success and bright future in her life.

For and on behalf of NFL

  
11/12/2023

(Puran Singh)  
I/c.

R&D Farm/STL, Naya Nangal  
Puran Singh  
Asst. Secy (Tech)/ AM (Mktg)  
Incharge  
Naya Nangal, N.F.L.  
R&D Farm & STL, Naya Nangal

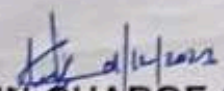
NO. RMU/ADMN/ 11 672

DATED: 01/12/2023

**TO WHOM IT MAY CONCERN**

It is to certify that **Ms. Nancy Sharma D/o Sh. Yashpaul**, Roll No. 200843 student of B.Sc. Agriculture (Hons.), Sri Guru Teg Bhadur Khalsa Collage, Sri Anandpur Sahib, Ropar (Pb.) has undergone in-plant training in Quality Assurance and Production Section at Verka Mohali Dairy.

During the training period from **01.11.2023 to 30.11.2023** her performance has been adjudged as 'Good'.

  
**IN-CHARGE (ADMN)**  
**VERKA MOHALI DAIRY**





NFL/Mktg/STL-R&D Farm/Nangal/ 761

Dated: 11.12.2023

### CERTIFICATE OF TRAINING

This is to certify that Miss Pooja Rani student of B.Sc. (Hons) Agriculture of Sri Guru Teg Bahadur Khalsa College, Anandpur Sahib, (Pb) has undergone Training programme at **National Fertilizers Limited**, Naya Nangal for project work entitled on Package practices of Paddy Crop, Soil testing and R & D work at Farm. The project has been completed by the student in our company at Soil Testing Lab, Naya Nangal (Punjab) from **01.11.2023 to 30.11.2023**.

She took keen interest in her training and her conduct and performance was **excellent**. We wish her all success and bright future in her life.

For and on behalf of NFL

*Puran Singh*  
11/12/2023

(Puran Singh)

I/c.

R&D Farm STL Naya Nangal  
Naya Nangal (Punjab) AM (M&D)  
अधीन/Incharge  
रासायनिक उर्वरक/ N.F.L.  
R&D Farm & STL Naya Nangal



NFL/Mktg/STL-R&D Farm/Nangal/ 765

Dated: 11.12.2023

### CERTIFICATE OF TRAINING

This is to certify that Miss Jasvir Kaur student of B.Sc. (Hons) Agriculture of Sri Guru Teg Bahadur Khalsa College, Anandpur Sahib, (Pb) has undergone Training programme at National Fertilizers Limited, Naya Nangal for project work entitled on Package practices of Paddy Crop, Soil testing and R & D work at Farm. The project has been completed by the student in our company at Soil Testing Lab, Naya Nangal (Punjab) from **01.11.2023 to 30.11.2023**

She took keen interest in her training and her conduct and performance was **excellent**. We wish her all success and bright future in her life.

For and on behalf of NFL

*Puran Singh*  
11/12/2023

(Puran Singh)

I / G.

R&D Farm / STL Naya Nangal

Mr. Puran Singh

Joint Secy (Agric) / AG (Mktg)

Joint / Incharge

Soil Testing Lab / NFL

At & to use of the above person for the

R&D Farm & STL Naya Nangal


NO. RMU/ADMN/ 11 675

DATED: 01/12/2023

**TO WHOM IT MAY CONCERN**

It is to certify that **Ms. Akanksha Devi D/o Sh. Sher Singh**, Roll No. 200810 student of B.Sc. Agriculture (Hons.), Sri Guru Teg Bhadur Khalsa Collage, Sri Anandpur Sahib, Ropar (PB.) has undergone in-plant training in Quality Assurance and Production Section at Verka Mohali Dairy.

During the training period from **01.11.2023 to 30.11.2023** her performance has been adjudged as '**Good**'.

  
**IN-CHARGE (ADMN)**  
**VERKA MOHALI DAIRY**







# verka

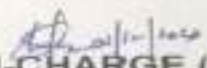
NO. RMU/ADMN/ 11674

DATED: 01/12/2023

**TO WHOM IT MAY CONCERN**

It is to certify that **Ms. Simran D/o Sh. Chain Singh**, Roll No. 200817 student of B.Sc. Agriculture (Hons.), Sri Guru Teg Bhadur Khalsa Collage, Sri Anandpur Sahib, Ropar (PB.) has undergone in-plant training in Quality Assurance and Production Section at Verka Mohali Dairy.

During the training period from **01.11.2023** to **30.11.2023** her performance has been adjudged as 'Good'.

  
**IN-CHARGE (ADMN)**  
**VERKA MOHALI DAIRY**

**THE ROPAR DISTRICT CO-OPERATIVE MILK PRODUCERS' UNION LIMITED**  
Verka Mohali Dairy, Industrial Area, Phase-VI, S.A.S. Nagar, Mohali -160 055  
PBX: 0172-2271784, 2271020, 2271021, 5039375  
Email: gm.moh@verka.coop Website: www.verka.coop  
GST No. 03AAAAT5977G1ZD



An ISO 9001:2015 Fax/Phone : 0172-2273247

E Mail : Mohali.agro@markfedpunjab.com

Website : [www.markfedpunjab.com](http://www.markfedpunjab.com)

MARKFED AGRO CHEMICALS

7 & 8-B, INDL. ESTATE, S.A.S.NAGAR, 160055,

DISTT. S.A.S.NAGAR (PUNJAB)

Plant GST No

03AAAAT3454G2Z5

No.MACM/EST/2023/ 1603

Dated: 2/12/2023

**TO WHOM SO EVER IT MAY CONCERN**

It is certified that Naina Sharma D/o Sh. Yogesh Kumar Sharma of BSc Agriculture (Hons.) Roll No. 200818 of Shri Guru Teg Bahadur Khalsa College, Sri Anandpur Sahib has successfully completed her Industrial training w.e.f 03.11.2023 to 02-12.2023 in **Markfed Agro Chemicals, Mohali.**

Her work and conduct during training period is found satisfactory. We wish her all the success for her future.

(S.S. Bajwa )

Supdt.

Markfed Agro Chemicals,  
S.A.S Nagar (Mohali)

**Sarbjit Singh Bajwa**  
Superintendent  
Markfed Agro Chemical  
Mohali.





NFL/Mktg/STL-R&D Farm/Nangal/ 764

Dated: 11.12.2023

### CERTIFICATE OF TRAINING

This is to certify that Miss Komal Sharma student of B.Sc. (Hons) Agriculture of Sri Guru Teg Bahadur Khalsa College, Anandpur Sahib, (Pb) has undergone Training programme at **National Fertilizers Limited**, Naya Nangal for project work entitled on Package practices of Paddy Crop, Soil testing and R & D work at Farm. The project has been completed by the student in our company at Soil Testing Lab, Naya Nangal (Punjab) from **01.11.2023 to 30.11.2023**.

She took keen interest in her training and her conduct and performance was **excellent**. We wish her all success and bright future in her life.

For and on behalf of NFL

(Puran Singh)

1/c

R&D Farm, STL, Naya Nangal

प्रधान/Incharge  
नया नंगल लिमिटेड, NFL  
जो & डी कार्ड पर हल परमाणु प्रयोगशाला परमाणु  
R&D Farm & STL Naya Nangal



NO. RMU/ADMN/ 11676

DATED: 01/12/2023

**TO WHOM IT MAY CONCERN**

It is to certify that **Ms. Ritika D/o Sh. Ashwani Kumar**, Roll No. 200833 student of B.Sc. Agriculture (Hons.), Sri Guru Teg Bhadur Khalsa Collage, Sri Anandpur Sahib, Ropar (PB.) has undergone in-plant training in Quality Assurance and Production Section at Verka Mohali Dairy.

During the training period from **01.11.2023 to 30.11.2023** her performance has been adjudged as '**Good**'.

  
**IN-CHARGE (ADMN)**  
**VERKA MOHALI DAIRY**





An ISO 9001:2015 Fax/Phone : 0172-2273247

E Mail : Mohali.agro@markfedpunjab.com

Website : [www.markfedpunjab.com](http://www.markfedpunjab.com)

Plant GST No  
03AAAAT3454GZZ5

MARKFED AGRO CHEMICALS

7 & 8-B, INDL. ESTATE, S.A.S.NAGAR, 160055,  
DISTT. S.A.S.NAGAR (PUNJAB)

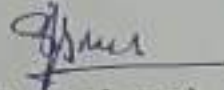
No.MACM/EST/2023/ 1602

Dated: 9/12/2023

### TO WHOM SO EVER IT MAY CONCERN

It is certified that **Priyanka D/o Sh. Devender Singh** of **BSc Agriculture (Hons.)** Roll No. **200835** of **Shri Guru Teg Bahadur Khalsa College, Sri Anandpur Sahib** has successfully completed her Industrial training w.e.f **03.11.2023** to **02-12.2023** in **Markfed Agro Chemicals, Mohali.**

Her work and conduct during training period is found satisfactory. We wish her all the success for her future.

  
(S.S. Bajwa )  
Supdt.

Markfed Agro Chemicals,  
S.A.S Nagar (Mohali)

**Sarbjit Singh Bajwa**  
Superintendent  
Markfed Agro Chemical  
Mohali.

NO. RMU/ADMN/ 11678

DATED: 01/12/2023

**TO WHOM IT MAY CONCERN**

It is to certify that **Ms. Shilpa Kumari D/o Sh. Kamal Dev Singh**, Roll No. 200839 student of B.Sc. Agriculture (Hons.), Sri Guru Teg Bhadur Khalsa Collage, Sri Anandpur Sahib, Ropar (PB.) has undergone in-plant training in Quality Assurance and Production Section at Verka Mohali Dairy.

During the training period from **01.11.2023 to 30.11.2023** her performance has been adjudged as '**Good**'.

  
**IN-CHARGE (ADMN)**  
**VERKA MOHALI DAIRY**



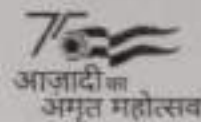
नेशनल फर्टिलाइजर्स लिमिटेड

(भारत सरकार का उपक्रम)

अधिकारिक कार्यालय : एस.सी.ओ. 76-79,

सेक्टर 17-डी, चण्डीगढ़ - 160017

दूरभाष : 0172-2703714, 2701693



NATIONAL FERTILIZERS LIMITED

(A Govt. of India Undertaking)

Zonal Office : SCO 76-79,

Sector 17-D, Chandigarh - 160017

Ph. : 0172-2703714, 2701693

NFL/Mktg/STL-R&D Farm/Nangal/ 755

Dated: 11.12.2023

### CERTIFICATE OF TRAINING

This is to certify that **Miss Rishika**, student of B.Sc. (Hons) Agriculture of Sri Guru Teg Bahadur Khalsa College, Anandpur Sahib, (Pb) has undergone Training programme at **National Fertilizers Limited**, Naya Nangal for project work entitled on Package practices of Paddy Crop, Soil testing and R & D work at Farm. The project has been completed by the student in our company at Soil Testing Lab, Naya Nangal (Punjab) from **01.11.2023 to 30.11.2023**.

She took keen interest in his training and his conduct and performance was **excellent**. We wish him all success and bright future in his life.

For and on behalf of NFL

(Puran Singh)

I/c.

R&D Farm / STL Naya Nangal





NFL/Mktg/STL-R&D Farm/Nangal/ 756

Dated: 11.12.2023

### CERTIFICATE OF TRAINING

This is to certify that Miss Sandeep Kaur student of B.Sc. (Hons) Agriculture of Sri Guru Teg Bahadur Khalsa College, Anandpur Sahib, (Pb) has undergone Training programme at **National Fertilizers Limited**, Naya Nangal for project work entitled on Package practices of Paddy Crop, Soil testing and R & D work at Farm. The project has been completed by the student in our company at Soil Testing Lab, Naya Nangal (Punjab) from **01.11.2023 to 30.11.2023**.

She took keen interest in her training and her conduct and performance was **excellent**. We wish her all success and bright future in her life.

For and on behalf of NFL

*Puran Singh*  
11/12/2023

(Puran Singh)

I/c

STL, NFL, Nangal  
R&D Farm  
Incharge  
N.F.L.  
R&D Farm & STL, Naya Nangal



NFL/Mktg/STL-R&D Farm/Nangal/ 757

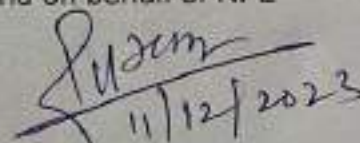
Dated: 11.12.2023

### CERTIFICATE OF TRAINING

This is to certify that Miss Riya student of B.Sc. (Hons) Agriculture of Sri Guru Teg Bahadur Khalsa College, Anandpur Sahib, (Pb) has undergone Training programme at **National Fertilizers Limited**, Naya Nangal for project work entitled on Package practices of Paddy Crop, Soil testing and R & D work at Farm. The project has been completed by the student in our company at Soil Testing Lab, Naya Nangal (Punjab) from **01.11.2023 to 30.11.2023**.

She took keen interest in her training and her conduct and performance was **excellent**. We wish her all success and bright future in her life.

For and on behalf of NFL

  
11/12/2023

(Puran Singh)

I/c.

R&D Farm / STL Naya Nangal

ਪੁਰਨ ਸਿੰਘ / Puran Singh  
ਕੰਪਨੀ ਮੈਨੇਜਰ (ਮਿਸ਼ਨ) / AM (Mktg)  
ਚਾਰਜ / Incharge  
ਨੈਸ਼ਨਲ ਫਰਟੀਲਾਈਜ਼ਰ ਲਿਮਟਿਡ / N.F.L.  
ਜਲਾ ਅਤੇ ਫੀ ਫਾਰਮ ਨਵਾ ਨੰਗਲ ਪੰਜਾਬ  
R&D Farm & STL Naya Nangal





An ISO 9001:2015 Fax/Phone: 0172-2273247

E Mail : Mohali.agro@markfedpunjab.com

Website : [www.markfedpunjab.com](http://www.markfedpunjab.com)

MARKFED AGRO CHEMICALS

7 & 8-B, INDL ESTATE, S.A.S.NAGAR, 160055,

DISTT. S.A.S.NAGAR (PUNJAB)

Plant GST No  
03AAAAT3454G225


No.MAGM/EST/2023/1599

Dated: 21/12/2023

**TO WHOM SO EVER IT MAY CONCERN**

It is certified that Tanjot Bedi S/o Sh. Gurwinder Singh Bedi of BSc Agriculture (Hons.) Roll No. 200808 of Shri Guru Teg Bahadur Khalsa College, Sri Anandpur Sahib has successfully completed his Industrial training w.e.f 03.11.2023 to 02-12.2023 in Markfed Agro Chemicals, Mohali.

His work and conduct during training period is found satisfactory. We wish him all the success for his future.

  
(S.S. Bajwa)

Supdt.

Markfed Agro Chemicals,  
S.A.S Nagar (Mohali)

Sarbjit Singh Bajwa  
Superintendent  
Markfed Agro Chemical  
Mohali.



An ISO 9001:2015 Fax/Phone : 0172-2273247

E Mail : Mohali.agro@markfedpunjab.com

Website : [www.markfedpunjab.com](http://www.markfedpunjab.com)

MARKFED AGRO CHEMICALS

7 & 8-B, INDL. ESTATE, S.A.S.NAGAR, 160055,

DISTT. S.A.S.NAGAR (PUNJAB)

Plant GST No  
03AAAAT3454G2ZS

No.MACM/EST/2023/1598

Dated: 2/12/2023

**TO WHOM SO EVER IT MAY CONCERN**

It is certified that Ratinder Singh S/o Sh. Surjit Singh of BSc Agriculture (Hons.) Roll No. 200821 of Shri Guru Teg Bahadur Khalsa College, Sri Anandpur Sahib has successfully completed his Industrial training w.e.f 03.11.2023 to 02-12.2023 in Markfed Agro Chemicals, Mohali.

His work and conduct during training period is found satisfactory. We wish him all the success for his future.

(S.S. Bajwa )

Supdt.

Markfed Agro Chemicals,

S.A.S Nagar (Mohali)

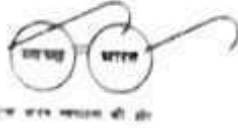
Sarbjit Singh Bajwa

Superintendent

Markfed Agro Chemical

Mohali.





नशनल फर्टिलाइजर्स लिमिटेड

(भारत सरकार का उपक्रम)

अंचलिक कार्यालय : एस.सी.ओ. 76-79,

सेक्टर 17-डी, चण्डीगढ़ - 160017

दूरभाष : 0172-2703714, 2701693



NATIONAL FERTILIZERS LIMITED

(A Govt. of India Undertaking)

Zonal Office : SCO 76-79,

Sector 17-D, Chandigarh - 160017

Ph : 0172-2703714, 2701693

NFL/Mktg/STL-R&D Farm/Nangal/ 760

Dated: 11.12.2023

### CERTIFICATE OF TRAINING

This is to certify that **Mr. Jashmeet Singh**, student of B.Sc. (Hons) Agriculture of Sri Guru Teg Bahadur Khalsa College, Anandpur Sahib, (Pb) has undergone Training programme at **National Fertilizers Limited**, Naya Nangal for project work entitled on Package practices of Paddy Crop, Soil testing and R & D work at Farm. The project has been completed by the student in our company at Soil Testing Lab, Naya Nangal (Punjab) from **01.11.2023 to 30.11.2023**.

He took keen interest in his training and his conduct and performance was **excellent**. We wish him all success and bright future in his life.

For and on behalf of NFL

(Puran Singh)

I/c.

R&D Farm / STL Naya Nangal


NO. RMU/ADMN/ 12274

DATED: 18/12/23

**TO WHOM IT MAY CONCERN**

It is to certify that **Mr. Narayan Sharma S/o Sh. Dinesh Sharma**, Roll No. 200836 student of B.Sc. Agriculture (Hons.), Sri Guru Teg Bahadur Khalsa Collage, Sri Anandpur Sahib, Ropar (Pb.) has undergone in-plant training in Quality Assurance and Production Section at Verka Mohali Dairy.

During the training period from **01.11.2023** to **30.11.2023** his performance has been adjudged as '**Good**'.

  
**IN-CHARGE (ADMN)**  
**VERKA MOHALI DAIRY**

**THE ROPAR DISTRICT CO-OPERATIVE MILK PRODUCERS' UNION LIMITED**

Verka Mohali Dairy, Industrial Area, Phase-VI, S.A.S. Nagar, Mohali -160 055

PBX: 0172-2271784, 2271020, 2271021, 5039375

Email: gm.moh@verka.coop Website: www.verka.coop

GST No. 03AAAAT5977G1ZD





एक कदम स्वच्छता की ओर

नेशनल फर्टिलाइजर्स लिमिटेड

(भारत सरकार का उपक्रम)

आंचलिक कार्यालय : एस.सी.ओ. 76-79,

सेक्टर 17-डी, चण्डीगढ़ - 160017

दूरभाष : 0172-2703714, 2701693



NATIONAL FERTILIZERS LIMITED

(A Govt. of India Undertaking)

Zonal Office : SCO 76-79,

Sector 17-D, Chandigarh - 160017

Ph. : 0172-2703714, 2701693

NFL/Mktg/STL-R&D Farm/Nangal/ 752

Dated: 11.12.2023

### CERTIFICATE OF TRAINING

This is to certify that **Mr. Mohit Kumar**, student of B.Sc. (Hons) Agriculture of Sri Guru Teg Bahadur Khalsa College, Anandpur Sahib, (Pb) has undergone Training programme at **National Fertilizers Limited**, Naya Nangal for project work entitled on Package practices of Paddy Crop, Soil testing and R & D work at Farm. The project has been completed by the student in our company at Soil Testing Lab, Naya Nangal (Punjab) from **01.11.2023 to 30.11.2023**.

He took keen interest in his training and his conduct and performance was **excellent**. We wish him all success and bright future in his life.

For and on behalf of NFL

(Puran Singh)

I/c.

R&D Farm / STL Naya Nangal

पंजीकृत कार्यालय : स्कोप कॉम्प्लेक्स, कोर - III, 7, इंस्टिट्यूशनल एरिया, लोधी रोड, नई दिल्ली - 110003 दूरभाष : 011-24361252 फैक्स : 011-24361553

Regd. Office : Scope Complex, Core-III, 7, Institutional Area, Lodhi Road, New Delhi - 110003 Ph. : 011-24361252 Fax : 011-24361553

CIN : L7489DL1974G01007417 Website : <http://www.nationalfertilizers.com> @nationalfertilizers



NO. RMU/ADMN/ 11 679

DATED: 01/12/2023

**TO WHOM IT MAY CONCERN**

It is to certify that **Mr. Aryan Aery S/o Sh. Jitender Aery**, Roll No. 200804 student of B.Sc. Agriculture (Hons.), Sri Guru Teg Bhadur Khalsa Collage, Sri Anandpur Sahib, Ropar (PB.) has undergone in-plant training in Quality Assurance and Production Section at Verka Mohali Dairy.

During the training period from **01.11.2023 to 30.11.2023** his performance has been adjudged as '**Good**'.

  
**IN-CHARGE (ADMN)**  
**VERKA MOHALI DAIRY**



# verka

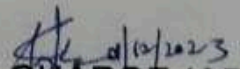
NO. RMU/ADMN/ 11680

DATED: 01/12/2023

**TO WHOM IT MAY CONCERN**

It is to certify that **Mr. Varun S/o Sh. Varinder Kumar**, Roll No. 200805 student of B.Sc. Agriculture (Hons.), Sri Guru Teg Bhadur Khalsa Collage, Sri Anandpur Sahib, Ropar (Pb.) has undergone in-plant training in Quality Assurance and Production Section at Verka Mohali Dairy.

During the training period from **01.11.2023 to 30.11.2023** his performance has been adjudged as '**Good**'.

  
**IN-CHARGE (ADMN)**  
**VERKA MOHALI DAIRY**

**THE ROPAR DISTRICT CO-OPERATIVE MILK PRODUCERS' UNION LIMITED**

Verka Mohali Dairy, Industrial Area, Phase-VI, S.A.S. Nagar, Mohali -160 055

PBX: 0172-2271784, 2271020, 2271021, 5039375

Email: gm.moh@verka.coop Website: www.verka.coop

GST No. 03AAAAT5977G1ZD





An ISO 9001:2015 Fax/Phone : 0172-2273247  
E Mail : Mohali.agro@markfedpunjab.com  
Website : [www.markfedpunjab.com](http://www.markfedpunjab.com)

Plant GST No  
03AAAAT3454G2Z5

MARKFED AGRO CHEMICALS  
7 & 8-B, INDL. ESTATE, S.A.S. NAGAR, 160055,  
DISTT. S.A.S. NAGAR (PUNJAB)

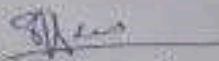
No. MACM/EST/2023/1600

Dated: 2/12/2023

**TO WHOM SO EVER IT MAY CONCERN**

It is certified that **Abhishek Bhardwaj S/o Sh. Mukteshwar Kumar** of **BSc Agriculture (Hons.) Roll No. 200806** of **Shri Guru Teg Bahadur Khalsa College, Sri Anandpur Sahib** has successfully completed his Industrial training w.e.f 03.11.2023 to 02-12.2023 in **Markfed Agro Chemicals, Mohali**.

His work and conduct during training period is found satisfactory. We wish his all the success for his future.

  
(S.S. Bajwa )  
Supdt.  
Markfed Agro Chemicals,  
S.A.S Nagar (Mohali)  
**Sarbjit Singh Bajwa**  
Superintendent  
Markfed Agro Chemical  
Mohali.


NO. RMU/ADMN/ 12269

DATED: 18/12/23

**TO WHOM IT MAY CONCERN**

It is to certify that **Mr. Gurpreet Singh S/o Sh. Harjap Singh**, Roll No. 200811 student of B.Sc. Agriculture (Hons.), Sri Guru Teg Bahadur Khalsa Collage, Sri Anandpur Sahib, Ropar (Pb.) has undergone in-plant training in Quality Assurance and Production Section at Verka Mohali Dairy.

During the training period from **01.11.2023 to 30.11.2023** his performance has been adjudged as '**Good**'.

  
**IN-CHARGE (ADMN)**  
**VERKA MOHALI DAIRY**

**THE ROPAR DISTRICT CO-OPERATIVE MILK PRODUCERS' UNION LIMITED**

Verka Mohali Dairy, Industrial Area, Phase-VI, S.A.S. Nagar, Mohali -160 055

PBX: 0172-2271784, 2271020, 2271021, 5039375

Email: gm.moh@verka.coop Website: www.verka.coop

GST No. 03AAAAT5977G1ZD



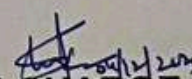
NO. RMU/ADMN/ 11811

DATED: 06/12/23

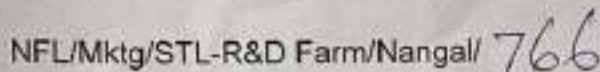
**TO WHOM IT MAY CONCERN**

It is to certify that **Mr. Nitish Thakur S/o Sh. Madan Gopal**, Roll No. 200820 student of B.Sc. Agriculture (Hons.), Sri Guru Teg Bahadur Khalsa Collage, Sri Anandpur Sahib, Ropar (Pb.) has undergone in-plant training in Quality Assurance and Production Section at Verka Mohali Dairy.

During the training period from **01.11.2023 to 30.11.2023** his performance has been adjudged as '**Good**'.

  
**IN-CHARGE (ADMN)**  
**VERKA MOHALI DAIRY**





## CERTIFICATE OF TRAINING

She took keen interest in her training and her conduct and performance was **excellent**. We wish her all success and bright future in her life.

(Puran Singh)

1/c

R&amp;D Farm / STL Naya Nangal

Dr. Puran Singh  
BSc, BEd, DipEd, MEd, PhD

Shift/Incharge

संयोजक: डॉ. वि. ए. शर्मा / N.F.J.

R&D Funding & Policy

**Full Path & ID:** Naya Nangal

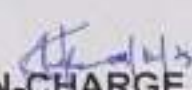
NO. RMU/ADMN/ 11810

DATED: 06/12/23

TO WHOM IT MAY CONCERN

It is to certify that **Mr. Anshul Sharma S/o Sh. Sandeep Sharma**, Roll No. 200824 student of B.Sc. Agriculture (Hons.), Sri Guru Teg Bahadur Khalsa Collage, Sri Anandpur Sahib, Ropar (Pb.) has undergone in-plant training in Quality Assurance and Production Section at Verka Mohali Dairy.

During the training period from 01.11.2023 to 30.11.2023 his performance has been adjudged as 'Good'.

  
IN-CHARGE (ADMN)  
VERKA MOHALI DAIRY



एक साथ पराक्रम की ओर

नेशनल फर्टिलाइजर्स लिमिटेड

(भारत सरकार का उपक्रम)

आंचलिक कार्यालय : एस.सी.ओ. 76-79,

सेक्टर 17-डी, चण्डीगढ़ - 160017

दूरभाष : 0172-2703714, 2701693



NATIONAL FERTILIZERS LIMITED

(A Govt. of India Undertaking)

Zonal Office : SCO 76-79,

Sector 17-D, Chandigarh - 160017

Ph. : 0172-2703714, 2701693

NFL/Mktg/STL-R&D Farm/Nangal/ 751

Dated: 11.12.2023

### CERTIFICATE OF TRAINING

This is to certify that **Mr. Ajay Kumar**, student of B.Sc. (Hons) Agriculture of Sri Guru Teg Bahadur Khalsa College, Anandpur Sahib, (Pb) has undergone Training programme at **National Fertilizers Limited**, Naya Nangal for project work entitled on Package practices of Paddy Crop, Soil testing and R & D work at Farm. The project has been completed by the student in our company at Soil Testing Lab, Naya Nangal (Punjab) from **01.11.2023 to 30.11.2023**.

He took keen interest in his training and his conduct and performance was **excellent**. We wish him all success and bright future in his life.

For and on behalf of NFL

(Puran Singh)

I/c.

R&D Farm / STL Naya Nangal





नया नंगल फर्टिलाइजर्स लिमिटेड  
(प्राइवेट लिमिटेड का उपाय)।  
आपका निवास - एन.डी.ओ. 74-79,  
सेक्टर 17-डी, चण्डीगढ़ - 160017  
दूरभाष - 0172-2701714, 2701693



NATIONAL FERTILIZERS LIMITED  
(A Govt. of India Undertaking)  
Zonal Office: SCO 16-19,  
Sector 17-D, Chandigarh - 160017  
Ph. : 0172-2701714, 2701693

NFL/Mktg/STL-R&D Farm/Nangal/ 754


Dated: 11.12.2023

### CERTIFICATE OF TRAINING

This is to certify that Mr. Shivam Banyal, student of B.Sc (Hons) Agriculture of Sri Guru Teg Bahadur Khalsa College Anandpur Sahib (Pb) has undergone Training programme at National Fertilizers Limited, Naya Nangal for project work entitled on Package practices of Paddy Crop Soil testing and R & D work at Farm. The project has been completed by the student in our company at Soil Testing Lab, Naya Nangal (Punjab) from 01.11.2023 to 30.11.2023.

He took keen interest in his training and his conduct and performance was excellent. We wish him all success and bright future in his life.

For and on behalf of NFL

  
11/12/2023

(Puran Singh)

I/c

R&D Farm/ STL Naya Nangal


NO. RMU/ADMN/ 12272

DATED: 18/12/23

**TO WHOM IT MAY CONCERN**

It is to certify that **Mr. Pawan Kumar S/o Sh. Darshan Singh**, Roll No. 200828 student of B.Sc. Agriculture (Hons.), Sri Guru Teg Bahadur Khalsa Collage, Sri Anandpur Sahib, Ropar (Pb.) has undergone in-plant training in Quality Assurance and Production Section at Verka Mohali Dairy.

During the training period from **01.11.2023 to 30.11.2023** his performance has been adjudged as 'Good'.

  
**IN-CHARGE (ADMN)**  
**VERKA MOHALI DAIRY**




NO. RMU/ADMN/ 12271

DATED: 18/12/23

**TO WHOM IT MAY CONCERN**

It is to certify that **Mr. Sourav Dhiman S/o Sh. Nirmal Singh**, Roll No. 200837 student of B.Sc. Agriculture (Hons.), Sri Guru Teg Bahadur Khalsa Collage, Sri Anandpur Sahib, Ropar (Pb.) has undergone in-plant training in Quality Assurance and Production Section at Verka Mohali Dairy.

During the training period from **01.11.2023 to 30.11.2023** his performance has been adjudged as 'Good'.

  
**IN-CHARGE (ADMN)**  
**VERKA MOHALI DAIRY**



# verka

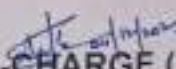
NO. RMU/ADMN/ 12273

DATED: 18/12/23

TO WHOM IT MAY CONCERN

It is to certify that **Mr. Harsh Rana S/o Sh. Rajesh Kumar**, Roll No. 200838 student of B.Sc. Agriculture (Hons.), Sri Guru Teg Bahadur Khalsa Collage, Sri Anandpur Sahib, Ropar (Pb.) has undergone in-plant training in Quality Assurance and Production Section at Verka Mohali Dairy.

During the training period from **01.11.2023 to 30.11.2023** his performance has been adjudged as '**Good**'.

  
**IN-CHARGE (ADMN)**  
**VERKA MOHALI DAIRY**

**THE ROPAR DISTRICT CO-OPERATIVE MILK PRODUCERS' UNION LIMITED**

Verka Mohali Dairy, Industrial Area, Phase-VI, S.A.S. Nagar, Mohali -160 055

PBX: 0172-2271784, 2271020, 2271021, 5039375

Email: gm.moh@verka.coop Website: www.verka.coop

GST No. 03AAAAT5977G12D

No.MACM/EST/2023/

Dated:

**TO WHOM SO EVER IT MAY**  
**CONCERN**

It is certified that **Harman Saini S/o Sh. Gogi Singh** of **BSc Agriculture (Hons.) Roll No. 200844** of **Shri Guru Teg Bahadur Khalsa College, Sri Anandpur Sahib** has successfully completed his Industrial training w.e.f 03.11.2023 to 02-12.2023 in **Markfed Agro Chemicals, Mohali.**

His work and conduct during training period is found satisfactory. We wish his all the success for his future.

**(S.S. Bajwa )**  
**Supdt.**  
Markfed Agro  
Chemicals,  
S.A.S Nagar (Mohali)







# verka

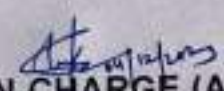
NO. RMU/ADMN/ 12270

DATED: 18/12/23

**TO WHOM IT MAY CONCERN**

It is to certify that **Mr. Hardeep Kumar S/o Sh. Sikander Pal**, Roll No. 200853 student of B.Sc. Agriculture (Hons.), Sri Guru Teg Bahadur Khalsa Collage, Sri Anandpur Sahib, Ropar (Pb.) has undergone in-plant training in Quality Assurance and Production Section at Verka Mohali Dairy.

During the training period from 01.11.2023 to 30.11.2023 his performance has been adjudged as 'Good'.

  
**IN-CHARGE (ADMN)**  
**VERKA MOHALI DAIRY**

**THE ROPAR DISTRICT CO-OPERATIVE MILK PRODUCERS' UNION LIMITED**

Verka Mohali Dairy, Industrial Area, Phase-VI, S.A.S. Nagar, Mohali -160 055

PBX: 0172-2271784, 2271020, 2271021, 5039375

Email: gm.moh@verka.coop Website: www.verka.coop

GST No. 03AAAAT5977G1ZD



An ISO 9001:2015 Fax/Phone : 0172-2273247

E Mail : Mohali.agro@markfedpunjab.com

Website : [www.markfedpunjab.com](http://www.markfedpunjab.com)

Plant GST No  
03AAAAT3434G225

MARKFED AGRO CHEMICALS

7 & 8-B, INDL ESTATE, S.A.S.NAGAR, 160055,  
DISTT. S.A.S.NAGAR (PUNJAB)

No.MACM/EST/2023/ 1596

Dated: 2/12/2023

### TO WHOM SO EVER IT MAY CONCERN

It is certified that Harpreet Singh S/o Sh. Ravinder Singh of BSc Agriculture (Hons.) Roll No. 200849 of Shri Guru Teg Bahadur Khalsa College, Sri Anandpur Sahib has successfully completed his Industrial training w.e.f 03.11.2023 to 02-12.2023 in Markfed Agro Chemicals, Mohali.

His work and conduct during training period is found satisfactory. We wish his all the success for his future.

  
(S.S. Bajwa)

Supdt.

Markfed Agro Chemicals,  
S.A.S Nagar (Mohali)

Sarbjit Singh Bajwa  
Superintendent  
Markfed Agro Chemical  
Mohali.





एक साथ पराक्रम की ओर

नेशनल फर्टिलाइजर्स लिमिटेड

(भारत सरकार का उपक्रम)

आंचलिक कार्यालय : एस.सी.ओ. 76-79,

सेक्टर 17-डी, चण्डीगढ़ - 160017

दूरभाष : 0172-2703714, 2701693



NATIONAL FERTILIZERS LIMITED

(A Govt. of India Undertaking)

Zonal Office : SCO 76-79,

Sector 17-D, Chandigarh - 160017

Ph. : 0172-2703714, 2701693

NFL/Mktg/STL-R&D Farm/Nangal/ 751

Dated: 11.12.2023

### CERTIFICATE OF TRAINING

This is to certify that **Mr. Ajay Kumar**, student of B.Sc. (Hons) Agriculture of Sri Guru Teg Bahadur Khalsa College, Anandpur Sahib, (Pb) has undergone Training programme at **National Fertilizers Limited**, Naya Nangal for project work entitled on Package practices of Paddy Crop, Soil testing and R & D work at Farm. The project has been completed by the student in our company at Soil Testing Lab, Naya Nangal (Punjab) from **01.11.2023 to 30.11.2023**.

He took keen interest in his training and his conduct and performance was **excellent**. We wish him all success and bright future in his life.

For and on behalf of NFL

(Puran Singh)

I/c.

R&D Farm / STL Naya Nangal



एन एफ एल लिमिटेड की ओर

नेशनल फर्टिलाइजर्स लिमिटेड

(भारत सरकार का उपक्रम)

आंचलिक कार्यालय : एस.सी.ओ. 76-79,

सेक्टर 17 - डी, चण्डीगढ़ - 160017

दूरभाष : 0172-2703714, 2701693



NATIONAL FERTILIZERS LIMITED

(A Govt. of India Undertaking)

Zonal Office : SCO 76-79,

Sector 17-D, Chandigarh - 160017

Ph. : 0172-2703714, 2701693

NFL/Mktg/STL-R&D Farm/Nangal/ 758

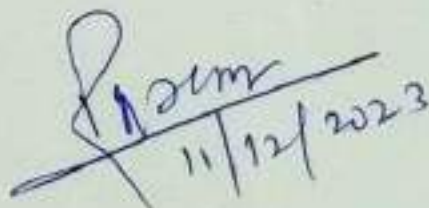
Dated: 11.12.2023

### CERTIFICATE OF TRAINING

This is to certify that **Mr. Raman**, student of B.Sc. (Hons) Agriculture of Sri Guru Teg Bahadur Khalsa College, Anandpur Sahib, (Pb) has undergone Training programme at **National Fertilizers Limited**, Naya Nangal for project work entitled on Package practices of Paddy Crop, Soil testing and R & D work at Farm. The project has been completed by the student in our company at Soil Testing Lab, Naya Nangal (Punjab) from **01.11.2023 to 30.11.2023**.

He took keen interest in his training and his conduct and performance was **excellent**. We wish him all success and bright future in his life.

For and on behalf of NFL

  
11/12/2023

(Puran Singh)

I/c.

R&D Farm / STL Naya Nangal

पंजीकृत कार्यालय : स्कोप कॉम्प्लेक्स, कोर - III, 7, इंस्टिट्यूशनल एरिया, लोधी रोड, नई दिल्ली - 110003 दूरभाष : 011-24361252 फैक्स : 011-24361553

Regd. Office : Scope Complex, Core-III, 7, Institutional Area, Lodhi Road, New Delhi - 110003 Ph. : 011-24361252 Fax : 011-24361553

CIN : L7489DL1974G01007417 Website : <http://www.nationalfertilizers.com> @nationalfertilizers





An ISO 9001:2015 Fax/Phone : 0172-2273247  
E Mail : Mohali.agro@markfedpunjab.com  
Website : [www.markfedpunjab.com](http://www.markfedpunjab.com)

Plant GST No  
03AAAAT3454G2Z5

MARKFED AGRO CHEMICALS  
7 & 8-B, INDL. ESTATE, S.A.S.NAGAR, 160055,  
DISTT. S.A.S.NAGAR (PUNJAB)

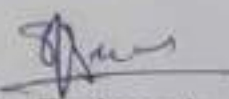
No.MACM/EST/2023/ 1601

Dated: 2/12/2023

### TO WHOM SO EVER IT MAY CONCERN

It is certified that **Kanchan Rana D/o Sh. Sanjeev Kumar** of **BSc Agriculture (Hons.) Roll No. 200856** of **Shri Guru Teg Bahadur Khalsa College, Sri Anandpur Sahib** has successfully completed her Industrial training w.e.f 03.11.2023 to 02-12.2023 in **Markfed Agro Chemicals, Mohali.**

Her work and conduct during training period is found satisfactory. We wish her all the success for her future.

  
(S.S. Bajwa )  
Supdt.

Markfed Agro Chemicals,  
S.A.S Nagar (Mohali)  
**Sarbjit Singh Bajwa**  
Superintendent  
Markfed Agro Chemical  
Mohali.



नेशनल फर्टिलाइजर्स लिमिटेड  
(भारत सरकार का उपक्रम)  
आधुनिक कार्यालय : एम.जी.ओ. 76-79,  
सेक्टर 17-डी, चण्डीगढ़ - 160017  
दूरभाष : 0172-2703714, 2701693



NATIONAL FERTILIZERS LIMITED  
(A Govt. of India Undertaking)  
Zonal Office : SCO 76-79,  
Sector 17-D, Chandigarh - 160017  
Ph : 0172-2703714, 2701693

NFL/Mktg/STL-R&D Farm/Nangal/ 750

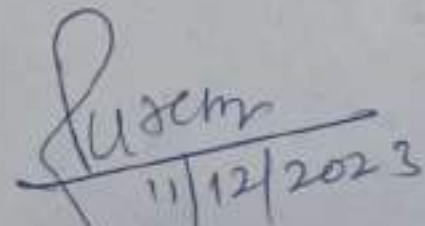
Dated: 11.12.2023

### CERTIFICATE OF TRAINING

This is to certify that **Mr. Nikhil**, student of B.Sc. (Hons) Agriculture of Sri Guru Teg Bahadur Khalsa College, Anandpur Sahib, (Pb) has undergone Training programme at **National Fertilizers Limited**, Naya Nangal for project work entitled on Package practices of Paddy Crop, Soil testing and R & D work at Farm. The project has been completed by the student in our company at Soil Testing Lab, Naya Nangal (Punjab) from **01.11.2023 to 30.11.2023**.

He took keen interest in his training and his conduct and performance was **excellent**. We wish him all success and bright future in his life.

For and on behalf of NFL

  
11/12/2023

(Puran Singh)

I/c.

R&D Farm / STL Naya Nangal





नेशनल फर्टिलाइजर्स लिमिटेड

(भारत सरकार का उपक्रम)

आंचलिक कार्यालय : एन.सी.ओ. 76-79,

सेक्टर 17-डी, चण्डीगढ़ - 160017

दूरभाष : 0172-2703714, 2701693



NATIONAL FERTILIZERS LIMITED

(A Govt. of India Undertaking)

Zonal Office : SCO 76-79,

Sector 17-D, Chandigarh - 160017

Ph. : 0172-2703714, 2701693

NFL/Mktg/STL-R&D Farm/Nangal/ 757

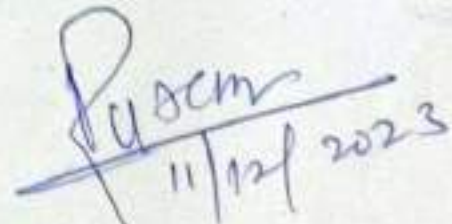
Dated: 11.12.2023

### CERTIFICATE OF TRAINING

This is to certify that **Mr. Abhishek Rana**, student of B.Sc. (Hons) Agriculture of Sri Guru Teg Bahadur Khalsa College, Anandpur Sahib, (Pb) has undergone Training programme at **National Fertilizers Limited**, Naya Nangal for project work entitled on Package practices of Paddy Crop, Soil testing and R & D work at Farm. The project has been completed by the student in our company at Soil Testing Lab, Naya Nangal (Punjab) from **01.11.2023 to 30.11.2023**.

He took keen interest in his training and his conduct and performance was **excellent**. We wish him all success and bright future in his life.

For and on behalf of NFL

  
11/12/2023

(Puran Singh)

I/c.

R&D Farm / STL Naya Nangal

पंजीकृत कार्यालय : स्कोप कॉम्प्लेक्स, कोर - III, 7, इंस्टिट्यूशनल एरिया, लोधी रोड, नई दिल्ली - 110003 दूरभाष : 011-24361252 फैक्स : 011-24361553

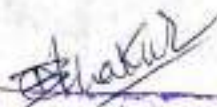
Regd. Office : Scope Complex, Core-III, 7, Institutional Area, Lodhi Road, New Delhi - 110003 Ph. : 011-24361252 Fax : 011-24361553

CIN : L7489DL1974G01007417 Website : <http://www.nationalfertilizers.com> @nationalfertilizers

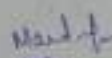


B.Voc. Food Processing Sem - VI  
Session- 2023-24

Sr. No	Name	University Roll No.
1	HARSIMRANJEET KAUR	14251
2	KANCHAN KUMARI	14253
3	TARANJEET KAUR	14254
4	JAGDEEP KAUR	14255
5	JASVEER SINGH	14258
6	DEEPAK	14260
7	HARSH KUMAR	14261

  
Head,  
Department of Agriculture  
SOTS Khales College  
Gri Anandpur Sahib

1.3.3	Percentage of programs that have components of field Projects / Research Projects/ Internships during the last five years				
	Department - Chemistry(2023-24)				
	Session (2023-24)				
S.NO.	Course Name	Course Code	Class Roll No.	Student Name	Project Title
1	M.Sc Chemistry	MC402	221730	Priyanka	Chemosensing Properties of a Benzimidazole Chromophore: Interplay Between Theory and Experiment
2	M.Sc Chemistry	MC402	221739	Jagjeet Singh	Spectrophotometric Analysis of Imidazole Based Chromomorphores
3	M.Sc Chemistry	MC402	221711	Shikani	Development of an Effective Indole Based Chemosensory for Cupric ions
4	M.Sc Chemistry	MC402	221712	Arun Kumar	Synthesis of Calcium Ferrite and it's application to Photocatalytic Degradation of dye
5	M.Sc Chemistry	MC402	221723	Gurmeet Kaur	Auto combustion - Promoted Synthesis of CdFe <sub>2</sub> O <sub>4</sub> Application as Photocatalyst in Environmental Remediation
6	M.Sc Chemistry	MC402	221706	Amandeep Kaur	Synthesis of Heterocyclic Compounds using of Manganese Iron Oxide Nanoparticles

  
 Head  
 P.G. Department of Chemistry  
 BATHINDA College  
 Bathinda-151001

# Chemosensing Properties of a Benzimidazole Chromophore: Interplay Between Theory and Experiment

A Project Report



Department of Chemistry

SRI GURU TEG BAHADUR KHALSA COLLEGE,

SRI ANANDPUR SAHIB

Affiliated to Punjabi University, Patiala

Submitted To

*Mandeep Kaur*  
Dr. Mandeep Kaur

*Priyanka*

Submitted By

Priyanka  
M.Sc Chemistry  
Roll No. 221730

# Spectrophotometric Analysis of Imidazole Based Chromophores

A Project Report



Department of Chemistry

SRI GURU TEG BAHADUR KHALSA COLLEGE,

SRI ANANDPUR SAHIB

Affiliated to Punjabi University, Patiala

Submitted To

*Mandeep Kaur*  
Dr. Mandeep Kaur

*Jagjeet Singh*  
Submitted By

Jagjeet Singh  
M.Sc Chemistry  
Roll No. 221739

# Development of an Effective Indole Based Chemosensory for Cupric ions

A Project Report



Department of Chemistry

SRI GURU TEG BAHADUR KHALSA COLLEGE,

SRI ANANDPUR SAHIB

Affiliated to Punjabi University, Patiala

Submitted To

*Mandeep Kaur*  
Dr. Mandeep Kaur

Submitted By

*Shivani*

Shivani

M.Sc Chemistry

Roll No. 221711



# Synthesis of Calcium Ferrite and its application to Photocatalytic Degradation of dye

A Project Report



Department of Chemistry

SRI GURU TEG BAHADUR KHALSA COLLEGE,

SRI ANANDPUR SAHIB

Affiliated to Punjabi University, Patiala

Submitted To

Dr. Gagandeep Kaur

Submitted By

Arun

M.Sc Chemistry

Roll No. 221712

# Auto combustion - Promoted Synthesis of $\text{CdFe}_2\text{O}_4$ : Application as Photocatalyst in Environmental Remediation

A Project Report



Department of Chemistry

SRI GURU TEG BAHADUR KHALSA COLLEGE,

SRI ANANDPUR SAHIB

Affiliated to Punjabi University, Patiala

Submitted To

Dr. Gagandeep Kaur

Submitted By

Gurmeet Kaur

Gurmeet Kaur

M.Sc. Chemistry

Roll No. 221723

# Synthesis of Heterocyclic Compounds using of Manganese Iron Oxide Nanoparticles

A -Project Report



Department of Chemistry

SRI GURU TEG BAHADUR KHALSA COLLEGE,

SRI ANANDPUR SAHIB

Affiliated to Punjabi University ,Patiala

Submitted To

Dr. Gagandeep Kaur

Submitted By

Amandeep Kaur  
Amandeep Kaur  
M.Sc Chemistry  
Roll No. 221706